THE FLOW OF PARTICULATE BULK SOLIDS IN AN AIR-ASSISTED GRAVITY CONVEYOR

by

C. R. Woodcock, DipTech(Eng) MSc CEng MIMechE MInstR AWP

(Thesis submitted for the degree of Doctor of Philosophy under the conditions for the award of higher degrees of the Council for National Academic Awards.)

School of Mechanical Engineering,
Thames Polytechnic, London.

October, 1978

ABSTRACT

The programme of work commenced with a thorough survey of the published literature relating to the air-assisted gravity conveying of bulk particulate solids. Aspects of the behaviour of fluidised powder in stationary beds were studied where it seemed possible that observations of such behaviour might be useful in predicting how the same powder would flow in an air-gravity conveyor. As a result, a simple chart was prepared allowing an estimate to be made of the minimum fluidising velocity and the velocity at which entrainment of fines could occur from a knowledge only of the density and particle size of the powder concerned.

The design and performance of air-gravity conveyors was examined in some detail, considerable effort having been made to bring together as much as possible of the published information on this method of bulk solids transport. Practical problems on the design and operation of conveying installations have been highlighted and techniques are suggested to simplify the preliminary stages of design.

One of the difficulties facing the designer of air-gravity conveyors has been the lack of a convenient mathematical model that would enable the performance of a given conveyor to be reliably predicted. A number of possible modelling techniques were therefore investigated and a new modelling approach, based on the uniform flow of a fluid in an inclined channel, has been proposed.

The experimental work was divided into two parts. In the first part various types of porous distributor material were examined and their relative merits discussed, and then a number of powders, having widely differing characteristics, were tested in a small fluidising rig. Significant features of the fluidisation behaviour of the powders in "stationary" (as opposed to "flowing") beds were recorded, notably their minimum fluidising velocities and bulk densities.

The second part of the experimental programme involved the flow of an aerated p.v.c. powder, of about 120 μm mean particle size, in an inclined channel. Two types of porous distributor were used in the channel, and it

each case the relationships amongst the solids mass flowrate, the channel slope, the superficial velocity of the fluidising air and the depth of the flowing bed were observed. Using the modelling approach proposed previously, the results of the tests on the channel rig were analysed and it was concluded that, although more experimental data was needed, the correlation between the model and the data obtained so far confirmed that further investigation would be justified.

"..... when you can measure what you are speaking about, and express it in numbers, you know something about it; but when you cannot measure it, when you cannot express it in numbers, your knowledge is of a meagre and unsatisfactory kind: it may be the beginning of knowledge, but you have scarcely, in your thoughts, advanced to the state of SCIENCE, whatever the matter may be."

(Lord Kelvin, as Sir William Thomson, speaking on "Electrical Units of Measurement" at the Institution of Civil Engineers, London, 3 May 1883.)

CONTENTS

AUTHOR'S NOTE

All the work in this thesis is the sole and original work of the author, except where indicated otherwise by acknowledgement or reference.

Substantial parts of the thesis have been presented at conferences, or have been prepared and accepted for presentation in the near future. Details are to be found in Appendix A.VII.

ACKNOWLEDGEMENTS

For his continued encouragement, advice and assistance throughout the programme of work I should like to express my sincere gratitude to my supervisor, Dr. J. S. Mason. It was largely as a result of his infectious enthusiasm, especially at times when progress seemed to be slow, that I was able to bring this work to a conclusion.

I owe debts of gratitude to many members of the academic and technician staff of the School of Mechanical Engineering at Thames Polytechnic; particularly to Dr. B. J. Jeffery and my colleagues in the Division of Fluid Flow and Thermodynamics for the various ways in which they have eased my teaching workload during the last two or three years, to Mr. N. A. Livermore for the design and construction of the mass flow meter, to Mr. I.R. Bittle for many helpful discussions, and to Mr. W. S. Churchill and his staff, notably Messrs. Wood, Curtis and Gray, for the construction of the experimental rigs. Some of the data relating to the fluidisation behaviour of sand were derived from test readings taken by a final-year undergraduate student, Mr. C. Goulding, and his assistance in this area is duly acknowledged. My thanks also go to the staff of the Polytechnic Central Services Unit, especially Mrs. S. Reed, who took all the photographs of the experimental rigs.

I would like to express my thanks to the various individuals and firms outside the Polytechnic who assisted in this work by providing helpful suggestions or materials or both. In this respect I should mention first and foremost Mr. R. B. Stacey for his valuable advice and assistance, especially with the initial design of the channel rig. Also I acknowledge with thanks the contributions of Mr. G. Dixon and I.C.I. Ltd., Messrs. Geo. W. King Ltd., Porvair Ltd., and Scandura Ltd.

For her magnificent efforts on the formidable task of typing this thesis I owe a special debt of gratitude to Mrs. Lesley Hopkins.

These acknowledgements would not be complete without a mention of the part played by my wife Angela. For the several years that I have been absorbed

in this work she has had to live with my moods of elation and depression which fluctuated much as the relative humidity from day to day! Through all this she has displayed patience and understanding far beyond the call of duty and my gratitude to her is immeasurable.

NOMENCLATURE

a	a variable index
A	cross-sectional area of packed or fluidised bed; constant in equation A.III.42 et seq.
Ar_b	Archimedes number for particulate bed (defined by equation 2.3.3)
A_{sp}	surface area of particle
A_{sm}	average surface area of a number of particles
b	width of conveying channel
B	constant in equation A.III.42 et seq.
C_d	drag coefficient for a particle in a gas flow
C_d'	modified drag coefficient defined by equation A.II.40a
d	diameter of spherical particle
d_A	particle size in sieve analysis
d_s	"surface diameter" of particle
d_{st}	Stokes diameter of particle
d_v	"volume diameter" of particle
d_{vsm}	volume-surface mean diameter of a collection of particles
d_{wm}	mass median particle size
f	friction factor (defined by equation 4.2.20)
F_D	drag force on particle
F_G	gravity force on particle
g	specific gravitational force, 9.81 N/kg
G	function in equation 4.3.14
h	height (or depth) of packed or fluidised bed
h_{mf}	height (or depth) of bed of particles at condition of minimum fluidisation
H	height of fall of particles in sedimentation tank
k	consistency coefficient of non-Newtonian (power law) fluid
k, k', k''	constants or coefficients as defined in text
k_b, k_w	shear stress/velocity coefficients (defined by equations 4.3.10 and 4.3.3)
k_f	friction coefficient for flow in packed bed
K, K', K_t	constants or coefficients as defined in text
K_1	parameter in equation 4.3.19, defined by $K_1 = u_s/\tau_b$
K_2	parameter in equation 4.3.19, defined by $K_2 = 2\tau_w$
L	length of channel

$\dot{m}$	mass flowrate of fluid
$\dot{m}_s$	mass flowrate of solids in suspension
n	exponent governing bed expansion; non-Newtonian fluid (power law) index
N	number of particles per unit volume of a bed
Δp	pressure drop ($p_2 - p_1$)
Δp_b	pressure drop across packed or fluidised bed
P, Q	constants in equation 4.1.2
r_a	aspect ratio (h/b)
r_e	expansion ratio of fluidised bed
R_b	flow resistance (force) per unit area of particulate bed surface
R_{bc}	flow resistance of particulate bed at onset of channelling
R_d	flow resistance of distributor
Re_b	Reynolds number for flow of a gas through a packed bed
Re_{mf}	Reynolds number for particulate bed at condition of minimum fluidisation (defined by equation 2.3.2)
Re_p	Reynolds number for a particle in a gas flow (defined by equation 2.5.4)
Re'	modified Reynolds number (defined by equation 4.2.17)
Re'_p	modified Reynolds number (defined by equation A.II.40b)
S_b	specific surface of a bed of particles
S_p	specific surface of a particle
t_o	elapsed time
u	fluid velocity
u_{av}	average velocity of flowing fluid
u_{max}	velocity on the surface of a flowing suspension
u_s	average velocity of flowing bed of powder
u_{slip}	slip velocity at boundary
U_c	superficial velocity in the continuous phase in a particulate bed
U_{fs}	minimum superficial velocity at which a bed of powder is fully supported
U_g	superficial velocity in a packed or fluidised bed
U_i	the value of U_c at $\varepsilon = 1$ (see equation 2.4.1)
U_{mb}	minimum superficial velocity at which spontaneous bubbling occurs
U_{mf}	superficial velocity at condition of incipient fluidisation
U_t	terminal velocity of a particle
$\dot{V}$	volumetric flowrate of fluid

V_b	total volume of packed or fluidised bed
V_p	volume of particle
$\dot{V}_s$	volumetric flowrate of solids
$\dot{V}_w$	volumetric flowrate of liquid
W_b	weight of bed of particles
x	mass fraction of component in mixture
x,y	space coordinates; indices in equation 3.2.1
α	slope of conveying channel
$\dot{\gamma}$	shear rate
$\dot{\gamma}_b$	shear rate at base of channel
$\dot{\gamma}_R$	shear rate at surface of viscometer rotor
$\dot{\gamma}_w$	shear rate at side walls of channel
ε	voidage, or porosity
ε_o	voidage of packed bed
ε_{mf}	voidage of bed at condition of minimum fluidisation
η	coefficient of rigidity of non-Newtonian fluid
λ	hydraulic mean depth defined by equation 4.2.16
μ	viscosity of fluid
μ_a	apparent viscosity of non-Newtonian fluid
μ_g	viscosity of gas
ν	kinematic viscosity of fluid
ρ	density of fluid
ρ_b	apparent density of bed of particles; bulk density
ρ_g	density of gas
ρ_p	"true" density of a particle
τ_b	shear stress at surface of plane or at bottom of channel
τ_o	average boundary shear stress
τ_R	shear stress at surface of viscometer rotor
τ_w	shear stress at side walls of channel
τ_y	yield stress in Bingham plastic model
ϕ_s	sphericity of a particle (defined in Section 2.2.2)
ω	angular velocity

LIST OF PHOTOGRAPHS

PART I

THEORETICAL STUDY AND LITERATURE SURVEY

CHAPTER ONE

INTRODUCTION

With the continually escalating costs of packaging and labour, the advantages of handling particulate materials in bulk are becoming ever more apparent. Amongst the various established methods of bulk solids transport, pneumatic conveying by pipeline has, in recent years, shown a considerable upsurge in popularity. The principal features of this type of conveyor are its cleanliness, convenience and ease of installation and low capital cost, but these advantages have to be balanced against the less desirable features which include high power consumption and risk of degradation of the particulate material (or erosion of the pipeline and fittings) when conveying at high velocities.

In order to combat the disadvantages of erosion and high power usage the current trend in the pneumatic handling industry is towards "dense phase" transport in which the ratio of particulate solids to conveying air is greatly increased. In this way the power consumption is reduced, and, since the transport velocities are much lower, the risk of erosion or degradation of the conveyed material is virtually eliminated. However, dense-phase conveying also has its problems, not least of which is the increased tendency of the pipeline to become blocked. A further difficulty stems from the fact that this type of conveying system operates at a high pressure difference. This means that conventional methods of feeding the particulate material into the line cannot be used, and the usual technique is to convey the material in batches from a pressurized "blow-tank". Furthermore, even these systems have a fairly high power requirement compared with say a belt conveyor.

Clearly then, there is a need for a pneumatic system that will operate continuously at high solids flowrates, with low power usage and with minimum risk of degradation or erosion damage. Such a system already exists, and has done so for many years, in the form of the air-assisted gravity conveyor, commonly known by the trade name, "air-slide". Yet in spite of the superiority of this type of conveyor

in many situations involving the transport of bulk particulate solids (its only major limitation being the need for a continuous slight fall in elevation over its whole length) it does not appear to have achieved in the industry the widespread acceptance that might have been expected. The reason for this hesitation on the part of the user industry is not really clear, but may stem from a few unfortunate experiences resulting from incorrect design or attempts to handle unsuitable materials. Certainly there is very little published information that is directly helpful to the designer of an air-assisted gravity conveying system, although there must exist a wealth of practical data collected by manufacturers and installers which, if it were to be made generally available, would be invaluable to the industry as a whole.

The air-assisted gravity conveyor relies for its successful operation on the use of air (or other gas), supplied through the porous base of a channel, to reduce the particle-particle and particle-wall contact forces so that the bulk solid in the channel will "flow" under gravity even when the inclination of the channel is very small. It is in fact a relatively simple matter to make an air-gravity channel that will work, but if it is to work efficiently and reliably as a conveyor, and especially if it is to handle "difficult" materials, the designer needs to have a good understanding of the nature of aerated solids flow. Because of the shortage of technical data in the literature (and the difficulty of locating what data there is) the designer has had to rely almost entirely on practical experience for his understanding of the subject. The main purpose of the present work is not to remove the need for such practical experience (for which there is really no substitute) but to reinforce it by assembling in one volume as much information as possible on sources of relevant data. To this end the present programme of work has included what is believed to have been the most extensive study yet undertaken of the literature relevant to the air-assisted gravity conveying of bulk particulate solids.

Two familiar phenomena that have been extensively investigated and modelled by many research workers are appropriate to the present study and may be helpful in the synthesis of models of powder flow. These are the fluidisation of particulate materials and the flow of liquids

in inclined channels. A knowledge of the fluidisation behaviour of a powder will obviously be valuable in assessing its suitability for air-assisted gravity conveying and also in estimating the quantity of air required, and therefore the present work includes a detailed discussion of the fluidisation phenomenon, particularly with regard to the methods of predicting the behaviour of a bulk solid from the basic properties of particle density and particle size. It is suggested that since powder handling is not now, and is never likely to be, an exact science, the very intricate models of powder behaviour that have been proposed from time to time are probably little more reliable than some of the much more straightforward models involving a minimum number of system variables. A simple chart is presented, which it is felt should provide a useful preliminary indication of the probable fluidisation and flow characteristics of a powder when aerated in an inclined channel.

In some senses the present programme of work was seen as the forerunner to a series of studies on different aspects of bulk solids flow in inclined channels and consequently there is perhaps a bias towards the collection and analysis of previously published data. However, there appeared to exist a need for a simple practical approach to the experimental study of flow in air-gravity channels and therefore a modelling technique was developed which it is hoped will eventually allow the conveying characteristics of bulk solids to be quite easily predicted by comparison with one of a group of documented types. This technique of examining the relationships between the main system variables is introduced towards the end of Part I of this work, and is later amplified and discussed in more detail in the light of the experimental data reported in Part II.

CHAPTER TWO

THE FLUIDISATION OF BULK SOLIDS

2.1 INTRODUCTION

If a fluid is passed upwards through a supported bed of solid particles or granules at a relatively low flowrate it will merely filter through the interstitial voids without disturbing the packing arrangement of the bed. For a given bed the pressure drop across it would depend only on the flowrate of the fluid, in most cases the relationship being approximately proportional. This system is termed a "fixed" or "packed" bed.

As the rate of upward fluid flow is increased a stage will be reached at which the individual particles or granules become buoyantly supported in the flow and the bed is said to be "fluidised". In this condition the bed exhibits many fluidlike characteristics; for example, it will flow from a hole in the side of the fluidising vessel, light objects can be "floated" on its surface, and the surface will remain horizontal if the vessel is tilted.

Further increase in the fluid flowrate will cause the bed of particles to expand, thus allowing additional space between the particles through which the fluid can pass. Alternatively, the excess fluid passes upwards through the bed as a series of voids or bubbles. Eventually, a point will be reached when the interstitial velocity of the upward flowing fluid approaches the terminal velocity of individual solid particles. These particles then tend to become entrained in the flow, being carried upwards from the surface of the bed; and the system approaches a state equivalent to that of pneumatic transport.

The fluidisation technique has found widespread acceptance in industry as a means of ensuring continuous contacting between a particulate or granular solid and a stream of gas or liquid, one of the first applications being for the gassification of powdered coal. Wartime fuel requirements provided the impetus for a rapid development in the petroleum industry of the fluid catalytic cracking process, and the knowledge gained during such development, combined with the results of technological research, led to a considerable improvement in the understanding of fluidised bed behaviour. Many other processes making use

of the advantageous properties of fluidised beds have been developed in industry, including drying, mixing, plastic coating, fluidised combustion and bulk solids transport. (For an interesting review of some of these applications, see Ref. K10.)

The various stages of the fluidisation process are considered in the following sections, from flow through a fixed bed to elutriation. Some of the main factors influencing the quality of fluidisation are then discussed. Theoretical analysis of fluidisation is always difficult because of the large number of variables involved and reliance has to be placed upon a combined approach of simple physical models blended with appropriate experimental data. For instance, even in the case of movement of gas or liquid through a fixed bed, the intermingling of fluid with solid particles of diverse size and shape creates a flow of extreme complexity; and yet the experimental determination of the relationship between pressure drop and flow rate generally presents few difficulties.

An enormous amount of literature is available on the subject of fluidisation and the following survey and discussion has of necessity been somewhat restricted. Although there are many obvious similarities between gas and liquid systems, the experimental study undertaken has been concerned with air-assisted gravity conveying of bulk particulate solids rather than with slurry transport, and the present review is therefore limited to aspects of gas fluidisation relevant to its use as an aid to bulk solids transport.

2.2 FLOW THROUGH A FIXED BED OF SOLID PARTICLES

2.2.1 Introduction

Flow of a fluid upwards through a supported bed of solid particles corresponds closely to flow through a porous medium, the difference between the two situations only really becoming evident when the fluid flowrate is of sufficient magnitude to cause movement of individual particles within the bed. It has been pointed out by Zabrodsky (Ref. Z1, page 1) that up to this state the permeation of fluid through the

fixed bed can be regarded either as an internal flow of fluid in the interconnecting channels between the particles, or as an external flow around the particles. According to Zabrodsky the latter approach is more easily justified, but probably the greater number of authors have chosen to treat permeation as an internal flow problem and that is the approach that is followed in this work. Keuneke (Ref. K3) gives a detailed review of attempts to develop theoretical and semi-empirical expressions for pressure drop in packed and fluidised beds. The work that seems to have achieved the greatest acceptance among those seeking to predict the flow behaviour in fixed beds is that of Carman (Ref. C2) whose extensive study has more recently been augmented by Ergun (Ref.E2). Upon their work is based much of the analytical modelling subsequently proposed by various authors leading to expressions for the pressure drop across a fixed bed in terms of the properties of the flowing fluid and of the solid particles within the bed.

2.2.2 Pressure drop across fixed beds

Ergun (Ref. E2) has listed the variables influencing flow behaviour in fixed beds as the rate of fluid flow, the viscosity and density of the fluid, the closeness and orientation of packing, and the size, shape and surface of the particles. The variables concerning the packed solids are the VOIDAGE (also called POROSITY or VOID FRACTION) defined as

$$\varepsilon_o = \frac{\text{volume of voids}}{\text{total volume of bed}} \qquad \text{.....2.2.1}$$

and the size and shape of the particles, which are conveniently characterised by defining a VOLUME DIAMETER and a SPHERICITY as follows:

VOLUME DIAMETER, d_v, is the diameter of a sphere having the same volume as the particle.

$$\text{SPHERICITY, } \phi_s, = \frac{\text{surface area of sphere having volume of particle}}{\text{surface area of particle}}$$

(Note that $\phi_s \leq 1$)

These parameters can be related by noting that, since the volume of solid particles in a bed of unit volume is $(1 - \varepsilon_o)$, we can write the number of particles per unit volume of the bed as

$$N = \frac{6(1 - \varepsilon_o)}{\pi d_v^3} \qquad \text{.....2.2.2}$$

and the surface area of particles in unit volume of the bed (that is, the SPECIFIC SURFACE of the bed) is then given by

$$S_b = N \frac{\pi d_v^2}{\phi_s} = \frac{6(1 - \varepsilon_o)}{\pi d_v^3} \cdot \frac{\pi d_v^2}{\phi_s}$$

$$\text{or} \qquad S_b = \frac{6(1 - \varepsilon_o)}{\phi_s d_v} \qquad \text{.....2.2.3}$$

(It should be noted that there are many other ways of characterising particle size, and the mean size of a collection of particles of different sizes, and some of these are introduced in Appendix A I.)

The analytical approach leading to the development of various forms of the so-called Carman-Kozeny equation for flow in packed beds is now well established (see for example, Ref. K2 page 262 et seq.) and can be extended to yield various expressions for the pressure drop in laminar flow through such beds, as described in Appendix A II. An alternative analysis leads to an expression for pressure drop in terms of the kinetic energy of the flowing fluid and combining these gives a general equation as

$$\frac{\Delta p_b}{h} = \frac{1 - \varepsilon_o}{\phi_s^2 \varepsilon_o^3} \cdot \frac{\rho_g U^2}{d_v} \left(\frac{100}{Re_b} + 1.75\right) \qquad \text{.....2.2.4}$$

in which U is the superficial velocity of the flowing fluid in a packed bed of depth h, and Re_b is a Reynolds number for the bed defined as

$$Re_b = \frac{2}{3}\left(\frac{\phi_s}{1 - \varepsilon_o}\right)\frac{d_v U}{\nu_g} \qquad \text{.....2.2.5}$$

Expanding equation 2.2.4 yields the familiar Ergun equation which

represents the pressure drop across a packed bed as the sum of viscous effect and kinetic energy effect,

$$\frac{\Delta p_b}{h} = 150 \frac{(1-\varepsilon_o)^2}{\phi_s^2 \varepsilon_o^3} \cdot \frac{\mu_g U}{d_v^2} + 1.75 \frac{1-\varepsilon_o}{\phi_s \varepsilon_o^3} \cdot \frac{\rho_g U}{d_v} \quad \text{.....2.2.6}$$

One of the main problems in the practical use of this and other expressions for pressure drop in a packed bed arises from difficulty in determining the actual voidage of the bed and the sphericity of the particles in it. Some discussion on this aspect of the work is to be found in Appendix A I.

2.3 MINIMUM FLUIDISING VELOCITY

2.3.1 The concept of minimum fluidisation

As the superficial velocity of a fluid upwards through a stationary bed of particles is gradually increased, the pressure drop across the bed increases in the manner predicted by correlating equations such as the Ergun equation. (Equation 2.2.6) A stage will be reached at which the pressure drop approaches the magnitude of the downward gravity force per unit cross-sectional area of the bed of particles. If the bed is not restrained on its upper surface, there will be a slight expansion of the bed accompanied by a rearrangement of the particles as each one tends to "float" separately in the upward flow of fluid. This rearrangement brings the particles towards a state corresponding to the loosest possible packing in a fixed bed, at which condition the voidage has increased from the original ε_o to a value denoted by ε_{mf}. The bed is now on the point of becoming fluidised and further increase in the superficial fluid velocity will cause little, if any, change in the pressure drop across it.

A log-log plot of pressure drop against superficial fluid velocity is conventionally used to illustrate the onset of fluidisation. (Fig. 2.1)

In an "ideal" bed of uniformly sized spherical particles the relationship between the pressure drop Δp and the superficial fluid velocity U

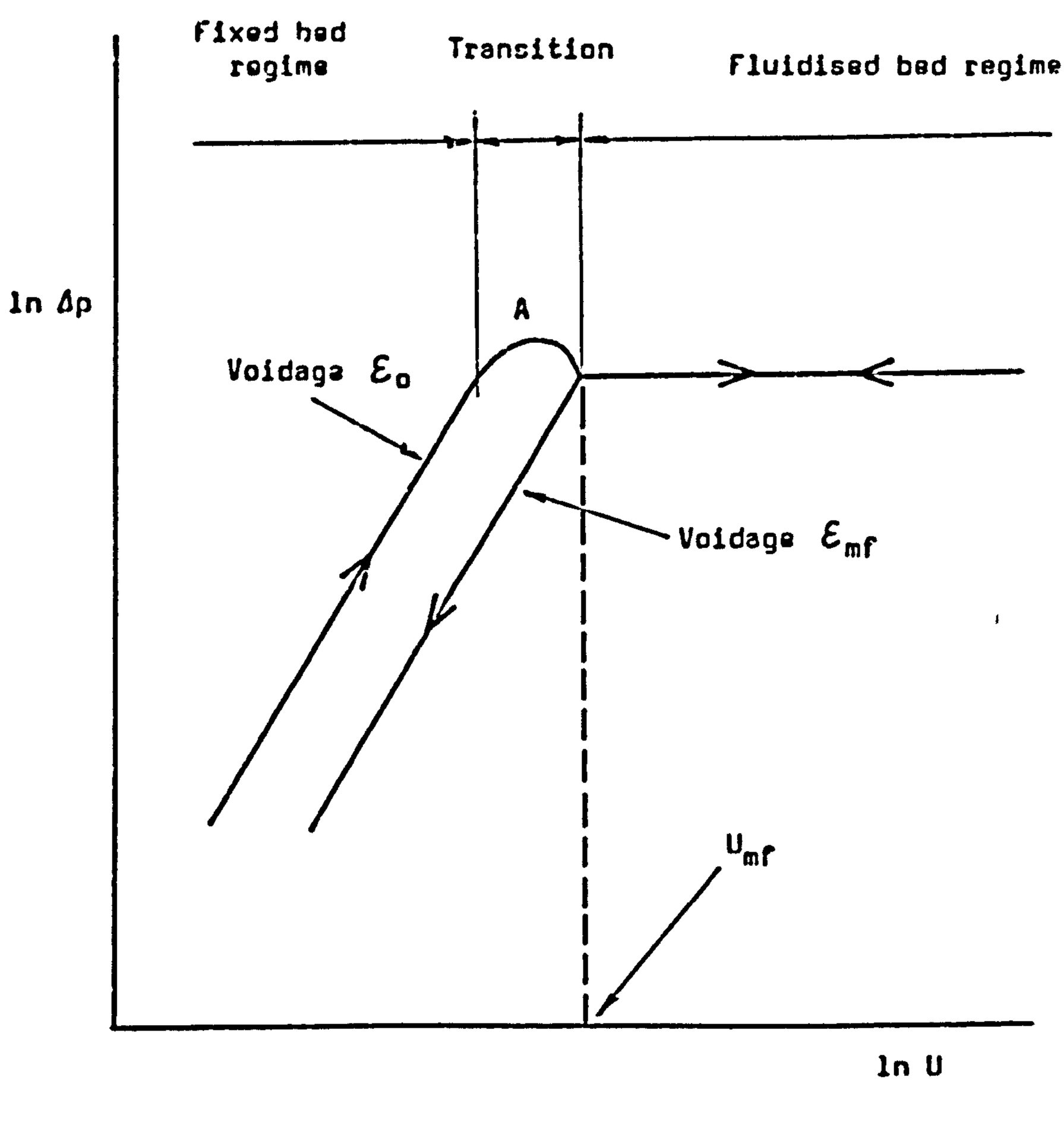

Fig. 2.1. TYPICAL RELATIONSHIP BETWEEN PRESSURE DROP AND SUPERFICIAL GAS VELOCITY FOR A BED OF SOLID PARTICLES.

might be expected to follow purely linear paths without the "peak" shown at A on Fig. 2.1. However, in practical beds there is likely to be some rise of the pressure drop above that required to maintain fluidisation, as the particles "unlock" themselves from their initial filling arrangement, and this may be followed by some fluctuation in Δp as a result of channel formation within the bed.

Figs. 2.2a to 2.2f give some typical relationships between Δp and U for a range of real bulk solids. (Based on diagrams in Refs. L3, K10, K3, and R1.)

The tendency of a bulk solid to form channels when fluidised usually decreases with increasing superficial velocity of the fluidising gas. (Fig. 2.2b.) However, materials that are particularly cohesive or "sticky" may be inherently unsuitable for fluidisation, exhibiting either severe channel formation (Figs. 2.2c, 2.2d) or a type of "slugging" behaviour in which whole sections of the bed rise from horizontal cracks and then fall back. (Fig. 2.2e.)

It would of course be expected that in a bed of randomly packed particles the voidage would not be uniform. As a result, therefore, of the variation in the local velocity of the fluidising gas in different areas of the bed, the whole bed will not become fluidised at a single value of the superficial gas velocity but will do so gradually over a range of velocity. When the bed is only partially fluidised its weight is shared between the fluidising gas and the gas distributor and therefore the pressure drop is less than that required to support the fully fluidised bed. (Fig. 2.2f.) It is usual still to define the minimum fluidising velocity as the point of intersection of the linear parts of the plot of ln Δp against ln U; (that is, for the fixed bed and fluidised bed regimes.) If required, a minimum superficial velocity at which the bed would be fully supported, U_{fs}, could be defined as shown in Fig. 2.2f. (Ref. R1)

The peak A (Fig. 2.1) tends to be more pronounced when a material is fluidised for the first time after being loaded into a vessel, although it will to some extent depend upon the method of loading and the degree

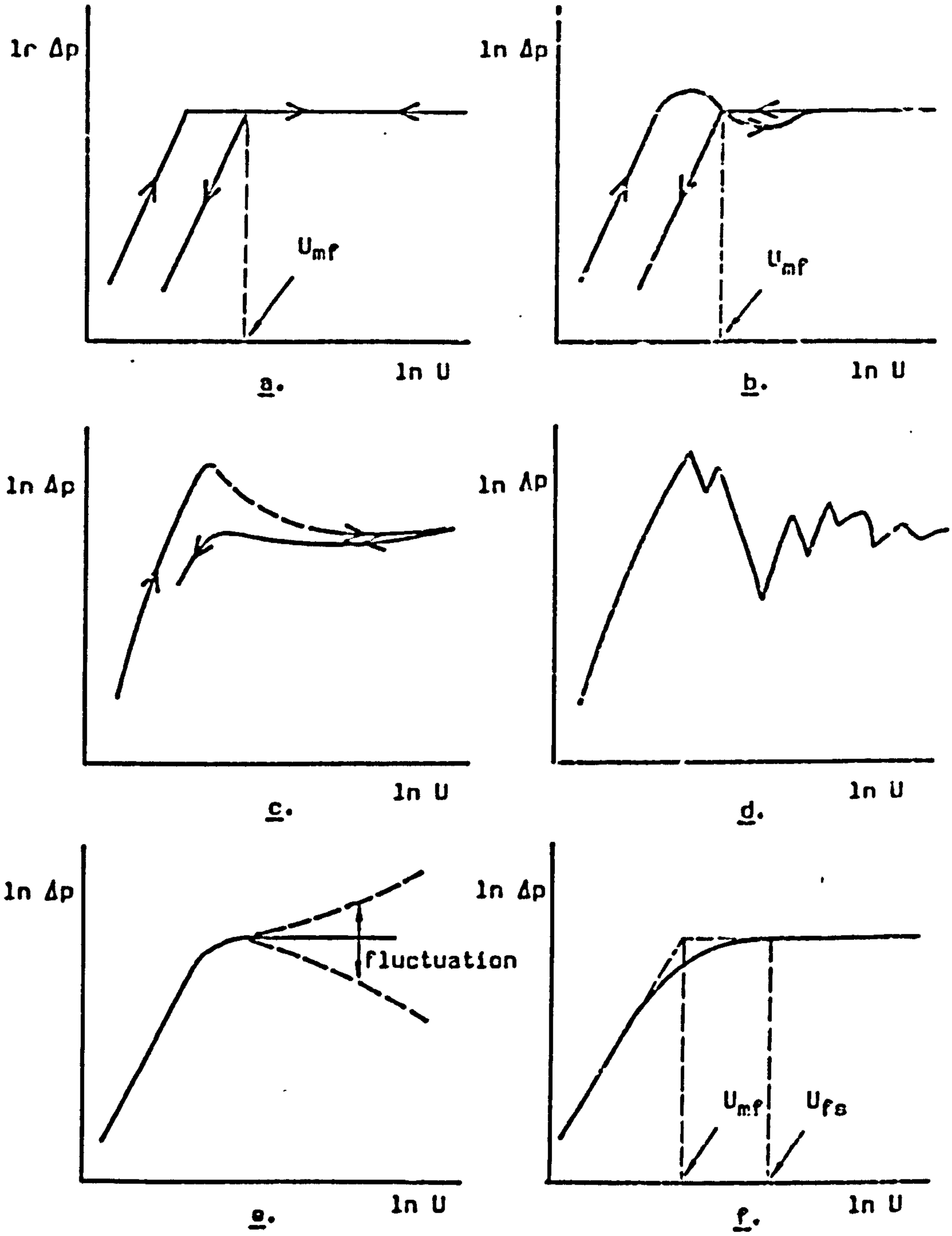

Fig. 2.2 TYPES OF BEHAVIOUR OF FLUIDISED BULK SOLIDS:-

a) ideally fluidising materials,

b) solids exhibiting moderate channelling,

c) and d) more severely channelling solids,

e) cohesive solids exhibiting "slugging" characteristics,

f) effect of lack of uniformity in the packing arrangement of the bed.

of compaction resulting from this. It has been suggested by Zabrodsky (Ref. Z1, page 26) that the peak results from the effect of adhesion of particles not only to one another, but also to the walls of the vessel. He points out that where this adhesion effect is small it is likely that the bed will not be uniformly fluidised at a single value of the superficial velocity of the upward flowing fluid, but rather will become fluidised either from the top downwards or from the bottom upwards over a transition range fluid velocity. (cf. Fig. 2.2f.) It could further be argued that if the bed is deep the packing of the particles might be "tighter" at the bottom than at the top causing higher interstitial velocities and consequently greater pressure drop per unit depth of the bed. Tending to counteract this effect is the variation in interstitial velocity resulting from the decrease in pressure and consequent decrease in density of the gas as it passes upwards through the bed. In spite of these effects and the effect of lack of uniformity of the bed structure discussed previously, the concept of a single "minimum fluidising velocity" (sometimes called the "upper minimum fluidising velocity" to distinguish it from the point at which the particles first begin to rearrange themselves) is now well established and is an important parameter in most design work involving the phenomenon of fluidisation.

Another form of irregular behaviour that can be a problem in some types of system occurs when there is a wide particle size distribution. (Ref. B15, page 73.) This is the segregation that may take place as a result of the finer particles becoming fluidised before the coarser ones, and which can cause several peaks to occur in the plot of Δp against U.

Various correlations have been proposed to enable the minimum fluidising velocity for a given bulk solid to be predicted. The most widely used approach is based on a force balance between the drag exerted by the upward flowing fluid and the weight of the bed acting downwards; that is, regarding the condition of incipient fluidisation as a limiting case of the packed bed model. An alternative approach clearly is to think of "minimum fluidisation" as a limiting case of the fully fluidised state by considering the superficial fluid velocity at

which the particles are on the point of settling.

None of the available correlations is entirely satisfactory: naturally they could hardly be expected to be so, for there are a number of variables such as particle shape, size distribution and (especially with fine particles) interparticle forces that are virtually impossible adequately to take into account. It is known also that U_{mf} can depend upon the height of the bed (Ref. F1) and upon the characteristics of the gas distributor. (See Section 2.6.) Perhaps it could be said that as the direct measurement of U_{mf} for a given sample of bulk solid is not usually difficult, there is little need to be excessively concerned with methods of predicting it. Nevertheless, a quick indication of the probable value of U_{mf} is certainly useful and a considerable amount of energy has been expended by a number of workers in searching for a reliable correlation. A discussion of some of these correlations is given in Appendix A.II.2 and a summary will now follow.

2.3.2 The prediction of minimum fluidising velocity.

From a force balance between the drag exerted by the upward flowing fluid and the downward gravity force on the bed, a convenient expression for minimum fluidising velocity can be developed in the form of a correlation between a Reynolds number and an Archimedes number for the bed. Thus, using the method of Wen and Yu (Ref. W4) to eliminate the particle sphericity ϕ_s and the bed voidage ε_{mf} as explained in Appendix A.II.2, the correlation becomes

$$Re_{mf}^2 + 67.3\, Re_{mf} - 0.041\, Ar_b = 0 \qquad \text{.....2.3.1}$$

where

$$Re_{mf} = \frac{\rho_g d_v U_{mf}}{\mu_g} \qquad \text{.....2.3.2}$$

and

$$Ar_b = \frac{\rho_g(\rho_p - \rho_g)\, g\, d_v^3}{\mu_g^2} \qquad \text{.....2.3 3}$$

Other similar correlations between Re_{mf} and Ar_b have been proposed, such as that of Baeyens and Geldart (Ref. B3),

$$Ar_b = 1823\,(Re_{mf})^{1.07} + 21.7\,(Re_{mf})^2 \qquad \ldots\ldots\ldots\ldots\ldots\ldots 2.3.4$$

Equations 2.3.1 and 2.3.4 are general ones endeavouring to cover the whole range of flow behaviour from laminar through transitional to turbulent. However, at normal atmospheric pressures and temperatures the gas flow through a bed of solid particles tends to be laminar for particles having diameters less than about 500 μm. For such relatively fine particles viscous effects predominate and the expressions for minimum fluidising velocity can therefore be simplified by ignoring the kinetic energy term. In effect of course, this is simply using Stokes Law for the drag force on an isolated particle in a laminar flow region, with an additional coefficient to take into account the difference between the drag on a single particle in a packed array and that on a single isolated particle.

This approach leads to an expression for U_{mf} of the form

$$U_{mf} = K d_v^{\,2} g \frac{\rho_p - \rho_g}{\mu_g} \qquad \ldots\ldots\ldots\ldots\ldots\ldots 2.3.5$$

Various values of K have been proposed (see Appendix A.II.2) but according to recent experimental data reported by Butt (Ref. B30), a value of K of about 8×10^{-4} should generally give the closest prediction.

2.3.3 Fluidisation with air at normal ambient conditions

Although the equation 2.3.5 represents the simplest form of the correlating equations considered, consistent with reasonable reliability of prediction of the minimum fluidising velocity, it is worth noting that for gas fluidisation $(\rho_p - \rho_g) \simeq \rho_p$. Furthermore, since the present work is concerned essentially with air-assisted gravity flow in which the air is used normally at a condition not far from standard atmospheric, it is possible to include μ_g in the constant to give,

$$U_{mf} = K' \rho_p d_v^2 \qquad \text{.....2.3.6}$$

where the constant K' has a value of about 420 to give U_{mf} in m/s with ρ_p in kg/m^3 and d_v in metres.

Baeyens and Geldart (Ref. B3) give for air at ambient conditions

$$U_{mf} = 1650\, d_v^{1.8} (\rho_p - \rho_g)^{0.934} \qquad \text{.....2.3.7}$$

where d_v is in cm, ρ_p and ρ_g are in g/cm^3 and U_{mf} is in cm/s. Noting that $\rho_g << \rho_p$ and bringing the expression to consistent SI units we have

$$U_{mf} = 104\, d_v^{1.8} \rho_p^{0.934} \qquad \text{.....2.3.8}$$

which may be compared with the reduced form of the equation of Leva et al. (equation A.II.30) for air as

$$U_{mf} = 134\, d_v^{1.82} \rho_p^{0.94} \qquad \text{.....2.3.9}$$

It is of interest also to compare here a rather different expression developed by Baerg et al. (Ref. B1) from a study of the heat transfer characteristics within air-fluidised beds. Their equation is

$$U_{mf} = 0.208\, (\rho_b d_v)^{1.23} \qquad \text{.....2.3.10}$$

where ρ_b is the bulk density of the particulate solid.

A preliminary comparison of equations 2.3.6, 2.3.8, 2.3.9 and 2.3.10 may be made by noting that $\rho_b = (1 - \varepsilon_o)\rho_p$ and for fine spheroidal particles, loosely packed, ε_o is about 0.4.

Thus $\rho_b \simeq 0.6\, \rho_p$ and substitution in equation 2.3.10 then gives

$$U_{mf} = 0.11\, (\rho_p d_v)^{1.23} \qquad \text{.....2.3.11}$$

Fig. 2.3 shows a plot of four of these correlating equations for minimum fluidising velocity of a typical material of density 2500 kg/m^3, fluidised with ambient air. It is clear from this that the expression of Baerg et al. (in the form of equation 2.3.11) tends to give a significantly higher prediction of U_{mf} for the finest particles whereas the simple equation 2.3.6 perhaps over-estimates U_{mf} for the materials of larger particle size. The effect of density is shown in Fig. 2.4 where equation 2.3.6 is plotted for a range of values of ρ_p.

In order to gain a visual impression of the level of confidence that can be placed in these simple correlating equations, some experimentally determined values of U_{mf} (from various authors) are plotted on Fig. 2.5 with corresponding values predicted by equations 2.3.6, 2.3.8 and 2.3.10. Whilst it is recognised that only a very limited selection of the available experimental data can be displayed in this way, it is felt to be helpful to compare directly the predictions of the various equations over a range of particle sizes. The experimental data used in this plot is listed in Table 2.1 with sources.

2.4 EXPANSION OF THE FLUIDISED BED

Further increase in the superficial velocity of the fluidising gas or liquid upwards through the particulate bed beyond the minimum fluidising velocity tends to cause the bed to expand without any appreciable change in the pressure drop across it. The actual behaviour of the fluidised bed depends upon the properties of the powder or granular material and of the fluidising medium, in particular the ratio of their densities. In general, where the particles and fluid have similar densities, and in other cases at conditions close to incipient fluidisation, the bed expands uniformly and has a virtually homogeneous structure throughout. This state is known as particulate fluidisation. At higher superficial velocities of the fluidising medium, and especially where its density is much less than that of the bed material, the structure of the bed ceases to be homogeneous as the fluidising medium tends to rise through the bed in the form of particle-free voids or "bubbles". The surface of the bed becomes similar in appearance to a boiling liquid and the bed then has the condition known as aggregative fluidisation.

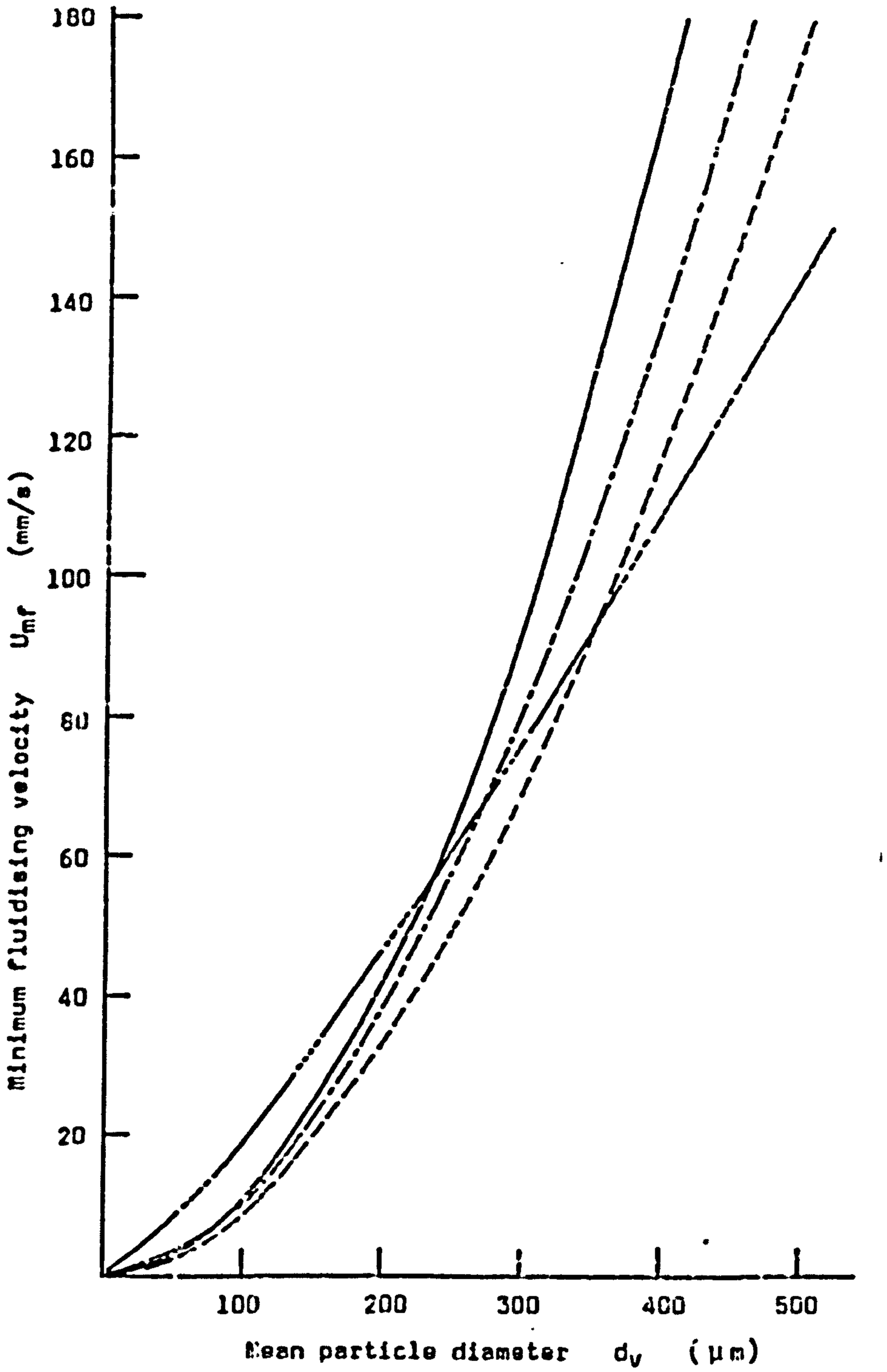

Fig. 2.3 PREDICTED VARIATION OF MINIMUM FLUIDISING VELOCITY WITH PARTICLE SIZE: for ρ_p = 2500 kg/m^3.

———— Equation 2.3.6 with K' = 42C

– – – – – Equation 2.3.8

———— Equation 2.3.9

———— Equation 2.3.11

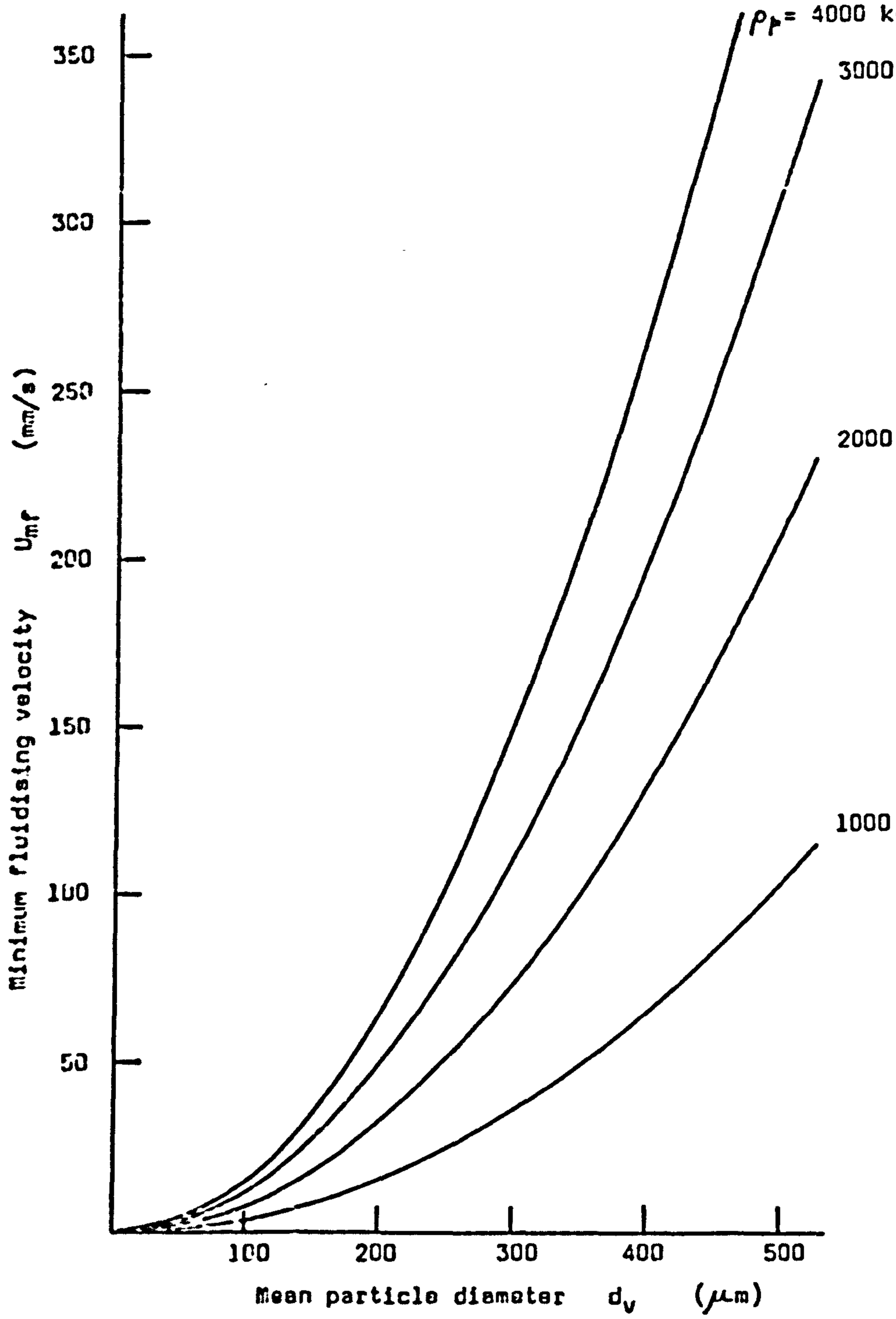

Fig. 2.4 PREDICTED MINIMUM FLUIDISING VELOCITIES FOR MATERIALS FLUIDISED WITH AIR AT NORMAL AMBIENT CONDITIONS: from Equation 2.3.6.

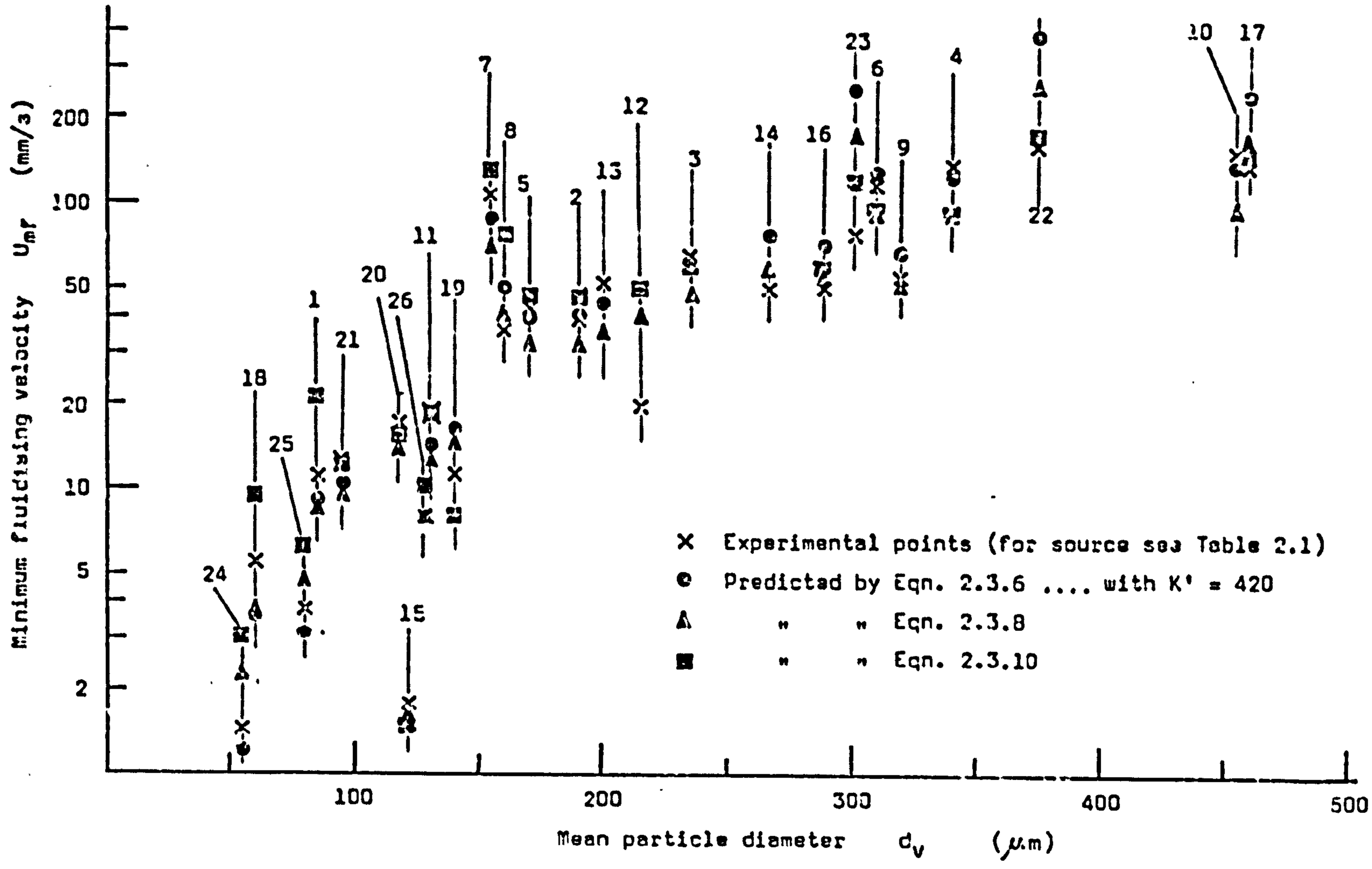

Fig. 2.5 CORRELATION BETWEEN PREDICTED VALUES OF MINIMUM FLUIDISING VELOCITY AND EXPERIMENTAL MEASUREMENTS FOR A RANGE OF DIFFERENT PARTICULATE MATERIALS. (See Table 2.1).

NO.	MATERIAL	ρ_p kg/m^3	ρ_b kg/m^3	d_v μm	U_{mf} mm/s	Ref.	Predicted U_{mf} (mm/s)		
							Eq 2.3.6	Eq 2.3.8	Eq 2.3.10
1	Lead glass ballotini	2963	1778	85	11	320	9.0	8.6	20.3
2	Soda glass ballotini	2643	1559	190	39.5	"	40.0	32.7	46.6
3	"	"	"	235	67	"	61.3	48.0	60.5
4	"	"	"	340	140	"	128.4	93.3	93.3
5	Silicon carbide	3204	1762	170	42.5	"	38.9	32.1	47.2
6	"	"	1698	310	119	"	129.3	94.6	94.5
7	Copper granules	8938	4469	154	109	"	89.0	70.0	131.4
8	Zircon sand	4709	2825	160	38	"	50.7	41.2	78.3
9	Sugar	1602	-	320	55	"	68.9	52.4	-
10	"	"	-	456	155	"	139.9	99.2	-
11	Potash	2000	1090	120	18.4	K3	14.0	12.6	18.6
12	Sand	2640	1452	215	19.7	"	51.3	40.9	49.7
13	"	2650	-	200	53	M4	44.5	36.0	-
14	"	2640	-	266	50.6	Q1	78.5	59.9	-
15	Phenolic resin	240	-	121	1.8	G7	1.44	1.6	-
16	Foundry sand	2275	1328	276	51.8	B1	72.7	55.7	60.5
17	Scotchlite beads	2819	1669	460	146.5	"	250.6	170.8	150.3
18	"	2371	1350	60	5.6	"	3.54	3.7	9.45
19	Cracking catalyst	1986	497	139	11.3	"	16.1	14.3	7.76
20	Alumina	2659	1025	117	16.9	"	15.2	13.3	15.3
21	"	"	1043	95	12.4	"	10.1	9.5	12.1
22	Iron powder	6776	2371	375	163.5	"	400.2	268.2	180.0
23	"	6663	2146	301	78.9	"	253.6	177.8	121.5
24	Catalyst	945	445	55	1.4	D3	1.20	2.17	2.92
25	PVC and catalyst	1200	570	80	3.7	"	3.23	4.66	6.22
26	Diakon	1167	682	128	7.9	"	8.03	10.36	10.7

Table 2.1 EXPERIMENTAL VALUES OF MINIMUM FLUIDISING VELOCITY FOR A SELECTION OF PARTICULATE MATERIALS, COMPARED WITH PREDICTED VALUES. (See also Fig. 2.5)

As might be expected, particulate fluidisation is found to be confined almost entirely to materials fluidised with liquid, although a corresponding state can be found in materials fluidised with a gas at velocities only slightly above the minimum fluidising velocity. It is relevant to the present work to study the behaviour of fluidised beds of powdered and granular solids at superficial gas velocities up to a few times the minimum fluidising velocity, and therefore both particulate and aggregative fluidisation will be discussed.

In a gas fluidised bed it is possible, with some fine solids of low density, to obtain particulate fluidisation with an even expansion of the bed over a fairly wide range of superficial gas velocity. (Ref. G7) The lower limit of this range is the minimum fluidising velocity U_{mf}, and the upper limit can be regarded as the minimum velocity for spontaneous bubbling, U_{mb}. Generally U_{mb} is only slightly above U_{mf}, but for fine light powders U_{mb} may be two or three times U_{mf}. For example, for a 55 μm cracking catalyst, having relative density 0.95, the ratio U_{mb}/U_{mf} has been measured at about 2.8 (Ref. D3), and for a 121 μm phenolic resin U_{mb} was about six times U_{mf}. (Ref. G7) However, it does seem probable that particulate fluidisation at these higher superficial velocities may be a somewhat unstable state, the bed immediately reverting to continuous bubbling if appreciably disturbed.

The regular expansion of the particle bed with increasing gas velocity is characteristic of particulate fluidisation and is usually modelled by the relationship due to Richardson and Zaki (Ref. R3)

$$\frac{U_c}{U_i} = \varepsilon^n \qquad \text{.....2.4.1}$$

where U_c is the superficial velocity in the continuous phase, U_i is the value of U_c at $\varepsilon = 1$ (approximately equal to the terminal velocity U_t of the particles in the fluid), and n is an index.

In an extensive investigation with diakon and phenolic resin Godard and Richardson (Ref. G7) have found that U_i is generally in excess of U_t, the ratio U_i/U_t varying between unity and 1.75 for particles fluidised

at atmospheric pressure, and the index n was shown to have values of about 5.3 for 125 μm diekon up to nearly 9 for the much lighter phenolic resin of similar particle size.

Much of the study of aggregatively fluidised beds has been founded on the work of Toomey and Johnstone (Ref. T1) and Morse (Ref. M10) who were instrumental in developing the model of two-phase fluidisation. In this model the bed is represented as a combination of a "dense phase" comprising solid particles uniformly distributed within the stream of gas supporting them in a condition of minimum fluidisation, and a "lean phase" of gas alone in the form of bubbles or channels. Although there is some doubt about the validity of the two-phase model in the lower region of the bed, experimental studies seem to confirm that, away from the gas distributor, the excess gas above that required for minimum fluidisation is in fact largely confined to discrete voids. (Refs. D9, B6, P2) Many authors have discussed in detail the complex phenomena inherent in the bubbling behaviour of fluidised beds. (For such discussion, and critical review of the relevant literature, see for example Refs. Z1, K10, R6, D1, B15.)

In tests with glass beads of about 200 μm diameter, Bakker and Heertjes (Ref. B4) identified three distinct zones in the centre of a fluidised bed: (i) close to the distributor where the voidage decreased with elevation, (ii) a zone of uniform voidage, and (iii) a zone where the voidage increased to unity at the surface. At the walls of their 90 mm diameter fluidising vessel Bakker and Heertjes found that the voidage tended to be significantly lower than in the centre of the bed - an interesting result that appears to conflict with the pattern of preferential gas flow at the walls reported by other authors. In shallow beds this effect of reduced voidage at the walls seemed to be less marked, and also the zone of uniform voidage tended to disappear so that, for example, in the case of a 50 mm deep bed fluidised at 407 mm/s (= 5 U_{mf}) there existed a region of about 15 mm depth which was influenced by the distributor, followed by a region of gradually increasing voidage up to the surface.

Probably the most useful recent work dealing with the fluidisation

characteristics of different types of particulate bulk solids has been that of Geldart (Refs. G1, G3, B3.) who showed that the behaviour of a solid fluidised by a gas can generally be classified into one of four recognisable groups. These groups are characterized by the difference in the densities of the solid and the fluidising gas, and by the mean particle size; and the salient features of the groups may be summarised as follows (Ref. G3):-

GROUP A Generally includes materials of small particle size and/or low particle density (less than about 1400 kg/m^3). Powders in this group show considerable expansion of the bed between U_{mf} and U_{mb}, and relatively slow settling of the bed when the fluidising gas is shut off. At velocities above U_{mb} the bed bubbles freely and at higher velocities axi-symmetric slugging tends to occur. At velocities higher still the slugging movement is continually collapsing so that the fluidising gas is forced to track upwards through angled crevices to the top surface of the vigorously turbulent bed.

GROUP B Including most materials in the mean particle size and density ranges 40 - 500 μm and 1400 - 4000 kg/m^3, this group would typify the generally accepted model of fluidised bed behaviour. At gas velocities above U_{mf} the expansion of the bed is small and bubbling occurs at or just above this minimum fluidising velocity. Collapse of the bed is rapid when the gas flow is shut off. As the velocity is increased the bed bubbles freely, and eventually tends to a form of asymmetric slug flow.

GROUP C Cohesive powders that are difficult to fluidise satisfactorily because of high interparticle forces resulting from very small particle size, electrostatic effects or high moisture content. Attempts to fluidise such materials usually result in the formation of stable channels or in the whole bed rising as a plug, although some success may be achieved with the aid of mechanical vibrators or stirrers.

GROUP D Including materials having large mean particle size and/or

high particle density. Fluidisation behaviour is in some respects similar to powders in Group B, but beds of Group D materials can generally be made to spout if the gas is admitted centrally.

Because of the complexity of the relationships amongst the various parameters it is not possible to lay down precise criteria for the placement of a material into a particular Group. Nevertheless, criteria have been proposed which should give a useful indication of the probable mode of behaviour. For example, Baeyens and Geldart (Ref. B3) suggest that for powders fluidised with air at normal ambient conditions, the class of behaviour is likely to be

$$\text{Group A if} \quad d_v < \frac{9.06 \times 10^5}{(\rho_p - \rho_g)^{1.17}} \qquad \ldots\ldots\ldots\ldots\ldots\ldots 2.4.2$$

$$\text{Group B if} \quad \frac{9.06 \times 10^5}{(\rho_p - \rho_g)^{1.17}} < d_v < \frac{3.15 \times 10^5}{(\rho_p - \rho_g)^{0.81}} \qquad \ldots\ldots\ldots\ldots\ldots\ldots 2.4.3$$

$$\text{and Group D if} \quad d_v > \frac{3.15 \times 10^5}{(\rho_p - \rho_g)^{0.81}} \qquad \ldots\ldots\ldots\ldots\ldots\ldots 2.4.4$$

where d_v is in μ_m, and ρ_p, ρ_g are in kg/m^3.

These zones of behaviour are conveniently illustrated on a plot of $(\rho_p - \rho_g)$ against d_v as shown in Fig. 2.6. The empirical boundary between materials of Groups A and C is rather indistinct as there are so many factors that can influence the cohesiveness of these fine powders, including electrostatic charging (discussed in Section 2.7), moisture content and particle shape.

Even after assessing the class to which a fluidised powder may belong, the prediction of the actual amount that a bed of the powder will expand is not at all easy. Bakker and Heertjes (Ref. B4) found that the expansion of their fluidised bed of glass beads (which falls comfortably into Geldart's Group B) showed linearity with the product of bed mass and superficial air velocity. However, this is perhaps

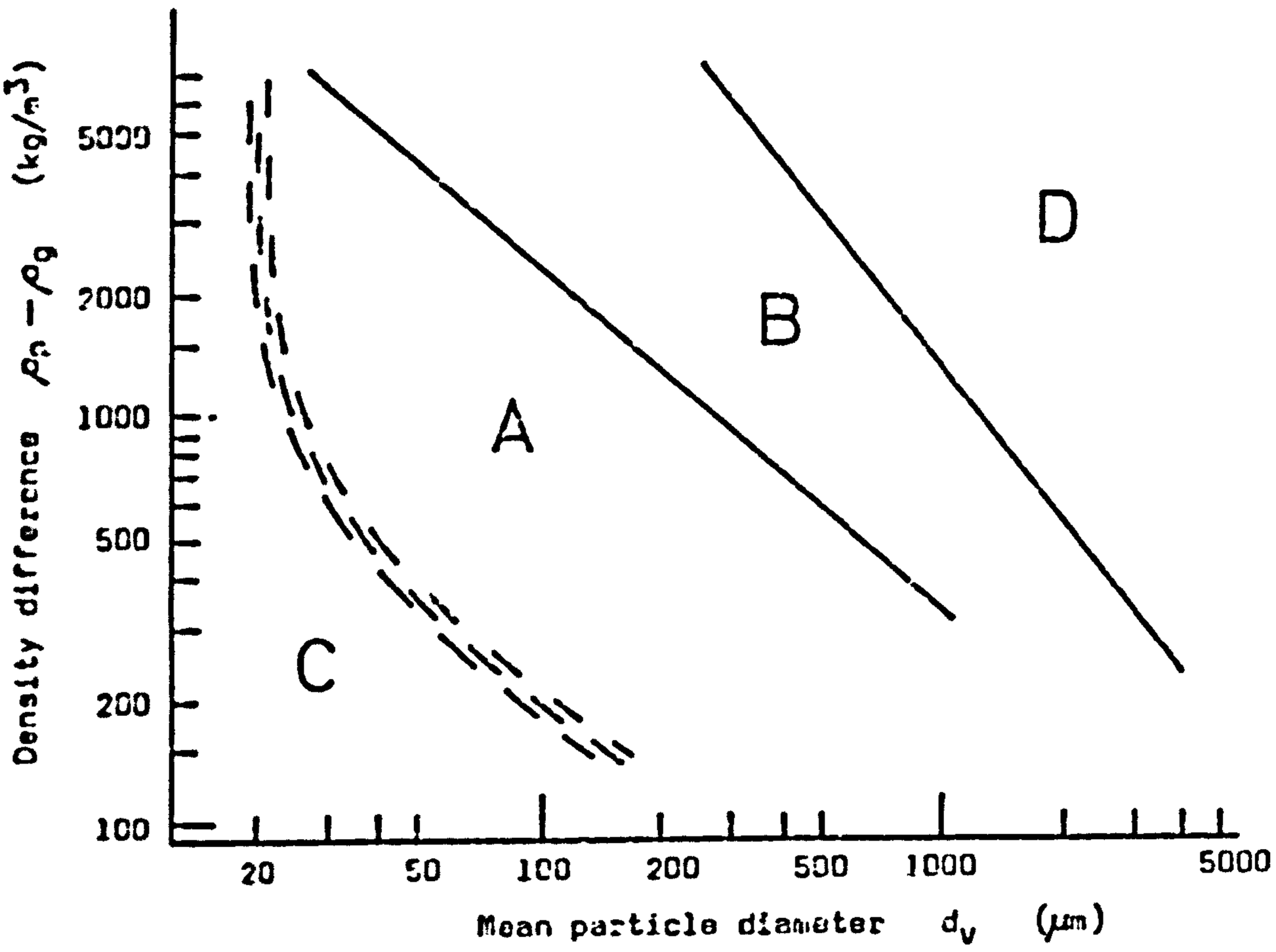

Fig. 2.6 GELDART'S CLASSIFICATION OF FLUIDISATION PROPERTIES ACCORDING TO SIZE AND DENSITY OF THE PARTICULATE MATERIAL; (Refs. G1, B3)

oversimplifying the case, and more detailed approaches have been proposed based on the criteria of the maximum stable size of bubble that can exist in the bed (Ref. G1) or the bubble-size distribution (Ref. P2). Both of these approaches of course suffer through requiring data on bubble behaviour which, although clearly an important factor in bed expansion, is generally not available.

2.5 ENTRAINMENT VELOCITY

Elutriation from fluidised beds, that is, the removal of fine particles as a result of entrainment in the gas stream leaving the top of the bed, is important insofar as it may effectively set the upper limit on the superficial velocity of the fluidising gas. In other situations there may be a positive requirement for unwanted fines in the material to be eliminated and one method of achieving this is by fluidisation at a gas velocity that is sufficient to carry over these smallest particles.

Above the surface of any fluidised bed there may be a region in which entrained particles tend to become separated from the upward flowing gas and then fall back into the main bed. Thus the quantity of material entrained and the size of the entrained particles decrease with height above the surface of the bed, until at some point (known as the "transport disengaging height") the entrainment levels off to an approximately constant value. If there is insufficient freeboard above the bed, for example, where the outlet from the vessel is below the transport disengaging height, the elutriation of particles may be sufficient to have a significant effect on the fluidisation quality of the material remaining in the bed.

The size of particles entrained in the upward flow of gas may vary across the section of the fluidising vessel as a result of the velocity profile that develops above the bed. (Ref. L5) Thus some of the finer particles near the wall of the vessel may tend to settle back into the bed.

It has been observed (Refs. J3, L7) that entrainment does not generally become significant until particles are fluidised at gas velocities well

in excess of the terminal velocity of a single particle. However, at higher fluidising gas velocities the quantity of material entrained can increase rapidly.

A useful review of several of the models that have been proposed for the prediction of elutriation from fluidised beds is given by Kunii and Levenspiel (Ref. K10, Chap. 10) but a first estimate can be made conveniently from basic fluid mechanics using the simple model for drag on a particle. (See Appendix A.II.3).

In this way approximate expressions for the prediction of the terminal velocity of spherical particles in air at normal ambient conditions can be developed as

$$U_t \approx 3 \times 10^4 \rho_p d_v^2 \quad \text{for } Re_p < 2 \qquad \text{.....2.5.1a}$$

$$U_t \approx 80 \times 10^4 \rho_p^{0.7} d_v^{1.4} \quad \text{for } 2 < Re_p < 500 \qquad \text{.....2.5.1b}$$

where ρ_p is in kg/m^3 and d_v is in metres, giving U_t in m/s, and Re_p is defined as $d_v \rho_g U_t / \mu_g$.

It is of interest to note that a comparison of equation 2.5.1a with equation 2.3.6 for minimum fluidising velocity suggests that the ratio U_t/U_{mf} may have a value of around 70. However, it has to be remembered that U_t should be estimated using d_v for the finest fraction of particles present, whereas U_{mf} is predicted using the mean particle diameter. Thus U_t/U_{mf} is normally less than 70 and its minimum value is around 10 (Ref. K10, page 78).

As with the correlations proposed for the prediction of minimum fluidising velocity, the limitations of the expressions 2.5.1a and 2.5.1b must be recognised. These equations are useful as a guide to the fluidising air velocity at which entrainment could begin from relatively shallow beds, as would be encountered in air-assisted gravity conveyors. However, for deep beds they would be unreliable as the pressure drop, and therefore the change in air density across the bed, may well be significant. Furthermore, the expressions are based on an analysis for

spherical particles: for irregular particles the values of U_t may be rather lower.

Comparatively little has in fact been published on the terminal velocities of non-spherical particles, and virtually nothing on such particles falling in air. Some discussion of the influence of particle shape is undertaken in Appendix A.II.3, and it is concluded that, in the absence of reliable detailed data, the approach of Hawksley (Ref. H3) is probably as good as any other. This involves the use of the relationship between drag coefficient and Reynolds number, as applying to spherical particles, but with both parameters modified to include particle sphericity.

The generally accepted form of the relationship between these parameters is that proposed by Schiller and Naumann (Ref. S3), expressed as the mathematical model

$$C_d = \frac{24}{Re_p}(1 + 0.15\,Re_p^{0.687}) \qquad \text{.....2.5.2}$$

where
$$C_d = \frac{4 g d_v (\rho_p - \rho_g)}{3 \rho_g U_t^2} \qquad \text{.....2.5.3}$$

and
$$Re_p = \frac{d_v \rho_g U_t}{\mu_g} \qquad \text{.....2.5.4}$$

A number of authors have pointed out the advantage of plotting $C_d Re_p^2$ against Re_p instead of the more conventional plot of drag coefficient against particle Reynolds number, since the group $C_d Re_p^2$ is independent of velocity. In fact, it is probably worthwhile going a stage further and, for work involving the prediction of terminal velocity, using a dimensionless plot of Reynolds number against Archimedes number. The Archimedes number (alternatively known as Galileo number) is defined as

$$Ar = \frac{\rho_g(\rho_p - \rho_g) g d_v^3}{\mu_g^2} \qquad \text{.....2.5.5}$$

and can therefore be determined easily from a knowledge of the powder

and gas properties. From a suitable Re_p vs. Ar plot a value of Re_p is read off allowing the terminal velocity then to be calculated directly.

Recalling that data for minimum fluidising velocity can also be correlated as a relationship between Re_p and Ar (see Section 2.3.2 and Appendix A.II.2) it would clearly be useful to prepare a combined plot of Reynolds number against Archimedes number from which predictions can be made of both minimum fluidising velocity and terminal velocity. Fig. 2.7 shows such a plot in which the minimum fluidising velocity U_{mf} is given by the correlation of Baeyens and Geldart (equation 2.3.4) and the terminal velocity U_t is given by a correlation based on the model of Schillar and Naumann (equation 2.5.2) modified for non-spherical particles in the manner suggested by Hawksley (see Appendix A.II.3).

2.6 INFLUENCE OF THE GAS DISTRIBUTOR

2.6.1 Introduction

In all processes involving the fluidisation of a bed of solid particles (other than spouting bed systems) some form of distribution device is needed to introduce the fluidising gas to the bed. Botterill (Ref. B15, p 80) lists the following requirements of a satisfactory distributor:-

1. It should promote uniform and stable fluidisation.
2. It should minimize attrition of bed material.
3. It should be designed to minimize erosion damage.
4. It should prevent flowback of bed material during normal operation and on interruption of fluidisation when the bed is shut down.

Although it is possible to distribute the gas through a pipe grid at the base of the fluidising vessel, for gas fluidisation the more widely used method is to construct the vessel with some form of gas plenum chamber at the bottom separated from the main container by a porous or perforated plate. The design of this distributor plate, particularly with regard to the material from which it is constructed and the pressure drop across it, can vary over a wide range. For example, some applications are

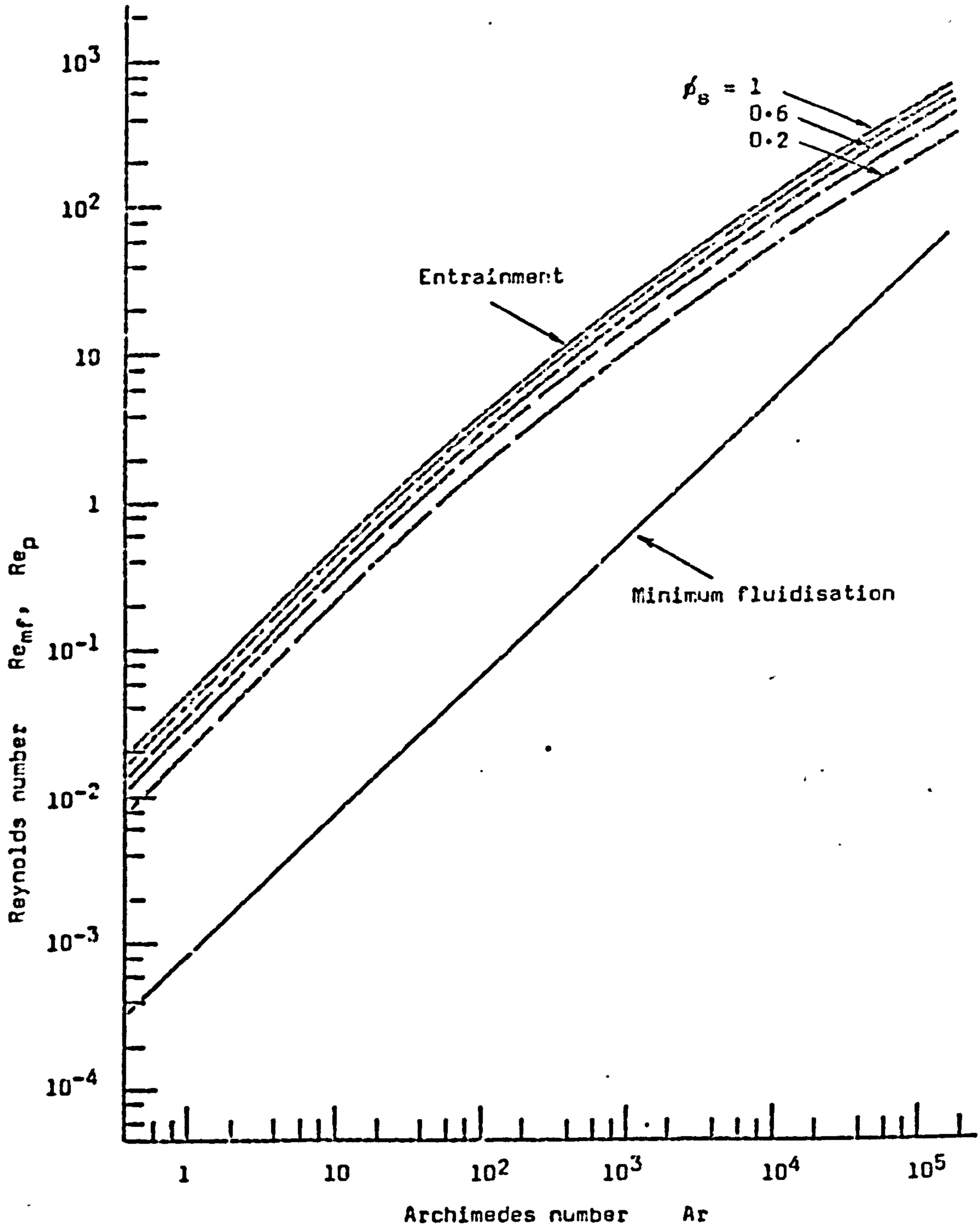

Fig. 2.7 PLOTS OF REYNOLDS NUMBER AGAINST ARCHIMEDES NUMBER FOR ISOLATED PARTICLES AT TERMINAL (FREE-FALL) VELOCITY, AND FOR A BED OF PARTICLES AT THE CONDITION OF MINIMUM FLUIDISATION

suited to the use of metal plates perforated with a small number of relatively large holes across which the pressure drop would be very small, whilst at the other end of the scale (that is, high pressure drop) would be found porous distributors such as ceramics, sintered metal and plastic, and woven cotton and polyester materials. Table 2.2 lists typical materials that have been used as porous distributors, and some sources of supply of these are given in Appendix A.IV.

There are, of course, factors other than pressure drop which may affect the choice of distributor, and Geldart and Kelsey (Ref. G5) list four variables involved in their design, pointing out however, that these are to some extent inter-related, making it difficult to isolate a particular effect. The variables are:-

1. The ratio of the distributor pressure drop to bed pressure drop.
2. The rate of change of distributor pressure drop with gas velocity.
3. The proportion of free area present.
4. The geometry of the plate.

The effect that the gas distributor has on the flow characteristics within a bed of fluidised solid particles has been given some attention by a number of authors in recent years and Geldart and Kelsey (Ref. G5) have pointed out that the investigations fall broadly into two categories. Firstly there are those concerned with hydrodynamic effects which include studies of density transients and uniformity of fluidisation, and also bubble size and frequency. Secondly, there are investigations involving problems in practical processes such as mixing and heat transfer.

2.6.2 Pressure drop

Probably most interest surrounds the pressure drop across the gas distributor and its effect on the "quality" of fluidisation. Many authors (for example, Refs. B15, G5, G10, H5, K10, L3, S11, T3, Z1, Z2) have discussed the influence of pressure drop across the distributor, or more specifically, the ratio of this pressure drop to that across the

MATERIAL	RELATIVE COST	FEATURES
Woven fabric:-		
cotton	low	light and fairly strong, but has little rigidity and may need supporting in wide ducts; may suffer deterioration of performance if fluidising air or conveyed solids are moist.
polyester	low	as for cotton, but less susceptible to moisture; unsuitable for use at elevated temperatures.
asbestos	low	particularly useful in high temperature applications.
Sintered plastic	medium	has smoother surface and greater rigidity than woven fabrics; appears very prone to deterioration through accumulation of atmospheric dust and fines in conveyed material, which cause decrease in air flow.
Sintered metal	high	hygenic (therefore useful in food industry); gives good fluidisation and can be made with high degree of uniformity; but very expensive.
Ceramic tiles	medium	perhaps less convenient than other materials in that tiles must be fitted together and sealed, but widely used; good fluidisation; ceramic is brittle and subject to impact damage, but is resistent to high temperatures.
Woven steel laminate	high	qualities similar to sintered metal; resistant to high temperatures.
Compound materials, e.g. filter cloth sandwiched between perforated steel plates	low to medium	combines good fluidisation qualities of fine filter cloth with strength of steel sheets; can be easily made up to any desired specification to suit user's application.

Table 2.2 SOME FEATURES OF MATERIALS COMMONLY USED AS THE POROUS DISTRIBUTOR IN AIR-ASSISTED GRAVITY CONVEYORS.

fluidised bed; several in the light of experimental observations. Clearly the "stability" of the fluid bed system is an important criterion and it is worth considering how this might be defined and how it depends upon the "distributor plate/bed resistance ratio".

Suppose that a disturbance occurs, in the nature of a localised increase in gas velocity, in a uniform bed of dry particles at a condition of incipient fluidisation. This disturbance will cause the bed in this region to expand, resulting in a fall in the local pressure drop through the bed, and consequent rise in pressure drop through the distributor plate as more gas tries to force its way through the potential "channel". The system is stable if the combined pressure drop across the bed and distributor rises with an increase in the local gas velocity in the bed. However, if this combined pressure drop were to fall there would be a further increase in the local gas velocity tending to establish a channel through which most of the fluidising gas could flow, causing the rest of the bed to defluidise. In general it may be said that the resistance to gas flow offered by the distributor should be great enough to ensure stability of the fluidised bed system without being so high that blower power becomes excessive; but there appears to be some disagreement as to how the optimum pressure drop should be determined.

Botterill (Ref. B15, p 81) states that 10% of the total pressure drop should be an adequate proportion for the distributor, and this figure is also quoted by Agarwal et al (Ref. A1) for deep beds or beds of high density materials, but Hiby's data (Ref. H5) implies that the pressure drop through the distributor should be at least 20% of that through the combined bed and distributor. This disagreement can in part be accounted for by the methods chosen to define bed stability, and also by the effect of differences in the sizes and densities of solid particles within the bed. An additional factor to be considered is the superficial velocity of the fluidising gas, since the data of Hiby suggests that where this is much greater than the minimum fluidising velocity, the pressure drop across the distributor can be a considerably lower proportion of the total pressure drop. The reason for this, put forward by Hiby, is that, as in the case of deep beds, the lower layers of material in the bed tend effectively to serve as a distributor of the fluidising gas to the upper layers.

For coudítions close to incipient fluidisation in 150 mm deep beds of fine and coarse sand, Geldart and Kelsey (Ref. G5) found that bed expansion ratios and bubble size did not vary appreciably for ratios of distributor pressure drop to bed pressure drop from 0.1 to 10. With lower resistance distributors larger bubbles and lower expansion ratios were observed, and with a distributor of negligibly small resistance it was found impossible to fluidise the beds.

Siegel (Ref. S11) attempted an analytical study of gas fluidised bed stability, describing a model from which he developed an expression for the ratio of the flow resistance of the distributor R_d to the flow resistance of the bed at the onset of channelling R_{bc} as

$$\frac{R_d}{R_{bc}} = \frac{1}{n}\left(\frac{U_{mf}}{U_t}\right)^{1/n} \frac{1}{1-\varepsilon mf} \qquad \text{.....2.6.1}$$

where n is an exponent governing bed expansion. For spheroidal particles $\varepsilon_{mf} \simeq 0.4$, and the form of the relationship between n and U_{mf}/U_t is given by Richardson (Ref. R1) who shows each parameter plotted against an Archimedes number. Thus for a given gas, equation 2.6.1 can be used to assist in the selection of a distributor of sufficient resistance to ensure bed stability. Fig. 2.8 given a plot, based on equation 2.6.1, of R_d/R_{bc} against particle size for beds fluidised with air at normal temperature and pressure.

It is worth noting that, although a better quality of fluidisation seems to be obtained with high pressure drop distributors, the use of such distributors does not guarantee smooth fluidisation with no channelling (Ref. G5). It was found for instance by Geldart and Kelsey (Ref. G5) that fitting a perforated metal sheet over a sintered plastic distributor eliminated the instabilities that tended to occur when the sintered plastic was used on its own. Also, Sutherland (Ref. S18) and Trivedi and Rice (Ref. T3) have pointed out that the pressure drop through the distributor may be different when there is a powder on it and when it is clear, even though the gas flowrate is the same. However, Sutherland's theoretical approach predicts that the pressure drop would be highest in the absence of a bed of powder on the distributor, which is quite the

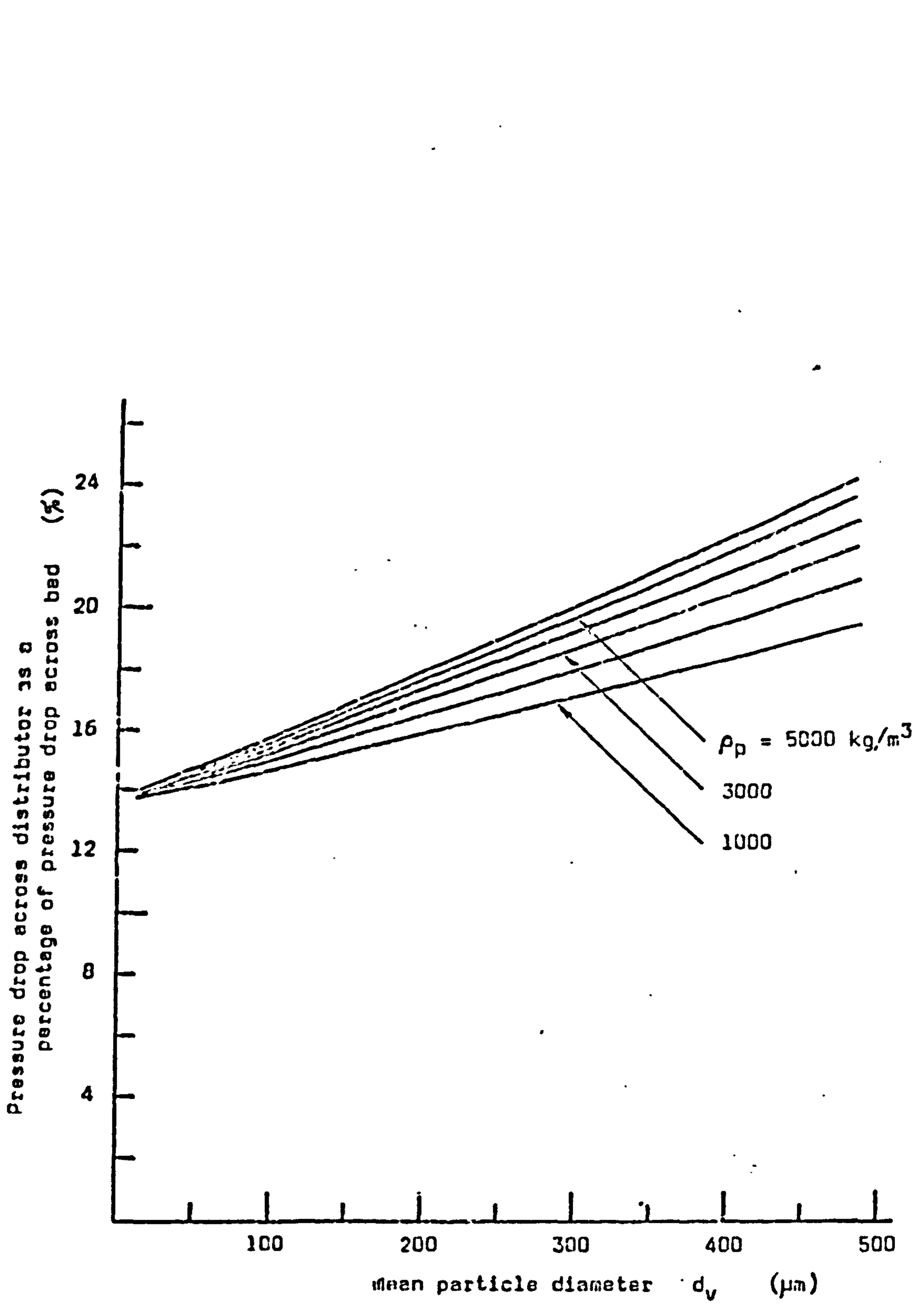

Fig. 2.8 MINIMUM PRESSURE DROP REQUIRED ACROSS DISTRIBUTOR FOR A BED OF SPHEROIDAL PARTICLES FLUIDISED WITH AIR AT A CONDITION CLOSE TO NORMAL AMBIENT - based on equation of Siegel (S11).

opposite of the effect observed experimentally by Trivedi and Rice. The reason for this remarkable discrepancy is not apparent, but it is clear that some caution should be exercised when following the conventional procedure of inferring the pressure drop across the powder bed by taking the difference between the total pressure drop across bed and distributor and that across the distributor alone.

2.6.3 Porosity (free area) and geometry of distributor

The type of gas distributor used in a fluidising vessel can have a marked influence on the behaviour of the fluidised material. According to Zabrodsky (Ref. Z1, p 45) such distributor effects tend to be confined to the lower part of the bed, and experimental work by Morse and Ballou (Ref. M11) using capacitance probes seems to confirm this. However, in shallow beds it appears probable that the effect on the whole bed could be significant. One reason for this is that in deep beds the particulate material can in part act as its own distributor, an advantage that is not available in shallow beds (Refs. H5, B15 p 86).

Working with a fine silicon powder, Grohse (Ref. G10) examined the differences in fluidisation behaviour when using multi-orifice, screen and porous plate distributors. Plots of bed pressure drop against superficial air velocity seemed to show a better quality of fluidisation with the porous distributor, with no channelling and with the point of incipient fluidisation clearly defined. Geldart and Kelsey (Ref. G5), in their experiments with sand supported on a sintered plastic sheet, found that segregation occurred at velocities close to U_{mf} causing unstable fluidisation, and they suggested that the instabilities tended to persist as a result of the very small bubbles produced at the surface of the porous plate. Fitting a perforated metal sheet on top of the porous distributor was found to restore stable operation, presumably as a result of the coalescence of the airflow into larger bubbles. The evidence of these and other workers (for example, Ref. G7) seems to suggest that distributors of moderate pressure drop, comprising a multi-orifice plate having a very large number of uniformly-spaced small drilled holes will eliminate the undesirable erratic bubbling that tends to be associated with porous media. There is of course a limit to the number of small holes that can economically be drilled in a metal plate,

and in fact there is nothing to be gained by so doing as a drilled plate with more than about 1000 holes per square metre has much the same drawbacks as a porous plate (Ref. G2).

2.7 OTHER INFLUENCES ON FLUIDISED BED BEHAVIOUR

2.7.1 Particle size and size distribution

It has long been accepted that both particle size and size distribution have a significant influence on the behaviour of a bed of fluidised material, notably with regard to the bubble size and velocity, and the bed "viscosity".

It is of course well established that, in general, minimum fluidising velocity decreases and bed expansion ratio increases with decreasing particle size, and these phenomena have been discussed at some length in Sections 2.3 and 2.4. However, it has been pointed out (Ref. G2) that the apparent influence of particle size can be distorted by the method of determining the mean size. Thus, for example, the use of the median size, defined by

$$d_{wm} \simeq \Sigma xd \qquad \text{.....2.7.1}$$

tends to under-emphasise the influence of the finer particles, which may in fact have a pronounced effect on the volume specific surface S_b of the bed, and therefore on its fluidisation behaviour. A more relevant size is the surface volume mean diameter, which is conveniently (though not exactly) expressed as

$$d_{vsm} \simeq \left(\Sigma \frac{x}{d_A}\right)^{-1} \qquad \text{.....2.7.2}$$

where d_A is the particle size from sieve analysis.

One of the ways in which particle size can influence quality of fluidisation is by altering the range of superficial gas velocity for which the bed is in a quiescent state. Thus $U_{mb} - U_{mf}$ tends to be greater

for small irregular particles than for large, closely-sized, spherical ones (Ref. G7). Once bubbling of the bed does start, the size, shape and rise velocity of the bubbles may all be influenced by the type of material in the bed (Ref. R6). However, there appears to be a lack of agreement in the published literature on the extent of this influence. Geldart (Ref. G2) describes as "part of the folklore of fluidisation" the belief that a better quality of fluidisation is obtained with a powder having a wide particle size distribution than with one having a narrow size range, and he goes on to show experimentally that for Group B powders (see Section 2.4) in a stable fluidised bed, the bubble size at a given bed level and excess gas velocity ($U_g - U_{mf}$) is independent of particle size and size distribution. It may be noted that Geldart considered the excess gas velocity $U_g - U_{mf}$ to be a more reliable criterion of the degree of fluidisation than the more usually employed ratio U_g/U_{mf}.

Because of the very complex nature of the phenomenon of fluidisation it is in any case difficult to isolate one aspect of bed behaviour from the others. Thus the quality of fluidisation, defined perhaps in terms of bubble frequency, size and rise velocity, may be linked with the presence of interparticle forces and with the "viscosity" of the fluidised bed, both of which are themselves dependent upon particle size. Before discussing these factors, however, some consideration will be given to the variation of particle size with position in the bed; that is, the stratification or segregation of particles.

2.7.2 Particle segregation

The variation of particle size with position in a fluidised bed is closely related to the variation of voidage within the bed - itself a problem that has exercised many experimenters (Refs. B4, B7, D9, G10). Bakker and Heertjes (Ref. B4) developed a voidage distribution plot which showed that a fluidised bed can be divided into three zones: the lower zone, dilute in solids, is dependent upon the nature of the distributor; the central zone, comprising most of the bed, is essentially at uniform voidage; the upper zone is dilute in solids due to entrainment of particles by the vigorous bubbling at the bed surface.

The occurrence of particle segregation - or stratification - in a fluidised bed will depend to some extent upon the operating condition of the bed (Ref. B15, p 48). Generally the denser particles will drift downwards to the lower part of the bed, but segregation by size can also occur in the bed, especially at low fluidising velocities, with the larger particles settling towards the bottom. Wen and Yu (Ref. W4) found that in a two-component mixture the particles tended to segregate into two distinct zones, with small particles fluidised separately above a layer of larger ones, if the particle size ratio was greater than about 1.3. They compared this result with the criterion found by Shannon that for segregation to occur the ratio of the minimum fluidising velocities of the two components should be greater than two. A mechanism for the segregation process is described by Leva (Ref. L3 p 108), but this is questioned by Zabrodsky (Ref. Z1 p 56) who modifies Leva's model, and also presents a separate model for segregation by density.

It is possible to use a bed, fluidised at low air flowrates, to classify material, best results being obtained if the segregated product is removed from the bottom of the bed rather than the top (Ref. B15 p 56). Whilst a uniform size distribution within the bed can usually be maintained with a sufficient air flowrate, it may be difficult to re-mix once segregation has been allowed to occur (Ref. B15 p 139).

Davies and Robinson (Ref. D2) have described how partial fluidisation of a segregated bed can occur as the superficial velocity of the air is gradually increased, causing minor peaks on a plot of bed pressure drop against air velocity. Whether the bed becomes fluidised altogether, or by zones over a range of air velocity may depend upon the humidity of the fluidising air (Ref. K1). Boland et al (Ref. B10) also report the influence of humidity on segregation. Zabrodsky (Ref. Z1 p 58) points out that segregation by size is significantly affected by variation of the cross-sectional area of the bed, the particles tending to settle to the level at which the superficial air velocity is equal to their minimum fluidising velocity. Katz (Ref. K1) reported some size segregation in the radial direction, with a higher proportion of coarse particles near the walls of the fluidising vessel.

2.7.3 Interparticle forces

Various authors have commented on the difficulty of fluidising fine particles where the interparticle forces tend to approach the magnitude of the forces transmitted to the particles by the fluidising gas (Refs. B2, D8, M10, P1). Such materials fall into Geldart's Group C classification (Fig. 2.6) suggesting that fine particles of low density may be less easily fluidised than those of high density. Morse (Ref. M10) has suggested that for a given material there is a limit of particle size below which fluidisation cannot be achieved.

The interparticle forces affecting the quality of fluidisation of a bed of powder are frictional forces and cohesive forces. Adhesive forces between the particles and the vessel wall may also make a contribution. According to Baerns (Ref. B2) the frictional forces are virtually negligible and Donsi and Massimilla (Ref. D8) have listed the cohesive forces as:-

Van der Waals forces.
Capillary forces, by surface tension of absorbed water.
Electrostatic forces, from charge separation in contacting between the solids and the wall of the fluidising vessel.

In a packed bed electrostatic charges are likely to be neutralised through mutually contacting particles (Ref. B2) but when fluidised the amount of contact between individual particles is reduced and electrostatic charges can develop. Baerns (Ref. B2) attempted to measure the interparticle cohesive forces for different materials by noting the angle at which a mass of the material would slide under gravity from an inclined flat plate. He then showed experimentally that where the cohesive force is large compared with the weight of the particles in a bed, there was an increased tendency for the particles to form agglomerates and also for stable channels to be set up. Instead of using an inclined flat plate, Rietema and Mutsers (Ref. R5) tilted the actual fluidised bed and noted the angle at which the surface of the bed ceased to remain perpendicular to the mean gas flow. From this work they developed the concept of elasticity of a fluidised bed, related to

the interparticle forces. They also pointed out that as a fine powder forms into agglomerates the ratio of cohesive force to the weight of the agglomerates would decrease. Thus, the tendency of a fine material to form into agglomerates when fluidised could be expected to persist until this ratio fell below unity. In a later paper Rietema and Mutsers (Ref. R4) reported further developments in their study of the concept of elasticity of fluidised beds, and suggested that from a knowledge of the elastic properties of the bed it should be possible to predict the critical bed expansion at which bubbling starts. Donsi and Massimilla (Ref. D8) found that the intensity of the cohesive forces depended upon the surface characteristics of the particles, being proportional to the radius of curvature of particle asperities at contact points.

Electrostatic charging in fluidised beds is well known though not well understood. It occurs as a result of the continual collision and separation of particles in a bed and can lead to agglomeration of the particles with consequent loss of quality of fluidisation. The phenomenon may constitute a safety hazard if there is the possibility of an explosion being initiated by a spontaneous discharge to an earth conductor (Ref. B10). Materials in the fluidised bed vary greatly in their ability to become charged, and in the effect that such charging has on their fluidisation behaviour. Thus, for example, fine powders of low density and low conductivity are generally less easily fluidised, although it is not clear whether this is as a result of static electrification or other interparticle forces (Ref. B2, D8).

A useful introduction to the subject of static electrification of solids is given by Montgomery (Ref. M15), and Boland and Geldart (Ref. B12) review the phenomenon as it occurs in particulate systems, suggesting that the charge is in fact generated by the motion of particles around gas bubbles. Various researchers (Refs. B12, K4,C4) generally using some kind of centrally mounted probe (Fig. 2.9) have attempted to measure the charges developed in fluidised beds of different powders under various operating conditions. Kisel'nikov et al (Ref. K4) observed that the potential on a centrally-mounted electrode rose gradually during the course of an experiment, reaching a steady level after a period of about twenty minutes. With the electrode situated near the

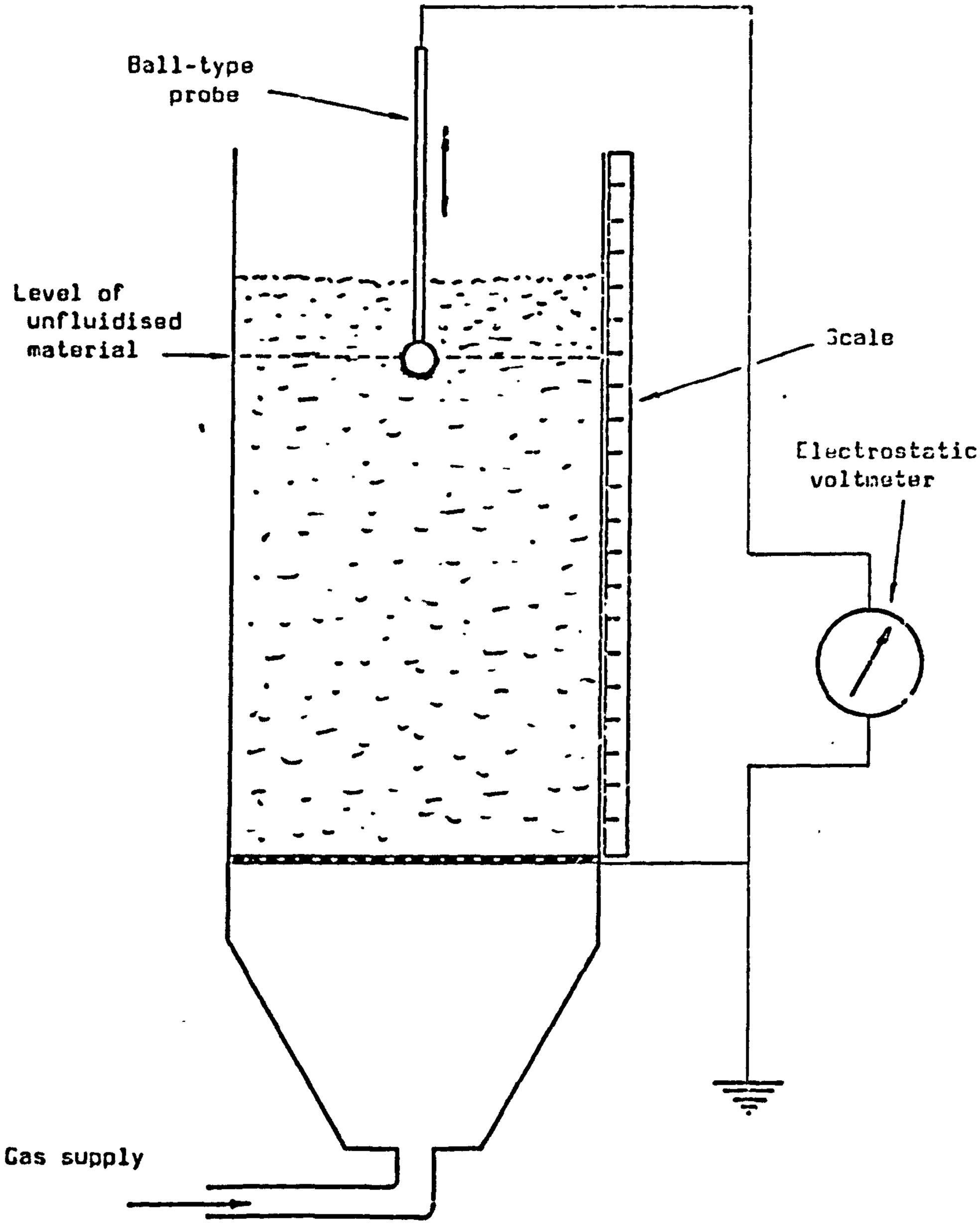

Fig. 2.9 A TYPICAL ARRANGEMENT FOR THE INVESTIGATION OF ELECTROSTATIC CHARGING IN GAS-FLUIDISED BEDS (Ref. K4). The electrode ends in a ball and is adjustable for depth in the bed. For most tests it is set so that the ball is level with the surface of the bed material when it is unfluidised.

surface of the bed the greatest potentials measured were about 1200 volts (with ammonium sulphate powder) but still higher potentials were found near the middle of the bed. The maximum potential recorded in any given bed was shown to increase significantly with increasing air velocity. Very much higher potentials - up to 15 kV - were recorded by Ciborowski and Wlodarski (Ref. C4) in their work with vinyl polyacetate, though again showing a marked dependence on fluidising air velocity. They too observed that the potential reached a steady maximum value after some twenty to thirty minutes of operation, but suggested that this was the time taken for the velocity and humidity of the fluidising air to become established. At the condition corresponding to the maximum potential the fluidised bed displayed peculiar behaviour which, from the description given by Ciborowski and Wlodarski, suggests that the presence of the electrode itself could have been exerting some influence. The tendency of the vinyl polyacetate powder to form into agglomerates, and of the bed to de-fluidise and form channels in a manner normally characteristic of very fine particulate solids, has been observed in the present work with p.v.c. powder, as described in detail in Part II. However, it is worth noting that, according to Kunkel (Ref. K11), even though a body of powder as a whole may be neutral, the individual particles could be positively and negatively charged, and therefore still have a tendency to form agglomerates.

Although increasing the humidity of the fluidising air seems to be the usual way of controlling the static electrification of particles in fluidised beds, some authors have reported the use of fine carbon powder (about 0.2% by weight; Ref. L8) or a graphite coating on the particles (Ref. H1) for this purpose. Virtually all the authors dealing with the phenomenon of static electrification of particulate bulk solids make some reference to the influence of moisture, and although there is general agreement that electrostatic potentials are reduced by the presence of moisture, some interesting and significant observations have been made. These are discussed in the next Section.

2.7.4 Moisture

The influence of moisture on the behaviour of a fluidised bed is, to a large extent, the result of changes in the rates of build-up and leakage

of electrostatic charge. It may be remarked at the outset of the discussion that it is not solely the moisture content of the fluidising air that has an effect. Ciborowski and Wlodarski (Ref. C4) in their detailed investigation, showed that increasing the humidity of the air surrounding their fluidising vessel caused a substantial reduction in the maximum potential reached on the electrode positioned centrally in the bed of fluidised material.

It is generally recognised that increasing the humidity of the fluidising air itself is sufficient to reduce the detrimental effects of static electrification to negligible proportions, and it is usual for researchers studying the fluidisation behaviour of different bulk solids to "eliminate" this awkward variable by operating with a relative humidity of 60% or more (Refs. B12, D2, K3, S13).

Several papers (Refs. A9, C4, P1) have reported on experimental studies of the effect of moisture on fluidisation behaviour. It is evident that the extent to which the fluidised material is affected by moisture depends upon the type of material, for example whether or not it is porous. Arai and Sugiyama (Ref. A9) found that for beds of non-porous particles the minimum fluidising velocity and the bed expansion ratio were not influenced significantly by moisture up to 0.1% by weight. However, the particles used - glass powder, silica sand, quartz and so on - are not especially susceptible to electrostatic charging, and where such particles have a significant moisture content it is likely to be a surface film of water that causes agglomeration and consequent loss in fluidisation quality. Although not as dramatic as with many plastics powders, some static electrification effects have been observed in beds of glass beads (Refs. B12, K1, L6). In his work with glass beads, Katz (Ref. K1) pointed out that the behaviour of the fluidised bed is extremely sensitive to variations in the humidity of the fluidising air, but it may not be easy to distinguish between electrostatic effects and the effects of moisture adsorption.

Whilst it is well known that the level of electrostatic charge reached is generally much lower if the humidity of the fluidising air is high, Boland and Goldart (Ref. B12) have shown that this is because the

humidity influences strongly the rate of charge dissipation, rather than the charge generation. Ciborowski and Wlodarski (Ref. C4) found that, with all the different bed materials they tested, decreasing the humidity of the fluidising air caused first a rapid increase in the charge picked up by the central electrode, and then a rapid drop. Further conclusions reached by Katz (Ref. K1) are that in a bed of particles of mixed size, the segregation of particles that can occur when the bed is fluidised is to some extent dependent upon static electricity and adsorbed moisture, and the control of static by the use of humidified air, or by other means increasing the conductivity of the fluidising gas, is not feasible if consistent behaviour of the fluidised material is required.

2.7.5 Wall effects

The presence of a vertical surface within a fluidised bed can significantly modify the bubbling behaviour, and this has been extensively investigated, particularly with regard to changes in heat transfer characteristics. Botterill (Ref. B15 p 40) gives a useful discussion of the influence of internal surfaces, citing the work of a number of different authors.

Close to the wall of a fluidising vessel the direction of movement of particles tends to be predominantly downward. This can usually be observed in small laboratory rigs in which the vessel is made of glass or Perspex, and is in accordance with the recognised pattern of particle circulation that normally occurs in fluidised beds. Variation in the bed voidage can usually be detected near to the walls (Refs. B4, B7) and there may also be preferential bubble flow up the walls.

Behaviour close to the free surface of the bed may be affected by the velocity distribution in the fluidising air in the free-board above the bed (Ref. L5), especially where the diameter of the vessel is small.

However, clear experimental evidence relating to the influence of the vessel wall, or more particularly of the vessel diameter, is not easy to find and McGuigan (Ref. M4) comments that any generalisations

concerning such effects "must be regarded with extreme caution".

2.8 APPARENT VISCOSITY OF FLUIDISED BEDS

2.8.1 Introduction

Because of the visible similarities in the behaviour of fluidised particulate solids and ordinary liquids, it is natural that attempts should have been made to investigate the resistance of fluidised particles to shearing forces by conceiving a property corresponding to "viscosity". A considerable number of investigations have been reported in the literature, different approaches to the problem including rotational viscometers (Refs. D3, F3, K8, L8, M3, M4, S10), torsional pendulum viscometers (Refs. A10, H1), falling ball methods (Refs. K3, L2, P5), channel flow methods (Refs. N1, N2, S8, S13), frequency methods (Ref. G6) and methods based on observations of bubble behaviour (Ref. C8).

In the case of Newtonian fluid behaviour the shear stress is of course a linear function of the rate of shear. Where this relationship is non-linear the behaviour is broadly classed as "non-Newtonian". Many mathematical models have been proposed for non-Newtonian fluids, the best known being the power-law fluids (pseudoplastic and dilatant) and Bingham plastics which are discussed further in Appendix A.III.

Unfortunately, viscosity is not a property that can be measured directly. It has to be inferred from measurements of other quantities, generally shear stress and shear rate. Thus for example, if the torque required to rotate a cylinder of known size at a given speed is determined, both the shear stress and the shear rate can be calculated, and hence a value can be found for the "apparent viscosity". Where the rotating element is not circular in section the relative movement between it and the fluid is not simple shear. Therefore rotors such as paddles (Refs. F3, M3, S10), dumb-bells (Ref. K8) and wire meshes (Ref. D5) need to be calibrated in fluids of known viscosity. Herein lies the difficulty of attempting to measure "viscosity" using an instrument that involves "stirring" in addition to shear, since different instruments calibrated together in the same fluids will often give different

readings when subsequently used in the same fluidised bed. As remarked by Davidson et al (Ref. D1), such instruments are therefore useful only in giving qualitative information on the rheology of fluidised particulate solids. Schugerl (Ref. S4) has stated that only with concentric rotating cylinders (the Couette viscometer) can the non-Newtonian behaviour of fluidised beds be estimated, whereas for Newtonian behaviour either the Couette viscometer or a torsional pendulum could be used. However, this implies that the fluidised suspension behaves as a continuous fluid in laminar flow, and furthermore, the slip between the rotating element surface and the fluidised material is very much an unknown quantity. Nevertheless, although the calculation of values of "viscosity" using these instruments is somewhat questionable, it is clear that useful data on the rheology of fluidised beds can be obtained, for example in the form of shear diagrams. As previously mentioned, the difficulties appear to lie in obtaining meaningful correlations between the different investigative techniques available.

2.8.2 Rotational viscometers

These form the largest class of viscometers used in investigations into the rheological behaviour of gas fluidised beds, and can be conveniently subdivided into instruments measuring pure shear and instruments measuring a combination of shear and form drag. The first group includes viscometers using hollow or solid cylindrical rotors, and as pointed out by Schugerl (Ref. S4) and McGuigan (Ref. M4), these are the only viscometers which will allow a valid theoretical analysis based on a non-Newtonian fluid model. Some of the different types of rotor that have been used are illustrated in Fig. 2.10.

The first serious investigation of the viscosity of fluidised beds was that of Matheson et al (Ref. M3) who used a Stormer-type viscometer in which a paddle 38 mm x 19 mm x 1.6 mm was rotated in the bed at 200 rev/min and the torque necessary to maintain this rotation was determined. As would be expected, and has since been confirmed by many researchers, Matheson et al found that the torque required to rotate the paddle was very high when the bed was unfluidised but dropped sharply as the superficial velocity of the fluidising gas was increased. A point was

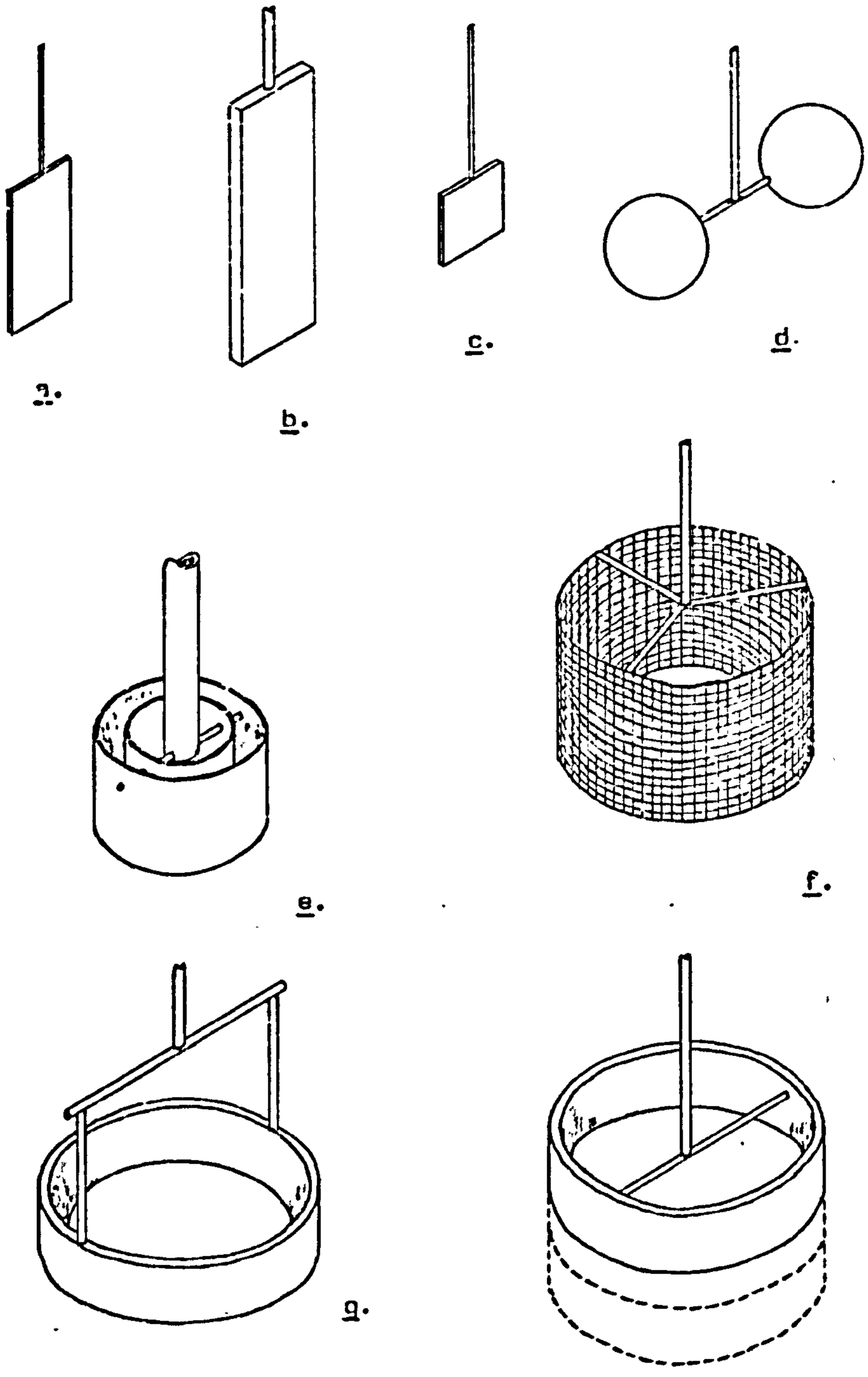

a - d and f - h approx. half full size;
e approx. full size.

Fig. 2.10 ROTATIONAL VISCOMETER ROTORS USED BY VARIOUS RESEARCH WORKERS FOR INVESTIGATING FLUID-BED "VISCOSITY".
a - c. Paddles (a. Matheson et al. Ref. M3, b. Furukawa and Ohmae Ref. F3; c. Shuster and Haas Ref. S10). d. Dumbell (Kramers Ref. K8). e. Concentric hollow cylinders (Liu and Orr Ref. L8). f. Hollow mesh cylinder (Diekman and Forsythe Ref. D5). g, h. Single hollow cylinders (g. Botterill et al Ref. B22; h. McGuigan Ref. M4).

reached at which the torque required was virtually independent of the superficial gas velocity, this "break point" being more clearly defined for fine particles than for coarse particles. Matheson et al in fact chose to define the viscosity of the bed in terms of this "minimum torque" condition.

It was found by Matheson et al that the "minimum viscosity" of the fluidised bed tended to increase with increasing particle size and density, and also was higher for spherical particles than for those of irregular shape. They commented that a relatively small amount of fines added to a bed can cause a sharp drop in the resistance of the bed to the rotating paddle. However, Geldart (Ref. G2) has pointed out that this conforms to the observed influence of particle size, since a small amount of fines could result in a significant reduction of the surface-volume mean diameter of the powder.

Stormer-type viscometers fitted with paddle rotors were also used by Furukawa and Ohmae (Ref. F3) and by Shuster and Haas (Ref. S10). Working with beds of glass beads of different sizes and at various fluidising conditions Shuster and Haas found that all their plots of "viscosity" against superficial air velocity showed the same general shape which could be explained in terms of three zones of behaviour (Fig. 2.11). Initially the viscosity of the bed decreases rapidly (Zone I) as the interparticle forces are reduced by the fluidising air. Then in Zone II particle activity increases with a resulting increase in momentum interchange between particles and paddle, and hence an increase in the measured "viscosity". Further increase in the superficial air velocity may result in a significant expansion of the bed so that fewer particles are present in the region swept by the paddle. This may outweigh the effect of increased particle activity, causing the "viscosity" of the bed once again to decrease (Zone III).

The influence of such variables as particle size, paddle position and type of gas distributor was investigated by Shuster and Haas, and from the results of this work they concluded that the measured "viscosity" of a fluidised bed depended very much on its bubbling behaviour. Thus, with a mesh distributor, which tends to introduce larger bubbles than

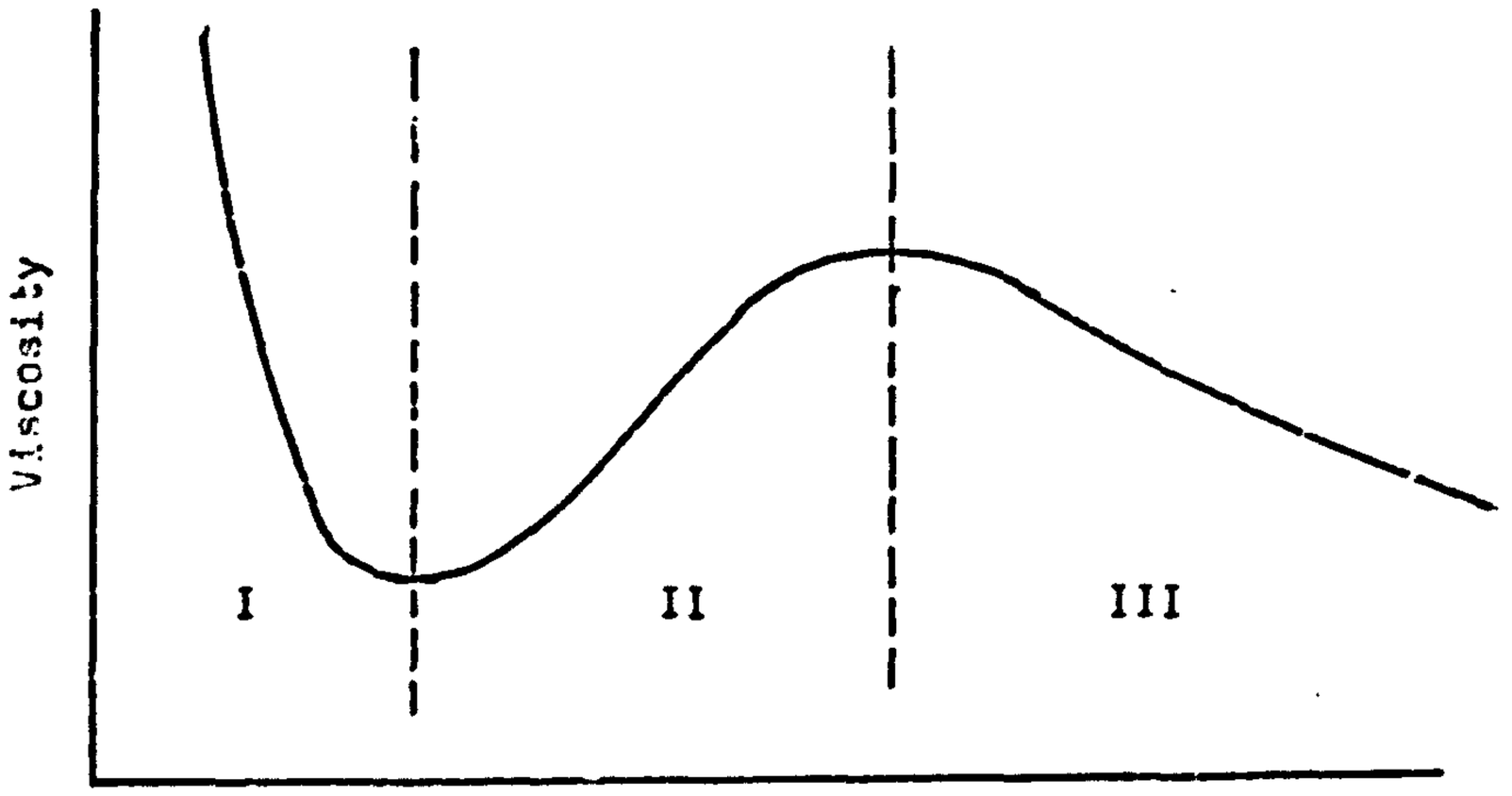

Fig. 2.11 VARIATION OF "VISCOSITY" OF A FLUIDISED BED WITH SUPERFICIAL GAS VELOCITY, SHOWING THE THREE ZONES OF BEHAVIOUR THAT MAY BE OBSERVED. (Ref. S10)

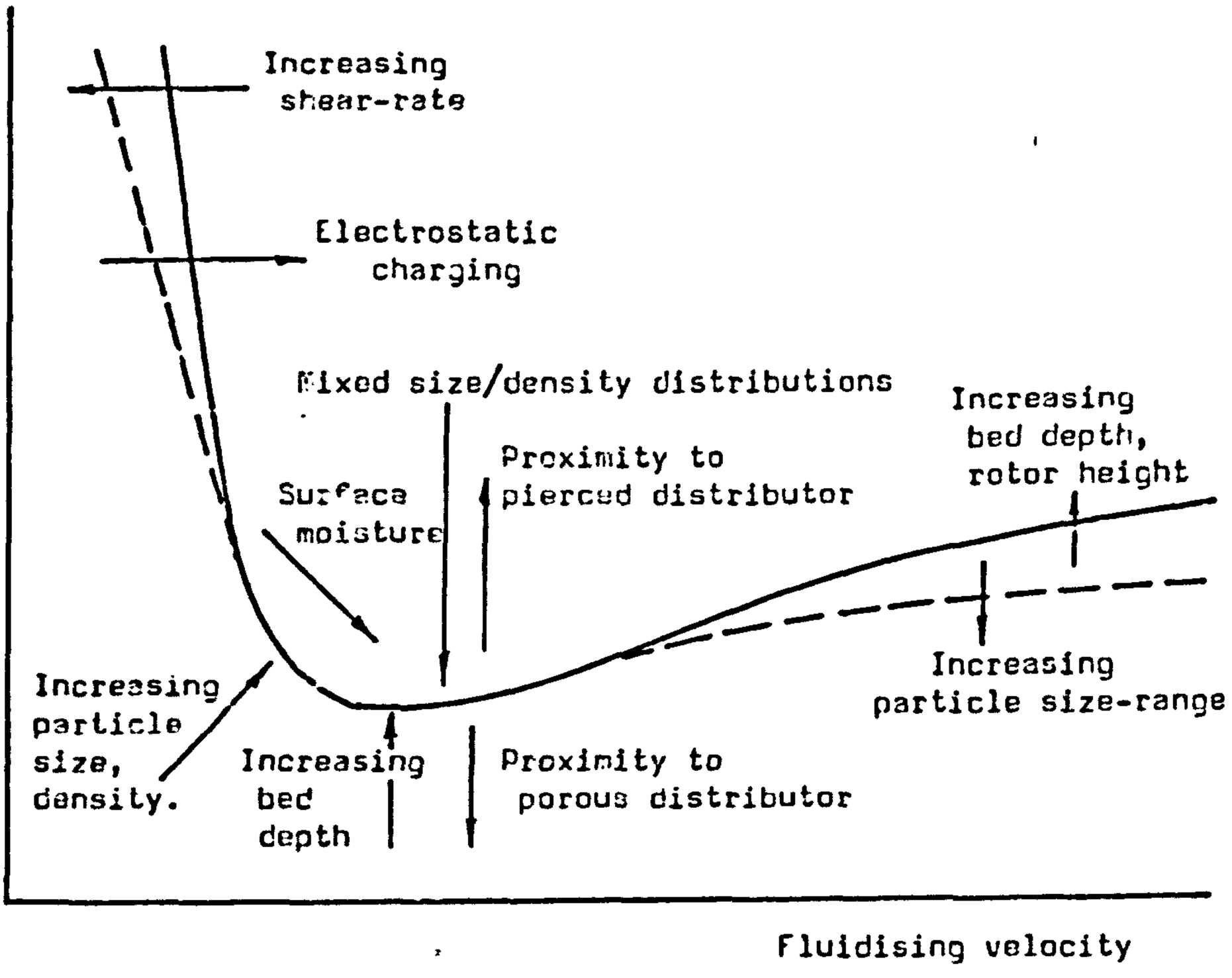

Fig. 2.12 SUMMARY OF THE INFLUENCE OF DIFFERENT VARIABLES ON THE "VISCOSITY" OF A BED OF FLUIDISED PARTICLES.(Ref. M4)

the porous plate type, the "viscosity" of the bed is generally higher. Also, because of the more uniform fluidisation produced by the porous plate, there was less radial variation of viscosity than with the mesh distributor.

In an attempt to minimize the disturbances caused by rotating paddles, Kramers (Ref. K8) used a dumb-bell, comprising two 25 mm diameter balls on 50 mm centres, rotating at a very low speed (less than 30 rev/min). By determining the relationships between the force on the spheres and their linear velocity in various fluidised beds, he was able to make a qualitative study of the "viscosity" of the bed materials. Kramers plotted curves corresponding to Zone I and part of Zone II on Fig. 2.11, the lowest viscosity being found generally at the bottom of the fluidised beds.

Rotating cylinder viscometers, usually having hollow cylinders, have been used by a number of research workers and in one case (Ref. D5) the cylinder was made of a 10-mesh wire screen (1.7 mm aperture size) in order to cause minimum interference with particle behaviour.

One of the most thorough studies of fluid-bed viscosity was that undertaken by McGuigan (Refs. M4, M5) for the purpose of establishing the parameters likely to influence the flow behaviour of shallow fluidised beds. He used a hollow cylinder of low aspect ratio (Fig. 2.10h) driven initially by a Brookfield Synchrolectric viscometer but in later tests by a Stormer-type arrangement. McGuigan showed that for a cylindrical rotor in an infinite fluid the shear rate at the rotor surface was given by

$$\dot{\gamma}_R = 2\tau_R \frac{d\omega}{d\tau_R}$$

where τ_R is the shear stress at the rotor surface and ω is the angular velocity of the rotor. In order to eliminate errors resulting from the ends of the cylindrical rotor and the supporting wires a calibration method was developed using two cylinders of the same diameter but different lengths.

The now familiar trend of sharply increasing "viscosity" of the fluidised material as the superficial air velocity is reduced towards U_{mf} was observed by McGuigan, and he also noted that the point at which this apparent viscosity was a minimum (termed by McGuigan the "flow deterioration velocity") was consistently greater than U_{mf}. Shear diagrams plotted for various particulate materials in beds of about 20 mm depth showed that flow behaviour generally showed pseudoplastic characteristics at superficial air velocities less than about $2U_{mf}$, but tended to become Newtonian at higher air velocities. Similar behaviour had previously been reported by Liu and Orr (Ref. L8) who used a Brookfield viscometer with a small rotor comprising two concentrically mounted thin-walled cylinders.

McGuigan carried out a series of interesting tests on materials of different mean particle size and on binary mixtures. He found that for single components the particle size had little influence on the apparent viscosity, but the viscosity of fine dense materials could be significantly reduced, without appreciably affecting the minimum fluidising velocity, by adding small quantities of larger lighter particles.

Similar distributor effects to those found by Shuster and Haas (Ref. S10) were reported by McGuigan; that is, with a perforated plate distributor the "viscosity" was generally higher than with a porous plate, and also tended to vary more with position in the bed. In deep beds it was again found that the viscosity tended to be higher, but also, it proved to be rather more sensitive to changes in superficial air velocity. Small variations in the moisture content of the fluidising air were found to significantly change the apparent viscosity of the fluidised material, although this could well correspond to changes in U_{mf}.

By comparing the results of tests with smooth and rough-surfaced rotors, McGuigan showed that at low shear rates the slip velocity between the rotor surface and the fluidised material was negligible. This conforms with the conclusion of Nimmo, cited by Hagyard and Sacerdote (Ref. H1), who used high speed photography to show that slip on a slowly moving boundary in a fluidised bed was very small, if it occurred at all. However, in other work mentioned by Hagyard and Sacerdote it was found

necessary to use roughened rotors in order to eliminate the effect of slip.

McGuigan concluded his work with a useful diagram summarising the trends observed in the relationship between apparent viscosity and superficial air velocity and this is reproduced here as Fig. 2.12.

2.8.3 Other techniques

A reasonable alternative to rotational viscometers is provided by instruments which involve oscillations of an appropriate bob suspended on a torsion wire. Such an approach has been described by Ashwin et al (Ref. A10) and by Hagyard and Sacerdote (Ref. H1), who obtained similar results to those of other workers using rotational viscometers, with the notable exception that they did not observe any decrease of viscosity with decreasing particle size.

Peters and Schmidt (Ref. P5) used a falling ball method to investigate the variation of viscosity in beds of fluidised sand of different particle sizes. They found that the viscosity was greater with larger particle sizes, and that the transition from high to low viscosity as the bed became fluidised was much less sudden than with the finer grain sizes; an effect previously reported by Matheson et al (Ref. M3). A falling ball was also used by Keuneke (Ref. K3), the 20 mm ball being attached to a thread and counter-weighted to fall at a rate of 0.2 m/s. Keuncke's work is of interest as he measured the apparent viscosity of fluidised materials with a rotational viscometer in addition to the falling-ball method and compared the results. With fine powders the falling ball tended to indicate higher viscosities than the rotational viscometer, but with materials of large particle size the readings from the rotational viscometer were the higher. In a variation of this method Leont'ev and Vakhrushev (Ref. L2) introduced a low density ball near the bottom of the bed and noted the time taken for it to float to the surface.

More unusual approaches have been tried by some researchers. Gel'perin et al (Ref. G6) applied harmonic circulatory vibrations to the fluidising

vessel and, using a sensitive pick-up, observed the resulting motion of the fluidised particles. However, this must cause considerable disturbance to the bed and Grace (Ref. G3) suggested that the shape of rising bubbles in the bed should be a function of the bed viscosity. From measurements of the included angles in spherical-capped bubbles Grace calculated values of viscosity for various fluidised materials. Good agreement was obtained with measurements by a rotating cylinder viscometer.

Observation of the flow characteristics of fluidised bulk solids in inclined channels provides yet another means of inferring the "viscosity" of such materials (Refs. N1, N2, S8, S13) and this possibility is discussed more fully in Section 3.2.10.

2.9 CONCLUSIONS

The fluidisation of particulate bulk solids has been studied in some depth insofar as it is felt to be relevant to the main theme of the present programme of work. The survey of the literature has therefore been concerned almost exclusively with fluidisation by air, and discussion of specific processes such as heat transfer has been largely avoided, although it is recognised that such processes may include some of the main applications of fluidisation.

Of particular significance to the flow behaviour of aerated bulk solids are the minimum fluidising velocity, the expansion of the fluidised material and the entrainment of particles in the stream of air leaving the fluidised bed. All these phenomena have therefore been discussed in considerable detail, especially with regard to methods of predicting how a given material will behave when aerated. For a preliminary estimate of minimum fluidising velocity it is recommended that the equation

$$U_{mf} = 420\ \rho_p\ d_v^2 \qquad \text{.....2.9.1}$$

should be used, where ρ_p is the particle density in kg/m^3 and d_v is the mean particle diameter in metres, giving U_{mf} in m/s. For practical convenience a chart has been prepared which, in addition to minimum

fluidising velocities, gives a guide to the conditions under which entrainment from the fluidised bed could occur. This chart (Fig. 2.13) which is restricted to fluidisation with air at normal ambient conditions, also shows the approximate classes of behaviour as described by Geldart (see Section 2.4). It is appreciated that equation 2.9.1 and Fig. 2.13 may not give as reliable prediction of fluidisation behaviour as some of the more rigorous treatments. However, even these rigorous analyses are of limited value if the fundamental data on, for example, particle size, shape and density are not wholly reliable. In practice a designer may find it as easy to obtain direct information on fluidisation behaviour from tests in a pilot plant as to measure accurately the more fundamental properties of the bulk solid concerned. Therefore a quick guide to the probable behaviour of a bulk solid, when aerated, could provide a useful aid to designers of air-assisted gravity conveyors.

Other influences have been considered insofar as they may affect the behaviour of stationary (that is, non-flowing) fluidised beds, in order subsequently to assess how they might be relevant to the flow of aerated bulk solids in inclined channels. Of special interest is the property characterising the resistance of the fluidised bed to flow, or more specifically, to shearing stresses. As a matter of convenience this property is called "viscosity" although it is recognised that the property may be significantly different from the viscosity as defined for homogeneous fluids. In general, quantitative data on the viscosity of fluidised materials is unreliable, showing a marked tendency to depend upon the way in which it is measured. Some authors, recognising this difficulty, have sought merely to establish trends, expressing viscosity in "arbitrary units". Of those that attempted to determine absolute values of viscosity, Siemes and Hellmer (Ref. S13) made a useful graphical comparison (reproduced in Refs. B15, K10) from which is is seen that there is a very wide variation in the data. There would appear to be some advantage in standardising the method used to investigate and characterise the rheological behaviour of fluidised beds in order to permit a meaningful comparison of data obtained by different workers under different conditions. Probably a Stormer-type viscometer using a hollow cylindrical rotor would prove to be the best candidate for such a standard method.

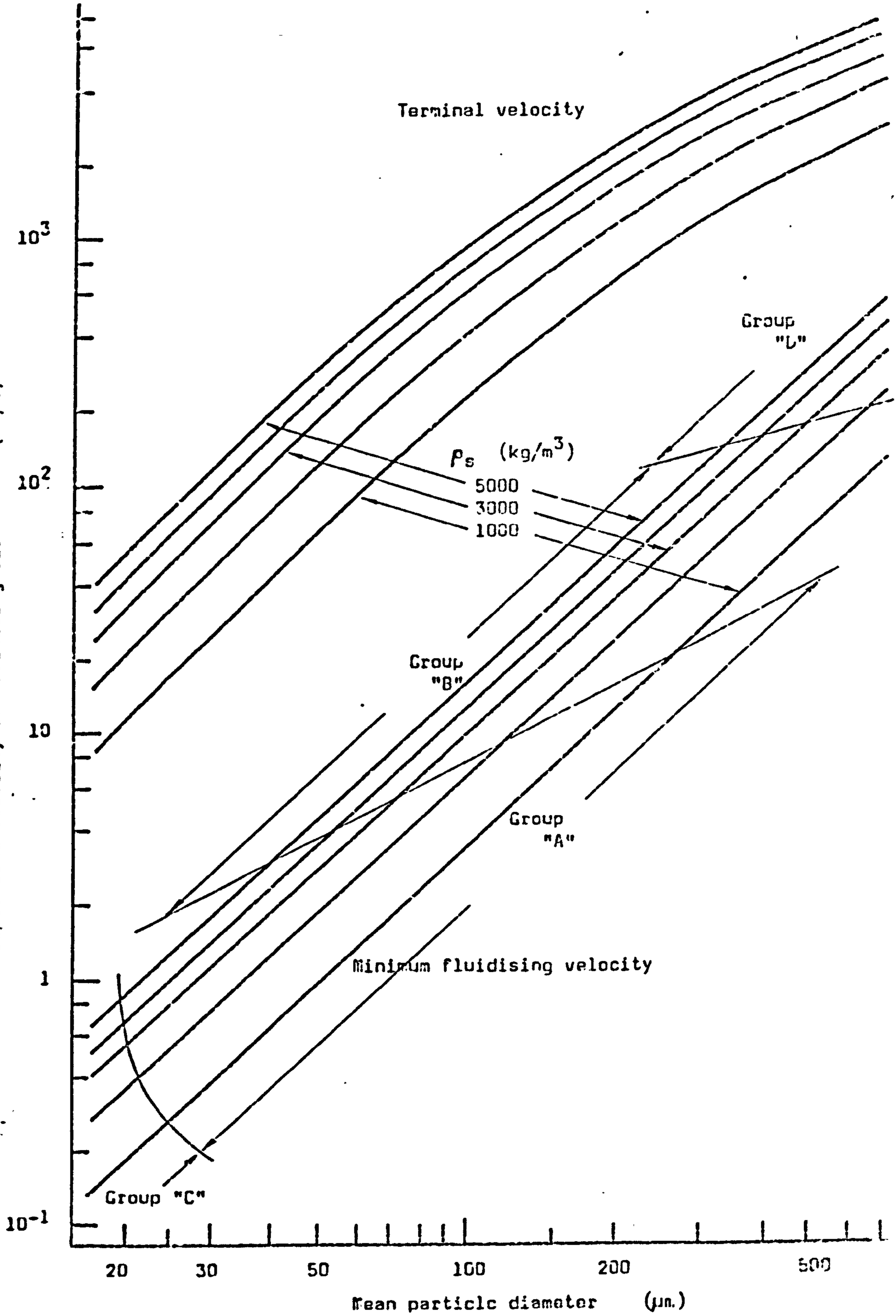

Fig. 2.13 MINIMUM FLUIDISING VELOCITY AND TERMINAL VELOCITY FOR A BED OF PARTICLES FLUIDISED WITH AIR AT NORMAL AMBIENT CONDITIONS.

CHAPTER THREE

THE FLOW BEHAVIOUR OF AERATED BULK SOLIDS

3.1 INTRODUCTION

3.1.1 General principles of fluidised flow

Most free-flowing particulate materials display a natural angle of repose of around 35^{o} to 40^{o}, this being the maximum angle of inclination of the free surface of a heap of the material (Fig. 3.1.). The angle of repose will in fact depend partly upon how the heap is formed and there is a certain amount of disagreement as to the most reliable method of measuring it. Amongst methods that have been proposed (Refs. B26, T2) are forming a heap of the powder by pouring or by draining, tilting a box filled with powder or rotating a horizontal cylinder half-filled with powder. In order to get even free-flowing materials to "flow" continuously, under gravity alone, in an inclined channel it would be necessary for the slope of the channel to be greater than about 35^{o}, depending upon the angle of repose and other properties which together might be termed the "flowability" of the powder, and also depending to some extent upon the roughness of the channel surfaces. Materials exhibiting some degree of cohesiveness have angles of repose much larger than the normal 35^{o} to 40^{o} and often will not flow, even on steeply inclined surfaces, without some form of assistance, such as vibration of the surface.

If a powder or granular material is to move freely along a channel when the slope is much less than the natural angle of repose, it is necessary either to improve the "flowability" or to reduce the frictional resistance between the bed of powder and the walls and bottom of the channel. Now the introduction of air to a bulk powder, for example by supporting the powder on a plate made of a suitable porous substance and allowing the air to flow upwards through it at low velocity into the powder, can significantly reduce the natural angle of repose (Fig. 3.2.). It is necessary then to incline the plate at only a very shallow angle for the powder to "flow"; for some free-flowing powders this angle being as little as 1^{o} or even less. It is not clear whether this results predominantly from the air filtering through the bed of solid particles and reducing the contact forces between them (thus perhaps causing partial fluidisation of the powder) or from the formation of an air

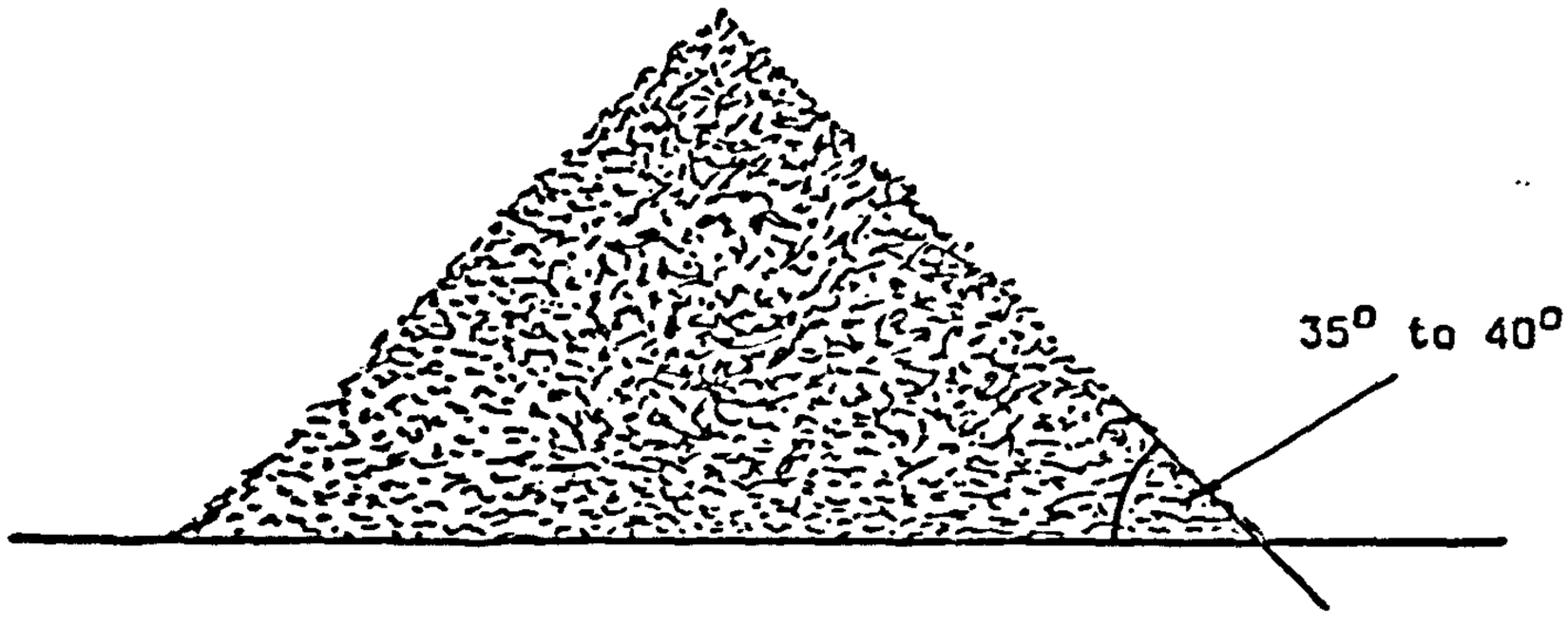

Fig. 3.1. THE NATURAL ANGLE OF REPOSE OF MOST FREE-FLOWING MATERIALS IS AROUND 35 TO 40°.

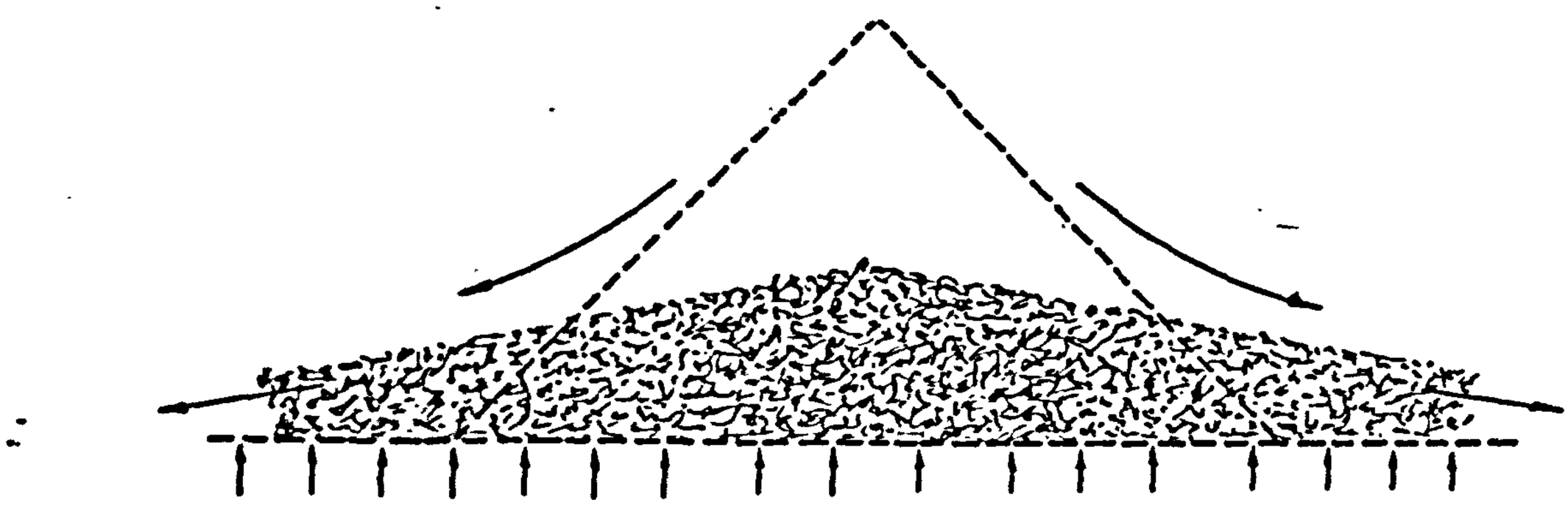

Fig. 3.2. AERATION OF THE MATERIAL CAN CAUSE A DRAMATIC REDUCTION IN THE ANGLE OF REPOSE.

layer between the bed of particles and the plate surface allowing slip to take place with consequent sharp reduction of the boundary shear stresses. However, it seems probable that with fine free-flowing solids, which can be easily fluidised, the former effect is the more significant, and it is these materials that will flow satisfactorily at extremely shallow slopes (Fig. 3.3.). Slightly cohesive powders, when aerated, will often "flow" down an inclined surface if the slope is rather greater; perhaps around 6^{o} to 10^{o}. Observation of such a material suggests that the particles are not fluidised, but move virtually as a solid mass sliding along the channel (Fig. 3.4.). It is probably because of the lack of knowledge on the way in which these two influences combine that prediction of the flow behaviour of one material from tests on another seem to have proved somewhat unreliable.

The ability of aerated bulk particulate solids to flow on a surface inclined at a very small angle to the horizontal can be utilised by constructing a conveying channel having a porous base through which air can flow at a uniform rate from some form of plenum chamber. In such a channel most kinds of bulk particulate solid (excluding very cohesive or "sticky" substances) can be transported continuously over useful horizontal distances with relatively little loss of elevation. Provided that this small loss of elevation can be accepted (and for free-flowing materials it may be as little as one metre in fifty) the "air-assisted gravity conveyor" would usually prove to be the most economical method of transport.

3.1.2 Historical development

It is not known when aeration of a bulk particulate solid was first used as an aid to conveying, but one of the earliest relevant patents appears to have been that of Dodge in 1895 (Ref. D7) who used air, entering an open channel through slits in the base, to transport coarse grained material. It is interesting to note that also around the turn of the century the air cushion principle was proposed for moving steel plates horizontally along a table on a series of vertical air jets (Ref. V2).

However, significant progress in the gravity conveying of aerated powders was not made until some thirty years later when it was found that the

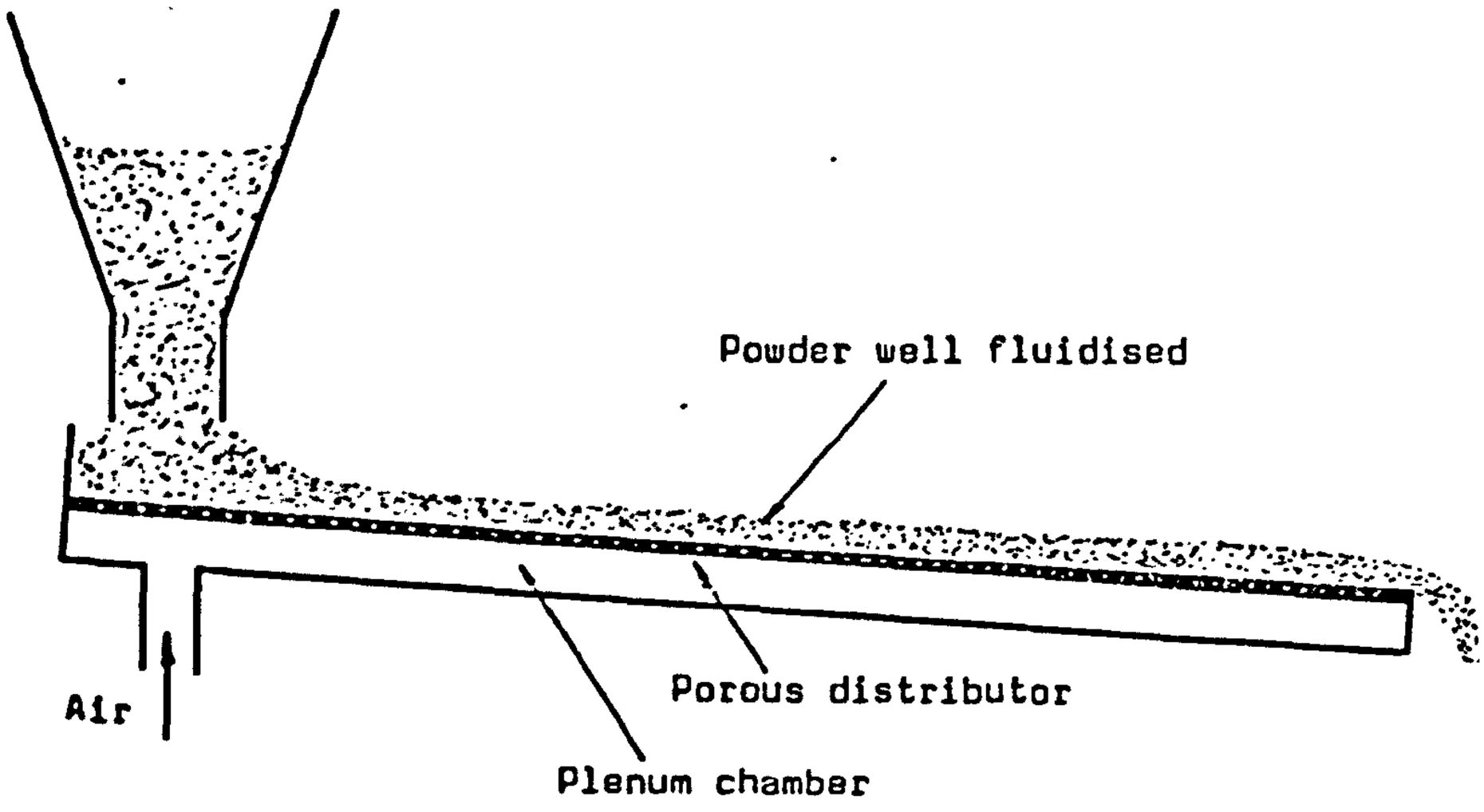

Fig. 3.3. FREE-FLOWING POWDERS BECOME FLUIDISED AND WILL NORMALLY FLOW ALONG THE CHANNEL WHEN THE SLOPE IS AS LITTLE AS 1^{o} OR LESS.

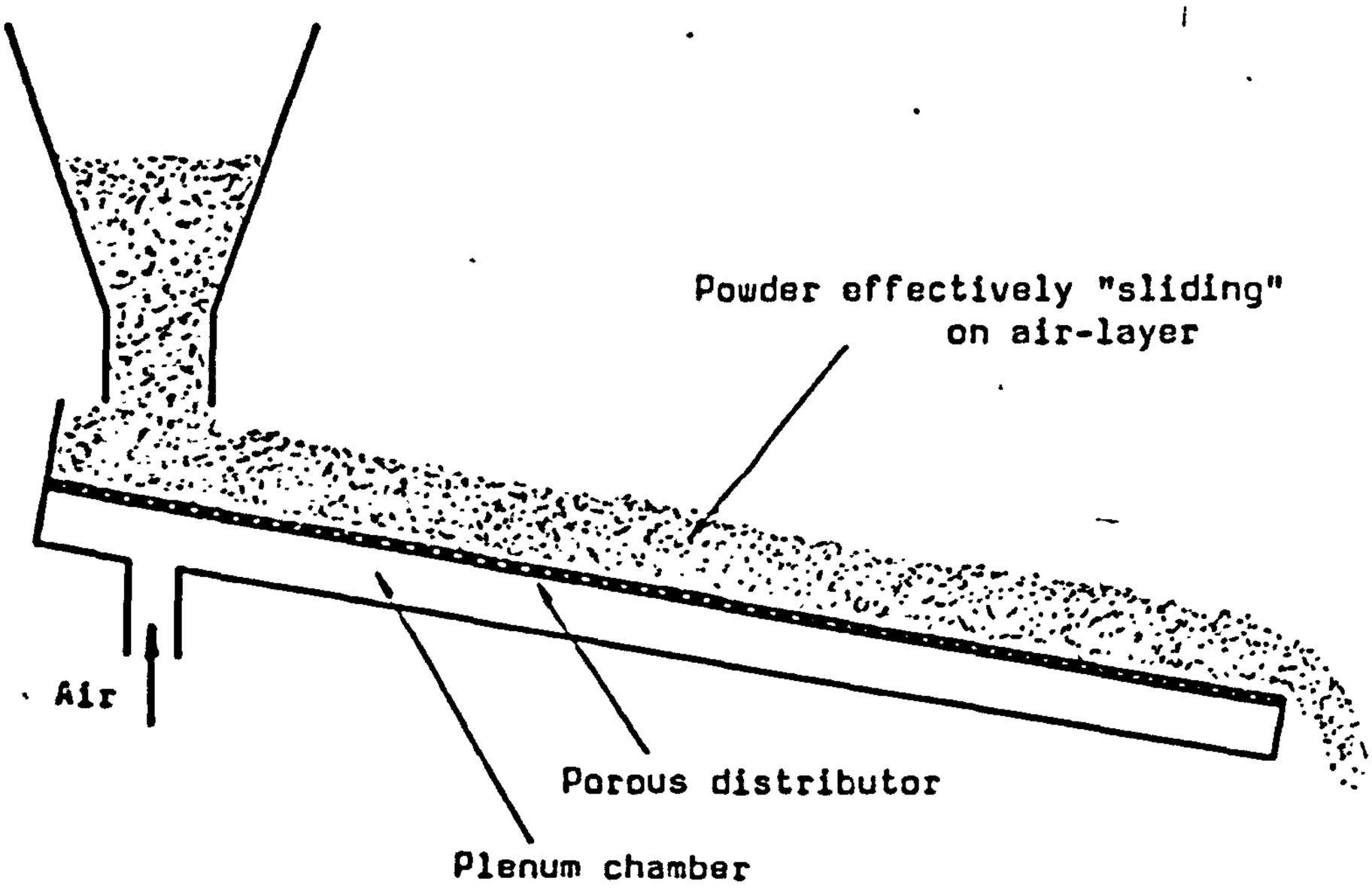

Fig. 3.4. SLIGHTLY COHESIVE POWDERS THAT DO NOT FLUIDISE WELL CAN OFTEN BE CONVEYED IF THE CHANNEL SLOPE IS GREATER (UP TO ABOUT 10^{o}). THE POWDER EFFECTIVELY SLIDES ON A LAYER OF AIR TRAPPED AGAINST THE TOP SURFACE OF THE DISTRIBUTOR.

method provided an excellent means of conveying cement. The German company Polysius was something of a pioneer in the development of air-assisted gravity conveying, but was followed into the field by the Huron Portland Cement Company of America which obtained the first British patent in 1949 (Ref. H8). Huron's plant at Alpena, Michigan was one of the first to make extensive commercial use of this method of conveying and employed "Airslides", as they came to be called, at various stages of the production process from grinding mill discharge to finished cement (Refs. A12, N3). The third organisation that played a prominent part in establishing air-gravity conveyors was the Fuller Company which manufactured them under license from Huron and which also held the rights to one of the main controlling British patents (Ref. F2). Further British patents, mostly taken out by Huron and by the Fuller Company, indicate the gradual development of air-assisted gravity conveying through changes to the design of the duct, feed and take-off points, air supply, porous base material, and so on, but rarely do these patents give any technical details on the performance of the conveyors.

Although the air-assisted gravity conveyor first came to prominence for the transport of cement - and this is still one of the main applications - many other types of material are now handled with relative ease, including such diverse substances as fly ash, coal dust, plastic and metal powders, washing powder, alumina and sand. Typical of the large installations described in some detail in the published literature are a 50,000 tonne storage plant and an 80,000 tonne ship loading plant, both handling alumina (Ref. L1) and a Canadian aluminium smelter capable of handling 160,000 tonnes of alumina per annum (Refs. B27, B28). These and other useful references to industrial installations handling various bulk solids are listed in Table 3.1.

Currently there are a number of different companies marketing air-gravity conveyors under a variety of different trade names such as Airslide, Flo-tray, Gravitair, Fluidor, Whirl-Slide and Fluid-Slide (see Appendix A.IV.). Nevertheless, considering the advantages that they can offer over other forms of bulk solids transport, the use of these conveyors today is not as widespread as might have been expected. To some extent this may be the result of a lack of confidence on the part of the

MATERIAL HANDLED	AUTHOR(S) AND REFERENCE
Cement, fluidised and conveyed on woven canvas belting in a trough inclined at about 4^{o}.	Avery, W.M. (Ref. A12) Nordberg, B. (Ref. N3)
Hot metallic sulphide dust, fluidised on a porous medium of refractory aluminium oxide.	Anon. (Ref. A6)
Alumina powder in a large Canadian smelting plant, conveyed on porous tiles at a 2.2^{o} slope. (Conveying rate about 200 tonne/h in 500 mm wide channel).	Bushell, E.; Maskell, R.C. (Refs. B27,B28)
Alumina transported on various sizes of air-gravity conveyor in ship loading and unloading plant.	Leitzel, R.E.; Morrisey, W.M. (Ref. L1)
Rockdust handled in bulk to reduce costs in mining applications. ("Airslide" with 6^{o} slope.)	Alston, G.L. (Ref. A3)
General information; and reference to sodium tripolyphosphate and silica flour.	Anon., EEUA Handbook (Ref. E1)
Various bulk solids conveyed on "airslides" in self-unloading rail-road car.	Hudson, W.G. (Ref. H6)

Table 3.1. SOME SOURCES OF INFORMATION ON INDUSTRIAL APPLICATIONS OF AIR-ASSISTED GRAVITY CONVEYING.

design engineer, since air-gravity conveying is still something of an art. Certainly the manufacturers of such conveyors have experience of transporting an extensive range of materials, and it is almost entirely upon the knowledge gained from this practical experience, supported where necessary with data from small-scale laboratory tests, that the design of air-assisted gravity conveying systems is based.

3.1.3 The construction and application of air-assisted gravity conveyors - current industrial practice.

The fundamental construction of a practical air-gravity conveying installation is very simple and indeed this is one of its main advantages over other methods of bulk solids transport. Essentially the conveyor consists of just two channels with the porous membrane clamped between them (Fig. 3.5.). Where the channel is fairly wide and the porous medium is not rigid (for example, woven fabrics) some additional support for the membrane may be required. The lower channel serves as a plenum chamber to which air is supplied at one or more points depending upon the overall length of the conveying system. The types of membrane that can be employed are discussed fully in Section 3.2.5.

The presence of the covered top channel renders the conveyor virtually free from problems of dust leakage, but naturally it would also operate satisfactorily as an open channel. In this form the device has been widely employed as flow assistors mounted at the bottom of silos, bunkers, bulk railway wagons and lorries, and so on, enabling these containers to be made with a virtually flat base and thus having a substantially greater capacity (Fig. 3.6). A good discussion of this type of application is to be found in Ref. L1.

Where the conveyor is covered it is necessary for the top channel to be adequately vented through suitable filters. With short conveyors it may be sufficient to rely on the air escaping with the powder from the outlet end of the channel and then through the vent system of the discharge hopper, if one is in use. If the conveying system is long, or if there is a possibility of the channel outlet becoming choked with powder, it is better to vent from two or more points between the inlet and outlet.

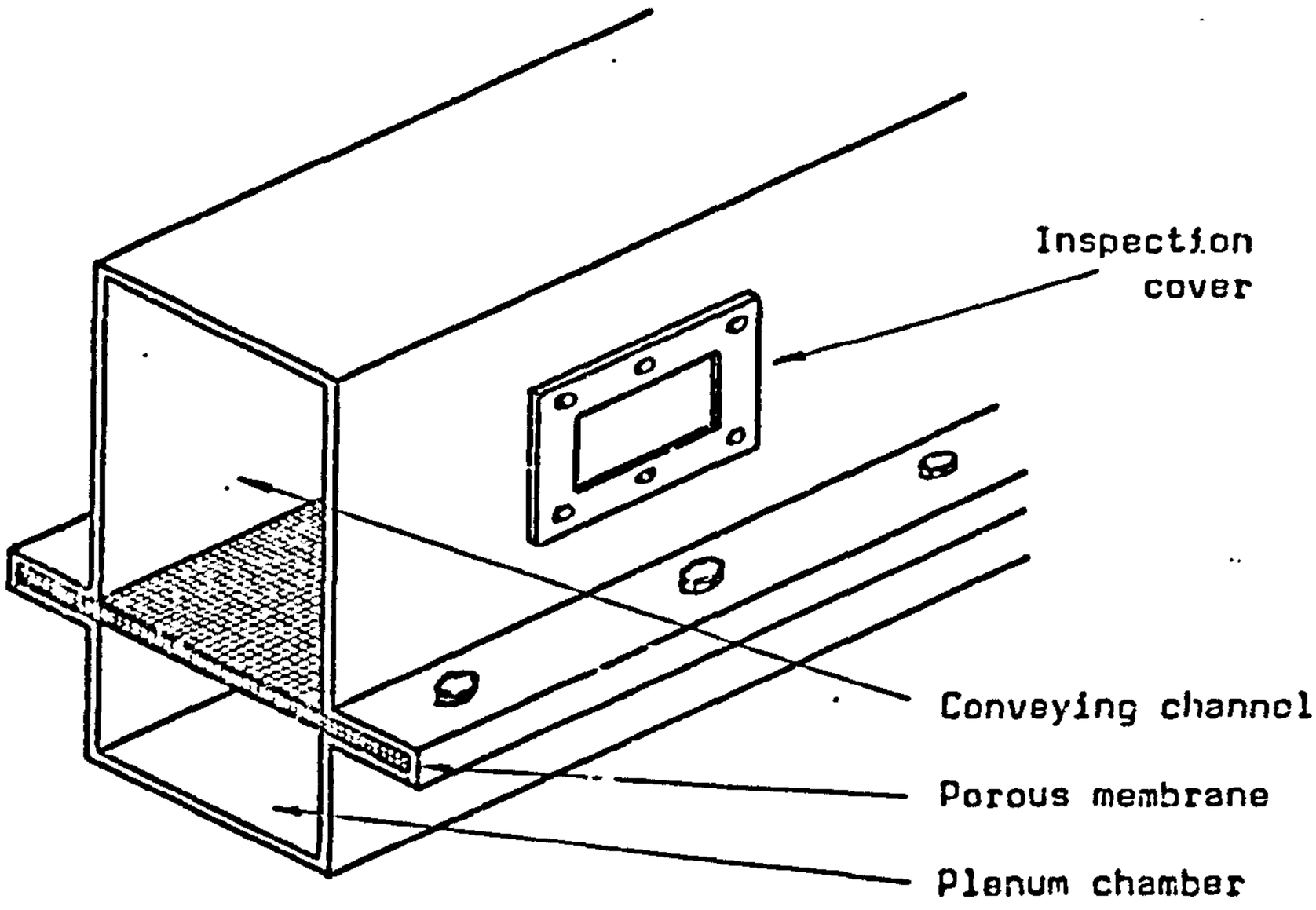

Fig. 3.5 THE BASIC CONSTRUCTION OF A PRACTICAL ENCLOSED AIR-ASSISTED GRAVITY CONVEYOR.

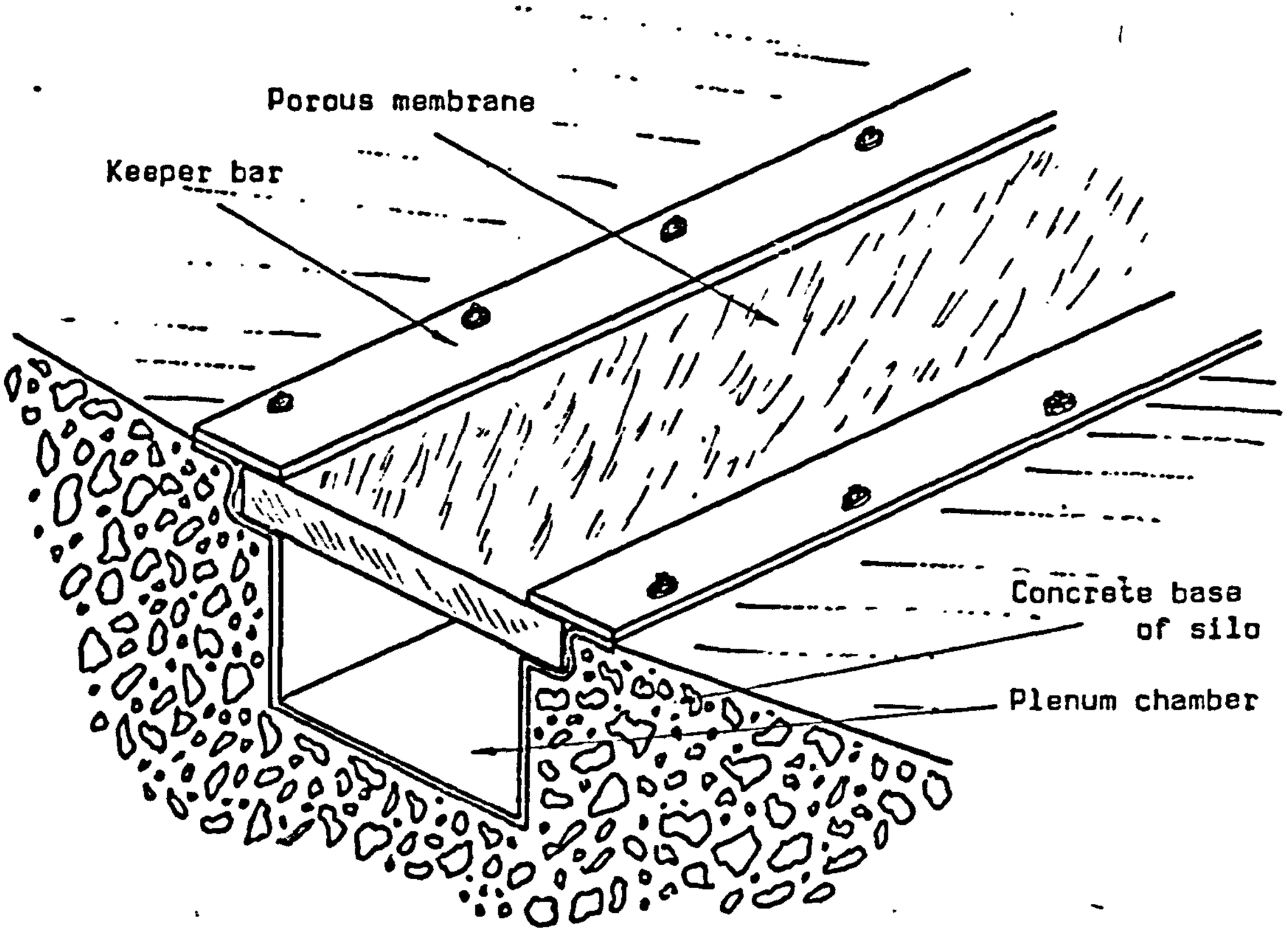

Fig. 3.6 A TYPICAL APPLICATION OF AN OPEN-TYPE AIR-GRAVITY CONVEYOR AS A FLOW ASSISTER IN THE BASE OF A SILO.

It is likely to prove useful to have inspection or access ports fitted at convenient positions along the duct, especially in the region of the inlet and outlet and in other positions where blockages may occur. Whilst it is possible to exercise some control over the flowrate of material in the conveying duct by the use of gates or baffles, it is likely to be more satisfactory to control the feed to the upstream end of the conveyor. Thus in the case of discharge from a hopper, for example, flow control can be achieved by the conventional use of a rotary valve, screw feeder or pinch valve. Where precise control of the solids flowrate is not required, flooded feed from the hopper to the conveying duct may be satisfactory. The system is then effectively self-regulating and with free-flowing powders there is little risk of the conveyor becoming choked provided that the slope of the channel and the flowrate of fluidising air are sufficient. The basic arrangement of a simple air-assisted gravity conveyor is illustrated in Fig. 3.7.

Most manufacturers of air-gravity conveying plant supply the equipment as standard components which bolt together to suit the user's particular requirement. In addition to the basic straight channel unit, components normally available include the following:-

Intake and discharge sections.
Bends (right-hand and left-hand).
Y-pieces to divide the flow from one channel into two or three streams (or to recombine streams into one).
Flow diverters, often used in conjunction with side discharge boxes, to allow the operative to divert the flow as required.
Flow control gates or baffles (for either manual or automatic operation).
Material traps for the collection and subsequent removal of heavy impurities in the flow.

Further information on these items can be obtained from Refs. A4, K9, L1, S16 or from manufacturers' sales literature (see Appendix A.IV).

As a postscript to these notes on the general construction of air-gravity conveying systems it should perhaps be remarked that they may need to

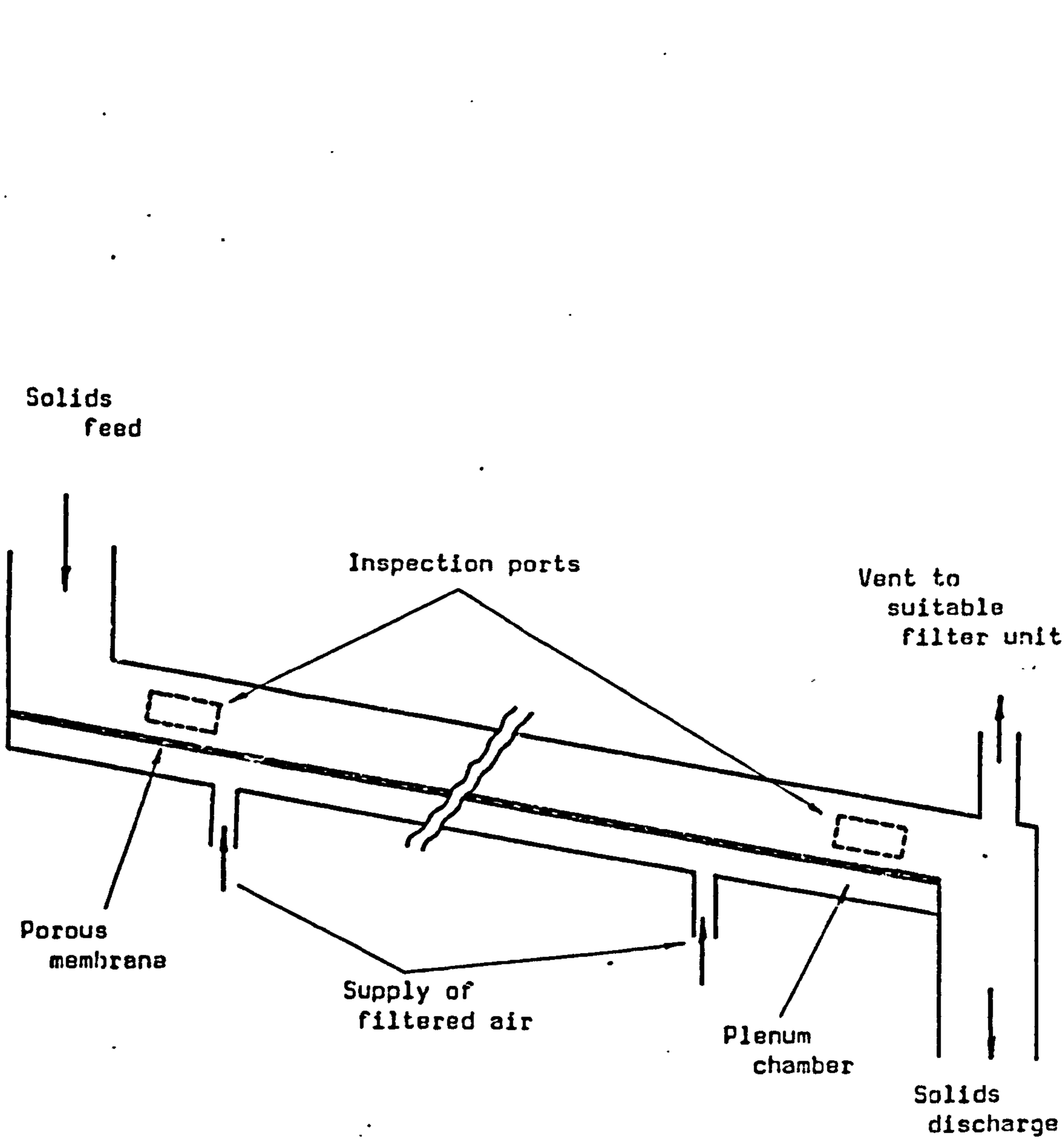

Fig. 3.7. THE GENERAL ARRANGEMENT OF A PRACTICAL AIR-ASSISTED GRAVITY CONVEYOR.

withstand a certain amount of ill-usage. It appears to be common practice for operatives to attempt to relieve suspected blockages with the aid of an iron bar or similar implement wielded against the outside of the channel or prodded through an inspection port, with the not uncommon result that the porous distributor is cracked (in the case of ceramic tiles) or punctured (woven fabrics).

Applications of the air-gravity conveyor are legion. Some examples have been mentioned briefly in the preceding section but the full range goes from the very small devices applicable to the drugs or cosmetics industries, to large conveyors up to a metre or so in width and 100 m or more in length. The list of materials that can be handled includes almost any particulate solid that is free-flowing or only slightly cohesive and the only real limitation on the installation is that there must be a small difference in elevation between the inlet and outlet ends of the conveying channel. (Even this restriction can sometimes be overcome with one of the specialised modifications described in Section 3.1.5).

A more detailed consideration of the advantages and disadvantages of air-gravity conveyors is undertaken in Section 3.1.6, and a full discussion of the design aspects, including a study of the types of bulk solids that can be handled and the problems that can arise is given in Sections 3.2.1 to 3.2.10.

3.1.4. Recent research

Published research into the flow of aerated powders in inclined channels is unfortunately rather scarce, and what data there is relates mainly to sand of around 200 μm mean particle size. A list of sources of experimental data is given in Table 3.2.

One of the main problems facing the prospective researcher into the performance of air-gravity conveyors is the size of the test rig required to be comparable to typical industrial installations. Even a small channel of 100 mm in width is capable of transporting fine sand at up to about 20 kg/s (72 tonnes/h) which requires a very substantial back-up

AUTHORS	CONVEYING CHANNEL		POROUS GAS DISTRIBUTOR	BULK SOLIDS CONVEYED			SLOPE OF CHANNEL	SOLIDS MASS FLOWRATE
	Breadth mm	Length m		MATERIAL	PARTICLE MEAN DIAM. μm	PARTICLE DENSITY kg/m³	degrees	kg/s
Mori, Y. et al. 1955 (Ref. M6)	50	0.85	canvas ("thick" & "thin")	sand	~200	2700	0 - 15	0 - 0.4
" "	"	"	" "	bauxite	95	3200	"	0 - 0.8
" "	"	"	" "	alumina	35	3900	"	0 - 0.1
Siemes, W.; Hellmer, L, 1962 (Ref. S13)	150	2	sintered metal plate	sand	200	2640	1 - 6	0.8 - 4
Keuneke, K. 1965 (Ref. K3)	50 - 100	6	ceramic plates	"Thomas phosphate"	64	3330	0.3 - 2.3	2.7 - 19.2
" "	" "	"	" "	cement	15	3000	0.9 - 3.2	1.4 - 7.4
" "	75 - 150	"	" "	gypsum	12	2500	3.4 - 4.0	1.0 - 5.0
" "	50 - 100	"	" "	potash	129	2000	0.6 - 2.8	1.4 - 10.9
" "	75 - 100	"	" "	"balancer meal"	80*	1427	2.6 - 4.0	1.1 - 4.2
Harris, W.F. 1965 (Ref. H2)	37 - 67	2.6	woven cotton fabric	sand	~180	2650+	1.6 - 10.6	0 - 3
Qassim, R.Y. 1970 (Ref. Q1)	84	0.18	porous plastic	sand	266	2640	0 - 10	0 - 0.6
Muskett, W.J. et al 1973 (Ref. M14)	75	2.4	sintered plastic ("Vyon D")	sand	150	2650+	0 - 8	0 - 1.5
McGuigan, S. J. 1974 (Ref. M4)	150	3	sintered plastic ("Vyon F")	sand	177	2700	0 - 9	0 - 7.3
Pugh, R.R. 1974 (Ref. P9)	100 - 150	3	sintered plastic ("Vyon F")	sand	200	2700	1 - 3	0 - 5
McGuigan, S.J., Pugh, R.R. 1978 (Ref.M6)	150	3	sintered plastic ("Vyon F")	sand	177	2700	0 - 9	0 - 7.3
Shinohara, K. et al 1974 (Ref. S8)	42	0.12	ceramic filter	glass beads	~210	2520	0 - 15	0.03 - 0.16
Singh, B. et al 1978 (Ref. S21)	150	9.15	"Pneudistributor" (circular pipe with orifices)	sand	~200	2630	0 - 3	1.4 - 28

* Mixture of coarse particles (groats and chaff) and very fine particles (meal)
\+ Approximate value (No value given in reference)

TABLE 3.2 SOURCES OF EXPERIMENTAL DATA RELATING TO THE FLOW OF SOLID-GAS SUSPENSIONS IN INCLINED CHANNELS

facility to provide either continuous circulation of solids or batch operation with a running period of reasonable duration. The majority of commercially available channels are 100 mm in width or wider and it is uncertain whether data from tests on narrower channels can reliably be extrapolated to predict the performance of conveyors on an industrial scale. The length of conveying channel that can be situated in an average laboratory also tends to be severely limited; in fact, as can be seen from Table 3.2, amongst the experimental programmes published, only that of Keuneke used a channel longer than 3 m. Whilst there may be some theoretical justification for the use of short channels (see for example Ref. M4), there does not appear to be any experimental evidence to confirm that uniform flow is so rapidly attained.

Additional problems are encountered when attempting to measure variables such as the depth of the flowing bed of suspended solids, the bulk density of the bed, the velocity of the bed and so on, with only partial success. In the case of "apparent viscosity" the problem is as much one of understanding and defining the property as of measuring it. However, these and other difficulties will be discussed more fully in subsequent Sections.

The most extensive programmes of work appear to have been those carried out by Keuneke (Ref. K3), Qassim (Ref. Q1), McGuigan (Refs. M4, M5, M6) and Pugh (Refs. P9, M6). That of Keuneke is especially interesting because of the number of different bulk solids investigated, which included cement, gypsum, potash and several typical agricultural products. He studied the fluidisation behaviour of these substances and then, using a 6 m long conveying channel, compared their flow characteristics at different channel slopes and fluidising air flowrates. A great deal of data is presented, mostly in graphical form, but unfortunately there is little mention of the depth of the flowing beds of material and consequently it is not possible to build up a comprehensive model which would allow the data to be correlated and extended.

Qassim (Ref. Q1), working at Imperial College, London, restricted his investigation to 266 μm sand flowing in a channel only 180 mm long. Despite the fact that in so short a channel fully developed flow

conditions are unlikely to be achieved, Qassim attempted to measure the depth of the flowing suspension at various solids mass flow rates and various channel slopes. However, he did not show graphs of bed depth against mass flowrate and when such graphs are plotted they seem to show some remarkable inconsistencies. Qassim chose to process his data to yield shear diagrams which largely mask these inconsistencies, and, as indicated by McCuigan (Ref. M4) the figures should be treated with some caution.

At the University of Aston a test rig based on a 3 m long channel was developed by McGuigan (Refs. M4, M5, M6) and Pugh (Refs. P9, M6). The programme of work undertaken by McGuigan concentrated on the "apparent viscosity" of the aerated sand that he used and attempted to find some correlation between values of this property as determined in the main flow channel and by a rotary viscometer in a small subsidiary fluidising rig. Both McGuigan and Pugh relied heavily on shear diagrams and friction factor/generalised Reynolds number correlations in the processing and display of their experimental data, and the outcome of the work is conveniently summarised in Ref. M6.

Consideration of research programmes involving the flow of aerated bulk solids would not be complete without a mention of the work of Botterill and various co-workers at the University of Birmingham (Refs. B16 - B22). Although this work was confined to flow in a horizontal channel in which a pressure gradient was maintained by a series of moving paddles, many of the reported results are obviously relevant to flow in inclined channels. A more detailed analysis of the published data from the work of Botterill, and from the various sources listed in Table 3.2, will be made as appropriate in later Sections of this report.

3.1.5 Novel variations for horizontal and upward conveying.

It has already been remarked that the one major limitation of the air-assisted gravity conveyor is that it requires a small decrease in elevation between the inlet and outlet ends of the flow channel. However, in view of the several positive features that this method of conveying has to offer it is not surprising that there have been a number of

attempts to devise modifications to the basic system that would permit material to be transported horizontally or on an upward slope.

One such modification has the air entering the channel through a series of louvres or angled slits in the base, and thus having a significant component of velocity in the horizontal direction (Fig. 3.8) (Refs. A7, F3, J1, K5, K6, M1). The velocity of the jet of air leaving these louvres may be quite high - up to around 30 m/s (Ref. F4) - and it is claimed that the conveyed material then "floats" on the resulting sheet of air. The size and spacing of the louvres would of course be selected to suit the material to be conveyed. This is the principle of the patented "Jetstream" conveyor which has been used successfully in a variety of applications handling granular and flaked materials. Naturally the quantity of air required tends to be much greater than when the product can flow under gravity, and the mass flowrate of product is lower. However, the disadvantage of the large volume of air required can be offset to some extent by combining the conveying with a degree of simultaneous processing using heated or cooled air (Ref. M1).

Shinohara and Tanaka (Refs. S7, S9) have described a device which has some affinity to the air-jet conveyors and which they called a "pneumatic escalator". In construction this device is similar to the conventional air-gravity conveyor except that plastic plates are fitted across the conveying channel to form a series of inclined cells (Fig. 3.9). Air passing through the porous membrane then lifts the particles up the inclined plates from one cell into the next. However, in common with the other forms of air-jet conveyor the quantity of air required tends to be large.

In an attempt to utilise the air-jet principle whilst reducing its relatively high power consumption, Stegmaier (Ref. S15) has proposed a system using a channel having a conventional porous base to fluidise the conveyed product, with the forward propulsion being provided by a series of separate forward-facing air-nozzles (Fig. 3.10). Other interesting variations on the air-jet principle (Refs. A8, E1, S15) are illustrated in Fig. 3.11.

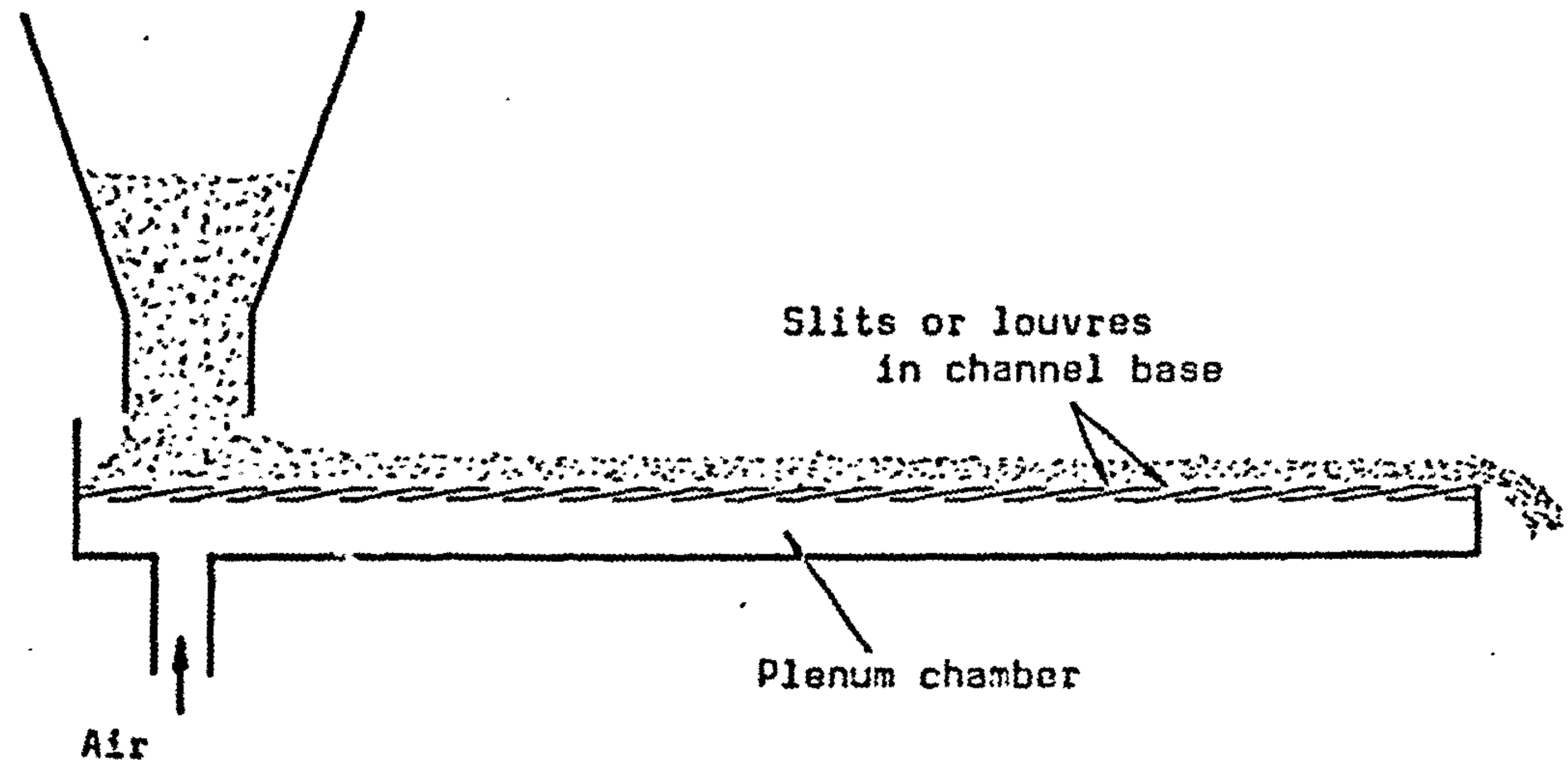

Fig. 3.8. LOUVRED-BASE CONVEYOR, DESIGNED TO PROVIDE THE CONVEYED MATERIAL WITH A FORWARD VELOCITY BY ANGLED AIR-JETS.

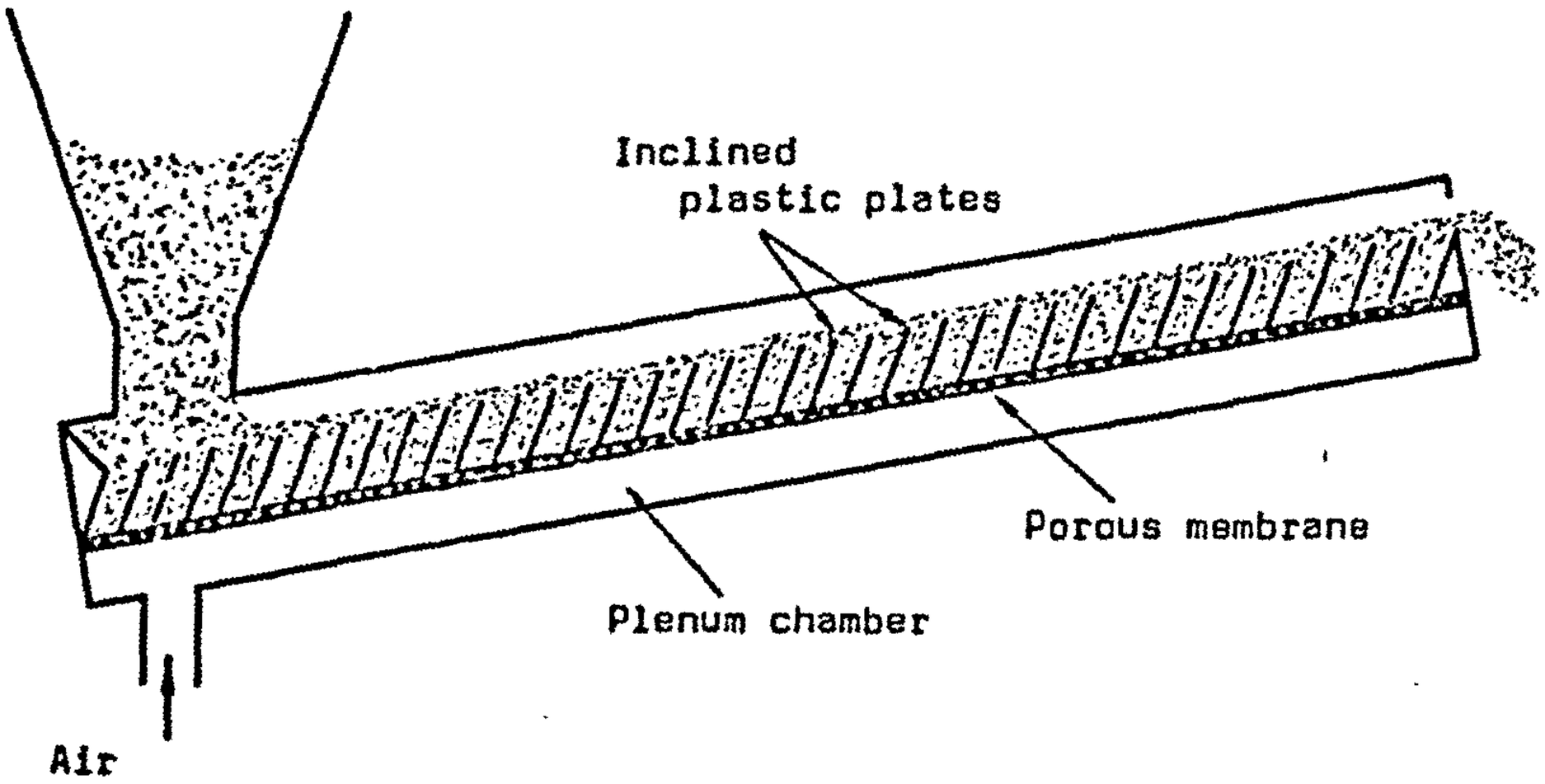

Fig. 3.9. THE "PNEUMATIC ESCALATOR" OF SHINOHARA AND TANAKA (Ref. S5)

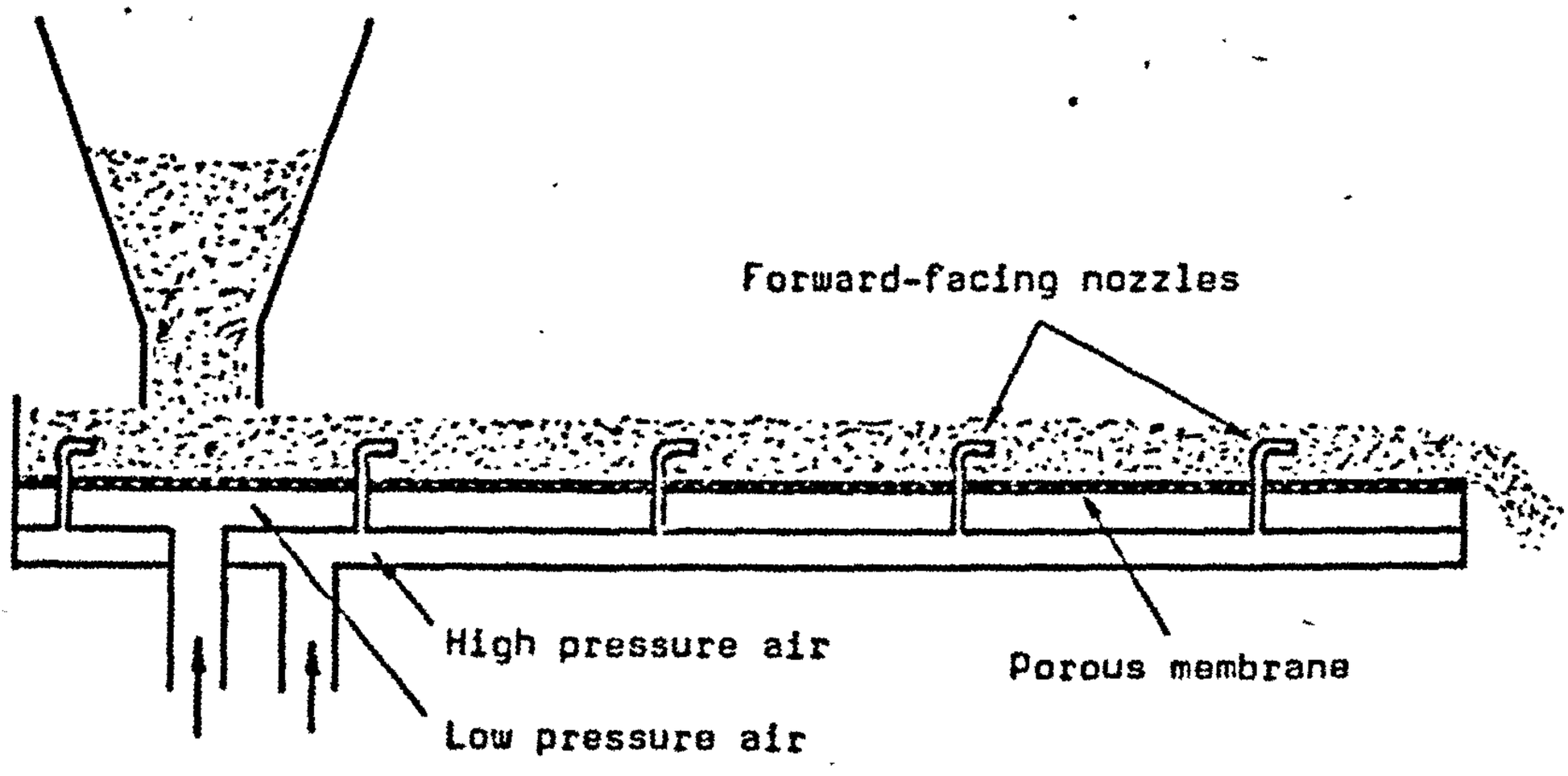

Fig. 3.10. ONE FORM OF STEGMAIER'S AIR-JET CONVEYOR (Ref. S15).

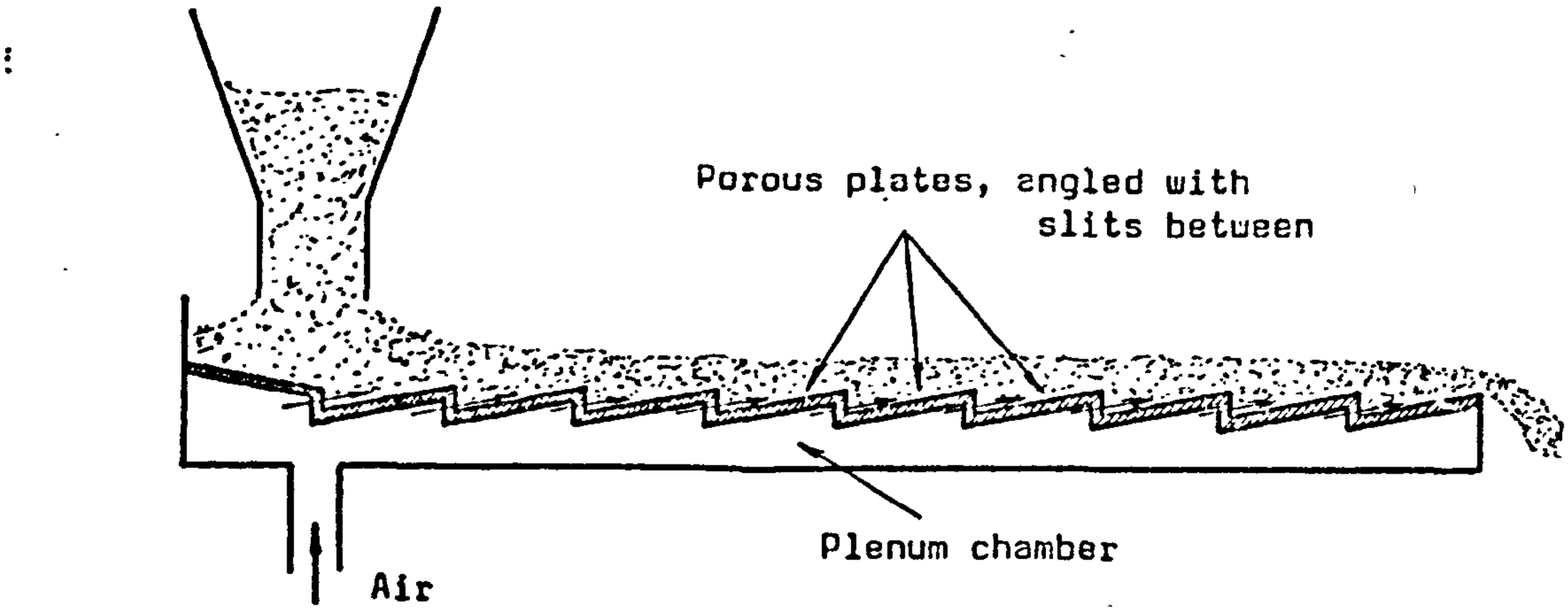

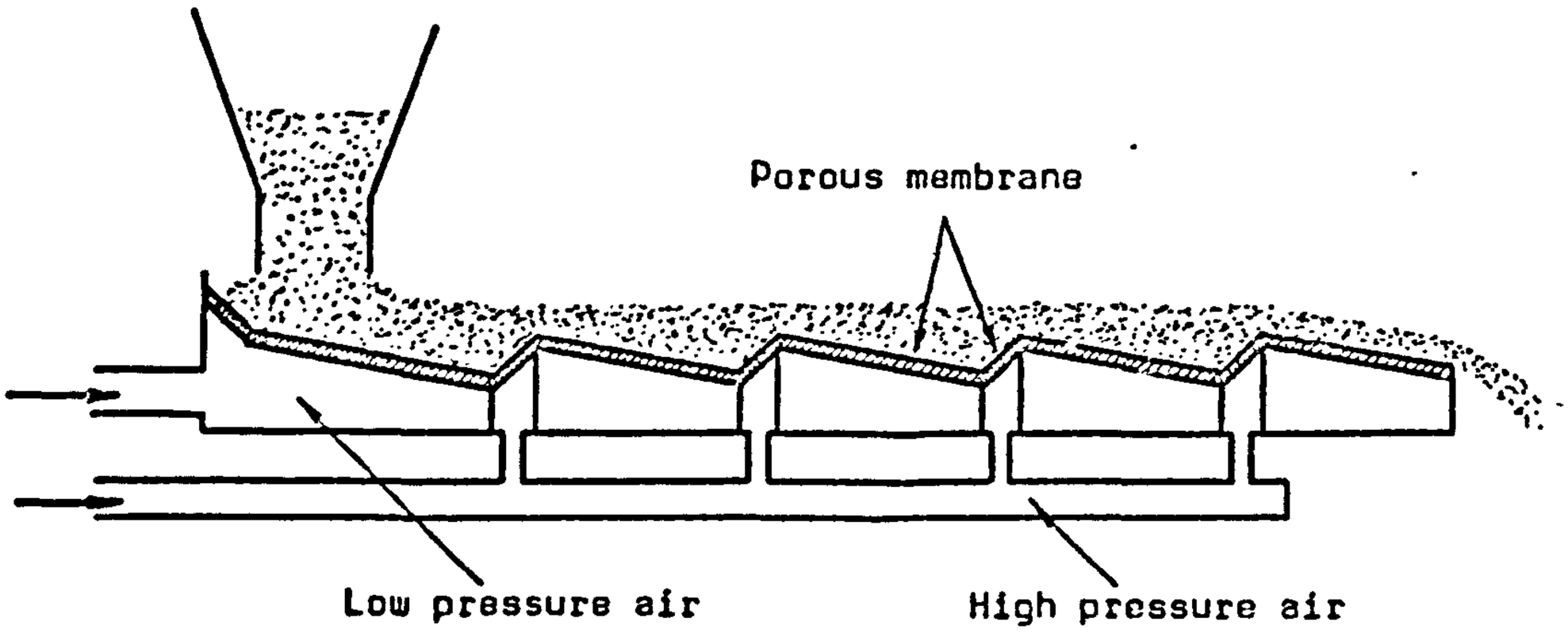

Fig. 3.11. TWO PATENTED VARIATIONS ON THE AIR-JET PRINCIPLE FOR CONVEYING HORIZONTALLY OR ON UPWARD SLOPES (Refs. A8, S15).

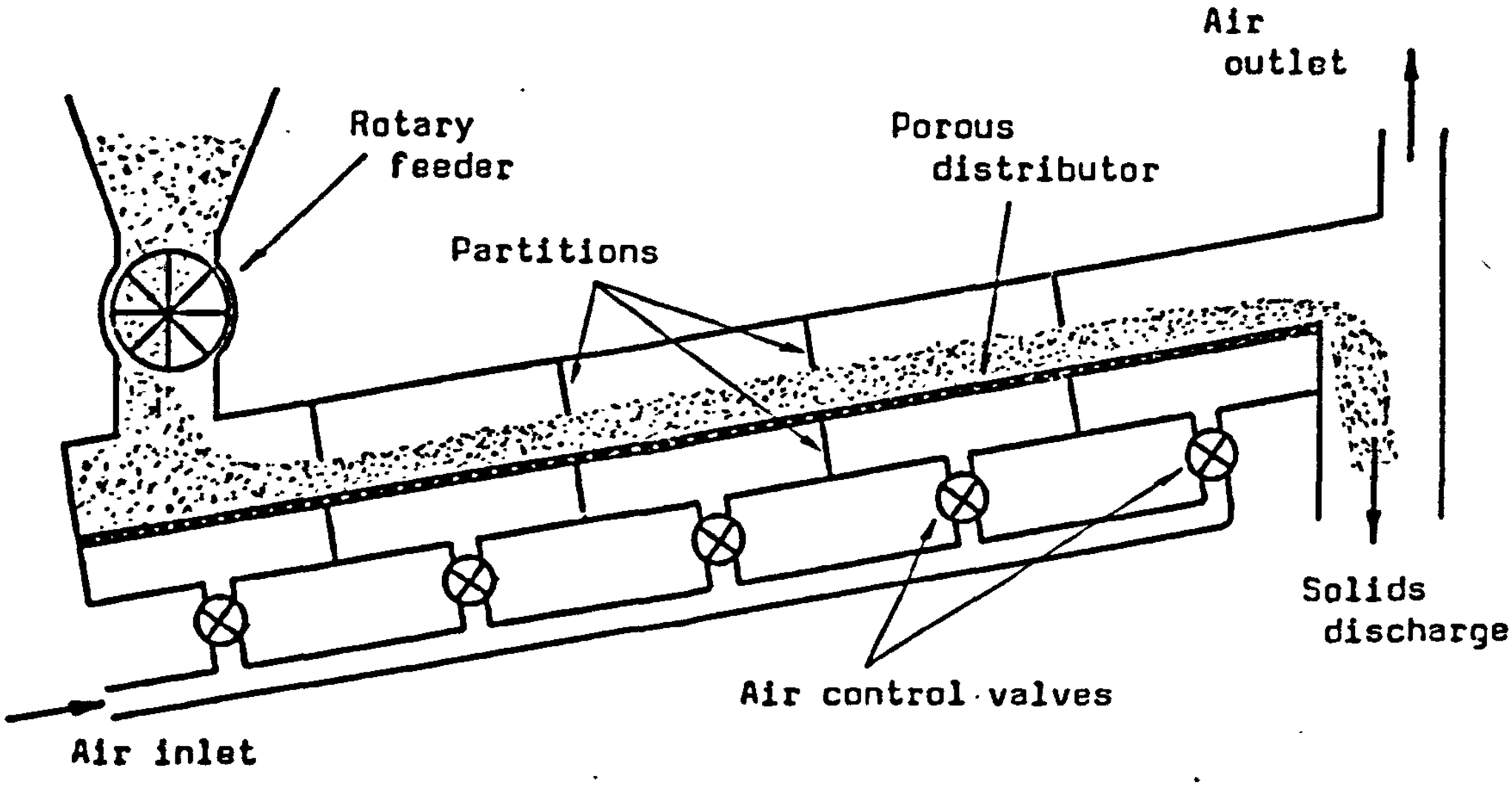

Fig. 3.12. CONVEYOR DESIGNED TO OPERATE ON AN UPWARD SLOPE BY MEANS OF AN INDUCED PRESSURE GRADIENT IN THE CONVEYED MATERIAL (Ref. I1)

A rather different approach to the problem of horizontal or upward conveying has been used by Islcr (Ref. I1) who developed a system in which a pressure gradient was set up in the conveyed material by dividing both the plenum chamber and the solids flow channel into separate compartments supplied with air at different flow rates (Fig. 3.12). Isler's test channel was 6 m long and 250 mm wide and conveyed cement at a rate of 20 tonne/h (although this was claimed to be well below the capacity of the channel). The maximum upward slope at which the channel was operated was about 12^{o}, when the "specific air consumption" was stated to be 70 m^3/h per m^2 (corresponding to an average superficial velocity of about 20 mm/s) at a pressure varying from 200 to 1200 mm H_2O. As pointed out by Stegmaier (Ref. S15) the pressurised conveying channel creates problems. Firstly, some form of air-lock feeder, such as a rotary valve, is required, and then the air control valves to the plenum compartments have to be carefully adjusted - and re-adjusted if the solids mass flowrate is altered. Also, because of the continual reduction of pressure and consequent expansion of the air the distance over which a practical conveyor would operate must be limited.

Summarising, these novel forms of conveyor would tend to have both a higher running cost and (with the exception perhaps of the "Jetstream" type) a higher capital cost than air-assisted gravity conveyors. However, in situations where a downward slope of the conveying channel is unacceptable, and where the distance to be conveyed is not great, these methods should be considered as possibly providing the best alternative.

3.1.6 Comparisons between air-assisted gravity conveyors and other methods of bulk solids transport

A number of authors (Refs. H6, H7, K9, S16, V1) have presented discussions of the main features of the various types of conveying system used for the transport of bulk particulate solids. Clearly the air-assisted gravity conveyor has established its place amongst recognised methods of conveying and in some situations it is an automatic choice as the "correct" method. The advantages and disadvantages of air-gravity conveyors are summarised below, with the question of power consumption

discussed in some detail as this is perhaps the most important single factor in their favour.

Conventional pneumatic conveying by pipeline has a number of advantageous features, including cleanliness and hygiene (of importance in the food industry), ease of installation, safe handling of explosive or toxic substances and low maintenance cost. However, it has the major disadvantage of large usage of air at relatively high pressure, and therefore a high power consumption. Among others, Masterson (Ref. M2) has pointed out that conveying by pipeline in dense-phase rather than dilute-phase can moderate this disadvantage since, although the air is still required at high pressure, the velocity is much lower. Further advantages of dense-phase conveying are reduced abrasion of pipes, elbows and valves, and less product degradation, but disadvantages mentioned by Masterson are that conveying is batchwise and that the headroom required is considerable.

The air-assisted gravity conveyor shares many of the advantages that the more conventional pneumatic conveyors have over mechanical systems; it is simple in concept, has no moving parts (except for the blower), it is virtually dustless, and it is of easy installation, operation and maintenance. It has to be admitted that the air-gravity conveyor is slightly less flexible in installation than the pneumatic pipeline, mainly through the requirement of a continuous downward slope, and may be rather more expensive in terms of capital cost. Also the range of materials that can be successfully conveyed is slightly more restricted. However, within these limitations the air-gravity conveyor has significant features that include little if any wear of the duct surfaces or degradation of the conveyed material, the possibility of the combination of transport with other functions such as drying or cooling of the conveyed material, and, most important of all, very low power consumption.

It is not easy to compare directly the performance of various types of pneumatic and mechanical conveyor since so much depends upon the type of material being conveyed, the distance, changes of elevation required during conveying, and so on. However, a few examples taken from the

published literature should serve to illustrate the kind of savings that can be made by using air-assisted gravity conveyors in situations where other conditions are appropriate.

The application of air-assisted gravity conveying to the handling of cement is discussed elsewhere (Section 3.3.2) but one of the examples quoted by Avery (Ref. A12) and by Nordberg (Ref. N3) relates to sixteen 400 mm diameter screw conveyors taking a total of 150 kW, which were replaced by eight air-gravity conveyors each using a 1.5 kW fan.

Descamps and Jodlowski (Ref. D4) give data on power consumption for the transport of cement in air-gravity conveyors operating with a plenum pressure of 510 mm H_2O, and their data are presented here as a plot of power consumption against solids mass flowrate (Fig. 3.13.).

Schauki (Ref. S2) also published a chart giving an indication of the power consumption of air-gravity conveyors operating with 500 mm H_2O plenum pressure. This chart, reproduced as Fig. 3.14, shows the approximate size of blower motor required for different lengths and solids volume flows, although naturally this could also depend upon the length and configuration of the airline to the plenum chamber.

Some comparison between the different types of pneumatic conveyor can be made from examples of specific power consumption quoted by Schauki (Ref. S2) for transport over a distance of 100 m. These examples are set out in Table 3.3.

CONVEYING METHOD	POWER CONSUMPTION FOR 100 m TRANSPORT DISTANCE (kW per kg/s)
Dilute-phase in pneumatic pipeline	5.6 to 11.2
Dense-phase in pneumatic pipeline	approx. 0.9
Air-assisted gravity conveyor	0.14 to 0.27

Table 3.3 POWER CONSUMPTION OF PNEUMATIC CONVEYORS (Ref. S2.)

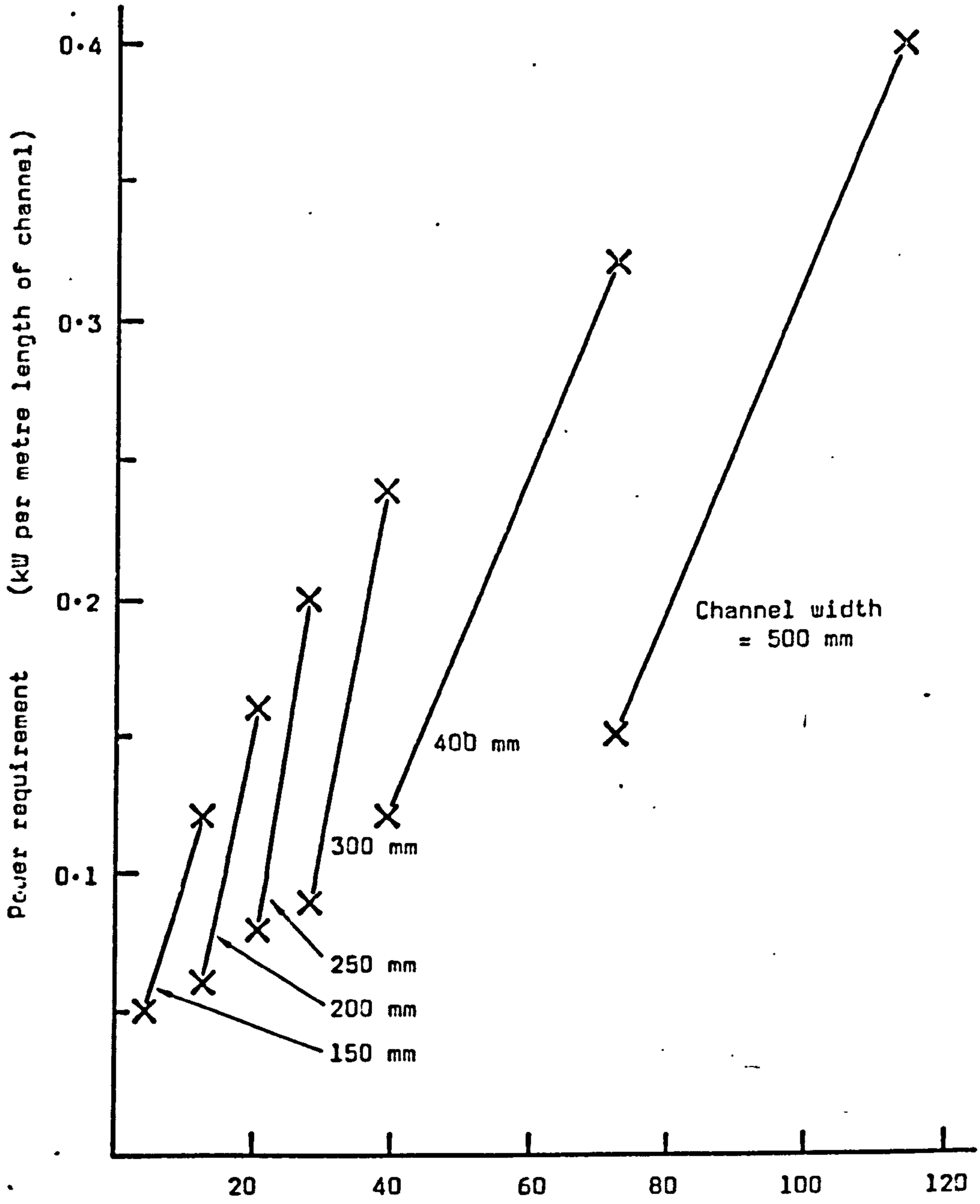

Fig. 3.13. VARIATION OF POWER CONSUMPTION WITH SOLIDS MASS FLOW-RATE FOR CEMENT TRANSPORTED IN AIR-GRAVITY CONVEYORS OF VARIOUS WIDTHS. (From data in Ref. D4).

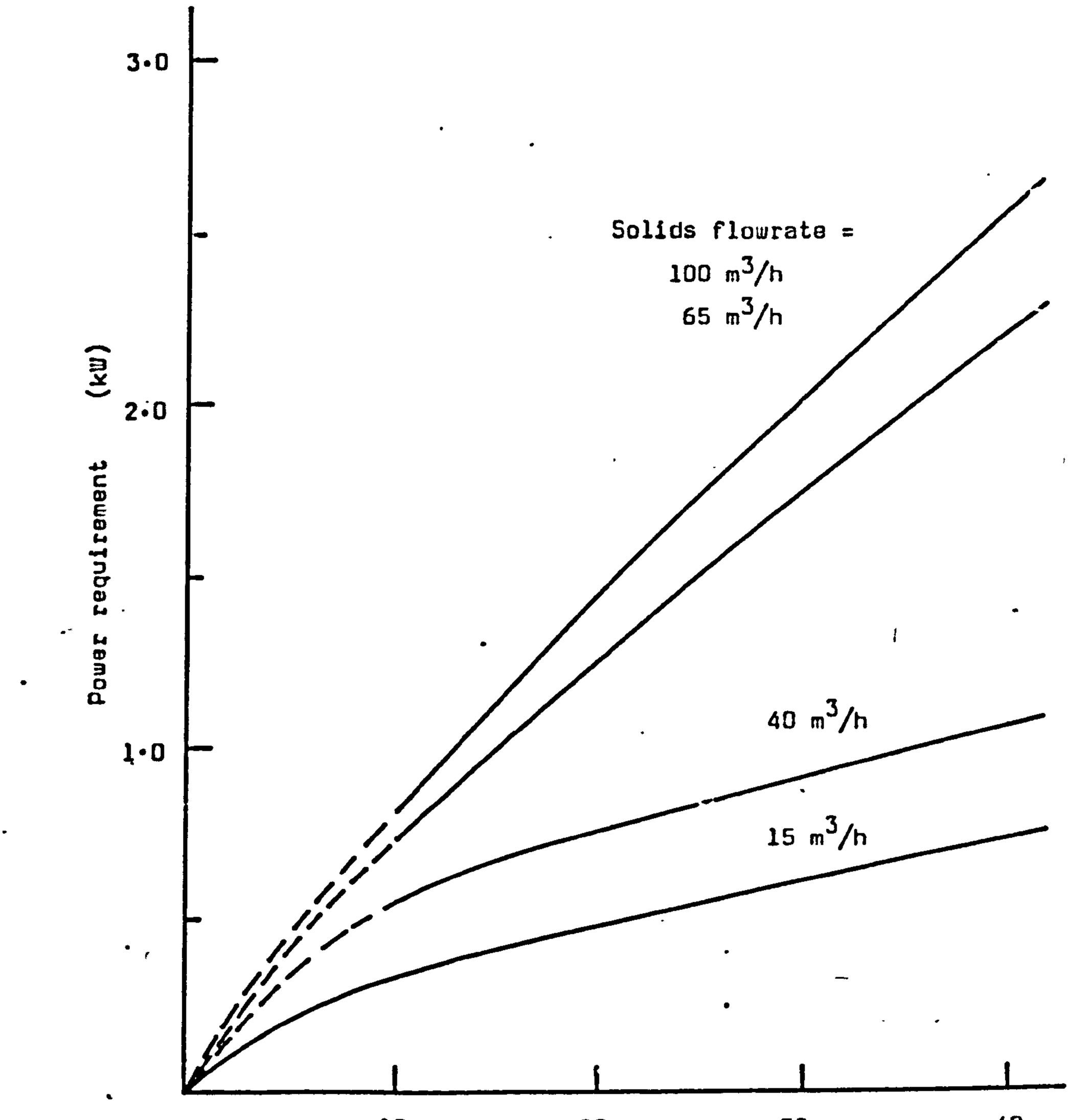

Fig. 3.14. RELATIONSHIP BETWEEN POWER CONSUMPTION AND TRANSPORT DISTANCE FOR UNSPECIFIED MATERIAL IN AN AIR-GRAVITY CONVEYOR (Ref. S2).

One example of the power savings that can be made by using air-gravity conveyors instead of screw conveyors has already been mentioned, and further evidence is provided by Mumby (Ref. M13) who published a plot of power consumption against handling distance for both types of conveyor handling cement at 40 tonne/h (about 11 kg/s). According to Mumby the ratio of power required for an air-gravity conveyor to that for a screw conveyor is about 1:8 for cement and about 1:5 for sand.

In terms of power consumption, probably the only serious rival to the air-assisted gravity conveyor is the belt-conveyor, which of course has the advantage that it can operate on upward gradients. However, the capital cost of the belt with idlers, supporting structure and housing is likely to be well in excess of that of the air-gravity channel.

Generally then, the air-assisted gravity conveyor provides a convenient, reliable and economical method of transporting particulate bulk solids, provided that a slight downward slope of the channel can be maintained. However, in order to make the most efficient use of these conveyors it is essential to have some understanding of the mechanism of the solids flow in the channel and of the factors influencing this flow, and some consideration will now be given to these.

3.2 FACTORS INFLUENCING THE FLOW BEHAVIOUR OF AERATED BULK SOLIDS IN INCLINED CHANNELS

3.2.1 Introduction

In Section 3.1.1 it was explained how the liquid-like behaviour of fluidised particulate bulk solids could be used to advantage in air-assisted gravity conveyors. It is in fact quite simple to construct a conveying channel which will work adequately with most free-flowing powders, but if a channel is to be properly designed to make the best use of available height and to provide trouble-free operation with maximum economy, it is essential to have a good understanding of the flow behaviour of aerated bulk solids.

A first step is to recognise the principal variables involved. Now for a given powder the mass flowrate in an inclined channel will depend

upon the width and inclination of the channel, the superficial velocity of the fluidising air and the depth of the powder bed in the channel. Of course there are other variables that should be recognised and there may be a complicated inter-relationship amongst them. Thus, for example, the superficial air velocity will affect the "viscosity" of the flowing powder, the shear stress between the flowing powder and the internal surfaces of the channel, and the bulk density of the powder. Also, the velocity of the flowing powder would be related to the bulk density and depth of the powder bed, but would be mainly influenced by the channel slope. Finally, it has to be appreciated that all these relationships are likely to be altered if there is any change in the nature of the conveyed powder, such as might occur as a result of attrition of the particles, electrostatic charging or variation in moisture content.

A good experimental approach should set out initially to obtain some insight to the relationships amongst the five basic parameters: solids mass flowrate, bed depth, width and slope of the channel and superficial air velocity. Investigation of these relationships for a number of different materials and correlation of the data should enable consistent behaviour patterns to be seen and physical models to be developed. However, a thorough survey of the relevant literature has yielded very little direct information on the flow of aerated solids in inclined channels. Whilst a considerable amount of data has been presented, mostly in graphical form, by various authors, this generally involves relationships between compound parameters such as modified Reynolds numbers and friction factors, and it is rarely easy to work back to the raw figures. Nevertheless, all the available data has been carefully sifted and compared, and insofar as it is relevant to the present work it is presented and analysed in this Section and in Section 3.3.

It is the intention to discuss in this Section in general terms the factors influencing the flow behaviour of aerated solids in inclined channels. Observations of the various research workers who have investigated the subject will be summarised where they help to throw light on the mechanism of the flow, although a more detailed analysis of their

results as these apply to various types of conveyed material will be deferred until Section 3.3. A full discussion of the relevance to flowing aerated powders of data obtained from studies of stationary fluidised beds will likewise be deferred until Section 3.4.

3.2.2 The material to be conveyed

Almost any bulk particulate solid having good fluidising characteristics will, when suitably aerated, flow easily down an inclined surface, and can therefore be transported satisfactorily in an air-assisted gravity conveyor. Many sources (Refs. E1, K9, L1, S16) state or imply that being easily fluidisable is an essential requirement for conveying in this manner, but it is in fact likely that many materials having slightly cohesive properties could also be conveyed. Leitzel and Morrisey (Ref. L1) set an approximate limit on the material to be conveyed by suggesting that its specification should lie within the range covered by:-

Particle size distribution	100% minus 850 μm
	10 to 15% minuse 75 μm
Free moisture content	less than 1%
Bulk density	80 to 3000 kg/m^3

Very cohesive (damp or "sticky") materials and powders of extremely fine particle size which "smear" over the channel surfaces and "blind" the porous membrane are, of course, generally unsuitable for air-gravity conveying (Ref. B29).

Clearly the "nature" of the conveyed material will have a profound effect on its flow behaviour in an inclined channel, particularly with regard to the minimum slope at which it could be transported and the quantity of air required to maintain its flow. The term "nature" is not easy to define in terms of measurable properties although it would be concerned with the ability of the material to become fluidised, as mentioned previously, and also with the cohesiveness or resistance of the material to shear. This consideration coupled with the observation of certain similarities between flowing fluidised solids and flowing liquids, has resulted in the use of the term "viscosity" or "apparent viscosity" for

fluidised solids. Further discussion of this concept is to be found in Section 2.8 (for fluidised beds) and in Section 3.2.10 (for flowing aerated bulk solids).

The work of Geldart in classifying bulk solids according to their fluidisation behaviour has been discussed previously (Section 2.4), and the chart illustrating the ranges of Groups A, B, C and D, reproduced as Fig. 2.6, provides a useful guide to the suitability of powders and granular materials for air-assisted gravity conveying. In general, materials in Group B, which includes most powders in the mean particle size and density ranges 40 to 500 μm and 1400 to 4000 kg/m^3, are the easiest to convey and will flow well at very shallow channel slopes. When the supply of fluidising air is shut off the bed collapses rapidly and flow stops, so that there are unlikely to be any problems with air retention. Materials of larger particle size and/or high density (Group D) can usually be conveyed in the same manner but the quantity of fluidising air required tends to become rather large and other forms of transport, such as belt conveying, might prove to be more suitable. Group A generally includes powders of small particle size and/or low density which should flow well in an air-assisted gravity conveyor; however, as a result of air retention, the material may have a tendency to continue flowing for a time after the fluidising air supply has been shut off. Finally, Group C includes cohesive powders that are difficult to fluidise satisfactorily because of high interparticle forces resulting from very small particle size, electrostatic effects or high moisture content. The dividing line between Groups C and A is very indistinct and the only way of properly assessing the suitability of doubtful materials for air-assisted gravity conveying is by practical experiment in a small-scale test rig. As previously mentioned, it may be found that apparently unsuitable materials will, by a combination of "flowing" and "sliding", move continuously along an inclined channel, provided that the slope and air supply are sufficient.

At the present time it is still necessary to rely heavily on experience when making an assessment of whether a given material is suitable for air-assisted gravity conveying, although Geldart's chart should help, and laboratory tests should provide confirmation in cases of doubt. A great

many different kinds of powders and granular materials have been and are being transported successfully by air-gravity conveyor, but the practical information obtained tends to be jealously guarded by the conveying equipment manufacturers. Some general information, culled from the published literature, on the handling characteristics of various materials, is given in Section 3.3.

3.2.3 The width of the channel

The main parameter governing the capacity of an air-gravity conveyor is the channel width. In the literature published by manufacturers of these conveyors, and in other sources giving basic design data (Refs. E1, L1, S16), quantities described as "typical capacities" are given as a function only of the channel width with little, if any, indication of how such figures would be modified for different types of conveyed material, and for different channel slopes and fluidising air flowrates. This is not as unreasonable as it first appears in view of the fact that, provided the slope and air flowrate exceed the required "minimum values" for the particular material being conveyed, they will have little influence on the solids flowrate.

It is of interest to plot, from the various sources available, the solids flowrate against the channel width (Fig. 3.15a). From the same data plotted to logarithmic scales (Fig. 3.15b) it appears that most authorities regard the volume flowrate as approximately proportional to the square of the channel width, for widths up to about 300 mm. However, at greater channel widths the index apparently increases from two to around three or even higher. The reason for this is not clear, unless it is being assumed that a wider channel should operate at a higher aspect ratio than a narrow one. There appears to be little justification for this, or for the alternative explanation of an increase in solids velocity.

Several authors (Refs. C3, D4, G9) supporting the use of an expression of the form

$$\dot{m}_s \propto b^x h^y \qquad \text{.....3.2.1}$$

appear to be suggesting that the influence of the channel width depends

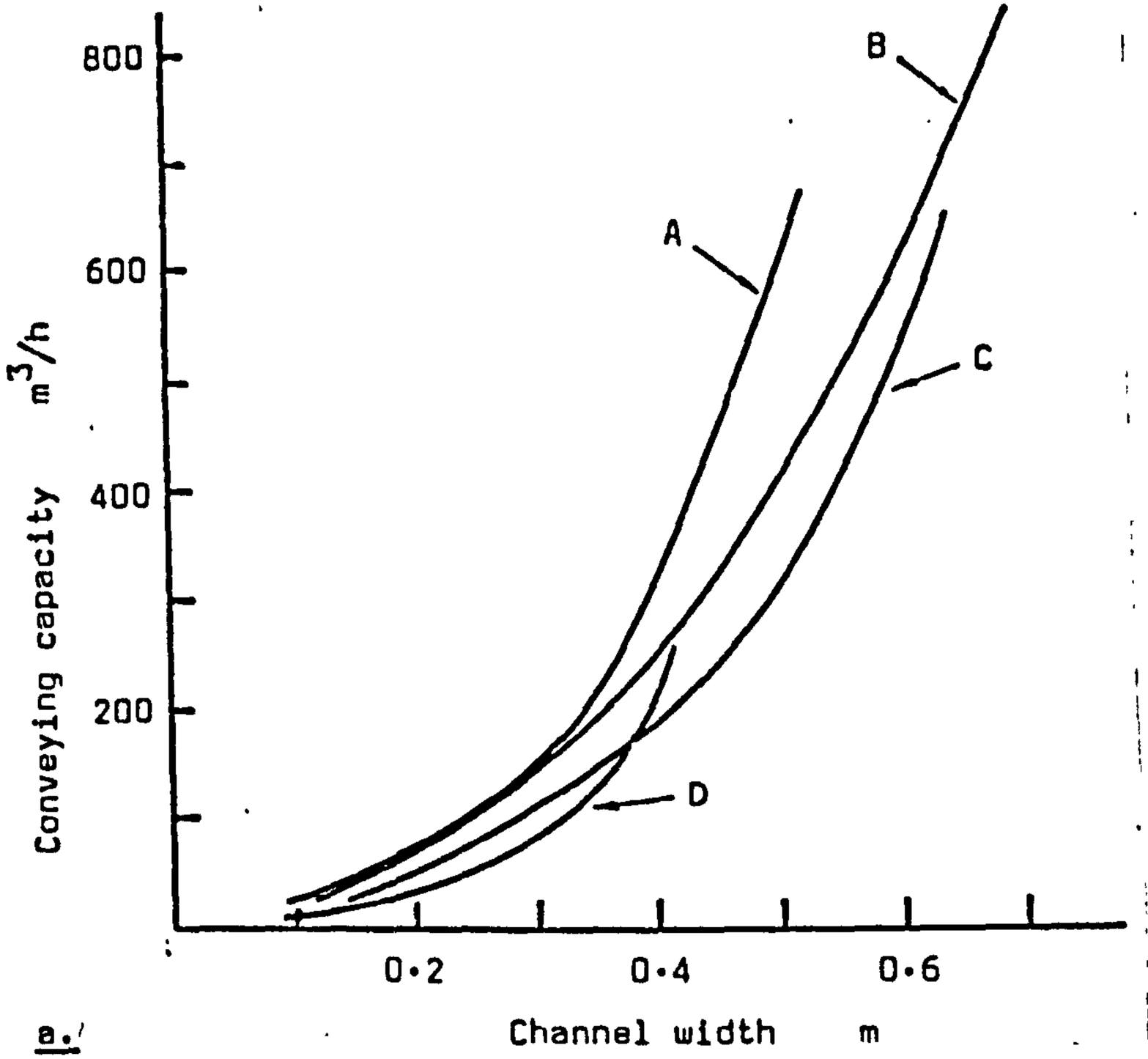

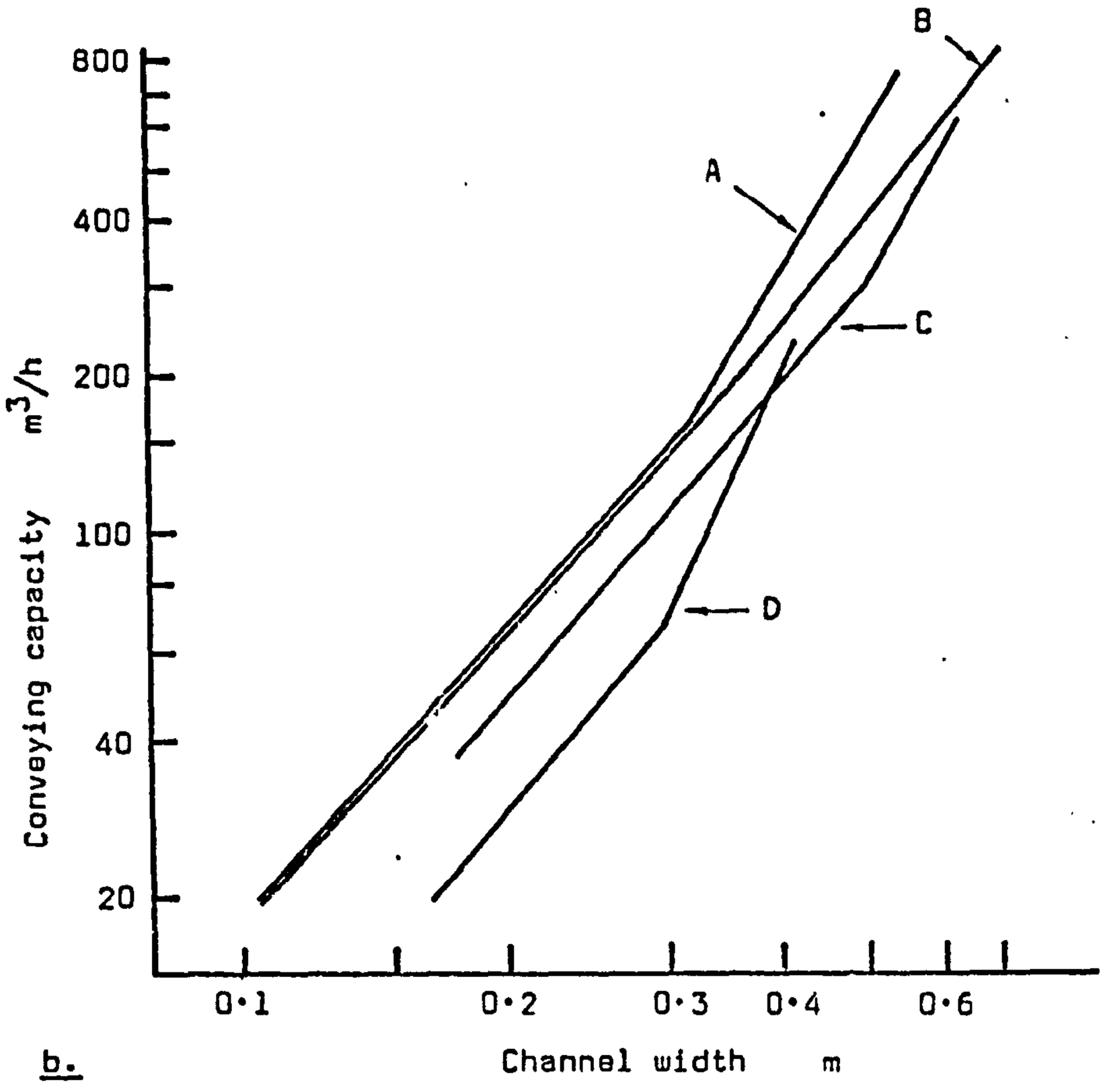

Fig. 3.15. RELATIONSHIP BETWEEN THE CONVEYING CAPACITY OF AN AIR-ASSISTED GRAVITY CONVEYOR AND THE WIDTH OF THE CHANNEL: a) to a linear scale, and b) to a logarithmic scale. Lines A, B, and C are plotted from representative sales literature of various manufacturers, and D is plotted from data in Ref. E1.

upon the aspect ratio at which the channel operates. Thus, according to Chandelle (Ref. C3) for $h/b \ll 0.5$, $\dot{m}_s \propto bh^2$; for $h/b \simeq 0.5$, $\dot{m}_s \propto b^2h^2$ and for $h/b > 0.5$, $\dot{m}_s \propto b^3h$. The discussion of Harris (Ref. H2) seems to imply that for the wider channels, the capacity should be more nearly proportional to the width. However, although Harris was one of the few researchers to have worked with channels of different widths, his range was unfortunately restricted to a maximum width of only 67 mm.

A useful preliminary estimate of the width of channel required for a given application may be made by regarding as constant the average velocity and the bulk density of the flowing suspension (both are functions of the channel slope and fluidisng air velocity). The ranges of values of these parameters will be discussed more fully later, but as a guide the average solids velocity would normally be between 1 and 4 m/s and the bulk density of the suspension between 10 and 50% less than that of the material when unfluidised. Furthermore, the optimum operating aspect ratio is around 0.5 (Ref. C3) since this corresponds to the maximum value of the hydraulic mean depth for a given cross-sectional area. However, many industrial conveyors are operated at a figure well below this. Clearly at constant aspect ratio, channel slope and fluidising air velocity, the conveying capacity of the channel would be proportional approximately to the square of the channel width.

Thus the width of conveyor required to handle a mass flowrate $\dot{m}_s$ of a material having bulk density ρ_b is given approximately by

$$b = \left(\frac{r_e \dot{m}_s}{r_a \rho_b u_s}\right)^{\frac{1}{2}} \qquad \text{.....3.2.2}$$

where r_a is the operating aspect ratio, r_e is the expansion ratio of the conveyed material (that is, the ratio of the bulk density of the unfluidised material to that of the suspension) and u_s is the average solids velocity along the channel. For many particulate bulk solid materials capable of being transported in air-assisted gravity conveyors a first estimate of the width of conveyor required can be obtained by simplifying equation 3.2.2. to a convenient "rule-of-thumb" as

$$b \simeq 1.6\left(\frac{\dot{m}_s}{\rho_p}\right)^{\frac{1}{2}} \qquad \text{.....3.2.3}$$

where $\dot{m}_s$ is the solids mass flowrate in kg/s, ρ_p is the true density of a particle in kg/m^3, giving the width b in metres.

3.2.4 The channel base (porous distributor)

In order to provide continuous aeration of a bulk particulate solid in an inclined channel, the channel must be fitted with a porous base extending to its full width and length, as described in Section 3.1.3. The requirements of this porous base are essentially those of the gas distributor in conventional fluidisation vessels, as listed in Section 2.6, to which may be added three further features:-

5. It should offer minimum resistance to the flow of an aerated powder over its surface.
6. It should offer minimum resistance to the flow of air through it, consistent with the need to promote uniform and stable fluidisation and to prevent flowback of bed material.
7. It should be reasonably resistant to impact damage.

The very low pressure-drop distributors (such as bubble-caps and pipe grids) that may be used in conventional fluidisation applications are generally not suitable for air-gravity conveyors because of the need for a smooth surface over which the conveyed material may slide. Flat plates with relatively large holes are also unsuitable because of possible flowback of the conveyed material. It has therefore become customary to use porous distributors, usually manufactured from one of the types of material listed in Table 2.2. Manufacturers can generally provide these porous media with permeability to suit the user's requirements, normally within the range 0.02 m^3/s per m^2 to 0.24 m^3/s per m^2 at 200 mm H_2O pressure difference. (This corresponds to a range of resistance to air flow from about 700 mm H_2O to 50 mm H_2O at an air flowrate of 0.07 m^3/s per m^2.) There may be some advantage in making up composite plates in order to combine the features of, for example,

sintered plastic and perforated steel sheet (Refs. S5, S6).

The most obvious influence of the porous distributor is on the quality of fluidisation of the conveyed material in the channel. The way in which the quality of fluidisation is related to the pressure drop across the distributor has been discussed in Section 2.6, and most of the information presented in that Section is relevant here. However, it is known that the fact that the bed is flowing has a significant modifying effect on the fluidisation behaviour, particularly in suppressing bubble development in the bed (Ref. B15, p 118). Presumably the formation of channels in the bed is also inhibited by the flow, and this would help to explain why many powders that do not fluidise well can still be transported by air-gravity conveyor.

Unfortunately there is very little published information on the flow of aerated solids on different types of distributor that would enable useful comparisons to be made. When designing an air-gravity conveyor the aim is to keep the power consumption to a minimum, and therefore the distributor should offer the lowest possible resistance to air flow. Naturally the resistance has to be sufficient to provide a uniform distribution of air into the conveyed material, not only to maintain the flow of the material but also to ensure that flow will restart after a shutdown. This requires that a sufficient pressure-drop exists across the distributor to guarantee that, even when a large part of it is uncovered, the minimum fluidising velocity will still be reached in the powder remaining on the distributor (Fig. 3.16). In the absence of other information, it would seem reasonable to select the distributor on the basis of pressure-drop data for stationary beds (see Fig. 2.8). Since the flow of the bed tends to suppress the formation of bubbles and channels it is probable that a distributor having a rather lower pressure drop than that required for "stationary" fluidisation would operate quite satisfactorily, provided that the distributor was completely covered by the flowing powder. However, with such a low pressure drop, it may prove difficult to re-start the powder flow after a shutdown and in order to avoid problems it may be advisable to select a distributor having a slightly higher pressure drop than might otherwise seem necessary. Some sources (Refs. E1, L1) state that the pressure drop through the porous membrane should be greater

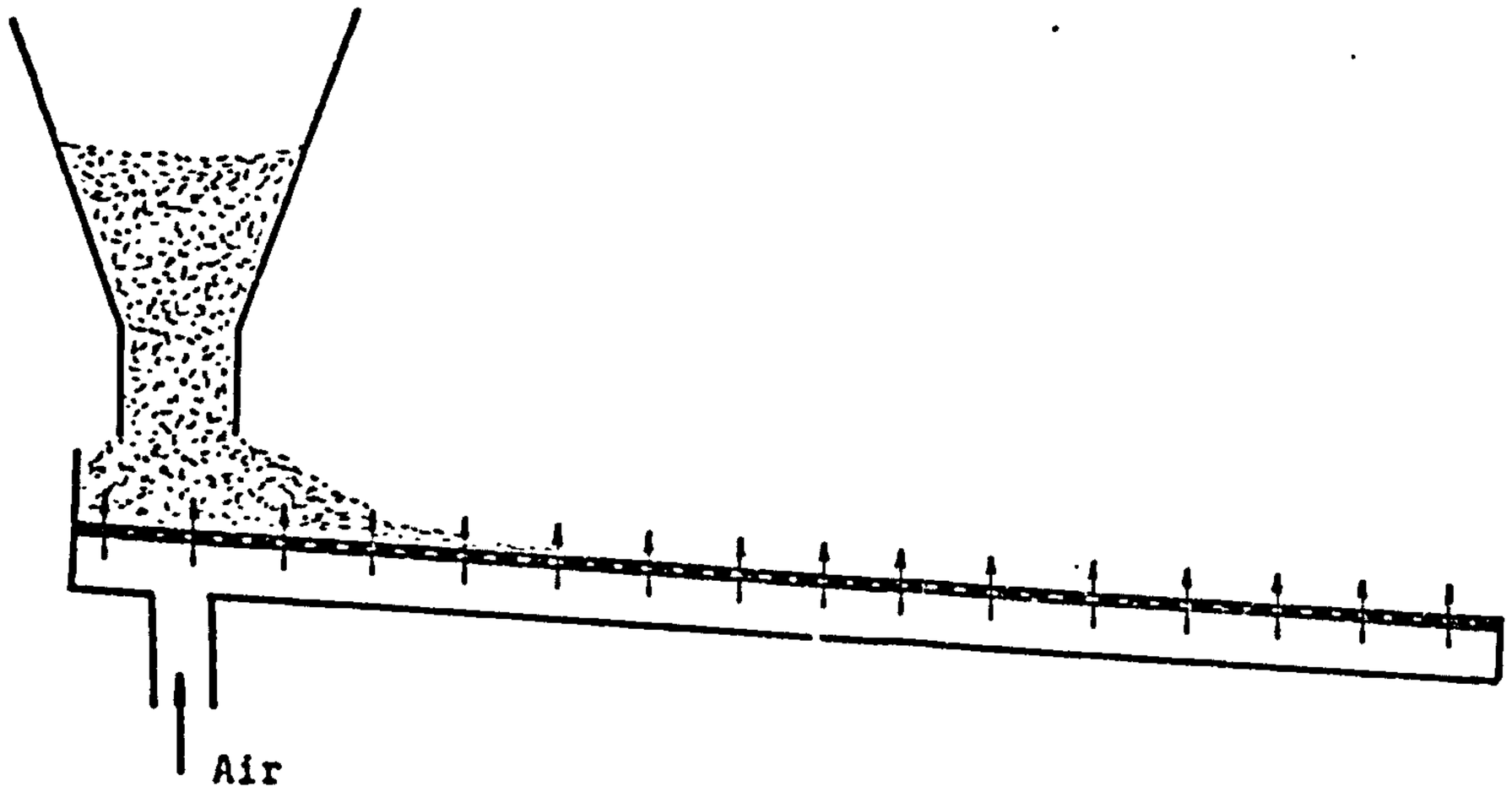

Fig. 3.16. STARTING THE FLOW; air velocity into the stationary powder must exceed U_{mf}, even when a large portion of the porous membrane is uncovered.

than 50% of the total pressure drop, but this is now known to be excessive. A more realistic proportion of the overall pressure drop is 17 to 23% as quoted by Weber (Ref. W2).

That the roughness of the channel base has an influence on the solids flow has been demonstrated by Siemes and Hellmer (Ref. S13) who placed a wire grid on the top surface of the porous distributor. They found that artificially "roughening" the base of the channel in this way tended to modify the solids flow condition by reducing the slip velocity. In effect the "viscosity" of the bed is increased and its dependence on the bed depth is reduced. No other reference has been found to the effect of roughness of the internal channel surfaces, but it seems reasonable to suppose that there is some advantage in selecting a distributor with a smooth top side.

For the dense-phase pneumatic conveying of particulate solids in pipelines, it has been suggested (Ref. A13) that flow may be improved by aerating the powder from an internal pipe containing a series of holes. In a very recent paper (Ref. S21) a similar idea has been proposed as the air-distributor in an air-assisted gravity conveyor, the 'Pneu-distributor' as it is called, running along the V-bottomed channel some 100 mm above its lowest point. The main advantage claimed for this type of distributor is that problems associated with backfilling or clogging are eliminated.

3.2.5 The inclination of the channel

In most industrial applications air-gravity conveyors are installed with a slope of 2 to 10° to suit the plant layout, the lower limit of inclination depending upon the type of material being transported. The degree of initial aeration of the conveyed powder and the nature of the porous membrane may also influence the minimum slope that can be used, but in general about 1° is sufficient for very free-flowing powders, whilst more cohesive substances may require a minimum of 6° to 10° for satisfactory transport.

For a constant solids mass flowrate and superficial velocity of the fluidising air the most obvious effect of an increase in the slope of

the channel is an increase in the velocity of the flowing suspension accompanied by a decrease in its depth. It follows that when operating at a constant aspect ratio an increase in the channel slope would permit an increase in the mass flowrate of solids. Most authors seem to agree that for a constant aspect ratio and superficial air velocity the solids flowrate is likely to be proportional to the sine of the angle of inclination of the channel (Refs. C3, D4, G9, S13). Experimental work with sand (Refs. H2, M4, M14, P9, S13) indicates that there may be a limiting slope beyond which there is little further increase in solids mass flowrate. However, it is not easy to collect reliable data on the maximum solids flowrates that can be handled by air-gravity conveyors because these tend to be very large and therefore the cost of ancillary equipment is prohibitive. There is also the problem of ensuring that the limit on the solids flowrate is a characteristic of the conveying channel and not of some other part of the test rig. This particular difficulty can arise when operating test rigs with flooded feed to the channel and, for some of the experimental data reported in the literature, appears to have given rise to misinterpretation of the plots of solids mass flowrate against channel slope and superficial air velocity. The problem will be examined further in the following Section.

At the present time there does not appear to be any way of predicting, for a given material, the minimum channel slope at which it can be conveyed, and the designer either relies on past experience or tries a sample of the powder in a small test rig. Alternatively the designer simply allows a slope of 10^{o} or more, since on slopes of this order virtually any powder can be conveyed, if it will flow at all!

3.2.6 Superficial air velocity

Except for some special applications (for example, in chemical processing or where there is an explosion hazard) air is used exclusively as the fluidising agent to assist the flow of bulk solids in channels at shallow inclinations. The pressure to be maintained in the air plenum chamber need not be treated as a separate variable as it would depend upon the type of porous distributor in use, the depth of powder on the distributor, and the superficial air velocity required. However, the

plenum pressure would normally be around 250 to 500 mm H_2O so that the air mover can be a simple fan or low-pressure blower, such as a Roots-type blower.

Just how the superficial air velocity affects the solids flow is not really understood, but its influence appears to be twofold. Firstly, the air filtering upwards amongst the particles reduces the contact forces between them so that the "viscosity" of the bed is decreased. This of course corresponds to conventional fluidisation behaviour in a stationary bed, and observation of such a bed should help to predict the flow characteristics of the material when fluidised in an inclined channel. A second way in which an increase in the superficial air velocity can increase the solids flowrate is by effectively providing a lubricating air layer between the bed of powder and the channel bottom, and possibly also between the powder and the channel walls. Pugh (Ref. P9) and McGuigan (Ref. M4) both reported evidence of preferential air flow close to the channel walls giving rise to a lubricating layer of better fluidised powder in this region, and Botterill and van der Kolk (Ref. B21) noted the presence of a layer of air just above the surface of their porous tile distributor.

Fundamentally, the superficial velocity of fluidising air that would be required for satisfactory conveying depends upon the slope of the channel and the mass flowrate of the bulk material to be conveyed, but primarily upon the nature of this conveyed material. Thus there is a clear relationship between the air flow required and the fluidisation characteristics of the material to be conveyed; in general, the lower the minimum fluidising velocity of the material the less air required to convey it.

As mentioned previously, some of the experimental data reported in the literature has been obtained from rigs operated with flooded feed to the conveying channel, as is common in industrial installations. This arrangement, shown diagrammatically in Fig. 3.17, is convenient in that it is to some extent "self-regulating", allowing the bulk solids to flow into the channel at the same rate as it is being emptied, and without risk of overflowing should the channel become blocked for any reason.

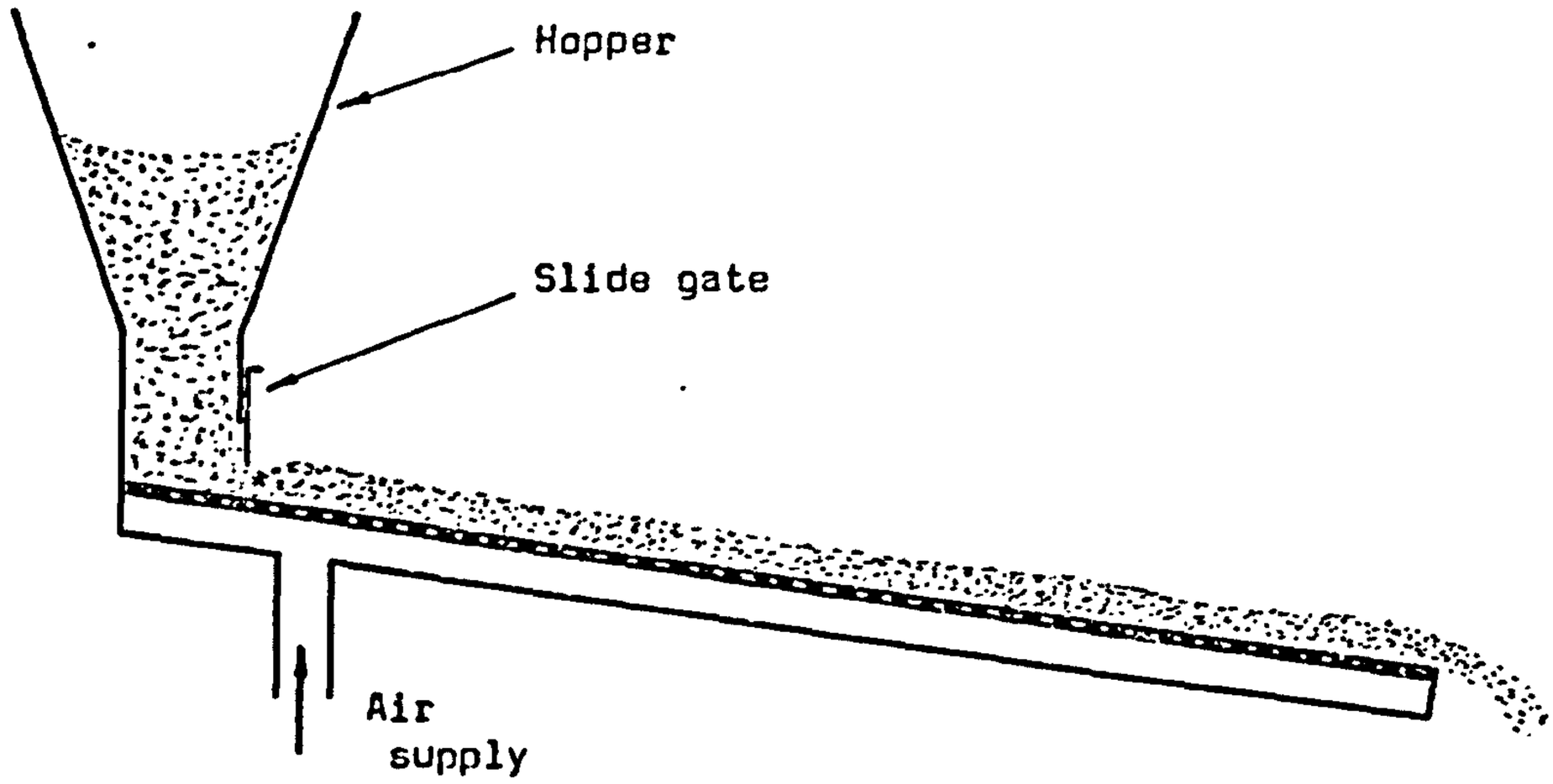

Fig. 3.17. AIR-ASSISTED GRAVITY CONVEYOR WITH FLOODED FEED.

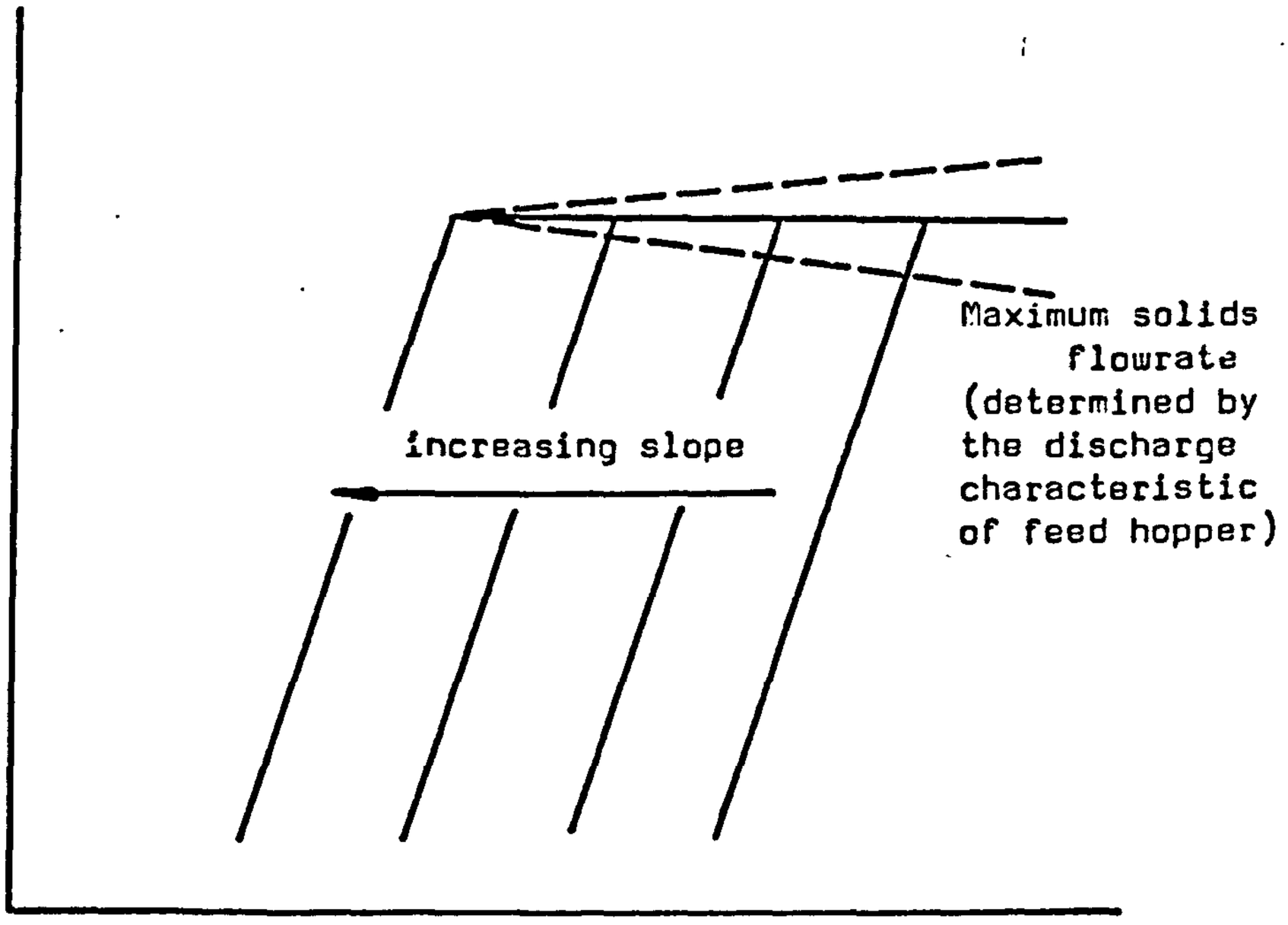

Fig. 3.18. RELATIONSHIP BETWEEN MASS FLOWRATE OF CONVEYED MATERIAL AND SUPERFICIAL VELOCITY OF FLUIDISING AIR, WITH FLOODED FEED TO CHANNEL.

The form of relationship between the solids mass flowrate, the superficial air velocity and the channel slope that would be anticipated for a conveyor with a flooded feed is shown in Fig. 3.18. A certain level of the superficial air velocity must be reached before the flow in the channel starts, this tending to be lower for larger inclinations of the channel. As the superficial air velocity is increased beyond this starting level, the solids flowrate increases rapidly until it becomes restricted at the transfer point from the supply hopper to the upstream end of the channel. Further increase in fluidising air flow causes no appreciable change in the solids flow, other than a possible slight variation resulting from the effect of the increased air flow on the discharge characteristics of the hopper outlet. There seems to be no obvious reason for the solids mass flowrate to become restricted in the channel itself, unless the slope of the channel is small or the aspect ratio is large.

The relationships between solids mass flowrate, superficial air velocity and channel slope shown in Fig. 3.18 correspond quite closely to the results achieved by Harris (Ref. H2) and by Muskett et al (Ref. M14), both working with fine sand. The shape of the graphs in Fig. 3.19, plotted from their data, with the limit on the solids flowrate shown on Fig. 3.19a, is not necessarily a characteristic of fluidised flow in an inclined channel, but rather of the complete hopper/channel system. A point of interest that is apparent in the data of Muskett et al concerns a phenomenon that can occur at air flows close to the condition of incipient fluidisation, where only the top layers of particles become fluidised, the remainder acting as an additional distributor (see for example Ref. Z1 p 26). The authors suggest this explanation to account for the change of slope of the lines in Fig. 3.19b, but whether the effect appears at all probably depends upon the experimental techniques used when operating the channel.

Thus, in order to gain an understanding of the mechanism of air-assisted gravity flow from experimental work, the design of the test rig should be such as to minimise the influence of the hopper discharge characteristics on the solids flow in the channel, or at least to allow any such influence to be recognised.

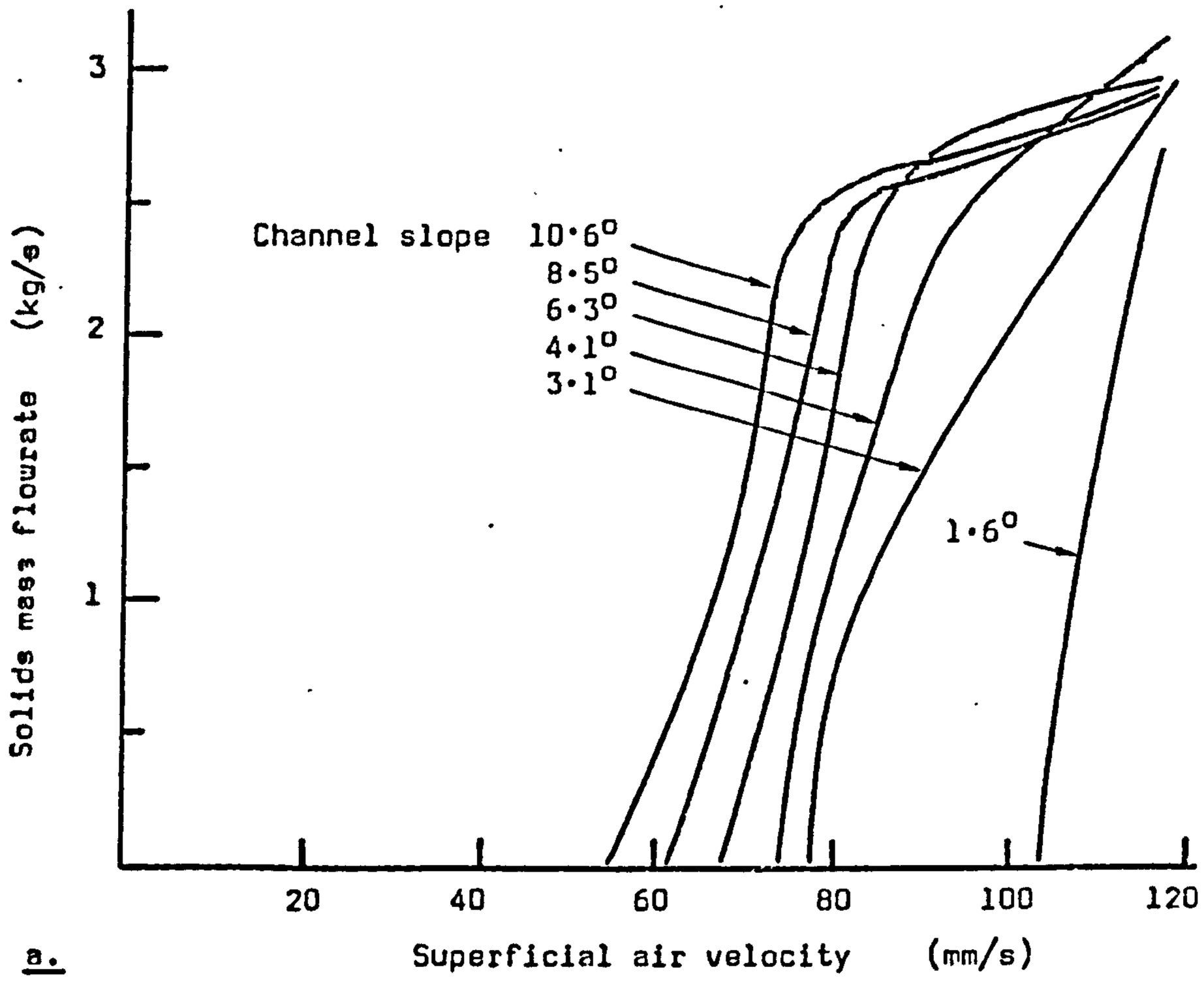

a.

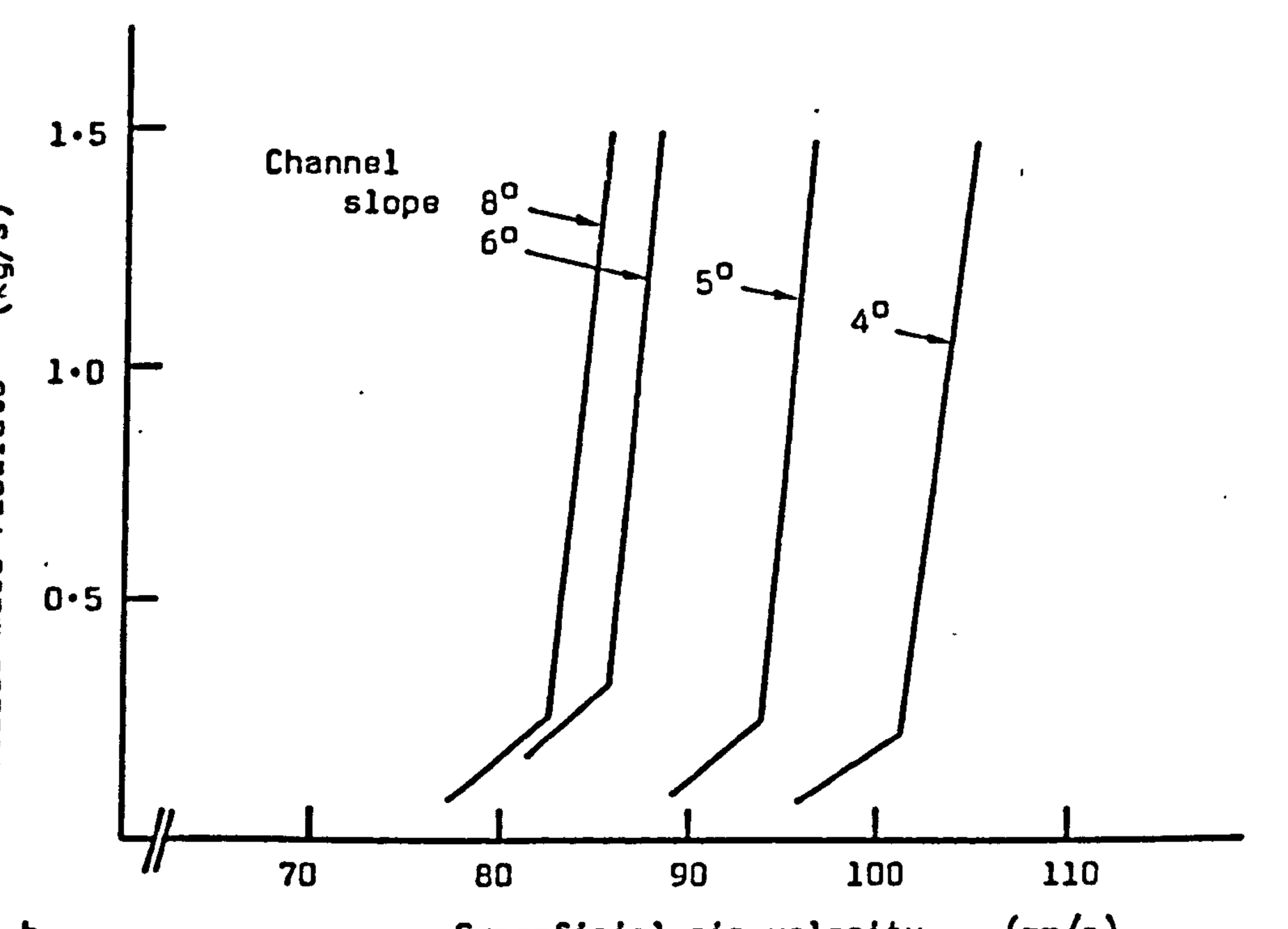

b.

Fig. 3.19. VARIATION OF SOLIDS MASS FLOWRATE WITH SUPERFICIAL VELOCITY OF FLUIDISING AIR:-

a) SAND, 180 μm, in 67 mm wide channel. From data of Harris (Ref. H2).

b) SAND, 150 μm, in 75 mm wide channel. From data of Muskett et al (Ref. M14).

Values of superficial air velocity required for satisfactory conveying can vary over quite a wide range, and it is probable that many industrial systems are operated at a higher air velocity than is necessary. Most authorities quote around 15 to 30 mm/s (Refs. B29, D4, L1, S14) although Descamps and Jodlowski (Ref. D4) give an example of cement conveyed at 15 tonne/h in a 150 mm wide channel with a superficial air velocity of only 4 mm/s. Much higher air velocities are recommended by the EEUA Handbook (Ref. E1) - from 50 mm/s up to as much as 300 mm/s for materials of low density and large particle size.

Whilst there are some differences in the values of the ratio of superficial air velocity to minimum fluidising velocity used or recommended by the various authors, most have worked at air velocities within the range 2 to 5 times U_{mf} (Refs. M4, P9, S13). Qassim's (Ref. Q1) range of operation was restricted to 1.5 to 2.5 U_{mf} as he reported that flow was unsteady at lower or higher air velocities. For most materials tested, Keuneke (Ref. K3) found that an air velocity between 2 and 6 U_{mf} was satisfactory, but for cement and gypsum at shallow slopes the figure had to be much greater; in the latter case, up to 30 U_{mf}.

Experimental investigation of a powdered or granular bulk solid in a stationary fluidised bed should enable a value of the minimum fluidising velocity U_{mf} to be determined. Alternatively a value can be predicted using one of the models discussed in Section 2.3, or using the chart (Fig. 2.13) which also gives an indication of the entrainment velocity. Thus, an air-gravity conveyor may be designed with fluidising air velocity at an optimum value, greater than the minimum necessary for satisfactory conveying (for most materials around 2 to 3 U_{mf}) but less than the velocity at which entrainment of fines from the surface of the bed may become a problem.

3.2.7 Electrostatic effects

Changes in the behaviour of bulk particulate solids as a result of electrostatic phenomena are known to occur in many situations, including conventional fluidised beds (see Section 2.7.3), pneumatic conveying (Refs. C5, D10, R2), the gravity flow of powders (Ref. D6), fine dusts

and aeroscls (a familiar examplc being electrostatic precipitators, for a discussion of which, see Ref. B13 p 221 et seq.) and air-assisted gravity flow - the subject of the present discussion.

In the pneumatic conveying of powders it is known that flow characteristics (especially pressure-drop) can vary with time, and it has been suggested (Ref. R2) that these effects are probably associated with the development of an electrostatic charge on the conveyed material. One of the first experimental investigations on this phenomenon was undertaken by Richardson and McLeman (Ref. R2) using sand of about 1.3 mm mean particle size. They found that during continuous conveying both the air velocity and the solids velocity decreased, while the relative velocity (air - solids) and the pressure drop increased. Similar behaviour was found with manganese dioxide, whilst with Perspex and polystyrene, although significant electrostatic effects were observed, they did not apparently increase with time. Richardson and McLeman suggest that these effects could be associated with a build-up of electrostatic charge on the dust layer adhering to the pipe walls. Cole et al (Ref. C5) and Duckworth and Chan (Ref. D10) have also carried out experimental studies in which they examined the possibility of predicting the effects of electrostatic charging. Other authors have investigated methods of taking advantage of the existence of static electrification in a flowing gas-solid suspension to measure particle velocities by cross-correlation of electrostatic signals (Refs. B14, M7).

From the foregoing comments, it is to be expected that static electrification could have a marked influence on the flow behaviour of aerated powders in inclined channels. Despite this, there is virtually no mention of the phenomenon in the relevant literature, other than passing references to the need to maintain the fluidising air at high humidity if electrostatic charging is to be minimized (Refs. M4, S13).

The influence of the humidity of the fluidising air naturally varies from one powder to another. Even with sand, some types are found to exhibit a strong dependence of the flow behaviour on moisture whilst others are virtually unaffected (Ref. B9). Potash has very good flow properties in dry warm air, but may not flow at all when the air is

cool and moist, even with high fluidising velocities (Ref. K3). Soluble crystalline powders may be particularly prone to a deterioration of flow properties if the moisture content is high (Ref. C6).

It may be prudent at this point to re-emphasise the risk of dust explosions being initiated by spontaneous spark discharge in an electrified gas-solid suspension. Boothroyd (Ref. B13 p 228) gives examples of potentially dangerous situations and discusses precautions that can be taken. Additional advice on procedures to minimise the hazard is given in a recent article by Pay (Ref. P3).

3.2.8 Particle segregation

The tendency for segregation to occur in fluidised beds was discussed in Section 2.7.2, where it was explained that at low fluidising air velocities coarse particles drifted downwards to the bottom of the bed. It could be anticipated that the same phenomenon might occur in air-gravity conveyors, especially in experimental rigs where the same material is continuously re-circulated.

McGuigan (Ref. M4) working with sand, found evidence that at low solids velocities there tended to be a gradual accumulation of larger particles close to the distributor. Since this layer was only partially fluidised it impeded the flow of the remaining bed over it, but increasing the slope of the channel, and therefore the average solids flow velocity, caused the segregated layer to be swept away. Pugh (Ref. P9) also commented on what he called the "segregated layer dissipation mechanism", and attempted to confirm the presence of this layer by observation through the transparent walls of the channel and by withdrawing samples of powder for size analysis. McGuigan and Pugh (Ref. M6) maintained that the existence of this segregated layer of coarse particles was responsible for the drastic changes in the flow behaviour of the aerated powder that occurred at low shear rates.

Keuneke (Ref. K3) worked with several different materials, and mentioned particularly the behaviour of "balancer meal", which consisted of a mixture of coarse particles (groats and chaff) and very fine ones (meal),

but tended to de-mix during conveying. The coarse material was deposited at the bottom of the channel and the finer particles moved over it until the deposit filled the channel and flow ceased. Keuneke commented that the problem might be overcome by continuously vibrating the channel.

The use of fluidisation as a means of classifying particulate materials has been mentioned by Botterill (Ref. B15 p 139) and it could well prove useful to extend this idea to flowing suspensions. Thus, for example, it might be possible to position a horizontal divider at the outlet of an air-gravity conveyor to split the flow into two components having predominantly fine and coarse particles respectively.

3.2.9 Velocity distribution

The velocity at which an aerated bulk solid flows along an inclined channel depends mainly on the slope of the channel, but will also be affected by the solids mass flowrate (that is, the rate of solids feed to the channel), the superficial velocity of the fluidising air, and, perhaps to a lesser extent, by the roughness of the internal surfaces of the channel. Weber (Ref. W2) and Chandelle (Ref. C3) state that the solids flow velocity in an inclined conveying channel is normally between 1 and 4 m/s, and Nordberg (Ref. N3) gives an example of cement flowing in an air-gravity conveyor at about 5.4 m/s. However, of the authors who actually measured the solids velocity under experimental conditions (Refs. K3, M9, P9, S8, S13) none has reported any measurement greater than about 1.6 m/s.

It is not easy to obtain direct measurements of the velocity of a flowing bed of aerated powder, especially at a point within the bed. Probes tend to be either too fragile to withstand the buffeting of the turbulently flowing solid particles or too large to provide "point" measurements without undue interference with the flow. External methods using, for example, lasers or ultrasonics give data for the surface particles only or average values for the whole cross-section of the bed. In all cases calibration presents a problem of considerable magnitude since it is almost impossible to provide a controlled environment that reproduces conditions within the flowing fluidised bed. There seems to be little point in trying to calibrate a velocity probe in oil as Keuneke did (Ref.

K3) and probably the best attempt so far has been that described by Botterill and Bessant (Ref. B16) who used a small annular rotating fluidised bed. However, even this method was not totally reliable because of differences in the flow behaviour between the calibration rig and the flow channel.

Perhaps the simplest method of obtaining an indication of the average velocity of a bed of moving particles is by observing the travel of a float placed on the surface of the bed (Refs. B16, K3, M4). Another very simple idea was that of Mori et al (Ref. M9) who estimated the velocity of particles along the channel by measuring the distance that they "jumped" from the downstream end.

Several workers (Refs. M9, P9, S8, S13) have investigated the velocity profile across the surface of the flowing bed by depositing coloured particles in a line on the moving surface and noting their distribution after a short interval of time. Mori et al (Ref. M9) and Shinohara et al (Ref. S8) observed the distribution of the tracer particles by the simple expedient of suddenly shutting off the supply of fluidising air so that the bed abruptly stopped and settled. In order to assess the validity of the mathematical model that they had developed, Shinohara et al required to measure the maximum solids flow velocity at various operating conditions. The velocities that they measured were generally in the range 0.5 to 1.2 m/s and their results showed a steady increase in maximum solids velocity with channel inclination and with superficial air velocity, although there was good evidence that above a certain air velocity the solids velocity ceased to increase. Shinohara et al also demonstrated that for constant slope and constant air velocity, the maximum solids velocity increased with increasing solids flowrate. In their paper published some twenty years earlier Mori et al (Ref. M8) had reached much the same conclusions regarding the variation of the solids flow velocity, but they also presented velocity profiles across the surface of flowing beds of alumina and sand. With alumina they found that the velocity profile was fairly uniform and the same trend towards a "flat" profile was evident in sand flowing in a steel-walled channel. However, with glass channel walls the velocity profile was modified as a result of sand particles adhering to the walls and therefore impeding slip.

Pugh (Ref. P9) and Siemes and Hellmer (Ref. S13) also used coloured tracer particles on the surface of the flowing bed, but recorded their distribution after a short interval by flash photography. Keuneke (Ref. K3) tried the same method but found that velocity vectors on the bed surface caused the tracer particles to move in from the sides of the channel to the middle. The technique was extended by Mori et al (Ref. M9) who investigated velocity distribution through the depth of the bed by inserting a vertical band of coloured particles into the static material, allowing it to flow for about 600 mm, and then examining the pattern of coloured particles in the section. They found that slip at the distributor was the controlling factor, above this zone the velocity being fairly uniform.

Probes to investigate the variation of velocity within the bed, instead of just at the surface, have been developed by Keuneke (Ref. K3) and by Botterill and Bessant (Refs. B9, B16, B17). Keuneke used a wire strain-gauge probe in which the force on the probe surface was a function of the solids flow velocity. However, the sensor was rather large (10 mm by 20 mm) for point velocity measurements, and the procedure for calibrating the probe in flowing oil appeared questionable. Nevertheless, Keuneke's velocity profiles seemed to confirm that the variation of velocity was more significant across the flowing bed than through its depth. In general, the velocity profiles were not parabolic and there was distinct slip at the walls and bottom of the channel. Furthermore, the maximum velocity was not at the bed surface but at a depth of one quarter to one half of the total depth. Mean velocities measured by Keuneke were generally about 1 m/s, but for gypsum and for cement were somewhat slower.

A small turbine-type velocity probe was used by Botterill and Bessant (Refs. B9, B16, B17) to determine velocity profiles in fluidised 200 μm sand flowing in a horizontal channel. At only 0.1 to 0.3 m/s the average solids velocities were considerably slower than is usual in inclined channels, but Botterill and Bessant still found that the velocity variation was predominantly across the channel, especially with deep beds (that is, having high aspect ratio). However, if the fluidising air velocity is reduced a significant variation of velocity

through the depth of the bed may develop, presumably as a result of an increase in the shear stress at the bottom of the channel.

3.2.10 Viscosity

The nature of the "viscosity" of fluidised particulate solids has been discussed at some length in Section 2.8, mainly with regard to its usefulness as a parameter descriptive of the rheological state of the materials and to problems in quantifying it. Of the various methods that have been employed to investigate the correlation between "viscosity" and the condition of fluidisation, it appears that a Stormer-type viscometer with hollow cylindrical rotor is the simplest with which to obtain repeatable results. The fact that there is little significance in the absolute measurements taken with this (or any other) instrument probably does not matter greatly, but there is a need to establish a standard instrument that will allow comparative tests to be made. Information from such tests is likely to prove valuable in predicting the flow behaviour of fluidised solids in inclined channels when more is known about the correlation between these two situations. Some preliminary investigation of this possibility has previously been undertaken for flow in horizontal channels (Ref. B22).

A number of authors (Refs. N1, N2, S8, S13) have taken an opposite approach; that is, they have attempted to use an air-gravity flow channel as an "instrument" with which to measure the "viscosity" of fluidised particulate solids. Siemes and Hellmer (Ref. S13) based their approach on a Newtonian fluid model for flowing fluidised sand, in which the viscosity depends only upon the superficial velocity of the fluidising air. Flexibility of the model was allowed by varying the amount of slip at the channel base. It was found that viscosity calculated on the basis of total slip at the channel bottom (that is, a two-dimensional model) showed a steady increase with increasing bed depth and decreasing channel slope. However, for the three-dimensional case with no slip at the channel bottom the viscosity showed a sharp decrease and Siemes and Hellmer concluded that slip in fact occurred in such a way as to give a constant viscosity at any given fluidising air velocity. These constant values of μ were calculated and plotted against air velocity, the result showing the same form of relationship

as had been obtained by other researchers using more conventional types of viscometer (see Section 2.8).

Neuzil and Turcajova (Ref. N1, N2) also believed that an air-gravity flow channel provided the most satisfactory method of investigating the viscosity of fluidised powders. They adopted a novel approach by attempting to find a correlation between the dependence of the viscosity of a Newtonian liquid on temperature, and the dependence of the viscosity of fluidised particles on the fluidising air velocity. Although they worked with relatively large particles (500 μm corundum) their experimental results compared quite well with the results of other workers and so Neuzil and Turcajova went on to develop a somewhat complicated expression for viscosity in terms of fluidising air velocities. However, their expression contained several constants which would presumably be specific to the particulate material they used, and possibly also to their conveying channel.

An empirical expression for viscosity in terms of superficial air velocity was also published by Shinohara et al (Ref. S8), which suffered from the same disadvantage of being specific to a single material; in that case, fine glass beads. Their study was based on a two-dimensional Bingham plastic model, and in fact the "viscosity" referred to is the property more commonly termed "coefficient of rigidity" (see Appendix A.III.6). From their model, Shinohara et al derived an expression for "viscosity" (or coefficient of rigidity) in terms of the maximum (free surface) velocity of the flowing bed, and from experimental values of this easily measured quantity they were able to study the relationship between the viscosity of the flowing fluidised glass beads and the fluidising air velocity.

In conclusion it may be said that there is good evidence of a qualitative correlation between the "viscosity" of a fluidised material flowing in an inclined channel and the property measured by more conventional viscometers in stationary fluidised beds. Clearly there exists some property of fluidised particulate solids, which for convenience we call "viscosity", which is an essential parameter governing the flow of such materials. However, a great deal more experimental data will have to be collected if the nature of this parameter is to be more fully understood.

3.3 DATA FROM OTHER SOURCES ON THE FLOW BEHAVIOUR OF VARIOUS AERATED SOLIDS

3.3.1 Introduction

As mentioned previously, from a study of the available literature it soon becomes clear that publications fall into one of two divisions - the first relating to purely experimental investigations, generally with sand as the conveyed material, and the second describing practical industrial installations, mostly handling cement or alumina products. Few research workers - Keuneke (Ref. K3) being a notable exception - have attempted to bridge the gap by studying the flow of materials that are of immediate industrial relevance or that are known to cause practical handling problems. Whilst it could reasonably be argued that there is a case for concentrating research on easily handled powders such as fine sand or glass beads in order to understand the mechanism of fluidised flow, it is nonetheless true that there is a need for practical data on the more difficult materials that are cohesive, friable, sensitive to moisture or static electrification, and so on.

This Section is the result of a search of the published literature for practical handling data on various powdered and granular solids in air-assisted gravity conveyors. Much of the data is very sketchy, and some goes to the other extreme being the outcome of detailed research programmes presented as complex functional relationships between abstract parameters. Whilst the latter may well be valuable from the research point of view, such data is often of little immediate use to engineers in industry who are involved with the design, installation and operation of practical conveyors. Nevertheless, an attempt is made here to summarize the main features of the various data available under the headings of some of the different materials handled.

3.3.2 Cement

Air-assisted gravity conveying as a means of transport of particulate bulk solids was mainly developed in the cement industries of Germany and America. Two early papers on the subject (Refs. A12, N3) concentrated almost entirely on the conveying installations at the Alpena, Michigan

plant of the Huron Portland Cement Company, and on a bulk cargo ship, the S.S. Samuel Mitchell, operated by the same organisation. A particular example quoted in these papers relates to 360 mm wide channels, 55 m long, conveying pulverized raw materials (kiln feed) on a 4^{o} slope at a rate of 220 tonne/h, or approximately 60 kg/s. Nordberg (Ref. N3) stated that the solids velocity was about 5.4 m/s, and commented that even at this rate the conveyors were not operating at full capacity.

Although apparently not based upon experimental work, a table is presented by Descamps and Jodlowski (Ref. D4) giving flowrates of cement in air-gravity conveyors of various widths, with superficial air velocities and power consumption. As it gives a useful indication of practical conveyor performance this table is reproduced here as Table 3.3, and the relationship between mass flowrate and channel width is shown plotted on Fig. 3.20. (Power consumption, from Table 3.4, had previously been plotted as Fig. 3.13.)

According to Keuneke (Ref. K3), working with cement of 15 μm mean particle size and 3000 kg/m^3 density, the flow is quite good although bed expansion (up to 60%) and air retention may be considerable. Some adhesion to the duct walls may occur, especially when the humidity of the air is high. Keuneke found that flow was possible at a channel slope of as little as 0.6^{o}, but his data shows that a more realistic "minimum" slope is around 2 to 2.5^{o}. Avery (Ref. A12) states that the minimum slope required is 2.5^{o}, although most practical conveyors handling standard portland cement operate at about 4^{o} slope. Special types of portland and other cements may require slopes greater than about 6^{o} (Ref. N3).

Keuneke (Ref. K3) gave the minimum fluidising velocity for cement as 1.3 mm/s, and although his measurements of minimum superficial velocities in channels of different widths were somewhat inconsistent, it appeared that for satisfactory conveying the air velocity had to be greater than about 8 U_{mf}. This corresponds to about 10 mm/s and is of the same order as the values given in Table 3.4.

Width of channel (mm)	150	200	250	300	400	500
Flowrate of cement (t/h)	15-45	45-72	72-100	100-140	140-260	260-410
" " " (kg/s)	4.2-12.5	12.5-20.0	20.0-27.8	27.8-38.9	38.9-72.3	72.2-113.9
Air flowrate (m^3/h per m^2)	14-36	18-48	24-60	26-70	36-96	45-120
Superficial air vel. (mm/s)	3.9-10.0	5.0-13.3	6.7-16.7	7.2-19.4	10.0-26.7	12.5-33.3
Power required (kW/m)	0.05-0.12	0.06-0.16	0.08-0.20	0.09-0.24	0.12-0.32	0.15-0.40

Table 3.4. DATA FOR THE TRANSPORT OF CEMENT IN AIR-ASSISTED GRAVITY CONVEYORS OF VARIOUS WIDTHS. The figures for power required are for air supplied at a pressure of 5 kN/m^2 (510 mm H_2O). (From Descamps and Jodlowski - Ref. D4)

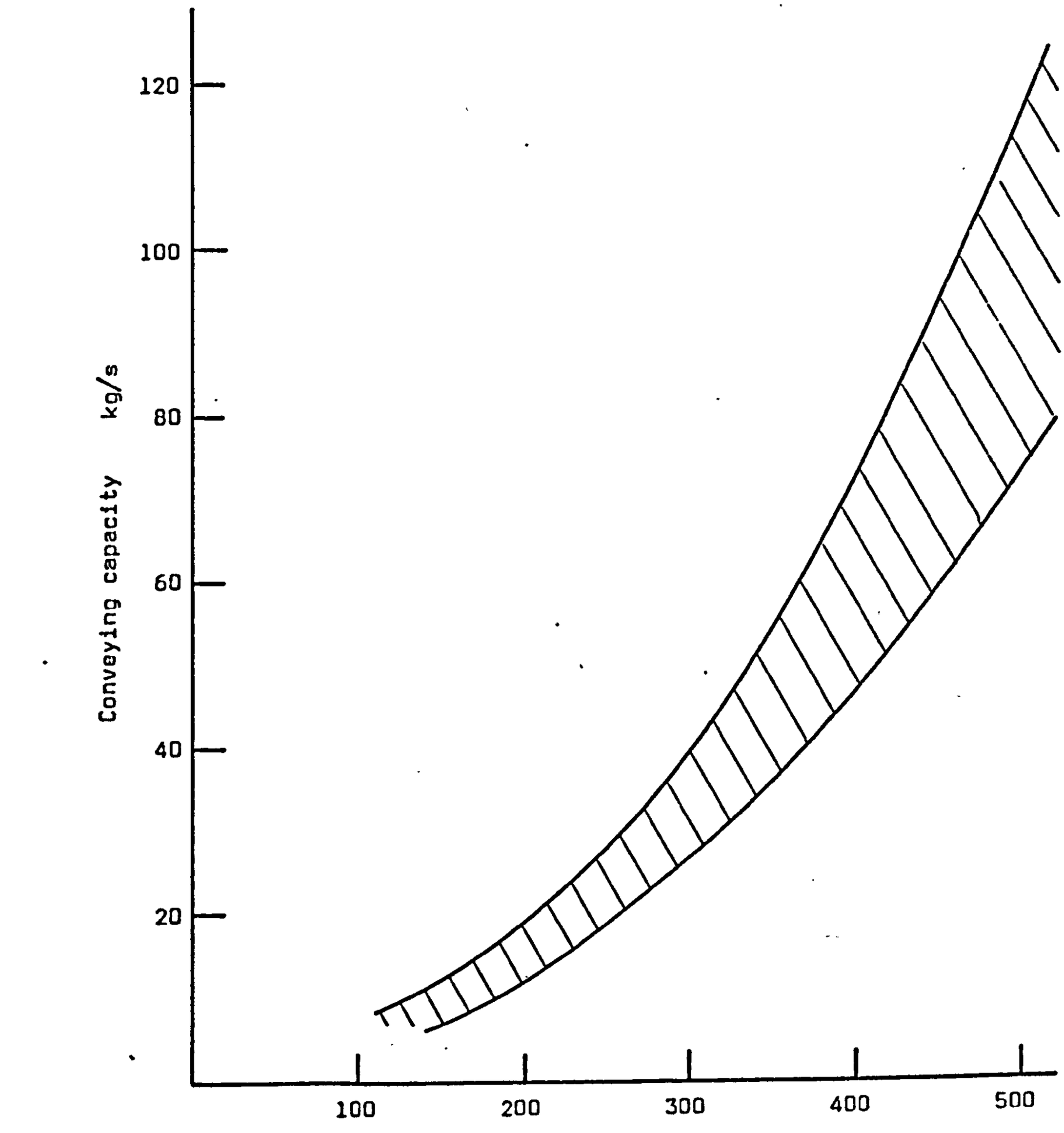

Fig. 3.20. APPROXIMATE CAPACITIES OF AIR-ASSISTED GRAVITY CONVEYORS CARRYING CEMENT. (From Ref. D4)

3.3.3 Alumina

It is probably true to say that, after the cement industry, the aluminium industry is the largest user of air-assisted gravity conveyors, and descriptions of some typical installations are to be found in Refs. B27, B28, L1, W5.

One of the largest operating air-gravity conveyors is the 915 mm wide channel mentioned by Butler (Ref. B29) which transports alumina from a surge hopper to a main silo at a rate of 1500 tonne/h (about 410 kg/s). Another 915 mm (3 feet) wide conveyor, carrying the somewhat lower quantity of 1000 tonne/h (275 kg/s) is described by Leitzel and Morrisey (Ref. L1). The same large plant, at Tacoma, Washington, which handles alumina by a combination of belt conveyors (for upward transport) and air-gravity conveyors, also used 460 mm wide channels carrying 350 tonne/h (96 kg/s). A second plant described by Leitzel and Morrisey is a ship loading installation in the U.S. Virgin Islands. Each of four storage silos is supplied with alumina at a rate of 100 tonne/h (28 kg/s) by 300 mm wide air-gravity conveyors. Similar conveyors, 610 mm in width, at the silo outlets, serve an inclined belt conveyor, but the final stage to the ship's hold is a 26 m long boom conveyor using a 610 mm wide air-channel. This channel transports 750 tonne/h (205 kg/s) of alumina. Unfortunately, no details are given of the particle size of the alumina or the air requirements, or even of the exact inclination of the channels.

Bushell and Maskell (Refs. B27, B28) provide a detailed description of a very large Canadian aluminium smelting plant. Air-assisted gravity conveyors are used to distribute the alumina powder from the service hopper to six storage silos. These conveyors are 500 mm in width, inclined at about 2.3^{o} and achieve mass flowrates of 200 tonne/h (55 kg/s). Once again, no details of air-requirements or particle sizes are given.

Fig. 3.21. shows an approximate relationship between conveying capacity and channel width for air gravity conveyors handling alumina, derived from the figures quoted above.

In sharp contrast to these industrial installations, the width of

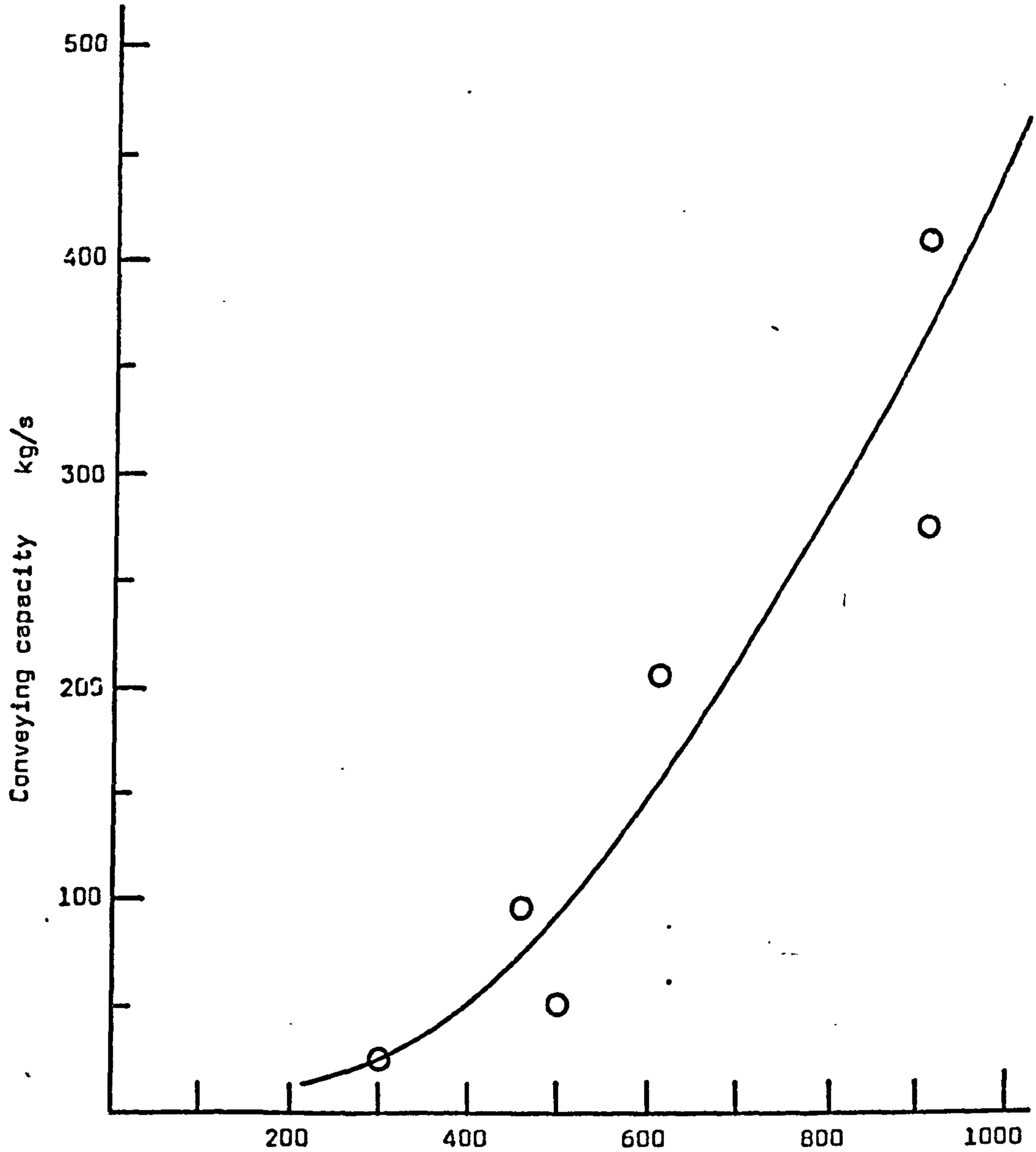

Fig. 3.21. APPROXIMATE CAPACITIES OF AIR-ASSISTED GRAVITY CONVEYORS CARRYING ALUMINA.

conveying channel used by Mori et al (Ref. M9) in experimental work on alumina was only 50 mm. They investigated the flow of 35 μm alumina powder having a true density of 3900 kg/m^3 and bulk density of 820 kg/m^3. The value of U_{mf} was found to be about 10 mm/s. The solids flow velocity was reported to vary from about 0.4 m/s at a channel slope of 3°, up to almost 1 m/s when the slope was increased to 7°.

No other data has been found on the flow of fluidised alumina in inclined channels. In their investigation of the flow properties of fluidised solids in a horizontal channel, Botterill and van der Kolk (Ref. B21) used 102 μm alumina (bauxilite) as one of the flowing powders. They found that the alumina flowed well when fluidised at air velocities from 2 to 3.5 U_{mf} and that it exhibited a wide range of rheological behaviour, depending to some extent on the dimensions of the channel.

Shinohara and Tanaka (Ref. S9) included 211 μm alumina particles as one of the bulk solids tested in their novel "Pneumatic Escalator" (see also Section 3.1.5), but no specific results were given.

3.3.4 Sand

In the first detailed experimental studies of fluidised flow in inclined channels reported in the literature, Mori et al (Ref. M9) included sand as one of the materials conveyed, and Siemes and Hellmer (Ref. S13) used it exclusively. Since then, because it is cheap, safe, easy to handle, available in a wide range of particle size and, not least, because it has good flow characteristics, sand has been widely used in research programmes on various aspects of fluidised flow. However, there appears to be no published information on the transport of sand on a commercial scale by air-assisted gravity conveyors.

The relevance of some of the reported experimental data to conveying on a commercial scale is unfortunately limited, either because of the very small size of flow channel used or because of incomplete information on the flow conditions in the channel. This applies particularly to situations where the solids mass flowrate is not controlled (and is thus a dependent variable) and yet the depth of the flowing bed is not recorded (Ref. H2).

Neither Mori et al (Ref. M9) nor Siemes and Hellmer (Ref. S13) give "raw" data in their published papers in a form suitable for direct comparison with fluidised flow data for sand from other sources. However, in the latter case, back-calculation from the graphical results presented does allow the preparation of approximate plots of bed depth against solids mass flowrate (Fig. 3.22) or bed depth against channel slope (Fig. 3.23). These relationships are only at a single superficial air velocity of 89 mm/s (4.5 U_{mf}) and for the one size of sand of about 200 μm. The plot of bed depth against channel slope for various constant solids mass flowrates (Fig. 3.23) shows the characteristic pattern of curves with the bed depth increasing, gradually at first, and then more steeply, as the channel slope is reduced. Fig. 3.22 is plotted from the same data on axes of bed depth against solids mass flowrate, but shows that artificially "roughening" the channel bottom causes a substantial increase in the bed depth.

Using a very short channel of 84 mm width, Qassim (Ref. Q1) investigated the flow of a 266 μm sand over a moderate range of flow conditions. Although raw data on solids mass flowrate, channel slope, fluidising air velocity and bed depth is presented in tabular form, it proves to be very inconsistent when plotted as bed depth against solids flowrate. At inclinations of 7, 6 and 5° the relationship between these parameters was more or less as expected, but it appeared that frequently there was a significant increase in the solids flow as the inclination was reduced to 4, 3 and 2°. The reason for the erratic results is not clear, but it is noteworthy that Qassim was working with extremely shallow beds, often less than 4 mm in depth, which is of the order of magnitude of the residual depths reported by Mori et al (Ref. M9) at which fluidised flow tends to become unstable, and eventually to cease. Furthermore, in view of the very short channel used, it seems probable that the flow was unduly influenced by the hopper discharge characteristics.

A considerable amount of data relating to the flow of sand in air-assisted gravity conveyors was collected by McGuigan and Pugh (Refs. M4, M6, P9) during their investigation undertaken at the University of Aston. They worked with a channel 3 m in length and having widths of either 100 mm or 150 mm. Much of their data was processed to yield shear diagrams

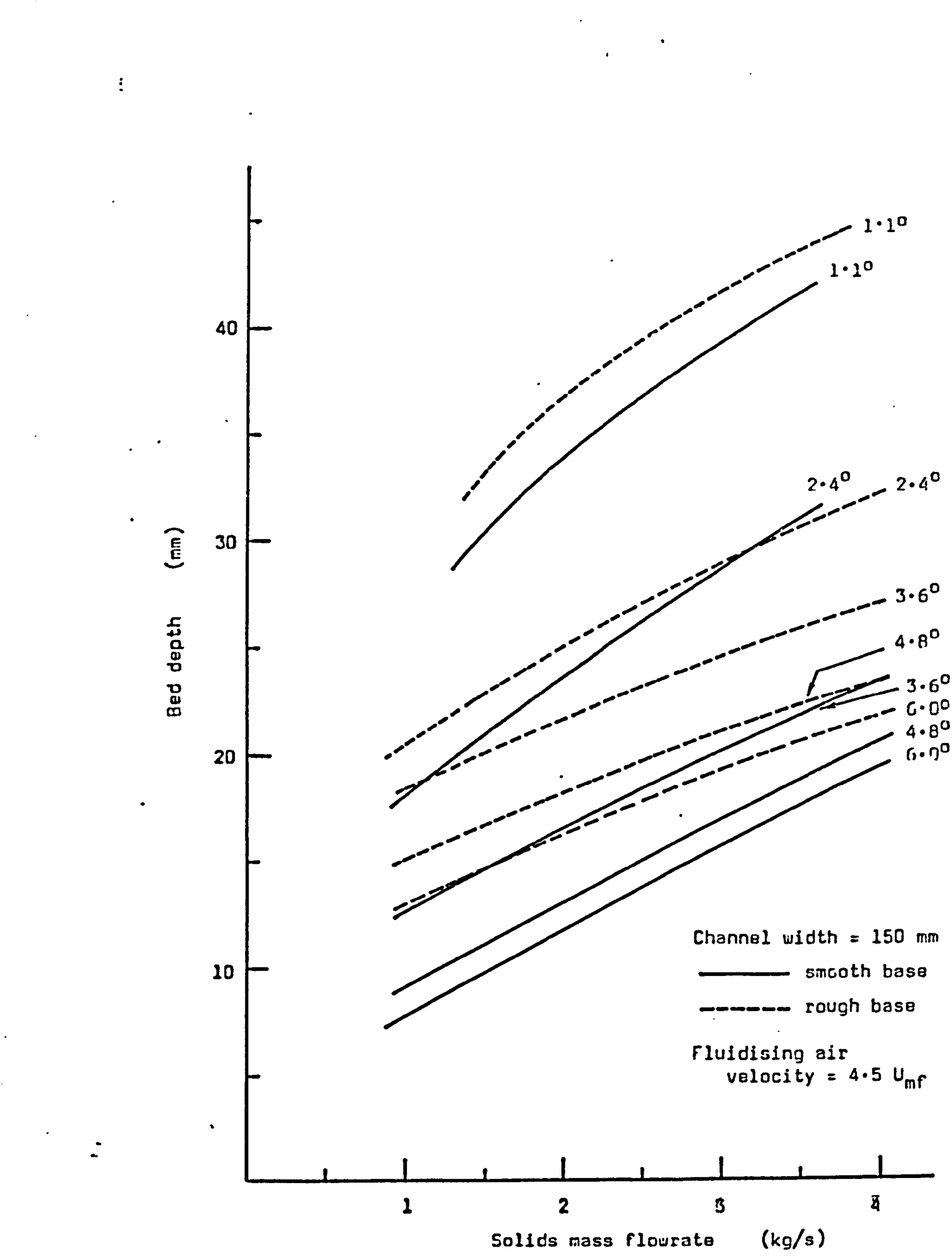

Fig. 3.22. VARIATION OF BED DEPTH WITH SOLIDS MASS FLOWRATE FOR 200 μm QUARTZ SAND, SHOWING THE EFFECT OF ROUGHENING THE CHANNEL BASE. (Based on the data of Siemes and Hellmer, Ref. S.13)

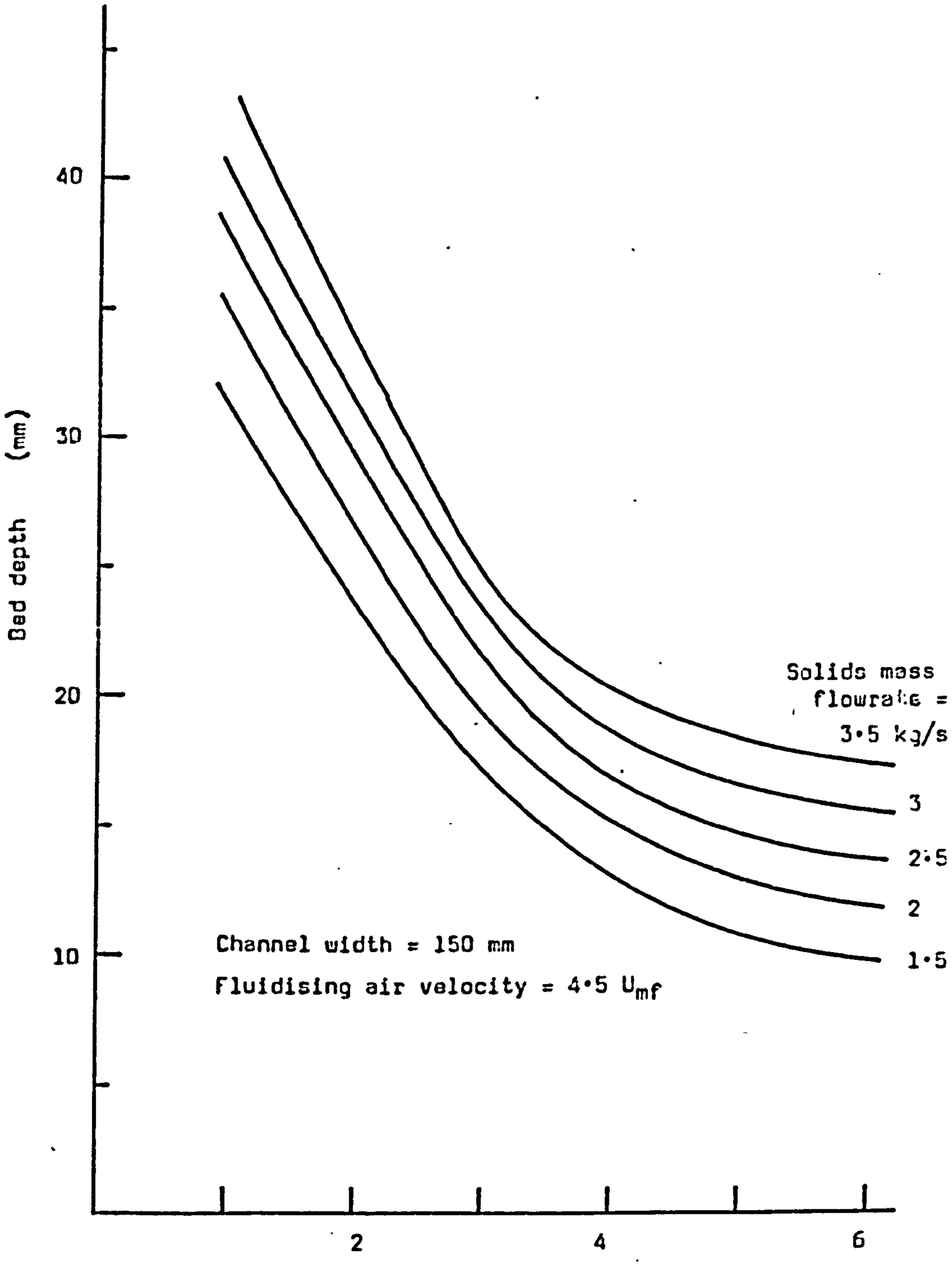

Fig. 3.23. VARIATION OF BED DEPTH WITH CHANNEL SLOPE FOR 200 μm QUARTZ SAND. (From Fig. 3.22; based on the data of Siemes and Hellmer; Ref. S.13)

and dimensionless plots of modified Reynolds numbers against modified friction factors. (A discussion of the reasoning behind this approach and of the model on which it is based is undertaken in Section 4.2.2.) However, sufficient information is given by both authors to enable the fundamental relationships between the solids mass flowrate, the channel slope, the fluidising air velocity and the depth of the flowing bed to be examined. Pugh (Ref. P9) does in fact present plots of flowrate per unit width against bed depth for three different fluidising air velocities and two different channel widths. Using Pugh's data for flow in the 150 mm wide channel, Fig. 3.24 has been prepared to illustrate the variation of bed depth with solids mass flowrate at three channel slopes and three fluidising air velocities. It can be seen that this graph compares quite closely with Fig. 3.22 prepared from the data of Siemes and Hellmer. Fig. 3.24 suggests that increasing the superficial velocity of the fluidising air has little effect, except at very shallow channel slopes, but it is likely that at air velocities below about $2\ U_{mf}$ the increase of the bed depth would become significant at all channel slopes. McGuigan (Ref. M4) also gives data for the flow of sand in the 150 mm wide channel, and from this data Figs. 3.25 and 3.26 have been prepared to illustrate the approximate form of the relationships amongst the basic flow parameters.

Once again the same general pattern emerges: a series of lines showing a gradual increase of bed depth with increasing solids flowrate, the rate of increase of bed depth tending to be greatest at shallow channel slopes. The tendency for the bed to thicken drastically at low channel slopes is perhaps more clearly illustrated by the "knee-type" curves of Figs. 3.23 and 3.26, which effectively indicate that there is a practical limit of channel slope at which conveying should be undertaken. It was the observation of the regular pattern of these curves, and the realisation of their significance, which led to the plan to construct a simple mathematical model to represent them. A detailed description of the steps taken in attempting to construct such a model is given in Section 4.3.

The only other published work of any importance dealing with the flow of fluidised sand is that undertaken by Botterill and various co-workers

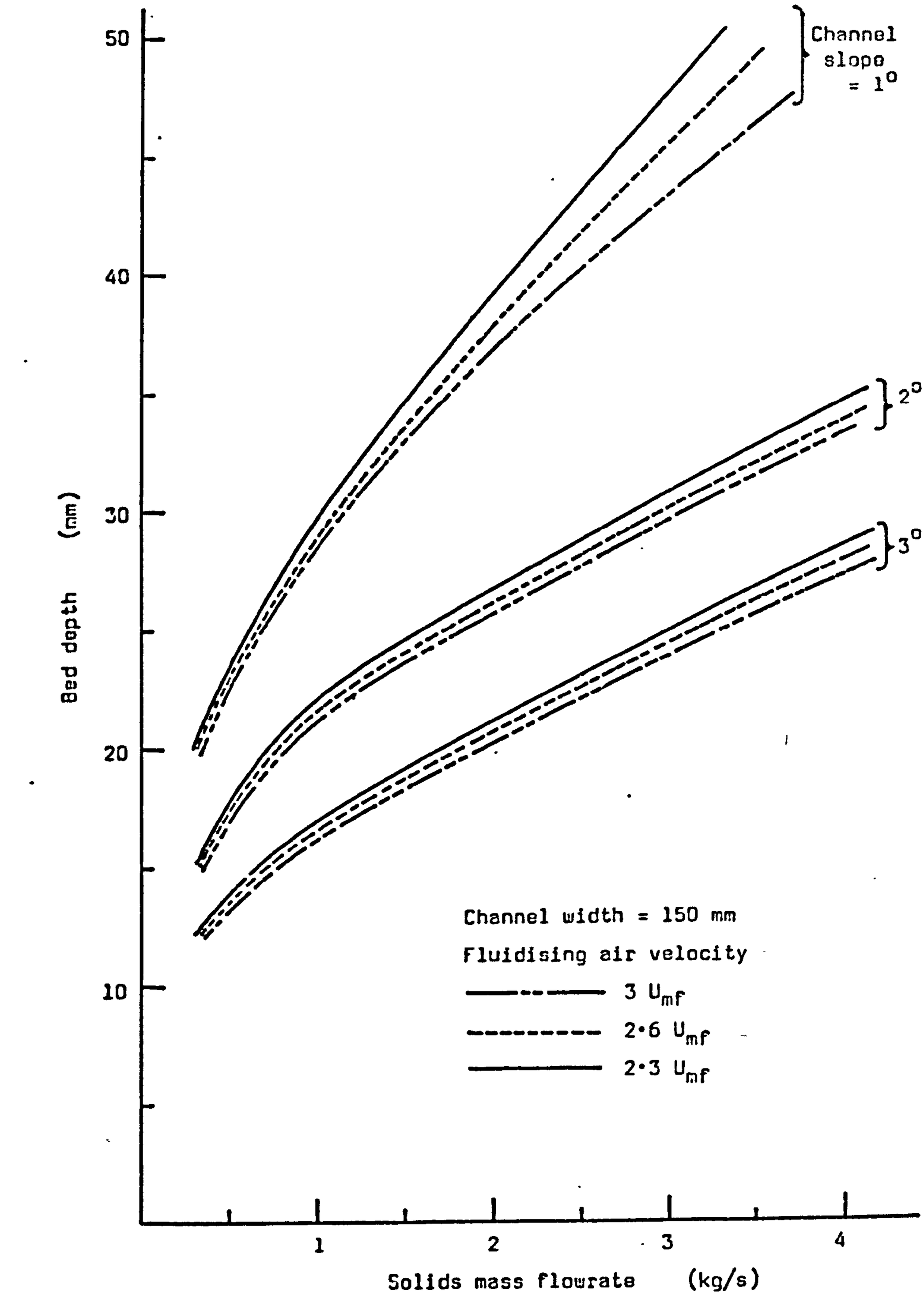

Fig. 3.24. VARIATION OF BED DEPTH WITH SOLIDS MASS FLOWRATE FOR 150 μm SILICA SAND. (Based on data of Pugh; Ref. P9)

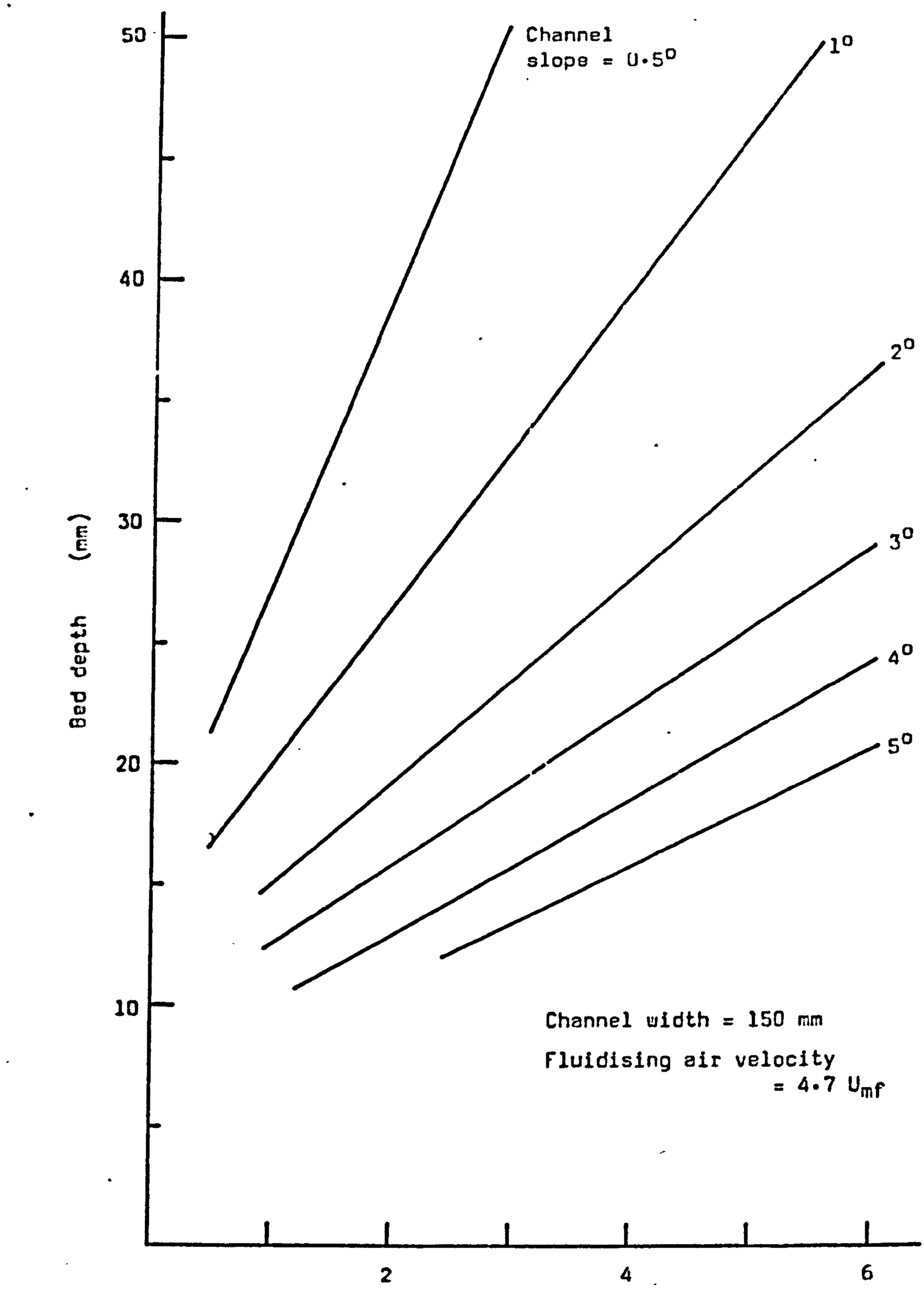

Fig. 3.25. VARIATION OF BED DEPTH WITH SOLIDS MASS FLOWRATE FOR 177 μm SAND. (Based on data of McGuigan; Ref. M4)

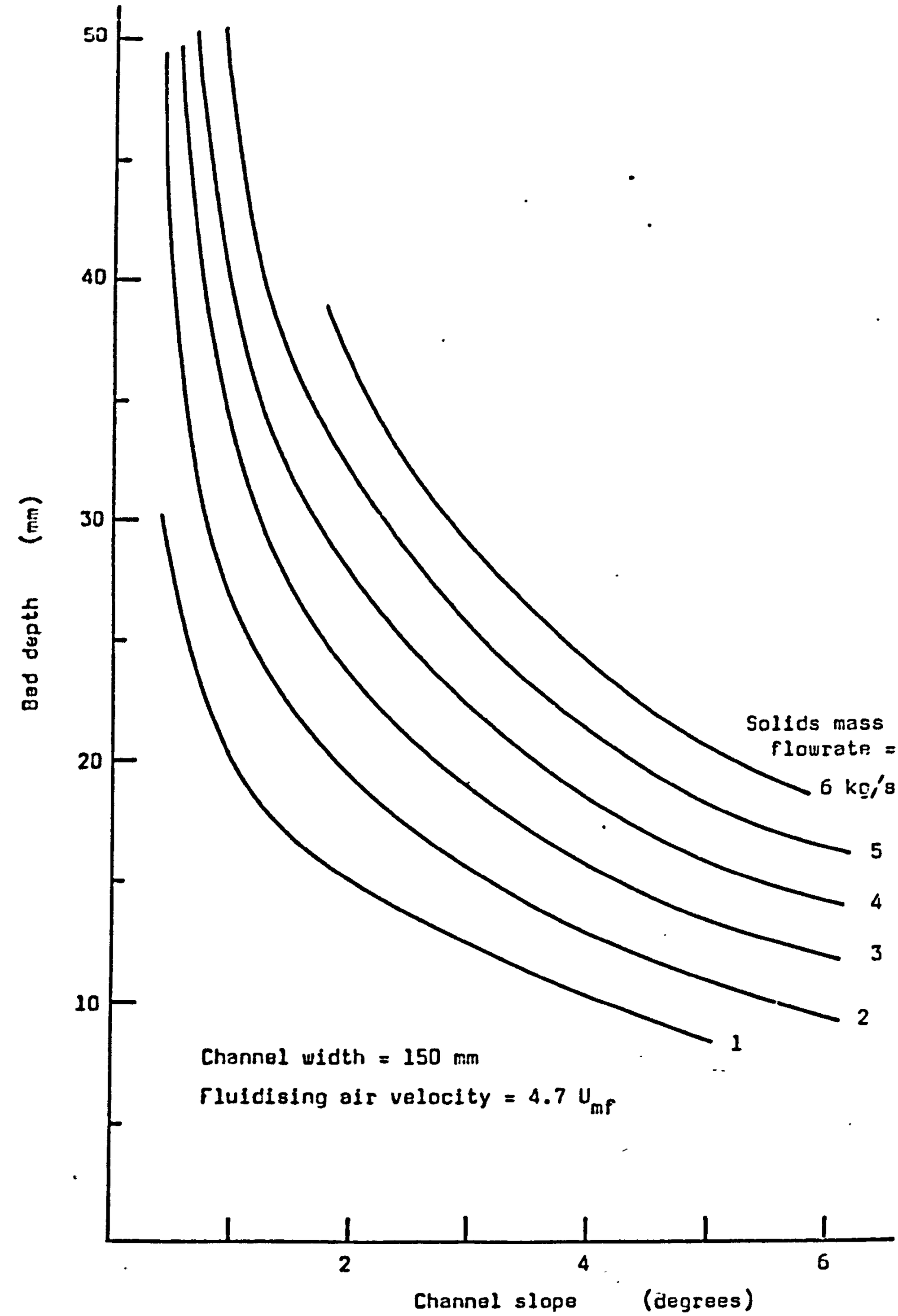

Fig. 3.26. VARIATION OF BED DEPTH WITH CHANNEL SLOPE FOR 177 μm SAND.
(From Fig. 3.25; based on the data of McGuigan; Ref. M4)

(Refs. B16-B22) and by Bessant (Refs. B8, B9). However, this work was almost exclusively concerned with flow in a horizontal channel in which the fluidised material was caused to flow by the action of a series of paddles. A great deal of useful information on the flow properties of fluidised sand (and other materials) is to be found in these publications, especially concerning velocity distributions, boundary shear stresses and general non-Newtonian flow characteristics. However, until a better understanding is obtained of the mechanism of air-assisted gravity flow, this information cannot be directly used to relate the basic parameters of solids mass flowrate, bed depth, channel slope and fluidising air velocity for uniform flow in inclined channels.

3.3.5 Other bulk solids

Many manufacturers' sales brochures, and other sources (for example, Ref. L1) provide lists showing the many kinds of bulk solid that can be transported by air-assisted gravity conveyor. Cement and alumina, as the two materials most commonly handled this way, and sand which is so often used in experimental studies, have been discussed at some length and attention will now be given, albeit briefly, to some of the other bulk particulate solids on which practical information may be found in the published literature.

The work of Keuneke (Ref. K3) has already been mentioned, particularly in connection with the flow of fluidised cement, and is valuable also for data on gypsum, potash and various other products including agricultural feedstuffs and fertilizers. For convenience, the main characteristics of the materials investigated by Keuneke are summarised in Table 3.5.

Gypsum, a material widely used in the building industry as the basis of plaster and also as an agricultural fertilizer, was found by Keuneke to fluidise only poorly. It would flow in an air-gravity conveyor provided that the channel slope was greater than about 4^{o}, although there was a tendency for the fine components to cling to the surfaces of the conveying channel. At low velocities the flow of gypsum is fairly uniform, but at higher velocities substantial deposits of fine particles formed on the

MATERIAL	DENSITY	MEAN PARTICLE DIAM. (μm)	MINIMUM FLUIDISING VELOCITY (mm/s)	MIN. AIR VELOCITY RATIO U_g/U_{mf}	MINIMUM CHANNEL SLOPE (°)	REMARKS
Cement	3000	15	1.31	6 to 18	1.5	Good fluidisation and expansion. High capacity for air retention. Will flow.
Sand	2640	215	19.7	-	1.5	Good fluidisation; low expansion; low air retention; will flow.
Gypsum	2500	12	1.52	8 to 32	6	Poor fluidisation; aggregation; channel formation. Particles very liable to slip. Low air retention; will flow.
Potash	2000	129	18.4	1.2 to 2.6	1	Good fluidisation; low expansion; low air retention. Will flow, but will not fluidise with moisture content > 1%.
Thomas phosphate (a fertilizer)	3330	64	8.04	2.5 to 6	0.5	Good fluidisation and expansion; vigorous particle motion; will flow.
Balancer meal	1427	80	17.2	1.8 to 5.3	4.5	Poor fluidisation; segregation; channel formation; elutriation of fines; low air retention; will flow.
Oilcake meal	1386	105	29.8	-	-	Poor fluidisation; channel formation; particles very liable to slip; low air retention. Probably capable of flow.
Wheat groats	1427	76	17.8	-	-	Poor fluidisation; segregation; channel formation; elutriation of fines; low air retention. Probably will flow.
Wheat	1332	3730	1070	-	-	Fluidisation possible at high air velocity; low expansion; low air retention. Particles very liable to slip; capable of flow.
Barley/oats	-	-	-	-	-	Fluidisation not possible; channel formation; hooking of large particles and elutriation of fines. Will not flow.

Table 3.5. SUMMARY OF FLUIDISATION AND CHANNEL FLOW CHARACTERISTICS OF VARIOUS BULK MATERIALS (Ref. K3).

channel walls causing partial obstruction and very uneven flow. The air flowrate required was 8 to 10 U_{mf} (about 12 to 15 mm/s) in a 150 mm wide channel, but two or three times this level in a channel of 75 mm width.

Other difficult materials investigated by Keuneke were potash and "balancer meal". The meal comprised a mixture of very coarse particles (groats and chaff) and fine particles of flour, and consequently problems were encountered with segregation during conveying. It was found that if the velocity of the fluidising air was too high the coarse particles tended to settle at the bottom of the channel, yet with too low an air velocity the mixture could not be fluidised. In the case of potash, the flow depended upon the condition of the fluidising air, being good in dry, warm air. In cool, moist air the hygroscopic nature of the material causes it to become wet rapidly so that the particles stick together and flow ceases to be possible. Even after drying, the potash does not flow until the lumps have been broken down.

References to many other materials are to be found in the literature, including coal (Refs. B29, S16), plastics (Refs. B29, H6, L1), rock dust (Ref. A3) and fly ash (Refs. B29, H6, L1, S16), but these give only minimal information, or none at all, on the conveying conditions required. Stoess (Ref. S16) gives a useful list of typical bulk solids; in which their handling characteristics are briefly summarised and attention is drawn to those suitable for air-assisted gravity conveying.

3.4 THE APPLICATION TO FLOWING AERATED SOLIDS OF DATA FROM STATIONARY FLUIDISED BEDS

3.4.1 Introduction

It has been pointed out elsewhere in this work that, because of the number and complexity of the parameters needed to fully specify a particulate system, it will never be possible to develop an absolutely rigorous treatment of the flow of aerated particulate bulk solids in inclined channels. Consequently the most useful analytical approach lies in the construction of physical models that will represent the flow behaviour of an aerated bulk solid with sufficient reliability to permit

the prediction of the flow of one material from experimental results on another. The chances of achieving success with such a prediction are of course greatest if the experimental work is carried out in a channel under similar conditions to those at which the product is to be conveyed, but consideration should be given to the possibility of making a reliable estimate of the flow from tests on a stationary fluidised bed (for example, in a simple cylindrical fluidising vessel).

The data that can be obtained from tests in a simple fluidising rig includes the minimum fluidising velocity (and, with a tall enough column and suitable instrumentation and filtration, the entrainment velocity), pressure drop across the bed, bed expansion and bulk density, bed "viscosity" and distributor performance.

3.4.2 Quality of fluidisation

Most of the features of fluidised beds will be considered under this heading, but bulk density and "viscosity" will for convenience be discussed in separate Sections.

Whilst the fluidisation of powders in stationary beds and in beds allowed to flow along an inclined channel are essentially the same process, there are some significant differences, the most important probably being the suppression of bubbling in the flowing bed. It would seem that there may be various consequences of this effect as a result of the alternative route that has to be taken by the air passing through the distributor. Thus, if this air does not pass through the bed as "bubbles" it must instead flow uniformly distributed within the bed, preferentially at the channel walls or along the channel bottom in a layer between the distributor and the powder. If the first of these alternatives occurred it might be expected that the pressure drop across the bed would be approximately proportional to the depth of the bed.

Working with a 200 μm sand, Mori et al (Ref. M9) found that the pressure drop per unit depth of the flowing bed was virtually independent of the depth. However, for 35 μm alumina the pressure drop per unit depth was found to be significantly lower for deep flowing beds than for shallow

ones, this effect being most pronounced at high air flowrates. The implication of these observations could be that with the very fine alumina, there was a tendency for the assisting air to form a layer beneath the moving bed instead of passing through it.

The difficulty of measuring the pressure drop across a flowing bed of material was discussed by Keuncke (Ref. K3) who reported that fine materials showing a degree of cohesion (such as gypsum) tended to cling to the distributor blocking up the pores so that the pressure drop across it often differed sharply before and after transport. Measurements of total pressure drop therefore could not be relied upon to give an accurate indication of the pressure drop across the flowing bed itself. Trivedi and Rice (Ref. T3) and Sutherland (Ref. S18) also cast doubts on this method of inferring the pressure drop across a fluidised suspension from the total pressure drop across the bed and the distributor, claiming that the pressure drop across the distributor was different when the distributor was covered with powder and when it was clear.

McGuigan (Ref. M4), Pugh (Ref. P9) and Singh et al (Ref. S21) all used measurements of the total pressure drop to infer the depth of the flowing particulate bed by comparison with observations on a stationary bed. In view of the preceding comments this method must be regarded as questionable, and it seems unlikely that the results would be any more reliable than direct measurements of the bed depth at a number of positions. Pugh in fact mentions the problem of blockage of the distributor and its "adverse effect on the quality of fluidisation", but does not relate this to the method used for determining bed depth.

The measurement of minimum fluidising velocity in a stationary fluidised bed provides in effect a stable reference characteristic for the particulate material concerned and is therefore a valuable part of the modelling process. The fact that the fluidisation behaviour may be modified when the powder flows in an inclined channel does not lessen the usefulness of U_{mf} as a basic property of the powder.

The influence of the porous distributor is less easy to assess experimentally. Some aspects of distributor performance have been considered in Sections 2.6 and 3.2.4 from which it was concluded that the best results

would be obtained if the distributor produced a stable and uniform fluidisation. However, it seems unlikely that this situation could readily be checked in an actual channel because of the manner in which the bubbling behaviour of the bed is modified by the flow. Whilst it seems fair to assume that a distributor which produces a good quality of fluidisation in a stationary bed would also work well in a flow channel, it is possible that apparently poor distributors will in fact work just as well with flowing materials. There appears to be little alternative to carrying out tests on distributors in an actual flow channel.

3.4.3 Bulk density

The degree of expansion experienced by a particulate bed when it is fluidised depends to a large extent on the manner in which the air flows through it; that is, its "bubbling behaviour". Since this bubbling behaviour can be significantly different in stationary and flowing fluidised beds, considerable caution must be exercised when attempting to apply data based on expansion of stationary beds to beds that are flowing in a channel.

The most important situation in which this problem arises is in the determination of the bulk density of a fluidised suspension. Various authors (Refs. K3, M4, P9) appear to have used this bulk density, along with the depth of the flowing bed and the mass flowrate, to calculate an average solids flow velocity. However, little indication is given by these authors of how the bulk density was determined, and presumably (with some justification in the case of sand, for which the expansion is quite small) changes of bulk density with air flowrate were neglected or assumed to be the same as for a stationary bed.

The two quantities bulk density and average velocity are both difficult to measure for aerated particulate solids flowing in an inclined channel and it is not possible to calculate either one of them without a reliable measurement of the other. The difficulties are compounded if reliable values of the depth of the flowing bed cannot be obtained. Clearly the results of any experimental work involving these variables should be subjected to very careful analysis.

3.4.4 Viscosity

Botterill et al (Ref. B22) point out that the main problem in small-scale determination of flow properties is in assessing the extent to which the fluidisation behaviour of the bed of particulate material is influenced by the presence of the viscometer element. They conclude from the results of their own work that whilst data obtained from such experiments is useful, it should be regarded as qualitative only. Nevertheless, although there is unlikely to be any significance in values of "viscosity" obtained on the basis of calibration of the measuring instrument in a liquid, the similarity of the flow situation at the vertical surface of a cylindrical viscometer rotor and at the vertical wall in an inclined channel is worth noting. The effect of the relative velocities between the vertical surface and the aerated powder in each case (which could be closely comparable if the diameter and rotational speed of the viscometer rotor have been chosen appropriately) is mainly apparent as an improvement in fluidisation resulting from the "stirring" action that occurs. Preferential bubbling at vertical surfaces in fluidised beds may occur and it is also known that flow of the fluidised material over the distributor can tend to suppress bubble formation in the bed. Both of these effects might be expected to cast doubts over the validity of applying viscosity data from stationary beds to the flow of aerated materials in channels.

Probably the main contributor of information on the correlation between viscosity data on fluidised powders in stationary and in flowing beds has been McGuigan (Ref. M4), but even his results were somewhat inconclusive. Perhaps the most significant difference in the two situations, as McGuigan himself pointed out, was that the rotational viscometer involved only vertical surfaces whereas the channel flow involved shear at the channel base in addition to the vertical channel walls. Inconsistencies in the correlation were put down to variations in shear behaviour at the channel base resulting from the presence there, under certain conditions, of a "segregated layer" of coarse particles.

The position can be summarised in the words of Botterill et al (Ref. B22) who said that "although the data obtained in viscometer experiments

cannot yet be extrapolated theoretically to give accurate predictions of deeper full-scale fluid bed flow situations, they are extremely useful in giving qualitative information about the effect of such variables as bed depth and fluidisation velocity on the flow properties of various particulate mixtures".

3.5 CONCLUSIONS

This Chapter has concentrated on the flow behaviour of bulk particulate solids when "fluidised" with air, with reference especially to the use of this method of reducing the natural angle of repose of the material to form the basis of a conveying system.

The construction of air-assisted gravity conveyors is quite simple and they are available from a number of manufacturers either as complete installations or as bolt-together components (see Appendix A.IV). Relatively little research into the operation of this kind of conveyor has been reported in the literature, probably because of the difficulty of financing and installing, in an academic environment, a test rig of sufficient size to be relevant to the requirements of industry. A significant proportion of the research has in fact been devoted to investigating the feasibility of conveying horizontally or on an upward slope by a combination of fluidising and blowing the powdered material. Whilst these novel forms of fluidised bed conveyor are interesting, they have a relatively high power requirement and, for the transport of powders, would seem to offer little advantage over dense-phase conveying by pneumatic pipeline. However, the true air-assisted gravity conveyor, operating at a downward slope of 3 to 10^{o} depending upon the material being conveyed, can prove to be a remarkably economical method of transport for powders and granular solids, using as little as 15 kW to transport 100 kg/s over a distance of 100 m.

The flow behaviour of an aerated powder in an inclined channel will depend very much on the nature of that powder and can be described in terms of a series of relationships amongst five basic parameters: solids mass flowrate, bed depth, width and slope of the channel and superficial air velocity. A study of published experimental data has given

some insight to the influence of each of these parameters and also to the influence of the porous air distributor that serves as the base of the channel. Almost any powdered or granular material that is free-flowing or only slightly cohesive can be conveyed, and the "nature" of the material would govern the optimum channel slope and the optimum flowrate of fluidising air. However, these optimum operating conditions may be modified by electrostatic effects, particle segregation, changing distributor characteristics as a result of blockage of the pores, changing moisture content of conveyed material or of fluidising air, and so on.

In addition to experimental data, which mainly relates to the flow of fluidised sand, a limited amount of information is available in the literature on practical industrial applications of air-assisted gravity conveyors. Most of this information concerns the transport of cement and alumina and gives a useful indication of the type of application to which these systems are suited.

The final Section of this Chapter was concerned with the question of using a small fluidising vessel to obtain experimental data for a powder which could be used to predict its flow behaviour when aerated in an inclined channel. It was concluded that whilst information on the quality of fluidisation, minimum fluidising velocity, bulk density, "viscosity" and distributor performance obtained from a stationary fluidised bed is valuable, much more work needs to be done in order to understand the correlation between the stationary and the flowing bed situations.

CHAPTER FOUR

MODELLING THE FLOW OF AERATED BULK SOLIDS IN INCLINED CHANNELS

4.1 INTRODUCTION

Several authors have attempted to develop physical models to represent the flow behaviour of aerated bulk solids in inclined channels; with only limited success. The main difficulty with the study of aerated solids flow, and the reason why it will never be possible to develop an exact mathematical analysis, is the large number of variables involved, and with some of them (such as particle shape) the lack of a precise and convenient definition. The shortage of experimental data on the influence of these more complex parameters adds to the already considerable problems.

In order to simplify the situation it is as well initially to set aside all the variables which contribute to what may be termed the "nature" of the bulk particulate solid. Thus, only a very general comparison will be made between the flow behaviours of different materials, with no attempt to investigate in depth the effects of characteristics such as particle size or shape, size distribution or particle density. The main influence of these variables is of course on the fluidisation behaviour of the bulk solid and has been discussed at some length in Chapter 2, and, more specifically with regard to flow behaviour, in Section 3.2.2. As previously mentioned, it is not possible to model these effects in any detail and they are accounted for by the use of appropriate coefficients.

The study thus becomes restricted to the flow of a given aerated powder in an inclined channel, and the significant variables are the mass flow-rate of the powder $\dot{m}_s$, the width of the channel b, the slope of the channel α, the depth of the flowing bed of powder h, and the superficial velocity of the supporting air U_g. Most of the experimental work and theoretical analysis carried out by various researchers have concentrated on the relationships amongst these five parameters, and the objective of this part of the present programme can be summarised as the investigation of the form of the functional relationship

$$\phi \left[\dot{m}_s, b, \alpha, h, U_g \right] = 0 \qquad \ldots\ldots\ldots\ldots\ldots 4.1.1$$

It is of course necessary to undertake some consideration of other variables which may or may not be independent of those listed above,

and here can be included shear stresses at the walls and base of the channel, the bulk density of the conveyed material, and, presupposing a similarity to the flow of liquids, the "viscosity" of the conveyed material. In addition to affecting the boundary shear stresses, the nature of the porous base of the channel may have some influence on the quality of fluidisation (see Sections 2.6 and 3.2.6) and, through effectively changing the "viscosity", will therefore also influence the flow behaviour of the conveyed material.

In common with work presented by other authors dealing with flow of aerated bulk solids in inclined channels, the present analytical study is restricted to the condition of uniform flow. This could be expected to correspond to the situation occurring in most practical air-gravity conveyors in which varying flow is confined to a short settling length at the inlet end of the channel and to a similar short distance at the outlet end. Over the major part of the channel flow takes place essentially at a uniform depth with constant velocity and with the gravity force on the flowing material balanced by the shear stresses at the walls and base of the channel.

In addition to the fluidisation of particulate materials, a second phenomenon that is clearly relevant to any study of the flow behaviour of such materials in air-assisted gravity conveyors is the flow of liquid in an open channel. Observation of an aerated or "fluidised" powder flowing down an inclined channel immediately suggests an affinity to a flowing liquid, especially with regard to the surface wave motion that can be set up, the plume that forms downstream of any obstruction on the surface, and also, under certain conditions, standing waves. Although it is perhaps unwise to overemphasise the liquid-like nature of the flow as there are significant differences, models derived from both Newtonian and non-Newtonian liquid behaviour show some promise. The main difficulty with such models lies in dealing with the properties density and viscosity, since with the flow of two-phase (air-solid) suspensions these properties depend very much on the quantity of air present. Furthermore, as explained in Section 3.4, it is not necessarily easy to determine values of "density" and "viscosity" applicable to a flowing suspension from tests on a stationary fluidised bed.

Again, possibly too much significance has been attached to values of Reynolds number, calculated as for flowing fluids and used as justification for the use of laminar flow models. In fact, the justification for the use of these or any other models lies in their ability to predict reliably the behaviour of the system concerned, and parameters such as Reynolds number are only useful if they can yield information on the relationships amongst the basic system variables in which the design engineer is interested; in this case, the solids mass flowrate, the width and slope of the channel, the depth of the flowing bed and the superficial air velocity.

Models that are constructed on a purely empirical basis are likely to be very restricted in application. One such example is the expression proposed by Harris (Ref. H2) from a limited range of tests on sand. The volumetric flowrate of sand is given in terms of the slope of the channel, its width, and the superficial air velocity as

$$V_s = P U_g b^2 (\tan\alpha)^{1.75} - Q \qquad \text{.....4.1.2}$$

in which P and Q are constants. Values of these constants given by Harris would correspond to P = 860 and Q = 0.0061, with the expression in coherent SI units.

In the following Sections some of the possible analytical models of aerated solids flow in inclined channels will be examined, leading to the introduction and development of a new modelling approach that it is believed will be of considerable usefulness in understanding and predicting the flow behaviour of bulk particulate solids in air-assisted gravity conveyors.

4.2 MODELS BASED ON THE FLOW OF LIQUIDS - A SURVEY

4.2.1 Models based on the laminar flow of Newtonian liquids

In view of the recognisable similarities between the flow behaviour of bulk particulate solids, when fluidised with air, and the flow of liquids, it is clearly of interest to examine the feasibility of using

physical models developed for liquids to represent flowing fluidised powders. A number of authors (Refs. N2, S12, S13, T4) have advocated models based on the laminar flow of liquids, although, because of the difficulty of carrying out an analysis in three-dimensions, attempts at modelling in this way have often involved a uniform velocity either in a lateral direction (across the flow) or vertically through the depth of the bed.

One of the earlier attempts at making an analytical study of air-assisted gravity flow was that of Siemes (Ref. S12). He based his approach on the two-dimensional laminar flow of a Newtonian liquid in an inclined channel, with no slip at the walls and total slip at the bottom (Fig. 4.1a). For this model the mass flowrate is given by

$$\dot{m} = \frac{\rho^2 g b^3 h \sin\alpha}{12\mu} \qquad \ldots\ldots\ldots\ldots\ldots 4.2.1$$

where ρ and μ are the density and viscosity of the liquid, b and α are the width and inclination of the channel and h is the depth of the flow. This expression is easily derived either by considering the equilibrium of a vertical elemental lamina of liquid in a two-dimensional flow with velocity varying only in the horizontal plane, or alternatively, as a special case of the corresponding non-Newtonian model as set out in Appendix A.III.3.

If the density and viscosity are regarded as constant, equation 4.2.1 may be written

$$\dot{m} = K b^3 h \sin\alpha \qquad \ldots\ldots\ldots\ldots\ldots 4.2.2$$

where the coefficient K includes ρ, μ and the specific gravitational force g. However, with K constant it has been found that this simple model does not reliably represent the relationships amongst $\dot{m}$, b, h and α for aerated bulk solids flowing in inclined channels over a range of operating conditions. The reason for this poor correlation between model and real system, as discussed by Siemes and Hellmer in a later paper (Ref. S13), was basically that, although there was likely to be significant slip at the channel base, the assumption of total slip

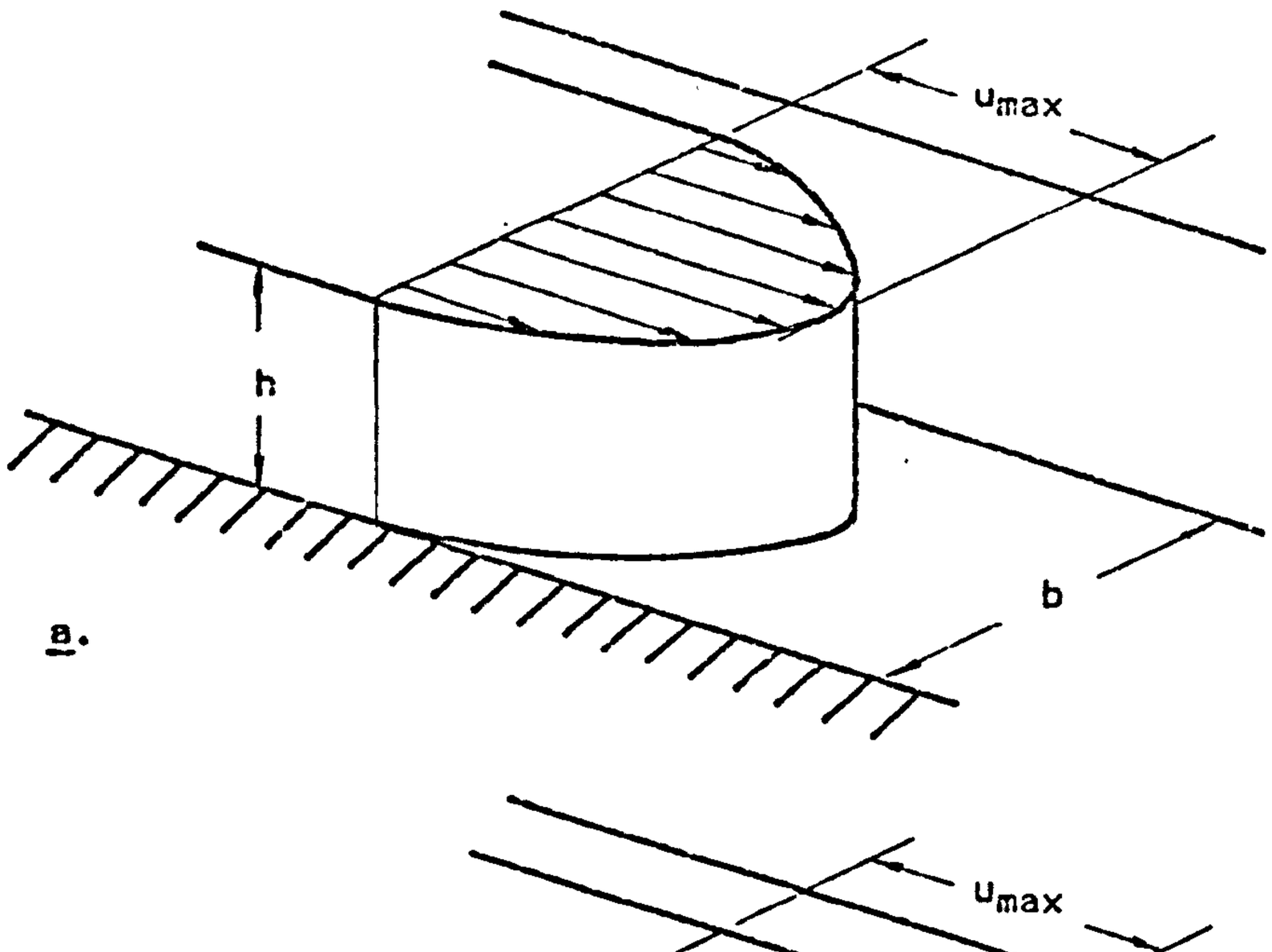

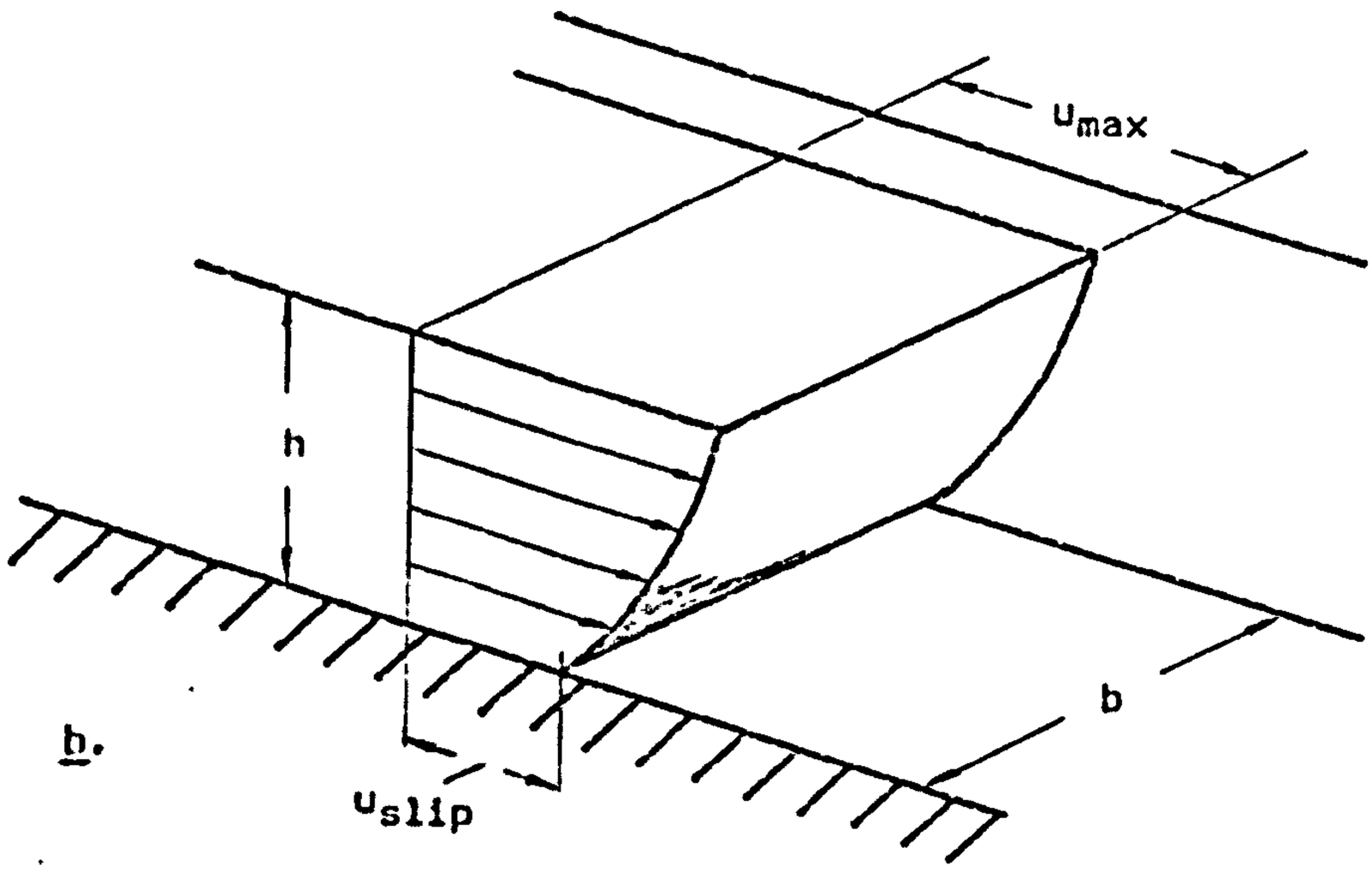

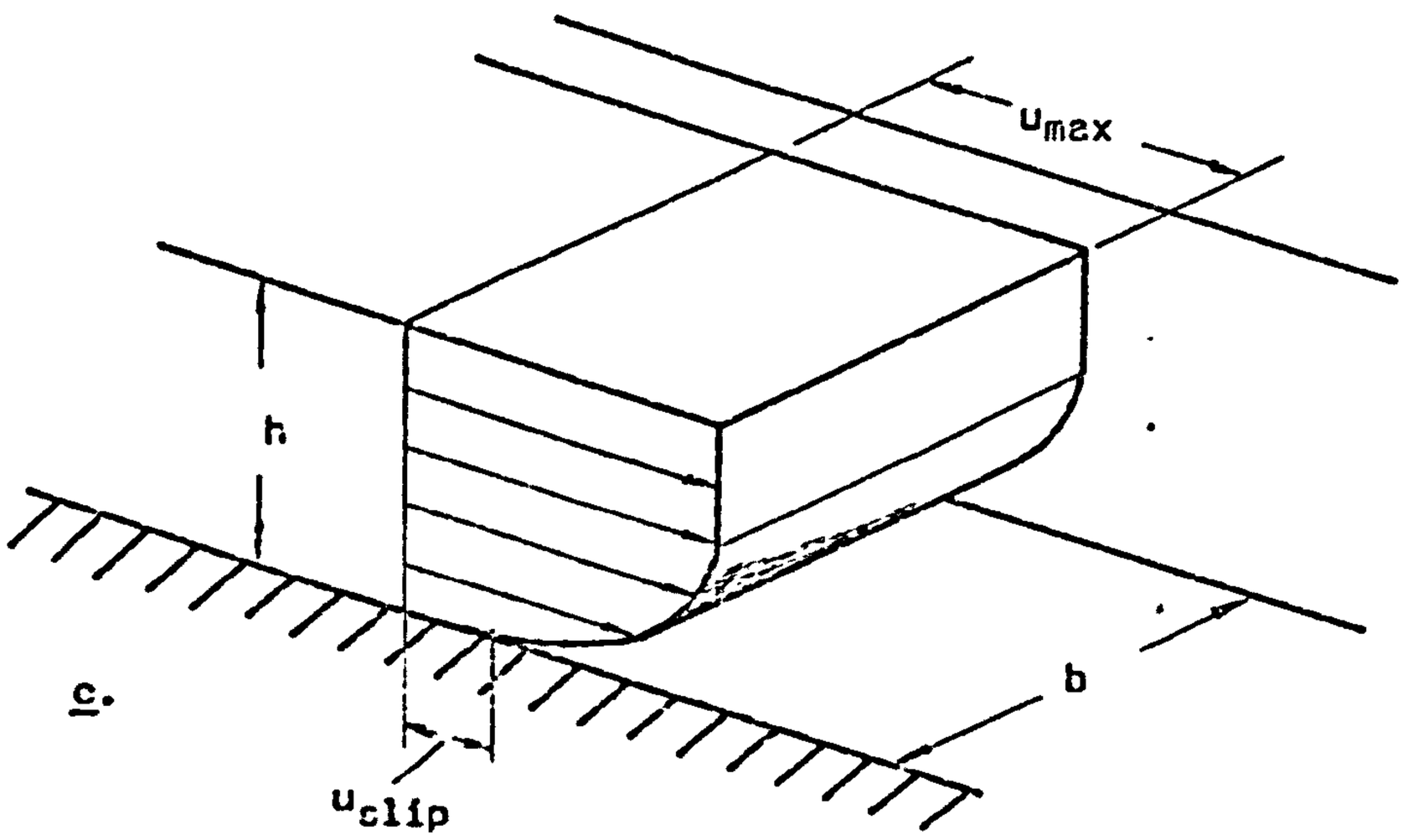

Fig. 4.1. MODELS OF LAMINAR FLOW IN AN INCLINED CHANNEL

a - Newtonian liquid; no slip at side walls.

b - Pseudoplastic; slip at channel bottom.

c - Bingham plastic; slip at channel bottom.

required by the two-dimensional model was too unrealistic. They attempted to overcome this difficulty by modifying equation 4.2.1 as

$$\dot{m} = \frac{\rho b^2 h^2 g \sin\alpha}{\mu} F\left[\frac{h}{b}\right] \qquad \ldots\ldots\ldots\ldots\ldots 4.2.3$$

where $F[h/b]$ is a function which for the simple two-dimensional model has the form b/12h, but which may be given a more complex form to represent three-dimensional flow with no-slip or with partial slip at the channel bottom. A similar approach, extended in an attempt to make it generally applicable to non-Newtonian fluids, has been proposed recently by Singh et al (Ref. S21).

A practical difficulty that occurs with equation 4.2.3, and with several other models, is the need to have some knowledge of the "viscosity" of the flowing fluidised powder. Siemes and Hellmer assumed that the viscosity of a given powder depended only upon the superficial velocity of the fluidising air, and thus, by operating their rig at various combinations of h, $\dot{m}$ and α, they were able to determine values of $F[h/b]$ to give a constant value of μ. However, this approach did not seem to lead to a convenient practical model, mainly because it tends to be found that the function depends upon the mass flowrate $\dot{m}$, and in any case the model has been called into question by a number of authors who have found that flowing fluidised solids have distinctly non-Newtonian characteristics (that is, the viscosity depends upon the rate of shear) (Refs. B22, M4, M6, P9).

An alternative method of modifying equation 4.2.1, supported by some authors (Refs. C3, D4, G9) is to adjust the indices of the bed depth h and channel width b. Thus Descamps and Jodlowski (Ref. D4) proposed a variable index 'a', writing the expression in the form of equation 4.2.2 as

$$\dot{m} = K b^a h^{4-a} \sin\alpha \qquad \ldots\ldots\ldots\ldots\ldots 4.2.4$$

where a = 1 for $h/b < 0.5$ and a = 3 for $h/b > 0.5$. The middle part of this range, that is $h/b \simeq 0.5$, was said by Chandelle (Ref. C3) to be covered by a = 2. Unfortunately, neither of these authors give any indication of the range of values of K, although Gregoraszczuk and

Fedoryszyn (Ref. G9) cited a Russian publication in which data characterising air-gravity conveyors were said to be tabulated. Furthermore, these authors failed to point out that, even for a single powder, K is a function of h/b. This is made clear by plotting the bed depth against the solids mass flowrate, as $\dot{m}/K$, for various channel slopes at a constant channel width (Fig. 4.2). The discontinuity of these relationships is clearly unsatisfactory and the model is considerably improved by expressing 'a' as a simple function of the aspect ratio of the flowing bed. A possible expression is

$$a = 3(h/b) + 0.5 \qquad \text{.....4.2.5}$$

and the effect is to allow equation 4.2.4 to be plotted as a smooth continuous curve relating the depth of the flowing bed to the solids flowrate (Fig. 4.3).

4.2.2 Models based on the laminar flow of non-Newtonian liquids

Greater flexibility of the model can be achieved by basing it upon the laminar flow of a time-independent non-Newtonian liquid as this allows a much wider range of possible flow behaviour, particularly with regard to the distribution of velocity within a cross-section of the flow.

Astarita et al (Ref. A.11) proposed a theory for the steady laminar flow of a non-Newtonian liquid down an infinite inclined plane (Fig. 4.1.b) and suggested that the inclined plane could be used to determine the rheological properties of the liquid in question at low shear rates. The approach used involved the derivation of expressions for shear rate and shear stress at the surface of the plane as follows:-

The velocity at distance y from the surface can be expressed as

$$u = u_{slip} + \int_0^y (\frac{du}{dy})dy \qquad \text{.....4.2.6}$$

and the volume flowrate per unit width of the plane as

$$V_w = h u_{slip} + \int_0^h y(\frac{du}{dy})dy \qquad \text{.....4.2.7}$$

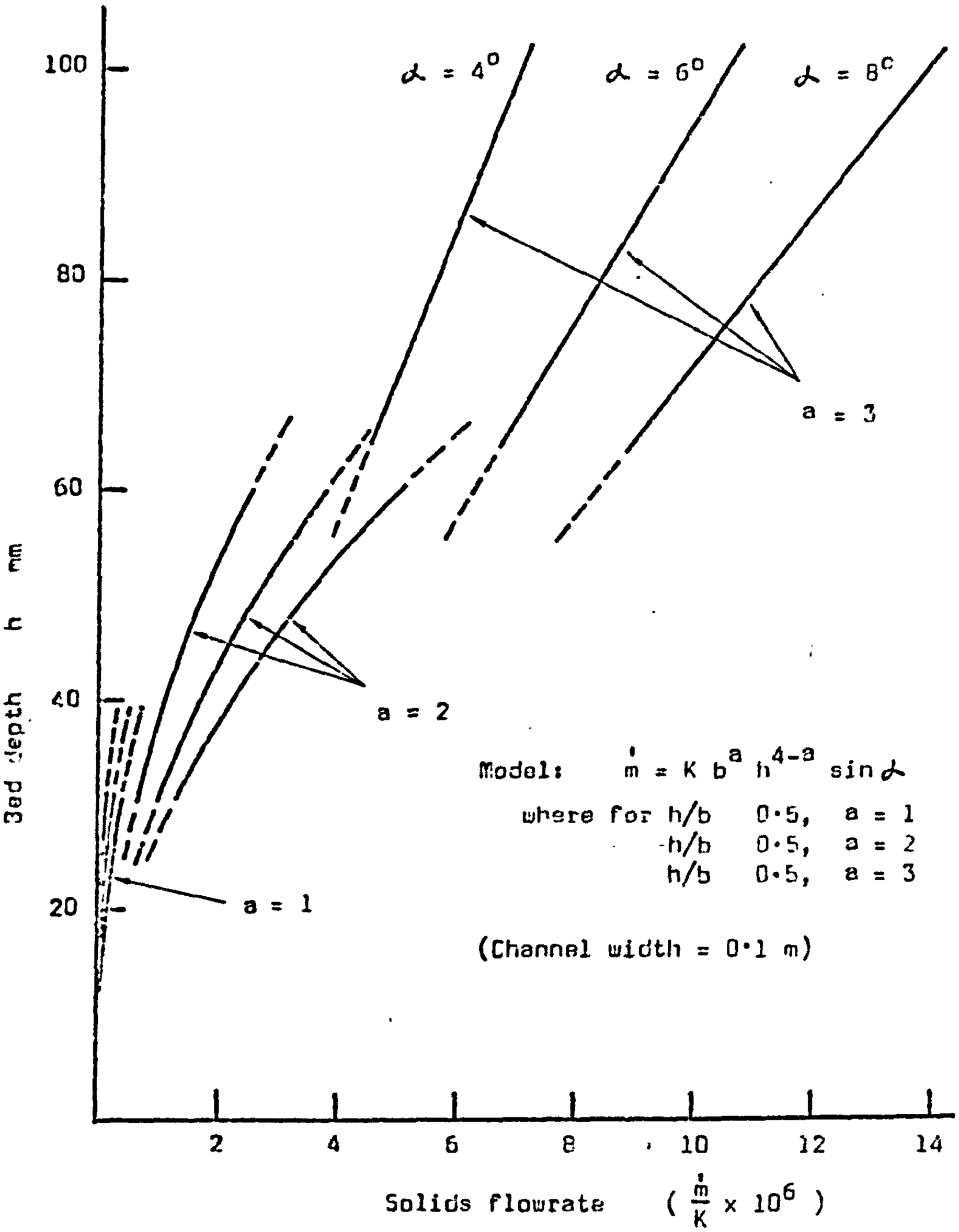

Fig. 4.2 PLOT OF BED DEPTH AGAINST SOLIDS FLOWRATE FROM THE MODEL OF CHANDELLE (Ref. C3) WITH CONSTANT K.

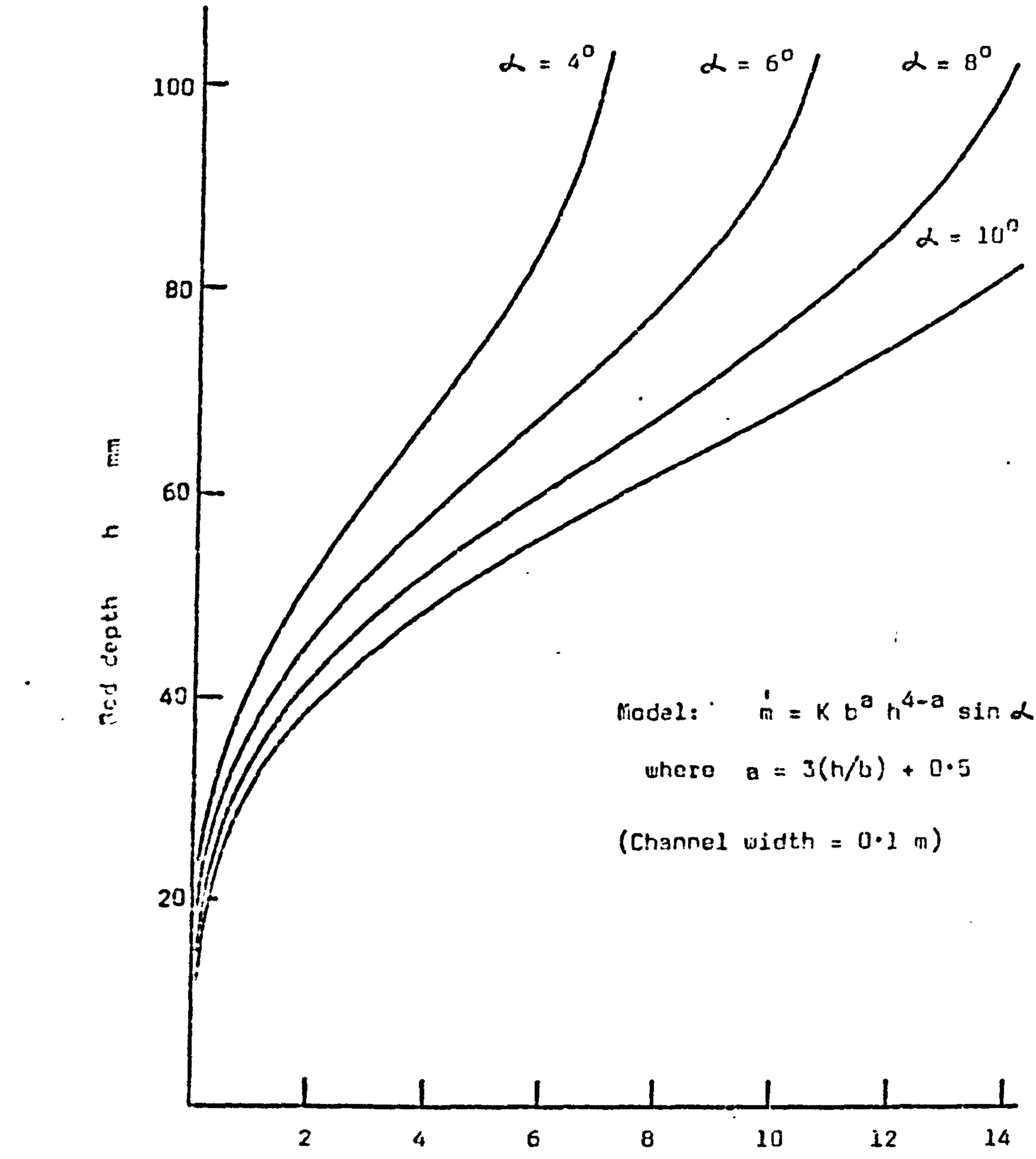

Fig. 4.3 PLOT OF BED DEPTH AGAINST SOLIDS FLOWRATE FROM IMPROVED MODEL WITH CONSTANT K.

where h is the thickness of the liquid layer and u_{slip} is the slip velocity at the surface of the plane. Manipulation of equation 4.2.7 leads to an expression for the shear rate at the plane surface as

$$\dot{\gamma} = \left(\frac{du}{dy}\right)_{y=0} = \frac{\dot{V}_w}{h^2}\left[\left(\frac{\partial \ln \dot{V}_w}{\partial \ln h}\right)_\alpha - \frac{u_{slip}\, h}{\dot{V}_w}\left\{1 + \left(\frac{\partial \ln u_{slip}}{\partial \ln h}\right)_\alpha\right\}\right] \quad \ldots\ldots 4.2.8$$

where the suffix α indicates constant slope of the plane.

Noting that the term $u_{slip}\, h/\dot{V}_w$ represents the fraction of the total flowrate which is due to slip at the plane surface, it is seen that for zero slip equation 4.2.8 simplifies to

$$\dot{\gamma} = \frac{\dot{V}_w}{h^2}\left(\frac{\partial \ln \dot{V}_w}{\partial \ln h}\right)_\alpha \quad \ldots\ldots 4.2.9$$

and for this case, with the aid of a log-log plot of experimental measurements of $\dot{V}_w$ and h, values of the shear rate at the plane can be determined.

The shear stress at the surface of the plane is given by

$$\tau_b = \rho g h \sin\alpha \quad \ldots\ldots 4.2.10$$

derived from a force balance, and thus curves of shear rate $\dot{\gamma}$ against shear stress τ_b may be plotted for the liquid.

Extending the analysis to cover different values of α, Astarita et al derive the expression

$$\left(\frac{\partial \ln h}{\partial \ln \sin\alpha}\right)_{\dot{V}} = \left(\frac{2\dot{V}_w - u_{slip}\, h}{\dot{V}_w}\right)\left(\frac{\partial \ln h}{\partial \ln \dot{V}_w}\right)_\alpha - 1 \quad \ldots\ldots 4.2.11$$

and noting that $0 < u_{slip} < \dot{V}_w/h$ it is clear that the parameters

$$\left(-\frac{\partial \ln h}{\partial \ln \sin\alpha}\right)_{\dot{V}} \quad \text{and} \quad \left(\frac{\partial \ln h}{\partial \ln \dot{V}_w}\right)_\alpha$$

must lie on the plot shown in Fig. 4.4 within the shaded region between lines LM, corresponding to $u_{slip} = 0$, and LN, corresponding to $u_{slip} = \dot{V}_w/h$.

Astarita et al also show that Newtonian fluids exhibiting no slip at the surface of the inclined plane are represented by the point $(\frac{1}{3},\frac{1}{3})$ on Fig. 4.4. Pseudoplastics for which there is no slip lie on the upper part of line LM and dilatant fluids lie on the lower part. A Newtonian fluid that does slip at the surface can be represented by line PQ for which the parameters

$$\left(-\frac{\partial \ln h}{\partial \ln \sin \alpha}\right)_{\dot{V}} \qquad \text{and} \qquad \left(\frac{\partial \ln h}{\partial \ln \dot{V}_w}\right)_{\alpha}$$

are equal. Pairs of corresponding values of these parameters obtained from experimental log-log plots of h against $\sin\alpha$ and h against $\dot{V}_w$ could thus be plotted on Fig. 4.4 where they should give a useful indication of the nature of the flow, and especially of the magnitude of the slip velocity.

A variation on this approach was adopted by Bessant (Ref. B3). He suggested that the slip velocity does not change significantly with variations in the depth of the flowing fluid and therefore the partial derivative of equation 4.2.7

$$\left(\frac{\partial \dot{V}_w}{\partial h}\right)_{\alpha} = u_{slip} + h\left(\frac{\partial u_{slip}}{\partial h}\right)_{\alpha} + h\left(\frac{du}{dy}\right)_{y=0} \qquad \ldots\ldots\ldots\ldots 4.2.12$$

can be written

$$\left(\frac{\partial \dot{V}_w}{\partial h}\right)_{\alpha} = u_{slip} + h\left(\frac{du}{dy}\right)_{y=0} \qquad \ldots\ldots\ldots\ldots 4.2.13$$

Plotting $\dot{V}_w$ against h then allows u_{slip} to be determined as the slope of the curve at h = 0, and the shear rate at the surface of the plane from

$$\dot{\gamma} = \left(\frac{du}{dy}\right)_{y=0} = \frac{1}{h}\left[\left(\frac{\partial \dot{V}_w}{\partial h}\right)_{\alpha} - \left(\frac{\partial \dot{V}_w}{\partial h}\right)_{\alpha,\ h=0}\right] \qquad \ldots\ldots\ldots\ldots 4.2.14$$

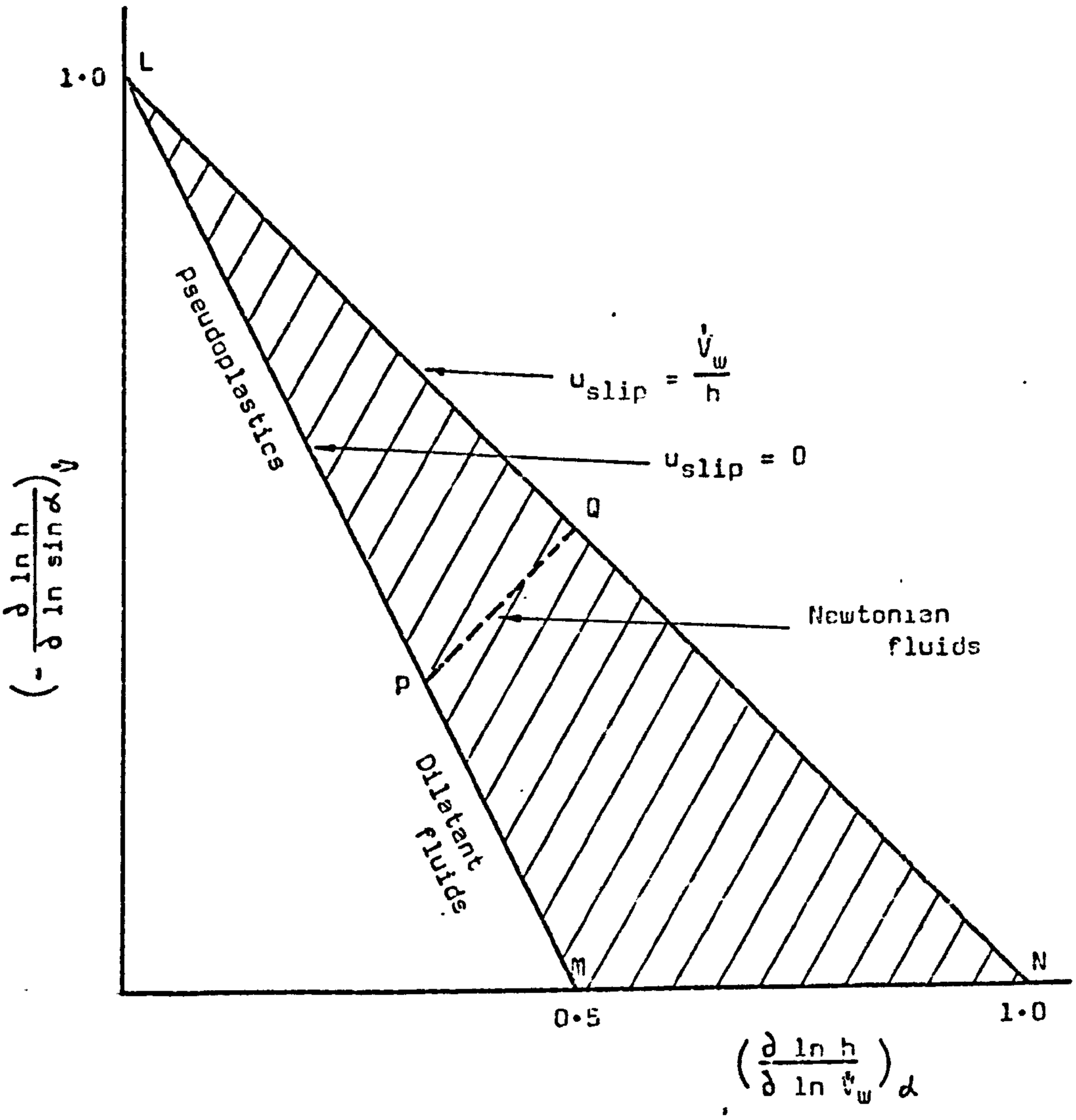

Fig. 4.4. RANGE OF POSSIBLE VALUES OF THE PARAMETERS

$\left(-\frac{\partial \ln h}{\partial \ln \sin \alpha}\right)_V$ AND $\left(\frac{\partial \ln h}{\partial \ln V_w}\right)_\alpha$ FOR THE LAMINAR FLOW

OF A NON-NEWTONIAN LIQUID ON AN INCLINED PLANE.

Suzuki and Tanaka (Ref. S19) extended the method of Astarita et al, outlined above, taking into account the variation of velocity across the width of a rectangular channel, in order to model the gravity flow of powders down steeply inclined channels (30 - 40^{o}). Their computation of shear rate was rather complicated and the resulting data very scattered, but there was evidence to suggest that the flowing powder tended towards Bingham plastic behaviour.

Other authors (Refs. B22, M4, P9, S8) have commented upon the tendency for aerated bulk solids to exhibit characteristics of Bingham fluids, especially when flowing in a channel at a low average velocity. Only Shinohara et al (Ref. S8) appear to have made any serious attempt to correlate the solids flow behaviour with a detailed model based on a Bingham plastic. They used a two-dimensional model in which the velocity varied only through the depth of the flowing material (Fig. 4.1.c, and see Appendix A.III.7 and A.III.9). For this model they derived an expression for mass flowrate in terms of density ρ, coefficient of rigidity η and yield stress τ_y of the flowing material, the depth of the bed h, the width b and slope α of the channel and the slip velocity u_{slip} as

$$\dot{m} = \rho b \left[\frac{\rho g \sin\alpha}{3\eta} h^3 - \frac{\tau_y}{2\eta} h^2 + u_{slip} h + \frac{\tau_y^3}{6\eta(\rho g \sin\alpha)^2} \right] \quad .....4.2.15$$

which corresponds to equation A.III.66, the derivation of which is discussed in Appendix A.III.9. However, because of the practical difficulties of measuring the depth of a shallow flowing bed of aerated particles, Shinohara et al rearranged equation 4.2.15, introducing u_{max}, the average velocity on the surface of the bed, as the dependent variable in place of h.

$$\text{Thus} \quad \eta = \frac{4.5 g \sin\alpha}{\rho_s (u_{max} - u_{slip})(2u_{max} + u_{slip})^2} \left(\frac{\dot{m}_s}{b} - \frac{u_{max} \tau_y}{g \sin\alpha} \right)^2 \quad .....4.2.16$$

and by substitution of sets of measured values of $\dot{m}_s$, u_{max}, and α, the authors were able to determine η, τ_y and u_{slip} at various superficial air velocities. However, there is little evidence to show the extent of the agreement between this model and the actual behaviour of the flowing bed of glass beads with which they worked.

Several authors (Refs. B17, B18, M4, M6, P9) have attempted to develop a general three-dimensional analysis by adapting the method used by Metzner and Reed (Ref. M8) for non-Newtonian flow in circular pipes (see Appendix A.III.6). In this method a modified Reynolds number is defined as

$$Re' = \frac{(4\lambda)^n u_{av}^{2-n} \rho}{k 8^{n-1}} \qquad \ldots\ldots\ldots\ldots\ldots\ldots 4.2.17$$

where λ is a hydraulic mean depth, the definition of which is

$$\lambda = \frac{bh}{b + 2h} \qquad \ldots\ldots\ldots\ldots\ldots\ldots 4.2.18$$

and n, k are respectively the power-law index and consistency coefficient as defined by the fundamental equation for the Ostwald power-law fluid

$$\tau = k\dot{\gamma}^n \qquad \ldots\ldots\ldots\ldots\ldots\ldots 4.2.19$$

An expression for friction factor can be derived in the usual way from the defining equation

$$f = \frac{\tau_o}{\frac{1}{2}\rho u_{av}^2} \qquad \ldots\ldots\ldots\ldots\ldots\ldots 4.2.20$$

in which τ_o is the average shear stress over the internal surfaces of the channel.

Writing $$\tau_o = \rho g \lambda \sin\alpha \qquad \ldots\ldots\ldots\ldots\ldots\ldots 4.2.21$$

then allows values of f to be calculated from experimental measurements of average velocity over a range of flow conditions, from

$$f = \frac{2 g \lambda \sin\alpha}{u_{av}^2} \qquad \ldots\ldots\ldots\ldots\ldots\ldots 4.2.22$$

Both McGuigen (Refs. M4, M6) and Pugh (Refs. P9, M3) processed most of their channel flow data in this way, plotting τ_o ($= \rho g \lambda \sin\alpha$) against $\dot{\gamma}$ ($\approx 8 u_{av}/\lambda$) in order to obtain values for the parameters k and n, and then using these values to calculate Re' from equation 4.2.17 so that a

dimensionless plot could be made of Re' against f. Although McGuigan and Pugh obtained good correlation of this dimensionless plot to the line $f = 16/Re'$, it is not easy to make practical use of the result because of a wide fluctuation of the power-law index n and the consistency coefficient k, particularly the latter. The range of values reported by these authors (Ref. MG) were (in coherent SI units):-

$$n = 0.72 \text{ to } 1.0 \quad \text{and} \quad k = 0.03 \text{ to } 0.40$$

Much of the difficulty encountered in this approach seems to stem from the adaptation of the relatively simple model of axi-symmetric flow in a circular pipe to the much more complex three-dimensional situation that occurs in a channel. Detailed derivations and discussions of power-law fluid and Bingham plastic models applied to non-Newtonian flow in inclined channels is undertaken in Appendix A.III. Attention is particularly drawn to the work of Kozicki and Tiu (Ref. K7) who show the development from the Rabinowitsch-Mooney equation of generalised expressions for average velocity and Reynolds number in non-Newtonian fluid flow in channels of various shapes.

An alternative approach, in which an attempt is made to allow for different shear behaviour at the walls and at the base of the channel is introduced in the following Section.

4.3 A NEW GENERAL MODELLING APPROACH

4.3.1 Introduction

Because of the complexity of the flow of aerated bulk solids it is very unlikely that a rigorous analytical treatment, taking into account the many variables, will ever be feasible. Some attempts at modelling, mostly based on the laminar flow of non-Newtonian fluids, have been discussed in the previous Section, and now a more general approach, albeit still employing the concept of the fluid continuum, will be introduced. The purpose of this tactic is to develop a modelling technique that will enable the flow behaviour of aerated particulate bulk solids in inclined channels to be described with acceptable accuracy by a minimum number of parameters. In this way, comparison of various types

of particulate materials is made easier and prediction of the flow behaviour of one material from the results of tests on another should be possible with much greater confidence than has hitherto been the case.

As remarked above, the construction of this model begins with a fluid continuum in uniform flow in an inclined channel. The width of the channel is b and the angle of inclination is α. At some given flow condition the depth of the flowing fluid is h, the average velocity is u_{av} and the average shear stresses are τ_w at the channel walls and τ_b at the channel bottom (Fig. 4.5). For steady uniform flow the gravity force on the fluid is balanced by the shear forces, so that for the element of length δL shown, the equation of motion is

$$(2\tau_w h + \tau_b b)\,\delta L - \rho g h b\,\delta L \sin\alpha = 0 \qquad \ldots\ldots\ldots\ldots\ldots\ldots 4.3.1$$

from which

$$h = \frac{b\tau_b}{\rho g b \sin\alpha - 2\tau_w} \qquad \ldots\ldots\ldots\ldots\ldots\ldots 4.3.2$$

where ρ is the density of the flowing fluid.

This can be regarded as the general expression giving the relationship between the depth of the flowing bed, the inclination of the channel and the boundary shear stresses. In order to develop the model further and subsequently to relate it to the real system of solids flow, we have to consider the relationships between τ_w, τ_b and other parameters such as the average solids flow velocity u_s and the superficial velocity of the fluidising air U_g.

For the moment the superficial air velocity will be regarded as constant so that in our fluid continuum model τ_w and τ_b are functions only of u_s. The flexibility of the model then allows these shear stresses to be zero (corresponding to total slip), constant, or proportional to the average velocity u_s raised to some power. Some of the variations on the basic model that could be investigated are:-

(i) τ_b constant and τ_w proportional to the velocity u_s.
(ii) τ_b and τ_w both proportional to u_s.
(iii) τ_w constant and τ_b proportional to u_s.

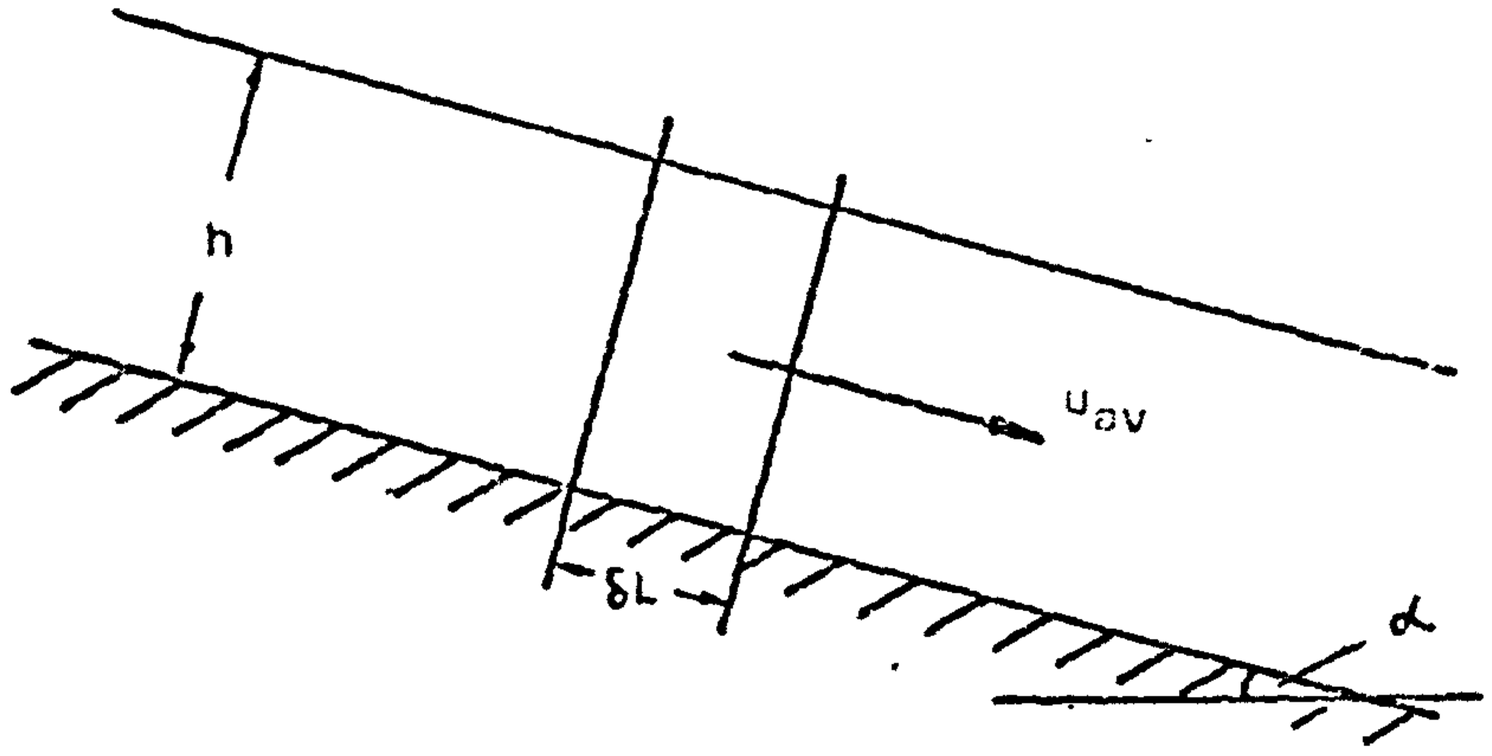

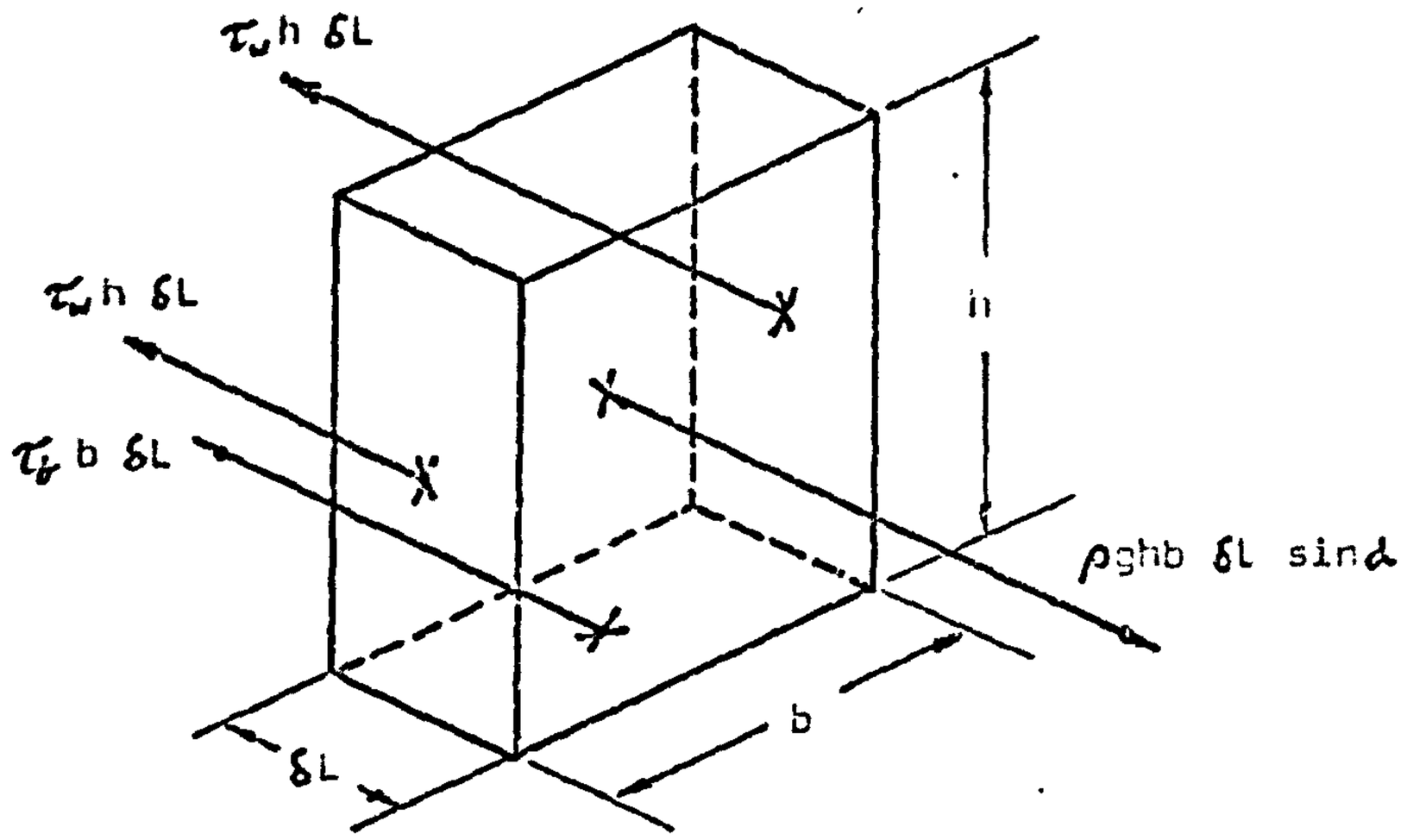

Fig. 4.5 FORCES ON AN ELEMENT OF FLUID IN STEADY UNIFORM FLOW ALONG AN INCLINED CHANNEL.

Clearly there are many other possible models and an infinite number of "shades" between them.

Very little is known about the way that the boundary shear stresses in an actual solids flow situation would be affected by the other parameters, and it is not easy to investigate this experimentally. Attempts have been made by Botterill and Bessant (Refs. B9, B16-18) to measure the wall shear stress using a movable section of wall mounted on a strain gauge measuring system. No quantitative results from these tests have been published which show directly the relationship between wall shear stress and solids flow velocity, but Botterill and Bessant do provide evidence that the wall shear stress is the dominant resistance except at low fluidising velocities and shear rates. There is thus little to indicate which of the above models might come closest to representing the actual solids flow behaviour in an inclined channel and in order to gain an insight to the influence of these parameters on each other, the above cases will be examined in more detail. It will become apparent that the modelling technique proposed really requires continuous comparison with experimental data. The numerical examples in the following Sections, based loosely on the flow of aerated sand, should therefore be regarded only as illustrative of the method; a more careful application to experimental data from the present programme will be developed in Part II.

4.3.2 Model with constant shear stress at the channel bottom and wall shear stress proportional to u_s.

Writing

$$\tau_w = k_w u_s \qquad \text{.....4.3.3}$$

or

$$\tau_w = k_w\left(\frac{\dot{m}}{\rho b h}\right) \qquad \text{.....4.3.4}$$

where $\dot{m}$ is the mass flowrate of the fluid (or suspension) and k_w is a constant, we have from equation 4.3.2

$$h = \frac{\rho b^2 \tau_b + 2 k_w \dot{m}}{\rho^2 b^2 g \sin\alpha} \qquad \text{.....4.3.5}$$

On rearranging, this becomes

$$\dot{m} = \frac{h \rho^2 b^2 g \sin\alpha}{2 k_w} - \frac{\rho b^2 \tau_b}{2 k_w} \qquad \text{.....4.3.6}$$

In the special case of total slip at the channel base, τ_b is zero, so that equation 4.3.6 reduces to

$$\dot{m} = \frac{h \rho^2 b^2 g \sin\alpha}{2 k_w} \qquad \text{.....4.3.7}$$

It is of interest to compare this equation with the expression for the mass flowrate of a Newtonian fluid in laminar flow in an inclined channel

$$\dot{m} = \frac{h \rho^2 b^3 g \sin\alpha}{12\mu} \qquad \text{.....4.2.1}$$

which may be written

$$\dot{m} = \frac{h^2 \rho^2 b^2 g \sin\alpha}{\mu} \left(\frac{1}{12} \cdot \frac{b}{h}\right) \qquad \text{.....4.3.8}$$

This is one of the expressions proposed by Siemes and Hellmer (Ref. S13) for the flow of aerated solids. (Note however, that the text of Siemes and Hellmer's paper gives the bracketed term of equation 4.3.8 incorrectly as 1/12.h/b).

Comparison of equations 4.3.7 and 4.3.8 shows that they are equivalent if the coefficient k_w is written as

$$k_w = \frac{6\mu}{b} \qquad \text{.....4.3.9}$$

It is worth also comparing equation 4.3.7 with that proposed by Chandelle (Ref. C3) and Descamps and Jodlowski (Ref. D4) as

$$\dot{m} = K b^a h^{4-a} \sin\alpha \qquad \text{.....4.2.4}$$

where K is a function involving ρ and μ, and the index 'a' takes a value of 1, 2 or 3 depending upon the aspect ratio h/b of the flow.

Whilst the exponents of h and b in equation 4.3.7 do not correspond exactly to equation 4.2.4, the form of the expressions is still the same.

Returning to equation 4.3.6, it is seen that this expression is of the same form as those just discussed, with the right-hand side reduced by a constant term to account for the shearing stresses on the bottom of the channel.

In order to make some preliminary assessment of the model defined by equation 4.3.6, plots can be made of h against $\dot{m}$ and h against α for typical (constant) values of ρ and b. It is convenient at this stage to select values of these parameters to correspond to the flow of aerated sand in a small channel. Thus we let $\rho = 1400$ kg/m^3 and b = 0.15 m.

Trial shows that the approximate order of magnitude of τ_b and k_w required in equation 4.3.5 (or 4.3.6) to yield plots approximating to the observed behaviour of sand would be

$$\tau_b = 3 \text{ to } 9.5 \text{ N/m}^2$$

$$k_w = 25 \text{ to } 55 \text{ N/m}^2 \text{ per m/s (or Ns/m}^3\text{)}$$

Taking values at the middle of these ranges, that is $\tau_b = 6.5$ N/m^2 and $k_w = 40$ Ns/m^3, Figs. 4.6 and 4.7 have been plotted from equation 4.3.5. Whilst they do give some confidence in this modelling technique through exhibiting the same patterns of lines seen in Figs. 3.22 to 3.26 for the flow of sand, it is clear that the correlations are not very satisfactory. Obvious discrepancies in this particular model are:-

(i) The lines on the plot of h against $\dot{m}$ are too spread out.

(ii) The curvature of the lines of h against α is too gradual.

(iii) The range of values of τ_b and k_w is too great. (They are intended to be constants)

(iv) The values of k_w are too high. (It is reasonable to expect τ_w and τ_b to be approximately the same, and since u_s is normally around 1 m/s, k_w should be of the same order of magnitude as τ_b.

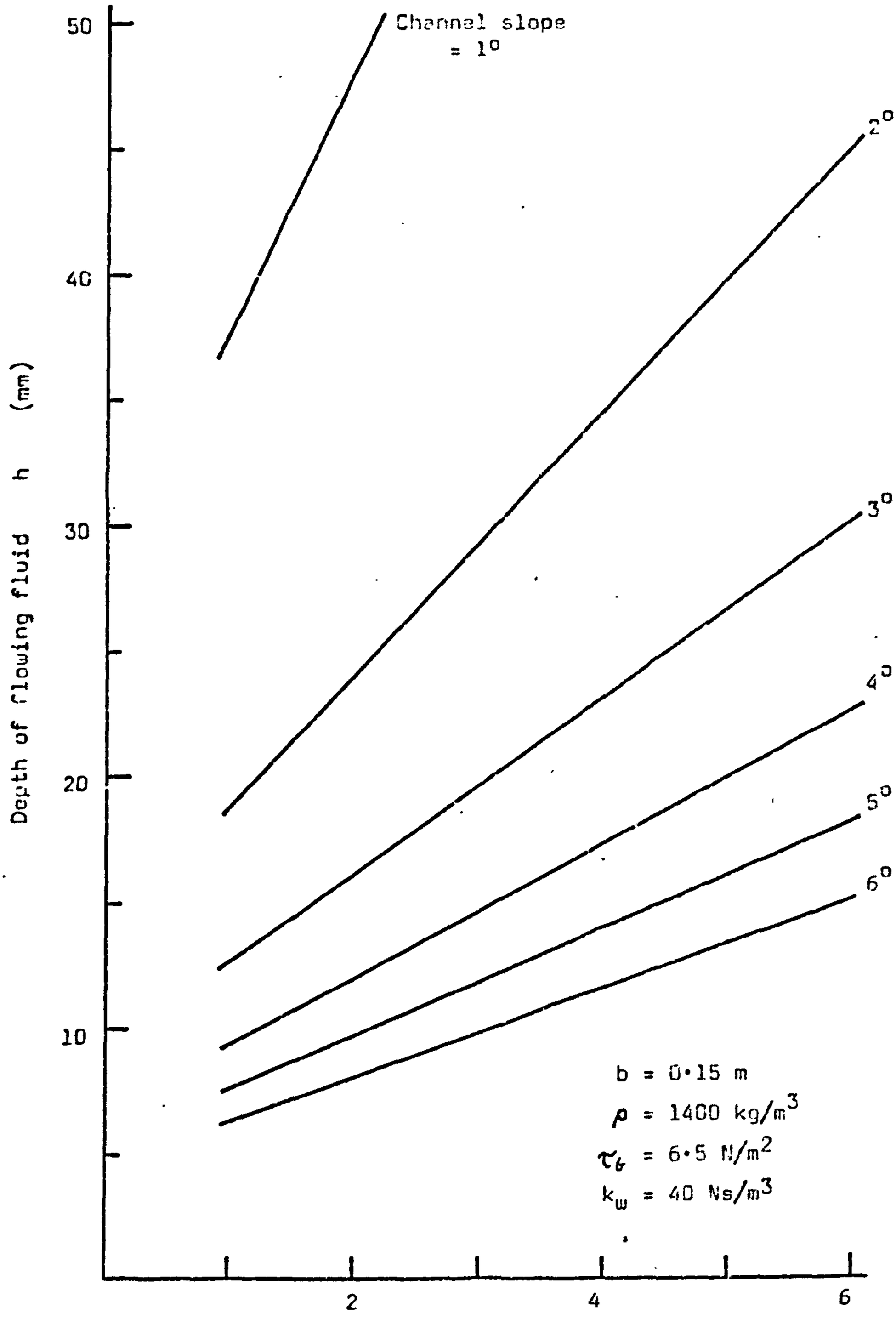

Fig. 4.6 PLOT OF EQUATION 4.3.5; model with constant shear stress at channel bottom and wall shear stress proportional to u_s.

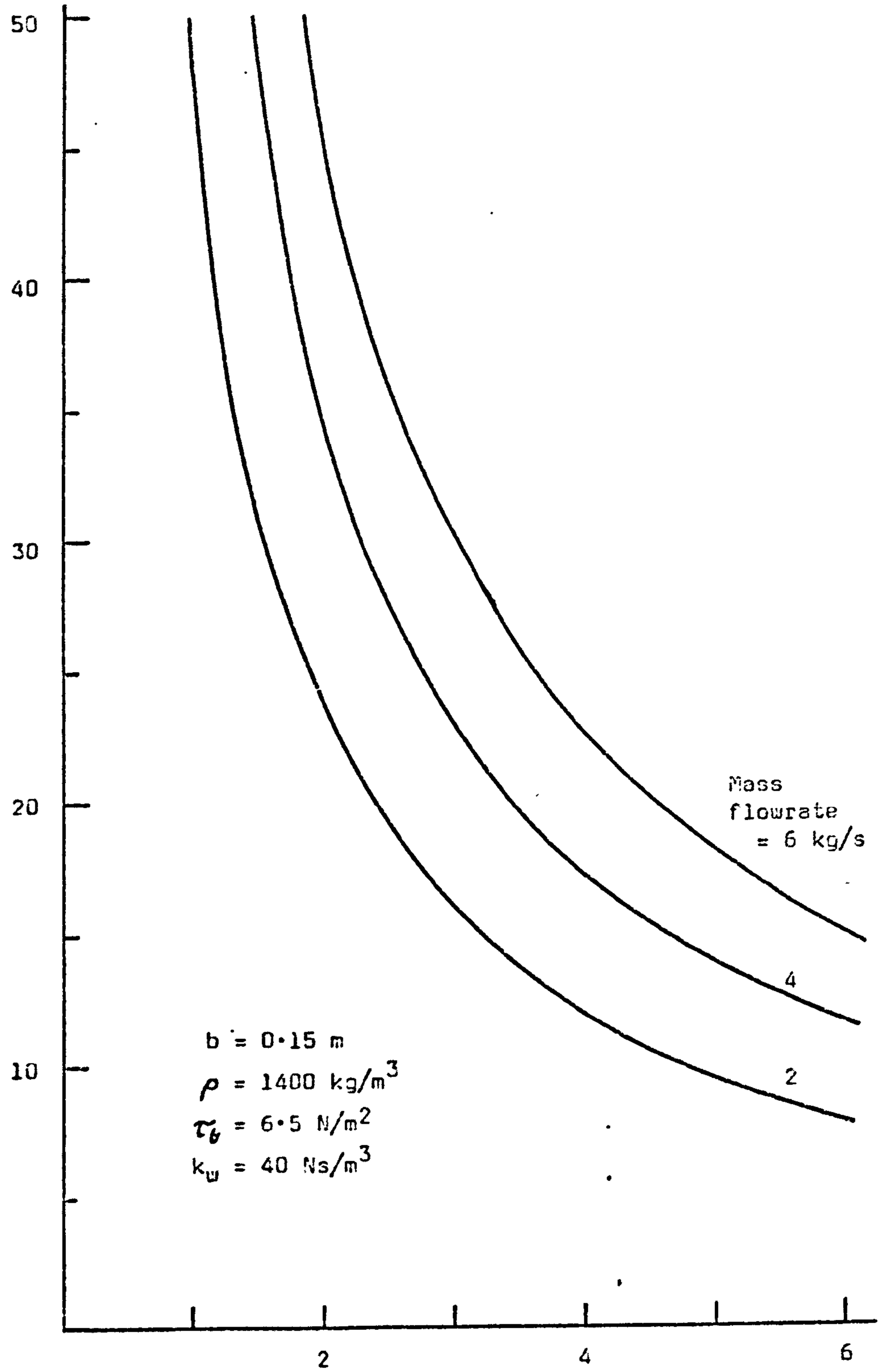

Fig. 4.7. PLOT OF EQUATION 4.3.5.

(v) The mathematical model (equation 4.3.6) suggests that, other parameters being constant, the mass flowrate is proportional to the square of the channel width, when a more reliable relationship would be $\dot{m} \propto b$.

Considerable "adjustment" can of course be made to this model by altering the values of τ_b and k_w. However, although in this way it might be possible to achieve a better "fit" to part of any given set of curves, it is unlikely that the net result would be satisfactory. At this stage it is felt to be prudent to examine another variation of the basic model.

4.3.3 Model with shear stress at the channel bottom and at the channel walls both proportional to u_s.

Substituting for τ_w as before, and also writing

$$\tau_b = k_b u_s \qquad \ldots\ldots\ldots\ldots\ldots\ldots 4.3.10$$

or

$$\tau_b = k_b \left(\frac{\dot{m}}{\rho b h}\right) \qquad \ldots\ldots\ldots\ldots\ldots\ldots 4.3.11$$

equation 4.3.1 becomes

$$\rho^2 g b^2 \sin\alpha h^2 - 2k_w \dot{m} h - b k_b \dot{m} = 0 \qquad \ldots\ldots\ldots\ldots 4.3.12$$

This is a quadratic in h, but may be more conveniently rearranged as

$$\dot{m} = \frac{\rho^2 g b^2 h \sin\alpha}{(2k_w h + k_b b)} \qquad \ldots\ldots\ldots\ldots\ldots\ldots 4.3.13$$

It may be noted that this expression is of the form

$$\dot{m} = G \rho^2 g b h^2 \sin\alpha \qquad \ldots\ldots\ldots\ldots\ldots\ldots 4.3.14$$

where

$$G = \frac{1}{(2k_w \frac{h}{b} + k_b)}, \quad \text{and is a function involving}$$

the boundary shear stresses and the aspect ratio h/b of the flow. Equation 4.3.14 is very close to that proposed by Chandelle (Ref. C3) and Descamps and Jodlowski (Ref. D4) for low values of the aspect ratio. Unfortunately, neither of these authors give any further information on the function G, and no typical values, and so further comparison is not possible.

Also, this was in essence the model used by Mori et al (Ref. M9) except that they chose to eliminate ρ as a variable and retain u_s by writing $\rho b h = \dot{m}/u_s$ in equation 4.3.13 so that

$$\dot{m} = b u_s^2 \left(\frac{2k_w \frac{h}{b} + k_b}{g \sin \alpha} \right) \qquad \text{.....4.3.15}$$

or

$$u_s = \frac{\rho g h \sin \alpha}{(2k_w \frac{h}{b} + k_b)} \qquad \text{.....4.3.16}$$

By plotting $\frac{h \sin \alpha}{u_s}$ against $\frac{h}{b}$, or by some similar method, it is then possible to determine values of k_w and k_b for any given superficial air velocity. Working with sand of about 200 μm mean particle size, Mori et al found that k_w and k_b varied with superficial air velocity as shown in Fig. 4.8. The extent to which these shear stress/velocity coefficients varied with other parameters was not indicated by Mori et al, except indirectly when determining graphically that the resistance to flow was proportional to the average solids velocity.

As in the previous Section, suitable values of the coefficients k_w and k_b may be determined by an iterative method to enable the model defined by equation 4.3.13 to represent the flow behaviour of sand. A reasonable correlation is obtained with $k_w = 20$ Ns/m^3 and $k_b = 10$ Ns/m^3, as is evident from plots made with these values, Figs. 4.9 and 4.10. Once again, some adjustment of the pattern of curves is possible by altering the values of k_w and k_b. Thus, for example, an increase in either of the coefficients would tend to reduce the depth at a given mass flowrate, with k_b having the greater influence at low flowrates (shallow beds). It should perhaps be remarked in passing that taking values of k_w and k_b to correspond to those given by Mori et al (see Fig. 4.8) results in a

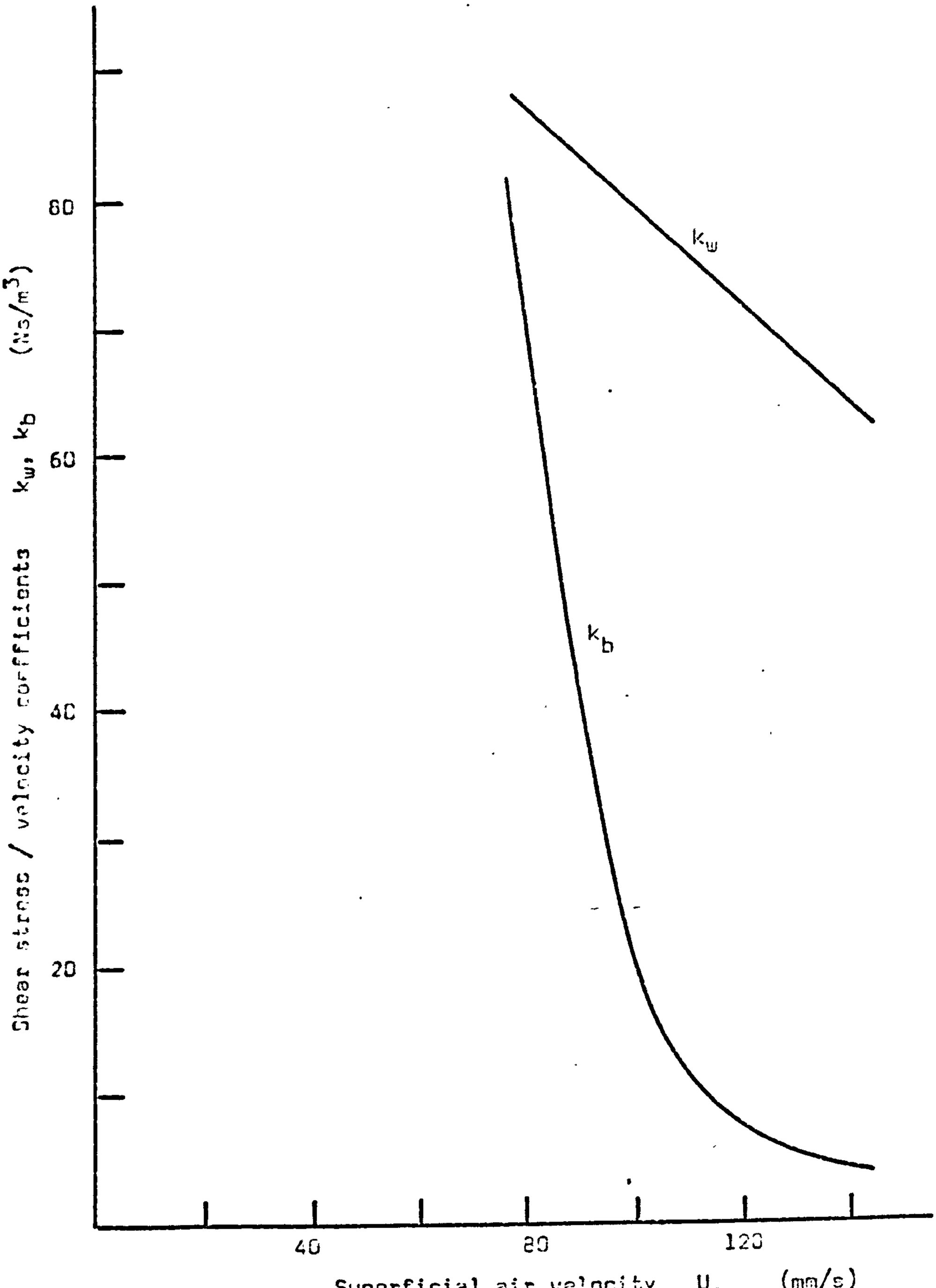

Fig. 4.8. VARIATION OF SHEAR STRESS/VELOCITY COEFFICIENTS WITH SUPERFICIAL AIR VELOCITY: from data of Mori et al for 200 μm sand (Ref. M9)

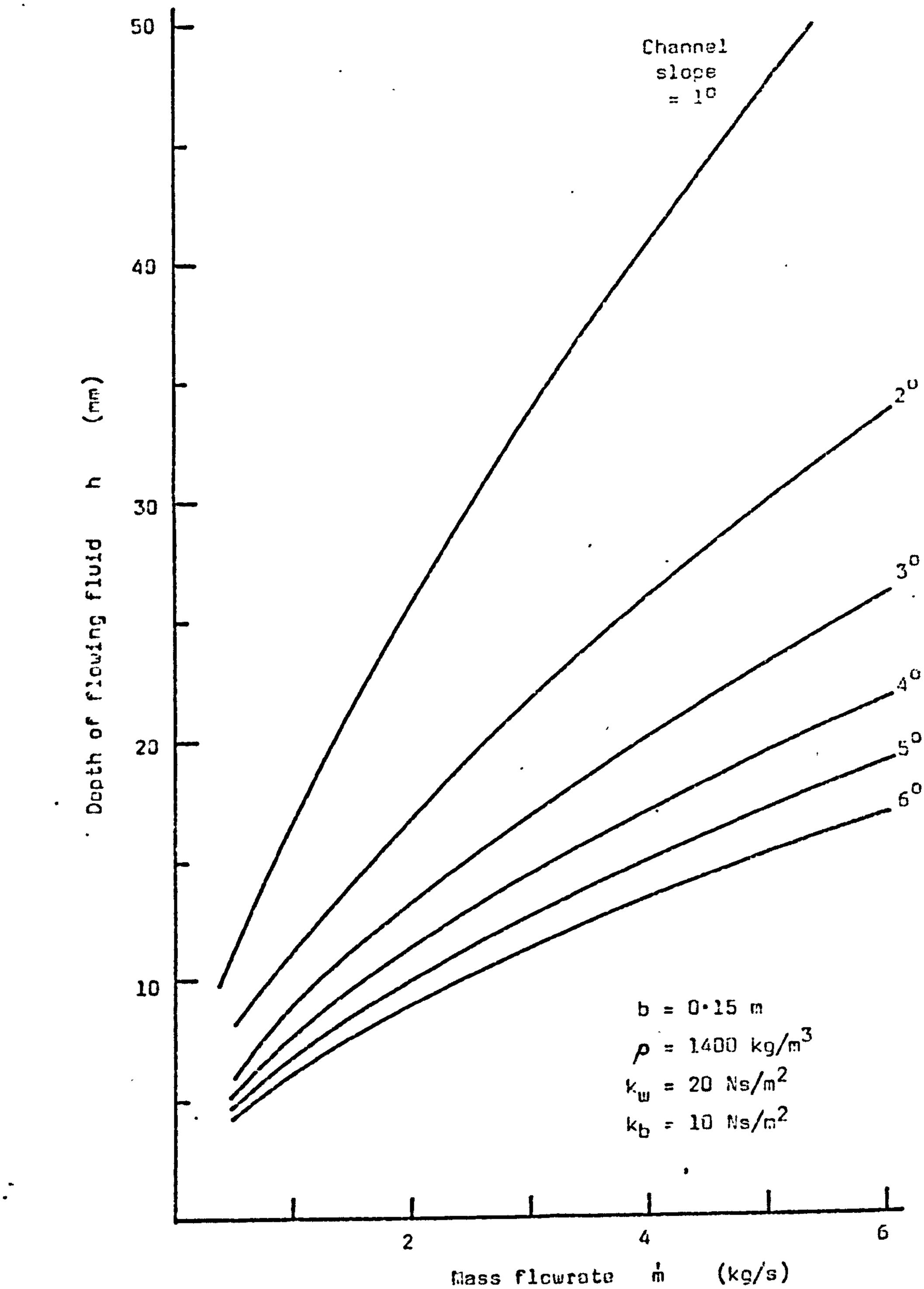

Fig. 4.9. PLOT OF EQUATION 4.3.13.

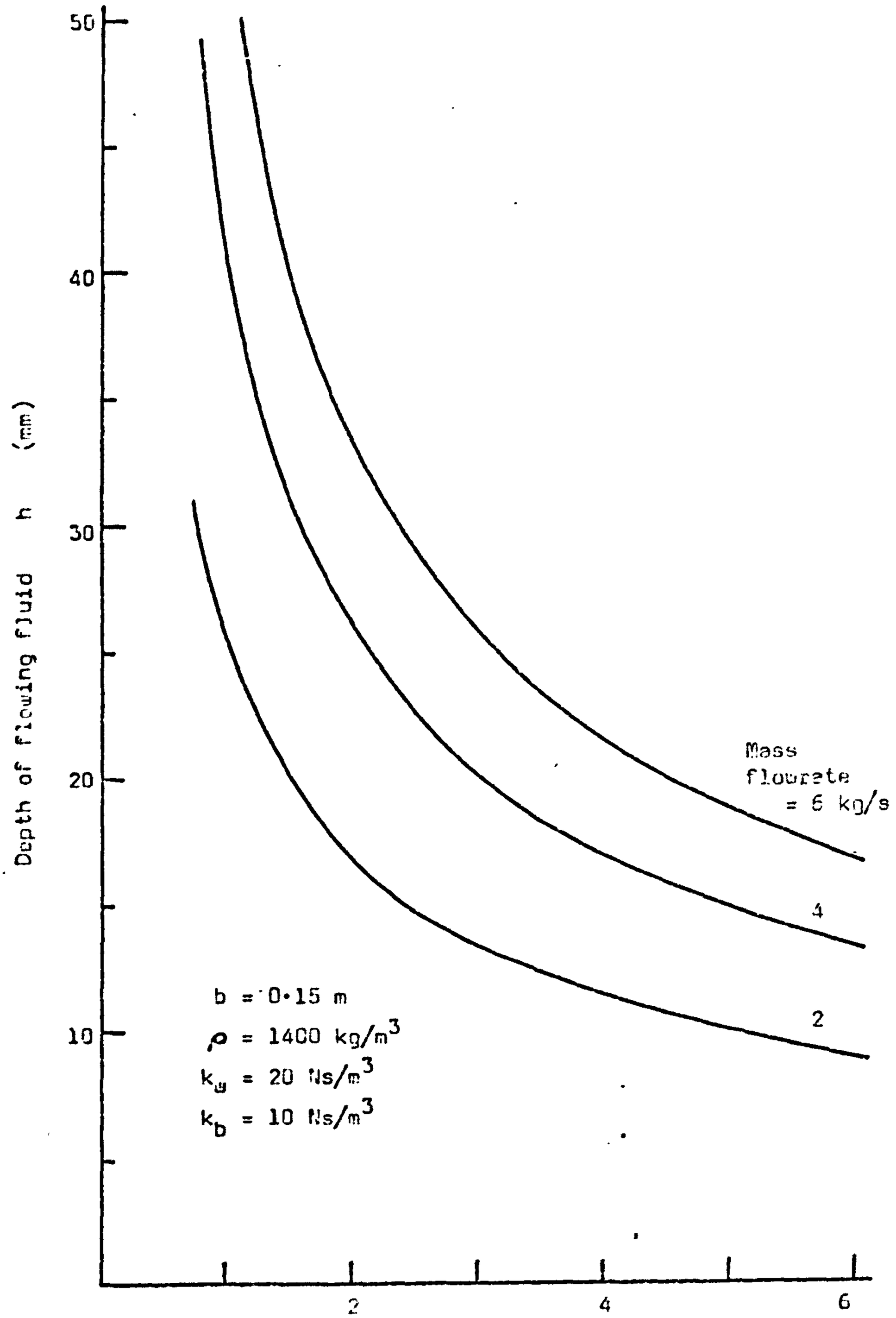

Fig. 4.10. PLOT CF EQUATION 4.3.13

substantial downward shift of the curves on Fig. 4.9. It may be significant that the channel used by Mori et al had a width of only 50 mm.

This mathematical model looks more promising than the previous one, but it still appears that the slope of the lines on the plot of h against $\dot{m}$ have a tendency to be too steep; that is, the model suggests that the bed depth is rather more sensitive to changes in mass flowrate than is in fact the case. However, before reaching any conclusion on this point, consideration will be given to another variant on the basic approach.

4.3.4 Model with constant shear stress at the side walls and shear stress at the channel bottom proportional to u_s.

Substituting for τ_b as in the previous case, but leaving τ_w as a constant, equation 4.3.2 now becomes

$$h = \left(\frac{k_b \dot{m}}{\rho^2 g b \sin\alpha - 2\rho\tau_w} \right)^{\frac{1}{2}} \qquad \ldots\ldots\ldots\ldots\ldots\ldots 4.3.17$$

from which

$$\dot{m} = \frac{\rho^2 g b^2 h \sin\alpha}{k_b} \cdot \frac{h}{b} - \frac{2\rho h^2 \tau_w}{k_b} \qquad \ldots\ldots\ldots\ldots 4.3.16$$

and again there are clear similarities between this mathematical model and those proposed by other authors, for example Siemes and Hellmer (equation 4.2.3). Equation 4.3.18 has a probable advantage over the models considered in Sections 4.3.2 and 4.3.3 in that the bed depth is less sensitive to changes in the mass flowrate ($h \propto \sqrt{\dot{m}}$), which seems to be in accord with observed flow behavicur.

A typical set of curves of h against $\dot{m}$ and h against α is plotted as Fig. 4.11 and 4.12, using $\tau_w = 3$ N/m^2 and $k_b = 12$ Ns/m^3 (which would correspond to an approximate range of τ_b from 3.5 to 20 N/m^2). With these values of τ_w and k_b the positions of the curves are similar to those constructed from equations 4.3.5 and 4.3.13.

In order to show how the positions of these model curves can be adjusted to match experimentally obtained data, graphs are plotted (Figs. 4.13 and

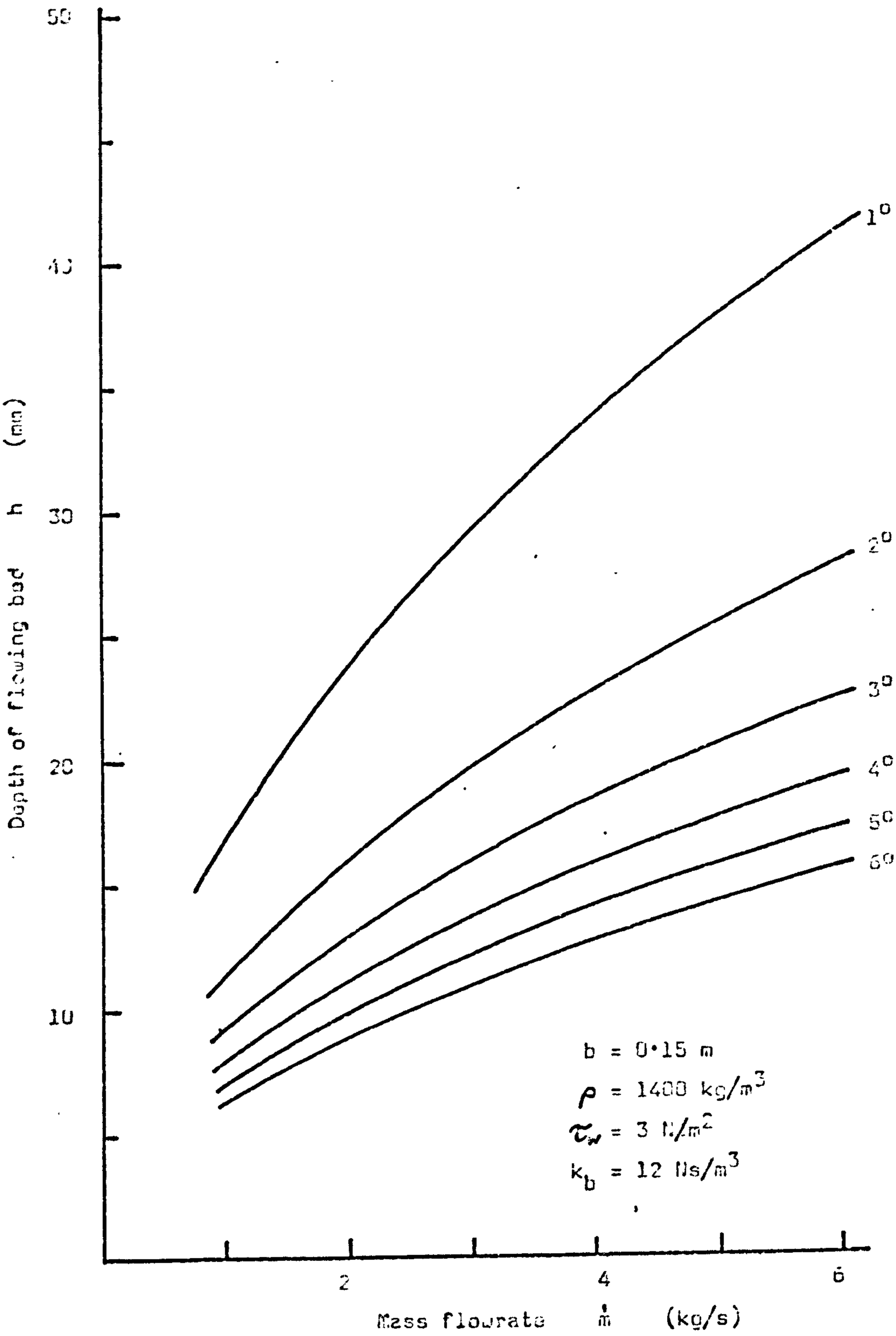

Fig. 4.11. PLOT OF EQUATION 4.3.18.

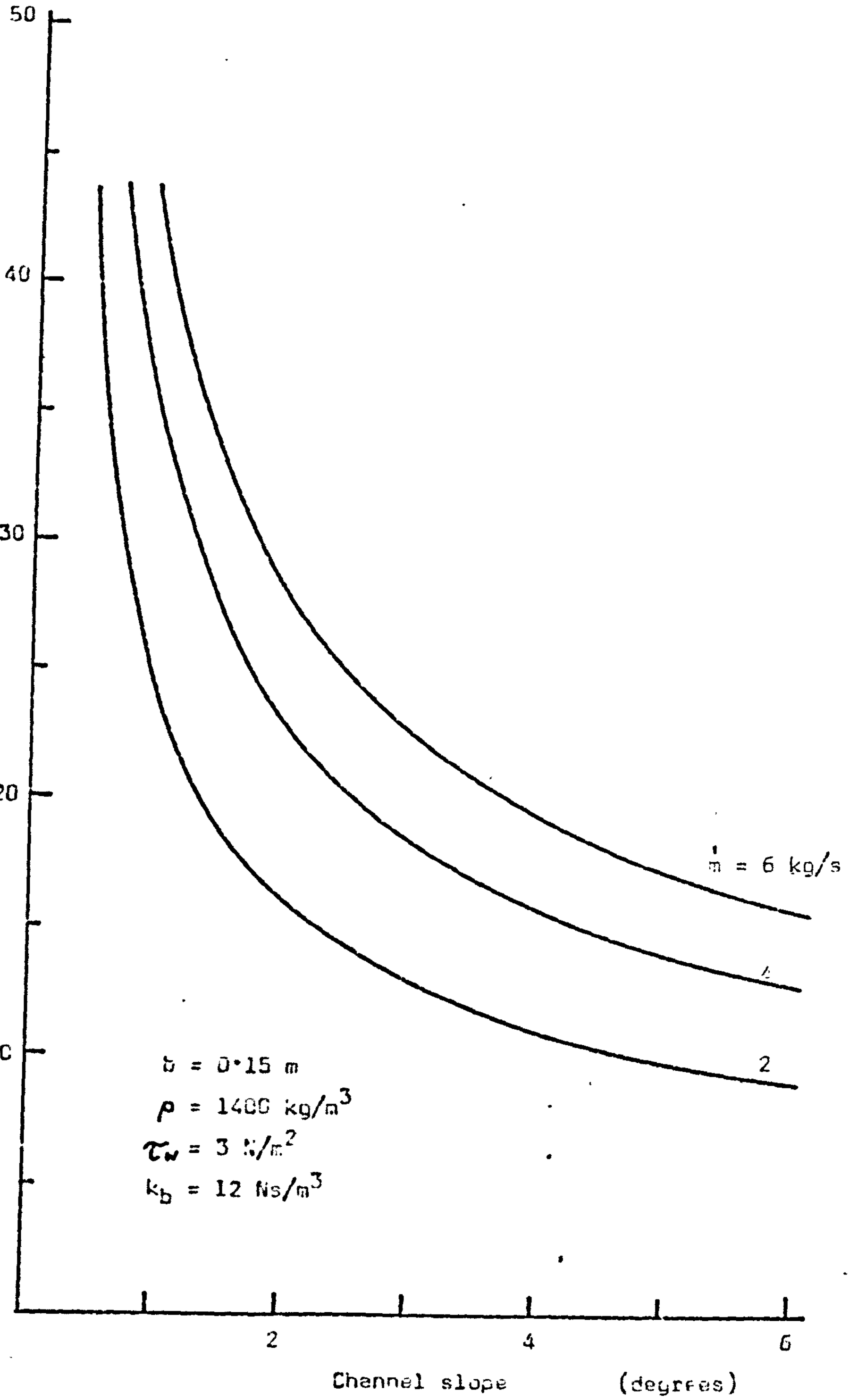

Fig. 4.12. PLOT OF EQUATION 4.3.18.

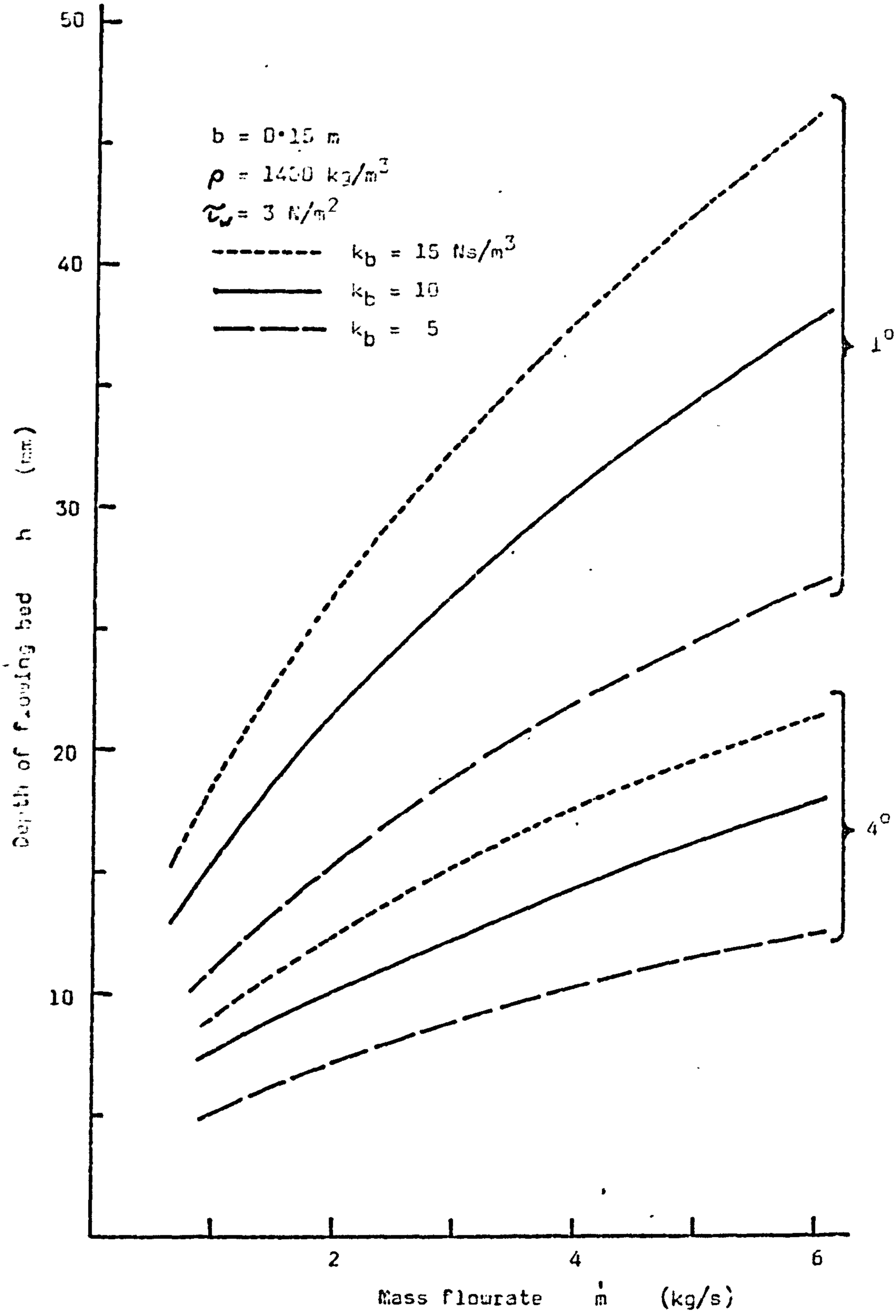

Fig. 4.13. PLOT OF EQUATION 4.3.18 SHOWING THE EFFECT OF VARYING THE SHEAR STRESS/VELOCITY COEFFICIENT, k_b.

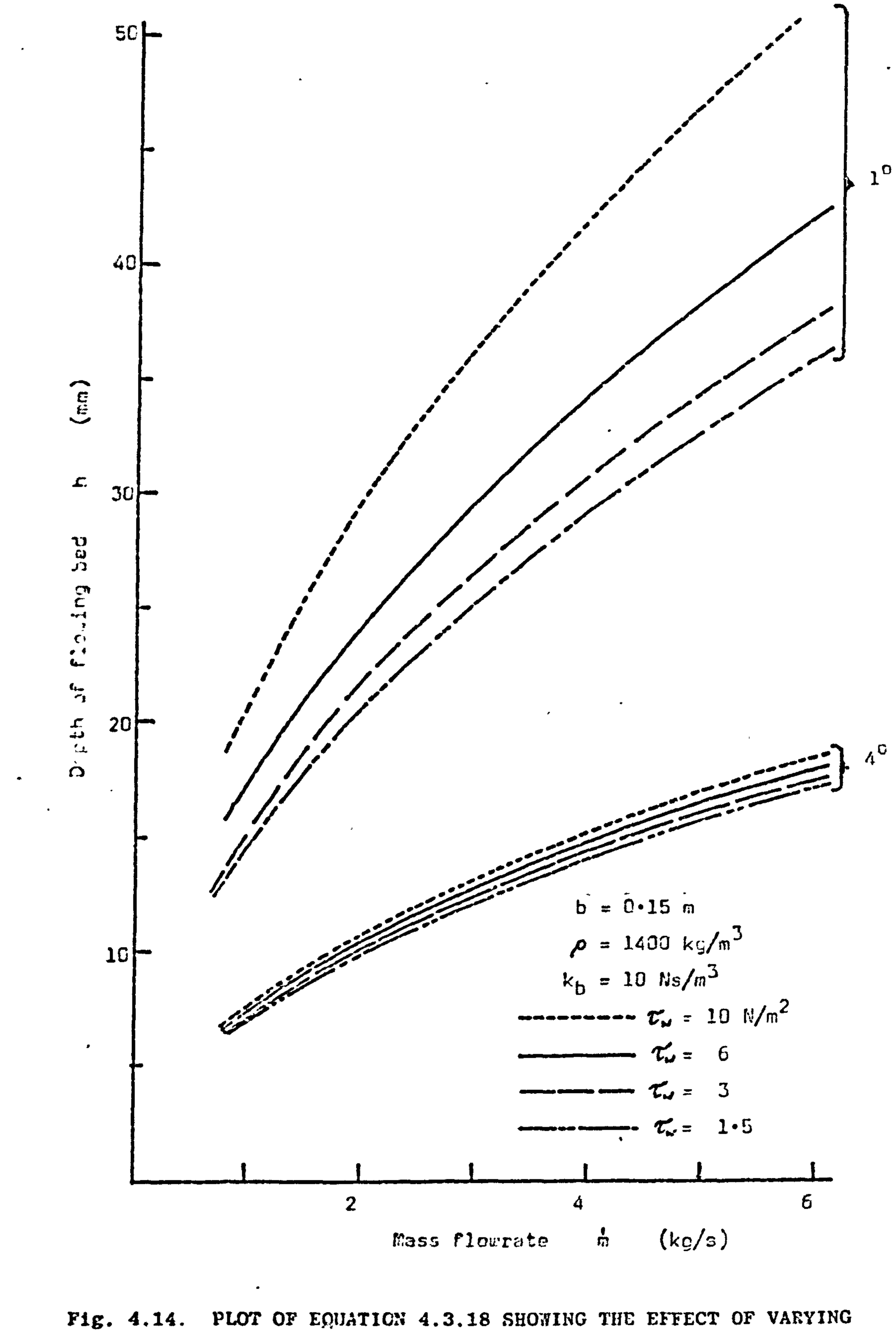

Fig. 4.14. PLOT OF EQUATION 4.3.18 SHOWING THE EFFECT OF VARYING THE SHEAR STRESS AT THE CHANNEL WALLS, τ_w.

4.14) with a range of values of the parameters τ_w and k_b. It is seen that whilst k_b has a significant influence on the depth of the flowing bed at all values of α considered, τ_w only gives rise to a significant shift of the curves at shallow channel slopes. Thus the procedure when matching experimental data would seem to be:-

1. Determine value of k_b to give correlation between model and experimental data on plot of h against $\dot{m}$ at relatively large angles of slope.
2. Adjust value of τ_w to give correlation between model and experimental data at shallow channel slopes.
3. Check value of k_b and then of τ_w to ensure correspondence of data.

It may be more convenient to express equation 4.3.18 in terms of two new parameters, K_1 and K_2, so that the mathematical model becomes

$$\dot{m} = K_1 \rho h^2 (\rho g b \sin\alpha - K_2) \qquad \text{.....4.3.19}$$

in which $K_1 = 1/k_b$ and $K_2 = 2\tau_w$.

For the model to be really useful, the parameters K_1 and K_2 should be approximately constant over a range of practical flow conditions and should bear some relationship to the size and density of the particulate material concerned so that a knowledge of these properties might allow a first estimate to be made of K_1 and K_2. Thus for instance, it might be anticipated that K_1 and K_2 would correlate with particle size and density in a manner corresponding to Geldart's classification of fluidisation behaviour.

Values of K_1 and K_2, and their dependence on other variables such as the superficial air velocity, will be discussed in more detail in Part II in the light of experimental data obtained, but as an example, for 200 μm sand, approximate values would appear to be around 0.08 and 5 respectively.

4.4. CONCLUSIONS

Although a full assessment cannot be made until the experimental data to be presented in Part II has been analysed, it seems at this stage that a mathematical model of the form

$$\dot{m} = K_1 \rho h^2 (\rho g b \sin\alpha - K_2) \qquad \text{.....4.3.19}$$

might conveniently represent the flow of an aerated particulate solid in an inclined channel. The parameters K_1 and K_2 are functions of the "nature" of the powder, the superficial velocity U_g of the fluidising air and the roughness of the channel.

A feature of this model is that for a given superficial air velocity, the shear stress at the channel wall is constant whilst that at the channel bottom is proportional to the average solids flow velocity. Other models involving variations on the dependence of boundary shear stresses on solids flow velocity have been considered, but this one appears initially to give the most satisfactory correlation with observed behaviour, consistent with ease of application.

Models of various forms proposed by other authors have been discussed at some length. Some, such as the purely empirical ones, seem to be of little value, whilst others, such as that of Chandelle/Descamps and Jodlowski (equation 4.2.4) suffers from a lack of information on the function K. The modelling approach based on a dimensionless plot of a modified Reynolds number against a friction factor is more promising, but suffers from the difficulty that the power-law index n and consistency coefficient k are not constant.

It is therefore concluded that the use of equation 4.3.19 is worth investigating further, particularly with regard to the values of parameters K_1 and K_2 and their dependence upon other system variables.

CHAPTER FIVE

CONCLUSION TO PART I

Perhaps the most striking single conclusion reached during the extensive survey of the literature relating to air-assisted gravity conveying is that the fundamental principle on which they operate is very simple and installations tend to work satisfactorily whether they have been carefully designed or not. The essential requirements are:-

1. The material to be conveyed must be free-flowing.
2. The width of the channel must be sufficient to handle the desired solids mass flowrate.
3. The slope of the channel must be sufficient to maintain the solids flow.
4. The fluidising air must be uniformly distributed and supplied at a sufficient rate to initiate and then to maintain the solids flow.

These requirements would usually be established by the manufacturer in pilot tests on a sample of the material to be conveyed, but unless care is taken at this stage, backed by an understanding of the mechanism of the flow of aerated solids, it is likely that the system will not be operating at its optimum condition. Furthermore, problems can arise through a gradual blinding of the distributor, through changes of moisture content of either the conveyed material or the fluidising air, or segregation in the conveyed material, and reliable control of the solids mass flowrate can also prove difficult to obtain. Thus there is clearly a need for a pooling of the considerable quantity of knowledge that has been obtained from practical experience with air-assisted gravity conveyors.

Part I of the present work endeavours to collect together such information as is available in the published literature. It is shown, for example, how an understanding of the phenomenon of fluidisation can be applied to the design of air-gravity conveyors in assessing the quantity of air required to transport a bulk solid of known density and particle

size. In this instance it is recommended that a very simple formula can give an adequate indication of the minimum fluidising velocity. There is probably nothing to be gained in attempting to use more complex methods of predicting U_{mf}, mainly because of uncertainty of the particle size and shape resulting from the difficulties of sampling, differences in definitions and methods of determining particle size and shape, and tolerances during production processes. At best the level of confidence that can be placed in predicted values of U_{mf} is quite low and there is much to be said for routine measurement of this quantity, for materials to be conveyed, in a suitable small fluidising vessel. Nevertheless, as a convenience to yield a first approximation to U_{mf} and to the terminal velocity U_t, a chart has been prepared (Fig. 2.13) showing these quantities plotted against particle size for a range of particle densities.

Study of the various parameters influencing the flow of aerated solids in inclined channels, or more generally, the parameters influencing the performance of air-assisted gravity conveyors, points again to the need for a better understanding of the relationships amongst these parameters. To this end, Chapter 3 involves a detailed discussion of the major influences on the performance of air-gravity conveyors, and is followed in Chapter 4 by a consideration of various approaches to modelling the flow of aerated powders in inclined channels. In this way the stage is set for further experimental programmes coupled perhaps with a partial re-analysis of previous research work. Part II of the present work will describe the design and construction of a major research facility, and will detail the first series of tests undertaken with a view to extending the knowledge available and gaining a deeper insight to the nature of the flow of aerated particulate bulk solids in inclined channels.

PART II

EXPERIMENTAL WORK

CHAPTER SIX

INTRODUCTION AND EXPERIMENTAL PLAN

The extensive survey of relevant literature undertaken within the framework of this research programme and described in Part I has shown that the amount of reliable data on the flow of aerated particulate bulk solids in inclined channels that is available for general reference is very small. Moreover, the prediction of the flow behaviour of powders under these conditions must be very doubtful as a design technique because of the lack of understanding of the mechanism of the flow. Similarities between the flow of aerated powders and the flow of liquids are of course well known, and have been used as the basis of models from which predictions can be made, but the number and complexity of the variables involved, and the shortage of experimental data, has limited the usefulness of such models.

The objectives of the current programme of work therefore include, not only the bringing together of published information and the introduction of possible modelling techniques (Part I), but also the development of a useful and practical experimental method for collecting, processing and correlating data on the flow of aerated particulate solids under realistic operating conditions.

The programme of experimental work in fact falls conveniently into two phases. The first phase deals with the behaviour of powders and granular bulk solids when aerated in a simple cylindrical vessel under conditions of no flow. Naturally this covers the familiar area of fluidisation and would therefore include some consideration of the porous fluidising media, characterisation of the particulate material, measurement of minimum fluidising velocity, bulk density and expansion of the fluidised bed, effects of electrostatic charging, and so on.

The second phase of the experimental programme involves the flow of the aerated powders in an inclined channel. One requirement here is to collect as much data as possible, in the time available, on the flow of one or more kinds of particulate material in order to correlate flow behaviour under different fluidising conditions with the behaviour of a

corresponding "stationary" bed. At the same time detailed consideration will be given to the relationships amongst the significant variables involved, with a view to assessing the modelling techniques discussed in Part I, Chapter 4. In this way it should be possible to obtain an indication of the most reliable combination of theoretical and experimental procedures for testing a particulate bulk solid in order to assess its suitability for transporting by air-assisted gravity conveyor.

CHAPTER SEVEN

FLUIDISATION STUDIES USING THE SMALL FLUIDISING RIG

7.1 INTRODUCTION

As previously mentioned, the first phase of the experimental programme described here involves conventional fluidisation tests on a range of different particulate solids in a small fluidising rig. The design and construction of the rig, described in detail in the next Section, is fairly standard and follows the general arrangement used by other researchers (for example, Refs. B30, C4, G5, K1, M4). Little information was available on the different types of porous distributor materials obtainable commercially and so some time was spent in acquiring a number of samples from manufacturers and assessing their advantages and disadvantages. The main features of the types of material are summarised elsewhere (Table 2.2 on page 33), and in this Chapter details of the comparative permeabilities of the various samples are given, along with some observations on the influence of the type of porous distributor on fluidisation behaviour.

Samples were also obtained of a representative range of different kinds of particulate material and the results of fluidisation tests on these samples are detailed in Section 7.4. It was on the basis of these test results that a decision was made on which powder to use for the experimental work in the main flow rig and, as described later, a powdered p.v.c. ("Corvic", supplied by I.C.I. Ltd.) was selected. However, before proceeding with the flow investigation a more rigorous series of tests was carried out on the Corvic in the small fluidising rig in order to learn as much as possible about its behaviour when aerated in a "stationary" condition. Section 7.5 gives details of these tests, and in the following Section is reported a similar series of tests undertaken on sand, by way of comparison. Although the p.v.c. powder was chosen as the main subject of the present programme, it was felt to be important to carry out a parallel study on a fine sand in view of the fact that this material is so familiar and has been used in the majority of previously reported experimental programmes. It is likely to be useful to compare the behaviour of these two quite different particulate solids and such a comparison should provide evidence which might be helpful when selecting other powders for future work.

7.2 DESIGN AND CONSTRUCTION OF RIG

The main purpose of the small fluidising rig was to permit preliminary tests to be carried out on samples of particulate solids in order to obtain information on their fluidisation characteristics and hence to assess their probable behaviour in an air-assisted gravity conveyor. Selected powders could then be tested in the main channel flow rig.

The small test rig, as constructed initially, is illustrated in Fig. 7.1 and consisted essentially of a cylindrical vessel of clear Perspex, separated from a lower plenum chamber by a flat sheet of porous material. The diameter of the vessel was 150 mm, which was felt to be small enough to enable realistic tests to be made with a minimum quantity of powder, without being so small that wall effects become significant. A scale fitted to the side of the cylinder allowed the depth of the powder bed to be estimated.

The porous base of the fluidising vessel was 200 mm square, and was supported by a cover plate having a hole 150 mm in diameter arranged to coincide with the cross-section of the vessel as shown in the diagram (Fig. 7.1). Four bolts secured the porous material and cover plate allowing easy removal so that different types of distributor could be investigated with minimum disturbance to the rig. Four more bolts, fitted with wing nuts, clamped the top part of the rig to the plenum chamber, thus enabling the cylinder and base to be lifted off as one unit in order to empty out the powder after each test.

The air supply to the plenum chamber originated from a Roots-type blower (the same blower that provided air for the main channel flow rig), the flowrate being controlled by manually-operated valves and measured by rotameters. The range of air flowrates that could be provided allowed the superficial air velocity in the fluidising vessel to be varied between 0 and 160 mm/s. The rotameters were calibrated using a water-displacement method as described in Appendix A.V, and charts were prepared to enable the rotameter scale reading to be converted directly to superficial air velocity in the fluidising vessel (Figs. 7.2 and 7.3).

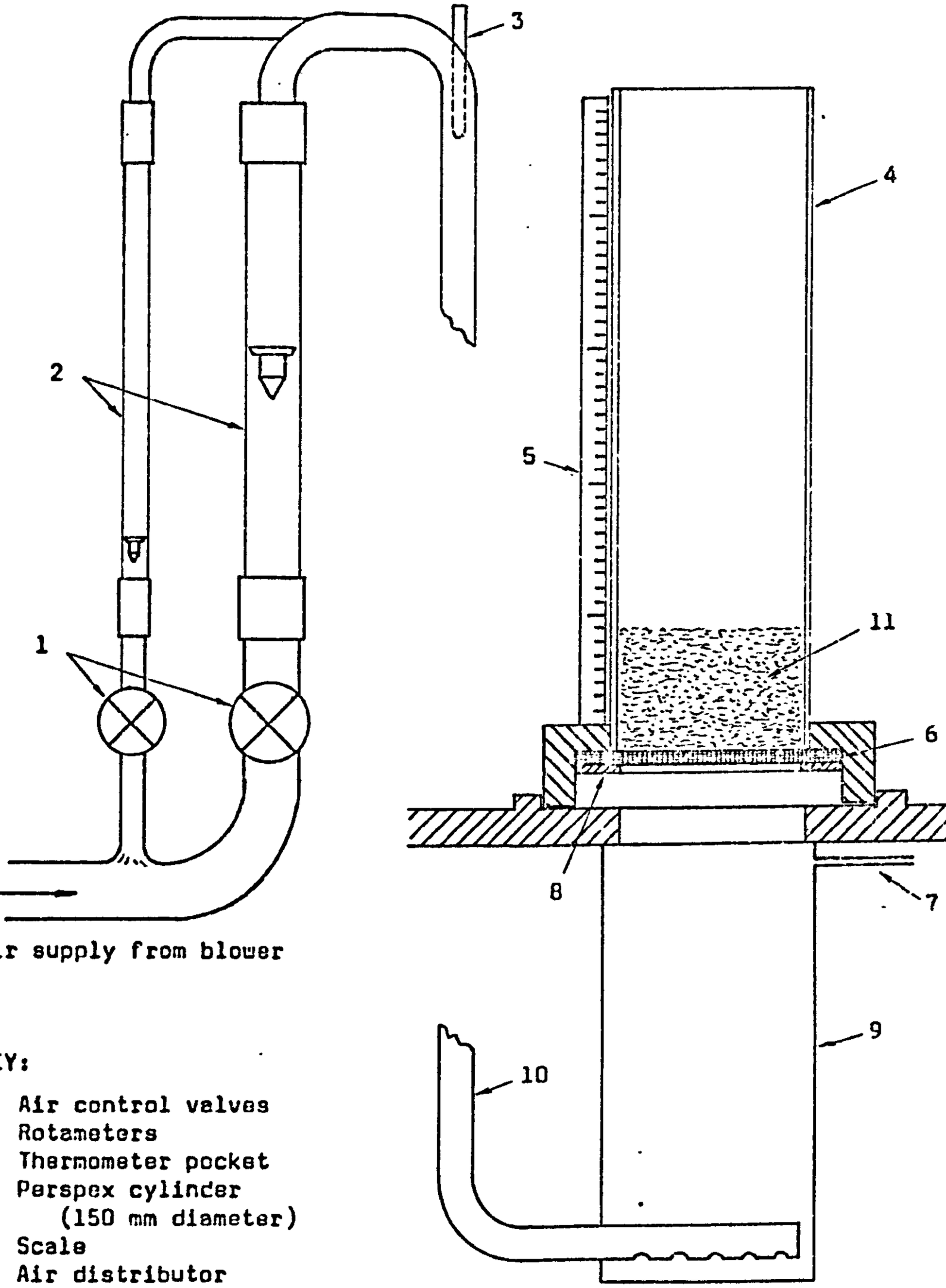

KEY:

1 Air control valves
2 Rotameters
3 Thermometer pocket
4 Perspex cylinder
(150 mm diameter)
5 Scale
6 Air distributor
7 Pressure tapping
8 Cover plate
9 Plenum chamber
10 Air supply to plenum chamber
11 Powder under test

Fig. 7.1. THE SMALL FLUIDISING TEST RIG

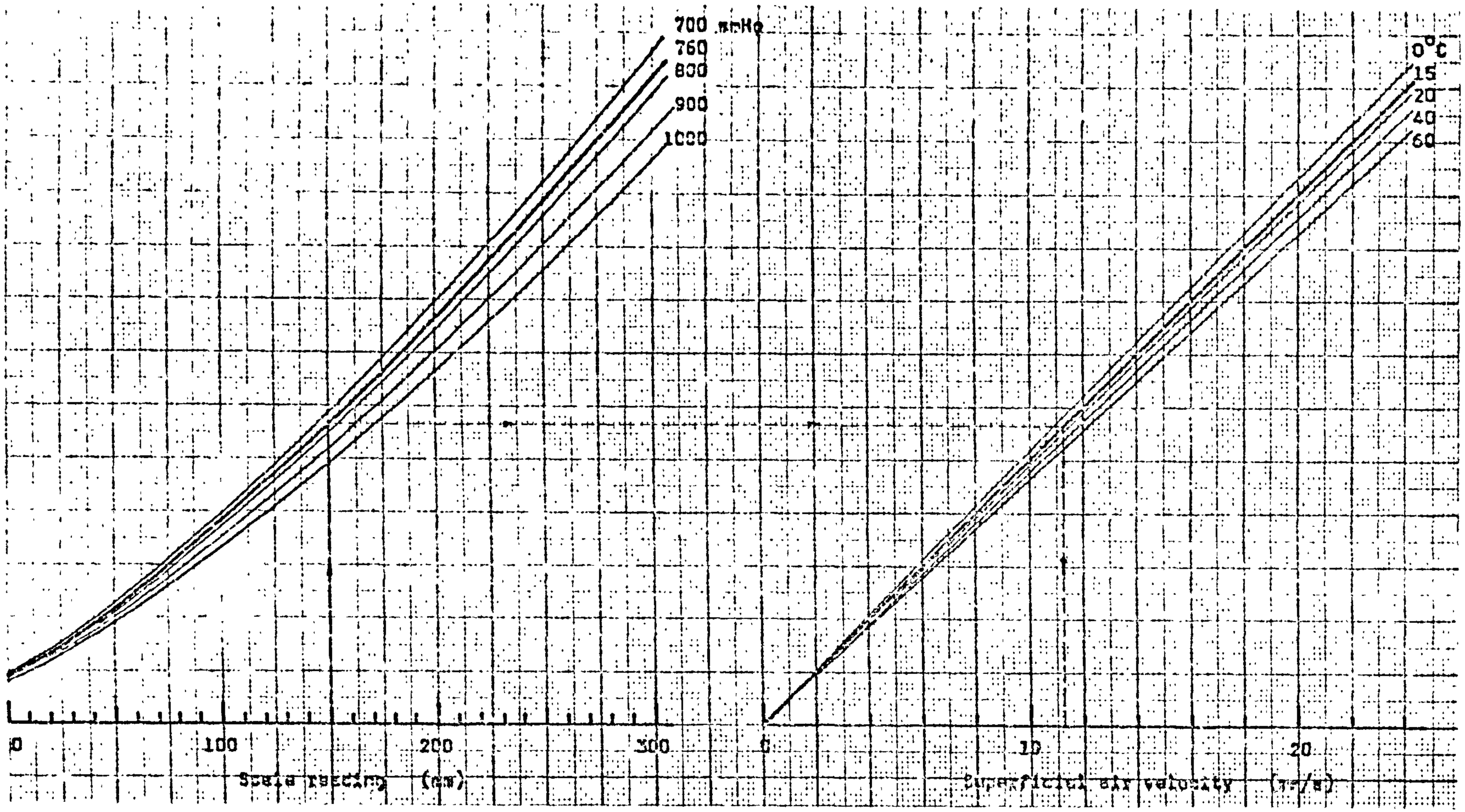

Fig. 7.2 CALIBRATION CHART FOR ROTAMETER 10A ON SMALL FLUIDISING TEST RIG

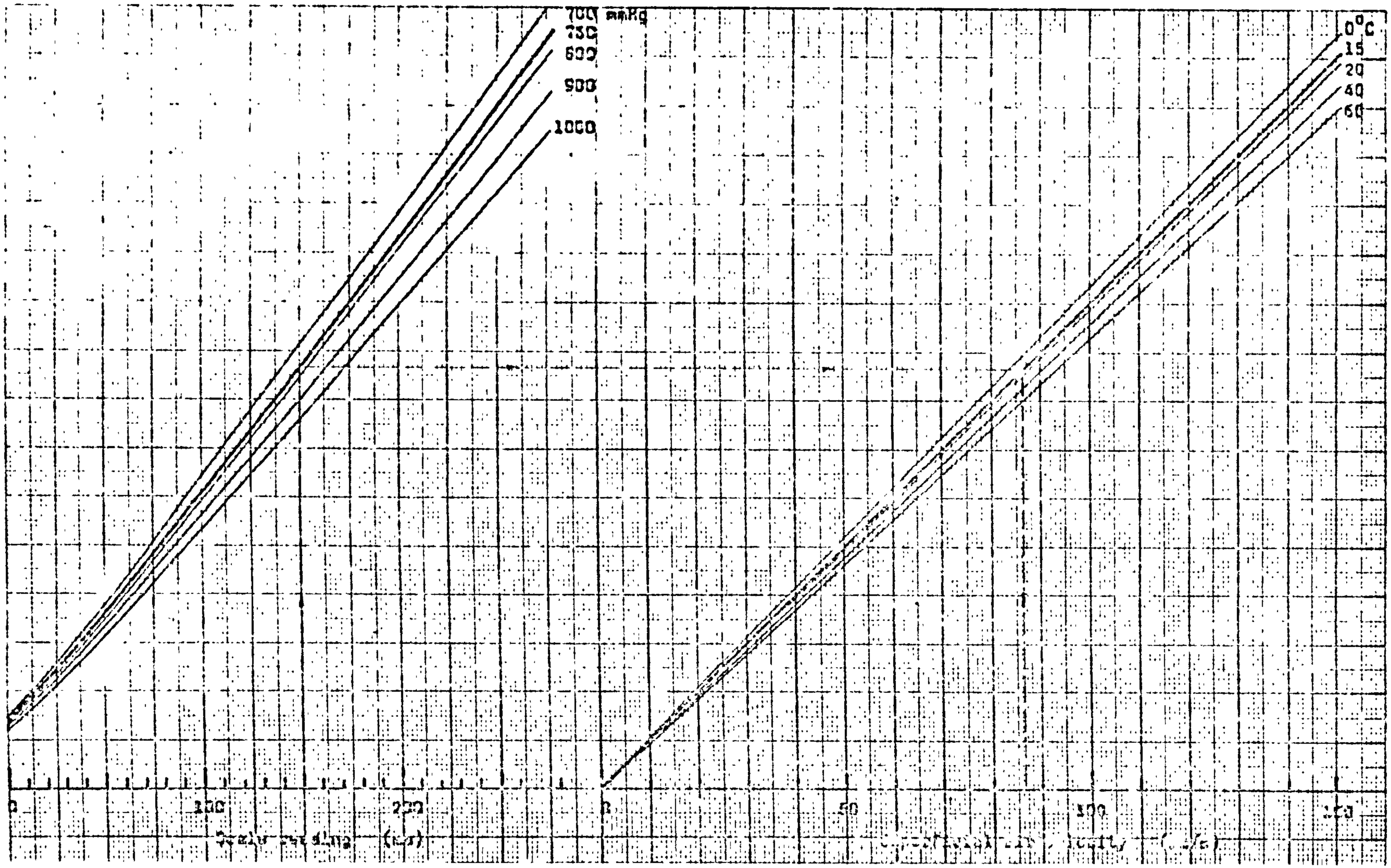

Fig. 7.3 CALIBRATION CHART FOR ROTAMETER 24XA ON SMALL FLUIDISING TEST RIG.

Considerable thought was given to the question of how to measure the pressure drop in the air as it flowed through the particulate bed. A pressure tapping in the plenum chamber, connected to a suitable manometer, allowed the pressure to be determined just below the porous distributor, and thus, with the fluidising vessel empty, the pressure drop across the distributor could be measured at any desired air flowrate. If the pressure in the plenum chamber is then measured again at the same air flowrate after powder has been put into the vessel, the increase can be presumed to correspond to the pressure drop across the powder alone. However, this simple presumption has been questioned by some authors (Refs. S18, T3) who claim that the pressure drop across the distributor is not the same in the presence of powder as it is when the upper surface is clear. Sutherland (Ref. S18) gives a theoretical explanation suggesting that the increase in pressure that occurs on the underside (upstream side) of the distributor when powder is placed on the top surface is less than the pressure drop across the powder itself. He comments that the discrepancy may not be significant where the resistance of the distributor is low, but for a distributor pressure drop of 500 mm H_2O the error could be about 4%. Trivedi and Rice (Ref. T3) used tappings immediately above and below the distributor in their 108 mm diameter fluidising vessel to measure the pressure drop across it, both in the absence of powder and in the presence of a 130 mm deep bed of glass beads. They found that the pressure drop was consistently greater when the powder bed was present, the error being about 7% when the distributor pressure drop was 500 mm H_2O. Thus the technique of measuring the pressure drop across the powder bed by subtracting the distributor pressure drop from the overall pressure drop could apparently give a result that is either too low (according to Sutherland) or too high (according to Trivedi and Rice)!

An obvious alternative to this technique is the use of pressure tappings located as closely as possible to the upper and lower surfaces of the distributor, especially the upper surface, so that the pressure drop can be measured directly whether powder is present or not. Trivedi and Rice (Ref. T3) did this, as mentioned above, and a similar method was used by McGuigan (Ref. M4) who developed from 1 mm diameter hypodermic tubing a probe which could be located with its open end just 0.05 mm above the

surface of the distributor.

In view of the somewhat surprising difference between the findings of Sutherland, and of Trivedi and Rice, it is not really clear which approach is at fault. For the purposes of the preliminary study of fluidisation behaviour of various powders to be undertaken in the small rig, the conventional technique using the single pressure tapping below the distributor was considered to be sufficiently reliable. There does however seem to be a need for a full investigation of the phenomena involved in flow through a porous grid with and without the presence of powder, although pressure on time unfortunately did not permit such a study during the current programme of work.

During the course of the research programme it became necessary to re-site the fluidising test rig and so the opportunity was taken to improve the arrangement of rotameters and manometers, and to modify the plenum chamber to make it more compact. This later arrangement of the rig is illustrated in Fig. 7.4 and much of the detail can be seen in the photographs, Plates I and II.

7.3 INVESTIGATION OF POROUS FLUIDISING MEDIA

7.3.1 Introduction

It has been pointed out previously (Part I, Section 3.2.4) that in air-gravity conveying applications the air distributor forming the base of the conveyor channel should normally have a smooth top surface, and, as a result of this requirement, the "porous membrane" type of distributor is used almost exclusively. It therefore seemed to be reasonable to restrict the study of different kinds of distributor to those which come into this category, and so samples were obtained of various sintered materials and woven fabrics recommended by the manufacturers for fluidising applications. Perforated plates, pipe grids and similar types of very low pressure drop distributors were excluded from the current investigation.

The most important single feature of a material used as the distributor in a fluidising vessel is its resistance to the flow of air and so the

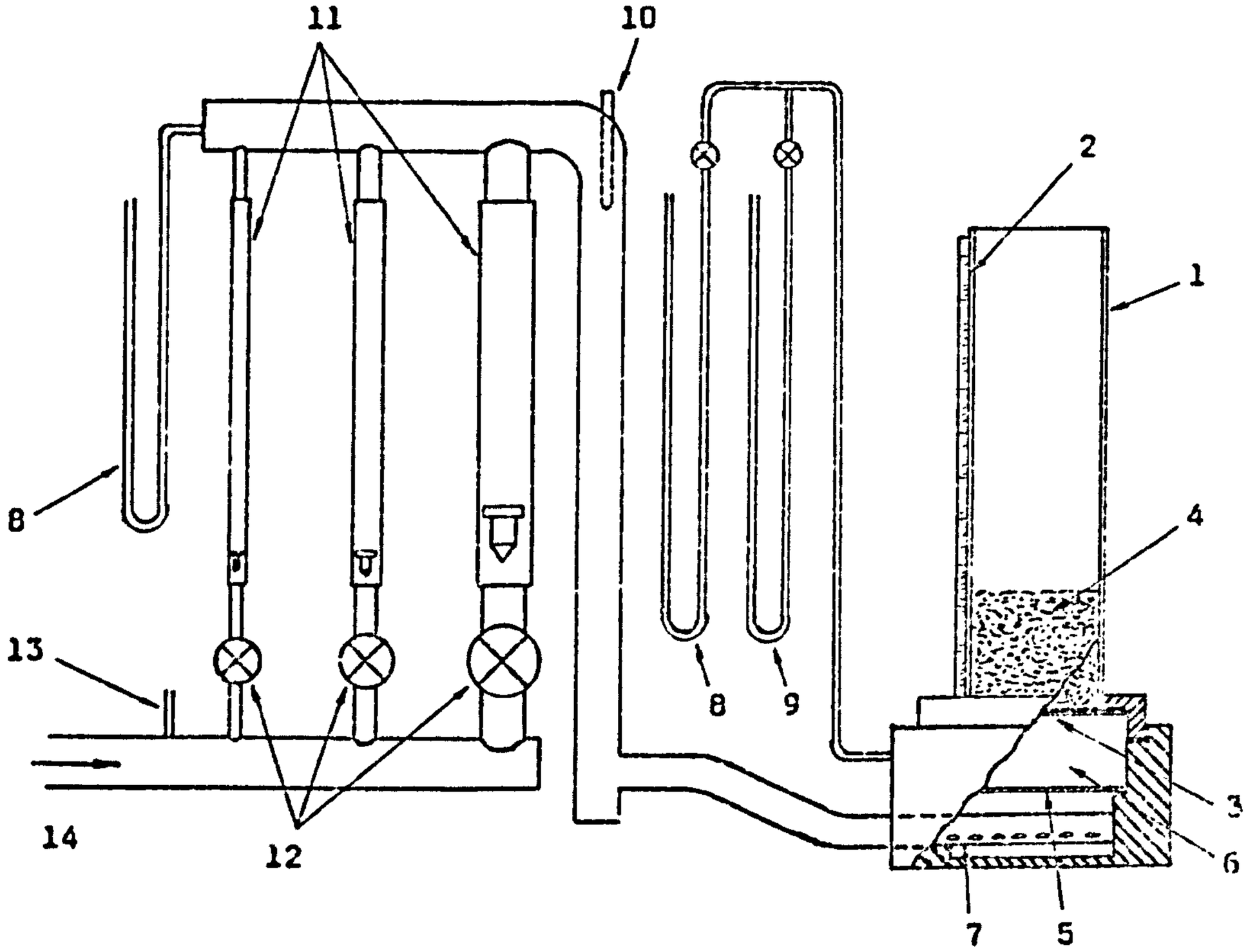

KEY:

1. Perspex cylinder (150 mm diameter)
2. Scale
3. Porous distributor
4. Fluidised powder
5. Baffle plate
6. Plenum chamber
7. Air supply to plenum chamber
8. Mercury manometers
9. Water manometer
10. Thermometer pocket
11. Rotameters
12. Airflow control valves
13. Tapping to hygrometer
14. Air inlet from blower

Fig. 7.4 LATER ARRANGEMENT OF SMALL FLUIDISING TEST RIG, SHOWING MODIFICATIONS TO INSTRUMENTS AND TO PLENUM CHAMBER.

Plate I. VIEW OF SMALL FLUIDISING TEST RIG.

Plate II. CLOSE-UP VIEW OF FLUIDISING VESSEL.

permeability of each sample was measured under controlled conditions. Various powders were fluidised on the different distributors in order to see whether any variation in performance could be detected, and from the results of this investigation recommendations were made on the kind of material to be used for the base of the channel in the main test rig.

7.3.2 Materials tested

A total of ten different porous materials were examined, of which five were woven fabrics, four were made of sintered particles and one was a steel mesh laminate. This selection was seen as being a fairly representative one from the materials commercially available, bearing in mind that many manufacturers are able to supply a particular type of membrane in a range of permeabilities.

The materials tested are listed in Table 7.1 and illustrated in Plate III.

Name	Manfrs. Ref. or grade	Manufacturer (see App.A.IV)	Type of material
Dynapore	P/N 401300	Michigan Dynamics	Stainless steel wire mesh laminate.
Nopol	-	Oy Nokia AB	Sintered polythene
Pyrolith	G628	Doulton Ind. Products Ltd.	Porous sintered ceramic tile
Scandura 'Topline'	P7	Scandura Ltd.	Woven polyester belting
" "	P22	" "	" "
" "	'Redstripe'	" "	Woven cotton belting
Vyon	'D'	Porvair Ltd.	Sintered polythene sheet
"	'DM'	" "	" "
Wocot	3/16" (5 mm)	Gandy Ltd.	Woven cotton belting
"	¼" (6.5 mm)	" "	" " "

Table 7.1 POROUS DISTRIBUTOR MATERIALS TESTED IN THE SMALL FLUIDISING RIG.

Pyrolith	Nopol	Vyon 'D'	Vyon 'DM'
Wocot 5 mm.	Scandura P7	Scandura 'Red-stripe'	Scandura P22	Dynapore

Plate III. POROUS DISTRIBUTORS USED IN SMALL FLUIDISING RIG.

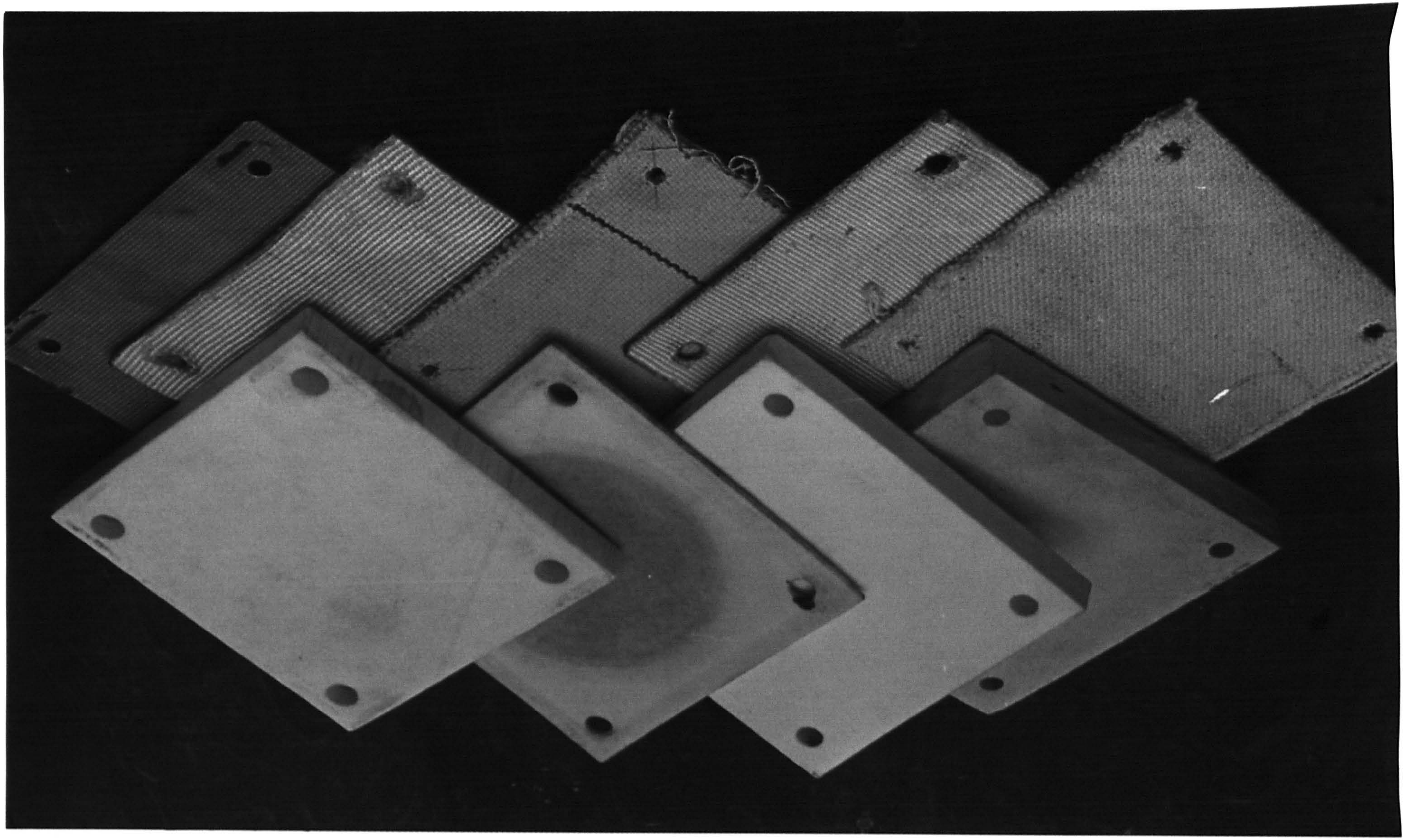

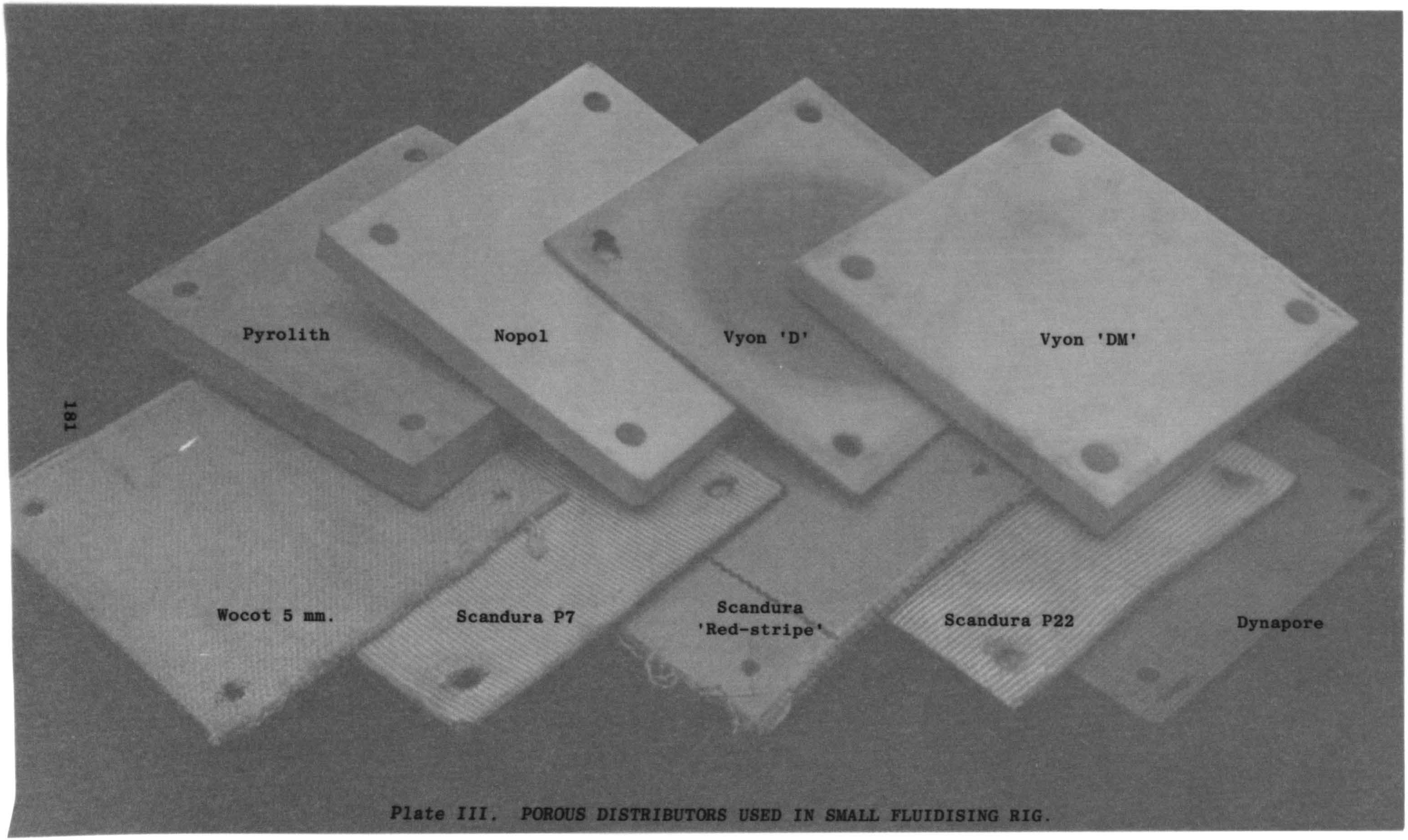

Plate III. POROUS DISTRIBUTORS USED IN SMALL FLUIDISING RIG.

7.3.3 Permeability

One of the requirements of a distributor used in fluidising applications is that it should provide uniform fluidisation, and it follows that the airflow through it should be uniform. For each of the porous materials investigated the manufacturer claimed that the porosity and permeability were uniform within a few percent over its whole area. It would perhaps have been of interest to have developed a convenient instrument for measuring the pressure drop and air flowrate through a very small area in the centre of a large sheet, in order to verify this claim. However, at this stage the measurement was restricted to an average permeability of a 150 mm diameter circle in a 200 mm square sample of the porous material.

All the samples were tested in the small fluidising rig, each in turn being sealed between the base of the empty fluidising column and the cover-plate in order to ensure that all the airflow passed through the same circular area of distributor, 150 mm in diameter. For each sample the airflow was gradually increased and readings were taken of the rotameters and manometers so that graphs could be plotted of superficial air velocity against pressure drop.

The results of these tests are presented on Fig. 7.5 for the porous materials which have relatively high pressure drop, and on Fig. 7.6 for the low pressure drop types. In order to provide a 'link' between the two ranges, the line for the Vyon 'D' sample is shown on both graphs. Of the samples tested it will be noticed that the highest pressure drops, that is, the lowest permeabilities, were exhibited by woven materials (the two thicknesses of Wocot and two of the three types of Scandura). The sample having the lowest resistance to air flow (highest permeability) was the 15 mm thick sintered plastic, Nopol.

Table 7.2 summarises the results of these tests, listing for each sample the pressure drop at an air flowrate of 0.05 m^3/s per m^2, and the permeability, or air flow through the material when the pressure drop is 200 mm H_2O.

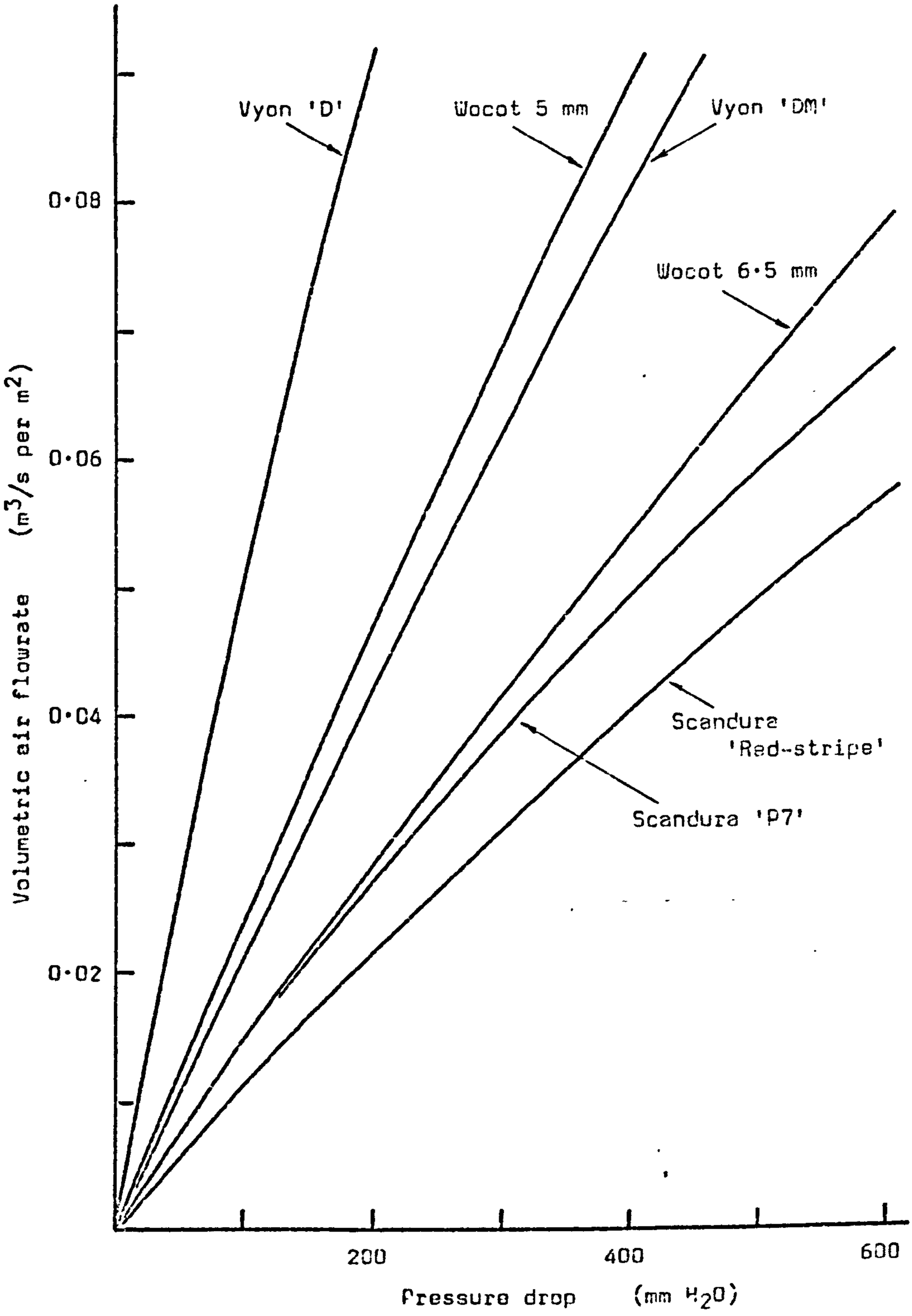

Fig. 7.5 PERMEABILITY OF VARIOUS DISTRIBUTOR MATERIALS (High pressure-drop types).

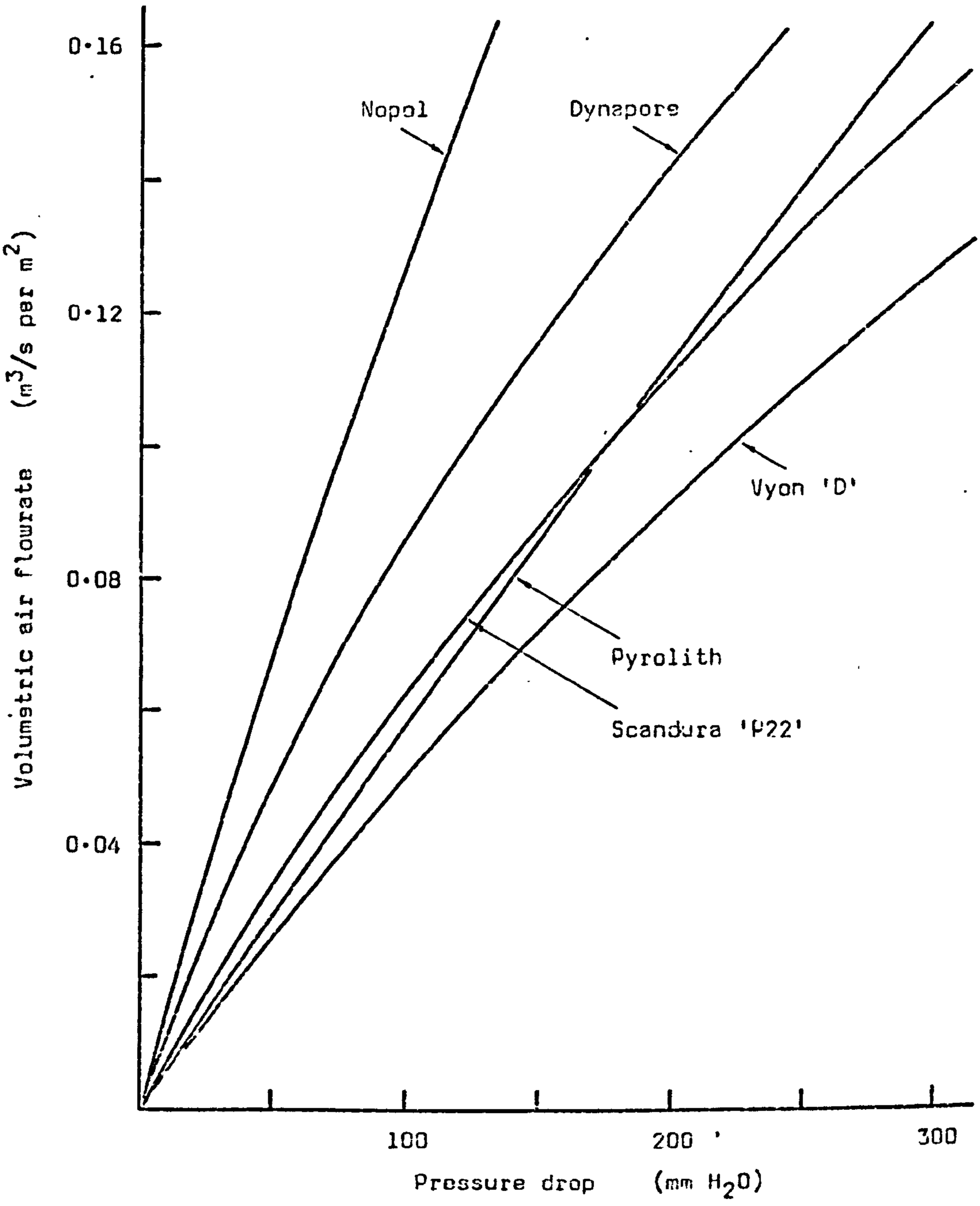

Fig. 7.6 PERMEABILITY OF VARIOUS DISTRIBUTOR MATERIALS (Low pressure-drop types).

Porous material	Thick-ness	Pressure drop at airflow of 0.05 m^3/s per m^2	Airflow at pressure drop of 200 mm H_2O
Nopol	20 mm	36 mm H_2O	0.22 m^3/s per m^2
Dynapore	1.2	52	0.142
Pyrolith	26	88	0.112
Vyon 'D'	4.5	100	0.091
Vyon 'DM'	19	240	0.042
Scandura P22	5	77	0.110
Scandura P7	5	410	0.027
Scandura 'Redstripe'	6	515	0.022
Wocot 5 mm	5	215	0.047
Wocot 6.5 mm	6.5	365	0.029

Table 7.2 PRESSURE DROPS AND AIR FLOWRATES FOR VARIOUS POROUS MATERIALS

7.3.4 General observations

No particular difficulties were encountered during these simple permeability tests. All the samples were sufficiently rigid to be fitted across the base of the fluidising column without additional support, although the Scandura P22 showed a tendency to bow upwards at high air flowrates. This material was of a much looser weave than the other types of Scandura and Wocot belting and would probably require support if used over a larger area.

It is well known that over a period of time the porous distributors used in fluidising and similar applications tend to suffer from blinding or blockage of the pores. It appears that this can occur on both sides; the underside with dust particles entrained in the air from the blower, and the top side with fines from the fluidised powder. Probably some types of distributor are more susceptible than others to blockage, with high pressure drop types presumably being worst affected. A very protracted series of tests would be needed to investigate this thoroughly,

but in the current investigation it was found that after several months in use the Vyon 'D' sample showed a marked deterioration. It had become noticeably discoloured (as can be seen in Plate III) and its resistance had increased by about 50%, which corresponds to a drop of around 30% in the air flowrate at any given plenum pressure. It is however unfair to single out the Vyon sample in this way as it was the distributor most frequently used in the fluidisation tests, and other materials would probably show similar deterioration after the same usage.

Some tests were carried out to see whether there were any discernable differences in the fluidisation behaviour of a given powder when supported on the different samples of distributor. The powders used were p.v.c. ("Corvic") and a fine sand, and the results of the tests are discussed in Sections 7.5 and 7.6 respectively.

7.3.5 Conclusions

Any of the materials examined would be suitable for the base of the channel in an air-assisted gravity conveyor, although naturally the low pressure drop types are more economical on power consumption. The woven materials and the thin plastic (Vyon 'D') would need supporting in a wide channel, but (except for the Scandura P22) should provide a firm enough base without additional support in channels less than about 150 mm in width.

Woven belting has the advantage of being available in considerable lengths, thus avoiding the jointing problems that can occur with some of the other materials. For example, the sintered plastics are normally available in sheets up to about one metre in length, and care has to be taken when welding pieces together that the non-porous area around the weld is kept to a minimum.

Consideration was given to all the samples tested when selecting the material to be used for the base of the channel in the main flow rig. Some, such as Dynaporc, Pyrolith, Nopol and Vyon 'DM' were ruled out on the ground of cost or difficulty of fitting to the narrow channel to be constructed. Finally it was decided to select two materials, of

different types and different pressure drops. Vyon 'D' was chosen as a medium to high resistance type, and Scandura P22 as a low resistance type to be representative of the woven beltings. The performance of these distributor materials in the main channel flow rig is discussed further in Chapter 8.

7.4 PRELIMINARY TESTS ON VARIOUS PARTICULATE MATERIALS

7.4.1 Introduction

Before selecting suitable particulate bulk solids for the investigation into flow in air-assisted gravity conveyors, a number of different powders were tested in the small fluidising rig. The purpose of these preliminary tests was to get a "feel" for some of the kinds of powders that might be encountered in industry, especially with regard to their fluidisation behaviour. Furthermore, by carrying out particle size analyses on the powders it should be possible to add to the evidence supporting the use of the simple equation for minimum fluidising velocity, presented in Section 2.3.3.

The choice of powders to be examined was made more or less arbitrarily from those that happened to be to hand or could be easily obtained. However, it was intended that the materials selected should be representative of a fairly wide range of types, including powders of both high and low density, and having particle sizes from fine to fairly coarse.

The powders examined are listed in Table 7.3 and the results of the size analyses and fluidisation tests are discussed in the following Sections.

7.4.2 Powder characterisation and fluidisation behaviour

For each of the samples of powder a size analysis was carried out by whichever method seemed to be the most appropriate. Then a quantity of each powder (around 1200 to 2000 cm^3) was placed in the Perspex cylinder of the small fluidising rig and its behaviour studied over a range of air flowrates. For most of the materials plots were made of the pressure drop across the powder bed against the superficial air velocity, and thus their minimum fluidising velocities could be observed. Also, the change

Sample No.	Material	Ref.	Manufacturer/Supplier
1	Sand	52/100	A.L. Curtis (ONX) Ltd., Chatteris, Cambs.
2	"	100/150	" "
3	"	120/170	" "
4	Pulverised fuel ash (PFA)	-	C.E.G.B., Ferrybridge Power Station.
5	Alumina ('Bauxilite')	F360/23	Universal Abrasives Ltd., Stafford.
6	P.V.C. ('Corvic')	D65/02	I.C.I. Ltd., Plastics Div., Welwyn Garden City, Herts.
7	Siliceous fillers ('Ultrasil')	VN.3	I.D. Chemicals Ltd., Northwich, Cheshire.
8	China clay ('Devonite')	-	English China Clays.

Table 7.3. PARTICULATE SOLIDS TESTED IN SMALL FLUIDISING RIG.

of bed depth (and hence of "bulk density") was noted so that the minimum bulk density with no air flow could be determined.

The observations made on each of the particulate solids examined will now be discussed separately.

SAND:

Since it is relatively inexpensive and readily available in a wide range of particle sizes, sand is commonly used in research work on the fluidisation phenomenon. In the present programme three samples of sand of different sizes were used, as received from the suppliers under reference codes 52/100, 100/150 and 120/170. Particle size analysis by sieving was carried out on each sample and the results are presented as plots of cumulative percentage undersize and percentage distribution by weight (Figs. 7.7 to 7.9). The mean particle sizes of the three samples were found to be 183 μm, 131 μm and 107 μm respectively.

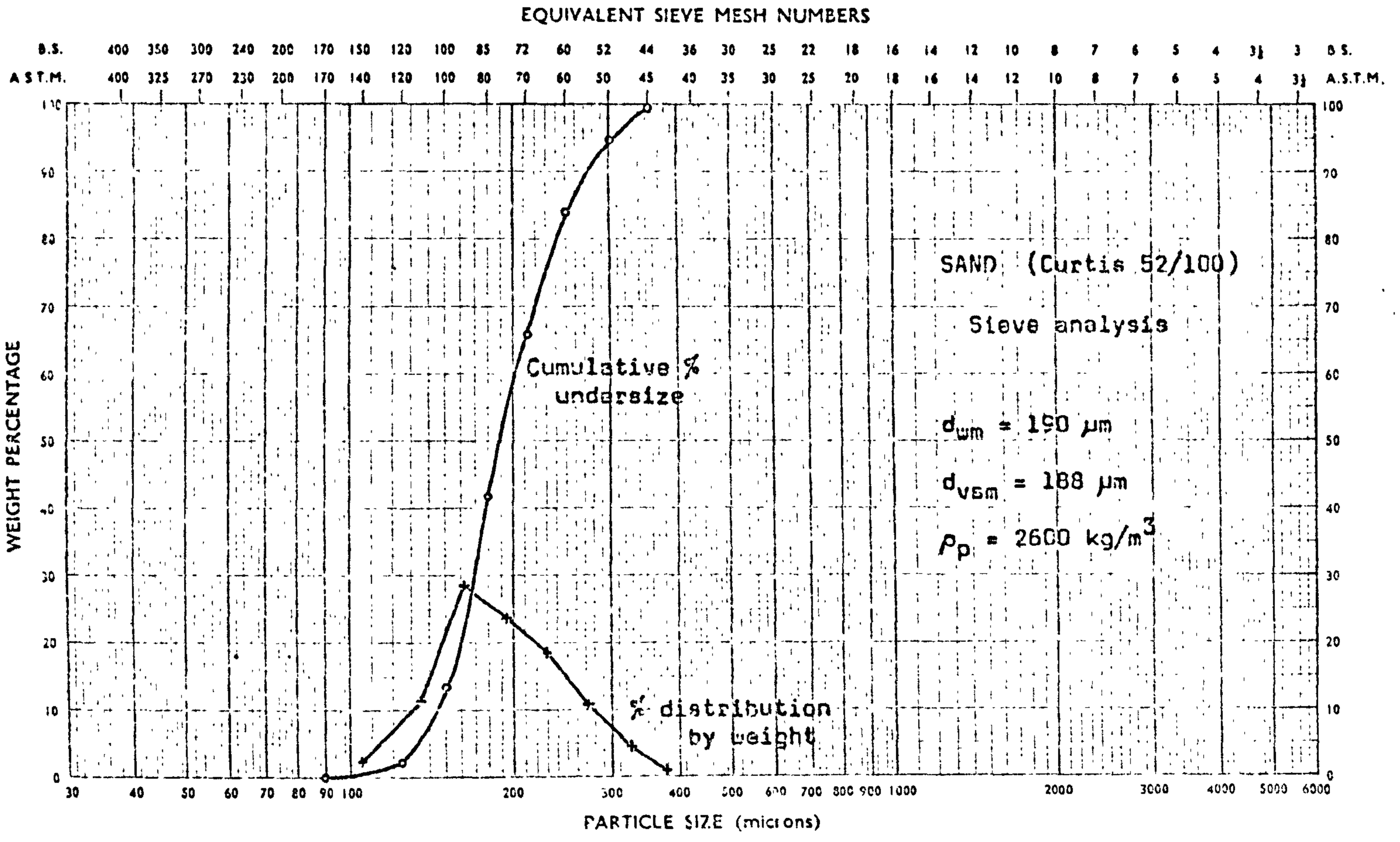

Fig. 7.7 PARTICLE SIZE ANALYSIS OF SAND SAMPLE No. 1 (Curtis 52/100)

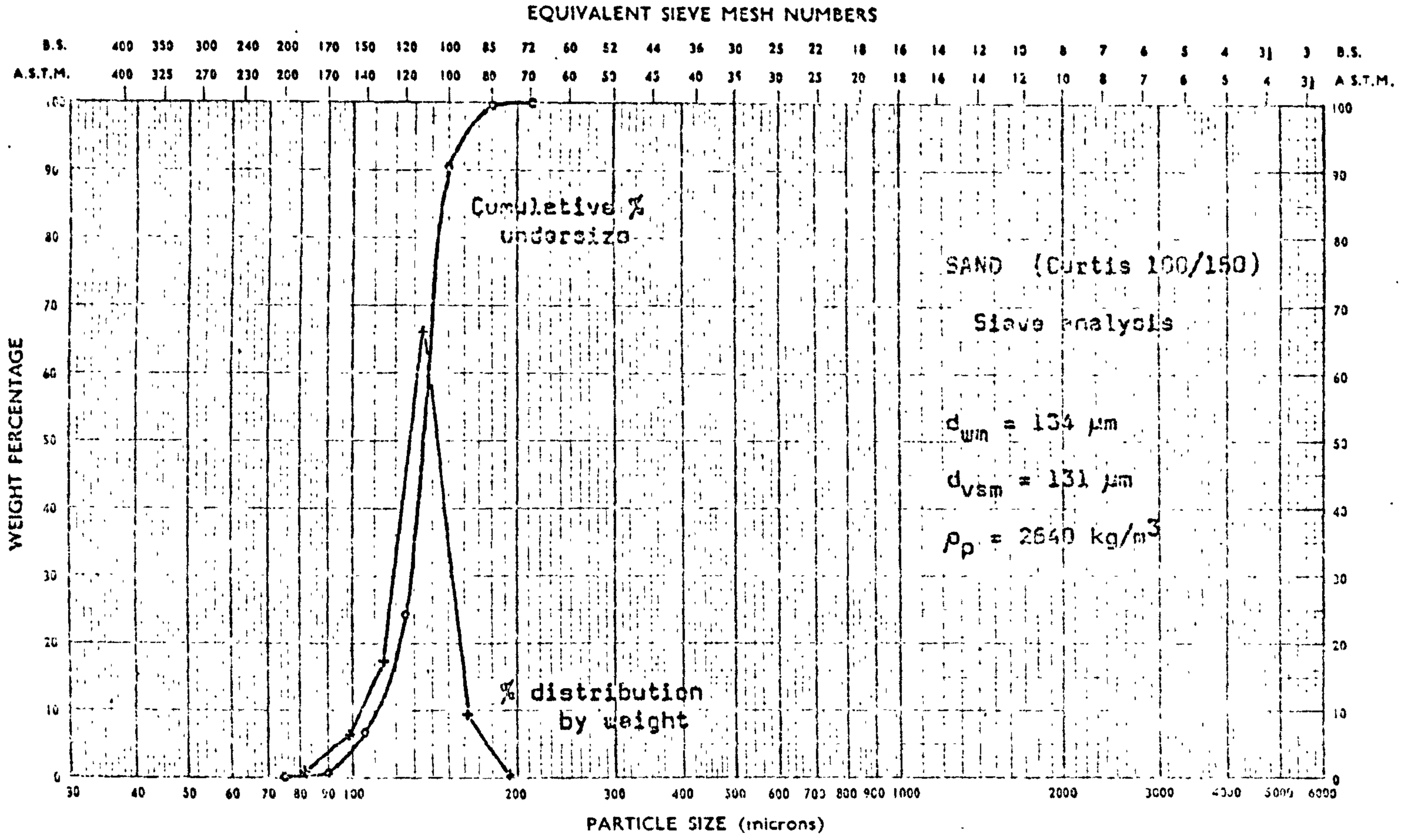

Fig. 7.8 PARTICLE SIZE ANALYSIS OF SAND SAMPLE No. 2 (Curtis 100/150)

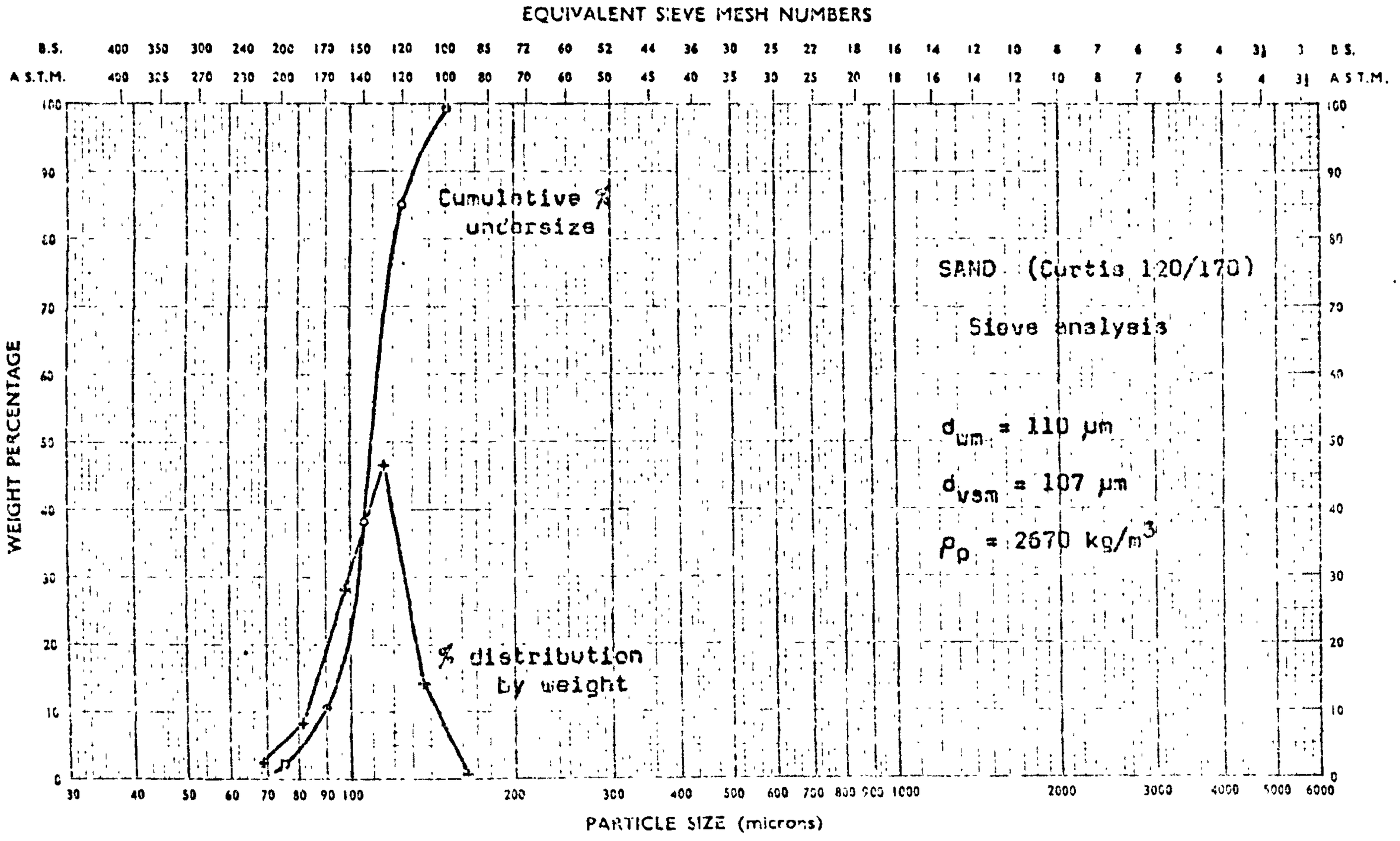

Fig. 7.9 PARTICLE SIZE ANALYSIS OF SAND SAMPLE No. 3 (Curtis 120/170)

As expected, the samples of sand were found to fluidise well, having minimum fluidising velocities of about 40 mm/s, 22 mm/s and 13.5 mm/s, but a more detailed discussion of the fluidisation behaviour of sand, as observed in these tests, is deferred to Section 7.6.

PULVERISED FUEL ASH (PFA):

Ash from power stations operating on pulverised coal presents considerable handling problems and air-assisted gravity conveying is one method that is used to move economically the large quantities of material involved. The sample of ash used in these tests came from the research facility at Ferrybridge Power Station and is believed to be a mixture of ashes from several other power stations.

The ash itself has the appearance of a rather fine "gritty" powder, containing a high proportion of very fine dust. Also present in the ash is a small amount of free coke particles and a significant quantity of fused hollow glass spheres known as "cenospheres" which have the property of extreme hardness and abrasiveness. Values of the true density of PFA must be somewhat ambiguous as it is not easy to assess the influence of the porous and hollow particles on the measurements. However, using the conventional method of density determination with a specific gravity bottle, an average particle density of the PFA was 1780 kg/m^3.

Particle size analysis was again by sieving, although the high proportion of fines meant that the result was a little obscure at the lower end of the size spectrum. However, the mass median size was found to be 108 μm and the volume-surface mean diameter (from equation A.I.9) was about 92 μm. Fig. 7.10 gives the full size analysis.

In the small fluidising rig it appeared that the PFA would fluidise quite well, although the point of incipient fluidisation was not clearly defined. In fact the bed became fluidised somewhat unevenly, one of the first visible signs being the segregation on the top surface of the larger, lighter particles of coke. Beds of PFA having three different initial depths were fluidised in turn and in each case the pressure drop across the bed was plotted against the superficial velocity of the fluidising air (Fig. 7.11). From these graphs an average value of the minimum fluidising velocity was about 5.3 mm/s.

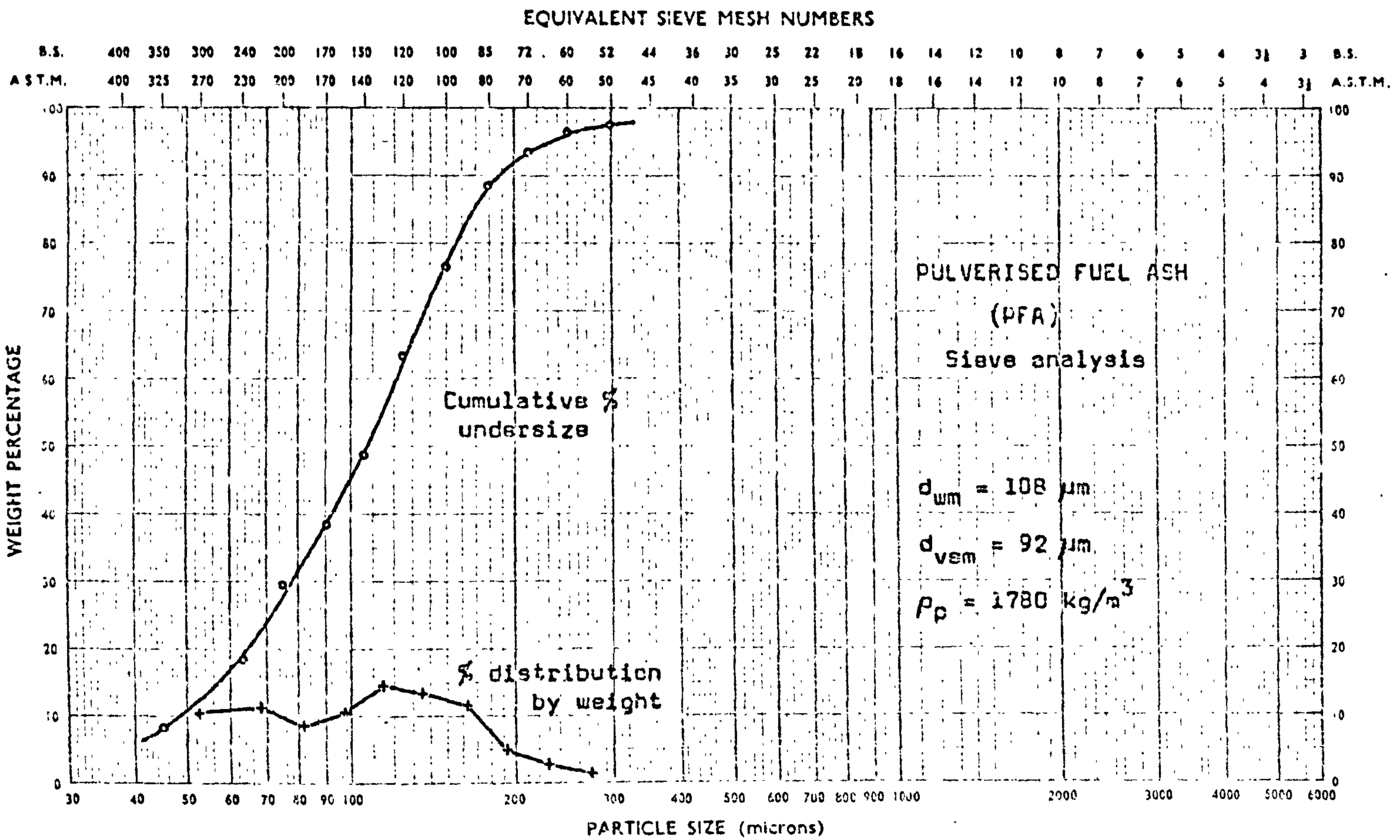

Fig. 7.10 PARTICLE SIZE ANALYSIS OF PFA SAMPLE No. 4

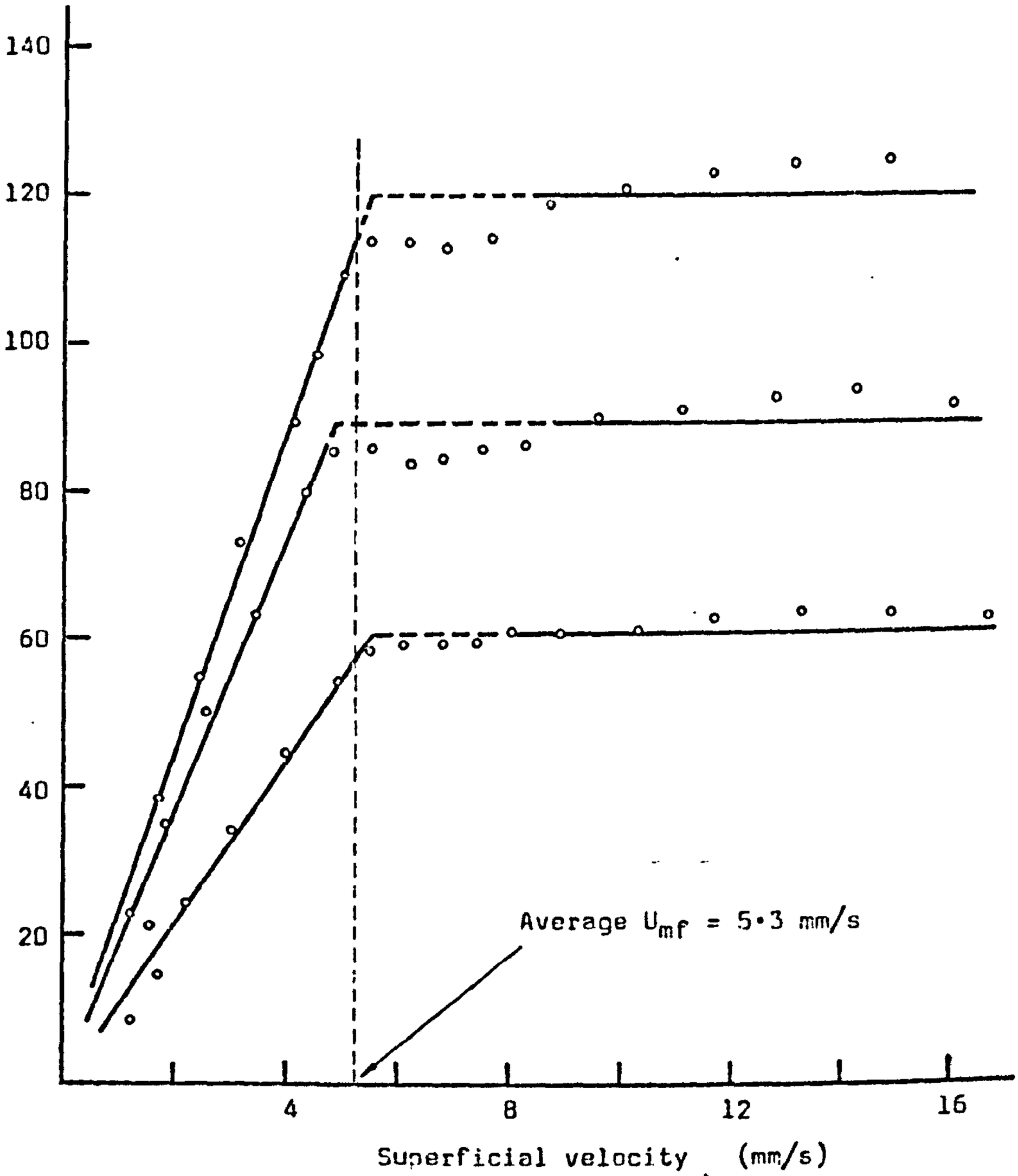

Fig. 7.11 FLUIDISATION BEHAVIOUR OF P.F.A.

d_v = 92 μm; ρ_p = 1780 kg/m^3

Distributor: VYON 'D'

R.H. = 72%

During these tests on the PFA the depths of the powder beds were recorded so that a graph could be plotted of the percentage expansion against the superficial air velocity (Fig. 7.12). The "minimum bulk density" with no air flow was also carefully measured by noting the depth to which the bed settled as the fluidising air was slowly shut off. The average of values determined with three different quantities of PFA in the fluidising vessel was 790 kg/m^3.

ALUMINA ('BAUXILITE'):

Another material of major industrial interest that is commonly transported in air-assisted gravity conveyors is alumina (see Section 3.3.3). This fine abrasive powder is available commercially in a wide range of closely graded sizes and the sample used in the present investigation was taken from a batch that happened to be available in the laboratory for use on another project. The true density of the powder, determined using an S.G. bottle, was 3830 kg/m^3.

Since the alumina was too fine for sieving, particle size analysis was carried out on a Microscal wide-angle scanning photosedimentometer (WASP) belonging to the School of Mechanical Engineering. (This instrument is described in Appendix A.I.) The resulting size analysis is presented as Fig. 7.13, from which the mass median size is seen to be about 25 μm.

Typical of free-flowing powders having high density and small particle size, the alumina was found to fluidise evenly at a very low superficial air velocity. Two different initial bed depths were tried and the average value of U_{mf} was about 4 mm/s (Fig. 7.14). The average "minimum bulk density" of the alumina (with no airflow) was found to be 1871 kg/m^3 and its expansion when fluidised was approximately the same as that of PFA. For instance, at a superficial air velocity of 10 mm/s the expansion of alumina was 13.5 % (Fig. 7.15) compared with about 11% for PFA (Fig. 7.12). However, a fairer comparison could perhaps be made by considering the expansions at the same degree of fluidisation; for example at 3 U_{mf} the expansion of alumina was 14.9 % whilst PFA expanded 15.6 %.

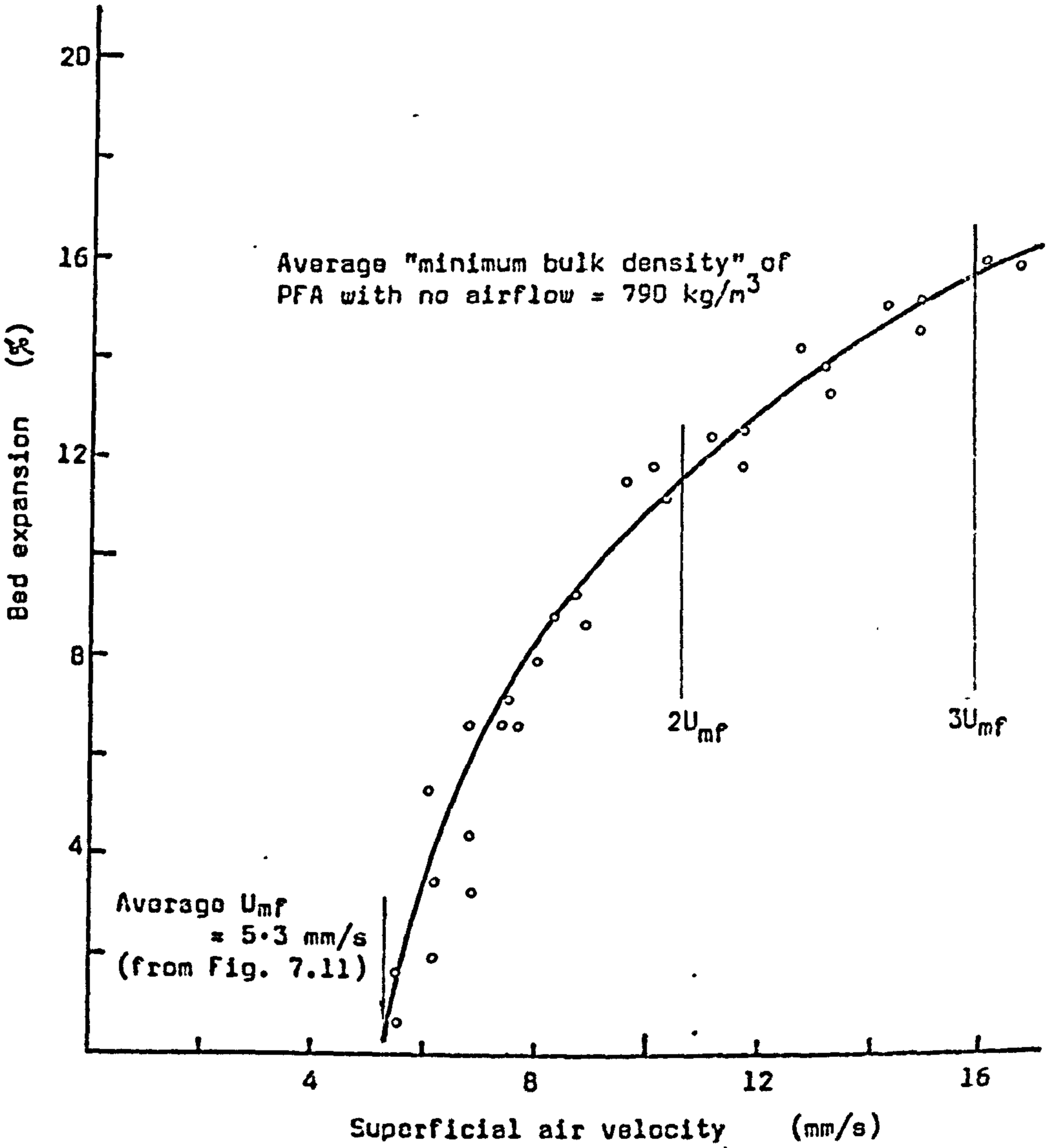

Fig. 7.12 EXPANSION OF FLUIDISED BED OF PFA AS A FUNCTION OF THE SUPERFICIAL AIR VELOCITY.
Distributor: Vyon 'D'; R.H. = 72%.

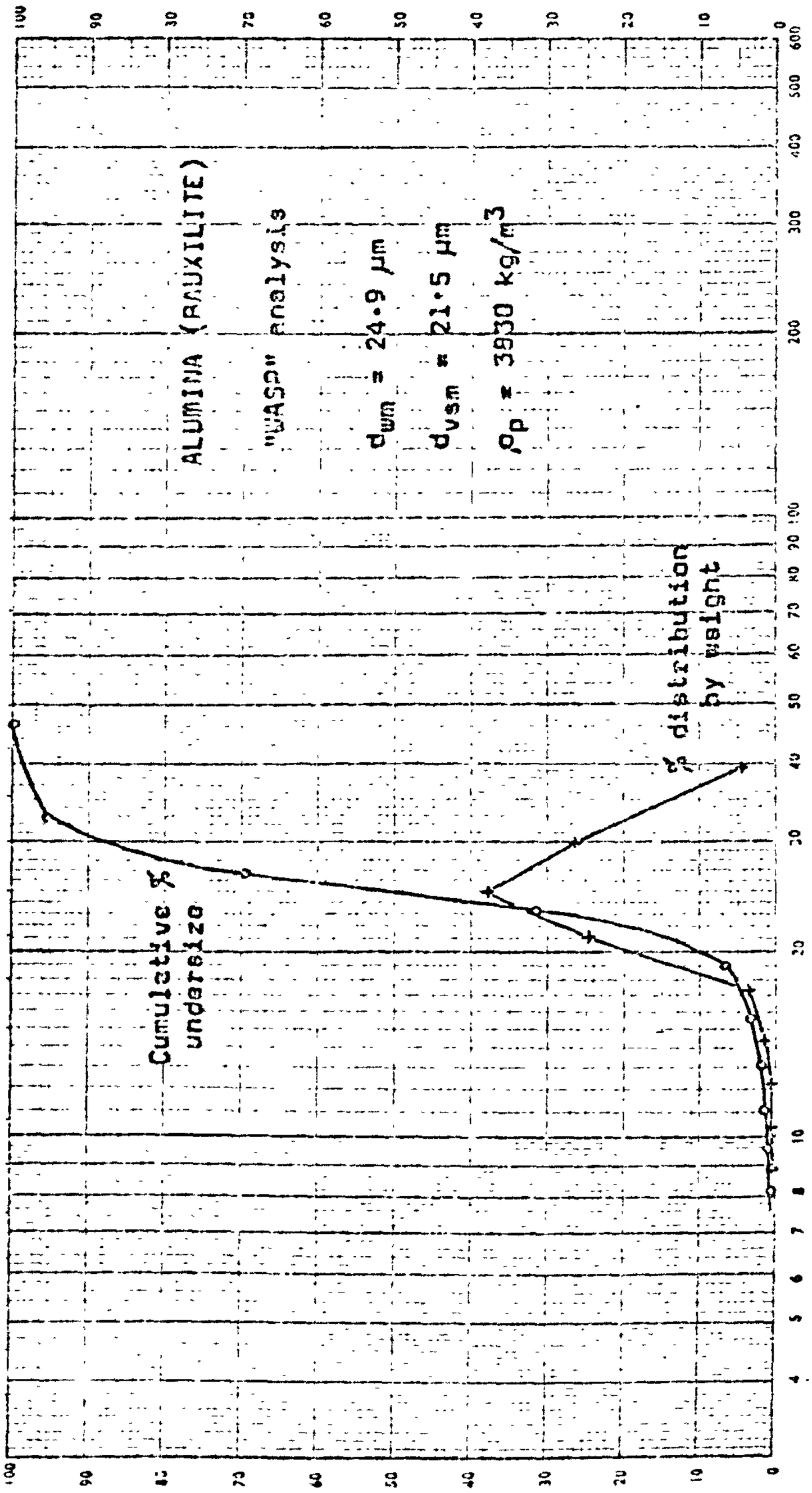

Fig. 7.13 PARTICLE SIZE ANALYSIS OF ALUMINA SAMPLE No.5

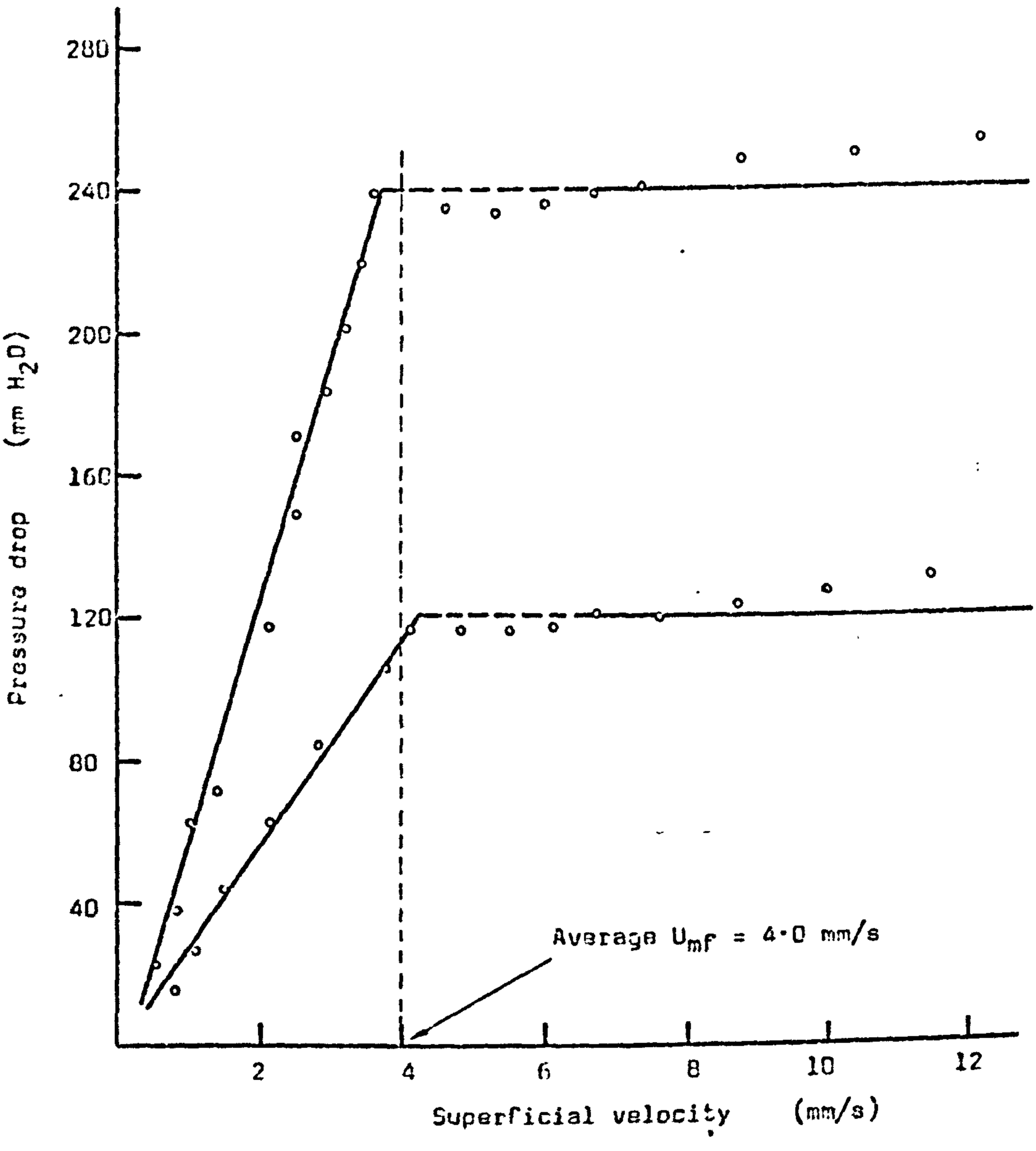

Fig. 7.14 FLUIDISATION BEHAVIOUR OF ALUMINA (BAUXILITE)

d_v = 21.5 μm; ρ_p = 3830 kg/m^3

Distributor: VYON 'D'

R.H. = 72%

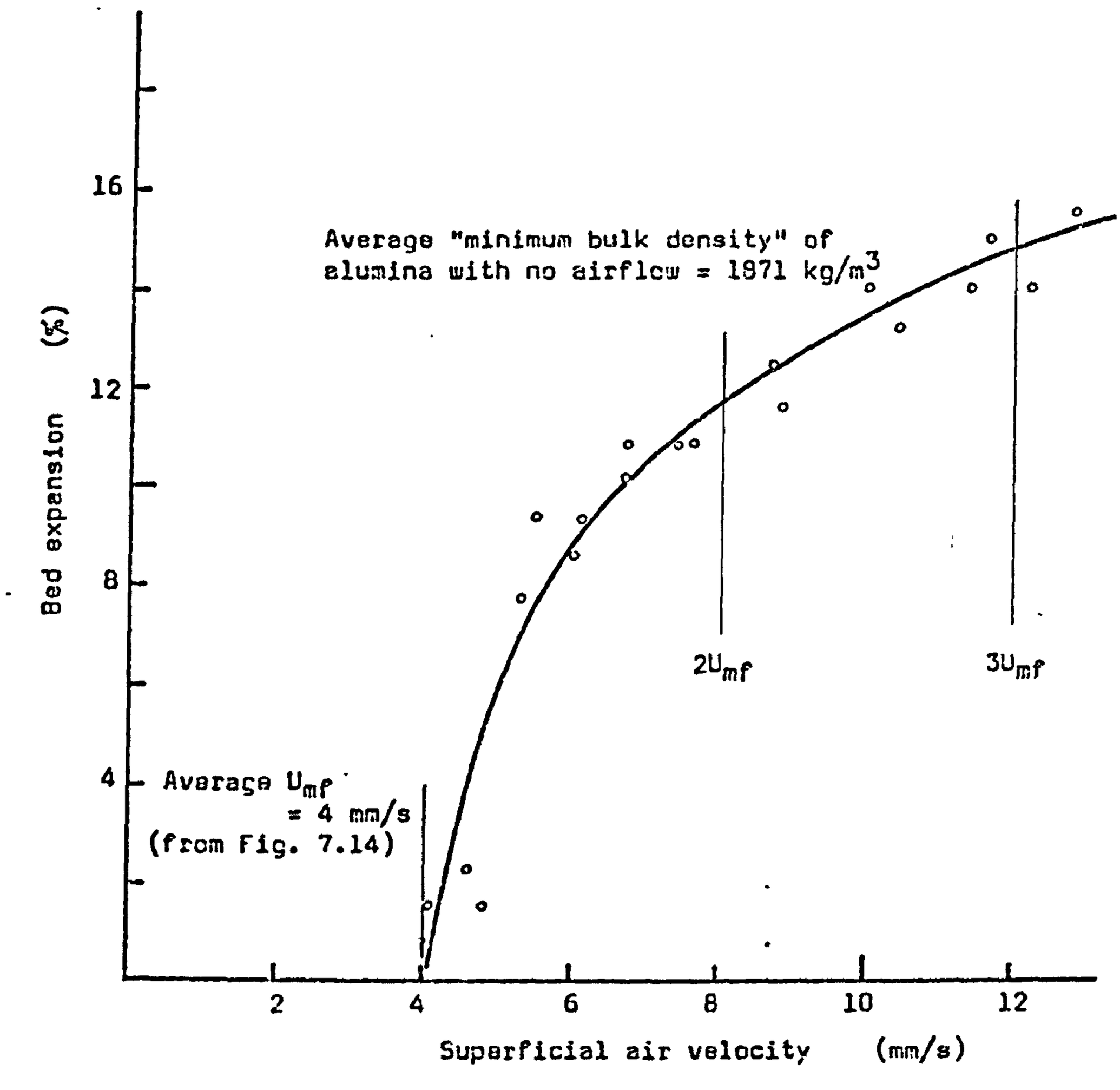

Fig. 7.15 EXPANSION OF FLUIDISED BED OF ALUMINA AS A FUNCTION OF THE SUPERFICIAL AIR VELOCITY. Distributor: Vyon 'D'; R.H. = 72%.

P.V.C. ('CORVIC'):

To represent materials of low density a typical plastic powder was chosen. "Corvic" is a general purpose, high molecular weight homopolymer of vinyl chloride, supplied by I.C.I. Ltd., and recommended for the manufacture of various plastic products. The true particle density of the powder was measured using an S.G. bottle with methanol as the displaced liquid. The measured value of 1430 kg/m^3 corresponds closely to the value of specific gravity quoted by the suppliers (1.4).

Particle size analysis of this material presented some difficulties as it was found impossible to get a reliable result either by dry sieving or by a sedimentation method. When shaken on the sieves' the Corvic particles appeared rapidly to acquire an electrostatic charge and the resulting agglomeration prevented them passing through the sieve meshes. Attempts with the photosedimentometer proved equally unreliable as the powder could not be properly dispersed in water or in ethylene glycol and in other liquids where dispersion was better it was found that the sedimentation rate was too high so that the top size could not be determined accurately. A result was obtained by Coulter analysis carried out on a sample of the Corvic by Dr. Rubinstein of Liverpool Polytechnic. Fig. 7.16 shows the size distribution plotted from Dr. Rubinstein's data, from which it is seen that the mass median diameter is about 120 μm.

Fluidisation tests on the Corvic showed that for the fresh, free-flowing powder the minimum fluidising velocity was around 10 to 11 mm/s, but if the powder became electrostatically charged its behaviour was drastically altered. The electrostatic phenomenon was interesting but caused a number of difficulties, not least of which was the near impossibility of obtaining closely repeatable results in the tests on fluidisation and on air-assisted gravity flow of Corvic. However, these problems and the results that were obtained in the tests are described fully in Sections 7.6, 8.4 and 8.5.

SILICEOUS FILLERS ('ULTRASIL' VN.3):

As a material of very fine particle size, but rather low density (compared with, for example, alumina) a sample of siliceous fillers was examined.

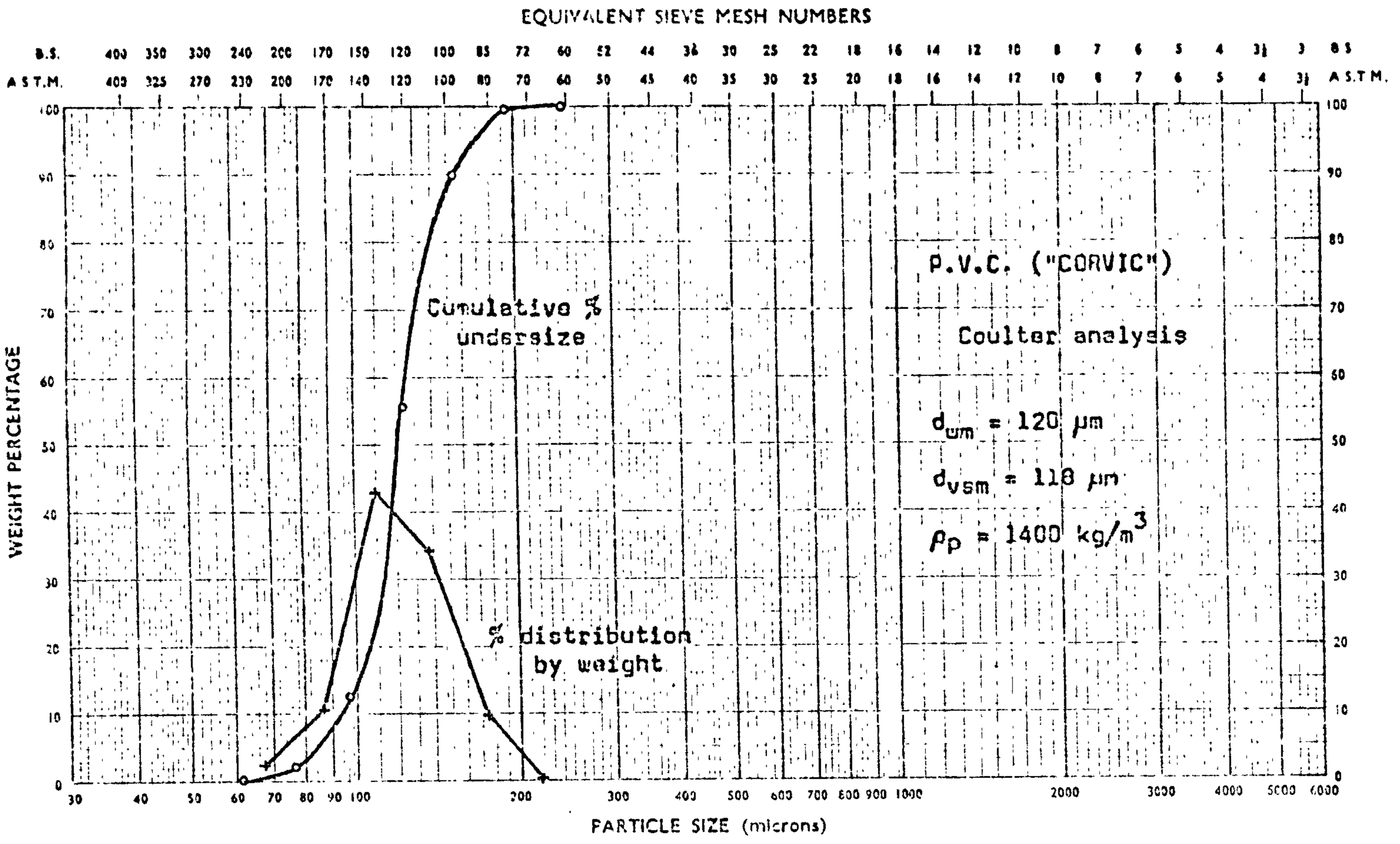

Fig. 7.16 PARTICLE SIZE ANALYSIS OF P.V.C. ('CORVIC') SAMPLE No. 6

"Ultrasil", supplied by I.D. Chemicals Ltd., is a precipitated silica having a specific gravity of 2.05 and is used as a reinforcing filler for natural and synthetic rubbers. Although the true particle density is slightly greater than that of the p.v.c. powder the bulk density is much less. The minimum bulk density was found to be about 190 kg/m^3.

A particle size analysis was undertaken by the School of Biology at Thames Polytechnic using a Coulter Counter and the resulting data is plotted as Fig. 7.17. The analysis shows that the sizes of particles are more or less evenly distributed from about 35 μm down to less than 6 μm, with a mass median size of about 13 μm.

The very fine particle size and rather low density of the siliceous fillers take this material into the class defined by Geldart as "Group C" (see Section 2.4) and it was therefore anticipated that fluidisation would be difficult. This prediction was confirmed when a sample of the powder was tested in the small fluidising rig. It was found to be impossible to get the powder properly fluidised as a result of persistent slugging and channelling.

CHINA CLAY ('DEVONITE'):

A sample of china clay was tested in the small fluidising rig and also proved to be difficult to fluidise. This material is again of very fine particle size, the mass median diameter being about 8.6 μm. The complete size analysis (by Coulter Counter in the Thames Polytechnic School of Biology) is shown in Fig. 7.18.

The true particle density was determined to be 2490 kg/m^3 and the average value of the bulk density of the unfluidised material was about 526 kg/m^3.

The china clay could not be satisfactorily fluidised since with increasing airflow there was a tendency for slugging to occur. As the slugs of powder collapsed back into the bottom of the vessel, 'cracks' formed through which the air channelled to the surface. A considerable amount of very fine dust was entrained in the airstream and could be seen leaving the top of the fluidising vessel.

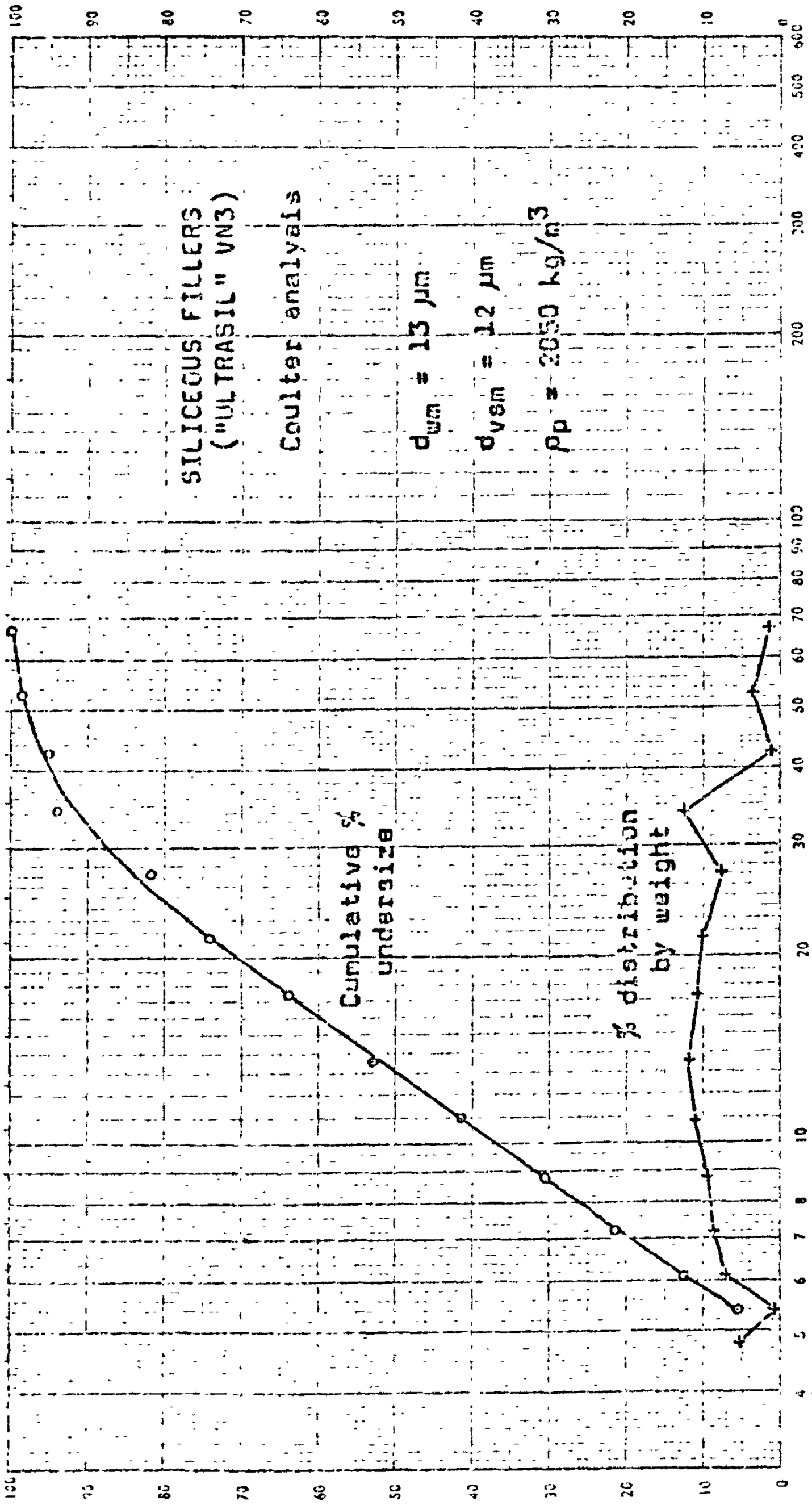

FIG. 7.17 PARTICLE SIZE ANALYSIS OF SILICEOUS FILERS SAMPLE No. 7

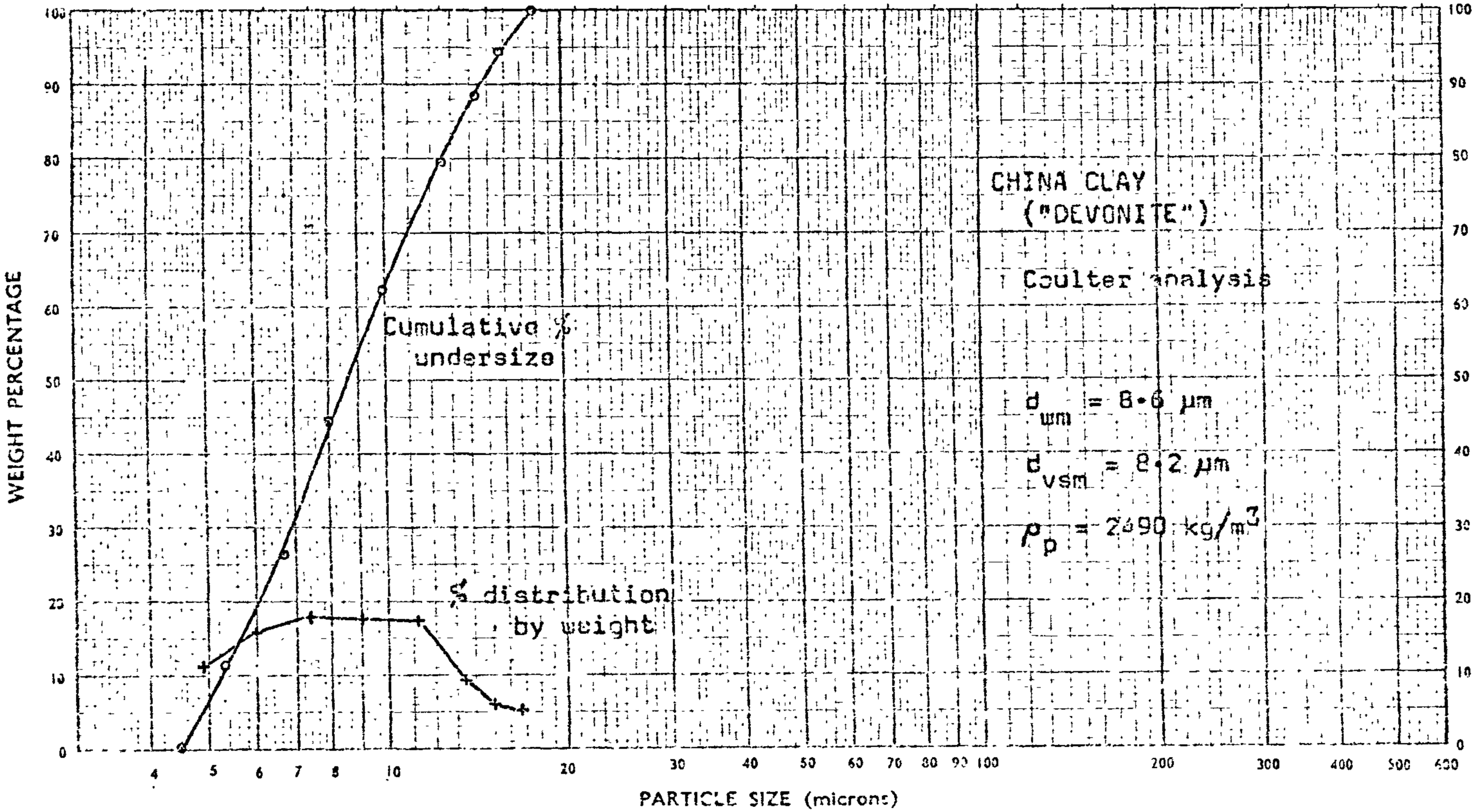

Fig. 7.18 PARTICLE SIZE ANALYSIS OF CHINA CLAY ('DEVONITE') SAMPLE No. 8

7.4.3 Conclusions

Of the eight samples of powder examined, three could be classified from their density and mean particle size as belonging to Geldart's Group A, three to Group B and two to Group C. These classifications were generally confirmed by observation of the behaviour of the powders in the small fluidising test rig, especially with regard to the Group C powders (siliceous fillers and china clay) which could not be satisfactorily fluidised. The classification of Corvic was perhaps questionable since it exhibited Group A behaviour in its fresh, free-flowing condition, but tended to behave in a manner more representative of Group C as it acquired an electrostatic charge.

Table 7.4 sets out the basic properties of the eight materials tested and allows a comparison to be made between values of minimum fluidising velocity predicted using equation 2.9.1,

$$U_{mf} = 420\ \rho_p\ d_v^{\ 2} \qquad \ldots\ldots\ldots\ 2.9.1$$

and values measured in the small fluidising rig. The two sets of figures compare quite closely, except for alumina where the predicted value of U_{mf} was much lower than that actually observed. It is perhaps significant that the alumina had the smallest particle size of the powders that could be satisfactorily fluidised, since equation 2.9.1, giving U_{mf} proportional to the square of the particle diameter, is inclined to be unreliable for very fine or very coarse powders. A better prediction in these cases might be given by an equation in which the particle diameter is raised to a lower power, such as equation 2.3.8 or 2.3.10:-

$$U_{mf} = 104\ \rho_p^{\ 0.934}\ d_v^{\ 1.8} \qquad \ldots\ldots\ldots\ 2.3.8$$

$$U_{mf} = 0.208\ (\rho_b\ d_v)^{1.23} \qquad \ldots\ldots\ldots\ 2.3.10$$

These equations give predicted values of U_{mf} for the alumina of 4.2 mm/s and 4.8 mm/s respectively, which compare rather more closely with the measured value of 4 mm/s.

Sample No.	Material	Particle density kg/m^3	Bulk density kg/m^3	Mean particle diameter μm	Group (Geldart)	Predicted U_{mf} mm/s	Measured U_{mf} mm/s
1	Sand 52/100	2600	1358	188	B	38.6	36-40
2	". 100/150	2640	1314	131	B	19.0	21.6
3	" 120/170	2670	1275	107	B	12.8	12.8-14.5
4	PFA	1780	790	92	A	6.3	5.3
5	Alumina	3830	1371	25	A	1.0	4
6	PVC (Corvic)	1430	450-500	120	A	8.6	10-11
7	Siliceous fillers	2050	190	13	C	-	-
8	China clay	2430	526	8.6	C	-	-

Table 7.4 PROPERTIES OF SAMPLES OF PARTICULATE SOLIDS. (Predicted values of U_{mf} are obtained using Equation 2.9.1.)

A more extensive investigation of the fluidisation behaviour of sand and of Corvic was then carried out and is described in the following Sections.

7.5 FLUIDISATION OF SAND

7.5.1 Introduction

It has been remarked previously that for experimental studies on the fluidisation phenomenon sand has the advantages of being cheap, clean, inert and readily available in a wide range of particle sizes. For these reasons sand has naturally been the material most frequently used by other investigators and there is a considerable amount of data available in the published literature. Where such data is relevant to the present work it has been reviewed in Part I. Despite the existence of this published information it was felt to be necessary to include sand as one of the materials to be tested in the small fluidising test rig since, in addition to adding to practical experience in handling a range of different materials, it would allow a direct comparison with the results of other investigators using sand and also with other materials in the same test rig.

The sand used was supplied by A.L. Curtis Ltd., of Chatteris, Cambridgeshire, in three grades under the codes 52/100, 100/150 and 120/170, indicating the particle size range by the limiting sieve mesh numbers. (These correspond respectively to the size ranges 150-300 μm, 106-150 μm and 90-125 μm. The complete size analyses obtained by sieving are shown in Figs. 7.7 to 7.9)

The tests carried out included observation of the fluidisation behaviour of each sample of sand and determination of their minimum fluidising velocities and bulk densities. The finest of the three samples was tested with two different kinds of porous air distributor fitted in the fluidising vessel (Vyon 'D' and Scandura P22). The effect on the fluidisation behaviour of a coarse material of adding a percentage of fines was examined by fluidising mixtures of coarse and fine sands in different proportions.

7.5.2 Minimum fluidising velocity - the influence of particle size.

Each of the samples of sand was tested in the small fluidising rig with the primary object of determining the minimum fluidising velocities. The main interest was in the finer sand (Sample No. 3, Curtis 120/170) because of the possibility of using this material subsequently in the channel flow rig.

The coarsest sand investigated had a mean particle diameter of 188 μm so that the predicted minimum fluidising velocity (using the simple equation 2.9.1) was 38.6 mm/s. A quantity of this sand was placed in the fluidising vessel (to an initial depth of about 135 mm) and a graph was plotted of the pressure drop across the bed of sand against the superficial air velocity. This graph (Fig. 7.19) gave a value of U_{mf} of 40 mm/s which compares closely with the predicted value. A later test with a slightly smaller quantity of the sand on a different distributor gave a value of 36 mm/s for U_{mf}.

The next sample of sand tested had a mean particle size of 131 μm, giving a predicted U_{mf} of 19 mm/s. In this case beds of three different depths were fluidised and a graph of the pressure drop against the superficial air velocity was plotted for each (Fig. 7.20). Although the sand seemed to fluidise evenly there was some fluctuation of the observed pressure drop across the bed. However, for each bed depth the value of U_{mf} was the same at 21.6 mm/s, slightly greater than the predicted value.

Finally, fluidisation tests were carried out on the finest sand (Curtis 120/170) which was of 107 μm mean particle size. Eight tests were made on this sample of sand: five with beds of different depth using the Vyon 'D' distributor in the fluidising vessel and a further three tests using Scandura P22. These two distributor materials were used to see whether there was any discernable difference in the fluidisation behaviour of the fine sand when supported on distributors having high and low pressure drops. It did appear that the fluidised state was reached rather more smoothly when the high pressure drop distributor was in use (Vyon 'D') and the measured minimum fluidising velocity was slightly greater in this case at 14.5 mm/s as compared to 12.8 mm/s for the Scandura P22 (Figs. 7.21 and 7.22). However, these difference are not regarded as particularly

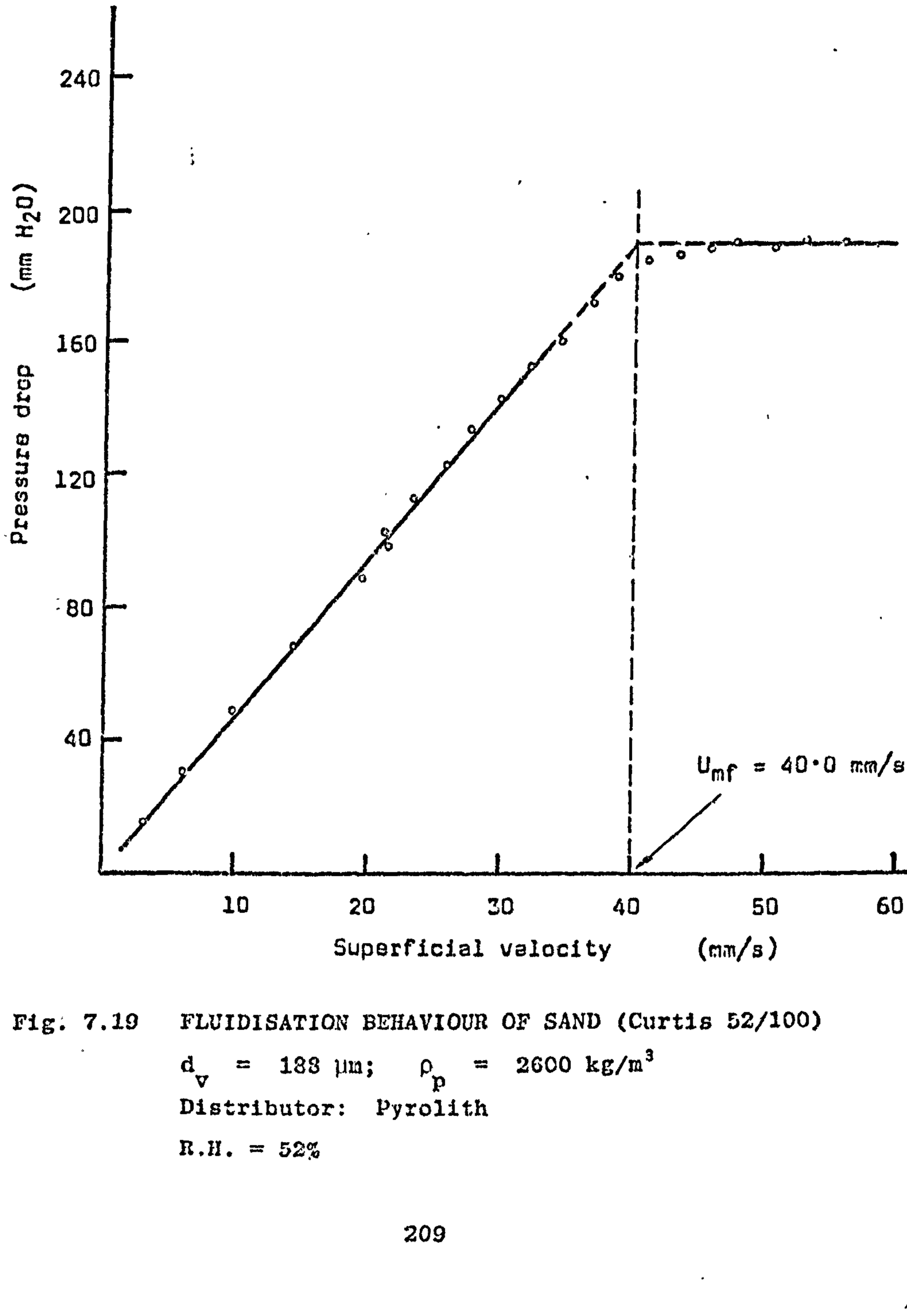

Fig. 7.19 FLUIDISATION BEHAVIOUR OF SAND (Curtis 52/100)

d_v = 183 μm; ρ_p = 2600 kg/m^3

Distributor: Pyrolith

R.H. = 52%

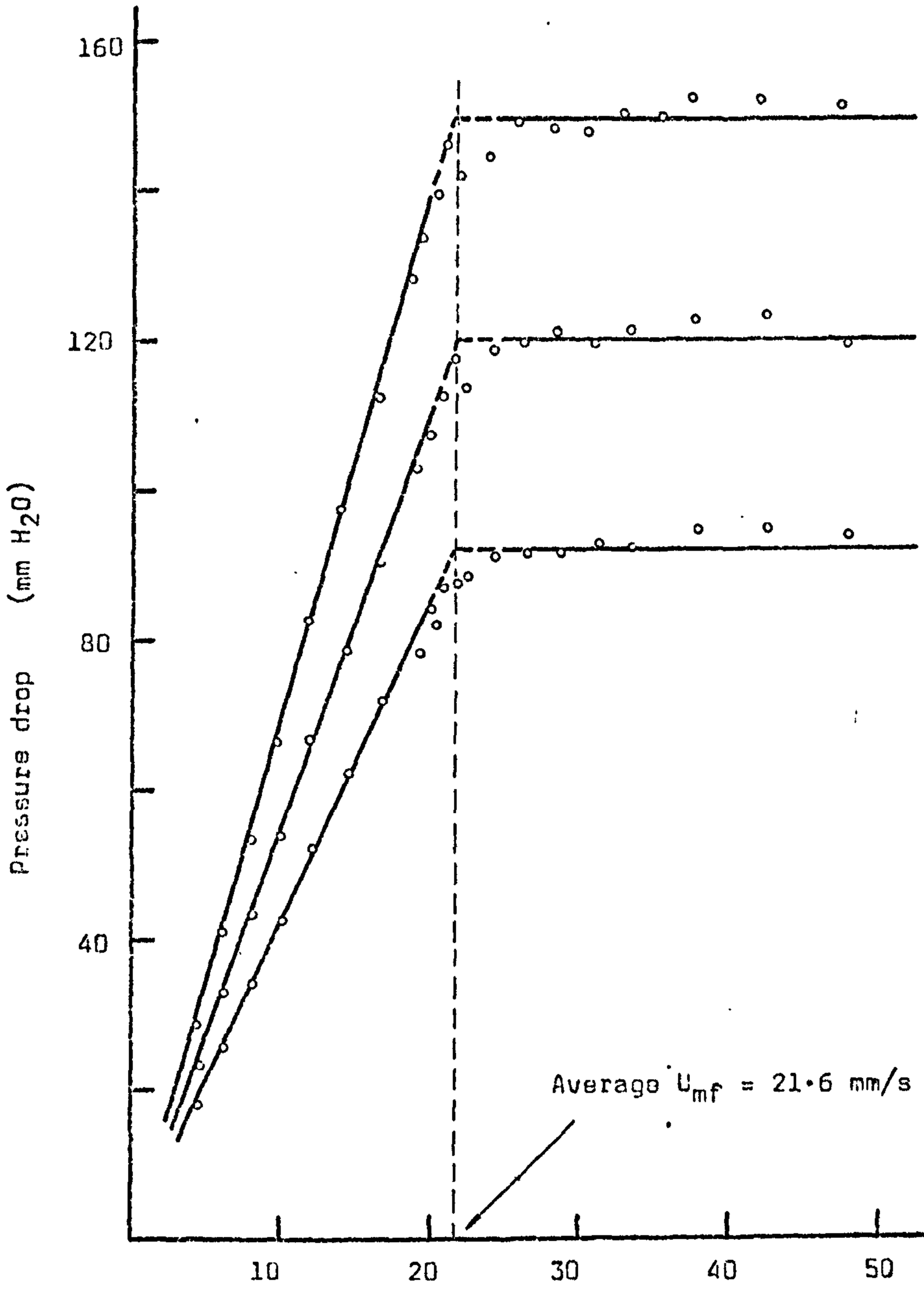

Fig. 7.20 FLUIDISATION BEHAVIOUR OF SAND (Curtis 100/150)

d_p = 131 μm; ρ_p = 2640 kg/m^3

Distributor: VYON 'D'

R.H. = 67%

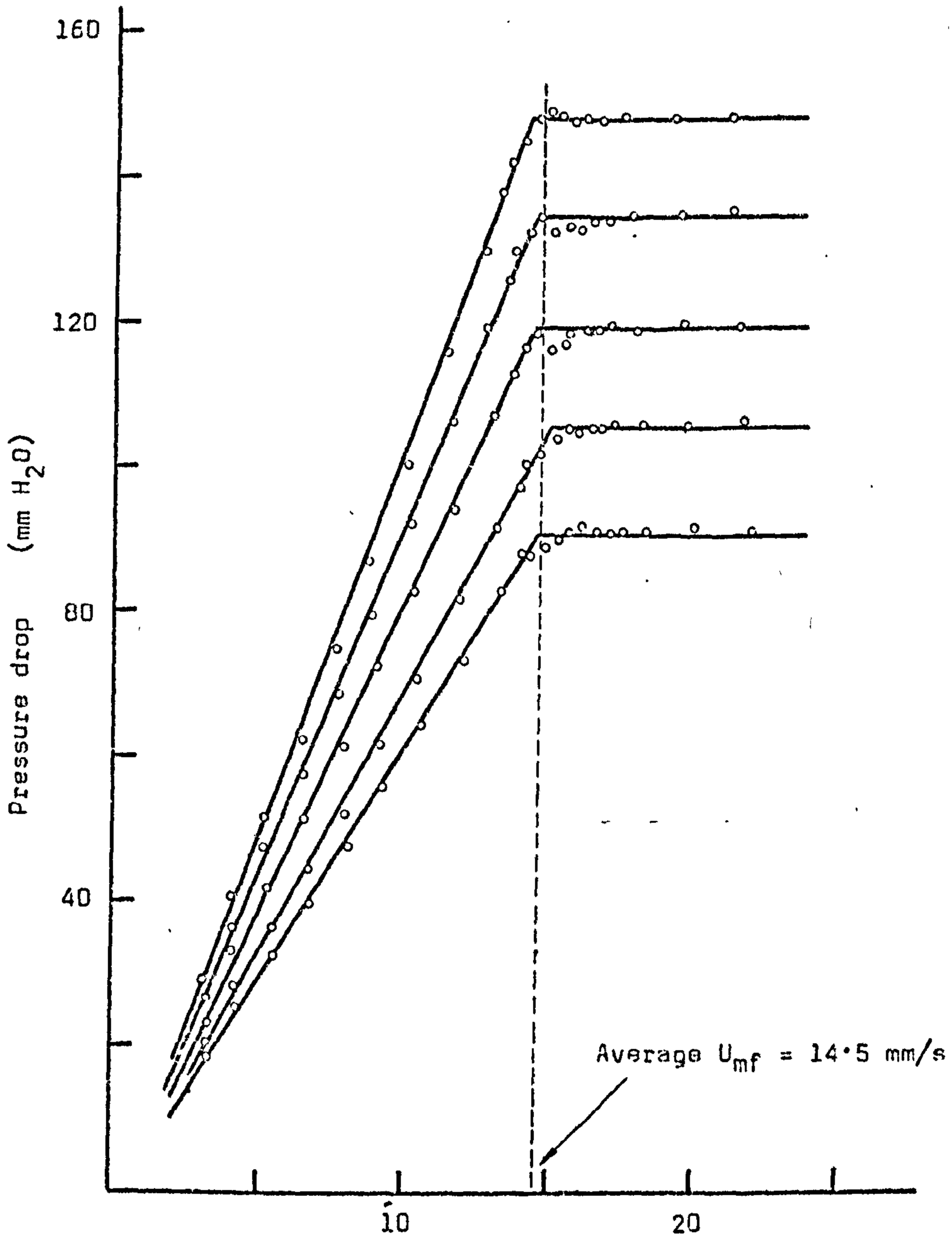

Fig. 7.21 FLUIDISATION BEHAVIOUR OF SAND (Curtis 120/170)

d_v = 107 μm; ρ_p = 2670 kg/m^3

Distributor: VYON 'D'

R.H. = 69%

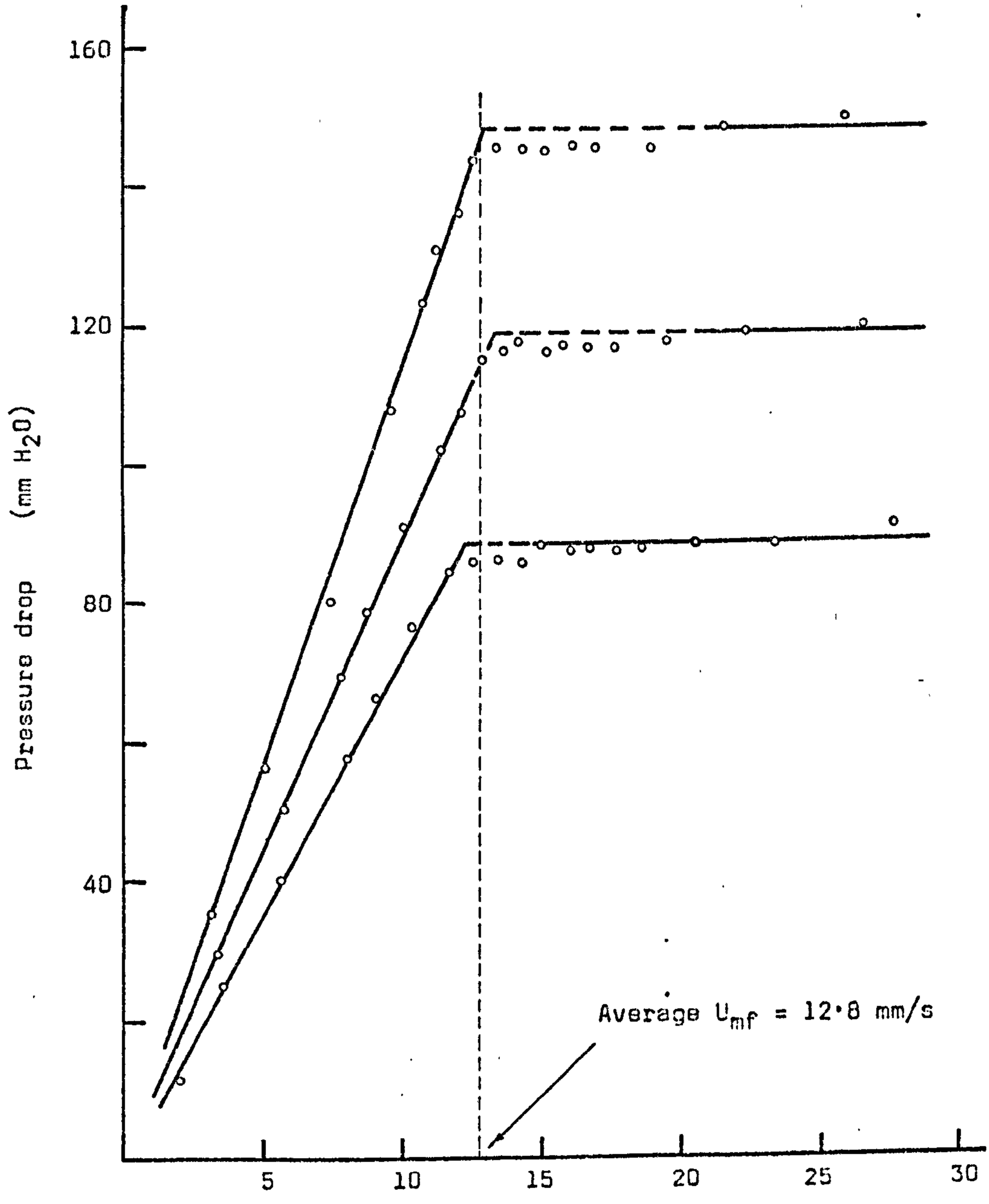

Fig. 7.22 FLUIDISATION BEHAVIOUR OF SAND (Curtis 120/170)

d_v = 107 μm; ρ_p = 2670 kg/m^3

Distributor: SCANDURA P22

R.H. = 72%

significant. The predicted value of U_{mf} was 12.8 mm/s, again comparing closely with the measured values.

An interesting extension of these tests was the investigation of particle size effects on minimum fluidising velocity. The coarse sand (Curtis 52/100) was used for this investigation, being first sieved into five component size fractions covering the ranges 150-180 μm, 180-212 μm, 212-250 μm, 250-300 μm and 300-355 μm. Approximately equal quantities of each of these fractions were placed in turn in the fluidising vessel and a set of graphs was plotted of pressure drop against superficial air velocity (Fig. 7.23). The increase in U_{mf} with increasing particle size is clearly evident from this graph, on which is plotted also the relationship for the 52/100 sand as supplied (that is, having the particle size distribution shown in Fig. 7.7) when fluidised with the same porous distributor (Scandura P22).

It had appeared that there might be a possibility of rendering a coarse material more easily fluidised by adding a small proportion of much finer powder. In order to examine this suggestion, some tests were undertaken in which varying amounts of 107 μm sand (Curtis 120/170) were added to the coarsest fraction of the 52/100 sand used in the previous investigation, and values of U_{mf} for the mixtures were determined. The results of these tests are plotted as a graph of U_{mf} against the proportion of fine sand in the mixture (Fig. 7.24). As was expected, the addition of fine sand caused a reduction in U_{mf}, but it was found that the bed did not always become fluidised uniformly at a single value of the superficial air velocity. There was a tendency over a period of time for segregation to occur with the coarse particles settling to the bottom of the fluidising vessel. A situation can then exist in which the fine material is fluidised on the top surface of the bed whilst the coarse material remains unfluidised, merely forming an extension to the air distributor.

7.5.3 Expansion of the fluidised bed and variation of "bulk density".

During the fluidisation tests on the three samples of sand described in the previous Section a record was kept of the variation in the depth of the bed of sand with increasing superficial air velocity. Firstly, the

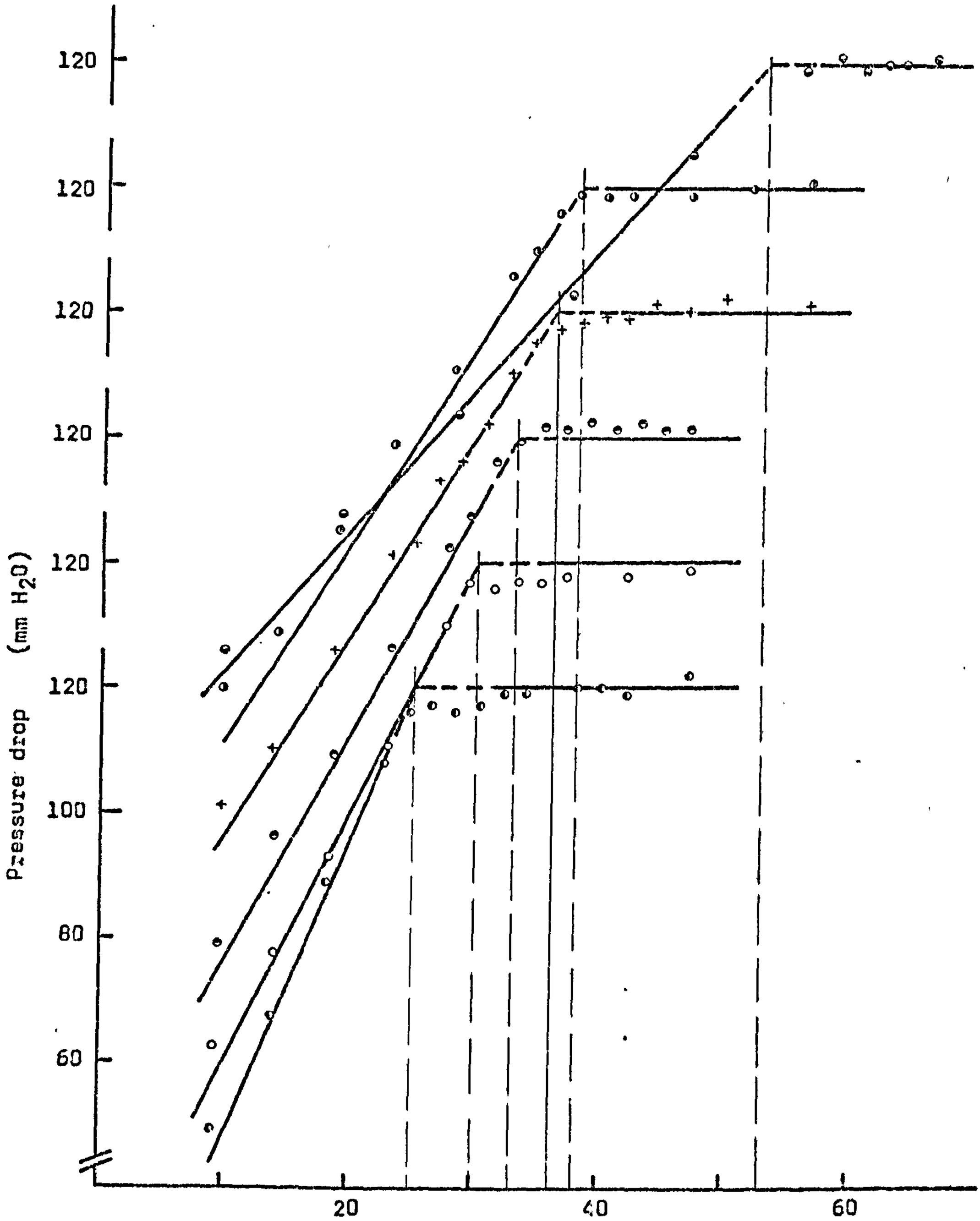

Fig. 7.23 FLUIDISATION BEHAVIOUR OF DIFFERENT SIZE FRACTIONS OF SAND

- ● 150-180 μm
- ○ 180-212 μm
- ● 212-250 μm
- ● 250-300 μm
- ● 300-355 μm
- \+ Mixture (as supplied)

Distributor: Scandura P22

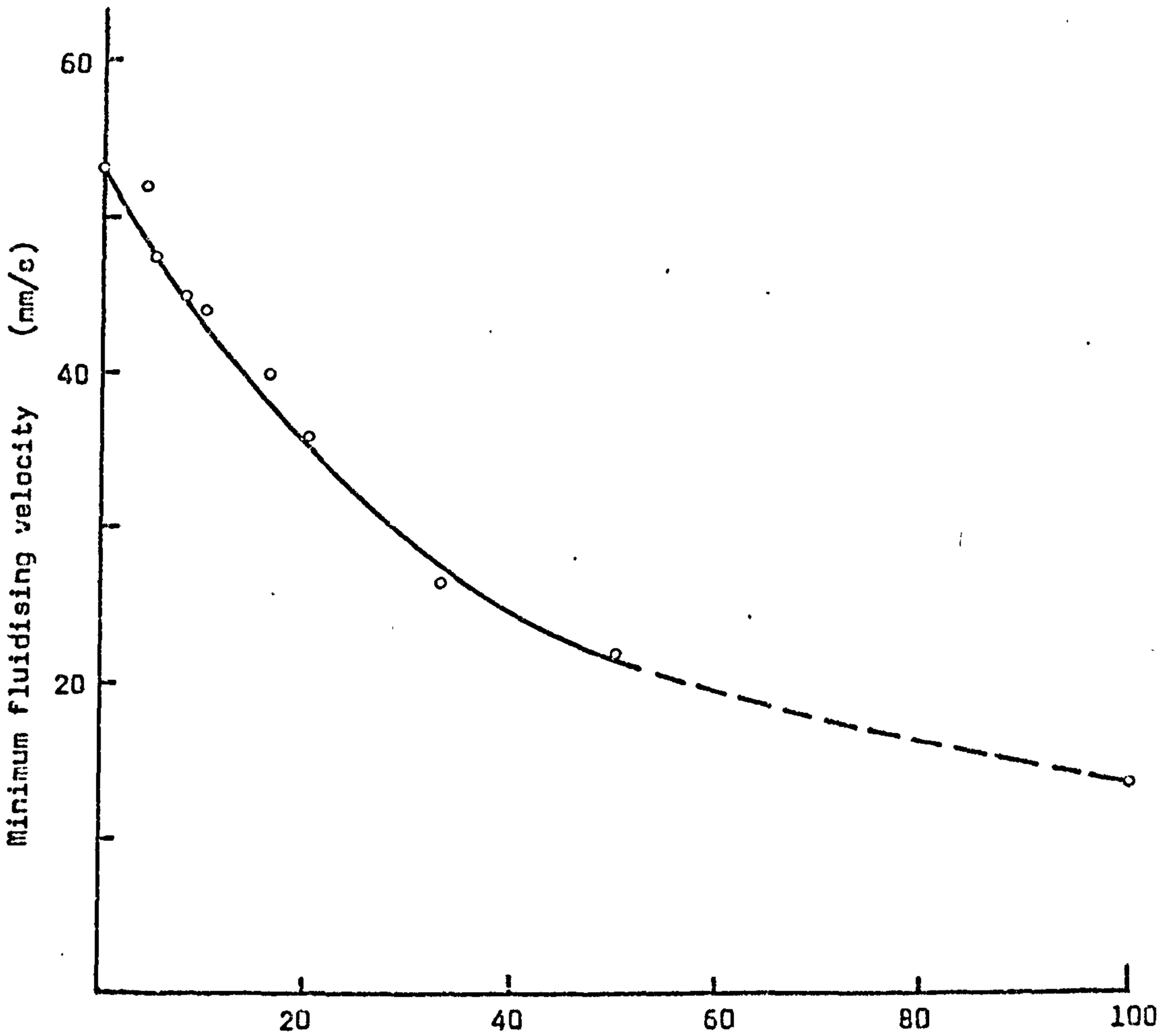

Fig. 7.24 MINIMUM FLUIDISING VELOCITIES OF THE COARSE FRACTION (300-355 μm) OF SAND, SHOWING THE EFFECT OF ADDING A PROPORTION OF FINER (107 μm) SAND.

initial depth was carefully determined by fluidising the sand and then slowly shutting off the air supply and observing the level to which the sand settled. An average of several such observations was taken for each sample of sand and, in the cases of the 131 μm and the 107 μm sands, for each of several different quantities in the fluidising vessel. Based on these initial depths the expansion of the beds could be determined and plotted against the superficial air velocity. Graphs showing the expansion of each sample of sand are plotted as Figs. 7.25 to 7.27. These graphs are not easy to compare except on the basis of minimum fluidising velocities. Thus for example at 1.5 U_{mf} the expansion of the 188 μm sand was 9.8%, for 131 μm sand it was 7.5% whilst beds of 107 μm sand expanded about 7.5% when the Vyon 'D' distributor was in use and apparently slightly more - up to about 8% - on the Scandura P22 distributor. It is interesting to note that these expansions were of very much the same order as in the cases of PFA (8.1% at 1.5 U_{mf}), alumina (8.9% at 1.5 U_{mf}) and Corvic (around 10% at 1.5 U_{mf}).

It has been suggested (Ref. B4) that the degree of expansion of a fluidised bed is a function of the mass of the bed (therefore, of course, of its initial depth) in addition to the superficial air velocity. However, for the two finer samples of sand, which were tested at several different initial depths, points on the plot of bed expansion against superficial air velocity were fairly scattered with no recognisable pattern which could be attributed to the effect of the initial depth of the bed.

The "minimum bulk density" of the samples of sand was determined simply by dividing the mass of material in the fluidising vessel by its volume after being allowed to settle slowly as the air was shut off. The average values of "minimum bulk density" quoted on Figs. 7.26 and 7.27 were averages of measurements with the various quantities of material in the vessel. There is a tendency for the measured bulk density to be lower as the mass of sand in the vessel is reduced. In most cases where the bulk density is required in order to predict conditions in a fluidised bed or in an air-assisted gravity conveyor the value at an appropriate bed depth and superficial air velocity should be used. However, for characterising a material, a more consistent property could perhaps be obtained by plotting the "minimum bulk density" against the initial depth

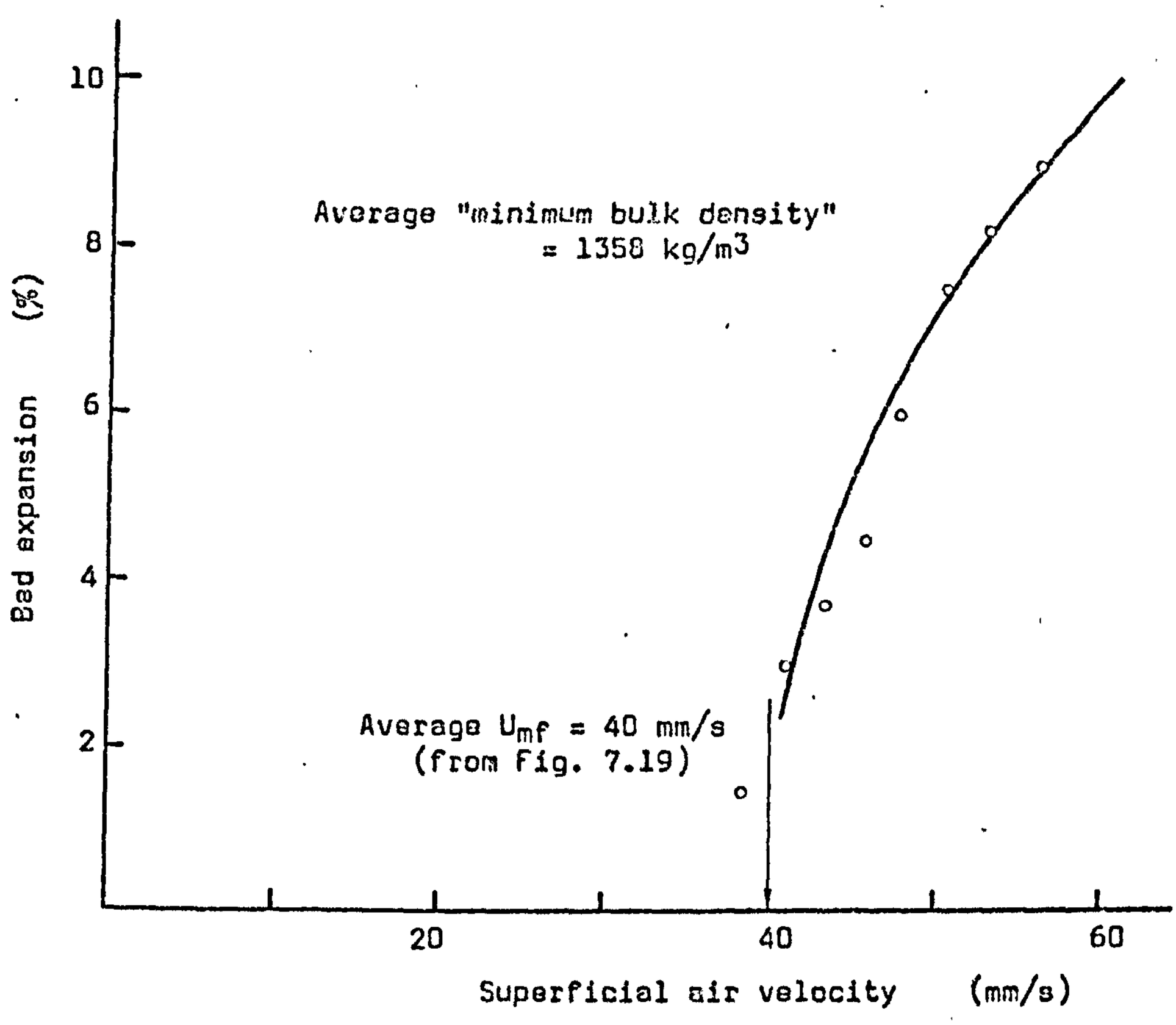

Fig. 7.25 EXPANSION OF FLUIDISED BED OF 188 μm SAND AS A FUNCTION OF THE SUPERFICIAL AIR VELOCITY. Distributor: Pyrolith.

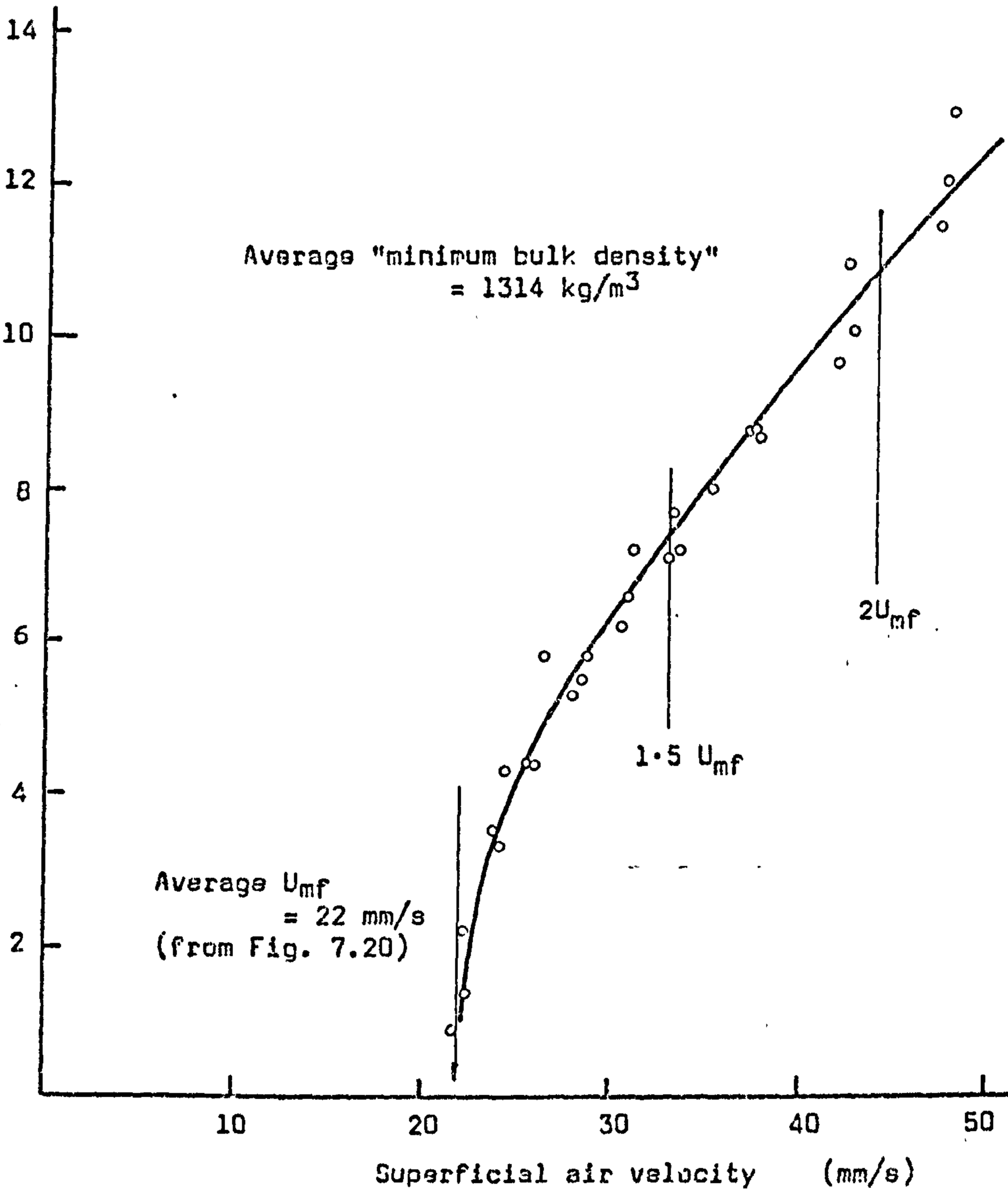

Fig. 7.26 EXPANSION OF FLUIDISED BED OF 131 μm SAND AS A FUNCTION OF THE SUPERFICIAL AIR VELOCITY.
Distributor: Vyon 'D'.

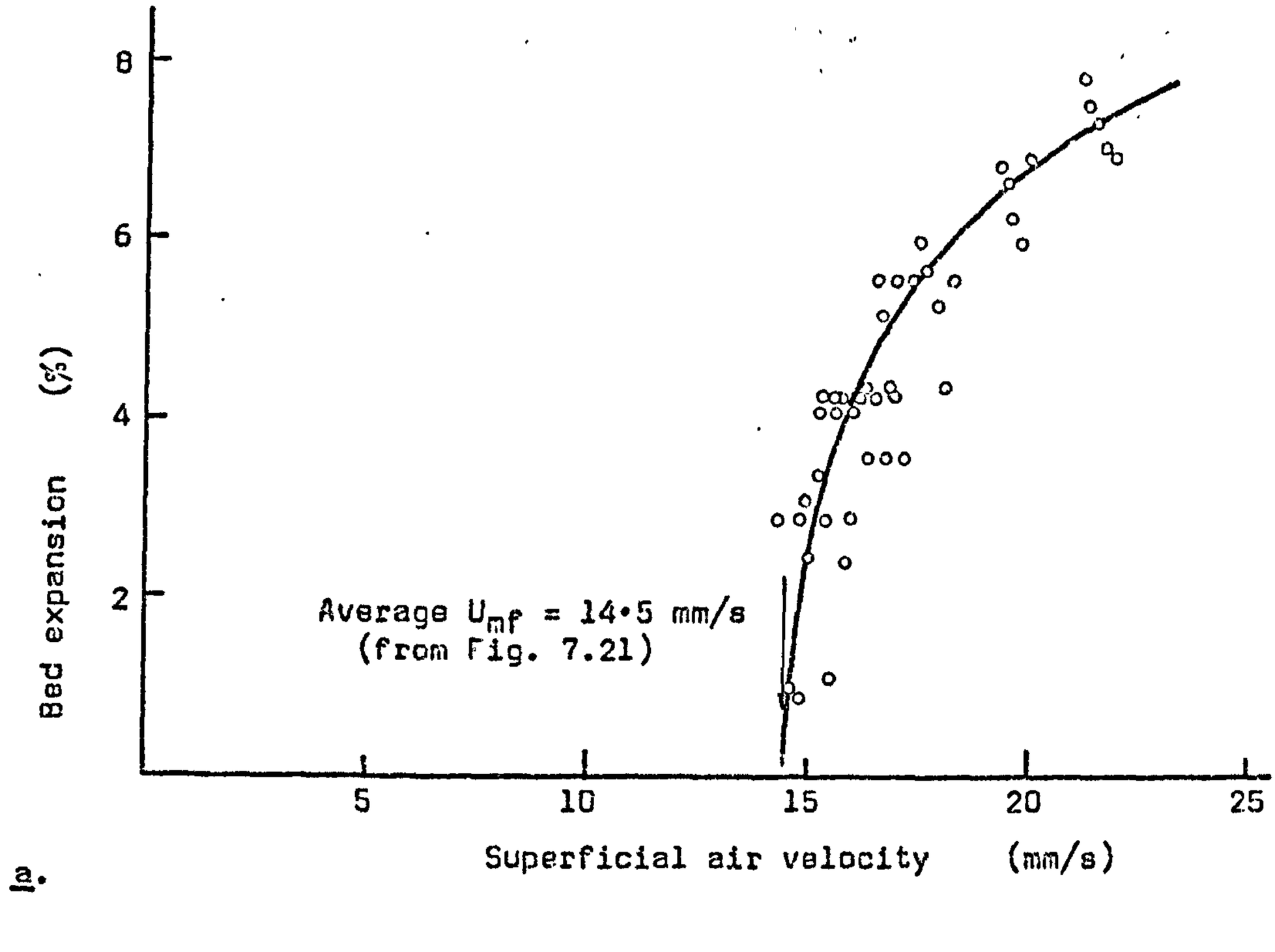

a.

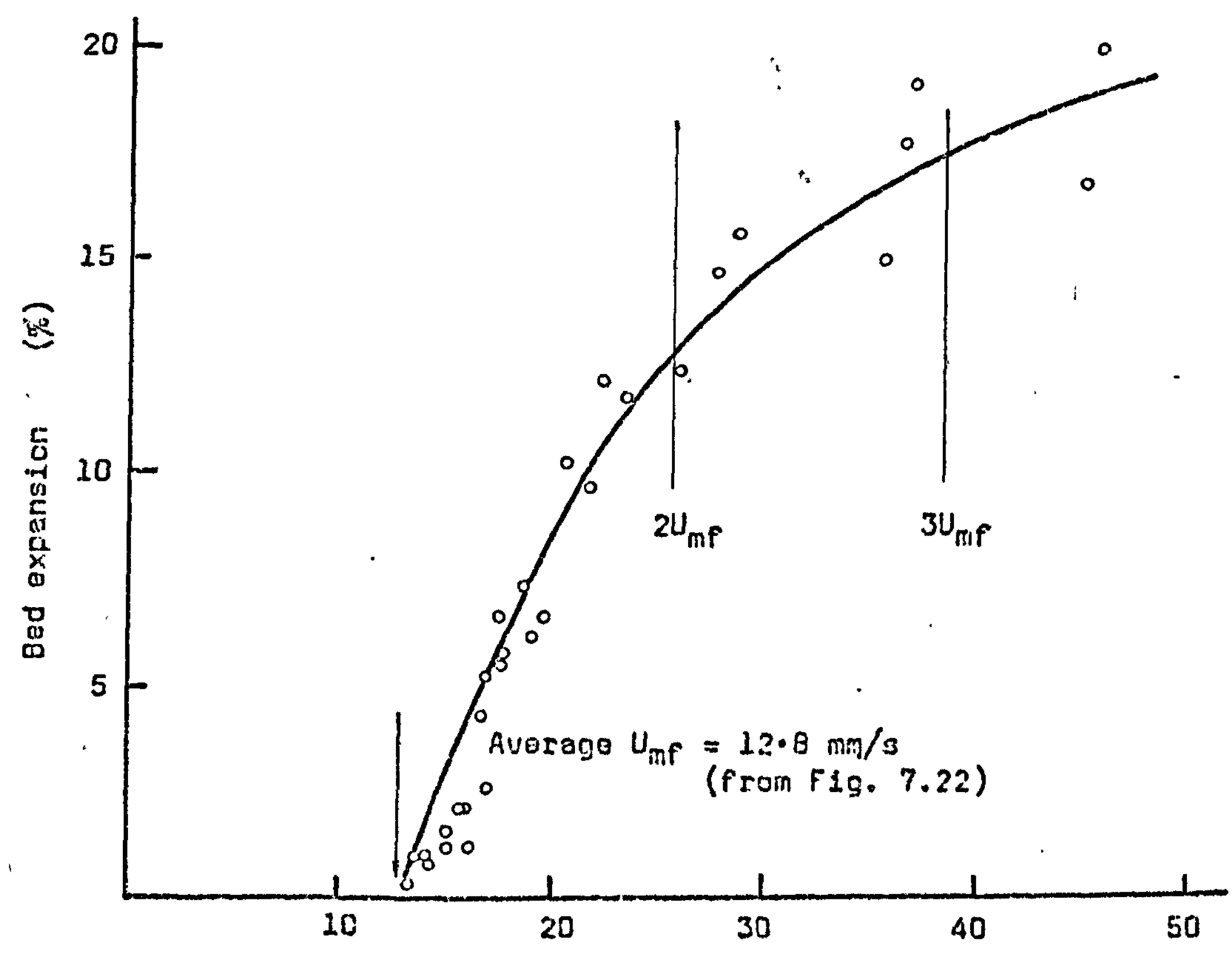

b.

Fig. 7.27 EXPANSION OF FLUIDISED BED OF 107 μm SAND AS A FUNCTION OF THE SUPERFICIAL AIR VELOCITY. Average "minimum bulk density" = 1275 kg/m^3. a) Distributor: Vyon 'D'; b) Distributor: Scandura P22.

of the bed and extrapolating to give a valuo corresponding to zero bed depth.

Although the term "minimum bulk density" is conventionally used for a material in its loosest packing arrangement when there is no airflow, the bulk density is obviously less when the material is fluidised. Under these conditions the definition of the term "bulk density" becomes questionable as it may depend on how voids ("bubbles") in the bed are accounted for, but an estimate can be made by dividing the "minimum bulk density" by the bed expansion ratio at the appropriate superficial air velocity. Thus, for the samples of sand tested, bulk densities over a range of fluidisation conditions could be estimated from Figs. 7.25 to 7.27.

7.5.4 Conclusions

The tests on various size samples of sand provided useful information on the behaviour of the material when fluidised in stationary (as opposed to flowing) beds. The measured values of minimum fluidising velocity compared quite closely with predicted values, showing how U_{mf} increases rapidly with increasing particle size and thus emphasising the fact that transportation of powders in air-assisted gravity conveyors may be less attractive for materials of large particle size because of the heavy air consumption.

One possible method of conveying coarse materials more economically might be to mix in a small proportion of finer material (which could be separated at a later stage, if necessary) thus reducing the minimum fluidising velocity and hence the quantity of air required by the air-gravity conveyor. Some evidence to support this idea was sought by carrying out simple fluidisation tests on mixtures of fine and coarse sand, but the results of these tests, summarised in Fig. 7.24, are not really conclusive. The proportion of fine sand that has to be added to produce a worthwhile reduction in U_{mf} is quite large and, furthermore, problems resulting from segregation of the fine and coarse fractions could well offset any advantage that might otherwise be gained.

One of the properties of a particulate material that should be known when designing air-gravity conveyors is the bulk density and, for the samples of sand tested, data was obtained which allows a reasonable estimate to be made of the bulk density over a range of fluidising conditions. However, as has been previously mentioned (Section 3.4.3.), some care should be taken when applying data from stationary beds to situations, such as occur in air-assisted gravity conveyors, where the aerated bed is flowing.

7.6 FLUIDISATION OF P.V.C. ('CORVIC')

7.6.1 Introduction

For the test programme to be undertaken on the air-assisted gravity conveying rig it was proposed to use some material other than sand in order to extend the range of detailed experimental data available. Of the many different particulate solids considered, some of which were tried in the small fluidising rig as described in Section 7.4, the p.v.c. powder ("Corvic") seemed to be a likely choice. This powder had the advantages of being clean, safe and easily fluidised and, through the generosity of I.C.I. Ltd., a suitable quantity was made available for the channel flow tests. The size analysis of the Corvic is given in Fig. 7.16, from which the mass median diameter is seen to be 120 μm.

As a preliminary to the investigation of the flow properties of the aerated powder, the small fluidising rig was used to test samples of the Corvic in order that its handling characteristics should become familiar. During these tests data was collected on the fluidisation behaviour of the Corvic on various types of porous distributor. At first these tests were confined to the powder in its fresh, free-flowing state, but after it had become obvious during commissioning of the channel flow rig that electrostatic effects could not be ignored, the investigation was extended to cover the fluidisation of a "stationary" bed of Corvic in its charged condition.

Finally a few measurements were made of the "viscosity" of a bed of fluidised Corvic in order to verify that changes in this property with

varying superficial air velocity followed the normally accepted pattern.

7.6.2 Minimum fluidising velocity

The first tests with Corvic in the small fluidising rig set out to determine the variation of the pressure drop across a bed of uncharged powder with the superficial velocity of the upward flowing air in the vessel. The exercise was repeated with various depths of Corvic in the vessel and with different porous distributors so that any influence of these factors on the fluidisation behaviour could be observed.

Fig. 7.28 shows the results of tests using Vyon 'D' as the porous distributor. Five different depths of Corvic were fluidised and the average of the minimum fluidising velocities for each depth of bed was found to be 10.8 mm/s. There does appear from this graph to be a tendency for U_{mf} to be less in the deeper beds but it is thought that a more likely cause for the variation of U_{mf} was changes in the electrostatic charge on the powder. Reference has been made elsewhere to the difficulty of obtaining repeatable results with the Corvic, because of fluctuations in interparticle forces that appear to be random, but presumably bear some relationship to the humidity of the fluidising air, or of the surrounding atmosphere, or both.

A further five depths of Corvic were fluidised on the Scandura P22 distributor, but the resulting graphs (Fig. 7.29) do not show any significant difference in the behaviour of the bed from that observed when fluidised on Vyon 'D'. Admittedly the average value of U_{mf} is slightly lower, which corresponds to the lower value of U_{mf} for 107 μm sand when fluidised on Scandura P22, but the difference in the values is quite small and it is not possible to state with any certainty that they are not caused by fluctuations in the electrostatic charge carried by the powder.

In fact, evidence to support the contention that interparticle forces resulting from electrostatic phenomena have a significant effect is provided by Fig. 7.30 which shows the outcome of tests completed on a different day when the humidity of the fluidising air was rather higher.

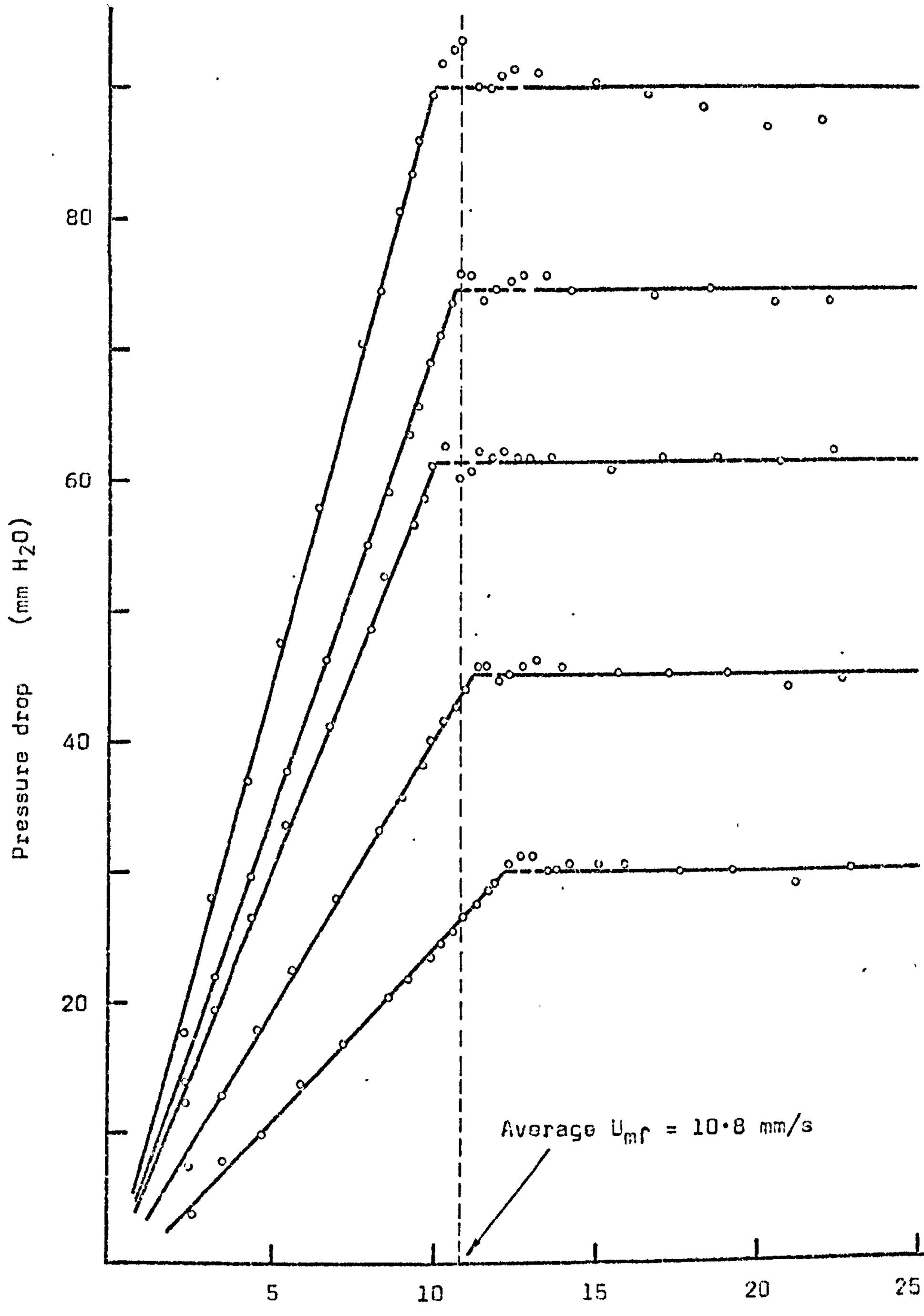

Fig. 7.28 FLUIDISATION BEHAVIOUR OF CORVIC

d_v = 120 μm; ρ_p = 1430 kg/m^3

Distributor: VYON 'D'

R.H. = 69%

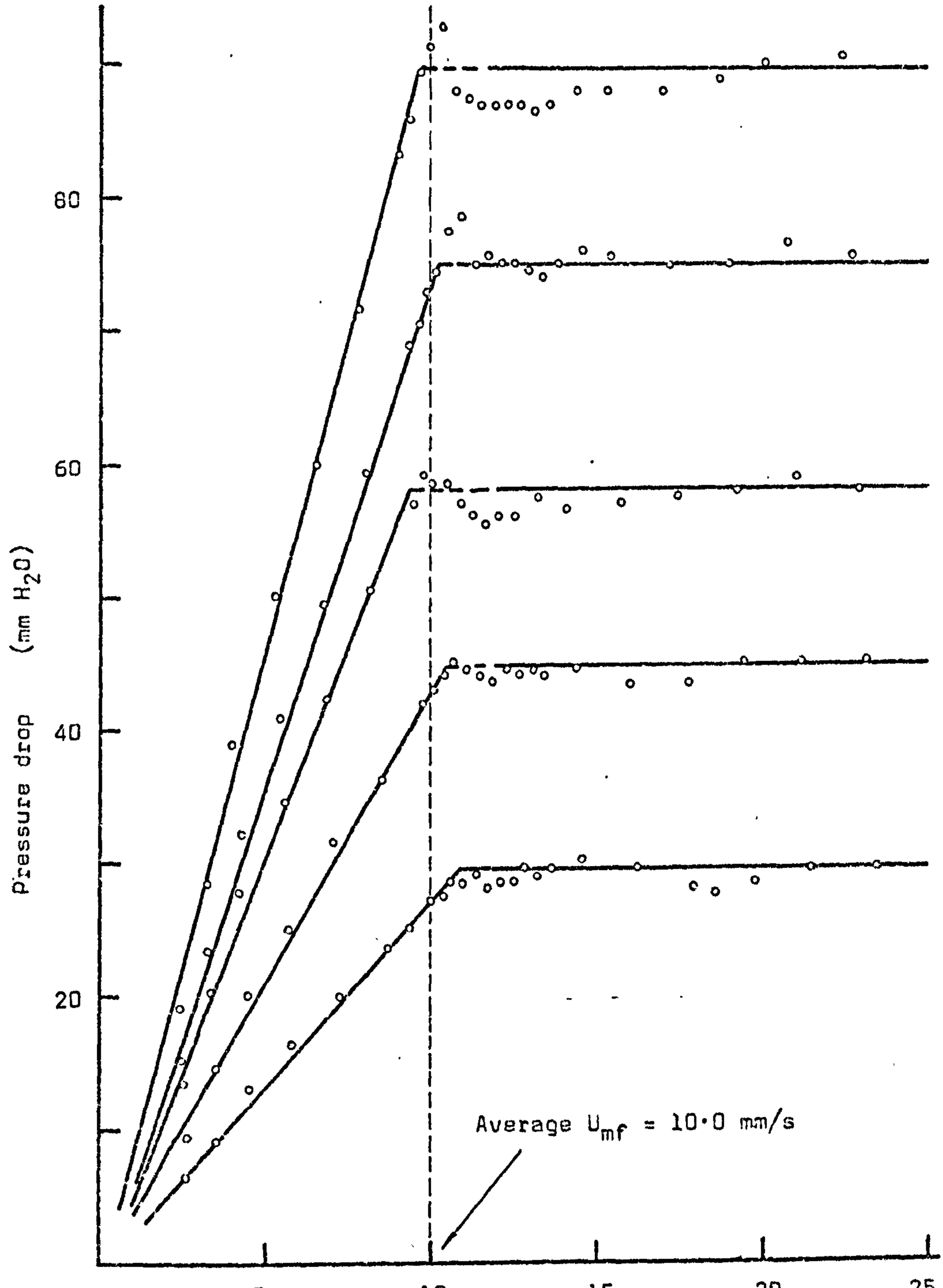

Fig. 7.29 FLUIDISATION BEHAVIOUR OF CORVIC

d_v = 120 μm; ρ_p = 1430 kg/m^3

Distributor: SCANDURA P22

R.H. = 60%

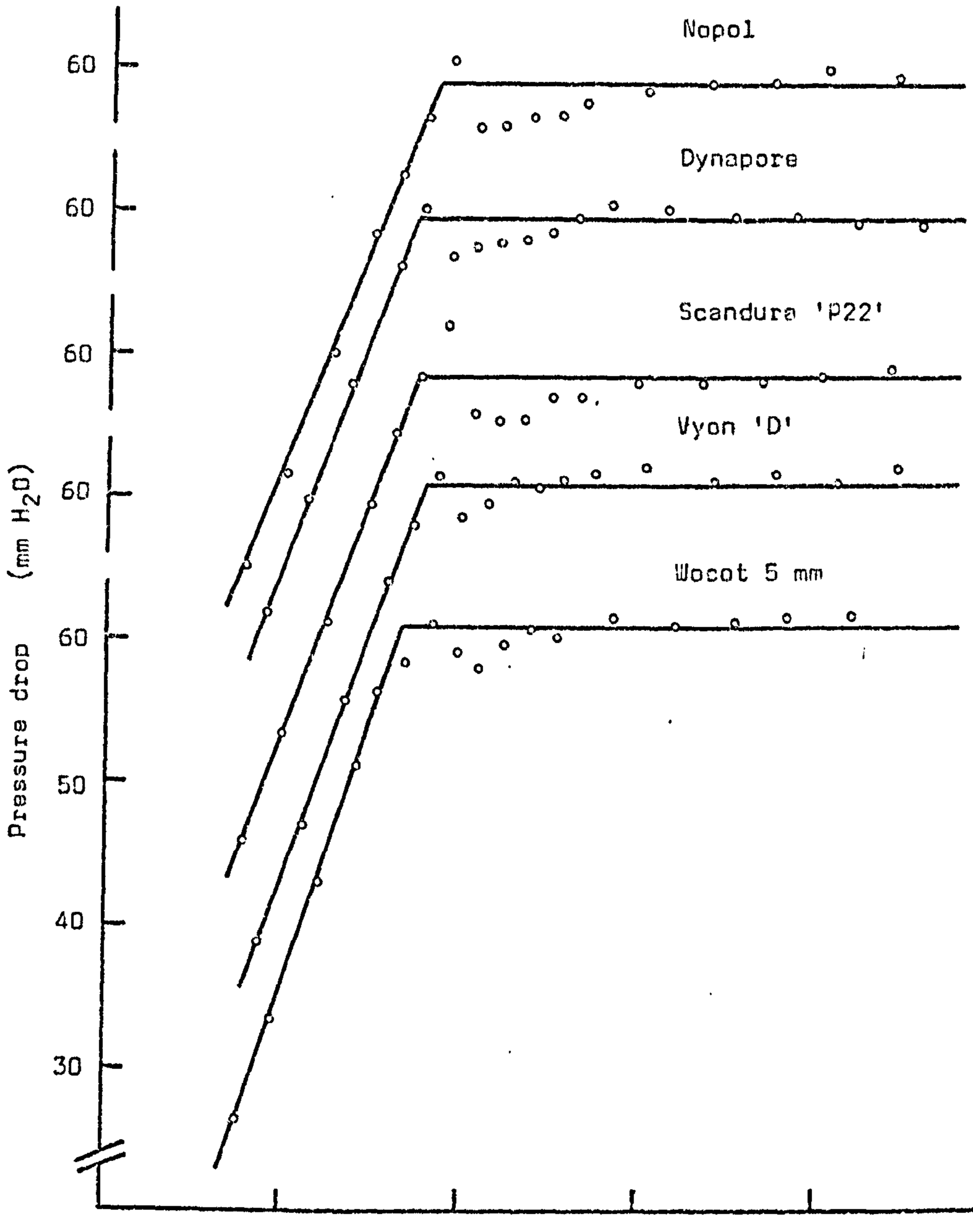

Fig. 7.30 FLUIDISATION BEHAVIOUR OF CORVIC, WITH VARIOUS TYPES OF DISTRIBUTOR.

d_v = 120 μm; ρ_p = 1430 kg/m^3

Initial bed depth ~ 132 mm

R.H. = 82%.

These tests sought to compare the behaviour of similar beds of Corvic when fluidised on various kinds of porous distributor, and in each case the value of U_{mf} was lower than those previously recorded. No consistent pattern can be seen to distinguish the behaviour of the Corvic amongst the various distributors, and the overriding trend towards the lower value of U_{mf} must be attributed to the powder carrying a lower electrostatic charge.

7.6.3 Expansion of the fluidised bed and variation of "bulk density"

As with the other particulate solids tested in the small fluidising rig, readings were taken of the depth of the bed of fluidised Corvic to enable plots to be made of the bed expansion against the superficial air velocity. Separate graphs were plotted for beds of Corvic fluidised on the Vyon 'D' (Fig. 7.31) and on the Scandura P22 (Fig. 7.32) distributors. In an attempt to detect the influence of the quantity of Corvic in the bed, points corresponding to different initial depths of the powder bed are distinguished. It does seem for both distributors, that the expansion of the beds is rather less when the initial depth of the bed is relatively small, the effect being most pronounced when the superficial air velocity is only slightly greater than U_{mf}. However, there is no obvious difference in the behaviour of the Corvic fluidised on the two distributors.

Taking a stage further the investigation of the influence of the type of distributor, a graph of bed expansion ratio (that is, the ratio of the actual depth of the bed to its greatest depth with zero airflow) against superficial air velocity was also plotted for a constant amount of Corvic (giving an initial bed depth of about 132 mm) on five different porous distributors (Fig. 7.33). As can be seen from this graph there is some scatter of the test points and unfortunately no pattern of behaviour emerges which could be attributed to the characteristics of the different distributors. It is worth noting however, that throughout this series of tests the expansion of the bed appeared to be significantly less than that shown on Figs. 7.31 and 7.32. It is thought that this was the result of the higher relative humidity of the fluidising air for the tests of Fig. 7.33 reducing the effects of electrostatic charging, but the matter is discussed in more detail in the next Section.

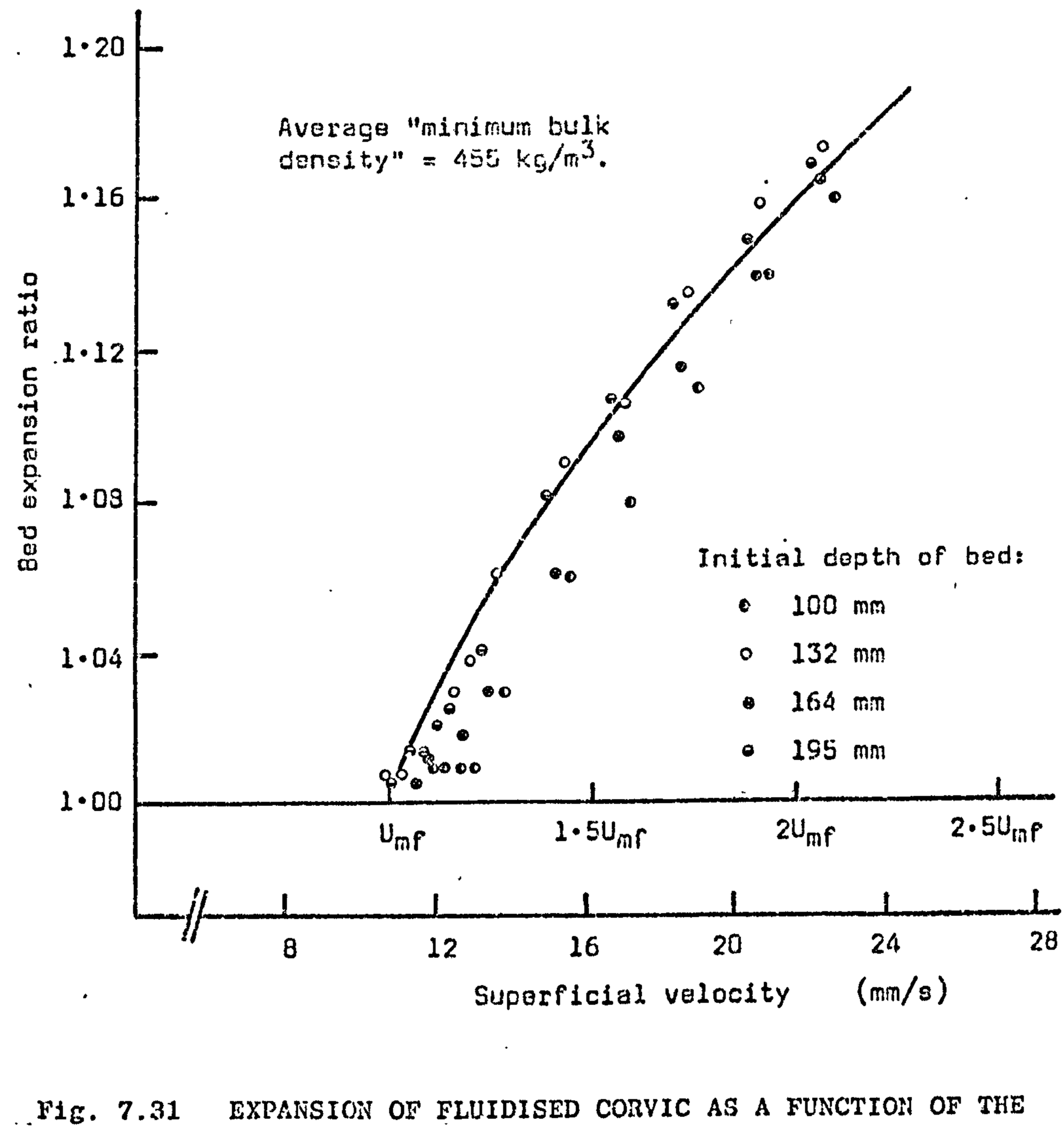

Fig. 7.31 EXPANSION OF FLUIDISED CORVIC AS A FUNCTION OF THE SUPERFICIAL AIR VELOCITY. Distributor: Vyon 'D', R.H. = 69%.

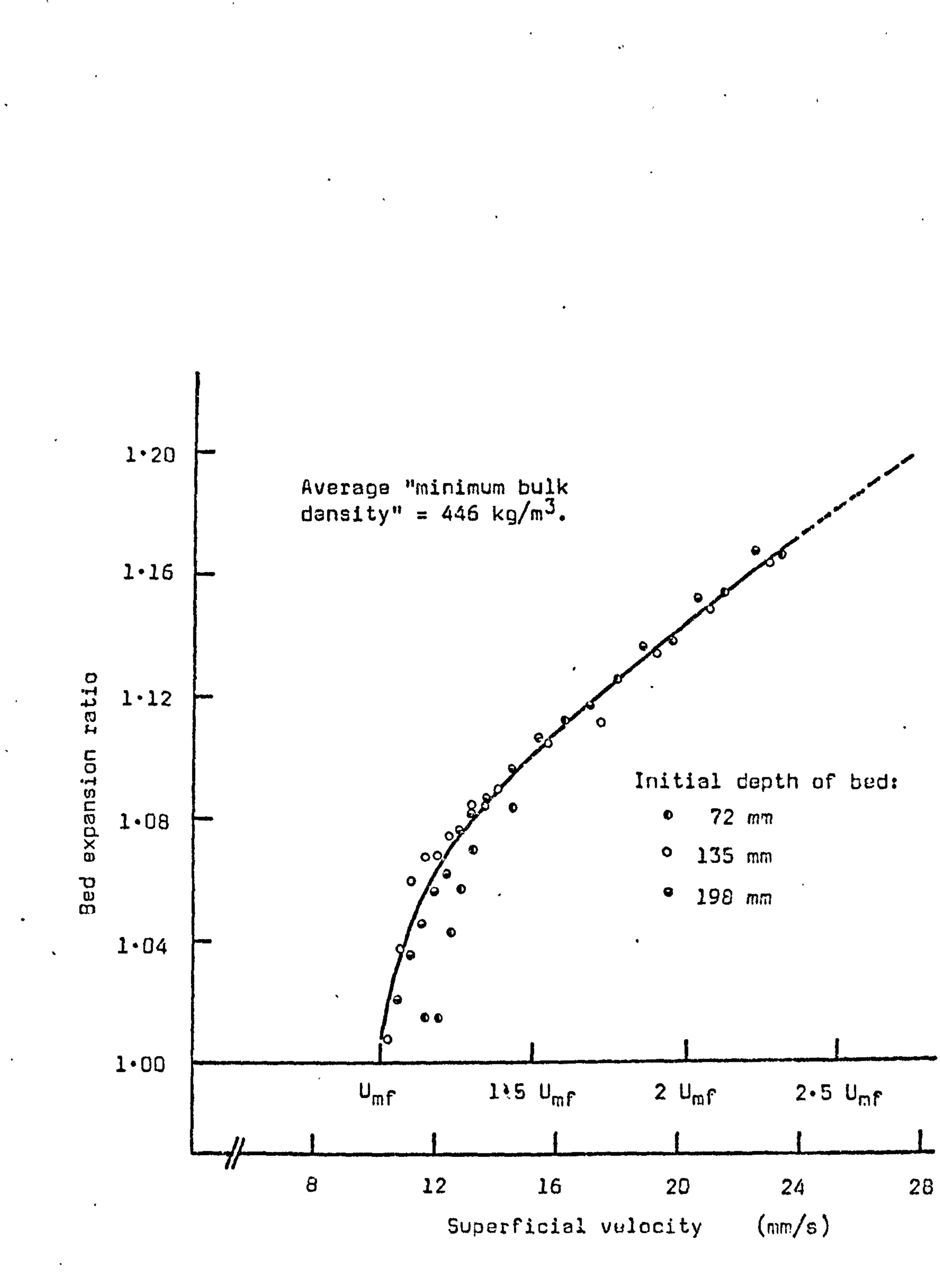

Fig. 7.32 EXPANSION OF FLUIDISED CORVIC AS A FUNCTION OF THE SUPERFICIAL AIR VELOCITY. Distributor: Scandura P22, R.H. = 60%

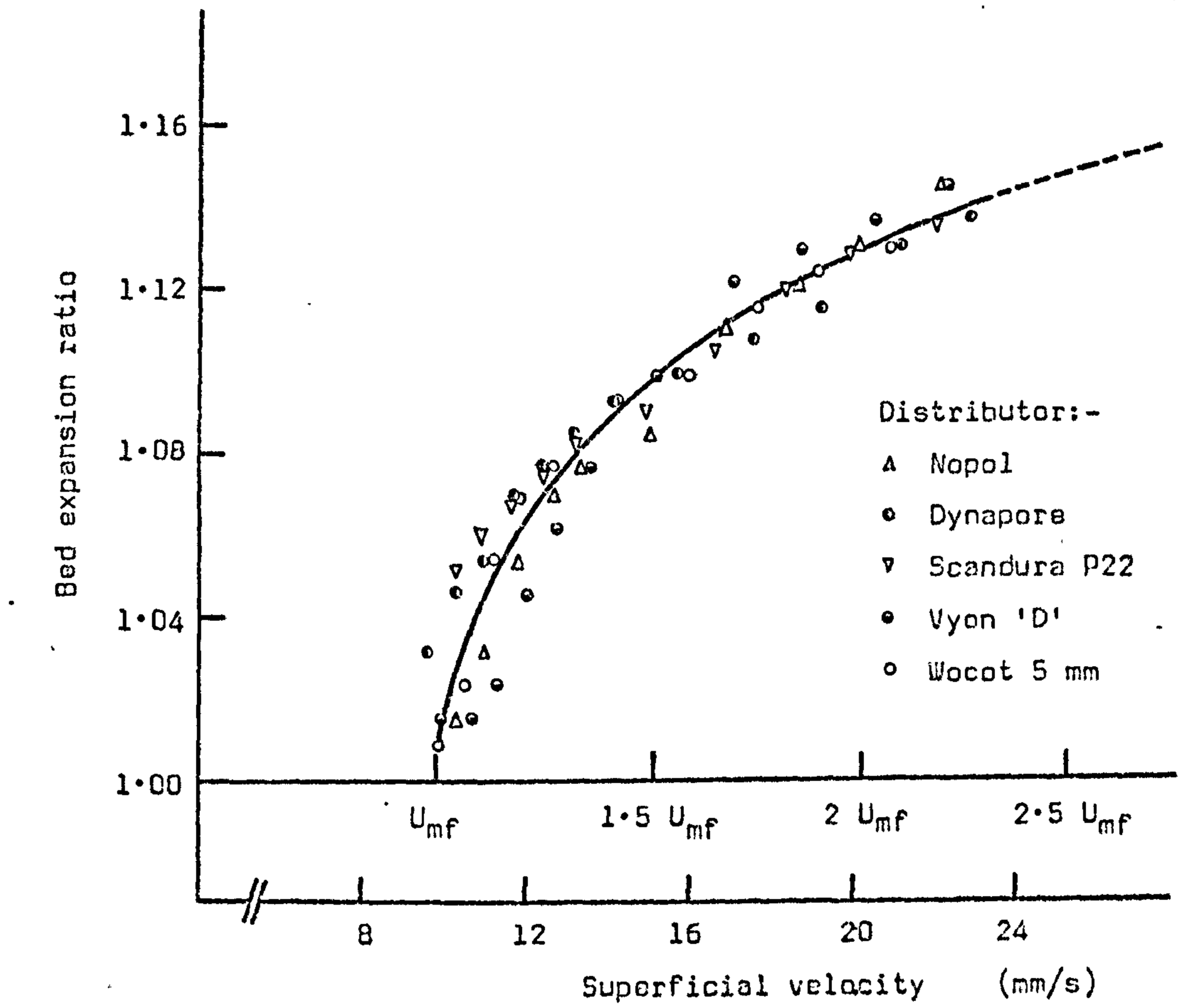

Fig. 7.33 EXPANSION OF FLUIDISED CORVIC AS A FUNCTION OF THE SUPERFICIAL AIR VELOCITY. Distributor: various. Initial bed depth = 132 mm, R.H. = 82%.

7.6.4 Electrostatic effects and relative humidity

It had been known from the outset that Corvic, in common with other plastics powders, was prone to changes in its nature as a result of electrostatic charging. However, it was only during the commissioning tests on the channel rig that the extent of the difficulties caused by these changes of behaviour began to be appreciated. Although there was a tendency for the electrostatic charges to develop in the Corvic whilst it was being fluidised, the process was quite slow, even when fluidisation was vigorous. That there was some increase in interparticle forces during the fluidisation tests was obvious from gradual changes in behaviour that occurred when the powder was fluidised for long periods of time, or from scattering of the test points when readings were taken in random sequence.

Fig. 7.34 is a plot of the variation of pressure drop across the bed at the lower end of the range of superficial air velocity, showing conditions in the region of minimum fluidisation. In this test, designed to demonstrate the way in which electrostatic charging could affect the value of U_{mf}, a sample of uncharged Corvic was placed in the fluidising vessel and the airflow was gradually increased until the material was clearly fluidised but not bubbling appreciably. On reducing the airflow the pressure drop is seen to be significantly lower than for increasing airflow. This was thought to be the result of particles settling into a different packing arrangement, perhaps influenced by the degree of electrostatic charging of the powder. The airflow was then increased and the bed of Corvic allowed to bubble vigorously for some time in order for it to reach a charged condition, corresponding, it was hoped, to the equilibrium charged condition attained by the powder in the flow tests on the main channel rig. The fluidising air was then shut off and gradually increased again whilst readings of pressure drop across the bed and air flowrate were taken. It was very evident that the charged powder did not become fluidised uniformly in the manner of the uncharged material. The point of incipient fluidisation was much less clearly defined, but seemed to occur at around twice the value of superficial air velocity at which the uncharged material became fluidised. Repetition of this procedure showed, as had by now come to be expected, that results varied considerably from one day to another, and recorded values of U_{mf} ranged between about 15 mm/s and

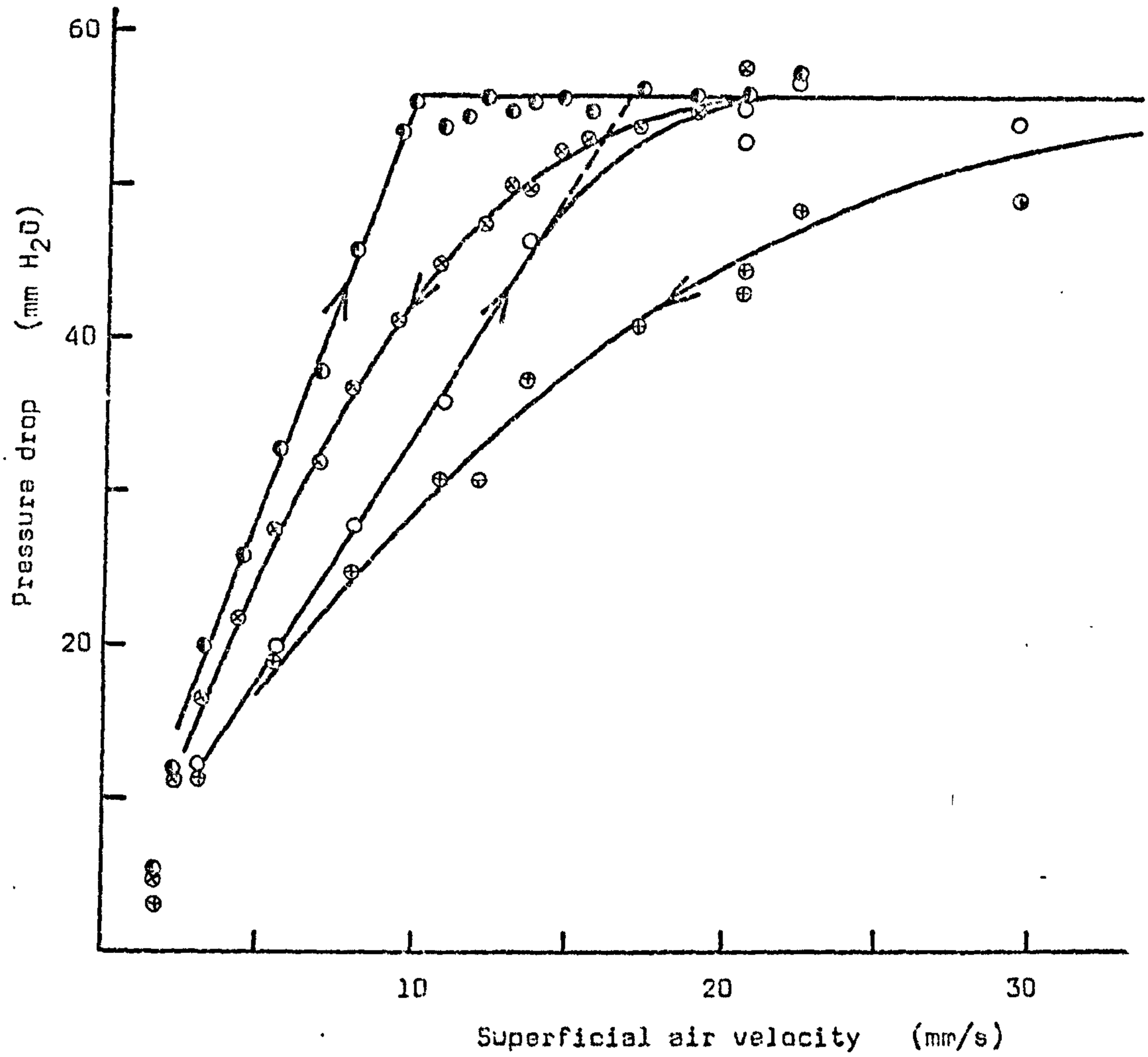

Fig. 7.34 FLUIDISATION BEHAVIOUR OF CORVIC, SHOWING THE EFFECT OT ELECTROSTATIC CHARGING.

- ⊙ Uncharged powder, fluidised from an initial bed depth of 107 mm.
- ⊗ Air flow reduced allowing powder to settle.
- ○ Same mass of powder, charged and fluidised from rest (120 mm initial depth).
- ⊕ Air flow reduced allowing charged powder to settle.

25 mm/s, depending evidently upon the level of charge acquired. On reducing the airflow the pressure drop across the bed of charged Corvic is again generally found to be well below that for increasing airflow, as shown in Fig. 7.34.

Powder taken from the channel rig after a lengthy period of running showed even more erratic behaviour in the small fluidising rig. Fig. 7.35 gives relationships between pressure drop and superficial air velocity for three different initial depths of such a sample. The Corvic appeared to be quite cohesive and could not be satisfactorily fluidised. There was a strong tendency for channelling and slugging to occur, particularly in the more shallow beds, and the measured pressure drop across the bed was often considerably greater than that corresponding to the bed weight. It seems probable that the effect of charged particles clinging to the Perspex wall of the fluidising vessel and to the plastic (Vyon) distributor could add a significant downward component of force to the weight of the powder bed.

The difficulties involved in predicting the bulk density of a flowing bed of aerated powder from tests on a stationary bed have already been mentioned and these difficulties are intensified when electrostatic charging of the powder appears as an independent variable. From measurements of the depth of beds of Corvic in the small fluidising rig taken during the various fluidisation tests a graph was plotted (Fig. 7.36) in an attempt to illustrate the range over which the bulk density could vary in the stationary aerated powder. From these results it was immediately clear that the charged powder could "hold" a lot more air than when uncharged, the "minimum bulk density" of the charged Corvic sometimes being recorded at less than 380 kg/m^3, compared with the normal range of 450 to 500 kg/m^3. As the superficial air velocity was increased and the beds expanded the difference in the bulk densities became less marked, but there was still a clear trend for the charged powder to occupy the greater volume. It should be noted that all the data on Fig. 7.36 is for increasing superficial air velocity. Much lower values of bulk density could be recorded with decreasing airflow, depending to some extent upon the time allowed for the Corvic to settle between test readings.

Some indication of the influence of humidity on the behaviour of fluidised Corvic is given by Fig. 7.37 in which the expansion of the bed of powder

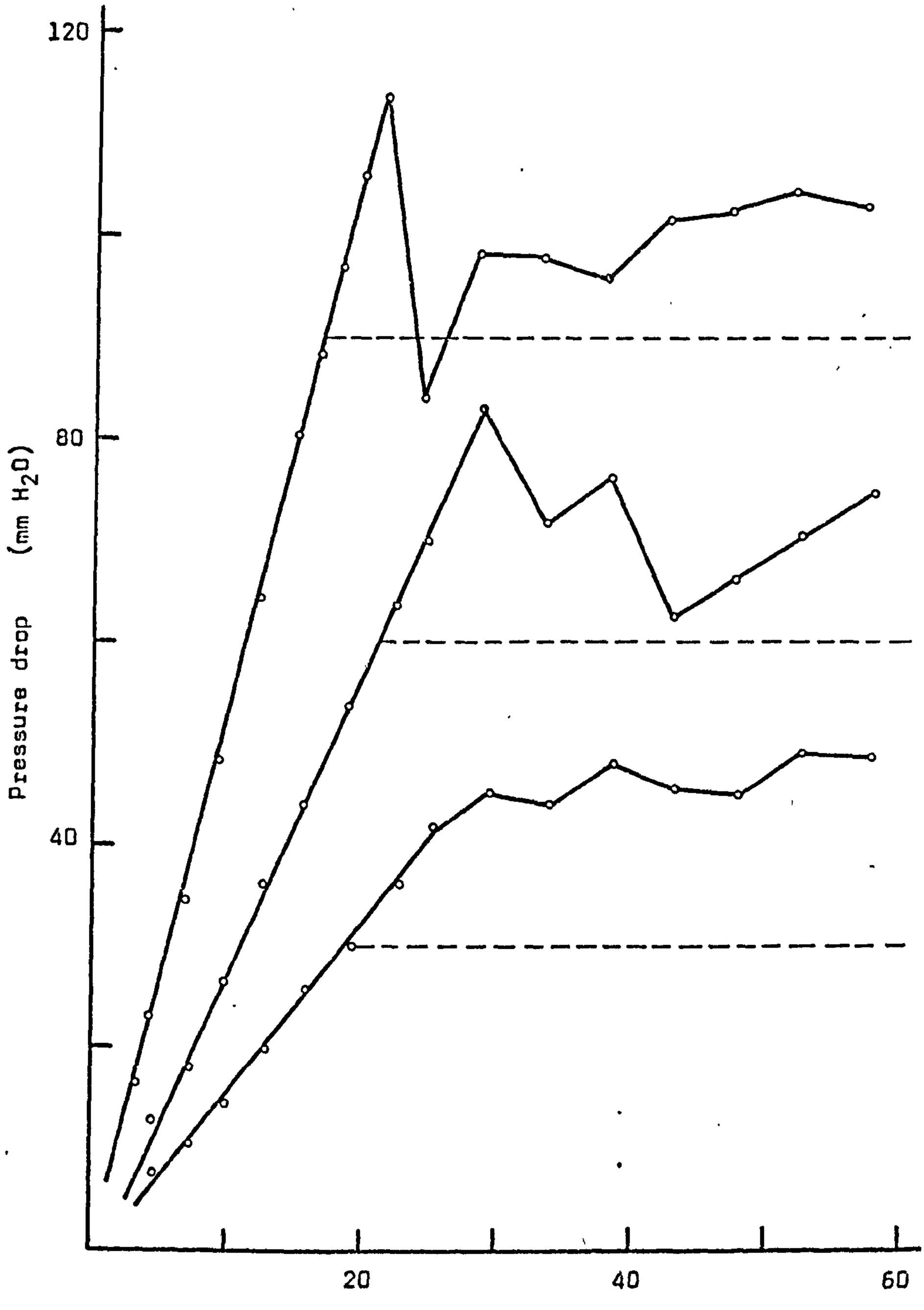

Fig. 7.35 FLUIDISATION BEHAVIOUR OF CORVIC WHEN ELECTROSTATICALLY CHARGED. (Broken lines indicate pressure drops corresponding to the weight of powder in each of the beds).

d_v = 120 μm; ρ_p = 1430 kg/m^3

Distributor: VYON 'D'; R.H. = 68%

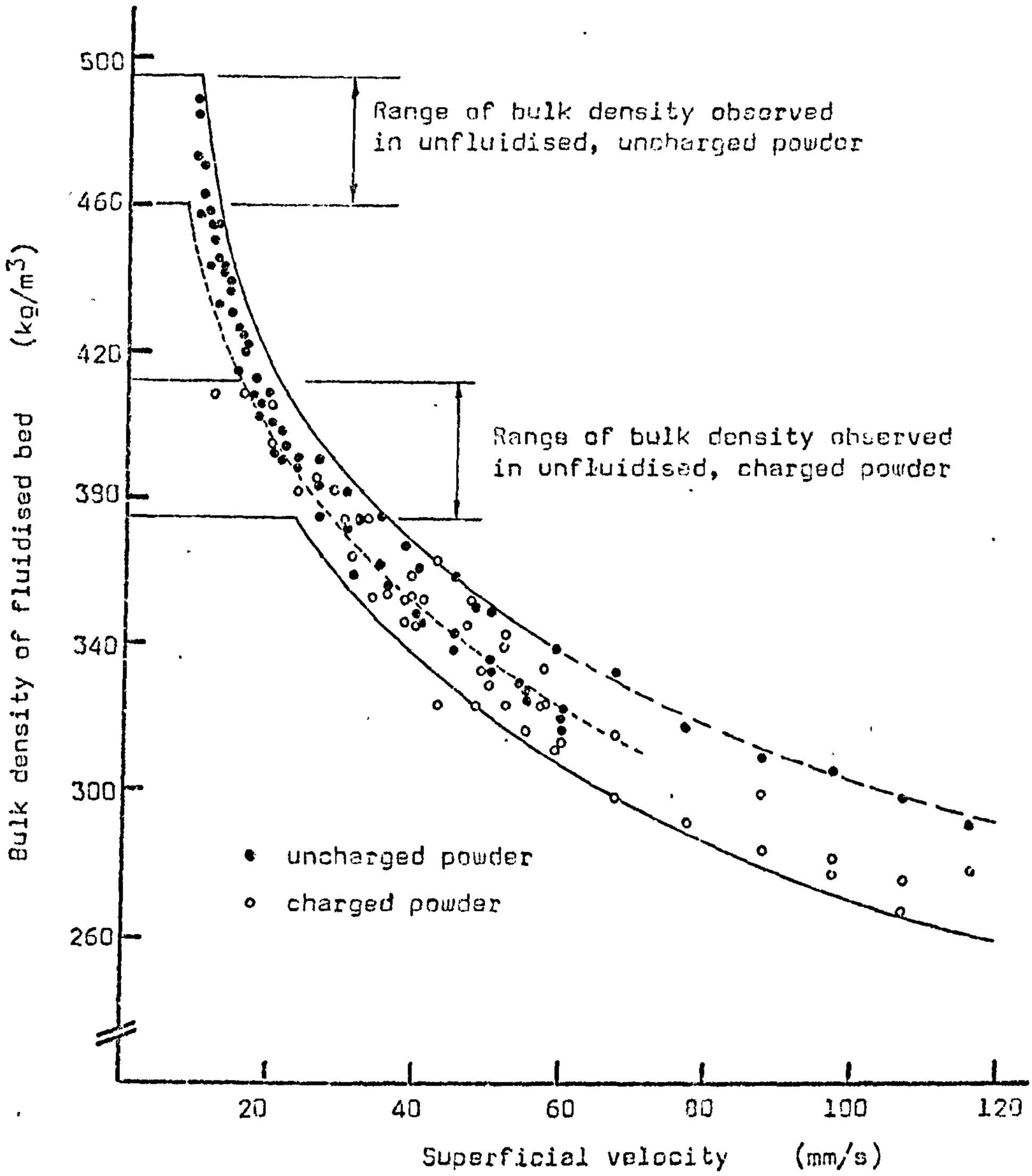

Fig. 7.3C VARIATION OF "BULK DENSITY" OF BED OF CORVIC WITH SUPERFICIAL VELOCITY OF FLUIDISING AIR, SHOWING EFFECT OF ELECTROSTATIC CHARGING. Various initial bed depths from 60 to 200 mm.
Distributor: VYON 'D'
R.H. 50 to 70%

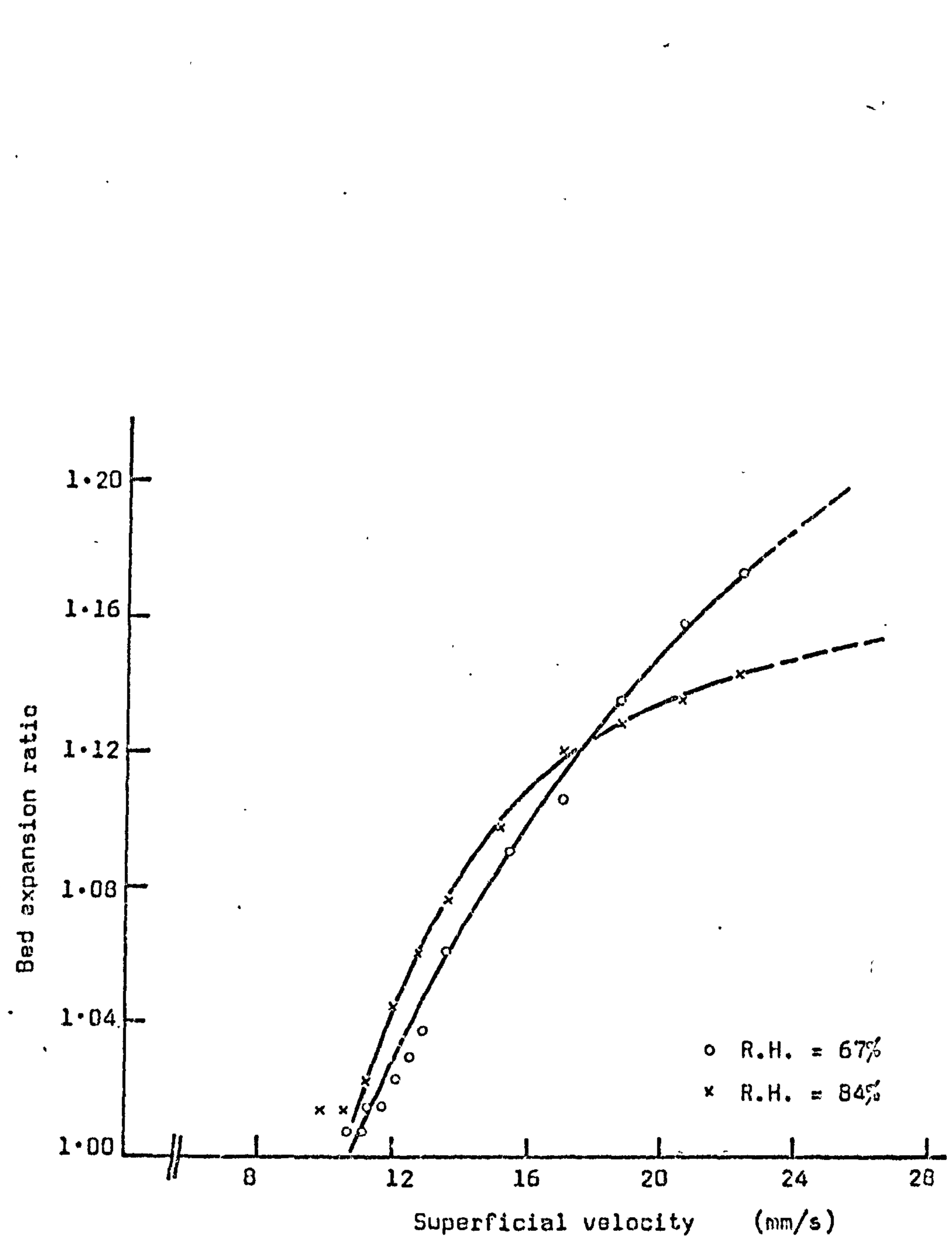

Fig. 7.37 EXPANSION OF FLUIDISED CORVIC AS A FUNCTION OF THE SUPERFICIAL AIR VELOCITY, SHOWING THE INFLUENCE OF THE RELATIVE HUMIDITY OF THE FLUIDISING AIR.

Distributor: VYON 'D'

Initial depth of bed ≈ 132 mm.

is plotted against superficial air velocity for two different R.H. values of the fluidising air. This graph shows that the degree of expansion of the bed is related to the humidity, presumably through a variation in the rate of electrostatic charging (or, more accurately, according to Boland and Geldart (Ref. B12), through a variation in the rate of dissipation of charge). At the higher R.H. the net charge acquired would be less and therefore the Corvic would become fluidised at a lower superficial air velocity. Also, at greater airflows the bulk density tends to be higher for uncharged than for charged Corvic, from which it would be expected that the expansion would be less when the fluidising air is at the higher humidity. Although the test data is insufficient to be fully conclusive, these effects seem to be confirmed by the trends shown on Fig. 7.37.

7.6.5 Apparent viscosity

The difficulties surrounding the concept of "viscosity" applied to a bed of fluidised powder, with regard both to definition of the property and to its measurement, have been discussed at some length in Part I (Sections 2.8.1 and 3.4.4). It was clear from the review of the work of other investigators that little further progress would be made on the establishment of a relationship between measurements of "viscosity" in a stationary fluidised bed and the flow behaviour of the same material in an air-gravity conveyor without undertaking a rigorous experimental study within this area. The present programme was intended to give a wider coverage of the flow characteristics of aerated powders in inclined channels, and viscosity measurements were therefore restricted to a few simple tests in a stationary fluidised bed to ascertain that the behaviour followed the pattern reported by other workers.

The instrument used for these tests was a Brookfield Synchrolectric Viscometer which was mounted centrally above the fluidising vessel. Various types of rotor were tried, including those supplied by the manufacturer of the viscometer and also some specially made hollow cylinders of the form described by Botterill et al (Ref. B22). The most consistent readings were obtained with a solid steel cylinder about 19 mm in diameter, suspended with its upper end level with the surface of the bed of powder. Even with this arrangement it was found that the scale

reading of the viscometer tended to fluctuate wildly, probably as a result of voids occurring on the vertical surface of the cylindrical rotor and affecting the resisting torque.

Fig. 7.38 gives the result of these tests as a plot of the "apparent viscosity" of the fluidised Corvic against the superficial velocity of the fluidising air. Following the example of McGuigan (Ref. M4) the viscosity is plotted on an arbitrary scale since there can be little justification for assuming a direct correlation between the viscosity of a liquid, as indicated by the viscometer scale, and that of a fluidised particulate solid. However, the trend shown by the graph is as expected, with the "viscosity" remaining approximately constant at superficial air velocities greater than about 2 U_{mf}, but increasing sharply as the airflow is reduced towards the point at which the powder ceases to be fluidised.

7.6.6 Conclusions

As with the tests on sand, reported in Section 7.5, these tests have provided information on the fluidisation characteristics of Corvic in stationary beds which can be correlated with observed features of the flowing aerated powder.

The predicted minimum fluidising velocity for the Corvic was 8.6 mm/s and, in general, beds of the powder in the small fluidising rig became fluidised at a superficial air velocity around this value or a little greater. The actual value of U_{mf} determined for a given bed of Corvic tended to vary from day to day, evidently depending not only upon the humidity of the fluidising air but also upon the ambient conditions. For "uncharged" Corvic values of U_{mf} of up to about 12 mm/s were recorded. However, once the powder acquired an electrostatic charge superficial air velocities of something like twice this figure were needed to fluidise it, and even then there was still a strong tendency for slugging and channelling to occur.

It was unfortunate that, as explained in Section 8.2.7, the humidity of the air supplied to the small fluidising rig and to the channel rig could not be satisfactorily controlled, especially at high levels, and

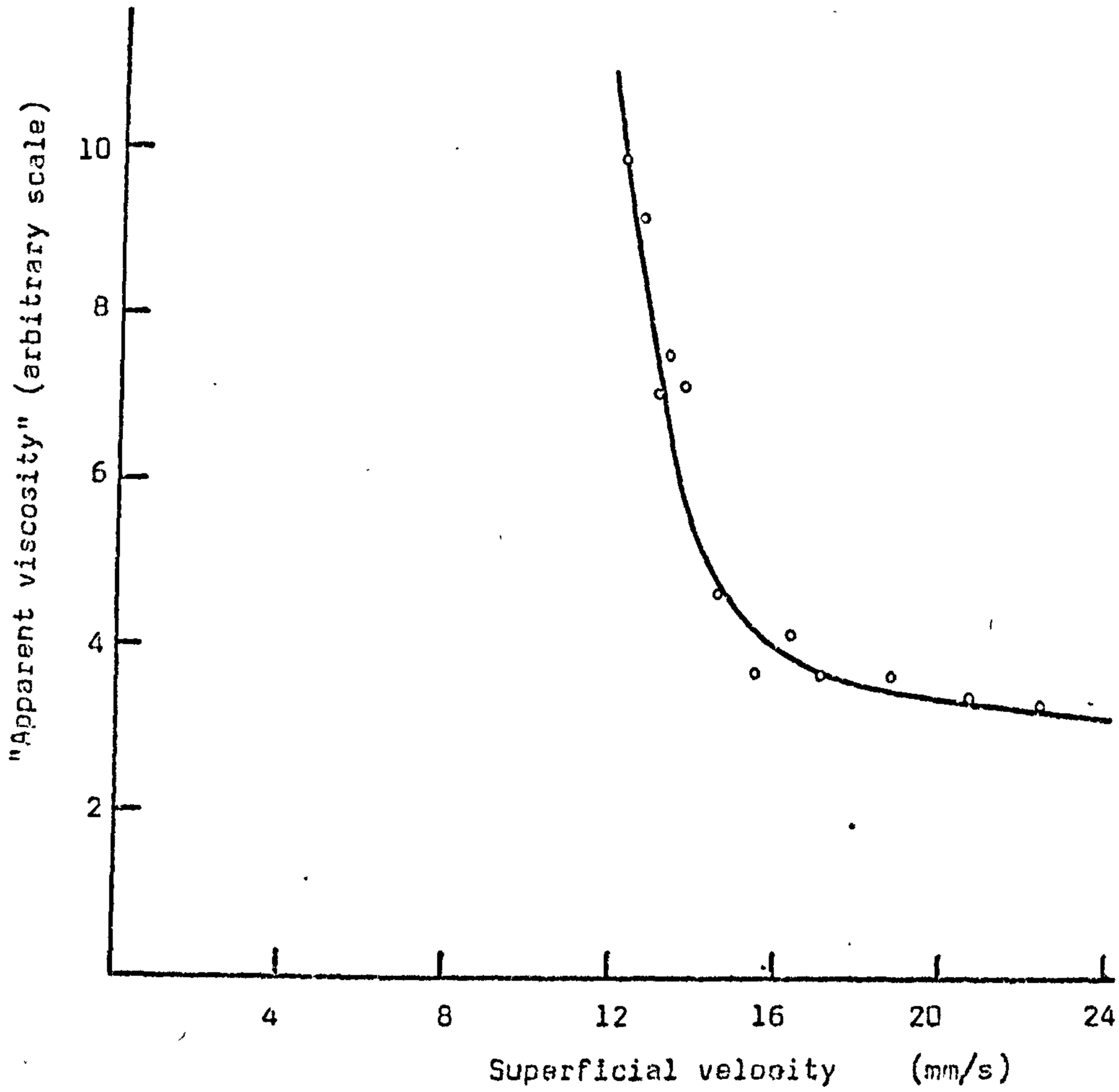

Fig. 7.33 VARIATION OF "APPARENT VISCOSITY" OF CORVIC, AS INDICATED BY VISCOMETER SCALE READING, WITH SUPERFICIAL VELOCITY OF FLUIDISING AIR.
(R.H. = 67%; initial depth of bed = 132 mm.)

this situation did not make the task of obtaining repeatable results any easier. Nevertheless, trends in the variation of the "fluidisibility" of the Corvic and in its bulk density were noted and proved to be relevant to the later tests on the channel flow rig.

No significant differences in fluidisation behaviour could be attributed to the type of distributor used. Visual observation of the fluidised bed of powder during such tests suggested that the higher resistance distributors gave a smoother fluidisation with less bubbling. However, the graphical results did not provide any further evidence to support either this or the suggestion that the degree of expansion of the fluidised bed was a function of the type of distributor used.

7.7 GENERAL CONCLUSIONS

Most of the conclusions that can be drawn from the work undertaken on the small fluidising rig have been discussed at the end of the separate Sections, but attention will be drawn again to a few of the points made.

In general the results obtained during this part of the experimental programme were successful in providing useful information on some of the types of porous air distributor available and on a selection of particulate solids. Whilst in most respects the simple test rig performed well there were some areas in which improvements could be made, especially with regard to the partial dismantling that was required whenever the powder had to be removed or the distributor changed. On some occasions the seals at the base of the fluidising vessel gave cause for concern and considerable care had to be taken to avoid errors occurring as a result of air leakage at this point. Plans are in hand for further modifications to the plenum chamber to allow rapid removal and replacement of the distributor when necessary. Attention will also be given to the method of determining the pressure drop across a fluidised bed of powder in the vessel, probably entailing the inclusion of pressure tappings directly above the top surface of the distributor.

All of the ten samples of porous material tried as distributors in the small fluidising rig were found to be suitable for use as the base of an

air-gravity conveying channel. Although they covered a considerable range of permeabilities (from 0.22 m^3/s down to 0.03 m^3/s at a pressure drop of 200 mm H_2O) there appeared to be no significant differences in the quality of fluidisation produced in beds of 107 μm sand and of Corvic at corresponding superficial air velocities. Advantages and disadvantages of individual porous distributor materials lay in more practical features such as cost, rigidity, brittleness, and susceptibility to deterioration through ingress of dust or moisture. For the experimental programme on the channel flow rig two porous materials having widely differing characteristics were chosen, these being Vyon 'D' (a sintered plastic of medium/high resistance) and Scandura P22 (a low resistance woven polyester belting).

The fluidisation behaviour was investigated of eight samples of powder selected to include representatives from each of the three Geldart Groups A, B and C. As described in Section 7.4 these behaved more or less as expected from their classification and the samples of sand and Corvic were then subjected to a more thorough examination. In each case useful information was obtained on the behaviour of the powders when fluidised in stationary (as opposed to flowing) beds, especially with regard to minimum fluidising velocity and bulk density. For sand the influence of particle size was investigated, and it was shown that, contrary to what might have been hoped, the suggestion of conveying coarse materials more economically by mixing in a small proportion of finer powder may not be viable. In the case of Corvic the phenomenon of electrostatic charging was at the root of most of the difficulties encountered during the experimental work. In most industrial situations the powder would not be continuously recirculated as it was in the channel test rig and therefore the problem of charging should not be so severe. Nevertheless, it was surprising how quickly the nature of the material could change from a free-flowing powder to a rather cohesive one. Consequently it was considered to be worthwhile to demonstrate in the small fluidising rig the extent to which the fluidisation behaviour of the Corvic could be altered. For instance, although the uncharged powder could be fluidised at less than 10 mm/s, when charged it became almost impossible to fluidise and, in addition, as a result of air retention within the charged powder, the bulk density was reduced by some 20 to 25%.

Much of this work on the small fluidising rig was undertaken in parallel with work on the main channel flow rig since it provided very necessary background information on the distributor materials and powders. As such it includes a significant proportion of the total programme of work, although the main purpose of the programme has been the investigation of powder flow in inclined channels as described in the next Chapter.

CHAPTER EIGHT

THE MAIN CHANNEL FLOW RIG

8.1 INTRODUCTION

The second and major part of the experimental programme involves a practical study of the flow of aerated particulate bulk solids in inclined channels and is intended to provide a significant contribution to current knowledge in this area of powder handling. It is hoped that this contribution might comprise not only direct experimental data but also the method of processing and the use of such data to support the development of suitable models giving a further insight to the mechanism of air-assisted gravity flow of bulk solids. An important requirement of this work was that it should have direct industrial relevance, and therefore the test rig had to be designed so that flow conditions in the channel could be seen to be representative of those that would be found in a typical industrial situation.

This Chapter begins with a detailed description of the design and construction of the channel test rig and its instrumentation, followed by a discussion of the extended series of commissioning trials that was undertaken using p.v.c. powder ("Corvic"). Problems encountered with the handling of this material are detailed and the various characteristics of the test rig are analysed.

The most important part of the practical study of the flow of aerated powders involves an investigation of the relationships amongst the principle system variables. These are the solids mass flowrate, the inclination of the channel and the superficial velocity of the fluidising air which are independent variables, and the average depth of the flowing suspension which is treated as the dependent variable. In this Chapter are reported the results of the extensive series of tests carried out, in which the influence of each of the three independent variables on the bed depth was observed. The significance of extraneous variables such as electrostatic charging and the moisture content of the fluidising air is also discussed.

Finally, comparisons are drawn between the flow behaviour of Corvic and of sand in preparation for the full analysis and correlation of all the experimental data, which will be undertaken in Chapter Nine.

8.2 DESIGN AND CONSTRUCTION OF THE TEST RIG

8.2.1 Overall plan

As explained in the introduction above, the purpose of the channel rig was to enable practical studies to be made of the flow of aerated particulate bulk solids under conditions representative of those that would occur in an industrial situation. The channel therefore had to be of a size that would be recognised and accepted by the manufacturing and user industry as being "realistic", which would have meant ideally a channel of width no less than 150 mm and a minimum length of around 5 m. Unfortunately however, both the floor space and the headroom in the laboratory were rather restricted, and the development of the rig was also hampered by the need to keep expenditure within reasonable limits. Thus, although the length of the channel ultimately constructed was an acceptable 6 m, the maximum width that could be accommodated was only 100 mm.

The reason for the limitation on channel width was bound up with the maximum feed rate of particulate solids that could be maintained to the channel, since it was considered to be more important to be able to operate the channel at somewhere near to its maximum capacity than to have a wide channel operating only at very small flow aspect ratios. In fact, although the 100 mm channel width was considered to be slightly less than ideal, relatively little of the previously published experimental work has been carried out on larger channels.

One of the main decisions that had to be made when planning the rig was whether to have continuous circulation of powder or to operate "batch-wise". Among previous investigators there are adherents to both methods. McGuigan (Ref. M4) for example, argues a strong case for continuous flow of powder around the test circuit, and Keuneke (Ref. K3) also constructed his rig for continuous operation, whereas Siemes and Hellmer (Ref. S13) preferred to operate batch-wise. The main factor against a rig for continuous operation on this current programme of research was the prohibitive cost of two pieces of equipment essential for such a system. These were the conveying facility to return the powder from the lower (discharge) end of the channel to the inlet at a rate corresponding to

the maximum capacity of the channel, and a suitable weigh-feeder to indicate continuously the mass flowrate in the channel. Even with batch-wise operation it was of course necessary to ensure that the maximum flowrate could be maintained in the channel for a reasonable period of time, which necessitated upstream and downstream hoppers of suitably large capacity, with all the attendant problems of space and headroom.

So it was decided to opt for something of a compromise between the two systems by planning for a conveyor return system that would allow continuous circulation of the powder at a moderate flowrate, albeit without any direct means of measuring it, and relying on batch-wise operation for test runs when investigating the flow behaviour in the channel.

The essential features of the channel test rig are shown digrammatically in Fig. 8.1 and may be summarised as:-

i) Main upstream storage hopper, to be of sufficient capacity to allow maximum powder flowrate to be maintained in the channel for a reasonable period of time. (Say, one minute minimum.)

ii) Means of adjusting the rate of discharge of powder from the hopper to the channel.

iii) Conveying channel, of maximum width and length within the constraints outlined above, and of variable slope.

iv) Downstream storage hopper, to double as a weigh-bin for the determination of powder mass flowrate.

v) Powder return system, to convey the powder from the lower to the upper hopper at a sufficient rate to ensure a reasonably short period between test runs, and also to allow continuous operation of the rig at moderate flows for demonstration purposes.

vi) Variable air supply to the channel.

Each of these features, together with the various refinements and the instrumentation, will be described in detail in the following Sections.

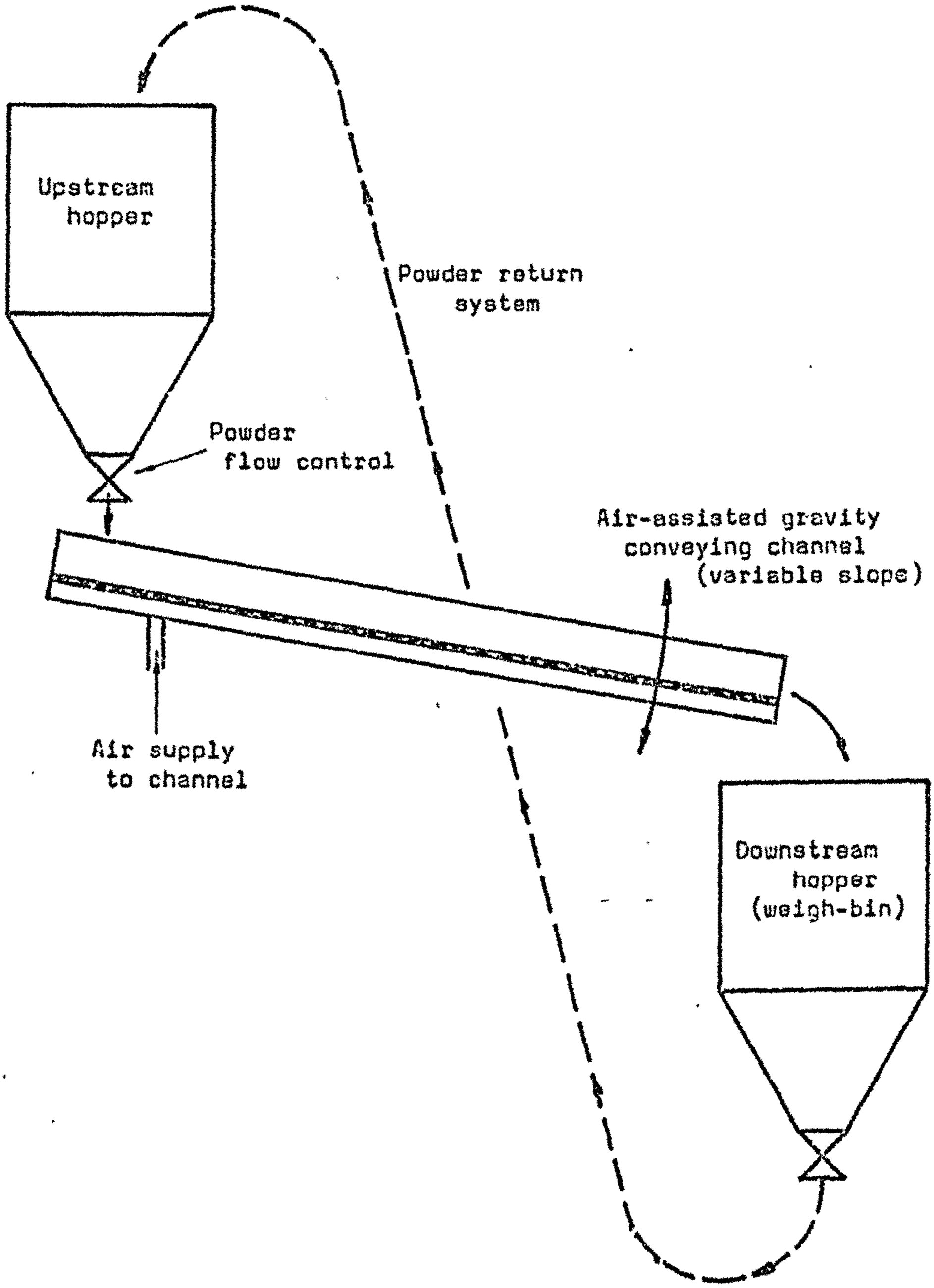

Fig. 8.1 OUTLINE PLAN OF CHANNEL FLOW TEST RIG.

8.2.2 Conveying channel

The reasoning behind the decision to make the width of the conveying channel 100 mm has already been mentioned. Although it would have been desirable to have had a rather wider channel, it has to be remembered that for a given aspect ratio the solids flowrate increases as the square of the channel width so that the difficulties of providing, under laboratory conditions, a sufficient quantity of powder soon become insurmountable.

The maximum length of channel was set by the space available, particularly the headroom. This was because of the need for the slope of the channel to be variable (up to about 15^{o}) which obviously required a difference in elevation between the inlet and outlet ends that was proportional to the channel length. Within this constraint, the greatest length that could be accommodated was 6 m and the main concern then was whether this would allow a long enough test section after the intake settling length. The magnitude of this settling length is not easy to predict with any degree of confidence. Siemes and Hellmer (Ref. S13) comment on this difficulty and, using an empirical equation for the laminar flow of liquids, suggest that the settling length should not be more than 0.15 m. However, McGuigan (Ref. M4) allowed an entry length of one metre on his 3 m long channel, and this figure seems to be a more reasonable one (a view subsequently confirmed by observation). Thus the decision was taken to construct a 6 m long channel with all observations of the "uniform" flow of the particulate suspension to be taken in a central test section of some three or four metres.

Most commercial air-gravity conveyors consist of two steel ⌐¬-section channels, the top one inverted, with the porous membrane clamped between them. Instead of following this pattern, it was decided to construct the research channel as an all-Perspex box-section supported in an aluminium framework. In this way it was intended to produce a channel that would be relatively light in weight, would ensure maximum visibility of the flowing powder and could be easily dismantled and reassembled with a different porous membrane or at a different width. Fig. 8.2 illustrates the cross-section of the channel showing the way that the porous membrane

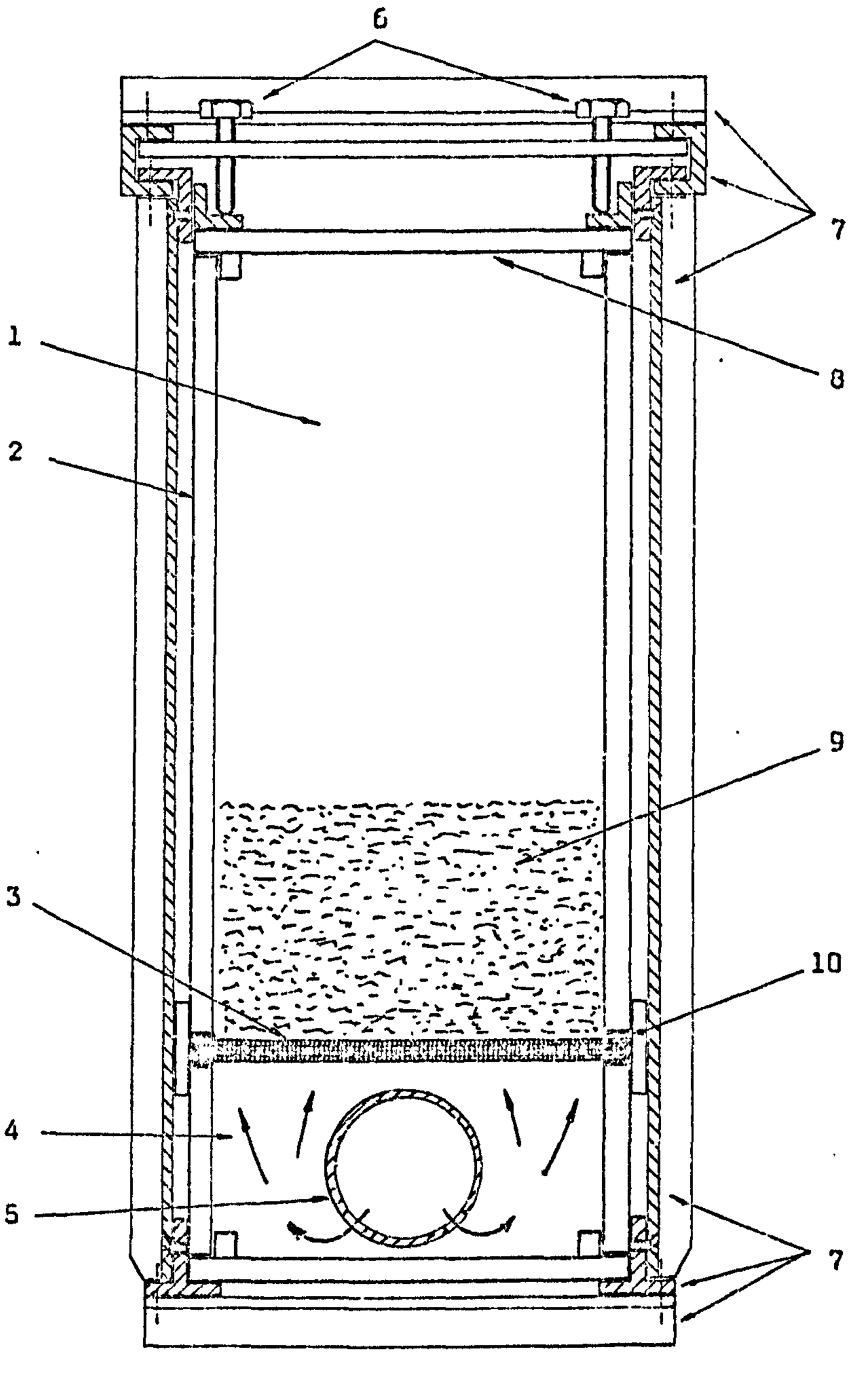

KEY:

1	Main flow channel	6	Clamping bolts
2	Perspex side walls	7	Aluminium framework
3	Porous base	8	Perspex top cover
4	Air plenum chamber	9	Conveyed material
5	Air distributor pipe	10	Rubber seal

Fig. 8.2 CROSS-SECTION OF THE CONVEYING CHANNEL

is clamped between the Perspex sides. The clamping bolts, which bear on the Perspex top cover of the channel and keep the whole assembly rigid within the aluminium framework, can be seen clearly in Plate IV.

As mentioned in the conclusion to Section 7.3, the porous materials that appeared to be most suitable for the present requirement were the thin sintered plastic sheet (Vyon 'D') and the low-resistance woven polyester belting (Scandura P22). Initially a Vyon distributor was fitted into the channel (Plate IV). After an extended series of commissioning tests and preliminary investigations on the flow of aerated p.v.c. powder ("Corvic"), this first distributor was replaced by a new one, also of Vyon 'D', and later still a length of Scandura P22 belting was installed. Since the Scandura was not rigid it had to be supported on the underside by a wire grid, but in spite of the support the surface of this distributor tended to be rather uneven.

Some care was taken when designing and constructing the channel to ensure that the free area of the porous distributor was the same on its upper and lower surfaces. This was so that the whole of the flowing powder bed would be uniformly aerated, the need for which has been pointed out by Keuneke (Ref. K3) and McGuigan (Ref. M4) among others. In contrast however, it is of interest to note the approach of Siemes and Hellmer (Ref. S13) who deliberately masked the edges of the underside of their porous membrane in order to "ensure that the flow velocity of the bed will fall to zero at the walls, a necessary condition for the flow equation"!

In an attempt to ensure that the air supplied to the plenum chamber beneath the porous base of the conveying duct was uniformly distributed, it was fed to a 38 mm diameter plastic pipe running the full length of the channel and having a series of holes along its under surface (see Fig. 8.2 and Plate IV). Although such an arrangement should not be necessary with high pressure-drop porous distributors, it was considered that some advantage could be gained when using low-resistance types.

As the top of the conveying channel was covered to prevent excessive emission of dust into the laboratory, some provision had to be made for

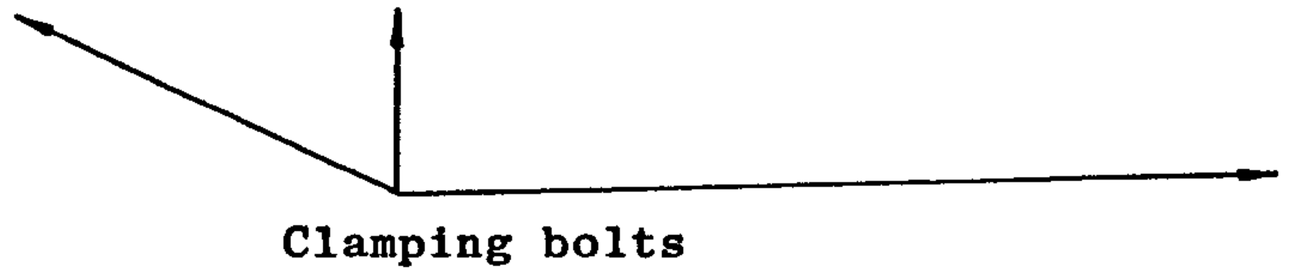

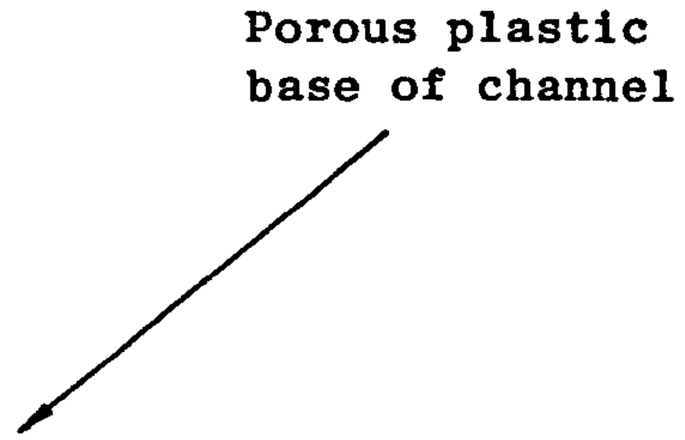

Plate IV. PART OF THE CONVEYING CHANNEL SHOWING THE CONSTRUCTION OF THE ALUMINIUM FRAMEWORK AND THE POROUS BASE.

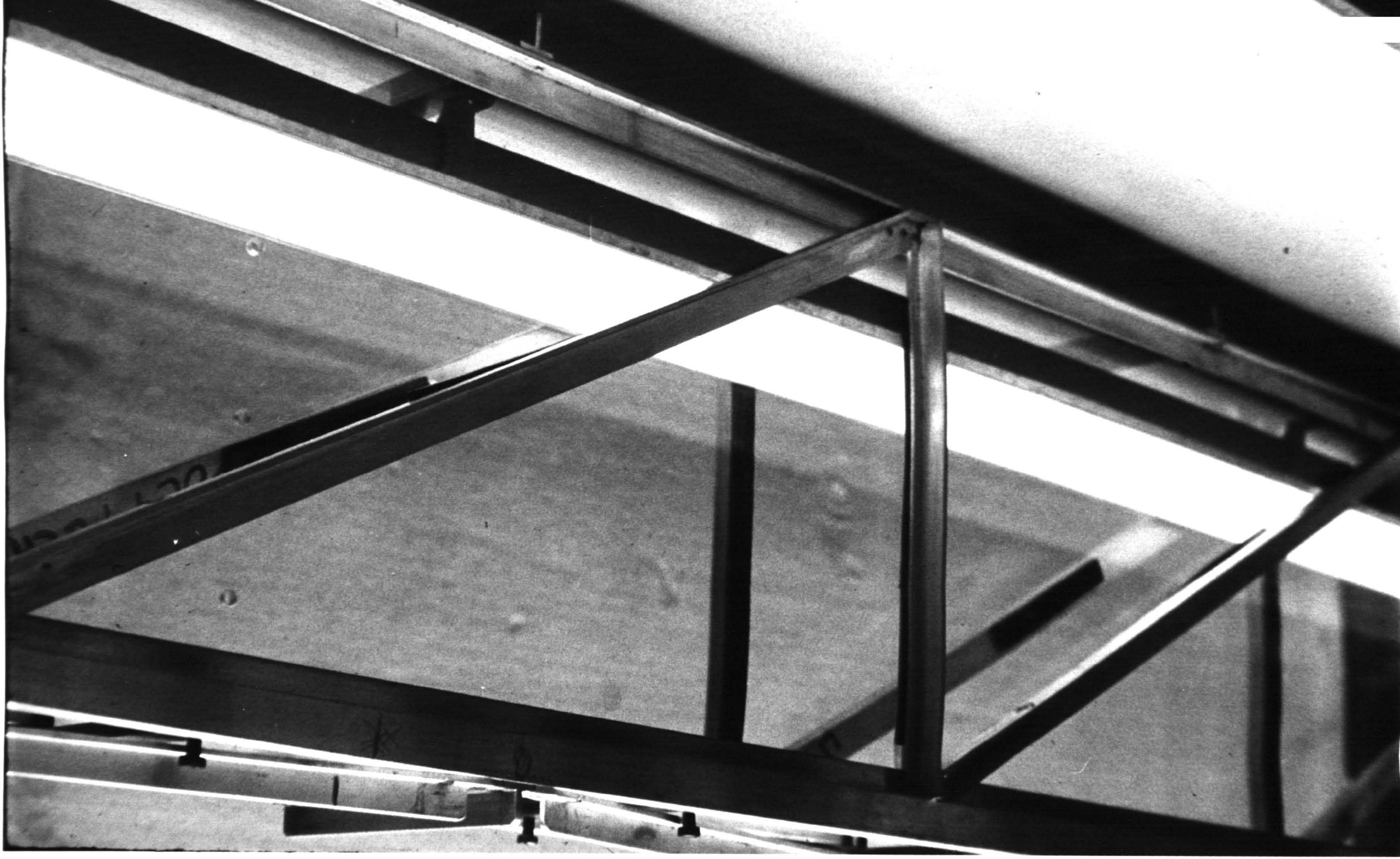

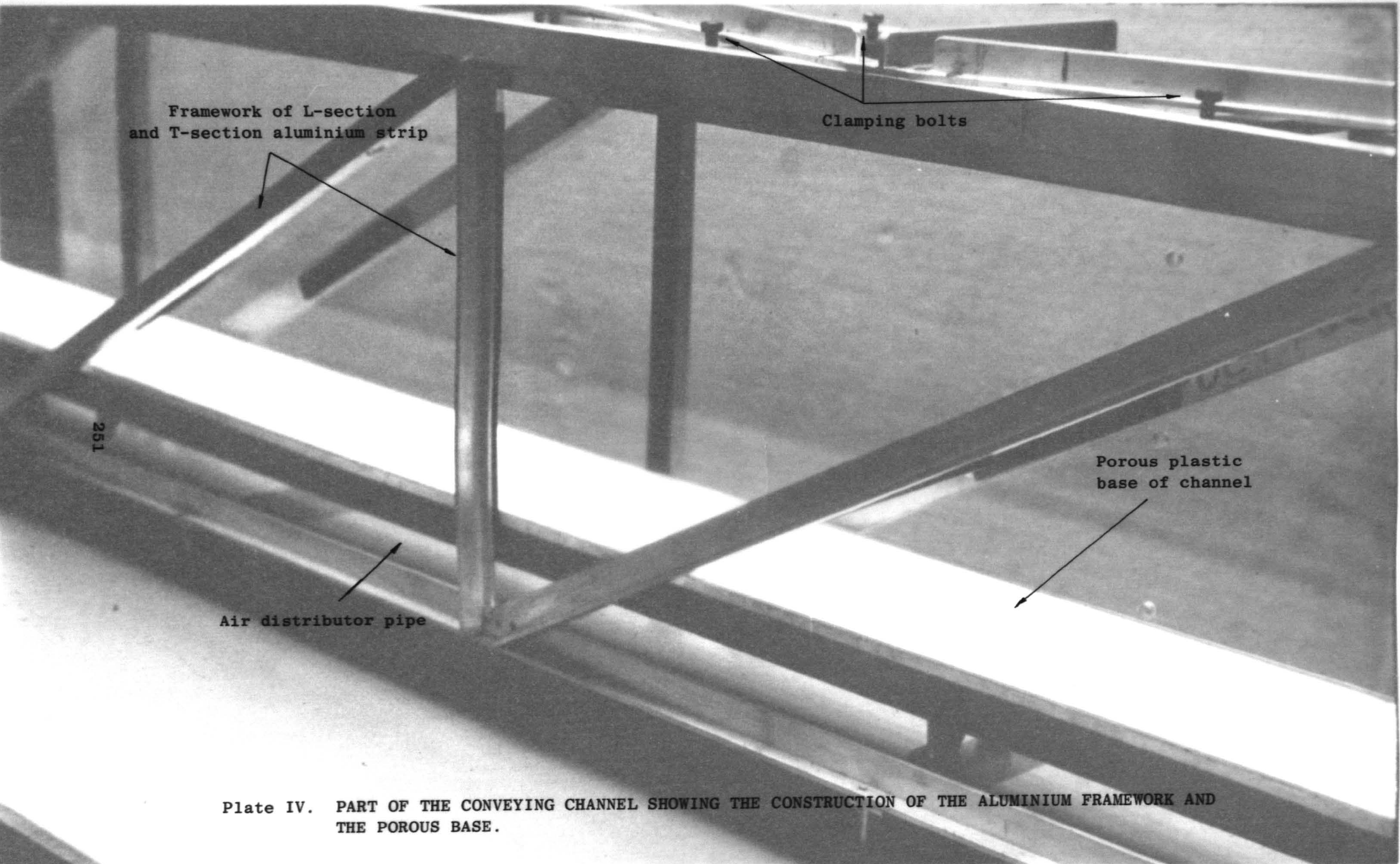

Plate IV. PART OF THE CONVEYING CHANNEL SHOWING THE CONSTRUCTION OF THE ALUMINIUM FRAMEWORK AND THE POROUS BASE.

the removal of the air after it had passed through the flowing powder bed. This air could not escape upstream because of the presence of the baffle plate at the inlet (described in the next paragraph) and in any case, it was considered to be more satisfactory to have the air flowing over the powder bed in the same direction as that of the bed itself. Thus it was intended that the exhaust air should flow from the duct with the discharging powder into the lower hopper, and thence through a suitable filter unit to the laboratory.

The majority of industrial installations and, for that matter, experimental rigs, have the air supplied to one continuous plenum chamber beneath the porous base of the conveying channel. However, it has been suggested (Ref. M14) that there could be some advantage in having a separate "preliminary fluidising chamber" at the upstream end of the channel, and therefore this arrangement was followed in the present design. The upstream fluidising chamber, extending for about the first half metre of the channel, has its own plenum with independent air supply and is divided from the remainder of the channel by an adjustable baffle or sluice-plate. The photograph of the inlet end of the channel (Plate V), taken during the construction of the rig, shows clearly the position of the baffle-plate and of the air inlet point for the separate upstream fluidising chamber.

Also visible in Plate V is one of the two bearings on which the upper end of the channel was supported. Corresponding bearings were mounted on A-frames fixed directly to the floor of the laboratory (that is, seperate from the main framework supporting the storage hopper and ancillaries) in order to avoid, as far as possible, the transmission of vibration to the channel from the rotary valve or from other equipment on adjoining test rigs. The lower end of the channel was attached to a block-and-tackle by means of which its slope could be varied from horizontal to about 12^{o} downwards. The angle of inclination was indicated by a plumb-line moving over a scale attached to the channel. The block-and-tackle arrangement and the top of the A-frame supporting the inlet end of the channel can be seen in Plate VI, which gives a general view of the test rig.

As the channel slope is changed from horizontal to its maximum value, the outlet end moves through a vertical distance of over one metre so that,

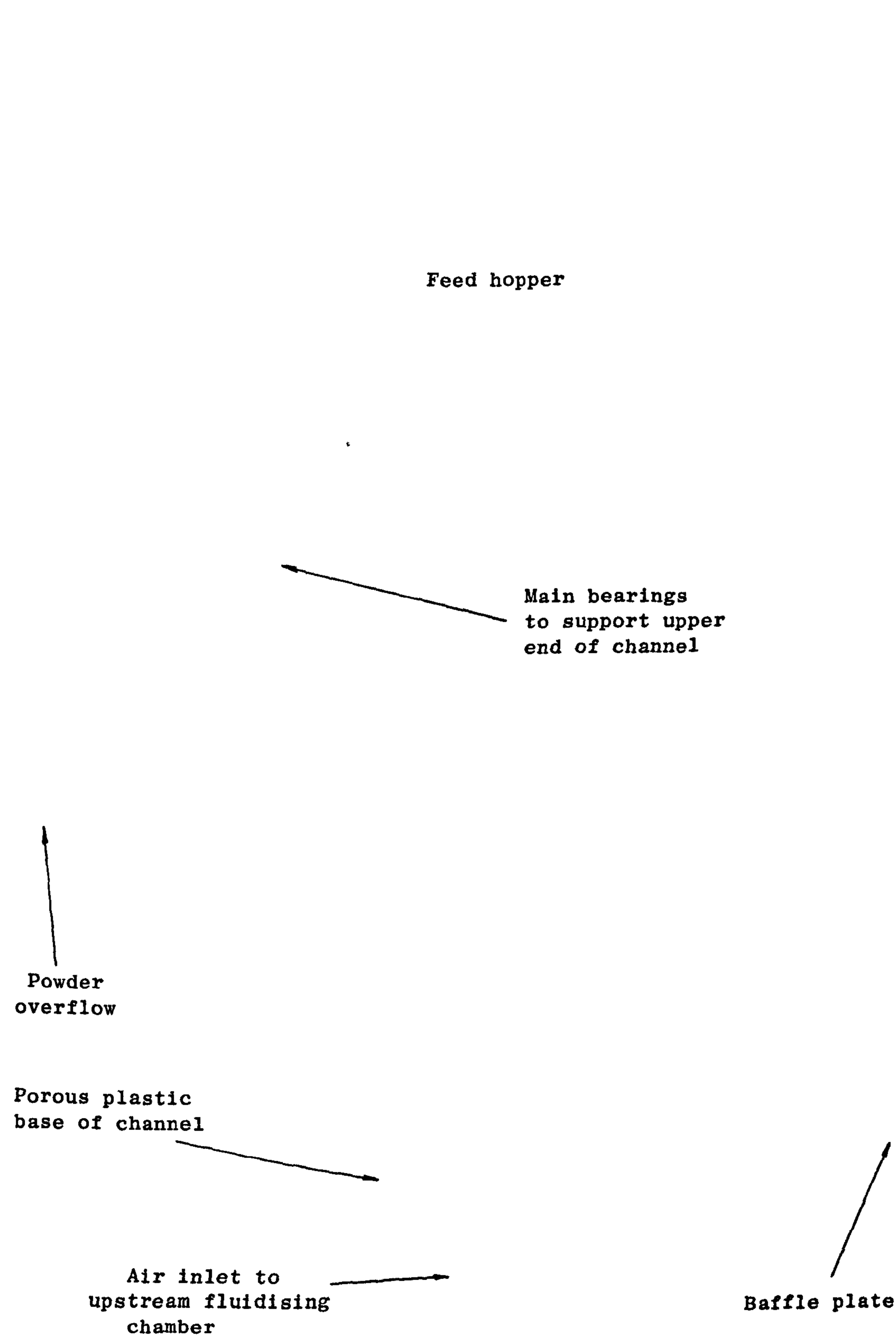

Plate V. THE UPSTREAM END OF THE CONVEYING CHANNEL.

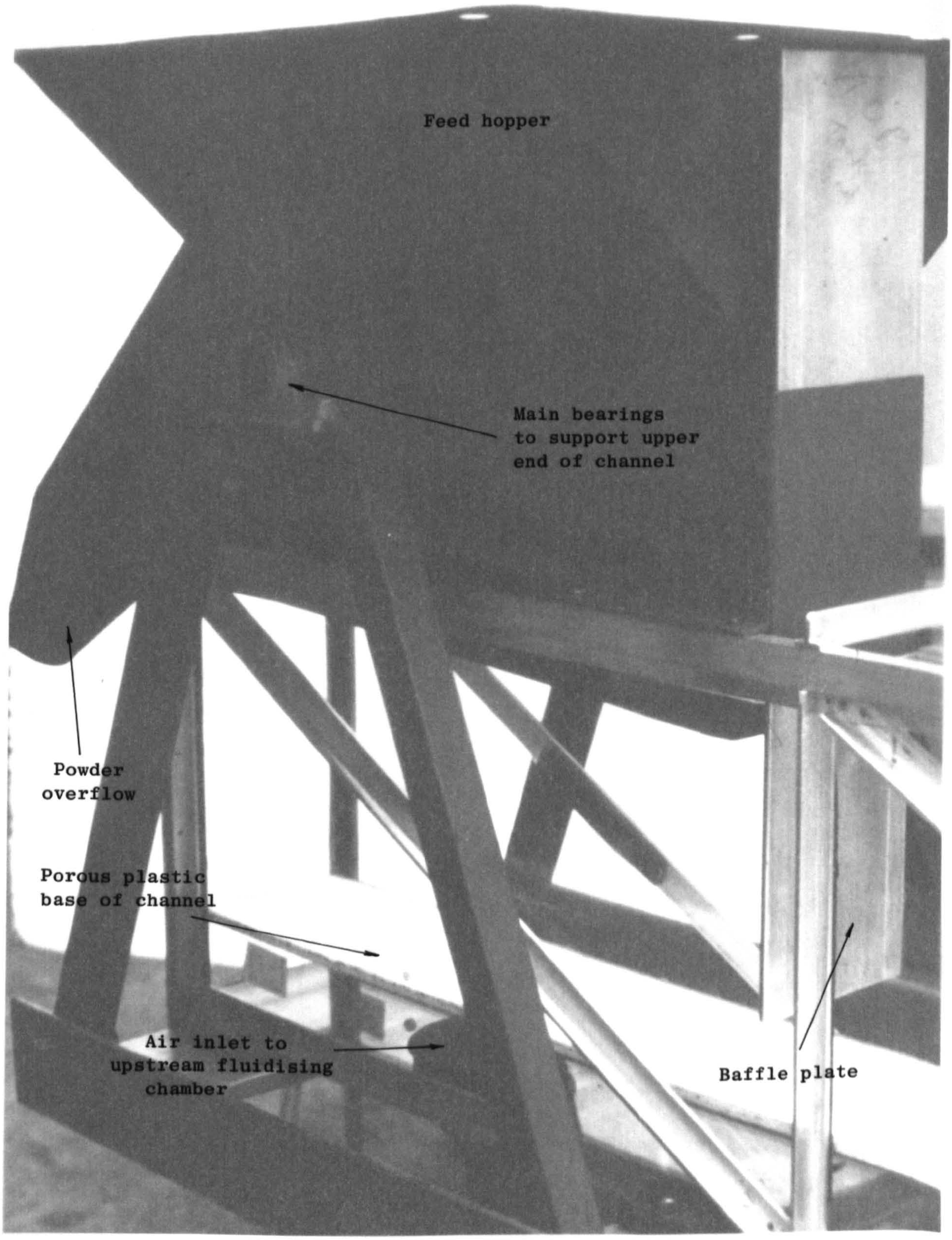

Plate V. THE UPSTREAM END OF THE CONVEYING CHANNEL.

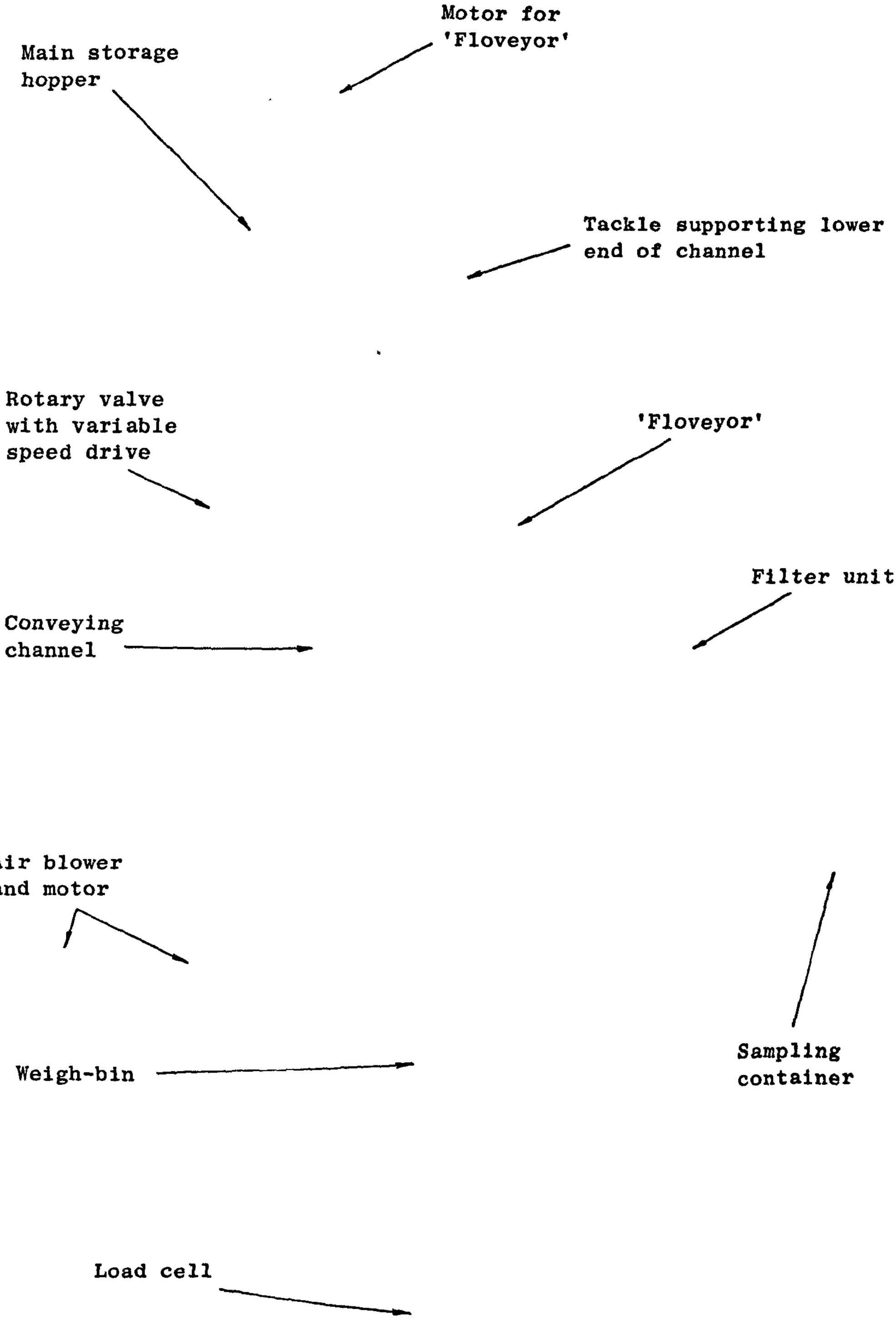

Plate VI. A GENERAL VIEW OF THE MAIN CHANNEL FLOW RIG.

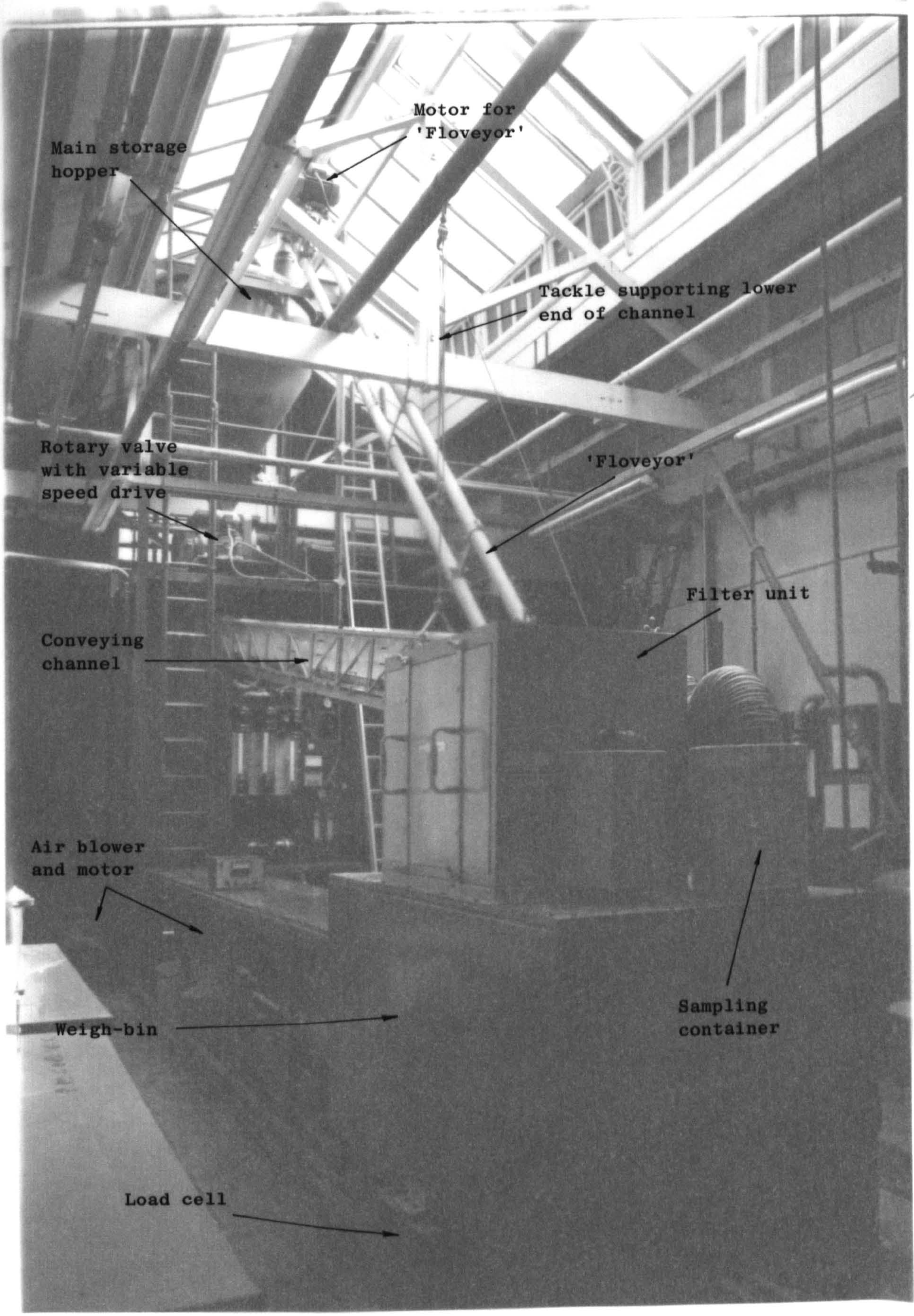

Plate VI. A GENERAL VIEW OF THE MAIN CHANNEL FLOW RIG.

in order to keep the system totally enclosed, it was necessary to dicharge the powder through a length of 150 mm diameter flexible trunking to the weigh-bin. A simple flap valve at the lower end of the channel allowed the flow of powder to be diverted into a separate container for sampling purposes.

The position of the channel in relation to the other major features of the test rig is illustrated diagrammatically in Fig. 8.3.

8.2.3 Main storage hopper

In order to give a test run of sufficient duration it was estimated that the capacity of each of the two hoppers would need to be at least one cubic metre, and preferably larger. It happened that at the time that the research programme was being planned a surplus hopper of suitable size became available and was therefore incorporated into the design of the rig as the main storage facility. This hopper was of conventional cylindrical/conical form, 1.4 m maximum diameter and 2 m overall height, having a capacity of approximately 1.1 m^3. The lower 0.46 m of the hopper consisted of a separate conical section fitted with an air connection which could be used for venting the hopper, balancing the pressure across the rotary valve, or for supplying air to assist the discharge of powder. This discharge cone and the air connection to it can be clearly seen in Plate VII.

The overall height of the main storage hopper was somewhat greater than had originally been planned and took up a significant proportion of the available headroom. The hopper had to be mounted as closely as possible to the roof of the laboratory, whilst allowing access for the conveyor returning powder from the lower hopper (weigh-bin), and so a substantial framework of rolled steel angle was designed and built for the purpose (see Plate VI).

In order to prevent any build-up of pressure within the storage hopper it was vented from the top cover through a filter bag which could be easily removed for cleaning.

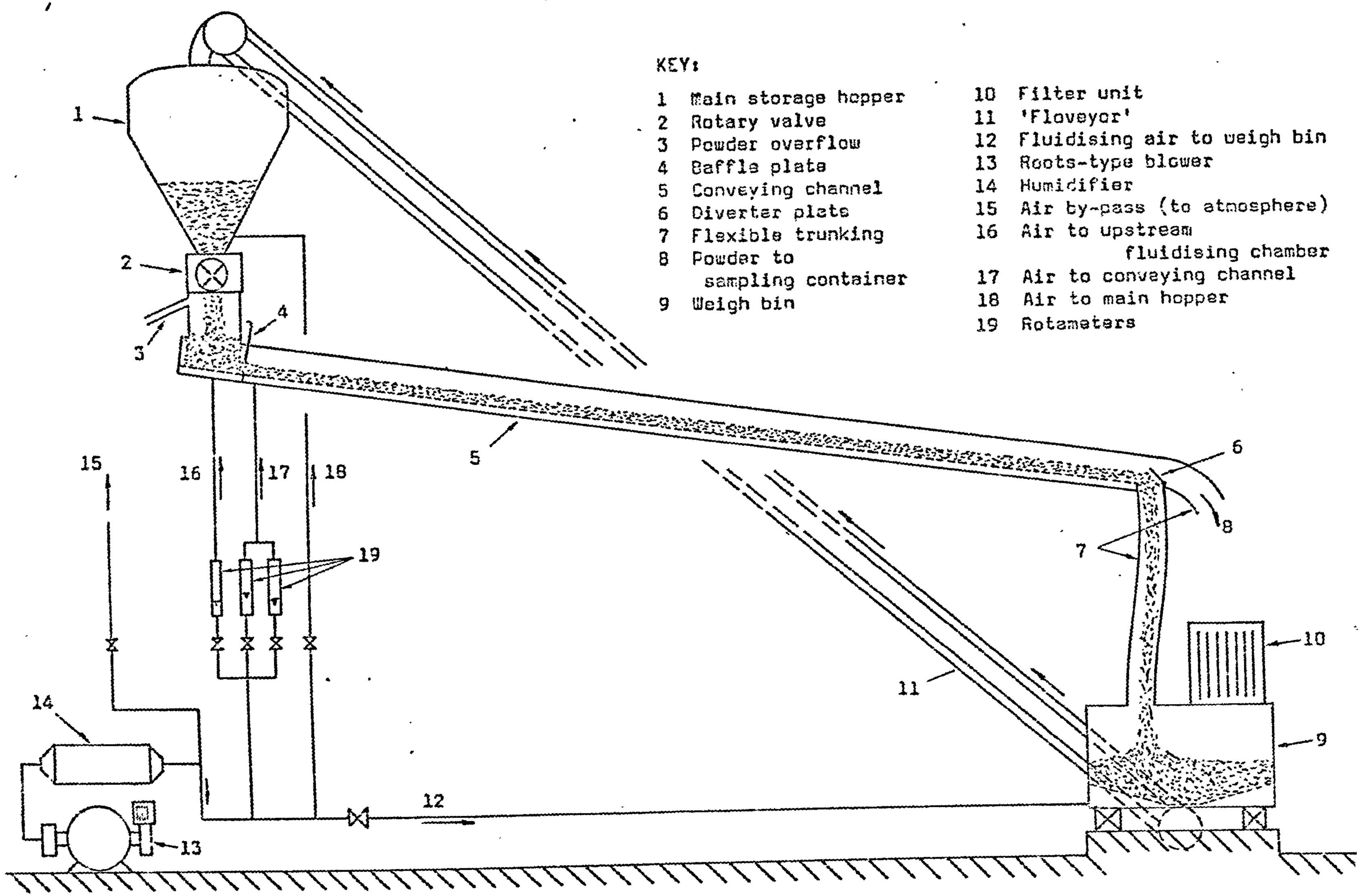

Fig. 8.3 DIAGRAMMATIC REPRESENTATION OF THE CHANNEL FLOW RIG.

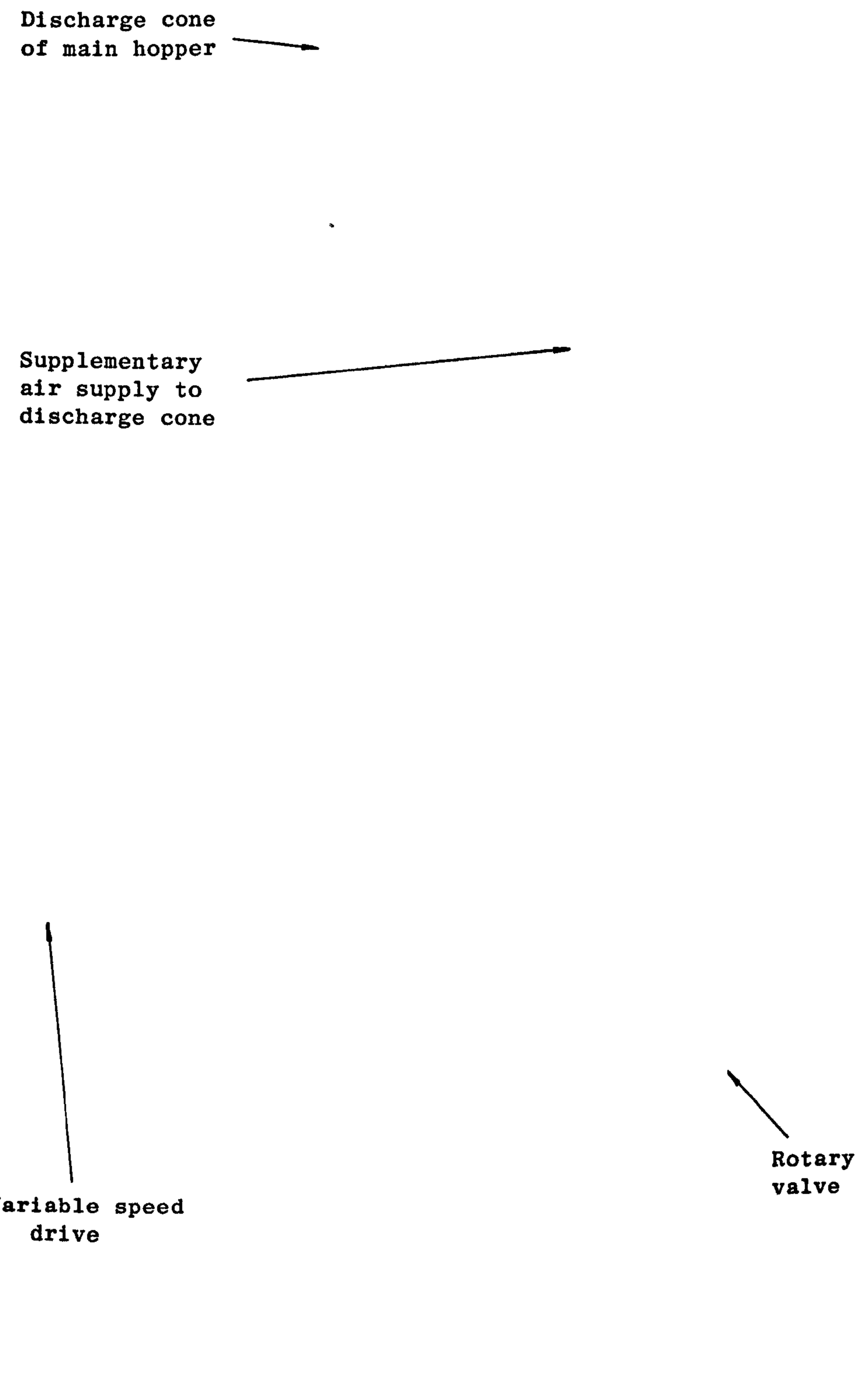

Plate VII. THE DISCHARGE POINT FROM THE MAIN HOPPER TO THE ROTARY VALVE.

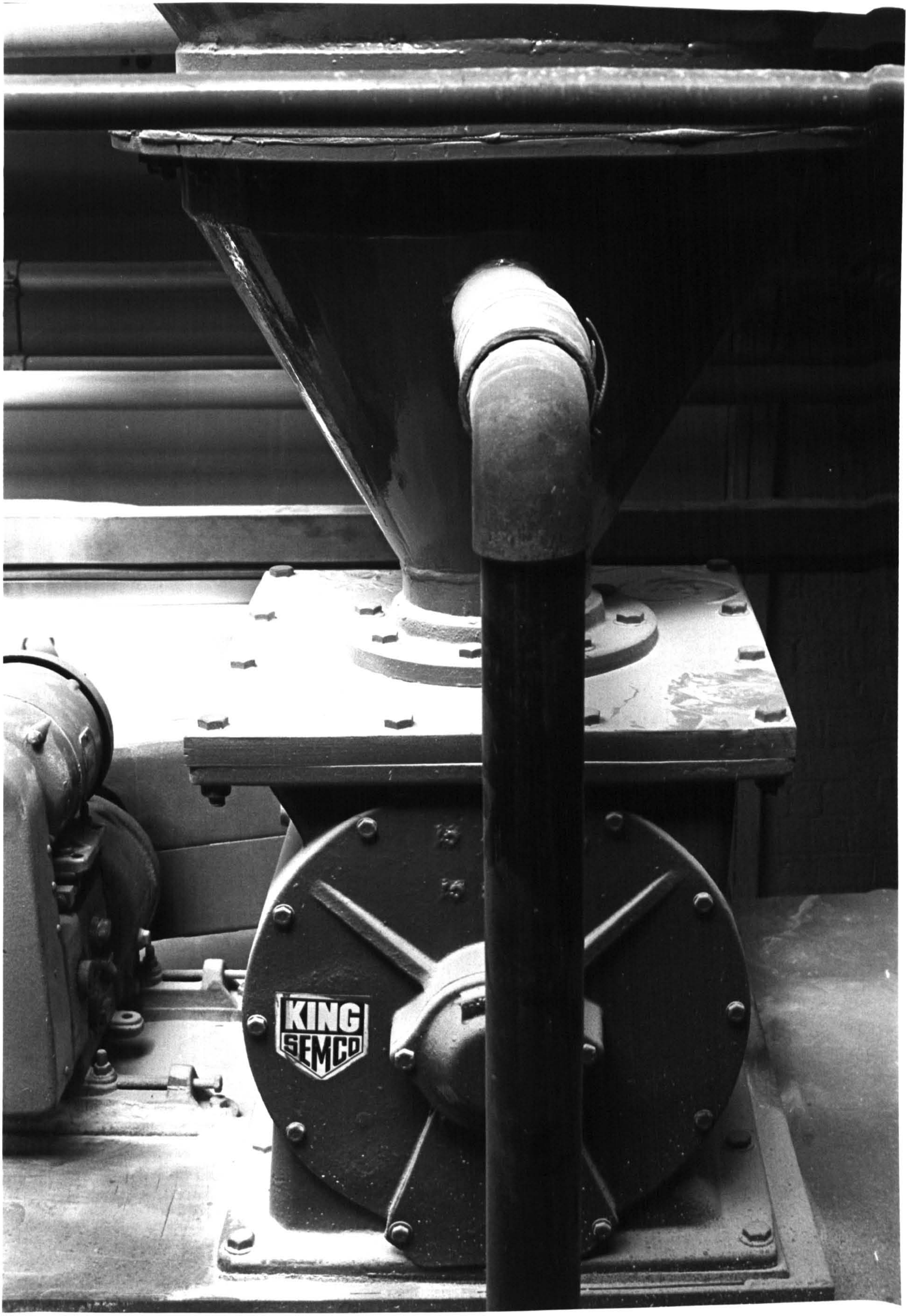
KING
SEMCO

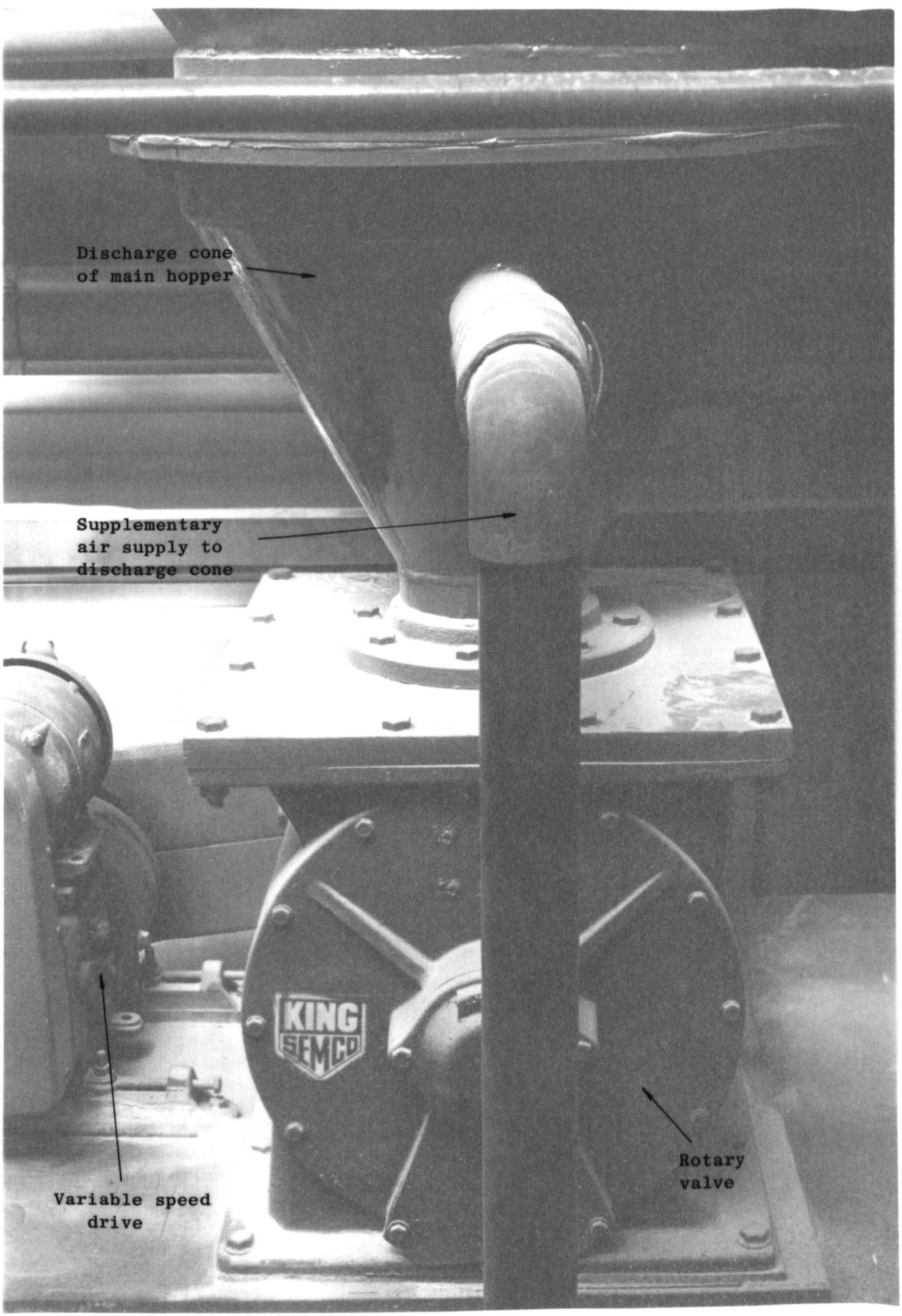

Plate VII. THE DISCHARGE POINT FROM THE MAIN HOPPER TO THE ROTARY VALVE.

8.2.4 Solids feed to the channel

Mention has been made elsewhere (Part I, Section 3.2.6) of the problems that may arise from the use of flooded feed of solids to the conveying channel in experimental rigs. Although some of the reported research has been carried out on rigs using flooded feed (Refs. H2, M14, Q1, S13), in one case (Ref. M14) an attempt was made to control the solids mass flow by means of a moveable baffle-plate. In the major programmes of work undertaken by Keuneke (Ref. K3), McGuigan (Ref. M4) and Pugh (Ref. P9) the need to control the solids flowrate was recognised at the design stage and suitable feeders were included in the test circuit. Keuneke chose to use a rotary valve, whereas McGuigan and Pugh preferred a weigh-belt feeder.

For the present programme a weigh-belt feeder was considered but was ruled out on the grounds of its high cost. The choice was then between a rotary valve and some form of variable orifice device such as a pinch-valve or iris-diaphragm valve. It appeared likely that a rotary valve would give a more precise control of the solids mass flowrate, whereas a variable orifice valve would permit an investigation of some of the peculiarities of flooded feed whilst allowing the maximum feed rate to be adjusted to some extent. It was decided that initially a rotary valve would be installed beneath the main storage hopper, with the possibility that an iris-diaphragm valve would be substituted at a later stage if time permitted. The valve selected was 300 mm in diameter and was driven through a Carter hydraulic variable-speed gear giving a range of rotational speed up to about 28 rev/min. The position of the valve and drive can be seen in Plates VI and VII.

It seemed that two problems could arise when using a rotary valve to feed the bulk solid into the channel: firstly there would be the effect of pulsations produced as each pocket of the valve discharged its contents into the channel, and secondly there could be undesirable effects if the valve were allowed to run with the flow stopped (as might occur if the channel became choked). The pulsations induced by the rotary valve should be damped, partially if not completely, by the separate chamber at the inlet end of the channel, referred to in Section 8.2.2. Depending

upon the setting of the baffle plate, the level of powder in this chamber could be significantly greater than in the main channel and also the degree of fluidisation could be different. Thus the chamber serves to some extent as a "buffer zone" between the rotary valve and the main channel. Naturally, if the baffle plate is too far closed or if the solids flow in the main channel is restricted in some other way, there will be a tendency for the upstream fluidising chamber to fill up, eventually blocking the rotary valve. To avoid this possibility, an overflow duct was fitted to the small feed hopper between the rotary valve and the channel inlet as indicated in Fig. 8.3. Since the powder in this region would normally be fluidised, the overflow (which can be clearly seen in Plate V) should give an immediate indication of an excessive discrepancy between the feed rate of the rotary valve and the conveying capacity of the channel.

8.2.5 Weigh-bin

For batch-wise operation of the test rig it is obviously necessary for the lower hopper to be of similar capacity to the main storage hopper. However, the requirement for the inclination of the channel to be variable up to about 15^{o} meant that the vertical space available for the lower hopper was restricted to a little over one metre. A rectangular galvanised steel tank was available which had a capacity of about one cubic metre, and it was decided to utilise this by fitting it with inclined porous base panels so that air assistance could be provided to discharge the powder (Fig. 8.4).

The lower hopper also had to serve as a weigh-bin in order to determine the mass of powder discharged by the channel during each test run, and for this purpose it was mounted on a set of three load cells as described in Section 8.3.1.

To prevent undue pollution of the laboratory by dust the top cover of the weigh-bin was sealed and fitted with a filter unit (Plate VI). In addition to the air used to assist the discharge of powder from the weigh-bin, most of the air from the conveying channel would exhaust through this filter unit.

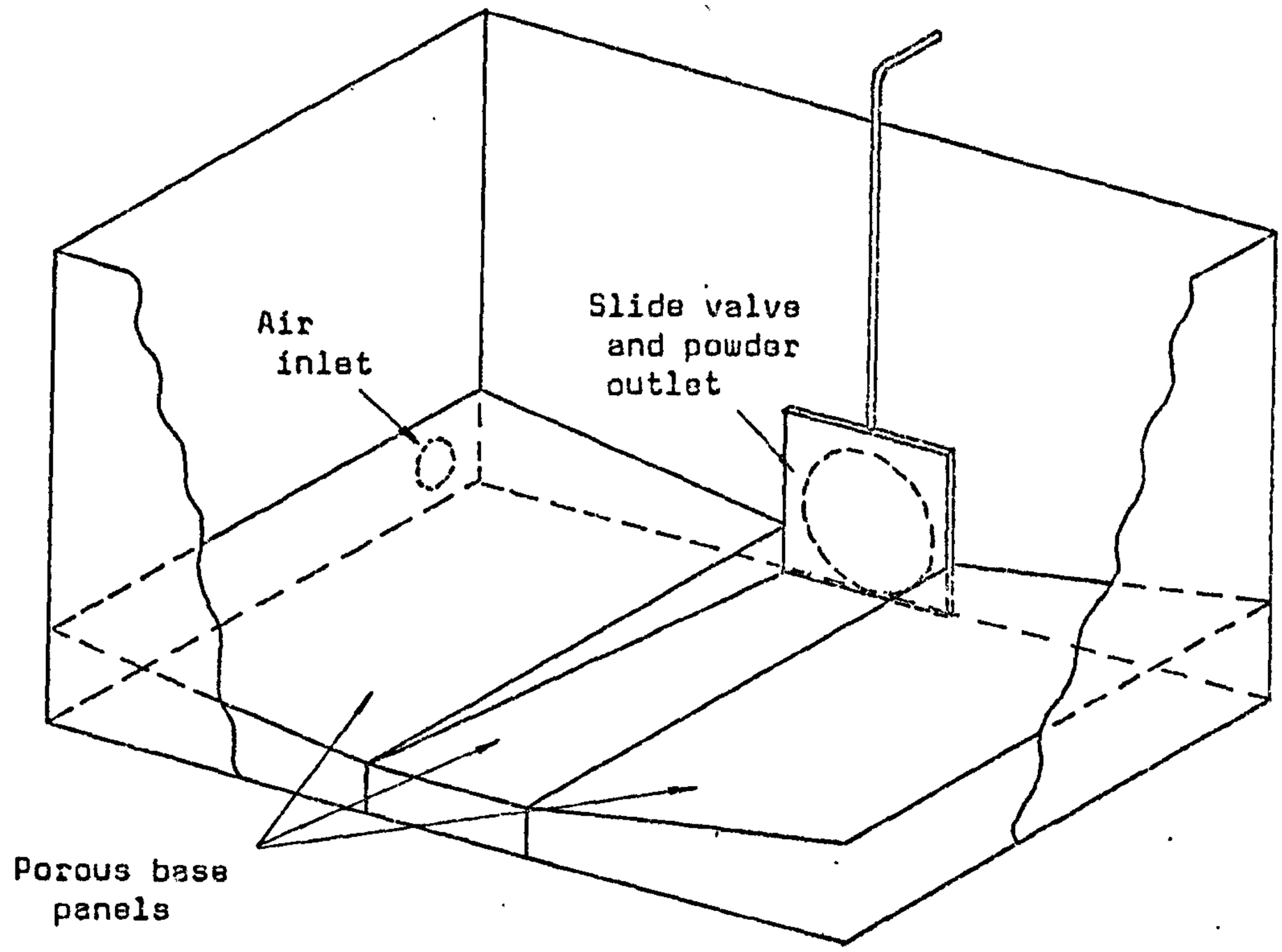

Fig. 8.4. CUTAWAY DIAGRAM OF THE WEIGH-BIN SHOWING THE ARRANGEMENT OF THE POROUS BASE PANELS.

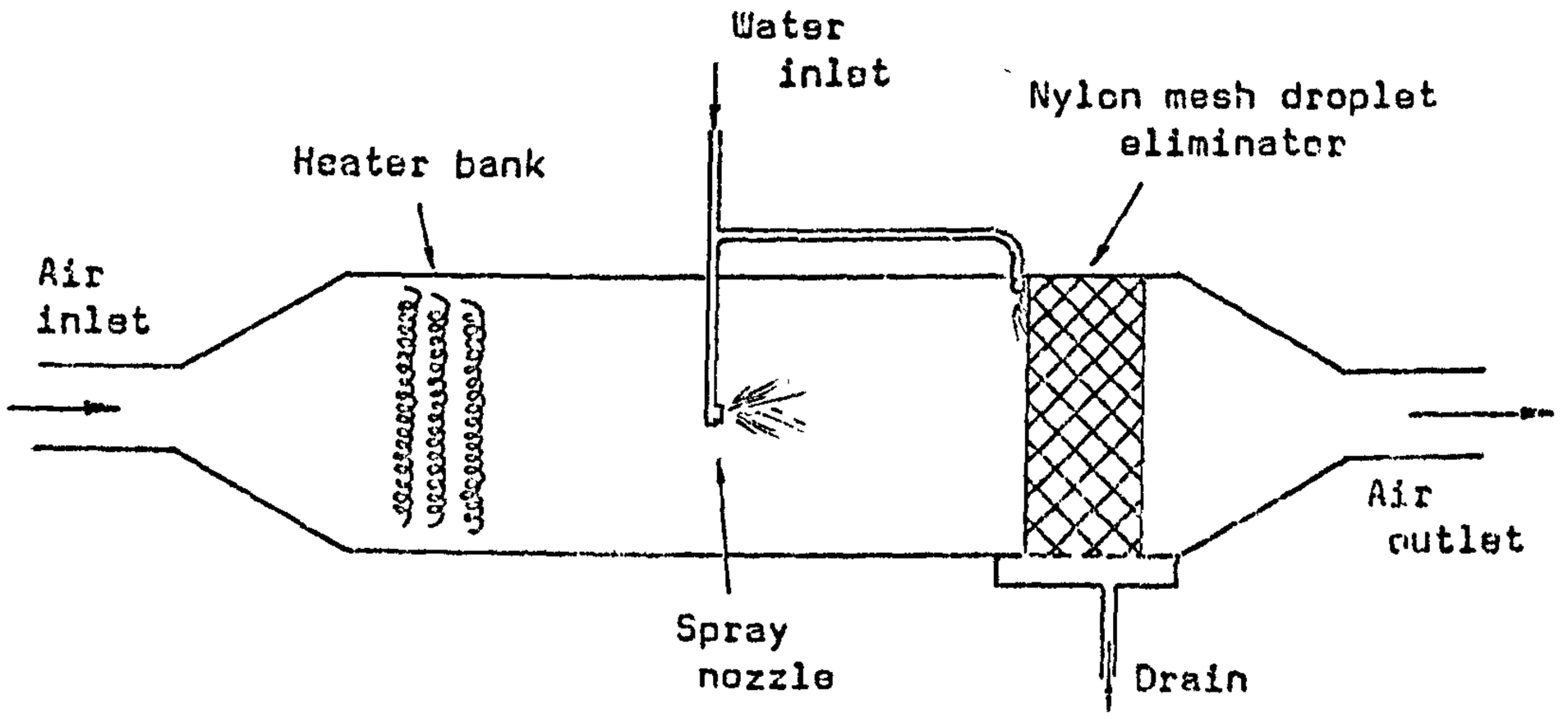

Fig. 8.5. THE HUMIDIFIER

8.2.6 Powder return system.

At the completion of each test run the powder in the weigh-bin had to be discharged through the outlet port (which could be closed by a simple slide-valve) and returned to the top hopper in readiness for the next run. Several alternative systems were considered but the one that appeared to offer the best combination of convenience and economy was the "Floveyor", an aero-mechanical tubular conveyor marketed at the time of installation by Entecon Ltd. (see also Appendix A.V). This conveyor was arranged to operate directly between the outlet port of the weigh bin and the inlet port in the top cover of the main storage hopper, as shown in Fig. 8.3. and in Plates VI and VIII.

8.2.7 Air supply system

All the air needs of the test installation were provided by a Godfrey MU1000 Industrial Blower, which was a Roots-type positive displacement machine, running at 1000 rev/min and (at this speed) capable of delivering up to 0.05 m^3/s of air at 52 kN/m^2 (390 mm Hg). (See also Appendix A.V.)

The layout of the air supply system can be seen from Fig. 8.3. The by-pass, necessary since the blower is a positive displacement type, discharges directly to atmosphere, and the air supply line then branches to feed the weigh-bin, the top hopper, and the two separate plenum chambers of the channel.

The air inlet to the blower is taken directly from the laboratory through a filter to minimize the amount of dust carried to the underside of the porous channel base. Some consideration was given to the need to condition this air before it reached the channel, complete control of both temperature and humidity being the ideal. Most previous investigators have worked with air at high humidities in order to eliminate problems of electrostatic charging of the conveyed material, and so it was decided that in the present study some attempt should be made to investigate the influence of humidity.

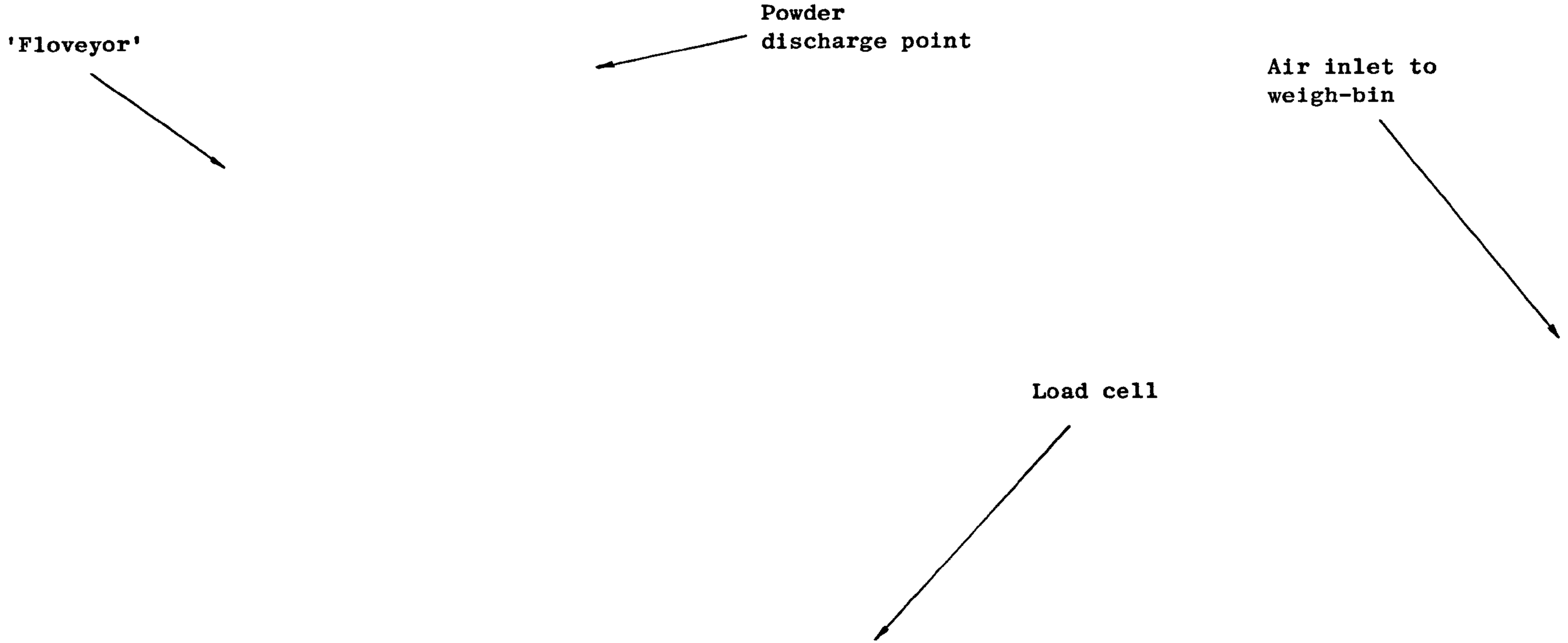

Plate VIII. A CORNER OF THE WEIGH-BIN, SHOWING ONE OF THE THREE LOAD CELLS AND THE DISCHARGE TO THE 'FLOVEYOR'.

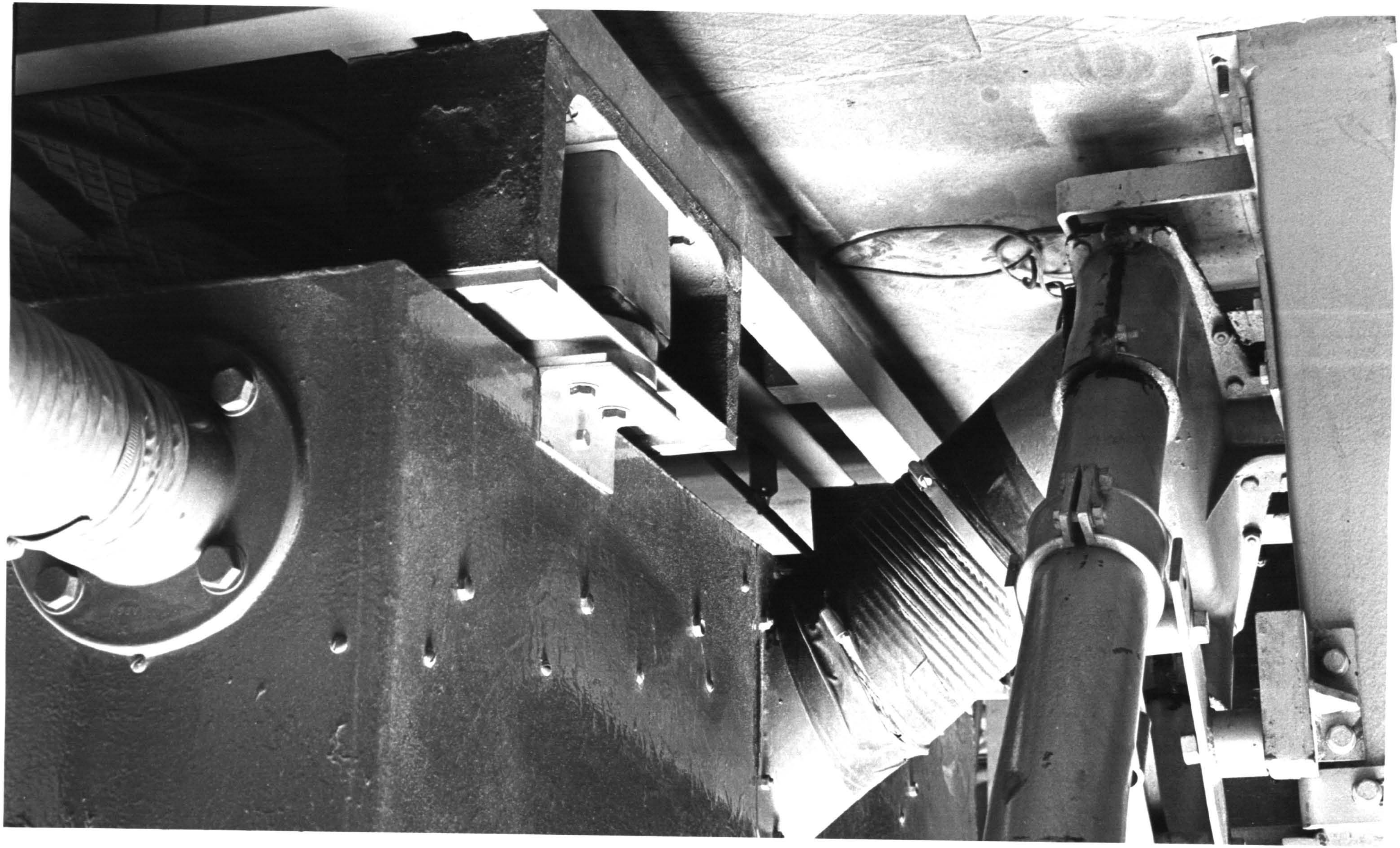

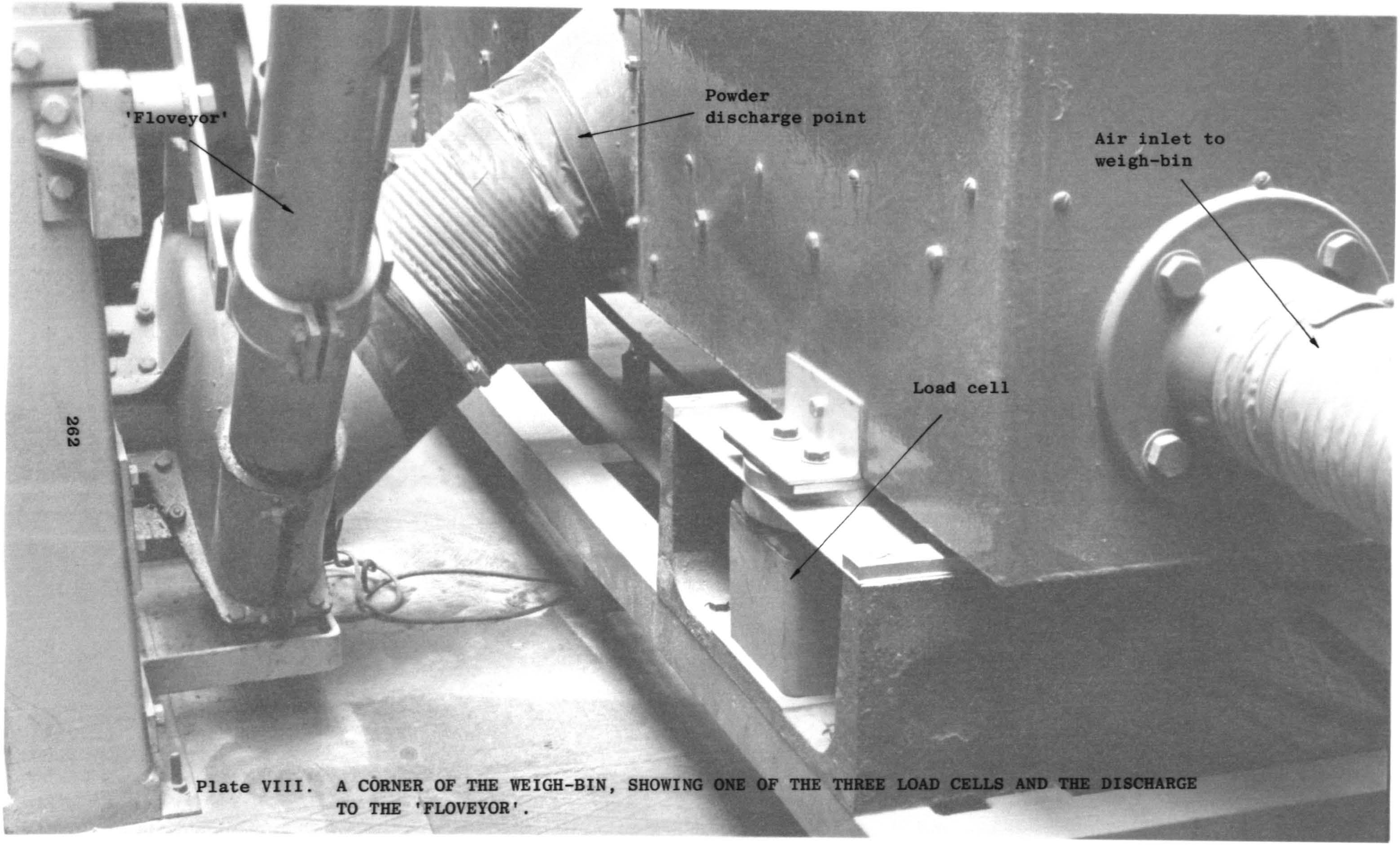

Plate VIII. A CORNER OF THE WEIGH-BIN, SHOWING ONE OF THE THREE LOAD CELLS AND THE DISCHARGE TO THE 'FLOVEYOR'.

Consultation with the air conditioning industry suggested that commercially available humidifiers, such as those working on steam injection, are very successful at maintaining steady low to moderate humidities, but might be less reliable on the high humidities required in this application, and in any case could not be expected to produce better than about 70% R.H. Also the pressure rise across the air blower was large compared with what would normally be encountered in air-conditioning systems and this could create additional difficulties with commercial humidifiers.

Various methods were considered of humidifying the air leaving the blower. (The significant rise in dry-bulb temperature across the blower would mean that, with humidification taking place on the suction side, even air with a high moisture content could have a rather low relative humidity.) Although there was doubt as to which method would be most likely to prove successful, it was decided to construct a water-injection system with a 3 kW pre-heater and nylon mesh droplet eliminator (Fig. 8.5). However, the actual performance of this humidifier was somewhat disappointing, for although it was capable of increasing the relative humidity of the fluidising air entering the plenum chamber of the channel, it proved almost impossible to control.

The arrangement of the air control valves and rotameters can be seen together with much of the other instrumentation on the control panel illustrated in Plate IX, and the humidifier is shown in Plate X.

8.3 INSTRUMENTATION

8.3.1 Solids mass flowrate

No provision was made for continuous measurement of the solids mass flow-rate, but the average value during a test run or part of a test run could be easily determined by observing the mass of powder collected in the weigh-bin in a given period of time.

Since it was felt to be advantageous to have a continuous indication of the mass of powder in the weigh-bin, the complete assembly of the bin,

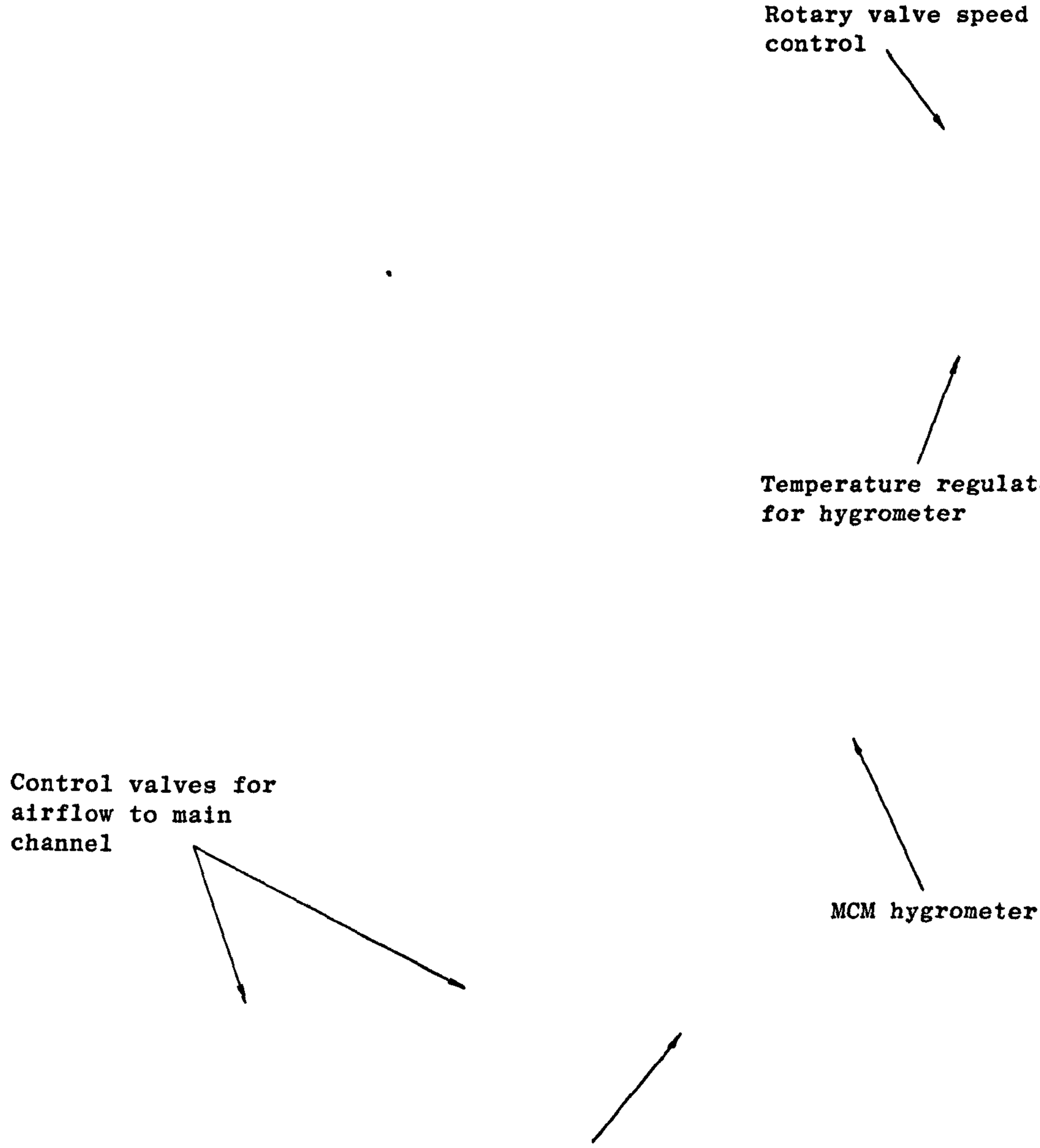

Plate IX. THE CONTROL PANEL FOR THE CHANNEL FLOW RIG.

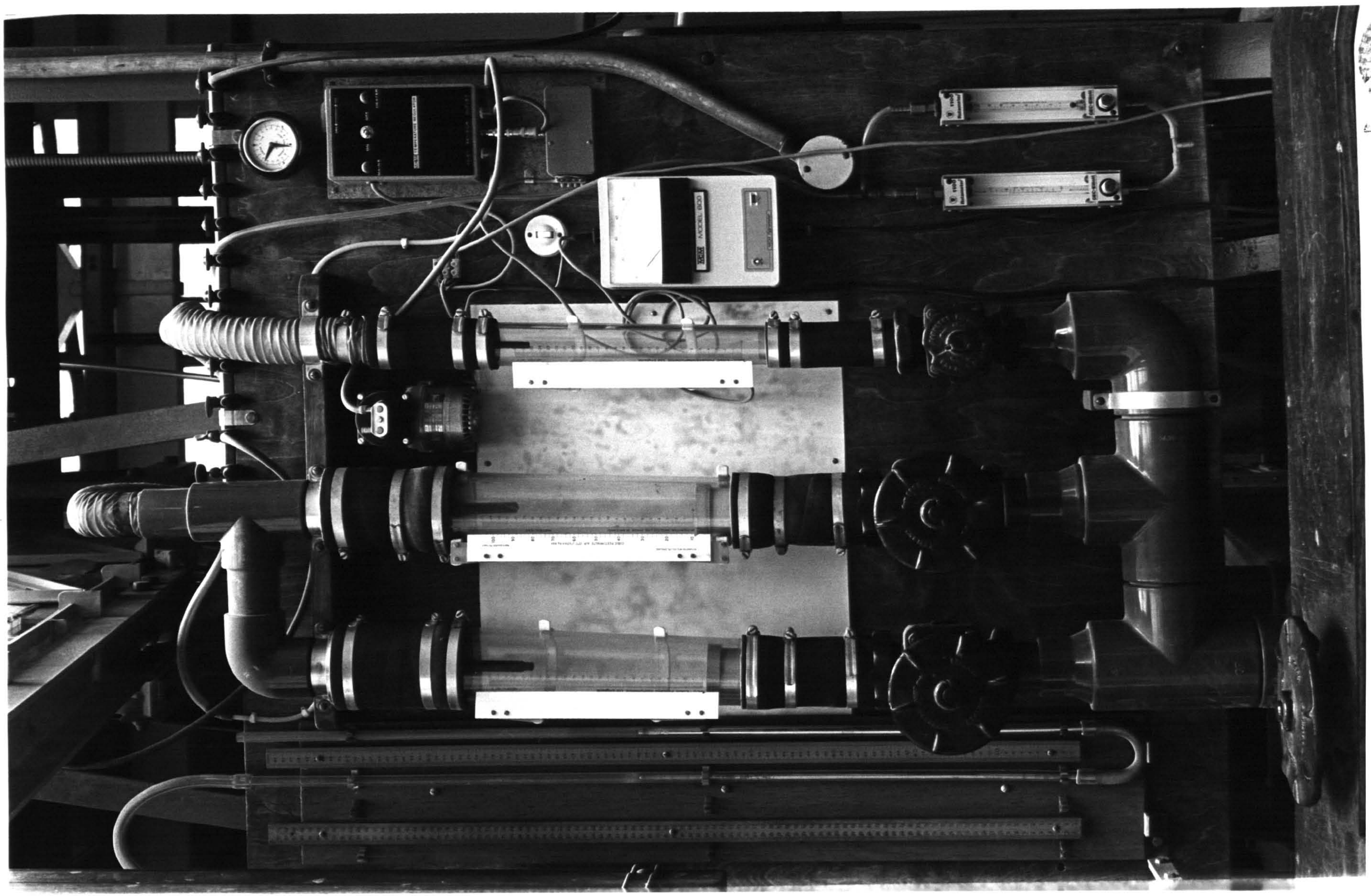

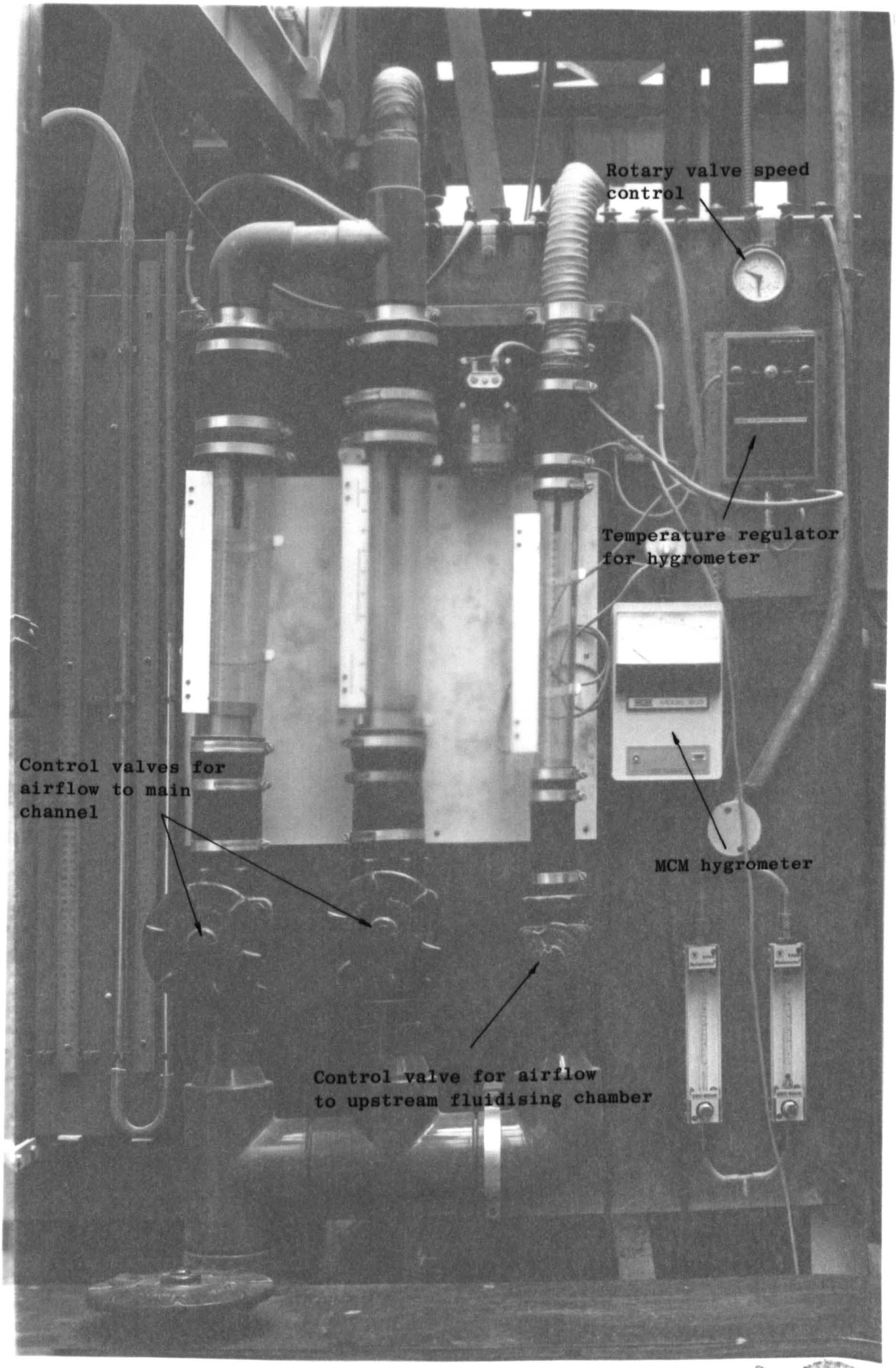

Plate IX. THE CONTROL PANEL FOR THE CHANNEL FLOW RIG.

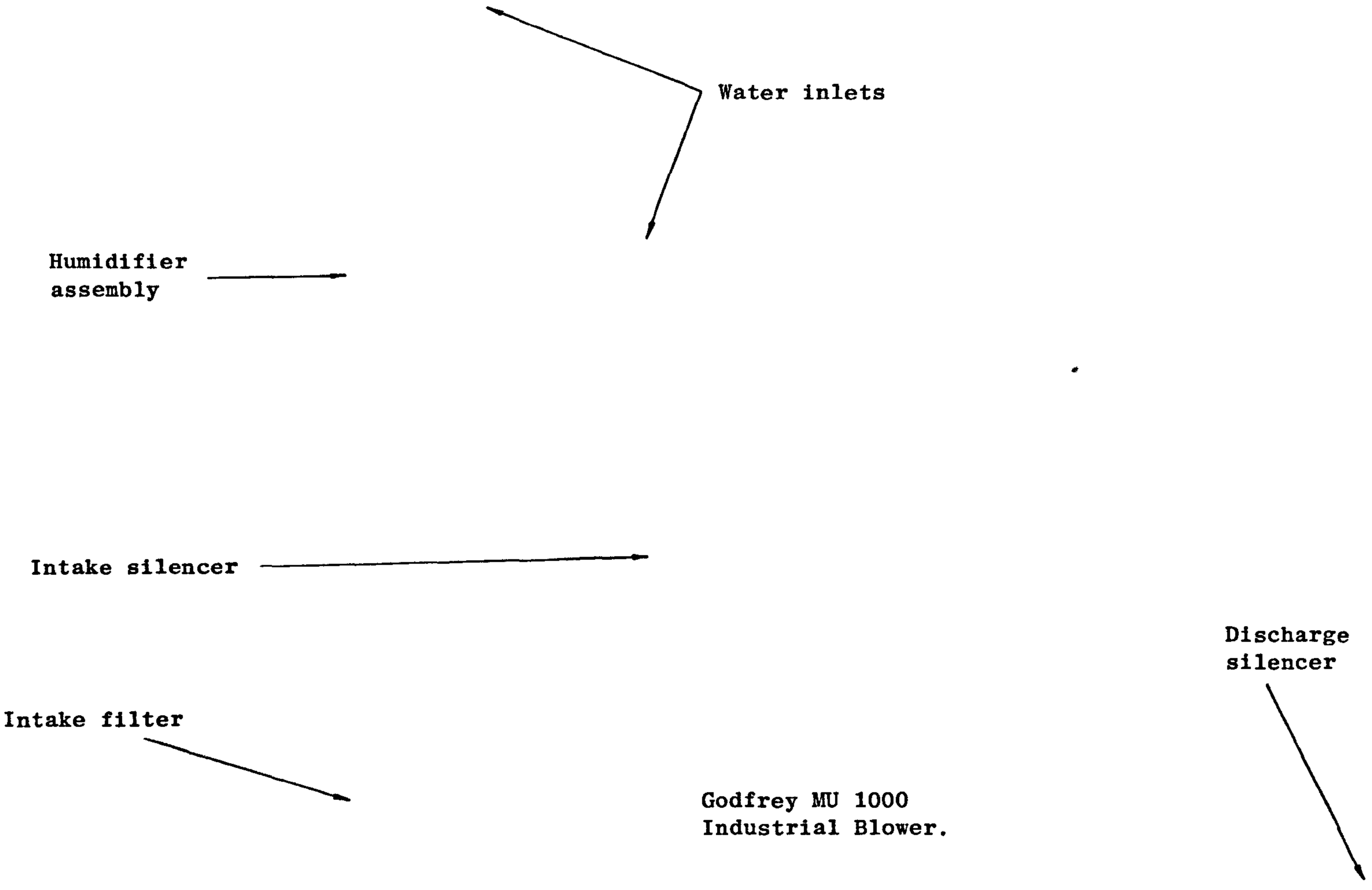

Plate X. THE HUMIDIFIER AND AIR BLOWER.

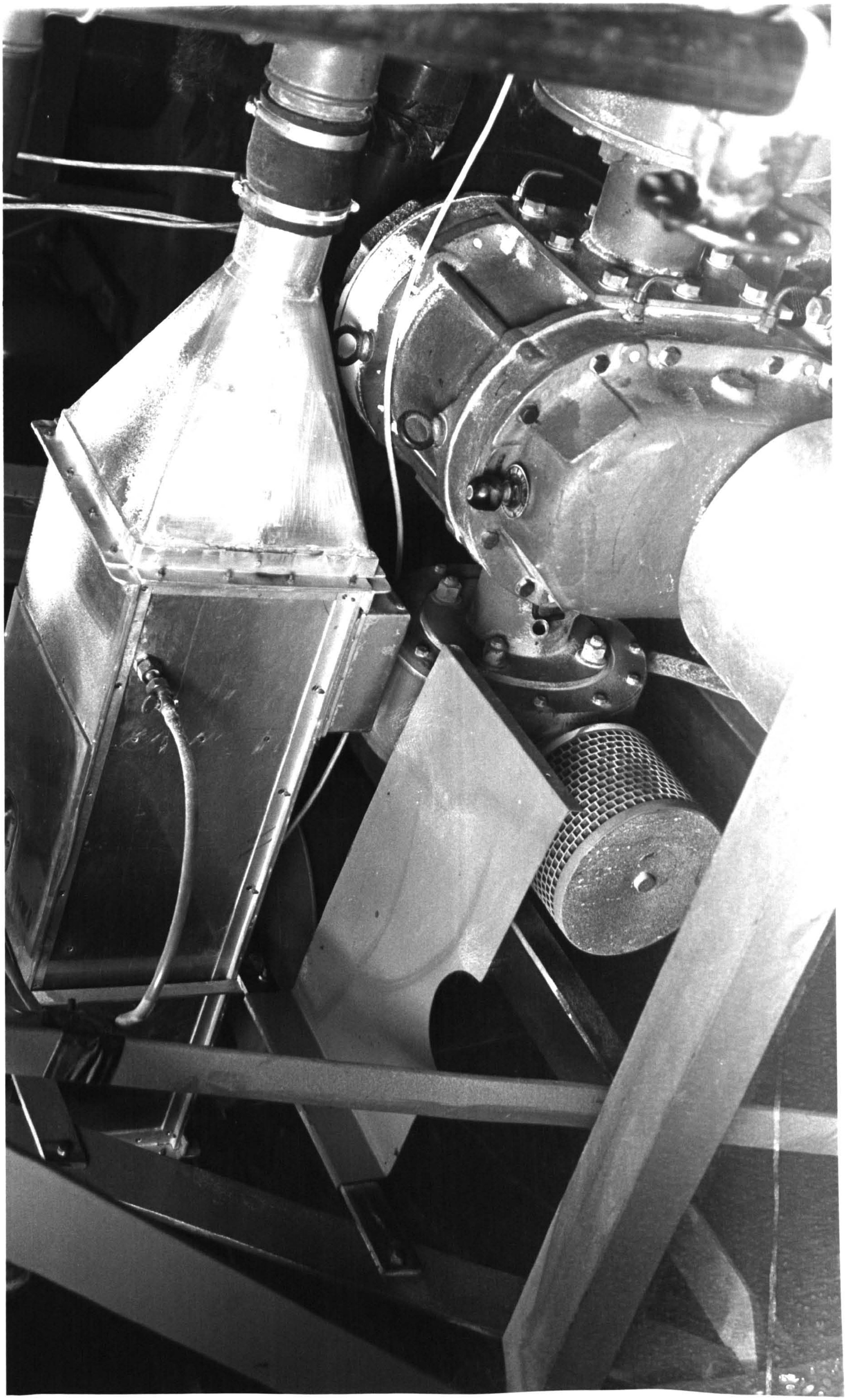

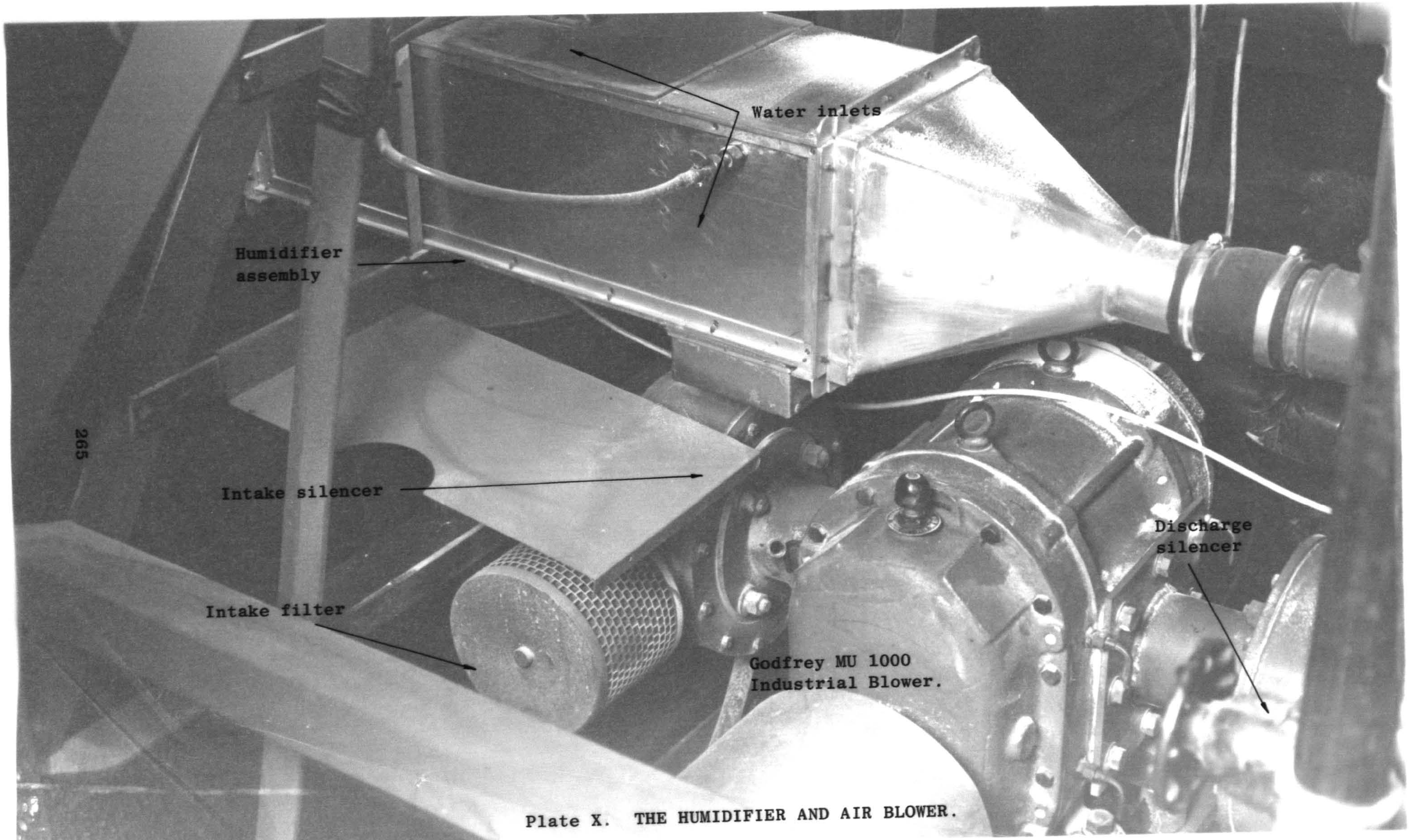

Plate X. THE HUMIDIFIER AND AIR BLOWER.

filter unit and sampling container was mounted on three load cells in triangular array (Plates VI and VII). The outputs from the load cells were taken to a summing and amplifying unit which gave a meter reading proportional to the combined load on the cells. Calibration of the system showed that the relationship between the total force on the load cells and the instrument scale reading was linear over the whole of the required working range of 0 to 500 kg(see Appendix A.V). Therefore the meter zero adjustment could be used as a tare set, allowing convenient indication of the mass of powder flowing into the bin during a test run, irrespective of the quantity of powder initially present in the bin. Calibration charts at the two range settings used are to be found in Appendix A.V (pages A-88 and A-89).

8.3.2 Depth of flowing bed

The measurement of the depth of the flowing suspension of powder has apparently caused considerable difficulties in previous experimental studies on the flow of fluidised particulate solids in inclined channels, and some investigators seem to have carefully avoided trying to measure it directly. McGuigan (Ref. M4) for example, states that the majority of his test data was collected at bed depths of 27.5 mm and 40 mm, but he does not make it clear how the depth of the flowing suspension was controlled at these values. Presumably McGuigan determined the bed depths by the same technique as Pugh (Ref. P9) who did not measure them directly, but deduced them from a pressure-drop correlation with readings from a small stationary bed. The accuracy of such a procedure might be acceptable when using relatively coarse solids, but must be questionable with fine powders because of unpredictable variations in the resistance of the porous distributor; a problem highlighted by Keuneke (Ref. K3).

Keuneke in fact determined the bed depth as an average of three direct measurements using sight glasses. Certainly, because of wave motion or bubbling on the surface of the flowing suspension, the direct measurement of the depth could not be expected to be very accurate. However, if the depth at several points is measured, the average should be no less reliable than that inferred from a measurement of the pressure drop across the bed.

The approach used in the present work was therefore to attach five vertical scales to the Perspex walls of the channel at equal intervals along its length, although to minimize any end effects only the readings of the middle three scales were used in estimating the average depth of the flowing suspension.

8.3.3 Air flowrates

The flowrate of air supplied to the main channel and to the upstream fluidising chamber were each measured by conventional rotameters. As with the small fluidising test rig, new calibration charts were prepared giving the relationship between the rotameter scale reading and the superficial air velocity. Fig. 8.6 gives this relationship for the separate upstream fluidising chamber, whilst Figs. 8.7 and 8.8 apply to the rotameters used on the main channel. The arrangement of these rotameters and their respective airflow control valves is clearly seen on Plate IX which shows the control panel for the channel test rig.

8.3.4 Pressure, temperature and moisture content of the fluidising air

The pressure of the air on the discharge side of the blower (or at the exit from the humidifier, when this was in circuit) was measured by a simple mercury manometer. A mercury-in-glass thermometer, inserted in a thermometer pocket, allowed the temperature of the air at this point to be measured.

Additional pressure tappings were made in the side walls of the conveying duct and the upstream fluidising chamber, and in the two separate plenum chambers, so that the pressure-drop across the porous base of the channel and also the combined pressure-drop across the base and the flowing suspension could be measured. In order to detect any variation in pressure along the length of the channel these pressure tappings above and below the distributor were repeated at five equally spaced positions. Pressures were measured with an Airflow Developments inclined manometer set.

At two points in the main plenum chamber, one near the air inlet and the other towards the lower end, horizontal thermometer pockets were built in

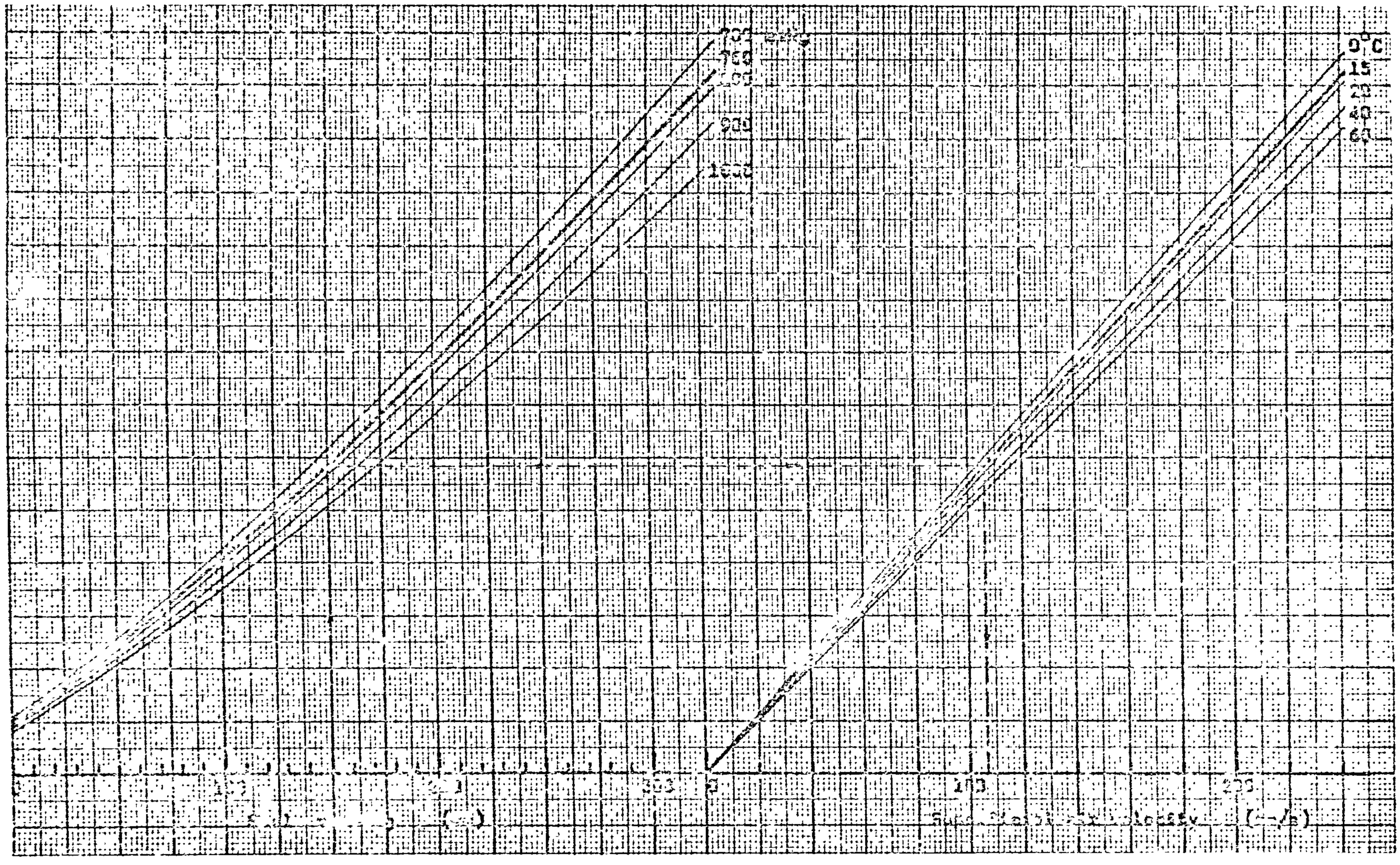

Fig. 8.6 CALIBRATION CHART FOR ROTAMETER 35A ON UPSTREAM FLUIDISING CHAMBER OF MAIN CHANNEL RIG.

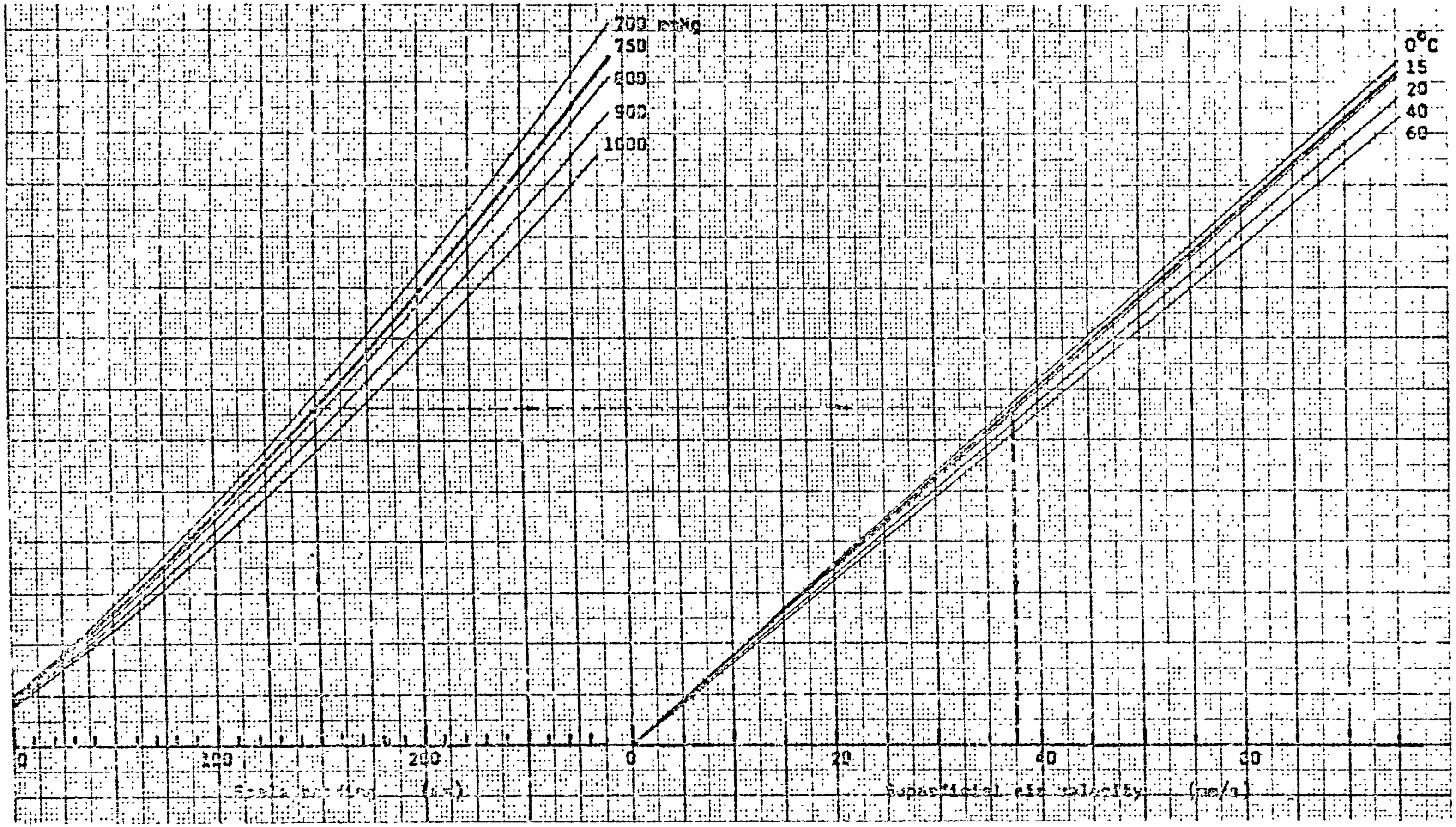

Fig. 8.7 CALIBRATION CHART FOR ROTAMETER 65A ON MAIN CHANNEL FLOW RIG.

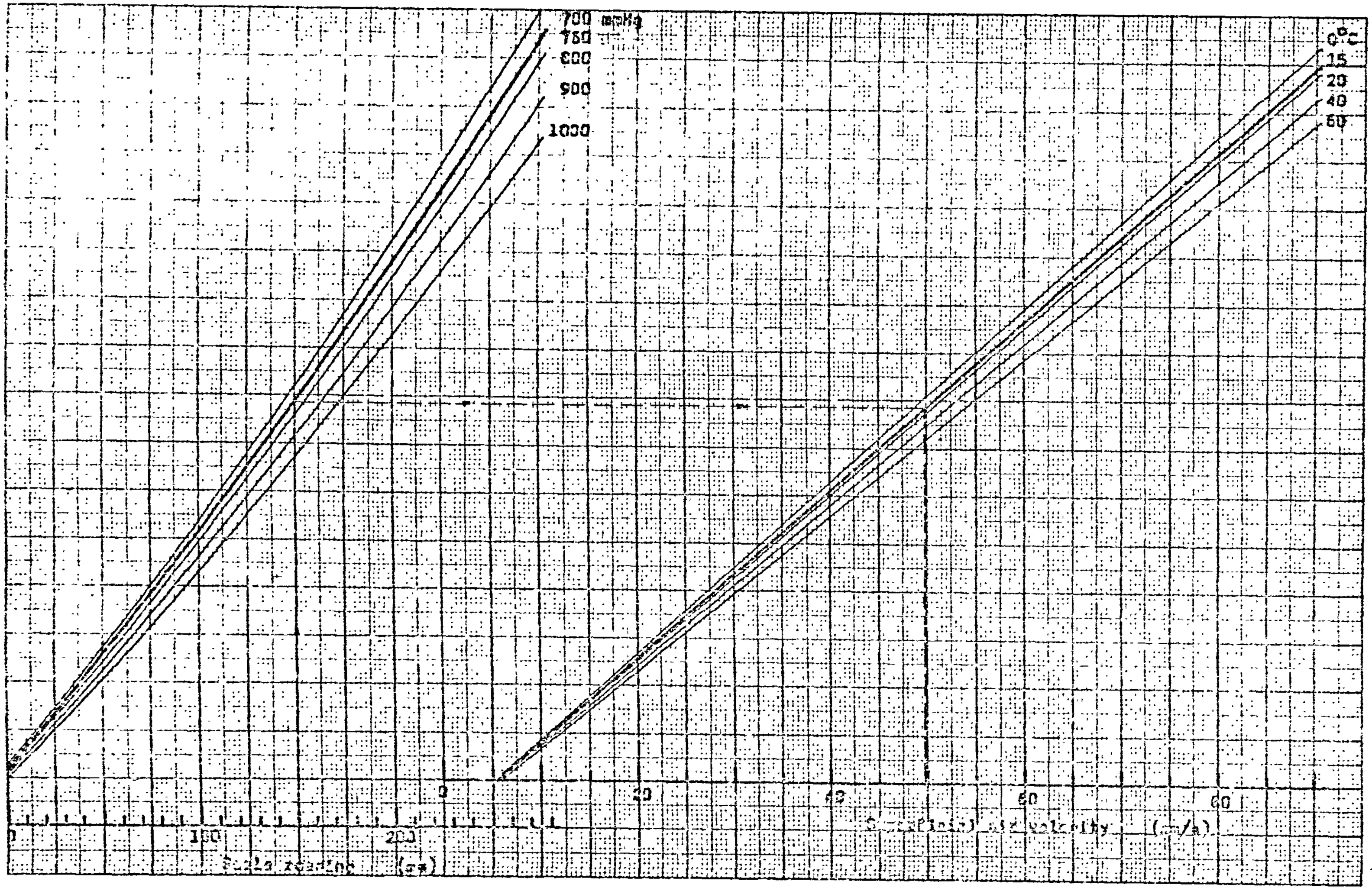

Fig. 8:8 CALIBRATION CHART FOR ROTAMETER 65XK ON MAIN CHANNEL FLOW RIG.

so that the temperature just beneath the porous distributor could be determined. Collets fitted in corresponding locations on the top cover of the channel supported mercury-in-glass thermometers which could be adjusted vertically to dip into the flowing suspension.

The pressure tapping points in the conveying channel and plenum chamber served as convenient sampling points to take off air for humidity measurement. A bank of small taps allowed selection of the required sample point and air from this point was thus piped to the sensor of the hygrometer. The MCM hygrometer is described in Appendix A.V, and in this application is used with a constant temperature regulator which ensures that the air coming into contact with the sensor is maintained at a constant dry-bulb temperature. This allows a simple calibration of the scale to give dew-point temperatures of the sampled air. The hygrometer and temperature regulator can be seen mounted on the control panel (Plate IX) and the manufacturer's calibration chart is reproduced as Fig. A.V.7 (page A-84). The humidity of the ambient air could be determined by passing a sample through the MCM hygrometer, but as a check, readings were also taken of a wet-bulb thermometer.

8.4 COMMISSIONING THE RIG

8.4.1 Introduction

As indicated in the previous Chapter, various particulate materials were considered for the first tests on fluidised flow, and the selection was eventually narrowed to a choice between sand and 'Corvic'. Sand clearly had the advantages of low cost and availability over a wide range of particle size, but its abrasive nature would have meant a somewhat harsh commissioning for the Floveyor and for the rotary valve.

Data on the flow of fluidised sand in the test rig would provide an interesting comparison with other materials, and also with the results of other investigators, but for the first series of tests the decision was taken to use the 'Corvic'.

The specification of Corvic, a p.v.c. powder manufactured by I.C.I. Ltd., has been given in Section 7.4.2 and its fluidisation behaviour in the

small fluidising rig has been described in some detail in Section 7.5. Basically this material is a free-flowing white powder of 120 μm mean particle size, having a true density of 1430 kg/m^3 and bulk density of around 500 kg/m^3. The minimum fluidising velocity of the fresh powder is about 10 mm/s, but as explained in Section 7.5, agglomeration of the particles as a result of electrostatic charging causes a drastic change in the fluidisation characteristics.

The next few Sections deal at some length with the extended series of commissioning tests that were undertaken on the rig using Corvic as the conveyed material. In addition to familiarising the operator with the characteristics of the test rig, the purpose of these tests was to investigate the influence of various features such as the air supply to the top storage hopper, the rotary valve and the baffle plate at the inlet to the main conveying channel. The effect on the flow behaviour of the aerated Corvic of extraneous variables, such as electrostatic charging and the pre-conditioning of the powder, was also investigated during these commissioning tests.

8.4.2 Operating procedure

The start-up procedure for the rig was quite straightforward and is summarised in the following steps:-

1. Check that air by-pass valve to atmosphere is open and switch on blower.
2. Open air control valves to supply air to upstream fluidising chamber and main conveying channel at suitable rates, closing by-pass valve as necessary. (In general, superficial velocities of about twice the minimum fluidising velocity of the conveyed material would be appropriate, or rather more for cohesive materials. Thus for Corvic, a value of around 30 mm/s should be sufficient to get the flow started.)
3. Check that baffle plate at channel inlet is open sufficiently.
4. Open air supply valve for weigh-bin just enough to fluidise the powder in it.

5. Check that slide gate on weigh-bin outlet is closed and switch on Floveyor. (It should be noted that starting the Floveyor when the lower end is choked with powder may put undue strain on the rope, and therefore the slide gate should always be closed and the Floveyor cleared of powder before it is switched off.)
6. Open the slide gate to begin conveying powder from weigh-bin to top storage hopper.
7. Set handwheel to required rotary valve speed using calibration chart (Fig. A.V.11, page A-90) and switch on rotary valve. (For batch-wise operation of the rig all the powder must of course be transferred to the top hopper before flow in the conveying channel is allowed to commence, but for continuous circulation of the powder the rotary valve can be started at any time.)

The shut down procedure is simply a matter of switching off the rotary valve and shutting the slide-gate on the weigh-bin (the order in which these steps are taken depending upon whether the powder is required in the top hopper or in the weigh-bin), and then switching off the Floveyor and the blower.

For the majority of test runs the rig was started up as outlined above and the powder was allowed to circulate continuously for a time while the hygrometer and the mass flow meter "warmed up". The rotary valve was then switched off and all the powder was transferred to the top hopper. The channel slope was set to the desired value and required settings were made of the rotary valve speed control and the superficial air velocity in the channel. The zero set on the mass flow meter was adjusted to give a meter reading just below the zero mark, and the rotary valve was switched on to start the powder flowing down the channel. As the mass flow meter needle passed the zero mark a stop-clock was started and then readings were taken of the bed depth, and the pressure, temperature and humidity of the fluidising air. As the meter needle passed another convenient mark (before all the powder was discharged) the clock was stopped and the time noted. Finally the powder was returned to the top hopper in readiness for the next run.

8.4.3 The flow of aerated p.v.c. powder - general observations and the effect of electrostatic charging.

During the first trial runs of Corvic in the channel two effects were immediately apparent. One was a wave motion on the surface of the flowing powder, and the other was a gradual change in the surface appearance of the powder from the smoothness characteristic of a free-flowing material to the rough craggy surface that is a feature of more cohesive ones.

The surface waves on the flowing suspension in the channel started at the baffle plate, the powder appearing to flow under it in pulses. The pulsations could be traced a stage further back to the effect of powder falling intermittently from the rotary valve into the fluidised bed in the separate upstream chamber. Since the frequency of the waves was generally around 1.5 to 2 Hz it seemed fairly obvious that they were initiated by the powder falling in discrete "parcels" from the pockets of the rotary valve. However, it was not clear why the effect should be so pronounced with Corvic, as no mention is made of this problem by Keuneke (Ref. K3) who also used a rotary feeder when working with several different particulate materials. By adjustment of the superficial air velocity in the upstream fluidising chamber, and of the position of the baffle plate, the amplitude of the waves in the channel could be significantly reduced, especially when the flowing bed was fairly deep. It was not thought that slight waves on the surface of the flowing bed would invalidate the investigation of the relationships amongst the bed depth, solids mass flowrate, channel slope and superficial air velocity, and therefore no decision was taken at this stage to replace the rotary valve with an alternative feed device.

A far more serious influence on the flow behaviour of the aerated Corvic was the change in its nature that became evident after just a few test runs. Suspicion was first aroused when it was found to be difficult to obtain repeatable readings of mass flowrate and average bed depth in the channel. Inspection of the Corvic showed a distinct change in its appearance and this was confirmed by examination of samples under a microscope. The photomicrographs (Plate XI) allow a comparison to be made of the fresh, free-flowing Corvic with a sample taken from the powder in the

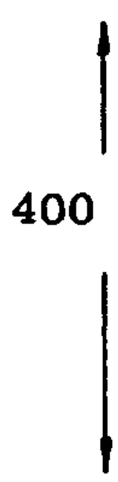

a) The separate particles in the free-flowing "fresh" condition.

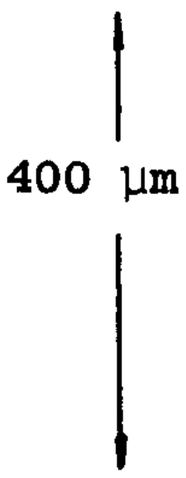

b) Showing the tendency to form loose agglomerates as a result of interparticle forces developed during test runs.

Plate XI. SAMPLES OF CORVIC AT A MAGNIFICATION OF X 84.

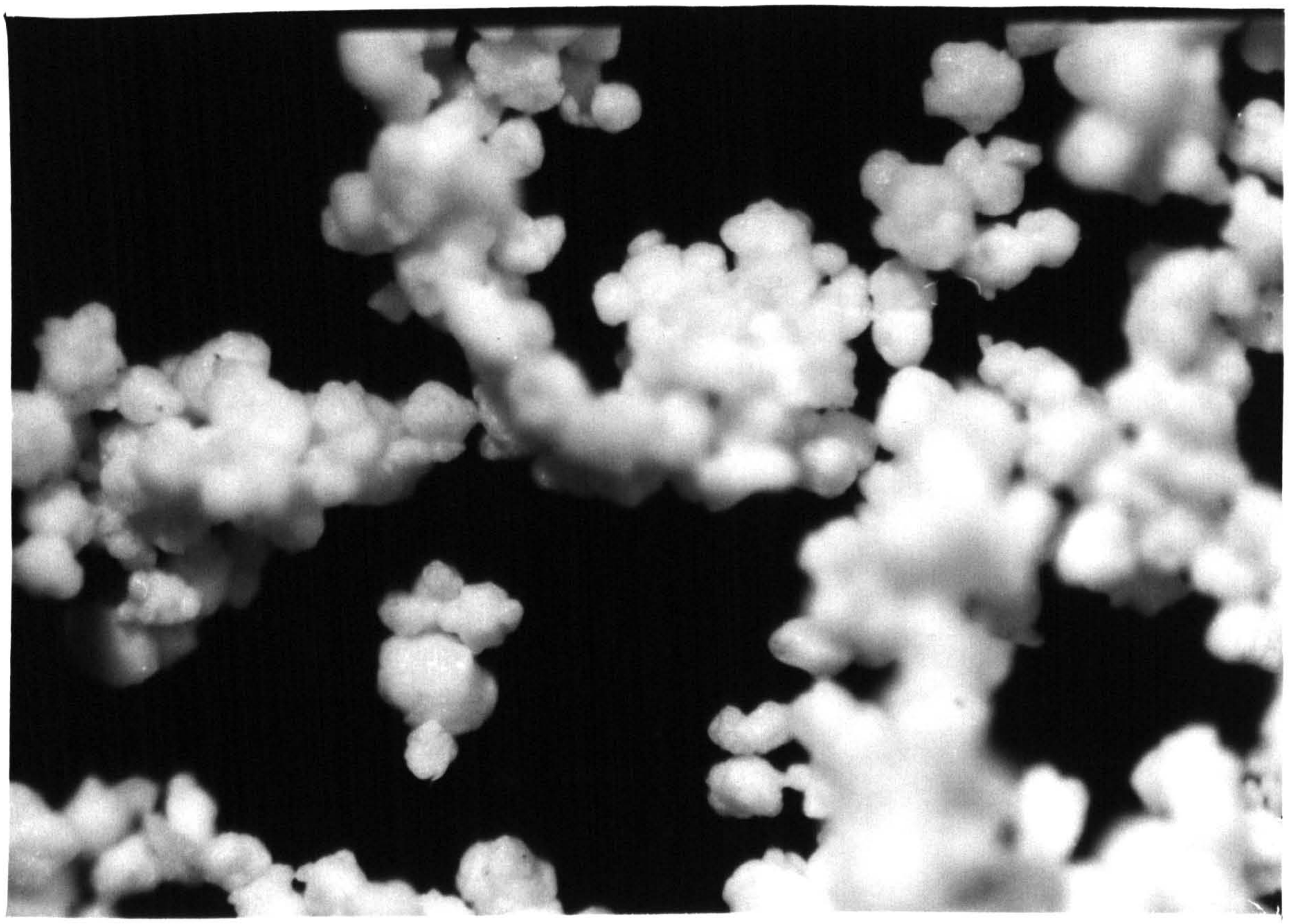

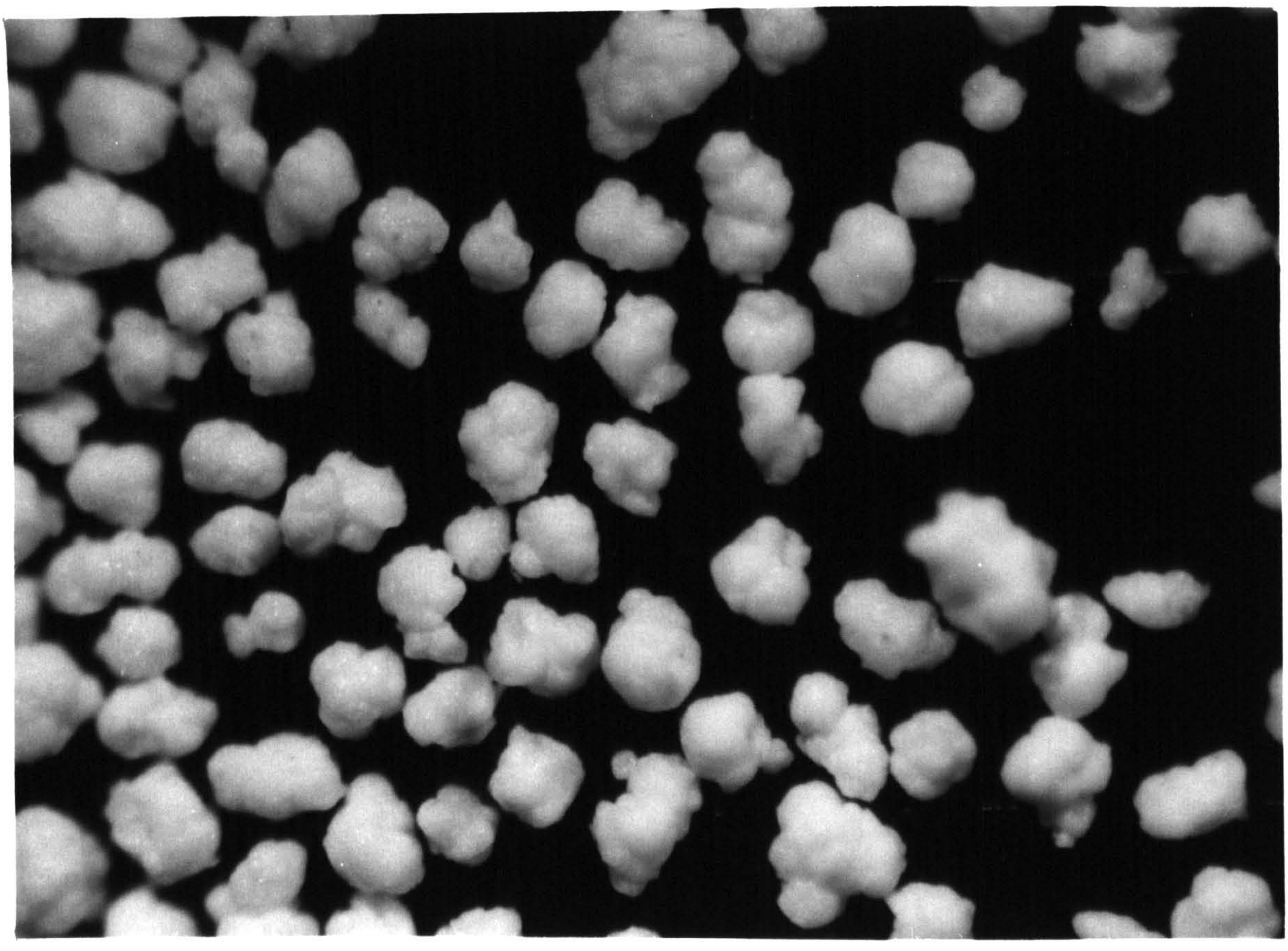

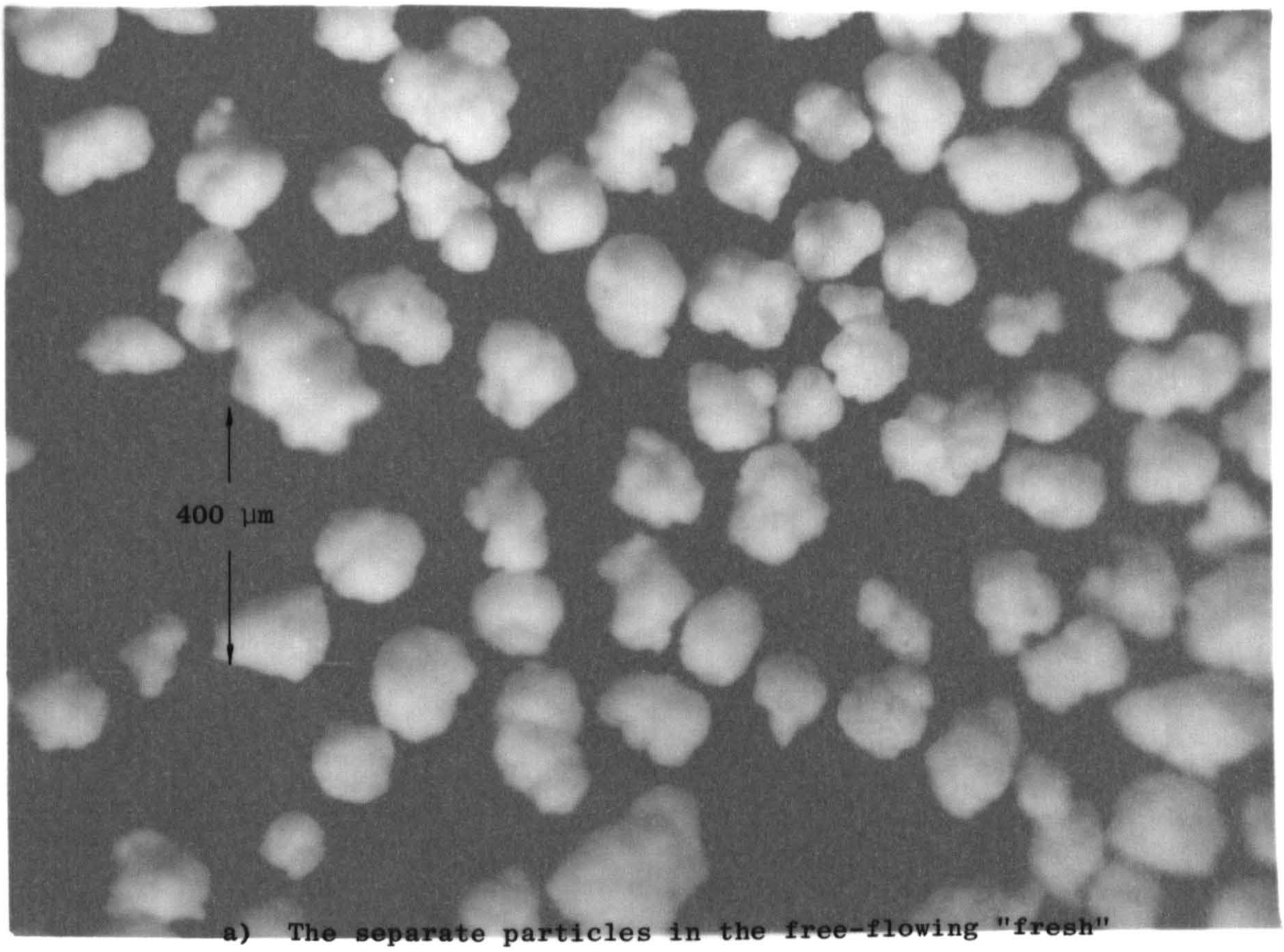

a) The separate particles in the free-flowing "fresh" condition.

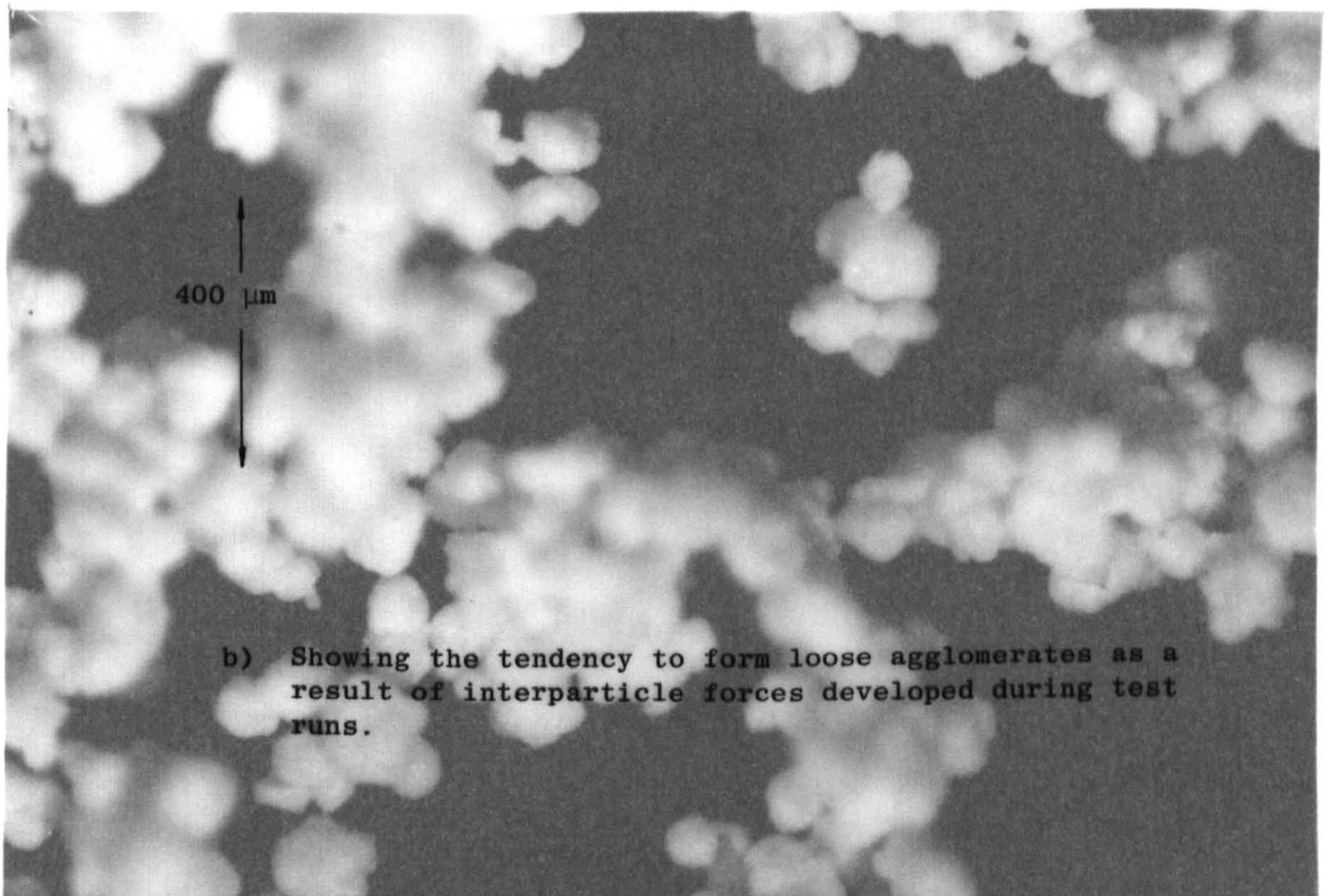

b) Showing the tendency to form loose agglomerates as a result of interparticle forces developed during test runs.

Plate XI. SAMPLES OF CORVIC AT A MAGNIFICATION OF X 84.

rig after about twenty test runs. The tendency for the particles of Corvic to form loose agglomerates is clearly seen and was assumed to be the result of electrostatic charging of the material. Whilst it was known that plastic powders of this type are susceptible to electrostatic charging, the severity of the effect in this case was somewhat unexpected.

In order to obtain a better appreciation of the time-dependent nature of the interparticle forces associated with the electrostatic phenomenon, several consecutive test runs were made at identical conditions (that is, at constant channel slope, rotary valve speed and superficial air velocity). Two effects were observed: a gradual decrease in the solids mass flowrate and a gradual increase in the depth of the flowing bed of Corvic. The variation in the solids mass flowrate can almost certainly be accounted for by the decrease in the bulk density of the Corvic that accompanies the development of an electrostatic charge. In Section 7.5.3 it has been suggested that the change in bulk density could be around 15 to 20% and this seems to correspond to the change in the mass throughput of the rotary valve, indicating, as would be expected, that the volumetric flow through the valve remained virtually constant.

The increase in the depth of the flowing bed of Corvic was perhaps more significant. It might have been anticipated that the bed depth would decrease if the solids mass flowrate decreased, but in this case the reverse was found to occur. This happens not only because of a decrease in the bulk density, but also because of the tendency of the Corvic to become defluidised as the interparticle forces build up. The result is in fact much the same as would be obtained by reducing the superficial air velocity; that is, the forward velocity of the flowing bed is reduced and its depth increases. Fig. 8.9a shows the way that the bed depth increased on successive test runs at two different superficial air velocities. At the lower air velocity, where the flow of the bed tends to be more sluggish, the rate of increase of the bed depth is much greater, and at still lower air velocities it was found that the powder initially flowed satisfactorily, but slowed up and then stopped flowing altogether as it became charged.

If the Corvic was left undisturbed it tended to lose the electrostatic charge, gradually reverting to its former free-flowing state. The time

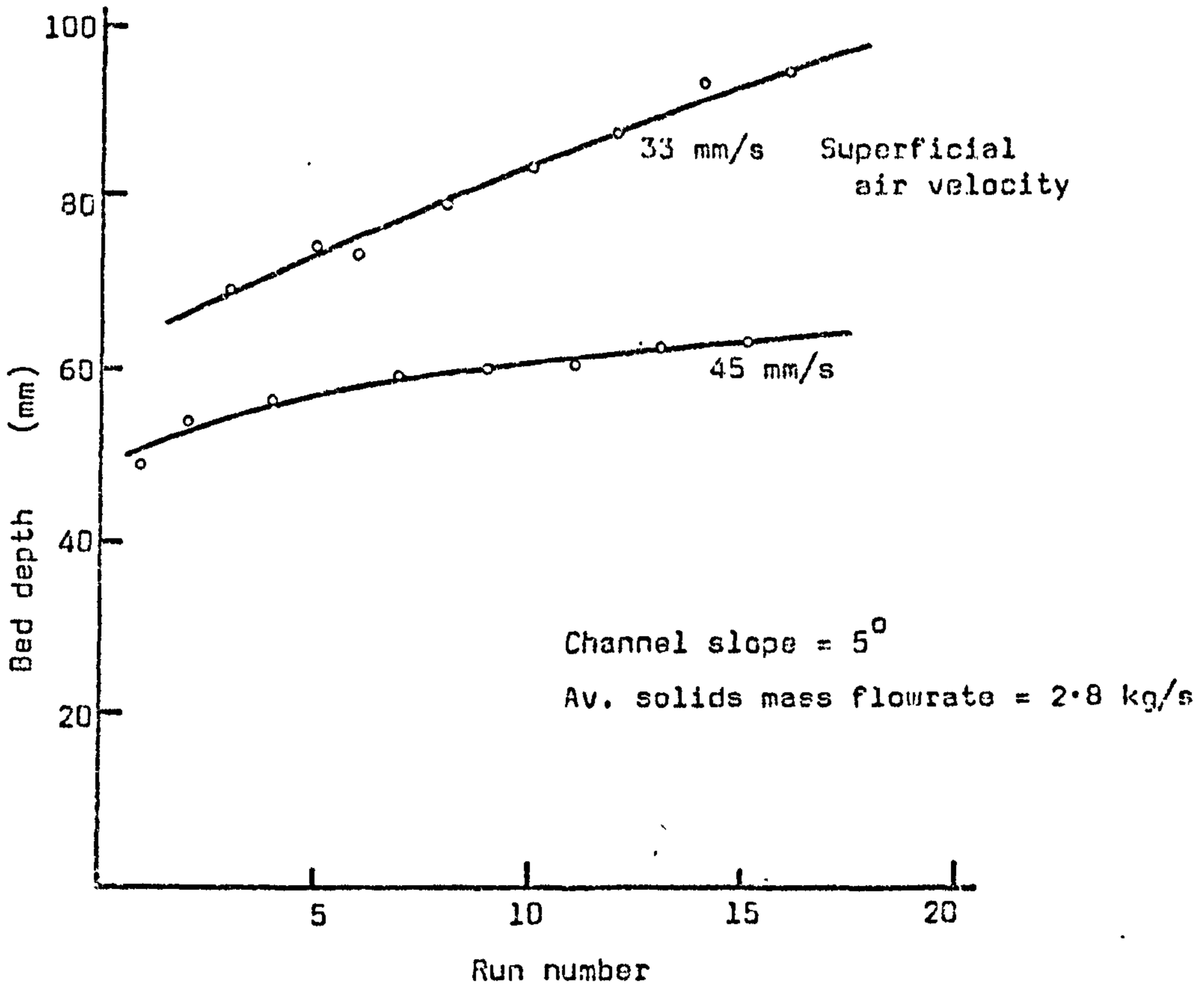

a.

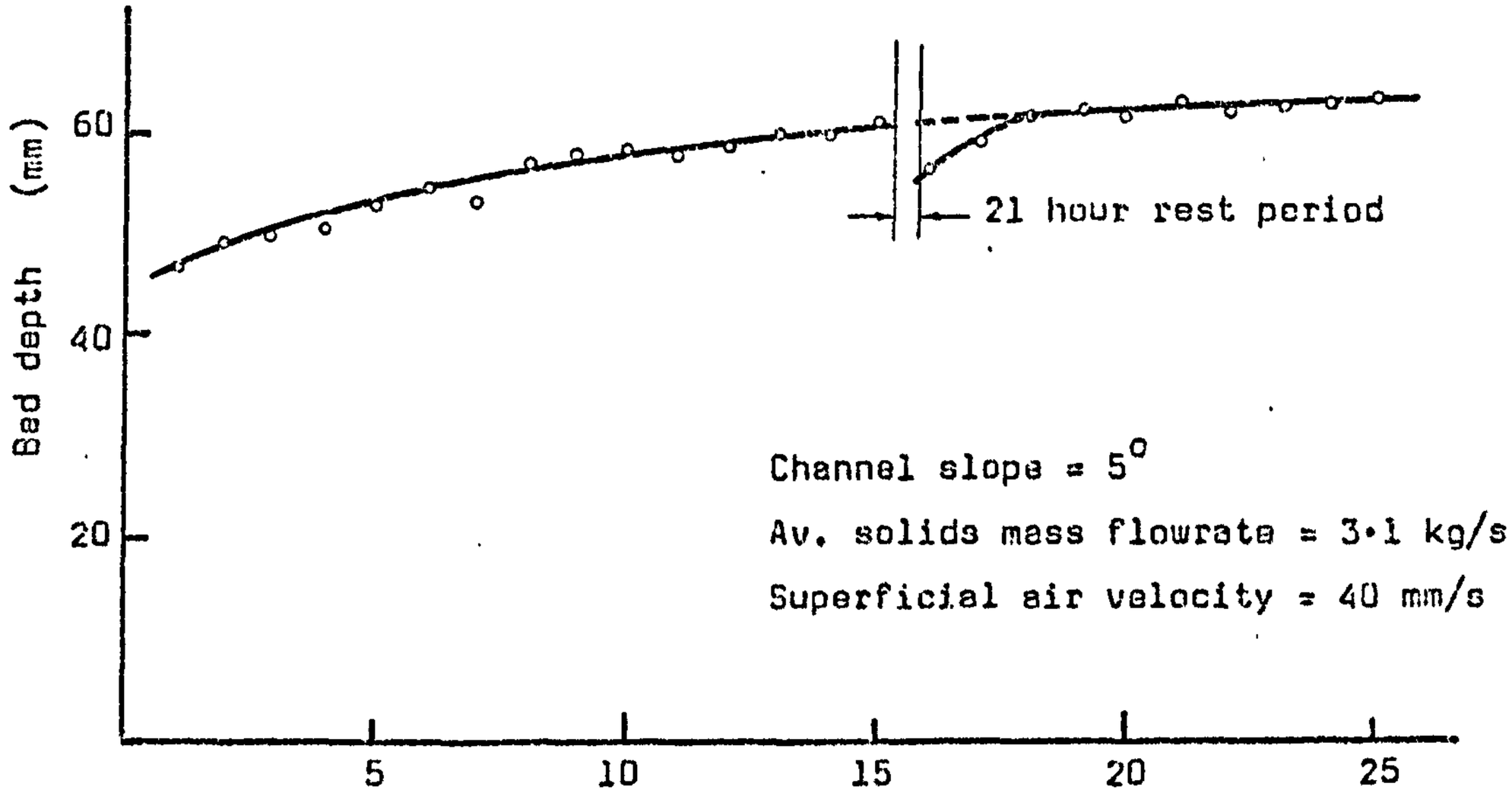

b.

Fig. 8.9 VARIATION OF BED DEPTH WITH CONVEYING TIME, SHOWING THE EFFECT OF ELECTROSTATIC CHARGING OF THE CONVEYED MATERIAL (CORVIC).

a) Runs at two different superficial air velocities.

b) Showing partial recovery after a period of rest.

for this to occur seemed to vary (presumably depending upon the humidity of the surrounding atmosphere) but was usually two or three days. However, even after a fairly lengthy rest period, the Corvic tended to become rapidly re-charged, as shown in Fig. 8.9b.

One of the main problems encountered as a direct result of the electrostatic phenomenon was the difficulty of obtaining repeatable data from the test runs carried out on different days under apparently identical conditions. Similar problems have been reported by other investigators (Refs. D6, R2) who found that experimental data relating to static electrification could be rather inconsistent. For example, Donald (Ref. D6) stated that "the charge acquired is never the same for two days running". One possible explanation for unexpected variations in test measurements has been pointed out by Ciborowski and Wlodarski (Ref. C4) is that levels of electrostatic charge reached in a fluidised powder can depend upon the humidity, not only of the fluidising air, but also of the atmosphere surrounding the test rig. In view of this, there is probably little to be gained from a detailed investigation of the influence of electrostatic charging unless the whole rig can be enclosed in a conditioned environment.

Some attempt was made in the present programme to vary the moisture content of the fluidising air supplied to the main channel. Using the humidifier described in Section 8.2.7, water was introduced into the air stream giving a significant increase in the relative humidity of the air in the plenum chamber of the channel. However, it was found to be impossible to obtain adequate control of the humidity, and although there seemed to be a trend towards more free-flowing behaviour as the humidity of the fluidising air increased, no consistent pattern could be recognised from the experimental results recorded.

Once some experience had been obtained in handling the Corvic in the test rig it became evident that, provided the powder did not completely defluidise and block the channel, the electrostatic charge tended to reach an equilibrium (maximum?) level, and in this condition the powder exhibited fairly consistent behaviour of the kind that would be expected of a slightly cohesive material. Most of the experimental data relating

to the behaviour of aerated Corvic and reported in this Chapter therefore apply to the powder in the charged condition, the relevant readings having been taken from trial runs begun only after the powder had been circulated continuously until it had acquired an "equilibrium" charge. Even for the Corvic in this fully charged state there was some variation in behaviour from day to day, again presumably depending upon the condition of the ambient air.

The general pattern of the dependence of the solids flow behaviour on the superficial velocity of the air supplied to the main channel became apparent during the commissioning of the rig. At high air velocities the flow was relatively fast in a shallow bed. Reducing the air velocity at first had little effect on the solids flow, but continuing reduction of the air flow soon caused the bed to thicken and to become noticeably slower flowing. If the air flow was reduced still further the thickness of the bed increased rapidly until it filled the channel and flow stopped. A more detailed quantitative investigation of the relationship between the depth of the flowing bed of Corvic and the superficial velocity of the fluidising air was subsequently carried out and is described in Section 8.5, along with the results of studies on the influence of other significant variables.

One further interesting problem that occurred during the commissioning trials concerned the discharge of the Corvic from the main storage hopper into the conveying channel. It was found at first that the maximum flowrate from the hopper was only about 1.8 kg/s, reducing to 1.4 kg/s as the Corvic became charged. This rate of discharge seemed to be well below the capacity of the rotary feeder and so some considerable time was spent in searching for the cause of the short-fall. One suggestion was that the diameter of the outlet at the lower end of the hopper discharge cone was too small so that the pockets of the rotary feeder were not filling properly. Another possible cause of trouble was the pressure difference across the rotary feeder, resulting in a reverse flow of air which could also prevent complete filling of the pockets. Since it was much easier to alter the pressure difference across the rotary valve than to increase the size of the hopper outlet, first attempts to remedy the situation involved supplying additional air to the hopper, as described in the next Section.

8.4.4 The effect of introducing additional air to the hopper discharge cone.

The provision of an air inlet pipe to the discharge cone of the main hopper has been mentioned elsewhere (see Section 8.2.3 and Plate VII). A valve on this line allowed some control of the air supply to the hopper, but there did not appear to be any need to know the actual flowrate and so no additional instrumentation was included at this stage. It was found immediately that with the hopper air valve open the discharge through the rotary valve was increased by some 70%. There did not at first seem to be anything to be gained by having the air valve fully open, and in fact there was a tendency for air to blow back through the Floveyor into the weigh-bin causing problems with the powder return. Many of the test runs were therefore made with the hopper air valve open just one turn, giving a maximum solids flowrate of about 3 kg/s (10.8 tonne/h).

At a later stage in the programme a chance occurrence of a substantially higher discharge rate from the rotary valve prompted a closer investigation of the influence of the additional air supply to the top hopper. Fig. 8.10 shows the variation of solids mass flowrate with valve opening at constant rotary valve speed and two different superficial air velocities. The solids flowrate was rather more sensitive to the air valve opening than had at first been thought, and interestingly there appeared to be an optimum amount of air for which the flowrate of Corvic was a maximum. Although the actual value of the maximum solids flow was somewhat erratic, figures of around 4 kg/s (14.4 tonne/h) could be obtained with careful adjustment of the air supply to the hopper.

For the test results plotted on Fig. 8.10 the pressure on the upstream side of the hopper air valve was held constant at 70 mm Hg. This might have been rather high if the requirement was simply to equalise the pressure across the rotary valve, but probably a certain amount of aeration of the charged Corvic in the hopper aided its discharge into the rotary valve. Excessive airflow to the hopper could tend to blow the powder away from the outlet and is probably the reason for the reduction in the solids discharge rate that is observed when the air valve is open more than about two turns.

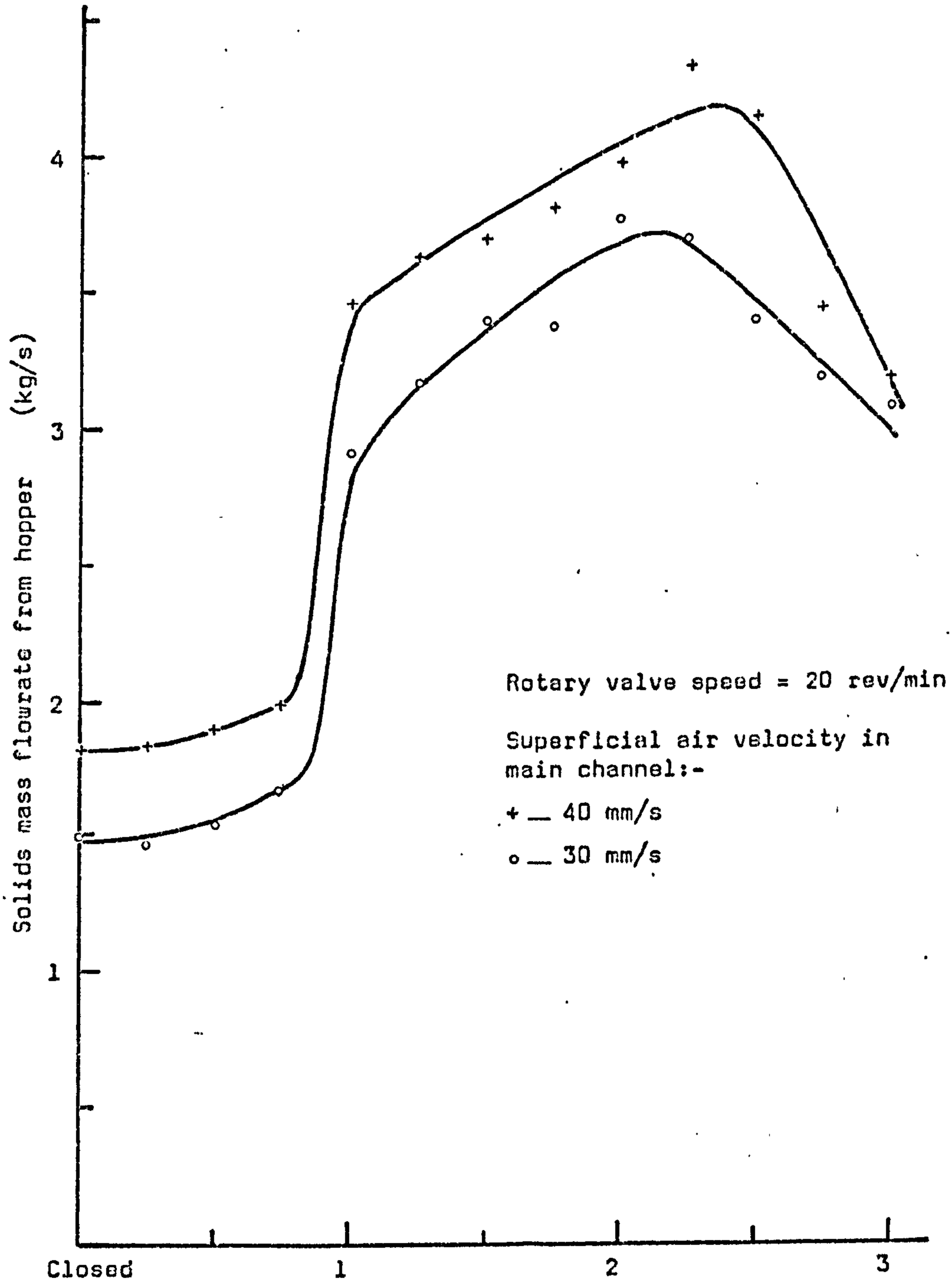

Fig. 8.10 THE DEPENDENCE OF THE MASS FLOWRATE OF CORVIC THROUGH THE ROTARY VALVE ON THE DEGREE OF OPENING OF THE HOPPER AIR SUPPLY VALVE.

The reason for the solids discharge rate being influence by the superficial air velocity in the channel is not clear, but probably results indirectly from a modification of the condition in the upstream fluidising chamber. In the tests on the feed rate of the rotary valve (described in the next Section) variation of the superficial air velocity appears to have rather less effect.

8.4.5 The variation of solids mass flowrate with rotary valve speed

A series of calibration tests was carried out in order to investigate the degree of control that could be exercised on the mass flowrate of Corvic in the channel using the rotary valve situated at the outlet of the main storage hopper. Preliminary test runs confirmed that the solids flowrate through the rotary valve was independent of the angle of inclination of the channel, provided that the valve outlet was clear, and all the subsequent runs were therefore carried out at the same channel slope of 10^{o}. It was also expected that the solids flowrate would not be influenced by the superficial air velocity in the main channel. However, some increase in the feedrate was observed with increasing air velocity and this was put down to a modification of the condition prevailing in the upstream fluidising chamber, somehow affecting the pressure drop across the rotary valve and thus the solids flow through it.

From the results of these tests a graph was plotted (Fig. 8.11) to show the variation of the flowrate of Corvic with increasing speed of rotation of the rotary valve. The minimum speed that could be obtained when feeding Corvic was 9 rev/min, and at this low speed there was considerable vibration transmitted from the valve through the rest of the rig. The maximum speed used was 25 rev/min. The solids mass flowrate at first increases linearly with valve speed and then levels off towards a maximum, the value of which depends upon the degree of opening of the supplementary air valve to the hopper. With this air valve open one turn the greatest flowrate of Corvic that could be obtained was about 3.2 kg/s. The observed flowrates were generally rather erratic, although the trend was for slightly greater flows to be recorded at the higher values of superficial air velocity in the main channel. With the hopper air valve open 2¼ turns, the amount giving the greatest discharge from the hopper, values

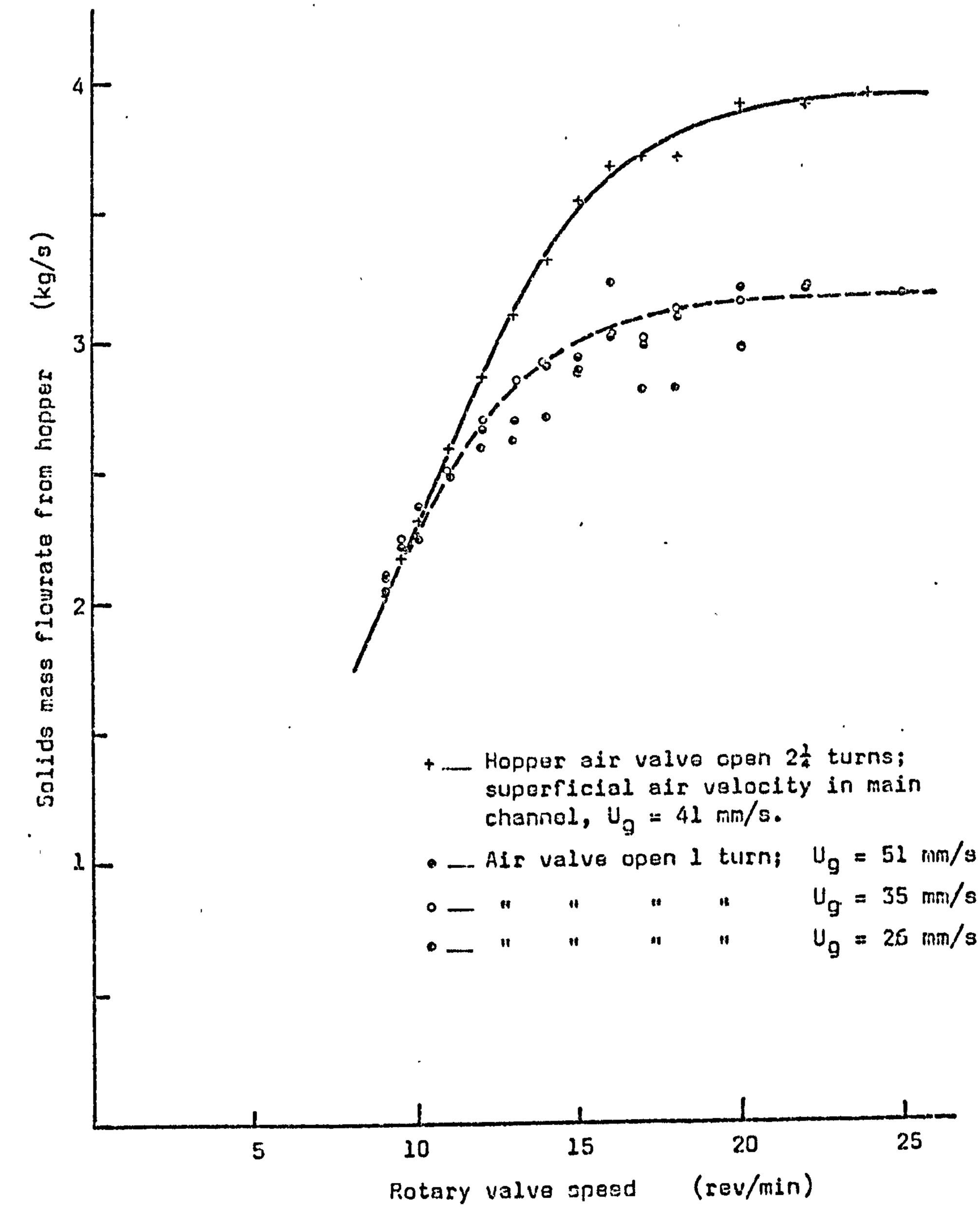

Fig. 8.11 MASS FLOWRATE OF CORVIC THROUGH ROTARY VALVE, SHOWING THE VARIATION WITH THE QUANTITY OF AIR SUPPLIED TO THE DISCHARGE CONE OF THE HOPPER.

of solids mass flowrate of up to about 4 kg/s were measured. In each case the rotary valve speed at which the maximum solids flow was first obtained was around 20 rev/min, with little further increase in flow at speeds above this figure.

Although it was not entirely clear whether the limitation of the solids flowrate to 4 kg/s was caused by the restriction at the hopper outlet or by the rotary valve, it seemed likely that the valve was approaching its full capacity and therefore no further modification to the rig was made at this stage.

8.4.6 The influence of the inlet baffle plate

Thorough investigation of the influence of the baffle plate on the flow in the main channel was difficult with the existing configuration of the test rig. It was found that over a wide range of settings of the baffle plate there was no obvious variation in the flow of the suspension in the central and downstream sections of the channel, although naturally there were changes in the surface profile of the flow in the region immediately downstream of the entrance. If the opening beneath the baffle plate was made too small the powder simply backed up in the upstream fluidising chamber until it flooded out of the overflow so that the test run had to be stopped. Thus it was decided to postpone a detailed study of the relationship between the open area under the baffle plate and the maximum flowrate of solids through it until such time as the rig could be modified to give flooded feed to the channel.

However, it was considered to be useful to look further into the variation of the surface profile of the flowing suspension with the position of the baffle plate. Profiles were recorded at baffle plate settings of 80, 60 and 30 mm for a channel slope of 10^{o} and various superficial air velocities. The profiles were obtained by attaching transparent graph paper to the Perspex walls of the channel, thus allowing coordinates of the surface of the powder to be read off directly. At this time the Corvic was continuously circulating around the rig and as a result the mass flowrate could not be directly measured. Figs. 8.12 to 8.14 illustrate to scale the surface profiles obtained at the three settings of the baffle plate.

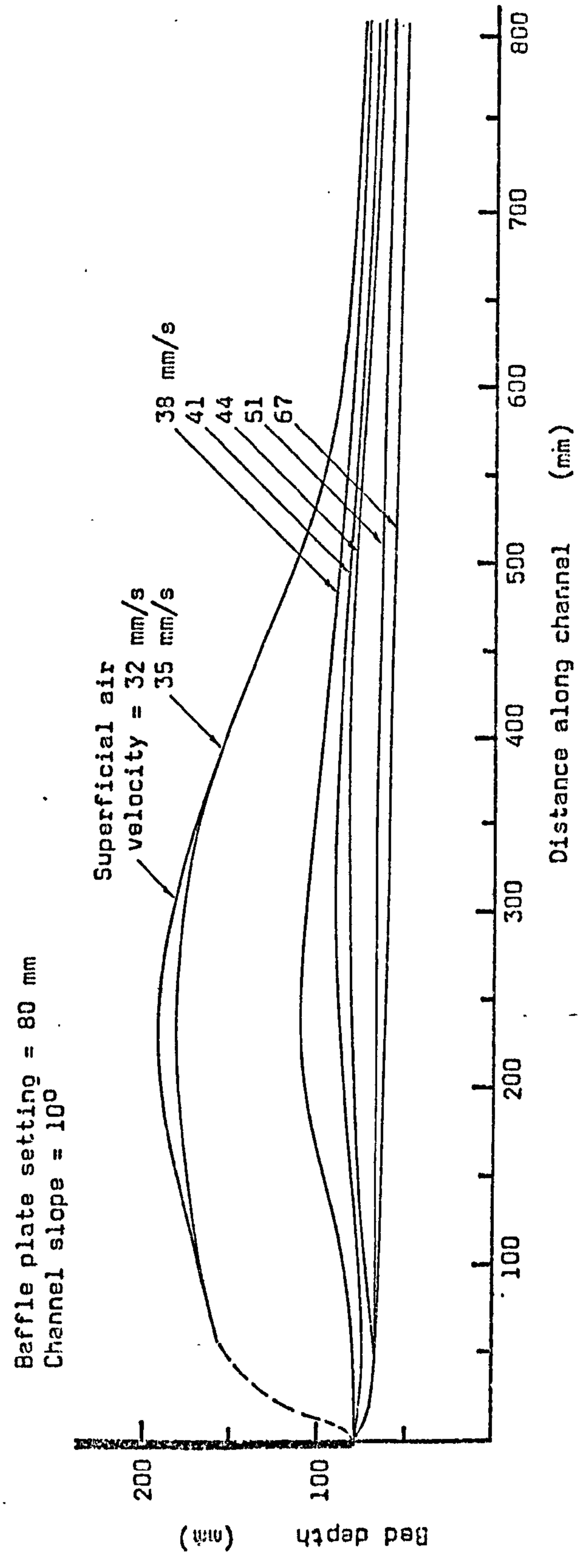

Fig. 8.12 SURFACE PROFILES OF FLOWING SUSPENSION OF CORVIC ON DOWNSTREAM SIDE OF THE BAFFLE PLATE AT VARIOUS SUPERFICIAL AIR VELOCITIES. (For 80 mm baffle plate opening.)

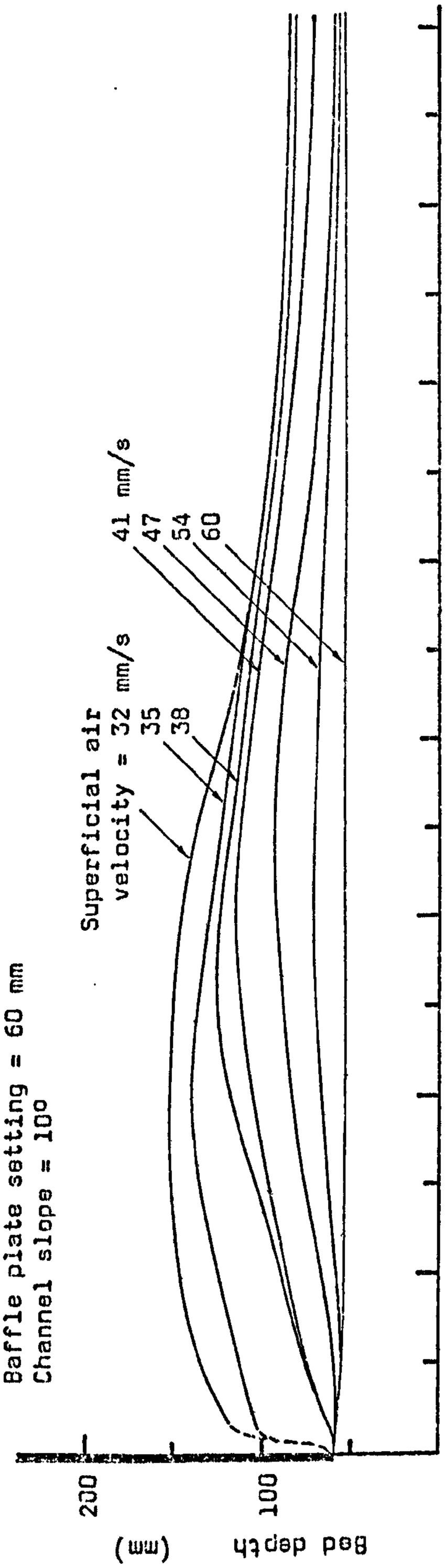

Fig. 8.13 SURFACE PROFILES OF FLOWING SUSPENSION OF CORVIC ON DOWNSTREAM SIDE OF THE BAFFLE PLATE AT VARIOUS SUPERFICIAL AIR VELOCITIES. (For 60 mm plate opening.)

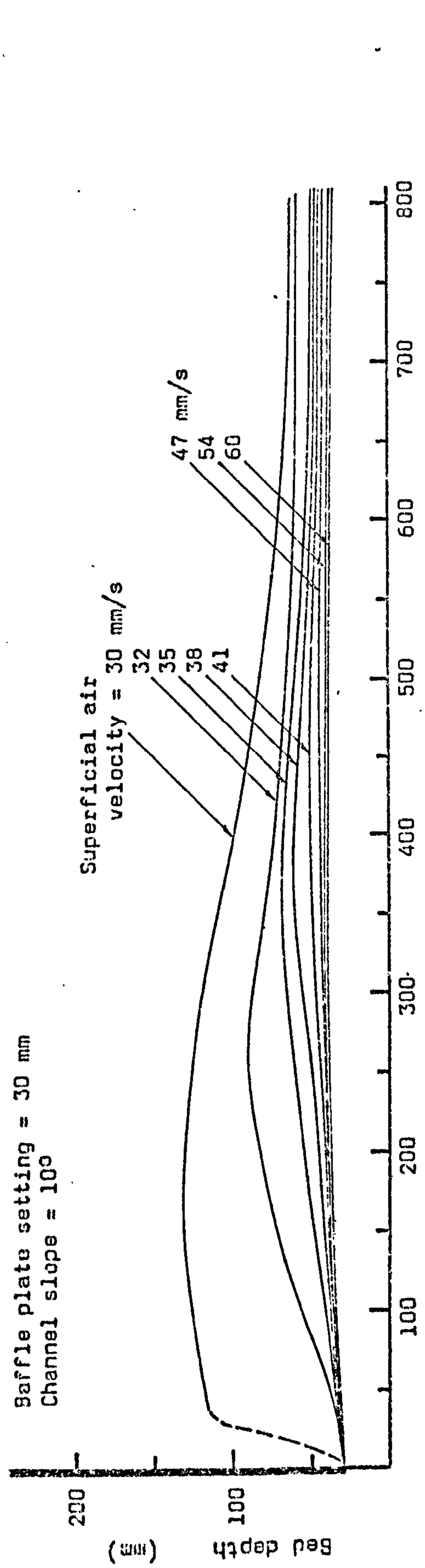

Fig. 8.14 SURFACE PROFILES OF FLOWING SUSPENSION OF CORVIC ON DOWNSTREAM SIDE OF THE BAFFLE PLATE AT VARIOUS SUPERFICIAL AIR VELOCITIES. (For 30 mm baffle plate opening.)

It is seen in each case that where the superficial air velocity is high the surface profile remains relatively flat, but as the air velocity is reduced the bed thickens and tends to back up against the baffle plate. In general it appears that where the depth of the uniformly flowing bed is less than the baffle plate opening the settling length remains short, but for the thicker beds the standing wave set up on the downstream side of the baffle plate causes the settling length to extend to a distance of around 0.7 m. In order to see more clearly the effect of the baffle plate setting Fig. 8.15 shows three profiles recorded at the same superficial air velocity of 35 mm/s. It is evident that at the wider baffle plate settings (60 and 80 mm) there is little difference in the mass flowrate since the final bed depth is the same, but when the baffle plate is lowered to 30 mm the mass flowrate is significantly reduced. Much the same pattern of behaviour, but with a less pronounced standing wave, occurs at higher superficial air velocities.

For the majority of the test runs carried out in the investigation described in Section 8.5 the baffle plate was set fairly high (80 mm opening) which seemed to provide the best compromise between minimizing the wave motion induced by the rotary valve and offering the least resistance to the flow of Corvic from the upstream chamber.

8.4.7 The effect of pre-conditioning the flowing powder

In at least one previous investigation (Ref. M14) pre-conditioning of the particulate solid was recognised as having a possible influence on its flow behaviour. It is reasonable to suppose that with solids capable of significant air retention the amount of air entering the powder, either in the upstream fluidising chamber or in the main hopper, could have a noticeable effect on the quantity of fluidising air required in the conveying channel to achieve the same flow behaviour. However, as implied by Muskett et al (Ref. M14), where there is a variation in the air supplied to a separate upstream fluidising chamber, it may be difficult to distinguish between the effect of varying the degree of initial fluidisation and the effect of pressurising the fluidised powder in the upstream chamber, thus tending to force it under the baffle plate.

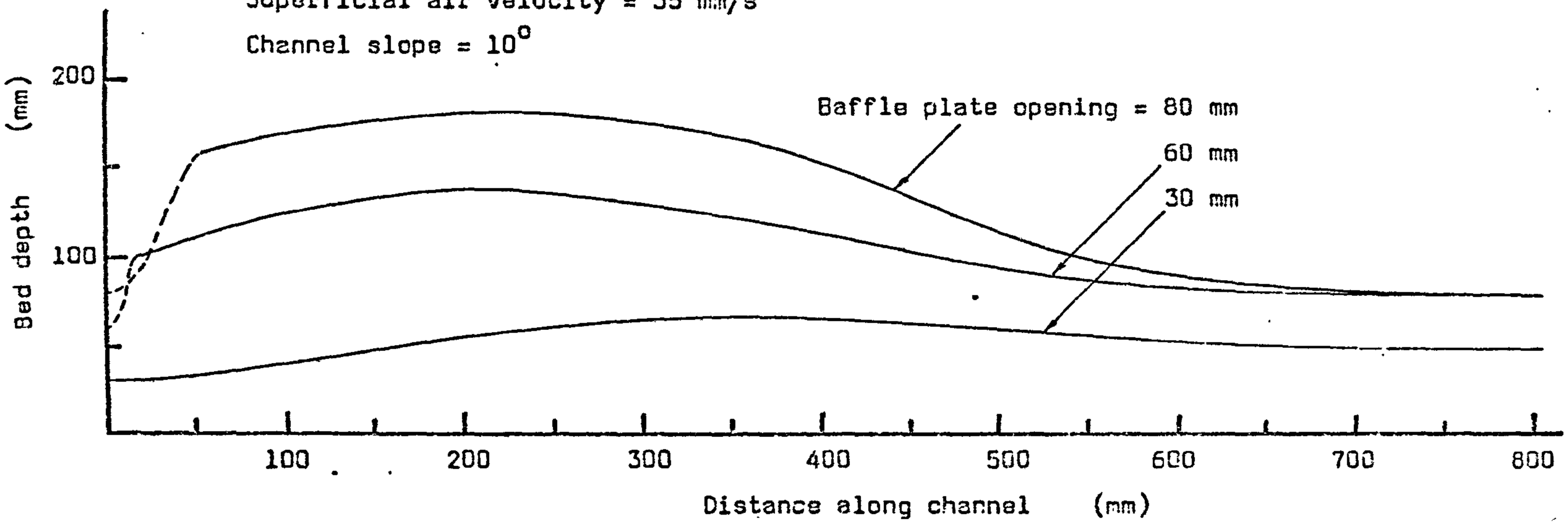

Fig. 8.15 SURFACE PROFILES OF FLOWING SUSPENSION OF CORVIC ON DOWNSTREAM SIDE OF THE BAFFLE PLATE SHOWING THE EFFECT OF VARYING THE BAFFLE PLATE OPENING AT CONSTANT SUPERFICIAL AIR VELOCITY.

With the test rig in its present form much the same difficulties are encountered in attempting to ascertain the effect of initial fluidisation of the Corvic as in determining the influence of the baffle plate. Thus, if the superficial velocity of the air in the upstream chamber was too low the powder filled up the chamber and flooded from the overflow so that the run had to be stopped, whereas at higher air velocities there was no consistent effect that could be observed, other than the change in amplitude of the surface waves on the flowing suspension that has already been mentioned. Any variation in the solids mass flowrate that occurred was in any case more likely to have been as a result of the change in pressure across the rotary valve than of the change in the degree of fluidisation (see Section 8.4.3).

Some thought was given to the most satisfactory method of dealing with the air supply to the upstream fluidising chamber during the investigation of powder flow in the main conveying channel. Obvious possibilities were either to keep it constant or to allow it to vary in some constant relationship with the air supply to the main channel. A rather high superficial air velocity in the upstream chamber appeared to give the best results with Corvic and it was therefore decided to maintain a constant value of around 70 to 75 mm/s for most of the test runs.

8.4.8 The velocity of the flowing suspension and the formation of standing waves

The measurement of velocity in a flowing bed of aerated powder has been discussed in Section 3.2.9 where it was pointed out that the accurate determination of velocity profiles from point measurements is extremely difficult, requiring specialised instrumentation and calibration procedures. However, some idea of the average velocity of a flowing suspension can be obtained by the simple technique of timing a float placed on the surface; a method used in several previous investigations (Refs. B16, K3, M4).

From visual observation of the Corvic (in its charged condition) flowing along the inclined conveying channel it appears that the velocity is virtually uniform across the width of the channel. Peaks and craggy ridges formed in the surface of the flowing powder bed can be visually

"followed" from the inlet end of the channel to the outlet, suggesting also that there is little air actually leaving the suspension through the top surface. This behaviour can be witnessed at all flow conditions but is especially evident when the bed of powder is deep and slow-moving (that is, when the channel slope is small or the superficial air velocity is low).

Visual observation of variations in the powder velocity through the depth of the bed was, of course, less easy because the flow had to be viewed through the transparent Perspex wall of the channel. The tendency of the Corvic to become electrostatically charged meant that particles of powder adhered to the channel walls so that there was always a thin coating over the inside surfaces of the channel. Whilst this coating did not entirely obstruct vision of the powder in the channel (for instance, it was still possible to see the position and condition of the top surface of the flowing bed) it did make it difficult to interpret observations of the movement of particles below the surface. It could clearly be seen that the layer of particles adjacent to the channel wall moved much more slowly than the bulk of the bed, and also that there was a velocity gradient in this layer from the surface of the bed down to the bottom of the channel close to the distributor. In fact, powder particles in the corners between the distributor and the channel walls often seemed to be almost stationary. However, beyond this layer of particles on the channel walls, the bulk of the bed seemed to move almost as a solid mass sliding (on a layer of air?) along the channel. Zig-zag cracks could usually be seen extending upwards through the flowing bed from the region of the distributor towards the surface, but it could not be said whether these cracks were confined to the edges of the flow or continued right across the bed.

In the present programme time was not available to tackle the formidable task of developing a probe capable of measuring point velocities in a flowing bed of Corvic. However, in order to determine the order of magnitude of the solids flow velocity in the channel a float was used, as mentioned in the opening paragraph of this Section. The float was about 30 mm in diameter and was timed over a 4 m length of the channel. Velocity measurements were not made during batchwise operation of the rig and consequently it was not possible to obtain corresponding measurements of

the solids mass flowrate. However, with the channel slope set at 10^{o}, and at two different settings of the upstream baffle plate (30 mm and 60 mm) a graph was plotted of the float velocity against the superficial air velocity in the channel (Fig. 8.16). Measured velocities were in the range 0.5 to 1.4 m/s which seemed to agree with observations reported by other investigators (Refs. K3, M9, P9, S8, S13; and see Section 3.2.9). The trend was for the solids flow velocity to decrease gradually with decreasing superficial air velocity, then falling sharply as the airflow approached the minimum necessary for satisfactory conveying. It was at first rather surprising that the solids velocity should be greater for the smaller baffle plate opening. However, the average depth of the flowing bed was much less with the smaller baffle plate opening and it was probable that the additional drag at the side walls would have had a significant influence.

The occurrence of standing waves in air-assisted gravity conveyors is a phenomenon that has generated some interest in other studies. Harris (Ref. H2) for example, reports a 50 mm high standing wave occurring in his conveying channel just downstream of the hopper outlet, and in the later work of McGuigan (Ref. M4) and Pugh (Ref. P9), also with sand, the authors discuss the differences between standing waves in fluidised solids and in liquids. With fluidised particulate solids changes in the quality of fluidisation, and therefore in the bulk density, occur across a standing wave and the resistance of the distributor may also influence the situation. Thus, as McGuigan points out, a standing wave may be less likely to occur when a high-resistance distributor is in use since the thickening of the bed downstream of the standing wave is less likely to affect the airflow on the upstream side of it.

During the present investigation standing waves were observed to occur in the conveying channel on many occasions. The most frequent situations in which they occurred were at the outlet end of the channel as a result of an obstruction to the flow at this point (the case reported by McGuigan and by Pugh) and at the inlet end immediately downstream of the baffle plate when the opening was quite small. Under some conditions it was found that a standing wave could be "triggered" in a steadily flowing bed of powder by temporarily inserting an obstruction into the flow. The wave

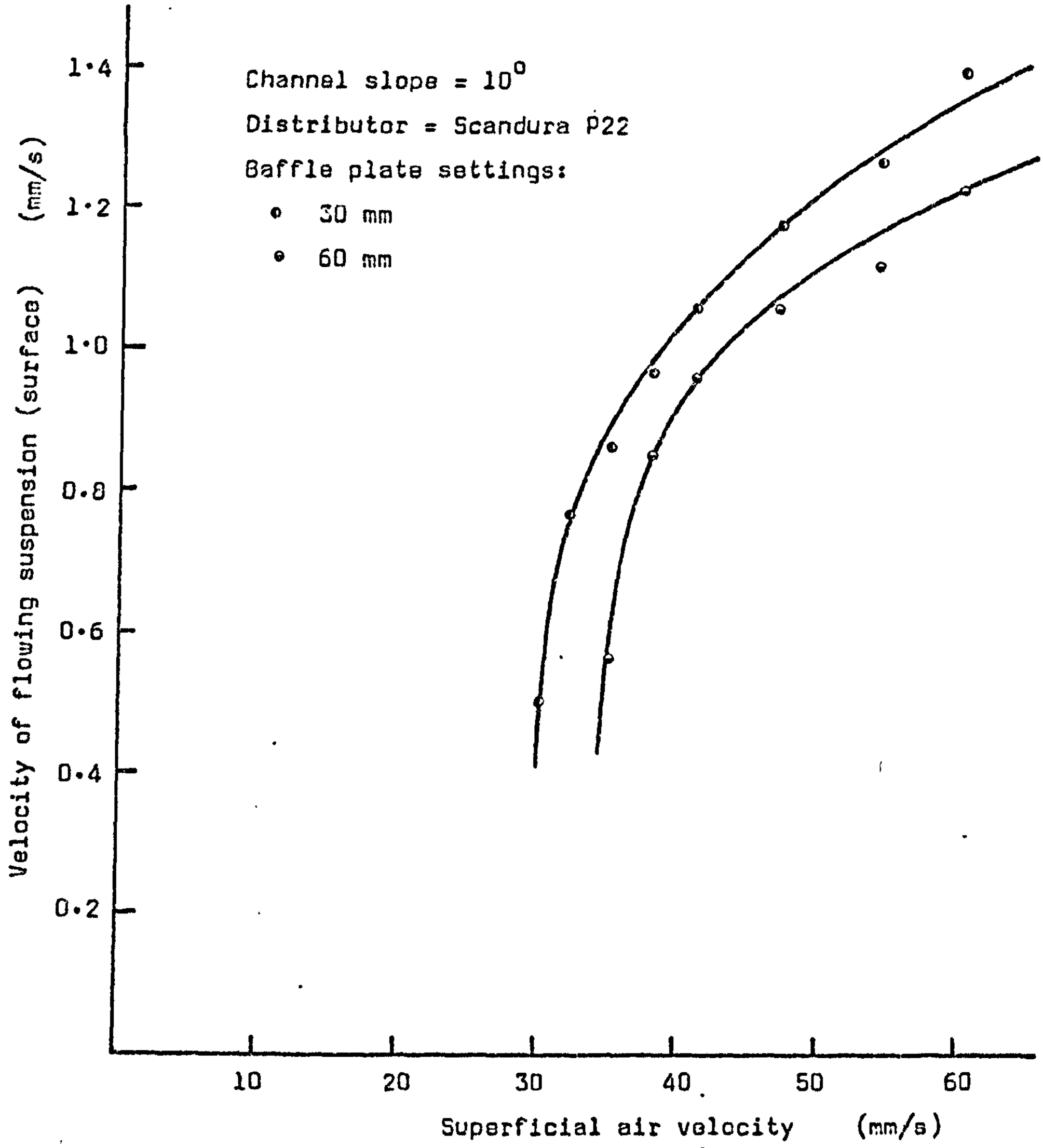

Fig. 8.16 PLOT OF THE VELOCITY OF A FLOAT ON THE SURFACE OF THE FLOWING BED OF CORVIC AGAINST SUPERFICIAL AIR VELOCITY AT TWO DIFFERENT BAFFLE PLATE OPENINGS.

would often persist after the obstruction was removed and sometimes the depth of the bed on the downstream side of the wave increased to such an extent that it completely blocked the channel causing the flow of powder to cease.

The fact that standing waves can occur in a flowing suspension of powder suggests that two distinct regimes of flow may exist corresponding to "rapid" and "tranquil" flow in liquids. In the present investigation there was evidence of such behaviour in the sudden increases of bed depth, coupled with slowing of the solids flow velocity, that tended to occur when either the channel slope was decreased or the airflow was reduced. In his work with sand Pugh (Ref. P9) reported observing the transition from one type of flow to another, which appeared as a sudden decrease in the depth of the flowing bed from one stable level to a lower stable level. An improvement in the quality of the flow was said to be "visually discernable". Again, in the present work a change in the quality of fluidisation of the flowing bed was also seen, albeit a gradual one, as the Corvic became electrostatically charged, and it is interesting to speculate on the manner in which the nature of the powder is related to the character of the flow.

8.4.9 Conclusions

During the extended commissioning trial of the channel rig a number of different aspects of the handling of Corvic were investigated. The operation of the rig generally presented no problems, the only major area of difficulty being the pronounced tendency of the Corvic to acquire an electrostatic charge which caused its behhaviour in the channel to vary noticeably from one day to the next. This meant that the procedure to be followed in test series investigating the relationships amongst the significant system variables would have to be rather carefully planned in order to eliminate, as far as possible, systematic errors resulting from the gradual change of humidity of the fluidising air and of the ambient air.

Since the purpose of this investigation in the channel rig was to observe the flow behaviour of a representative powder which could be expected to exhibit characteristics different from those of sand, it did not matter particularly what powder was selected. The fact that the Corvic used in

the investigation carried an electrostatic charge would therefore not be of any consequence provided that fluctuations in its behaviour when in the charged condition were not sufficient to make the test results worthless. Information on the flow behaviour of the charged Corvic could be taken to be representative of a slightly cohesive powder just as information on the behaviour of sand in this rig or a similar one could be regarded as typical of free-flowing powders. Once the decision had been taken to concentrate the investigation on Corvic in a charged condition instead of attempting to eliminate the influence of the electrostatic phenomenon, the normal procedure before each series of tests was to allow the powder to circulate continuously for a time to "charge it up" to an equilibrium condition, after which there would be little further change in its nature.

The use of the rotary valve to control the flow of powder to the inlet end of the channel seemed to be quite satisfactory, the only disadvantages in restricting the flow at this point being that it was not possible to examine fully the influence of the inlet baffle plate and the effect of pre-conditioning the powder in the upstream fluidising chamber. Whilst it was in some respects disappointing that the solids flowrate could not be controlled at less than about 1.5 kg/s (because the rotary valve would not run at less than 8 or 9 rev/min) this was not seen as a great disadvantage since the low flowrates would not be really relevant to an industrial situation. At flowrates of charged Corvic from 1.5 kg/s up to the maximum of about 4 kg/s the rotary valve gave quite consistent control as indicated by the "calibration curve" of Fig. 8.11.

The baffle plate at the inlet end of the conveying channel was not used in the current investigation as a means of controlling the solids flow since the rotary valve performed this duty adequately. Indeed, attempting to operate the rig with the baffle plate too far closed simply resulted in powder spilling from the overflow at the hopper outlet. Much the same comment applied to the use of the separate air supply to the upstream fluidising chamber. Both of these alternative methods of solids flow control will be examined more thoroughly when the rig is modified to flooded feed by replacing the rotary valve with an iris diaphragm valve. In an industrial situation there would seem to be no purpose in duplicating the method of controlling the solids flowrate and either the rotary valve or the baffle plate should give satisfactory results.

Measurements of solids flow velocity by the crude but convenient method of timing a float along the channel gave a range of velocity from 0.5 to 1.4 m/s. As mentioned previously, this was of the same order as values determined by other investigators, although considerably higher figures have been quoted in the literature (Refs. C3, N3, W2 and see Section 3.2.9). It seems likely that free-flowing powders could flow at somewhat higher velocities than the rather cohesive Corvic.

The principle series of tests on the flow of aerated Corvic, in which are investigated the relationships amongst the solids mass flowrate, the slope of the conveying channel, the superficial velocity of air supplied to the channel and the depth of the flowing bed, is described in the next Section.

8.5 THE FLOW BEHAVIOUR OF AERATED P.V.C. POWDER ('CORVIC')

8.5.1 Introduction

As stated elsewhere, one of the chief objectives of the current programme of work is to establish the form of the relationship amongst the significant variables governing the flow of an aerated bulk particulate solid in an inclined channel. The majority of similar work carried out by other investigators has been concerned with the flow of fluidised sand and it was considered likely to be beneficial to the general study of the flow of aerated powders to obtain data on a different type of material. From the several powders considered, the 120 μm p.v.c. powder (supplied by I.C.I. Ltd. under the trade name of 'Corvic') was selected for the investigation and various preliminary tests on its fluidisation characteristics and on its flow behaviour in an inclined channel were carried out as described in Sections 7.6 and 8.4. A discussion of the problems created by the electrostatic charging of the Corvic as it circulated around the rig has been already undertaken (Section 8.4.3) and will not be repeated here. Suffice it to say that care was taken before each of the tests to ensure that the powder was, as far as could be ascertained, fully charged. In this state the Corvic exhibited characteristics typical of a slightly cohesive material and information on its flow behaviour in the air-gravity conveyor should therefore provide a useful and interesting comparison with previously reported data on the flow of sand.

After the commissioning trials on the channel rig the porous base was replaced with a new piece of Vyon 'D'. It was clear that very considerable deterioration of the original distributor had occurred as a result of the blinding of the pores, although it was not certain whether it was the underside of the Vyon that had become choked with air-borne dust or the top side affected by the finer particles of Corvic. Once a substantial quantity of test data had been collected the distributor was again removed, this time being replaced by a length of Scandura P22 woven polyester belting. The test procedure was then repeated in order to obtain a second set of data so that the performance of the two different kinds of distributor could be compared.

All the test readings were taken while the rig was on batchwise operation, following the procedure detailed in Section 3.4.2. On most of the test runs 164 kg of Corvic (corresponding to a meter scale reading of 7.0 on Range 4) was discharged from the top hopper through the channel to the weigh-bin, taking from about 40 to 100 seconds depending upon the setting of the rotary valve speed control. Each set of test data taken during a "run" consisted of:-

i) the slope of the conveying channel,
ii) the superficial velocity of the fluidising air supplied to the main channel (determined from the reading of the appropriate rotameter),
iii) the mass flowrate of powder (determined from the time taken for a known quantity of powder to be collected in the weigh-bin),
iv) the average depth of the flowing bed (from measurements of bed depth at three stations along the channel),

and supplementary data that was recorded included the superficial air velocity in the upstream fluidising chamber, the baffle plate setting, the pressure, temperature and relative humidity of the fluidising air in the main plenum chamber and the speed of rotation of the rotary valve.

In most cases, where the effect of a single variable, such as channel slope, superficial air velocity or solids mass flowrate was being

investigated, different values of that variable were taken in random order so that systematic errors arising from gradual changes in electrostatic charge should be minimized. The results of these tests are presented in graphical form as plots of the average depth of the flowing bed (the dependent variable) against the mass flowrate of the Corvic and against the superficial velocity of the fluidising air. From these graphs additional useful information, especially concerning the relationship between the bed depth and the slope of the conveying channel, can be obtained by cross-plotting as described in Section 8.5.3.

8.5.2 Relationships between bed depth and solids mass flowrate

The first tests investigating the effect of varying the solids mass flowrate, whilst the channel slope and the superficial velocity of the fluidising air were held constant, were carried out at a slope of 4^{o} and at two different air velocities, 44 and 63 mm/s. At this rather shallow slope the air velocity of 44 mm/s was barely sufficient and the Corvic tended to flow somewhat sluggishly in a deep bed of around 110 to 130 mm. Nevertheless, in this case and at the higher air velocity there was a clear trend of increasing bed depth with increasing solids mass flowrate (Fig. 8.17) but, although the relationship was approximately linear, the bed depth was not directly proportional to the solids flowrate. If it can be supposed that the bulk density depends only upon the superficial velocity of the fluidising air we must conclude that the average velocity of the flowing suspension is a function of the solids mass flowrate and therefore of the bed depth. Thus, at a constant channel slope and air supply rate, an increase in the feed rate of powder to the channel results in a thickening of the flowing bed and a speeding up of its average flow velocity.

Fig. 8.18 illustrates the results of an extensive series of tests carried out at the higher of the two superficial air velocities mentioned above. At this constant air velocity of 63 mm/s test runs were made with varying solids flowrates at constant channel slopes from 3^{o} to 9^{o}. The effect of varying the mass flowrate of Corvic is seen to be much the same as that shown on Fig. 8.17, the relationship being approximately linear but not a direct proportionality. It is of interest to note that the linear plots

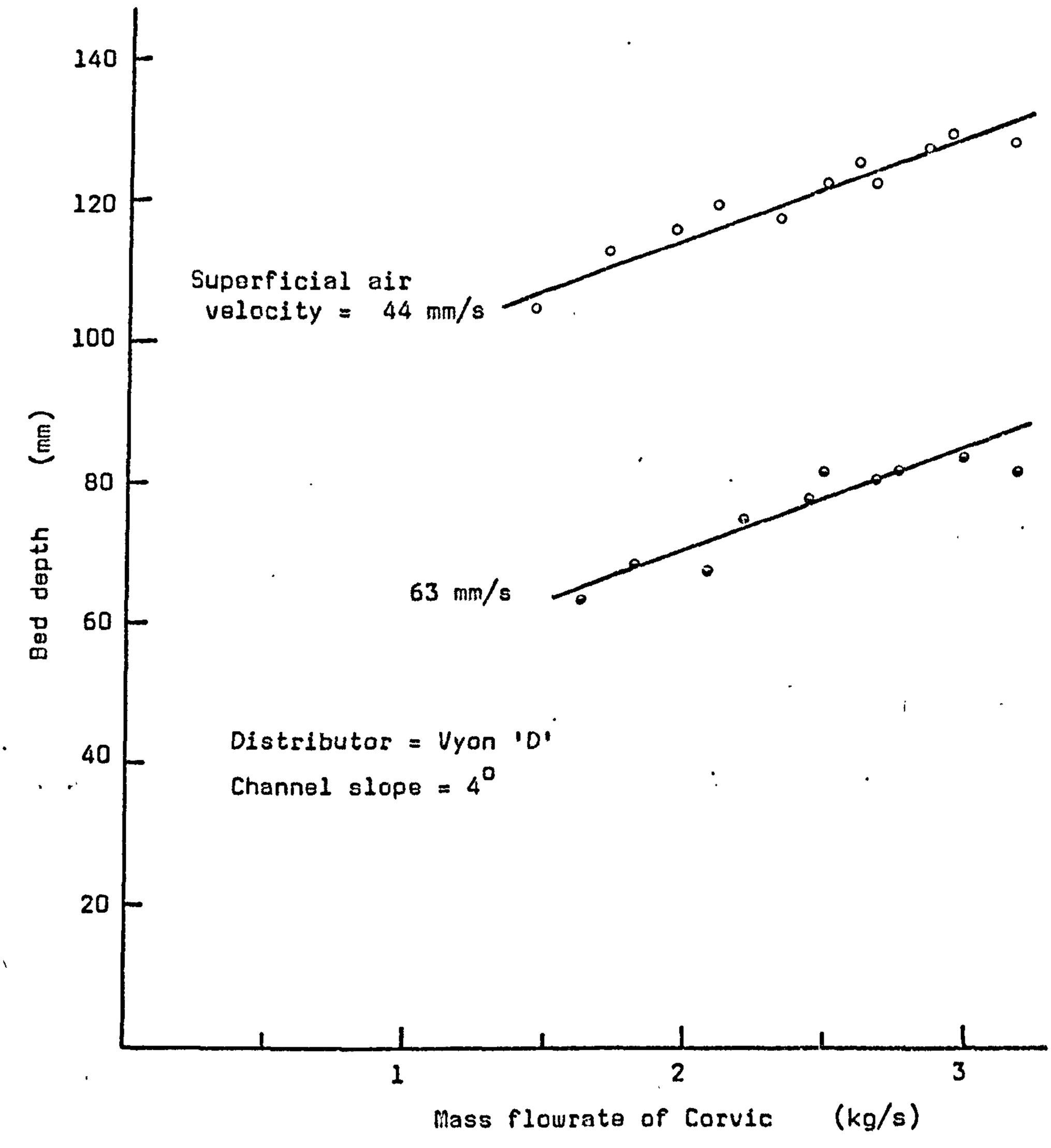

Fig. 8.17 THE VARIATION OF BED DEPTH WITH THE MASS FLOWRATE OF CORVIC AT CONSTANT CHANNEL SLOPE AND SUPERFICIAL AIR VELOCITY (VYON DISTRIBUTOR).

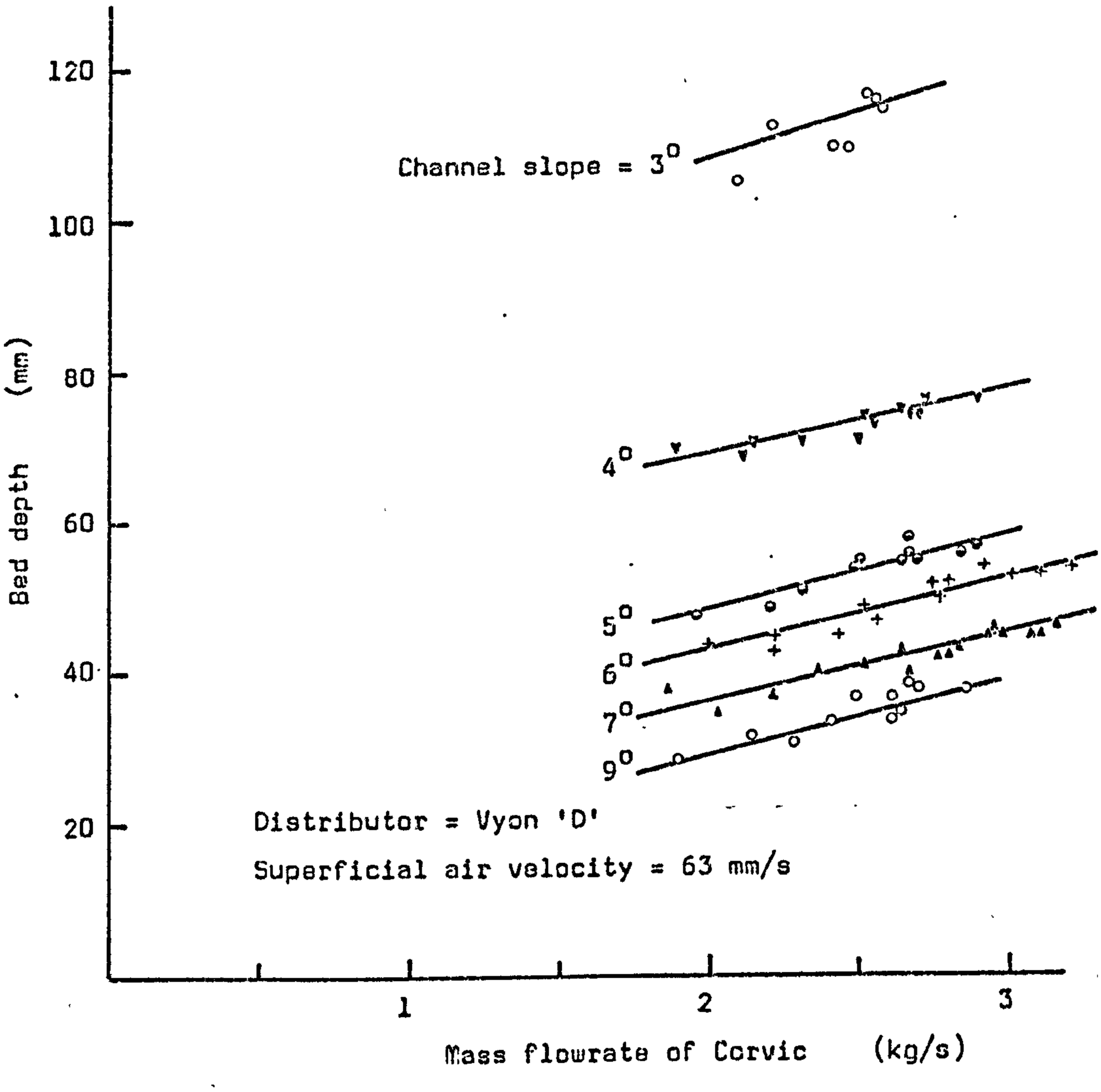

Fig. 8.18 THE VARIATION OF BED DEPTH WITH THE MASS FLOWRATE OF CORVIC AT CONSTANT CHANNEL SLOPE AND SUPERFICIAL AIR VELOCITY (VYON DISTRIBUTOR).

corresponding to the different channel slopes appear to be parallel and also become closer together at the steeper slopes. This would suggest that at these steeper slopes the bed depth is more nearly proportional to the solids mass flowrate; that is, the average velocity of the flowing suspension approaches a maximum as the channel slope is increased to around 10^{o}. The very pronounced thickening of the flowing bed as the channel slope is decreased is clearly evident from Fig. 8.18 for the tests at 3^{o} and 4^{o} slopes. At the 3^{o} slope the powder flow became extremely sluggish and at the higher solids feedrates there was a tendency for the flow to cease altogether as the channel became choked.

Generally similar results were obtained when investigating the effect of increasing solids mass flowrate with Scandura P22 as the distributor. Fig. 8.19 shows the test results for a coustant channel slope of 10^{o} and three different superficial air velocities and Fig. 8.20 shows results in a form corresponding to Fig. 8.18 for the Vyon 'D' distributor. The general pattern of the lines of Fig. 8.20 is similar to that of Fig. 8.18, except that they show an upward shift which is slight at the steeper channel slopes but becomes more marked at the slopes of 4^{o} and 5^{o}. In fact, at a channel slope of 3^{o} no results could be obtained as the powder would not flow along the channel but merely flooded from the overflow at the inlet end.

Three factors could contribute to the tendency for the depth of the flowing bed to be greater during the test runs on the Scandura P22 distributor than for those on Vyon 'D'. Firstly there is of course the influence of the distributor itself. The Vyon distributor offers a much greater resistance to airflow and therefore it might be expected that the quality of fluidisation produced would be better (although it must be stated that there was little hard evidence of any such difference in the tests on "stationary" fluidised powders reported in Chapter 7). Also the upper surface of the Scandura P22 was very rough in comparison with Vyon 'D' and therefore increased drag on the powder flowing over it could be expected to have the effect of slowing and thickening the bed. The two additional contributing factors are the slightly lower superficial air velocity in the tests with Scandura, and possible changes in the Corvic as a result of its continual re-circulation around the test rig. Each of these effects would tend to

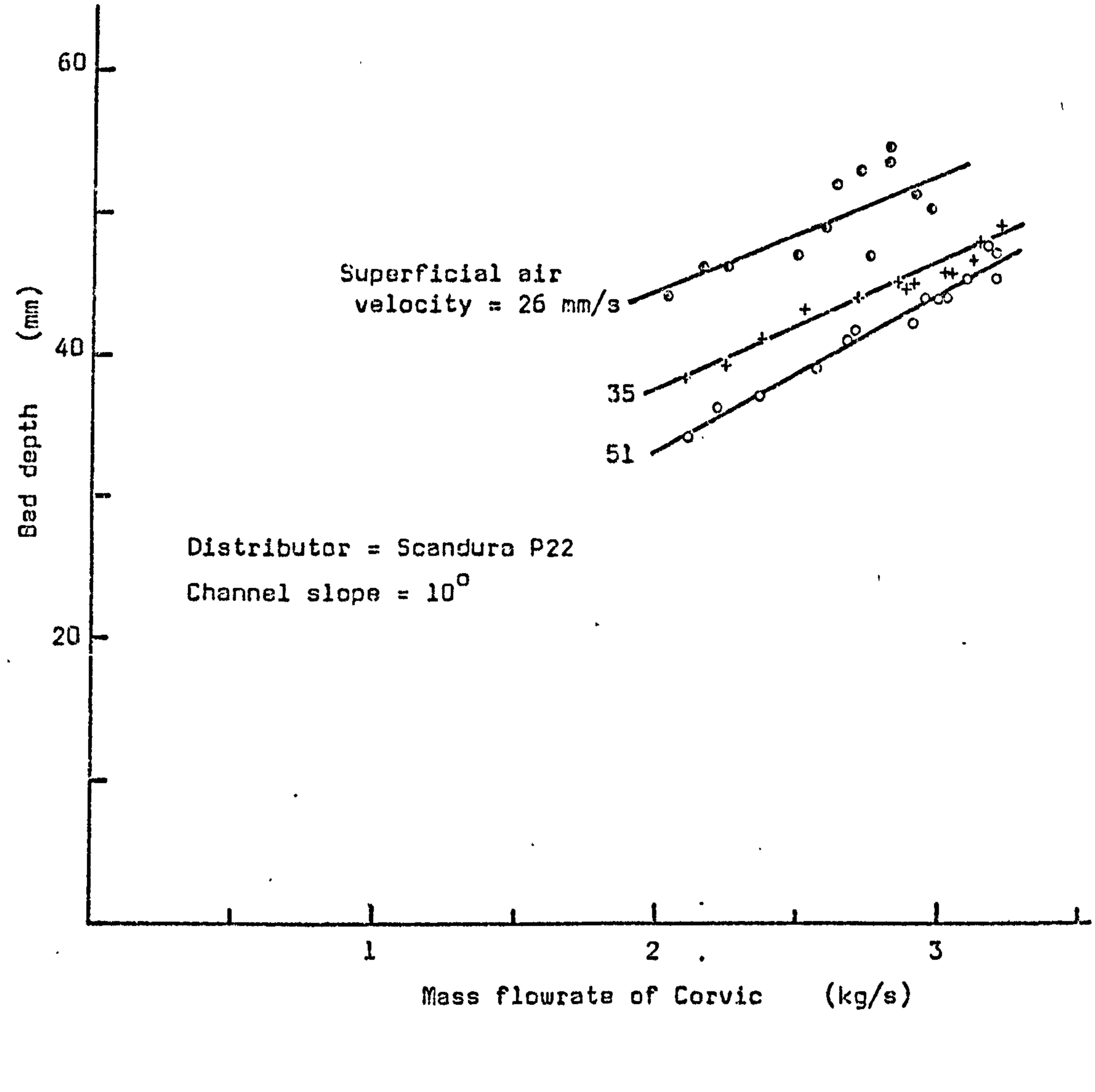

Fig. 8.19 THE VARIATION OF BED DEPTH WITH THE MASS FLOWRATE OF CORVIC AT CONSTANT CHANNEL SLOPE AND SUPERFICIAL AIR VELOCITY (SCANDURA DISTRIBUTOR).

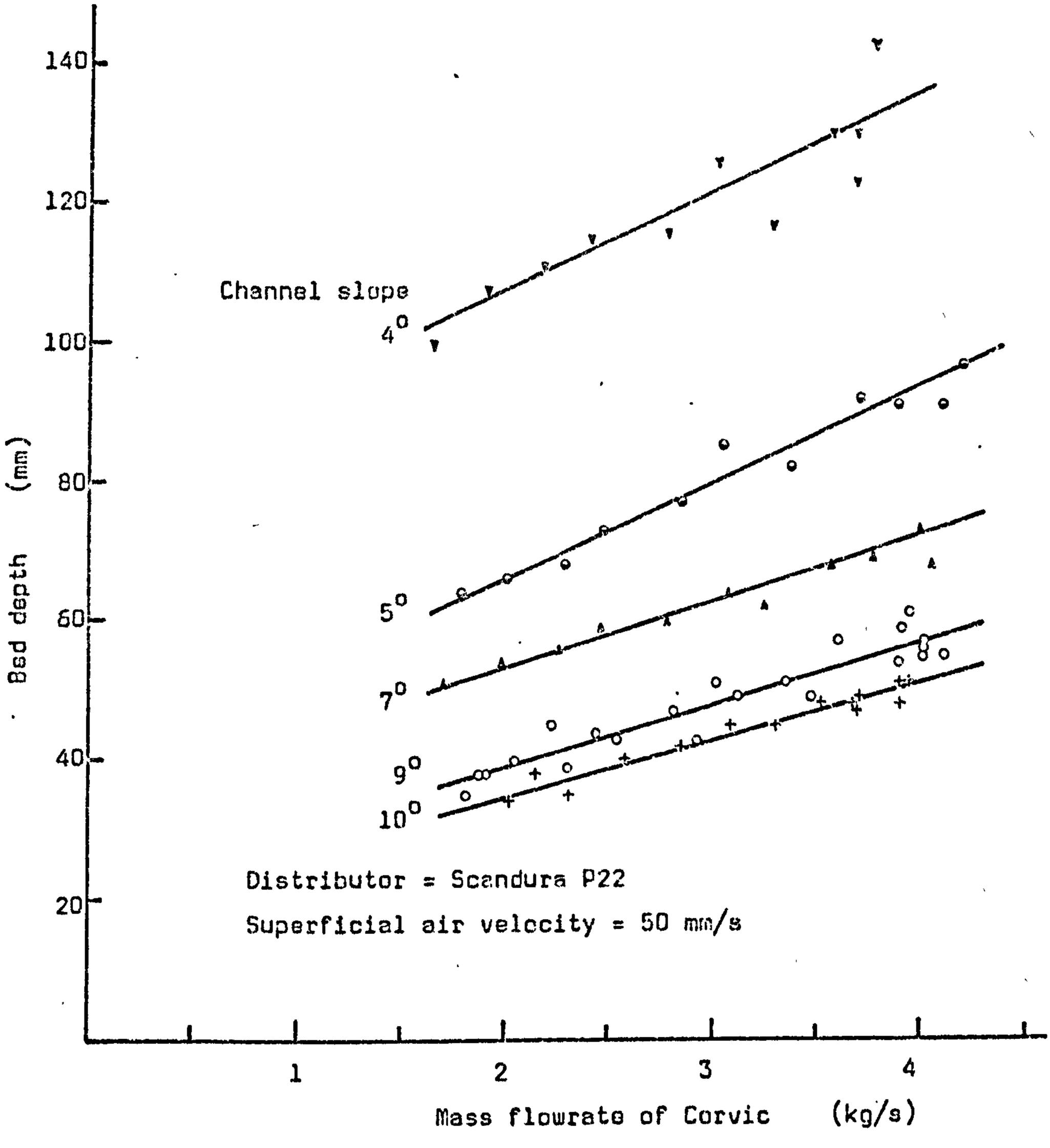

Fig. 8.20 THE VARIATION OF BED DEPTH WITH MASS FLOWRATE OF CORVIC AT CONSTANT CHANNEL SLOPE AND SUPERFICIAL AIR VELOCITY (SCANDURA DISTRIBUTOR).

reduce the quality of fluidisation which would in turn cause a thickening of the flowing bed. However, later tests suggest that the change in the flow behaviour between 50 mm/s and 63 mm/s superficial air velocity is not great enough to account for the difference in Figs. 8.18 and 8.20. Also, although examination under a microscope shows the presence of some fine dust in the Corvic, it is not thought likely that this small variation in the nature of the powder could produce a significant change in its flow behaviour.

8.5.3 Relationships between bed depth and channel inclination

Some indication of the influence of the slope of the channel is given by Figs. 8.18 and 8.20 from which it can be seen that a reduction in slope from greater than about 10^{o} at first has little effect, but then causes a thickening of the bed which becomes very pronounced as the channel slope falls below about 5^{o}. This relationship is illustrated more clearly by cross-plotting to yield a graph of the average depth of the flowing bed against the slope of the channel. Fig. 8.21 shows the resulting plot for the channel fitted with the Vyon 'D' distributor and Fig. 8.22 is a similar plot for the channel with Scandura P22 as its base. The shapes of the two sets of curves are similar, showing the drastic thickening of the flowing bed that occurs if the channel slope is too shallow. However, it is noticeable that the gradient of the curves is generally steeper for the channel with the Scandura base showing that the flow behaviour of the Corvic in that situation was more sensitive to changes in the slope of the channel. As mentioned previously, the slightly lower superficial air velocity and changes in the nature of the Corvic could be contributory factors but seem unlikely to be the major cause of this difference in the flow behaviour.

The familiar "knee" type of curve, which is admittedly more evident in Fig. 8.21 than in Fig. 8.22, suggests that there may be an "optimum" slope at which the channel should be operated when conveying charged Corvic or similar materials. Operating at a slope greater than the optimum value (which in this case could be said to be around 6^{o} to 7^{o}) gives little practical advantage and simply results in a greater loss of elevation than is necessary. However, if the channel is operated at a lower slope than

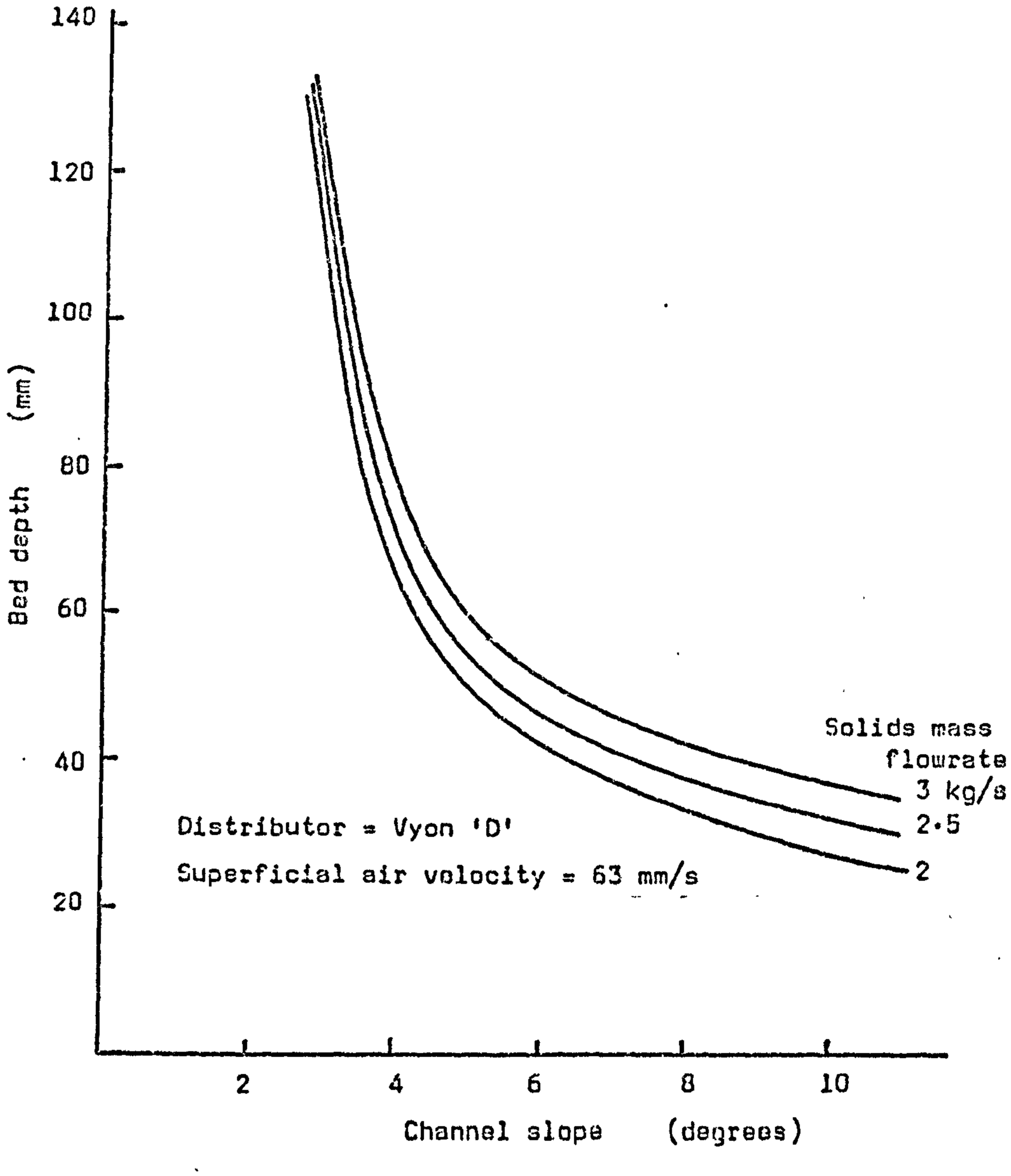

Fig. 8.21 DATA FROM FIG. 8.18 RE-PLOTTED TO SHOW THE VARIATION OF BED DEPTH WITH CHANNEL SLOPE AT CONSTANT SUPERFICIAL AIR VELOCITY AND SOLIDS MASS FLOWRATE (VYON DISTRIBUTOR).

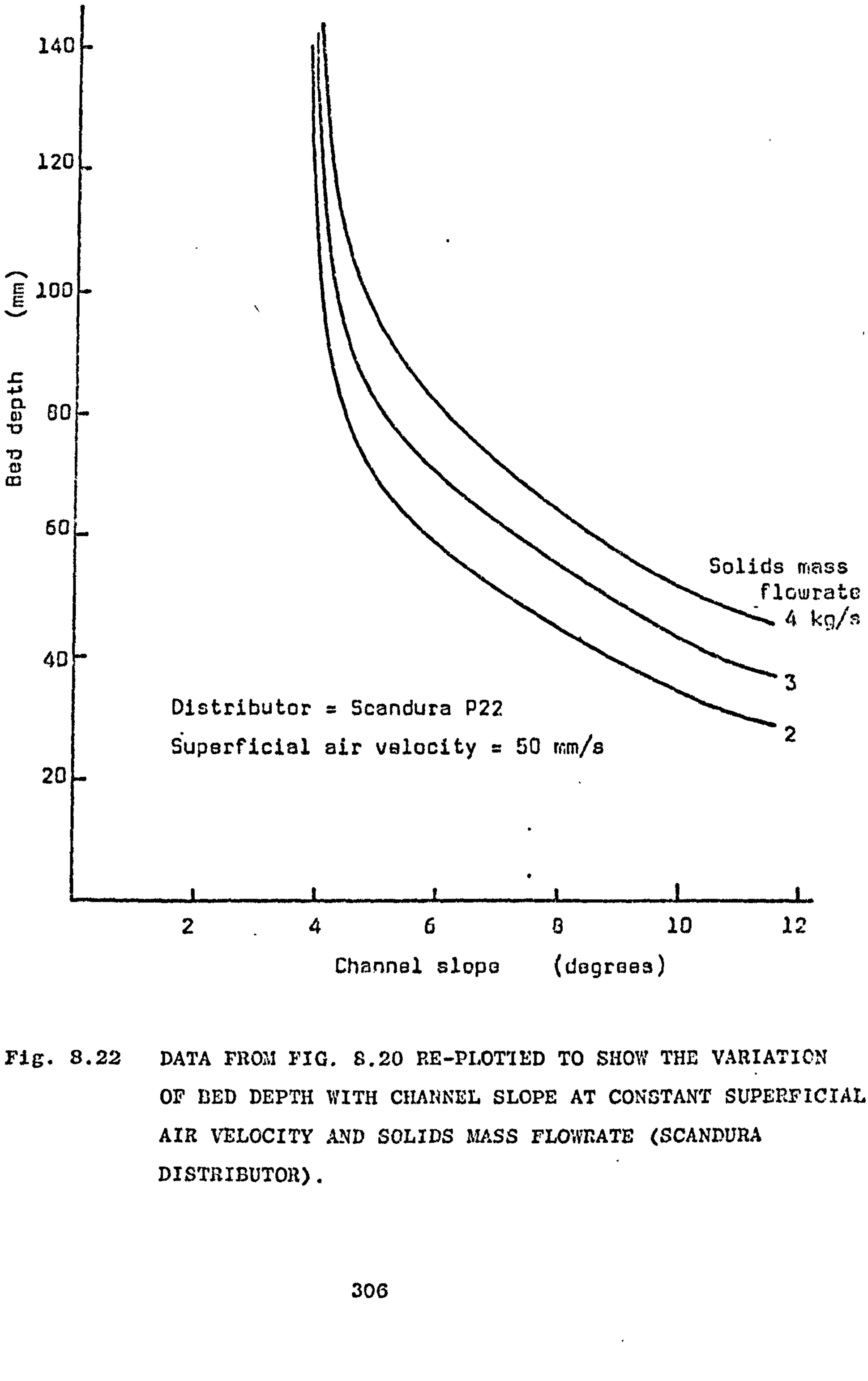

Fig. 8.22 DATA FROM FIG. 8.20 RE-PLOTTED TO SHOW THE VARIATION OF BED DEPTH WITH CHANNEL SLOPE AT CONSTANT SUPERFICIAL AIR VELOCITY AND SOLIDS MASS FLOWRATE (SCANDURA DISTRIBUTOR).

the optimum there is risk of the bed depth increasing excessively, even to the point where the channel becomes choked and flow ceases altogether.

8.5.4 Relationships between bed depth and superficial velocity of the fluidising air

During the foregoing discussion mention was made of the fluidising air and its obvious influence on the quality of fluidisation and therefore on the flow behaviour of the aerated Corvic in the inclined channel. In order to obtain a much more detailed picture of the influence of the superficial air velocity a series of test runs was made with the solids mass flowrate constant at about 2.8 kg/s. At various constant channel slopes from 11^{o} down to 3^{o} the superficial air velocity was varied and its effect on the average depth of the flowing bed was recorded. Fig. 8.23 illustrates the results of these tests carried out with the channel fitted with the Vyon 'D' distributor. These curves are interesting in that again they show the "knee" shape, suggesting that in addition to an optimum conveying slope there exists also an optimum superficial air velocity at which to convey. At air velocities less than the optimum the depth of the flowing bed tends to increase (as it does when the conveying slope is too shallow) whilst operation at too high an air velocity gives little improvement in performance and is wasteful of energy. It will be noted that the rapid thickening of the powder bed to the point at which flow ceases altogether corresponds approximately to the superficial air velocity at which a stationary bed of charged Corvic becomes defluidised (see Section 7.6.4). The "optimum" superficial air velocity for satisfactory conveying appears to range from about 2 U_{mf} up to 3 U_{mf} at shallower channel slopes, although with a material that does not fluidise properly the value of U_{mf} is itself somewhat speculative.

The spacing of the curves on Fig. 8.23 shows again that flow behaviour becomes more sensitive to changes in superficial air velocity as the channel slope is reduced. Cross-plotting from this graph onto axes of average bed depth against channel slope would result in a set of curves very similar to those of Fig. 8.21.

Similar tests at a constant solids mass flowrate of about 3 kg/s and constant channel slopes of 4^{o}, 5^{o}, 6^{o} and 9^{o} were carried out after the

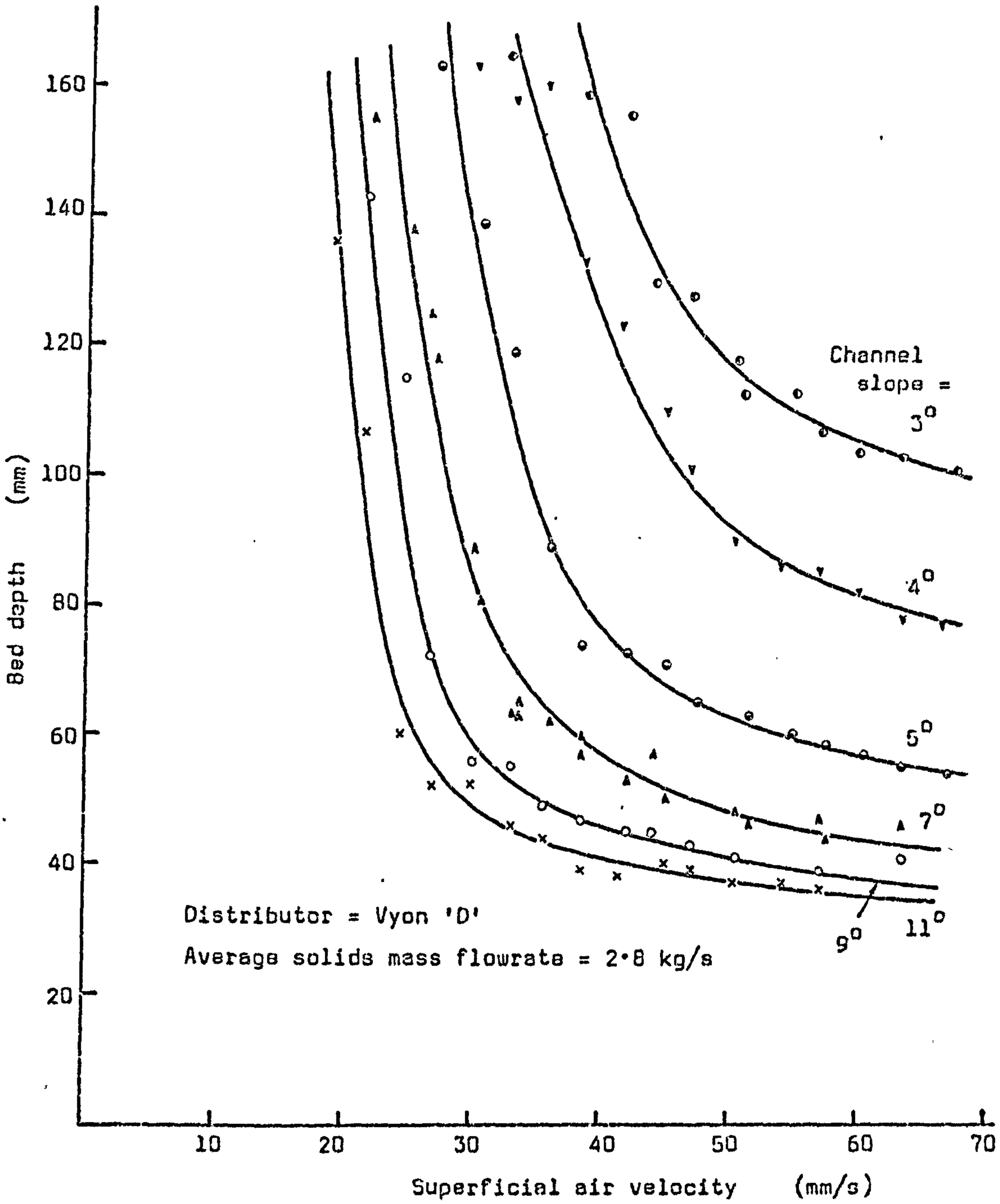

Fig. 8.23 THE VARIATION OF BED DEPTH WITH SUPERFICIAL AIR VELOCITY FOR CORVIC AT CONSTANT MASS FLOWRATE IN A CHANNEL OF CONSTANT SLOPE (VYON DISTRIBUTOR).

Vyon 'D' distributor in the channel had been replaced by the Scandura P22 type. Fig. 8.24 illustrates the results of these tests, again presented as a plot of the average depth of the flowing bed against the superficial air velocity. The most obvious difference between the two sets of curves of Figs. 8.23 and 8.24 is that the latter does not show the sharp upturn as the superficial air velocity is reduced towards the point at which the Corvic becomes defluidised. Also it is noticeable that all the curves of Fig. 8.24 are significantly higher than the corresponding ones on Fig. 8.23. The reasons for these differences are not clear. It was found during the tests that when the superficial air velocity was reduced to too low a value the channel would quite suddenly fill up as the flow stopped and powder spilled from the overflow. This suggests that Fig. 8.24 should in fact show the curves upturning even more sharply than those of Fig. 8.23. The greater bed depths evident from Fig. 8.24 seem to indicate that the quality of fluidisation of the Corvic was poorer during these tests and that the flow of the bed of powder was more sluggish. Whilst these effects are likely to be partly attributable to the Scandura distributor, it seems probable that varying electrostatic charging would also have contributed. Evidence for this supposition is provided by comparing the results of tests plotted as Fig. 8.20 with those of Fig. 8.24 (both of which were for the Scandura P22 distributor). For corresponding sets of conditions there is quite close agreement between the bed depths at the steeper channel slopes, but as the slopes are reduced to 5^{o} and 4^{o} the bed depths on Fig. 8.24 are significantly greater.

8.5.5 Conclusions

A considerable quantity of experimental data has been presented on the graphs discussed in the preceding paragraphs and provides a useful overall picture of the flow behaviour of aerated Corvic in an inclined channel. The main features of the flow of this material, which in its charged condition is probably representative of a typical slightly cohesive material exhibiting rather poor fluidisation qualities, are:-

1. An increase in the solids feedrate to the channel causes an increase in the average depth of the flowing bed (accompanied by an increase in the solids flow velocity).

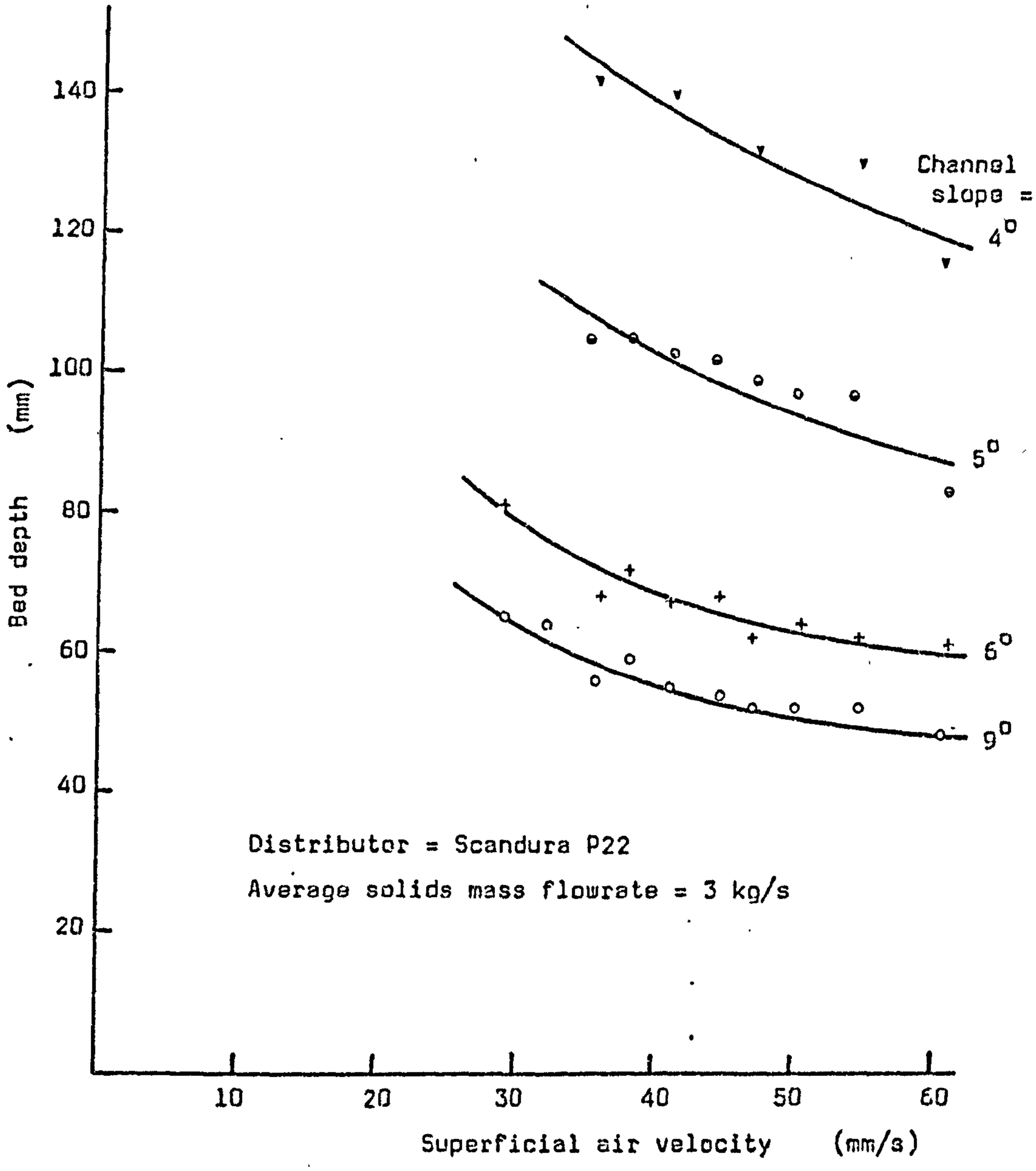

Fig. 8.24 THE VARIATION OF BED DEPTH WITH SUPERFICIAL AIR VELOCITY FOR CORVIC AT CONSTANT MASS FLOWRATE IN A CHANNEL OF CONSTANT SLOPE (SCANDURA DISTRIBUTOR).

2. There is an optimum value of the slope of the conveying channel. (Steeper slopes offer little practical advantage, whilst attempting to convey at shallower slopes may cause complete blockage of the channel.)
3. There is an optimum value of the superficial velocity of the fluidising air. (Operating at air velocities that are too low may cause the flowing bed to thicken to the point at which the channel becomes blocked, whilst using a higher air velocity is simply wasteful of energy.)

Fig. 8.25 is a reproduction of the graph of bed depth against superficial air velocity for various channel slopes with an "optimum operating band" superimposed on it. It is seen from the position of this optimum band that the best air flowrate at which to operate the conveying channel depends to some extent upon its angle of inclination. In general, the channel should thus be installed at a maximum slope that can be accommodated within the available headroom (although it should be noted that there is little to be gained from angles greater than about 10^{o}) and satisfactory operation at the most economical air consumption should then be possible.

The apparent differences in the performances of the two types of distributor are interesting although not easy to explain. It does seem that the quality of fluidisation produced by the Scandura P22 distributor is rather less than that with the higher resistance Vyon 'D'. This is evidenced chiefly by the significantly greater depths of flowing beds of Corvic at conditions that are otherwise equal for the two cases. However, no appreciable difference was observed during the tests in the small fluidising rig, and in any case, what difference there is may be more than compensated by the lower power consumption (because of the lower resistance to airflow) and by the seemingly lower tendency for the pores to become blocked.

8.6 GENERAL CONCLUSIONS

As with any experimental programme of this kind it was not possible to fully assess the design of the channel test rig until it had been in use for a period of time and, not unexpectedly, it soon became clear that there were areas in which improvements could be made. However, once the

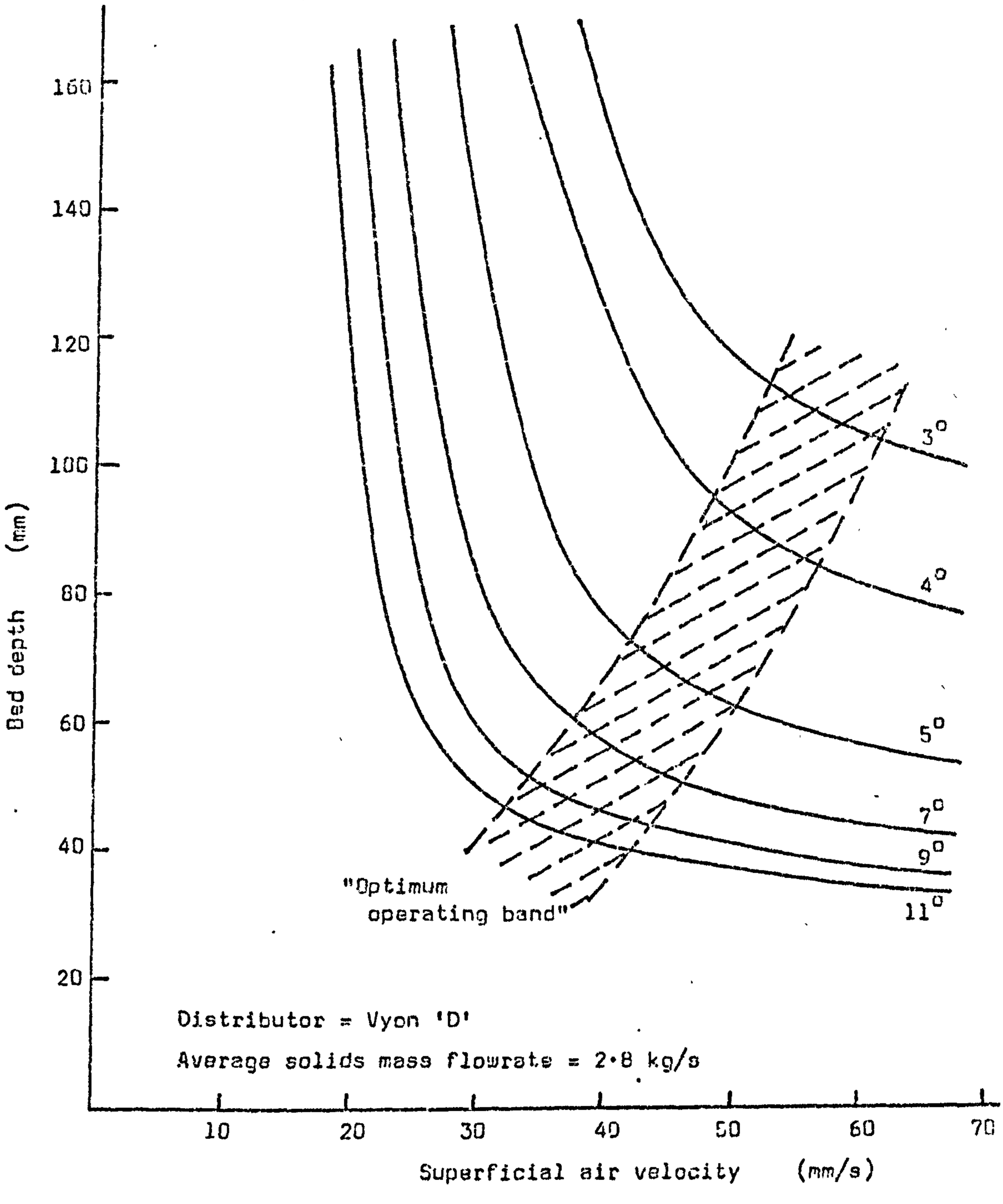

Fig. 8.25 THE RELATIONSHIP BETWEEN BED DEPTH AND SUPERFICIAL AIR VELOCITY FOR CORVIC FLOWING AT A RATE OF 2.8 kg/s, SHOWING THE SUGGESTED "OPTIMUM OPERATING BAND".

minor troubles had been put right at the start of the programme the rig performed very satisfactorily in most respects and improvements that would have involved major structural alterations were postponed until the first stage of the work had been completed.

One constant source of irritation stemmed from the difficulty of sealing the porous plastic (Vyon) sheets in the base of the weigh-bin (Section 8.2.5). The bin was designed with these sheets inclined at an angle of about 4^{o} which should have been just sufficient, even for the Corvic in its charged condition, to permit easy emptying of the bin. However, the constant occurrence of air leaks, aggravated by flexing of the sheets, whilst in no way affecting the accuracy of any test results, caused severe channelling in the powder and continual difficulty in discharging it into the Floveyor.

The design of the channel itself, although entirely original, has proved to be quite successful. Despite the tendency of the Corvic particles to adhere to the Perspex walls, visibility of the flowing powder was adequate to within about a millimetre of the top surface of the distributor. Unfortunately the dismantling and re-assembly of the channel (for example, to replace the distributor) was found to be less easy than had been intended. However, once the components of the channel had been carefully assembled with all the seals in position there were no significant problems with leakage, either of powder from the conveying channel or of air from the plenum chamber.

In fact the only places where leakage of powder created a nuisance were from the joints of the Floveyor and from the entry point to the upstream fluidising chamber from the rotary valve. In the latter case the problem was with the design of a suitable flexible seal that would allow the slope of the channel to be altered. It is intended at a later date to modify the powder feed to the channel to incorporate a flexible bellows arrangement, if this can be done within the very limited headroom available. Combined with this modification would probably be the changeover from controlled solids feed to flooded feed through a variable orifice. It had been hoped to install a Mucon iris-diaphragm valve in place of the rotary valve in order to provide a comparison between the two systems at

this stage of the work. However, this interesting aspect of the study of air-gravity conveying has been postponed to form the basis of a future programme.

Two other developments that would be desirable, or even essential, in a future programme of research concern the humidity of the fluidising air and the velocity of the flowing bed of powder. Difficulties with the control of the air humidity proved to be a considerable handicap since, although the dewpoint (and therefore the relative humidity) could be measured with some confidence, there tended to be a slow but noticeable drift throughout a day's tests. The whole question of the provision of air to the rig at high pressure (by normal air-conditioning standards) and steady high humidity needs a careful and thorough re-appraisal. The second development mentioned, measurement of the velocity of the bed of flowing powder, has been discussed in Section 3.2.9. Here too there is a need for detailed consideration to be given to the many difficulties involved in determining accurately the velocity distribution within a flowing bed of fluidised powder.

The results of the experimental work undertaken on the channel rig have been discussed in detail in Sections 8.4 and 8.5 and summaries appear at the end of each of these Sections. In preparing this report it was found to be convenient to include in Section 8.4 under the title "Commissioning the rig" observations made during subsidiary tests carried out at various stages of the experimental programme and therefore these notes do not follow a strictly chronological order. Nevertheless, the overall planning of the programme remains more or less unaltered, beginning with a general study of the flow of aerated Corvic in order to get a "feel" for the control of the rig and the handling of the powder, following with a more detailed look at the influence of some of the features of the rig and of external effects such as electrostatic charging, and finishing with an investigation of the relationships amongst the main system variables.

The results of this final part of the programme have been analysed only in a somewhat superficial manner in Section 8.5.5 and to complete the work it is necessary to take a closer look at the relationships observed with regard to their comparison with experimental data from other sources and also their correlation with appropriate analytical models. This analysis is described in Chapter Nine.

CHAPTER NINE

ANALYSIS OF EXPERIMENTAL RESULTS

9.1 INTRODUCTION

The detailed discussion of the analytical modelling of the flow of aerated bulk particulate solids in inclined channels, undertaken in Part I, Chapter 4, led up to the suggestion that a new approach, based on a simple force balance equation for steady uniform flow, might have some advantages over other techniques. Using data reported by other investigators for the flow of fluidised sand it was shown that the relationships amongst the solids mass flowrate, the angle of inclination of the conveying channel and the depth of the flowing bed of sand could be represented by a fluid model in which the shear stress at the side-walls of the channel is constant whilst that at the channel base is proportional to the average solids flow velocity (Section 4.3.4). The mathematical model proposed was of the form

$$\dot{m} = K_1 \rho h^2 (\rho g b \sin\alpha - K_2) \quad . . . . . 4.3.19$$

in which the parameters K_1 and K_2 are functions of the "nature" of the powder, the superficial velocity U_g of the fluidising air and the roughness of the channel.

One of the objectives of the experimental work carried out in this programme was to obtain data with which to test the modelling approach referred to above for a particulate solid exhibiting flow behaviour different from that of sand. If the model is to be of practical use it would be expected that values could be found for the parameters K_1 and K_2 such that curves plotted from equation 4.3.19 would match the curves obtained experimentally.

In this Chapter the correlation between the experimental data obtained for the flow of aerated Corvic and the proposed model is examined. The analysis is then taken further as a study of the influence of the superficial velocity of the fluidising air on the flow characteristics of the Corvic and how the model is affected by this variable. Attention is specially given to the shear stresses at the base of the channel and at the side walls, and although direct measurements of these stresses were not made, some indication of the way in which they vary with the flow condition may be obtained from a consideration of the model.

9.2 VALUES OF THE PARAMETERS K_1 AND K_2

A possible procedure to be followed when attempting to match experimental data to the model represented by equation 4.3.19 has been outlined in Section 4.3.4. It was pointed out that varying the parameter K_1 tends to shift all the curves on a plot of bed depth against channel slope (or against solids mass flowrate) upwards, whilst K_2 has a more pronounced influence at the shallower channel slopes. Therefore the value of K_1 to give the best fit of the model to the experimental data should normally be chosen first. An iterative method of determining a suitable value for the parameter K_1, and then for K_2, would be perfectly satisfactory, but a graphical method is perhaps more elegant and has the advantage of indicating where the model may deviate from the experimental data.

The mathematical model (equation 4.3.19) can be re-arranged as

$$\frac{\dot{m}}{h^2} = K_1 \rho^2 g b \sin\alpha - K_1 K_2 \rho \qquad \ldots\ldots 9.2.1$$

and it can be seen that a plot of $\dot{m}/h^2$ against $\rho^2 g b \sin\alpha$ should yield a straight line of slope K_1 and from which K_2 can be found by the intercept on the abscissa. The linearity of the experimental data plotted this way should provide evidence in support of the model.

Fig. 9.1 shows a plot of $\dot{m}/h^2$ against $\rho^2 g b \sin\alpha$ for the flow of charged Corvic in the channel fitted with a Vyon distributor. (It should be noted that this plot has been simplified by using points from the experimental graph, Fig. 8.18, rather than actual test readings. However, this is of little consequence as it is the correlation between the test readings and the mathematical model that is the more important, and Fig. 9.1 is merely an aid to the determination of the most suitable values of the parameters K_1 and K_2 in the model.) The scatter of the points on Fig. 9.1 was quite small and therefore a straight line was drawn from which values of K_1 and K_2 were calculated.

Values of the parameters from Fig. 9.1 were:-

$K_1 = 0.23$ $\qquad$ ($k_b = 4.3$ Ns/m^3)

$K_2 = 11.2$ $\qquad$ ($\tau_w = 5.6$ N/m^2)

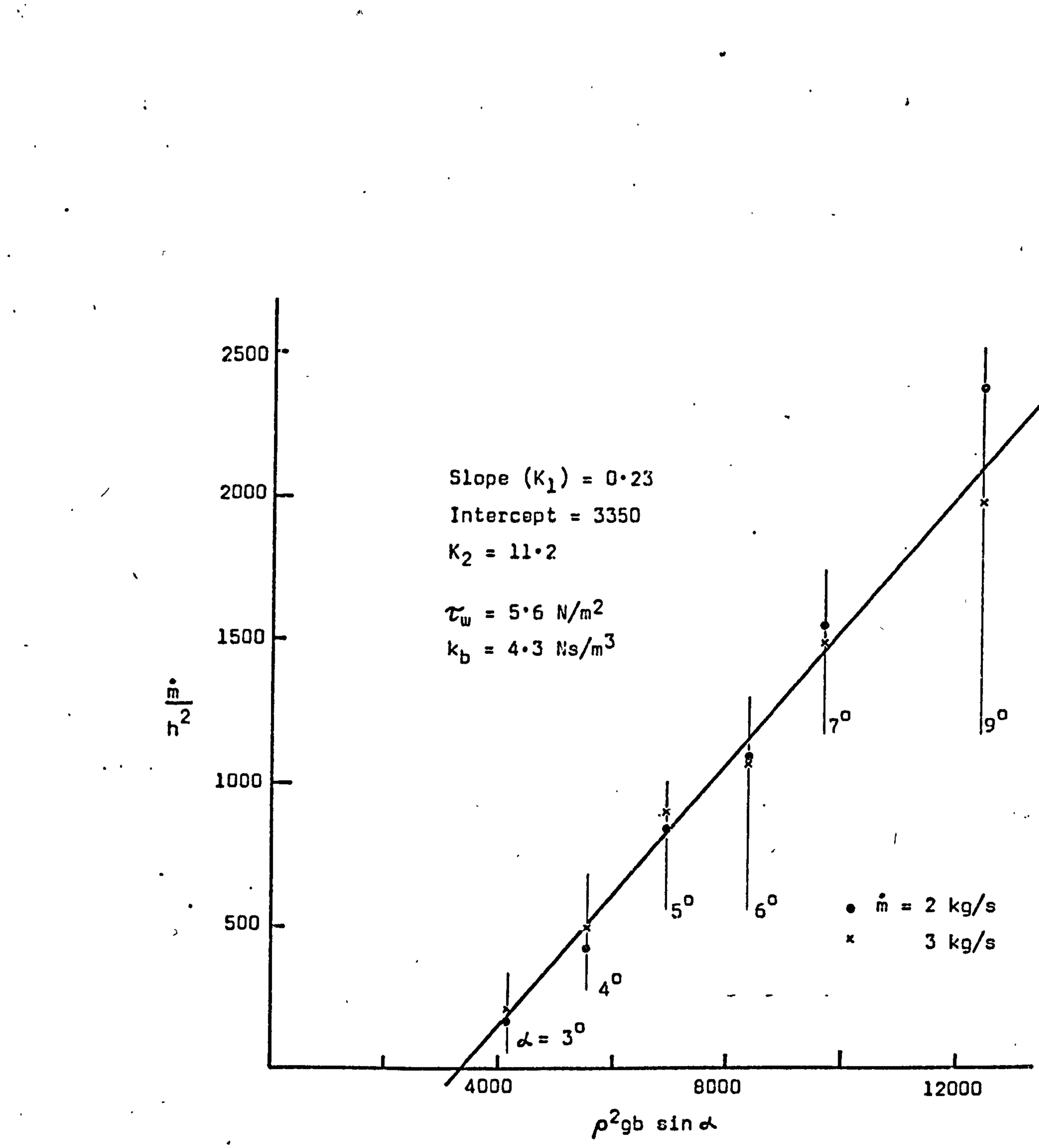

Fig. 9.1 PLOT OF $\dot{m}/h^2$ AGAINST $\rho^2 g b \sin\alpha$ FROM WHICH CAN BE CALCULATED APPROXIMATE VALUES OF THE PARAMETERS K_1 AND K_2 IN EQUATION 4.3.19. (Data from Fig. 8.18 for Corvic flowing on Vyon distributor.)

Substitution of these values in the equation 4.3.19 (or in equation 9.2.1) yields an expression relating the solids mass flowrate $\dot{m}$, the slope α of the conveying channel and the depth h of the flowing bed of powder. From this expression it is therefore possible to plot sets of curves of, for example, h against $\dot{m}$ and h against α.

Such a set of curves is presented as Fig. 9.2 in which the bed depth is plotted for solids mass flowrates up to 4 kg/s and for channel slopes from 3^{o} to 10^{o}. Whilst these curves are interesting and seem to bear some similarities to the lines plotted on Fig. 8.18 for the corresponding experimental data, it is only when the actual test readings are plotted on the same axes that the extent of the agreement becomes apparent. Thus Fig. 9.3 has been prepared, being identical to Fig. 9.2 but showing experimental points taken from Fig. 8.18. It is of course unfortunate that it was not possible to obtain solids mass flowrates over a wider range; or perhaps it is unfair to plot the predicted curves over the wider range. Nevertheless, it does appear that the model under consideration, with appropriate values of the parameters K_1 and K_2, gives an acceptable prediction of the relationship amongst h, $\dot{m}$ and α for charged Corvic in the conveying channel at the constant superficial air velocity of 63 mm/s.

It is possible alternatively to illustrate this relationship as a plot of bed depth against channel slope as shown in Fig. 9.4. This graph compares very closely with Fig. 8.21 which was produced by cross-plotting from the experimental data of Fig. 8.18; in fact, the curves for 2 kg/s and 3 kg/s on Figs. 8.21 and 9.4 are virtually coincident.

Two areas of doubt in the mathematical model surround the superficial air velocity and the bulk density of the flowing bed of powder. The effect of the former has been investigated experimentally and will be discussed in more detail in Section 9.4. The bulk density, however, presented something of a problem. The difficulty of deciding on a value of this property for a flowing bed of "fluidised" Corvic has not really been overcome and herein lies a weakness of the proposed model. For the present analysis the values of bulk density used have been determined from Fig. 7.36, although strictly this graph applies only to fluidised beds that are stationary (non-flowing). Despite misgivings about this approach, it is the one apparently used by

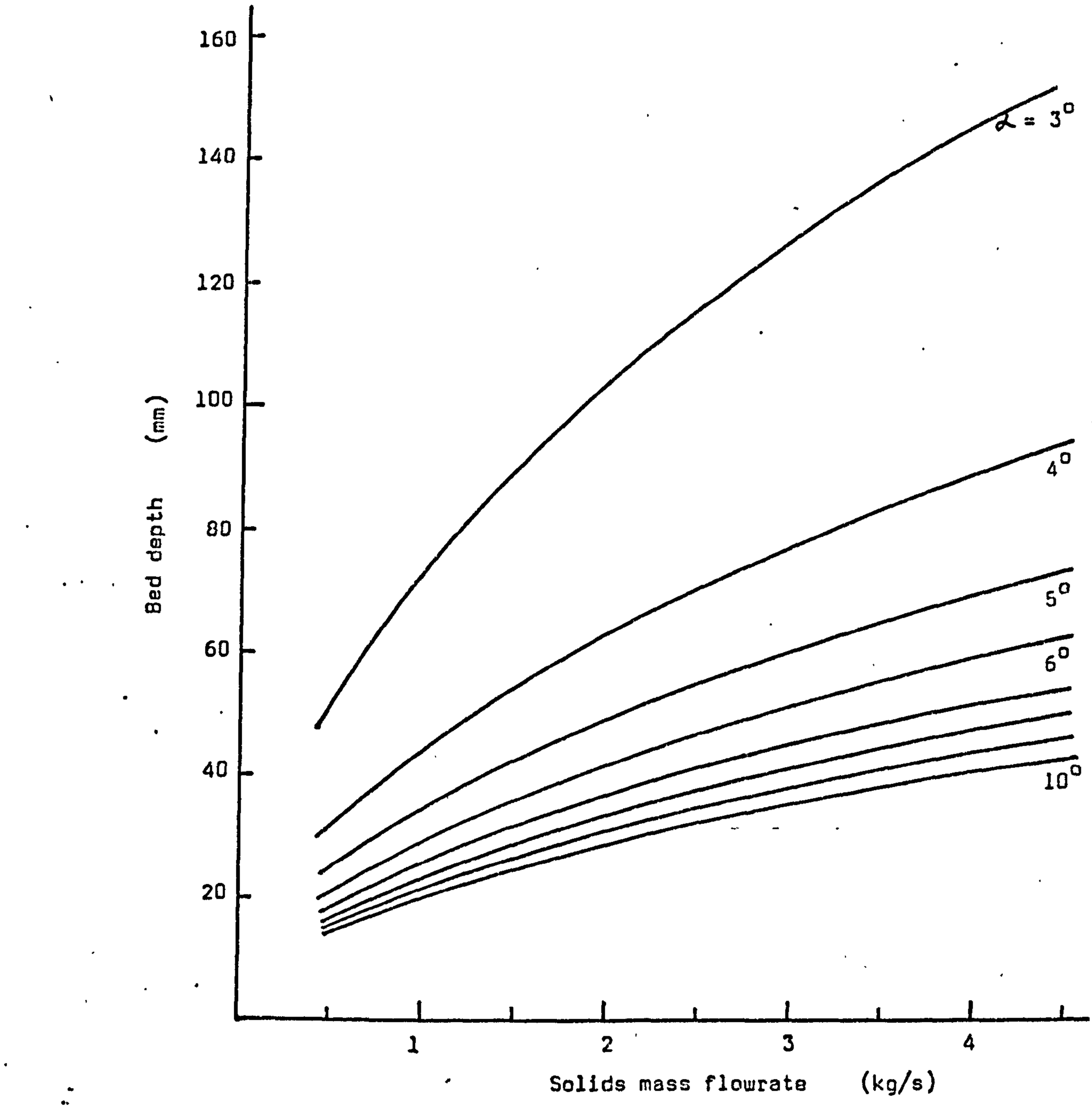

Fig. 9.2 THE RELATIONSHIP BETWEEN DEPTH OF THE FLOWING BED AND THE SOLIDS MASS FLOWRATE, AS PREDICTED BY EQUATION 4.3.19 WITH b = 0.1 m, ρ = 300 kg/m^3, K_1 = 0.23 and K_1 = 11.2.

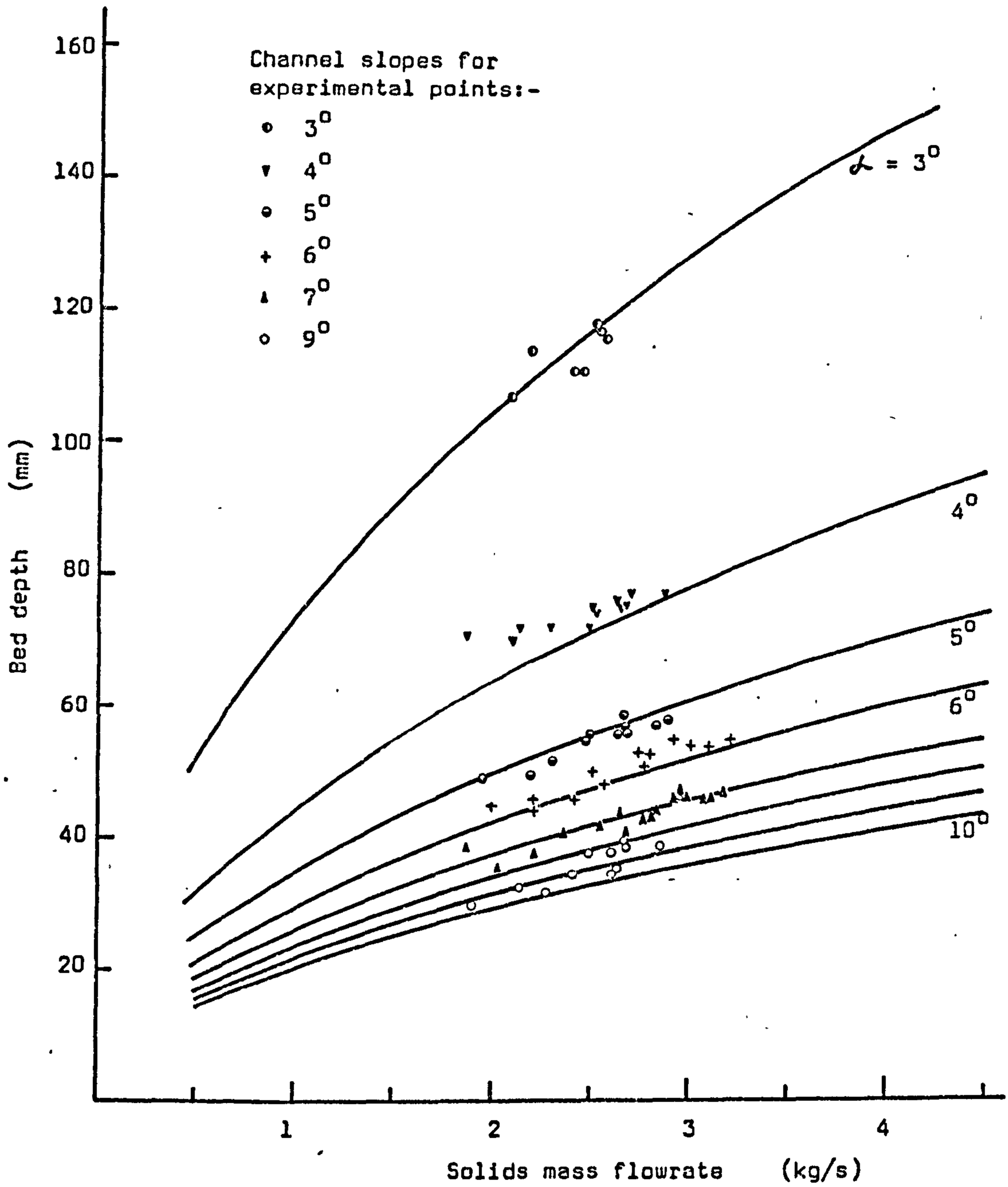

Fig. 9.3 THE PREDICTED CURVES OF Fig. 9.2 COMPARED WITH EXPERIMENTAL READINGS FROM Fig. 8.18.

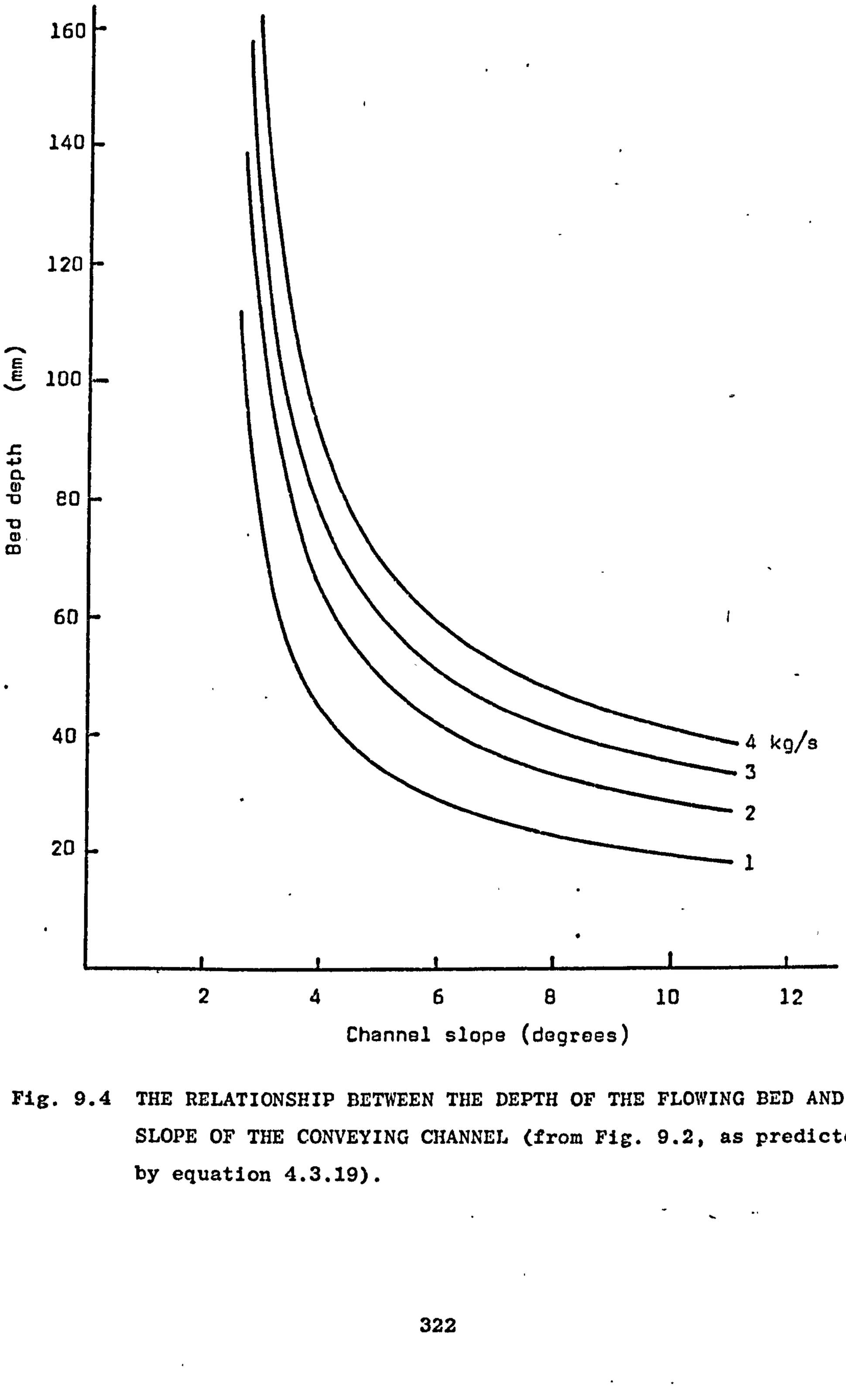

Fig. 9.4 THE RELATIONSHIP BETWEEN THE DEPTH OF THE FLOWING BED AND THE SLOPE OF THE CONVEYING CHANNEL (from Fig. 9.2, as predicted by equation 4.3.19).

most other investigators and there seems at this time to be little alternative.

An identical analytical procedure to that described above was followed for the second set of experimental data relating h, $\dot{m}$ and α for Corvic flowing in the channel fitted with the Scandura P22 distributor, and at the slightly lower superficial air velocity of 50 mm/s. Inspection of Fig. 8.20 suggested that, although the data covered a wider range of solids mass flowrate than that obtained for the Vyon distributor, the results were rather less consistent. It was therefore not surprising to find that it was more difficult to place a straight line through the points on a plot of $\dot{m}/h^2$ against $\rho^2 g b \sin\alpha$ (Fig. 9.5). In fact, such was the latitude available that this plot was of little benefit in determining the best values of the parameters K_1 and K_2 and greater reliance had to be placed on an iterative procedure, which gave the following results:-

$K_1 = 0.136$ $\quad (k_b = 7.4\ Ns/m^3)$

$K_2 = 14.4$ $\quad (\tau_w = 7.2\ N/m^2)$

As before, these values were substituted into the mathematical model so that sets of curves could be plotted to show the variation of h with $\dot{m}$ (Fig. 9.6) and of h with α (Fig. 9.8). The result of the higher value of K_2 and the lower value of K_1 on the plot of h against $\dot{m}$ is to shift all the curves upwards and to "spread out" the curves for the shallower channel slopes. This of course is in accordance with the observed behaviour of the Corvic in the tests with the Scandura distributor fitted to the channel, as is illustrated by Fig. 9.7 in which the experimental points are compared with the predicted curves. It is seen that correlation is not as good as with the first set of data (Fig. 9.3), and at the shallow slope (4^o) the test points lie well off the modelled curve, any attempt to rectify the situation by adjustment of K_1 or K_2 merely resulting in a greater deviation at the steeper slopes. Likewise, the correlation between the plots of h against α (Figs. 9.8 and 8.22) is not as good as previously. Nevertheless, the similarities between the patterns of experimental data and modelled curves are sufficiently close to give considerable confidence in the method of analysis.

It is interesting now to look at the significance of the differences in the values of the parameters K_1 and K_2. Firstly, it must be recalled that

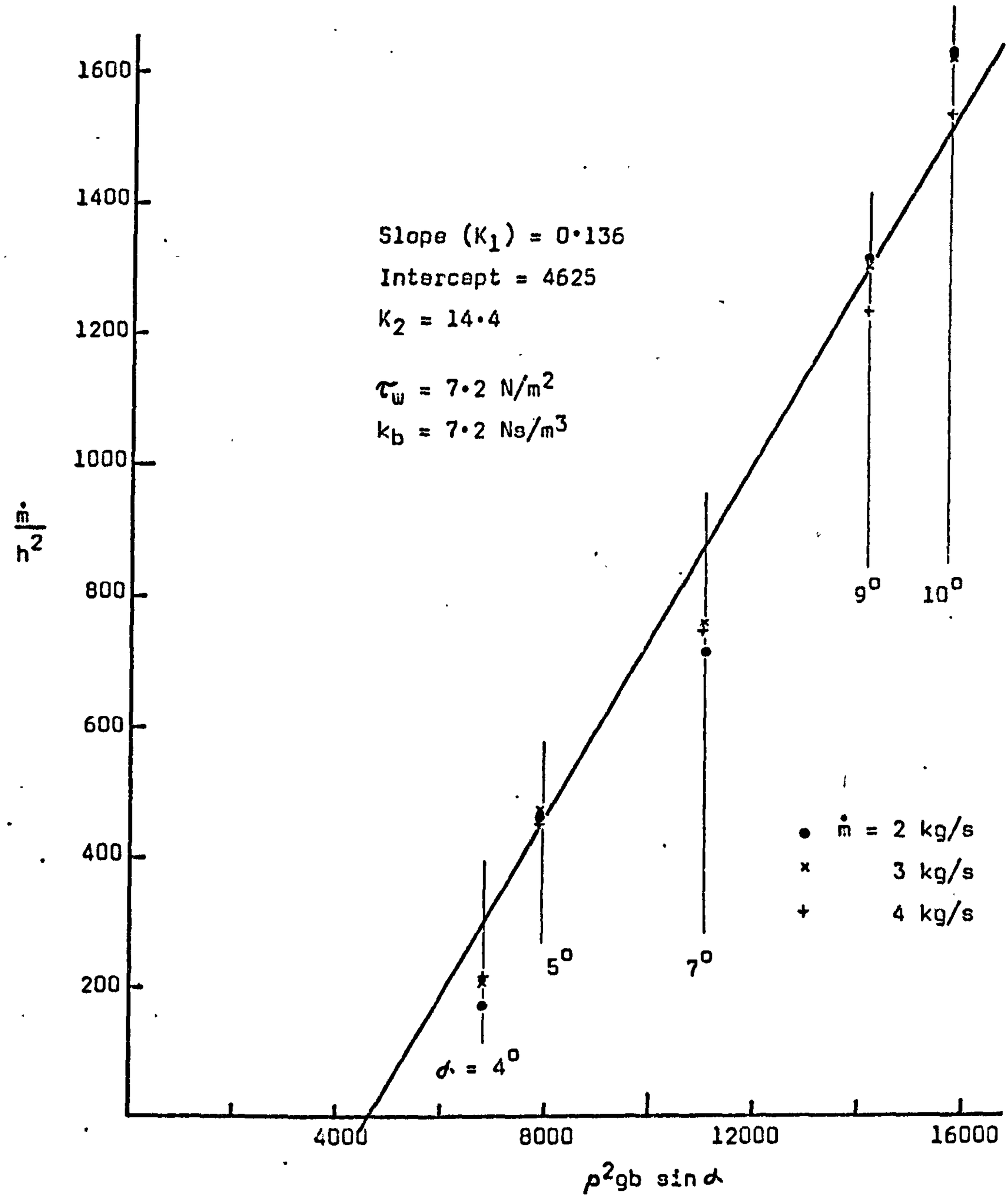

Fig. 9.5 PLOT OF $\dot{m}/h^2$ AGAINST $\rho^2 g b \sin\alpha$ SHOWING APPROXIMATE VALUES OF THE PARAMETERS K_1 AND K_2 IN EQUATION 4.3.19. (Data from Fig. 8.20 for Corvic flowing on Scandura distributor.)

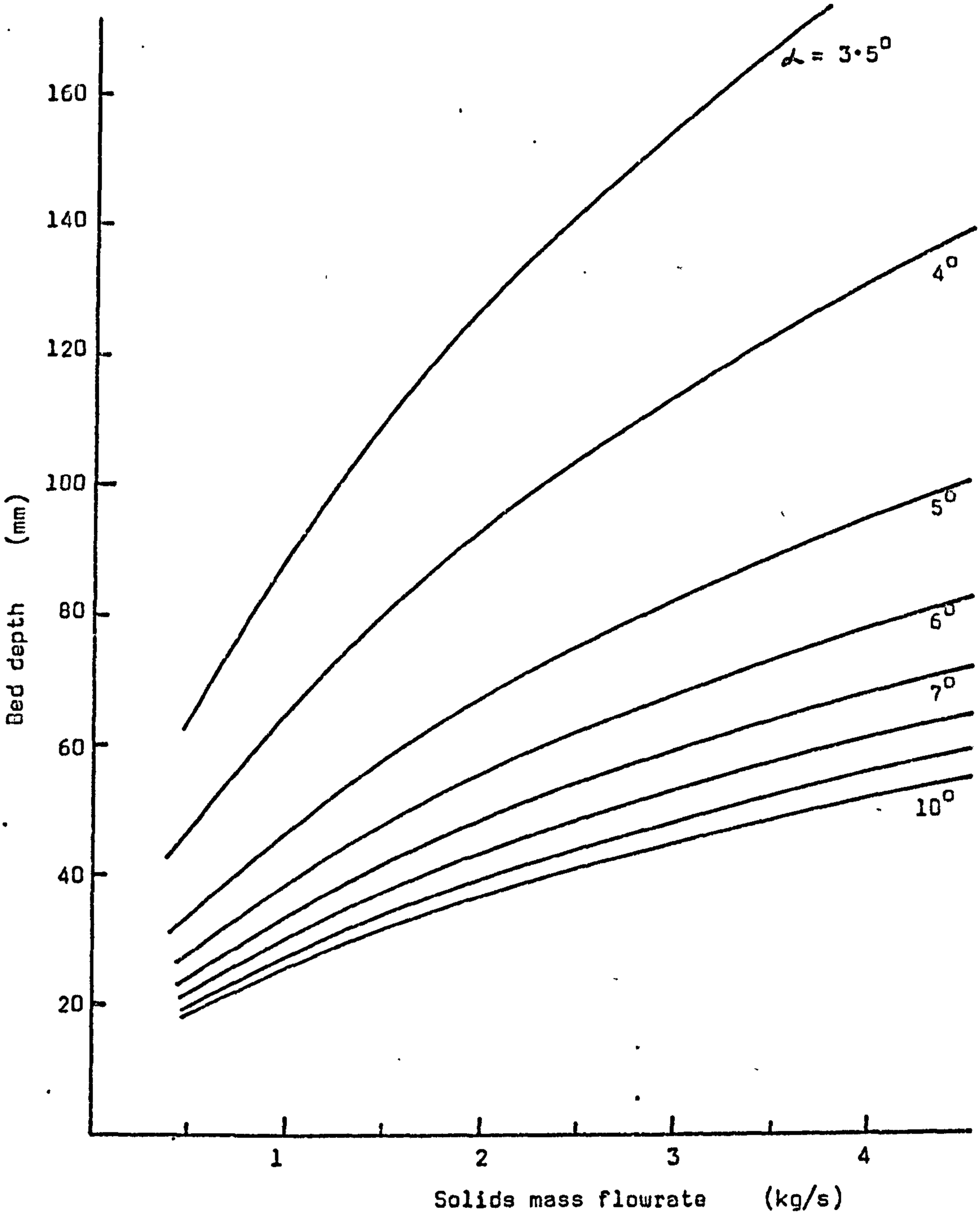

Fig. 9.6 THE RELATIONSHIP BETWEEN DEPTH OF THE FLOWING BED AND THE SOLIDS MASS FLOWRATE, AS PREDICTED BY EQUATION 4.3.19 WITH $b = 0.1$ m, $\rho = 320$ kg/m^3, $K_1 = 0.14$ AND $K_2 = 14.4$.

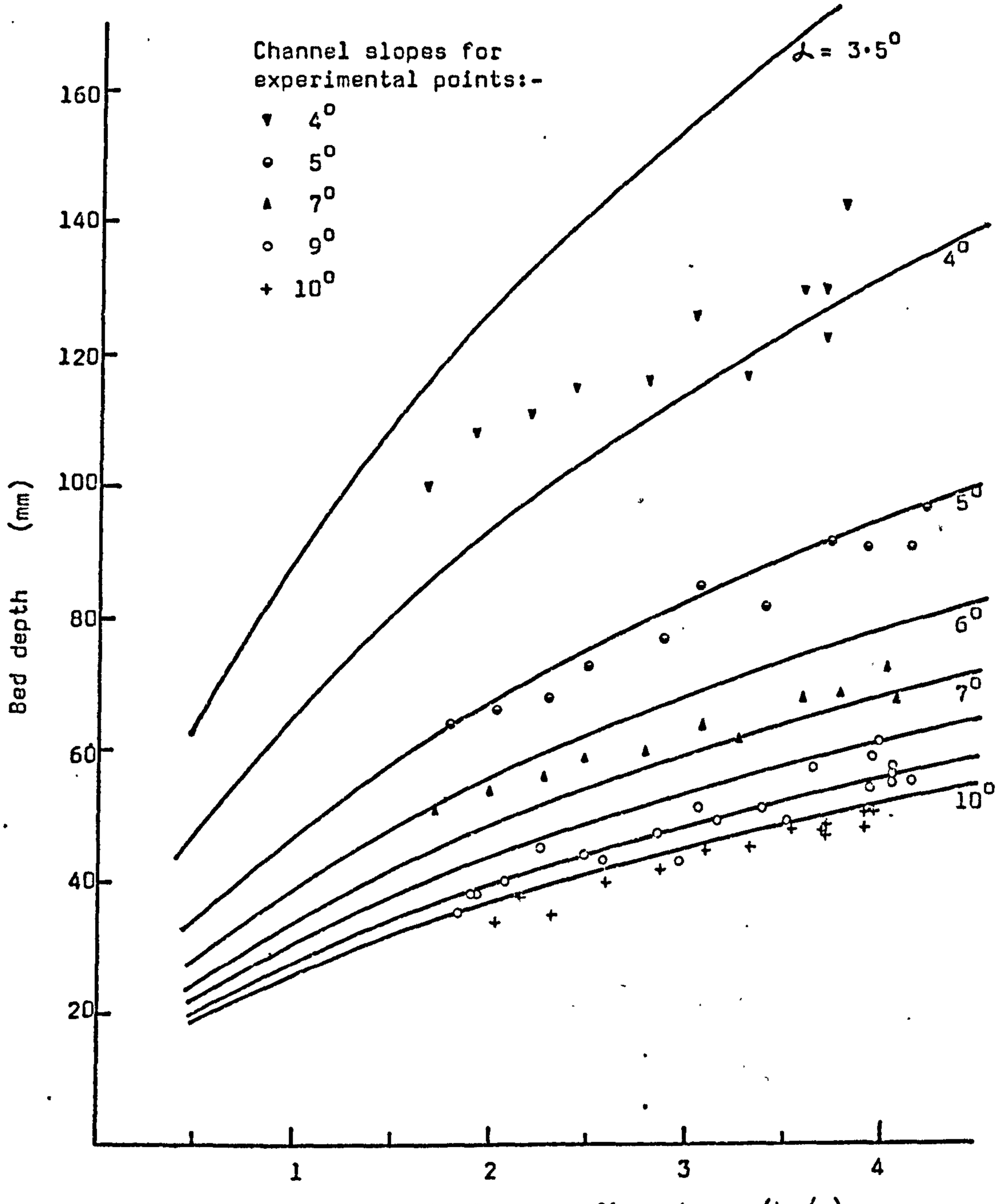

Fig. 9.7 THE PREDICTED CURVES OF Fig. 9.6 COMPARED WITH EXPERIMENTAL READINGS FROM Fig. 8.20.

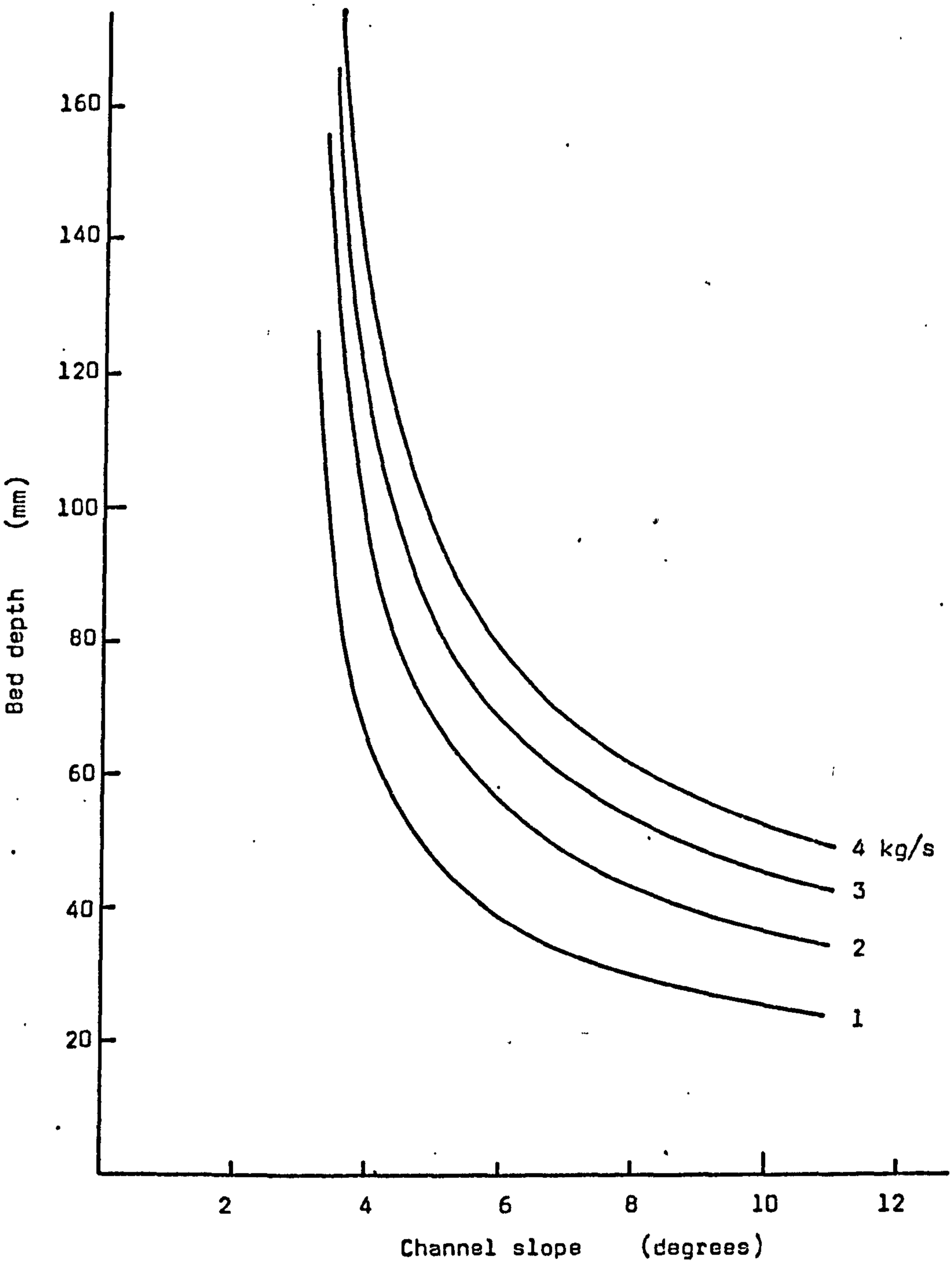

Fig. 9.8 THE RELATIONSHIP BETWEEN THE DEPTH OF THE FLOWING BED AND THE SLOPE OF THE CONVEYING CHANNEL (from Fig. 9.6, as predicted by equation 4.3.19).

these parameters were defined in terms of the shear stress at the channel wall, τ_w, and a shear stress/velocity coefficient, k_b, in order to simplify the mathematical model which was originally written

$$\dot{m} = \frac{\rho^2 g b^2 h \sin\alpha}{k_b} \cdot \frac{h}{b} - \frac{2\rho h^2 \tau_w}{k_b} \quad \ldots\ldots 4.3.18$$

The coefficient k_b was itself a function of τ_b, the shear stress at the base of the channel, so that

$$K_1 = \frac{1}{k_b} = \frac{1}{\tau_b} \frac{\dot{m}}{\rho b h} \quad \ldots\ldots 9.1.2$$

and

$$K_2 = 2\tau_w \quad \ldots\ldots 9.1.3$$

and clearly an increase in the parameter K_1 would be associated with a decrease in the shear stress at the base of the channel, whilst an increase in K_2 would be associated with an increase in the shear stress at the side walls.

In the case under consideration it appears that the set of experimental data relating to flow on the Scandura distributor can be represented by the same mathematical model (equation 4.3.19) as the data relating to flow on Vyon, provided that K_1 is reduced and K_2 increased by appropriate amounts. Thus it seems that during the tests in which the Scandura distributor was used the shear stresses at the side walls and at the base (that is, at the surface of the distributor) were both greater than for the tests using Vyon.

It should be noted that the superficial air velocity was slightly lower in the second series of tests (using Scandura) and this could account partly for the poorer fluidisation which was evidenced by the greater shear stress at the side walls. The same explanation could apply to the shear stress at the base of the channel, but it seems likely that an additional contribution would be made by the much rougher surface of the woven polyester Scandura distributor.

Finally, it is worthwhile to compare the values of parameters K_1 and K_2 for Corvic with those suggested previously for the flow of fluidised sand.

When introducing the model, use was made of experimental data reported by various other investigators to estimate values of K_1 and K_2 that gave reasonable correlation with the observed behaviour of the sand which, in contrast to Corvic, could be regarded as representative of a range of free-flowing materials. Table 9.1 sets out the three pairs of values of K_1 and K_2, and also the wall shear stress τ_w and the shear stress/velocity coefficient k_b, allowing comparison between those for Corvic and those for 200 μm sand.

CONVEYED MATERIAL	K_1	K_2	τ_w	k_b
P.V.C POWDER (CORVIC) (electrostatically charged and therefore exhibiting some degree of cohesiveness)				
i) First series of tests; channel fitted with Vyon 'D' distributor.	0.23	11.2	5.6	4.3
ii) Second series; Scandura P22 distributor.	0.136	14.4	7.2	7.4
SAND (approximately 200 μm mean particle size)	0.08	5.0	2.5	12.5

Table 9.1 VALUES OF THE PARAMETERS K_1 AND K_2 (AND τ_w AND k_b) TO GIVE REASONABLE CORRELATION OF THE MODEL WITH THE OBSERVED BEHAVIOUR OF CORVIC (TYPICAL OF A SLIGHTLY COHESIVE MATERIAL) AND SAND (A TYPICAL FREE-FLOWING MATERIAL).

It appears that the value of K_2 (and therefore of τ_w) for the sand is much less than that for Corvic, a result that was at first somewhat surprising, although it is perhaps reasonable to suppose that adhesion of the charged Corvic particles to the channel walls could have had a significant influence on the overall wall shear stress. Direct comparison of the values of K_2 (or k_b) is again interesting, but may be misleading because of the different densities of the two materials and also because of the relative effects of the superficial air velocity in each case. It is clear of course that changes

in the superficial air velocity would require changes in the parameters K_1 and K_2 if the correlation between the mathematical and the experimental data is to be maintained, and this aspect of the modelling will therefore be discussed more fully in Section 9.4.

9.3 THE SOLIDS FLOW VELOCITY

It was unfortunate that in the present programme of work measurement of the velocity of the flowing bed of aerated Corvic was restricted to a few values obtained using a float on the surface of the powder (see Section 8.4.7). Nevertheless, it is of interest to compare the values of velocity measured (mostly in the range 0.5 to 1.4 m/s) with those that would be expected from a consideration of the mathematical model.

Thus, writing the average solids flow velocity in the channel as

$$u_s = \frac{\dot{m}}{\rho b h} \qquad \ldots\ldots\ldots\ldots \quad 9.3.1$$

it is seen that lines of constant velocity may be plotted on the graphs relating the depth of the flowing bed to the solids mass flowrate. Figs. 9.9 and 9.10 are identical to Figs. 9.2 and 9.6 respectively, showing the variation of h with $\dot{m}$, but in addition some lines of constant solids velocity are superimposed. These lines are derived from the simple equation 9.3.1 and it will be noted that the density, ρ, representing the bulk density of the flowing suspension, is taken to be constant. (That is, any variation of the bulk density of the aerated Corvic with the depth of the flowing bed is ignored.)

The general way in which the solids flow velocity increases with increasing channel slope is well illustrated by these plots, but it is of perhaps greater interest to compare the two; Fig. 9.9 with 9.10. It is evident that for a given mass flowrate of Corvic at a given channel slope the average solids flow velocity should have been significantly less in the second series of tests when the Scandura P22 distributor was in use. This appears to confirm visual observations of the more sluggish behaviour of the flowing Corvic during this second series of tests although, as previously

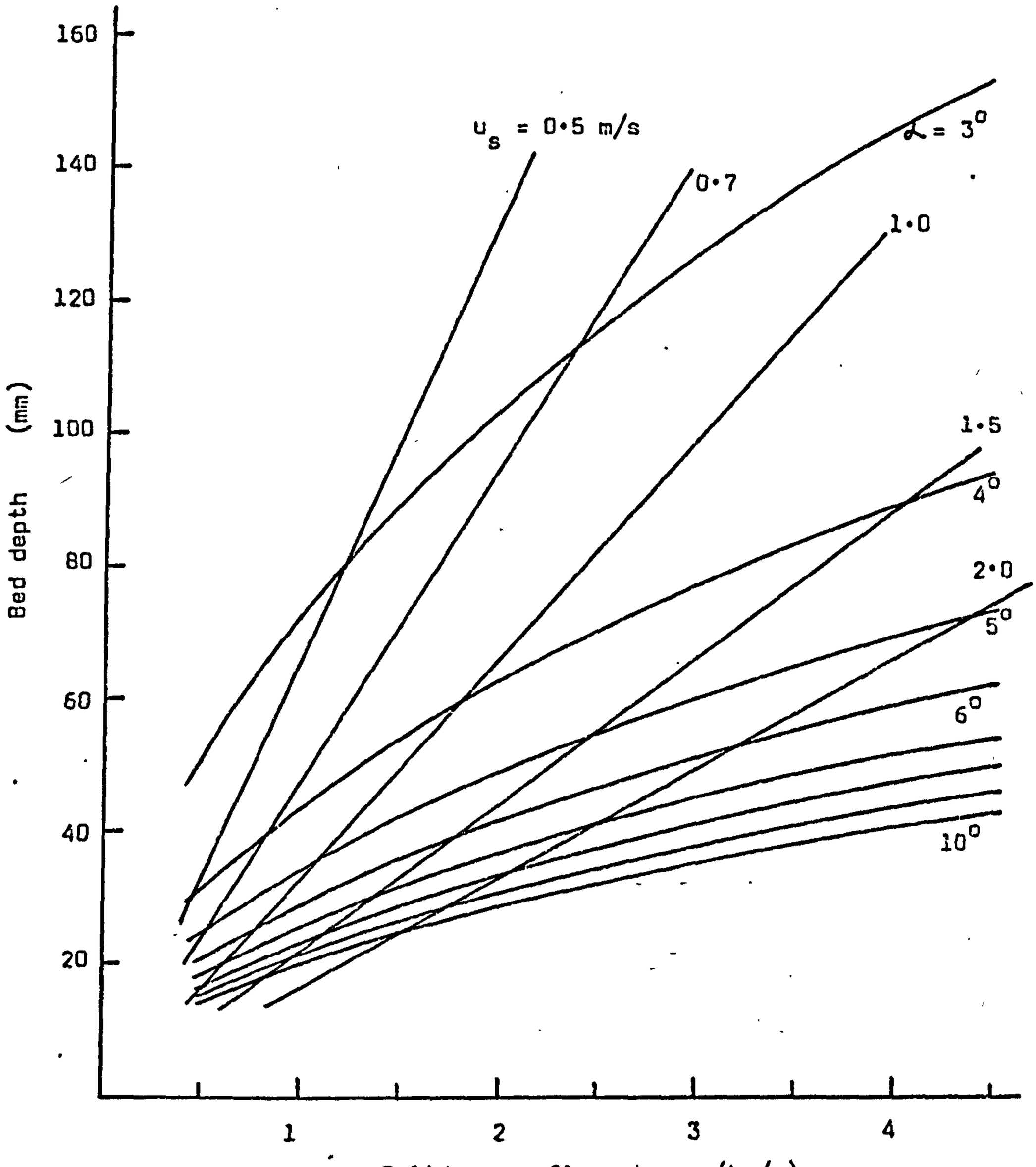

Fig. 9.9 THE PREDICTED CURVES OF Fig. 9.2 SHOWING LINES OF CONSTANT SOLIDS FLOW VELOCITY.

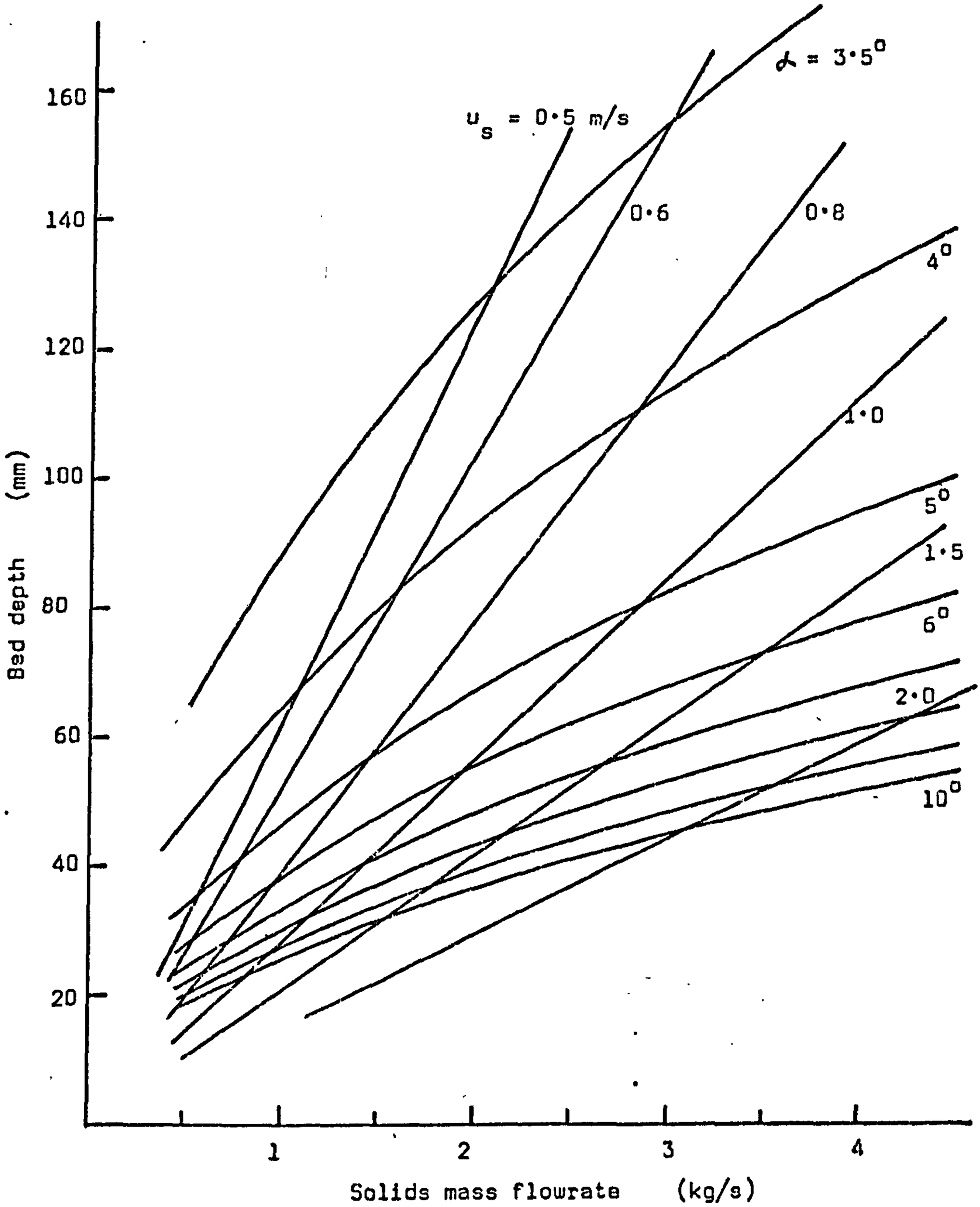

Fig. 9.10 THE PREDICTED CURVES OF Fig. 9.6 SHOWING LINES OF CONSTANT SOLIDS FLOW VELOCITY.

mentioned, no detailed measurements of velocity were made at the time.

9.4 THE INFLUENCE OF SUPERFICIAL AIR VELOCITY

The effect of variations in the superficial velocity of the fluidising air is not easy to model as it is likely that a change in U_g would influence the density ρ, the wall shear stress τ_w and the shear stress at the base of the channel τ_b (and hence k_b). If it is assumed that the relationship between the bulk density of the flowing suspension and the superficial air velocity is similar to that between the bulk density of a stationary fluidised bed and the velocity of the fluidising air (and this is a somewhat dubious assumption in view of the different bubbling behaviour in each case) then an estimate of the variation of ρ can be made and included in the calculation of the model.

The relationship between the depth of the flowing bed and the superficial air velocity has been investigated experimentally and the results presented as Figs. 8.23 and 8.24. However, there does not appear to be any advantage in attempting to find a mathematical model directly linking these two variables. Instead, the approach should be through matching the equation 4.3.19 to sets of curves of h against $\dot{m}$, and h against α, for various values of the superficial air velocity U_g in order to determine the variation of the parameters K_1 and K_2 with U_g.

Examination of the graphs, Figs. 8.23 and 8.24, which show the bed depth plotted against superficial air velocity for constant solids mass flowrate and channel slope, indicates that the effect of variation in U_g on the plot of h against $\dot{m}$ would be to shift all the lines upwards (for a decrease in U_g) or downwards, the movement being greatest at the lowest angles of inclination. It is possible to obtain further information on the influence of U_g by plotting a series of lines of $\dot{m}/h^2$ against $\sin\alpha$ for different values of U_g, using the experimental data presented graphically on Figs. 8.23 and 8.24. From the slopes of these lines and their intercepts on the abscissa, values of K_1 and K_2 (and hence of k_b and τ_w) can be determined, taking due account of the variation of the bulk density with U_g. Fig. 9.11 shows such a plot of $\dot{m}/h^2$ against $\sin\alpha$ prepared using data from the first series of tests (in which the channel was fitted with the Vyon distributor).

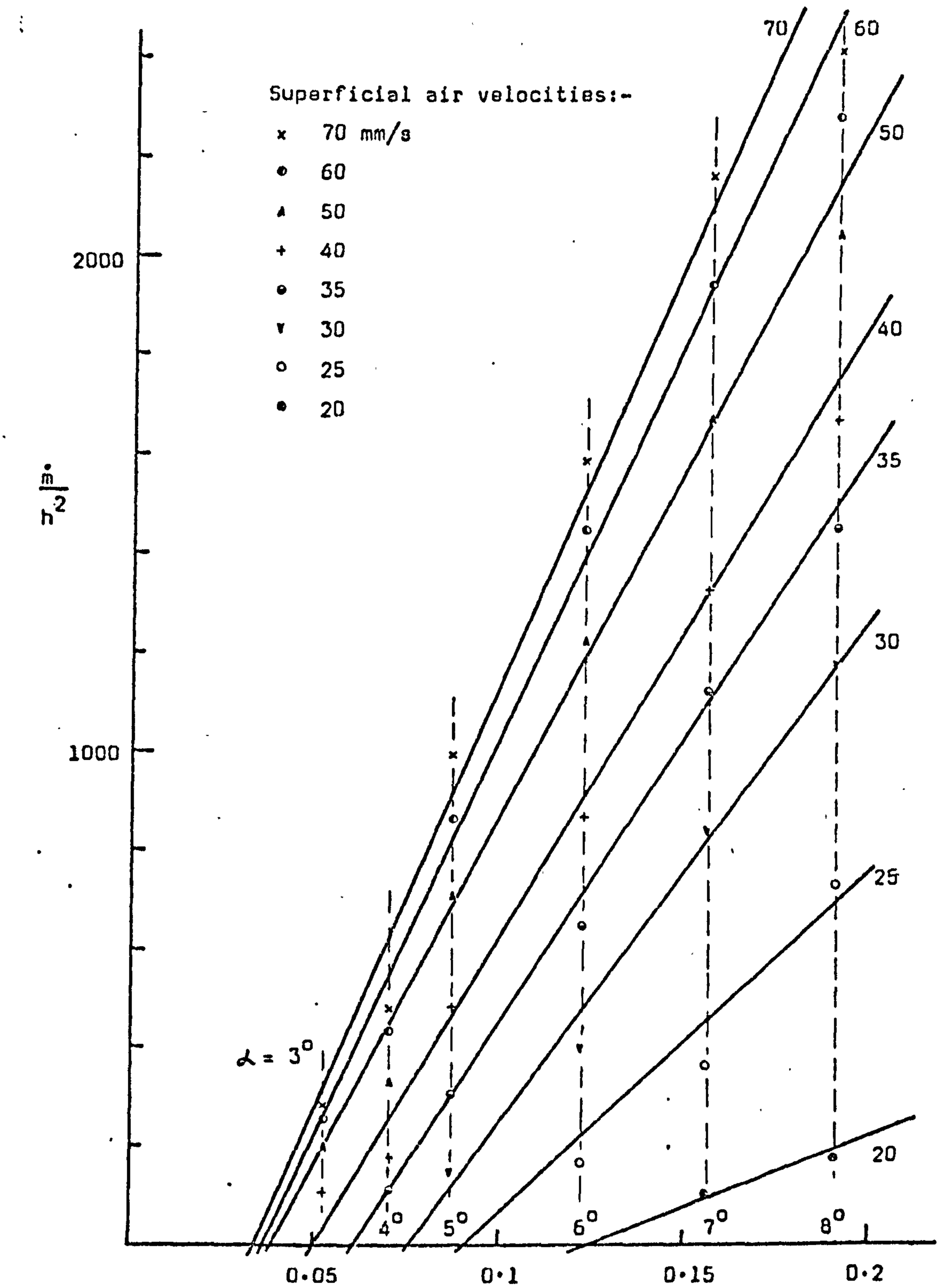

Fig. 9.11 PLOT OF $\dot{m}/h^2$ AGAINST $\sin\alpha$ FOR VARIOUS SUPERFICIAL AIR VELOCITIES.
(Data from Fig. 8.23 for Corvic flowing on a Vyon distributor.)

Although there is some scattering of the points, which are taken from the curves shown on Fig. 8.23, it is possible to construct a set of lines through them enabling values of K_1 and K_2 to be calculated.

Table 9.2 sets out the results of these calculations, thus giving an indication of the way in which K_1 and K_2 have to be varied in order to maintain a correlation between the mathematical model and the experimental data for h, $\dot{m}$ and α as the superficial air velocity is altered.

U_g (mm/s)	ρ (kg/m^3)	Intercept (at $\dot{m}/h^2 = 0$)	K_2	τ_w (N/m^2)	Slope	K_1	k_b (Ns/m^3)
70	295	0.033	9.6	4.8	1.70×10^4	0.20	5.0
60	305	0.036	10.8	5.4	1.60	0.18	5.7
50	320	0.038	11.9	5.9	1.41	0.14	7.1
40	335	0.050	16.4	8.2	1.24	0.11	8.9
35	345	0.061	20.6	10.3	1.15	0.098	10.2
30	360	0.076	26.8	13.4	1.02	0.080	12.5
25	370	0.090	32.7	16.4	0.68	0.051	19.7
20	390	0.12	45.9	22.9	0.29	0.019	51.5

Table 9.2 RESULTS OF CALCULATIONS OF K_1, K_2, τ_w and k_b FROM FIG. 9.11 USING THE DATA OF Fig. 8.23.

Fig. 9.12 shows the variation of K_1 and K_2 plotted against the superficial air velocity, but it is possibly easier to interpret the influence of U_g from a plot of the variation of τ_w and k_b (Fig. 9.13). It is seen from this graph that at relatively high superficial air velocities both τ_w and k_b show only a limited variation and, coincidentally, both have approximately the same numerical value. As U_g is reduced towards the level at which the flowing powder would tend to become defluidised both τ_w and k_b increase rapidly. Thus Fig. 9.13 illustrates the kind of behaviour that would be expected, with the shear stresses at the channel walls and at the base both increasing as the quality of fluidisation is reduced.

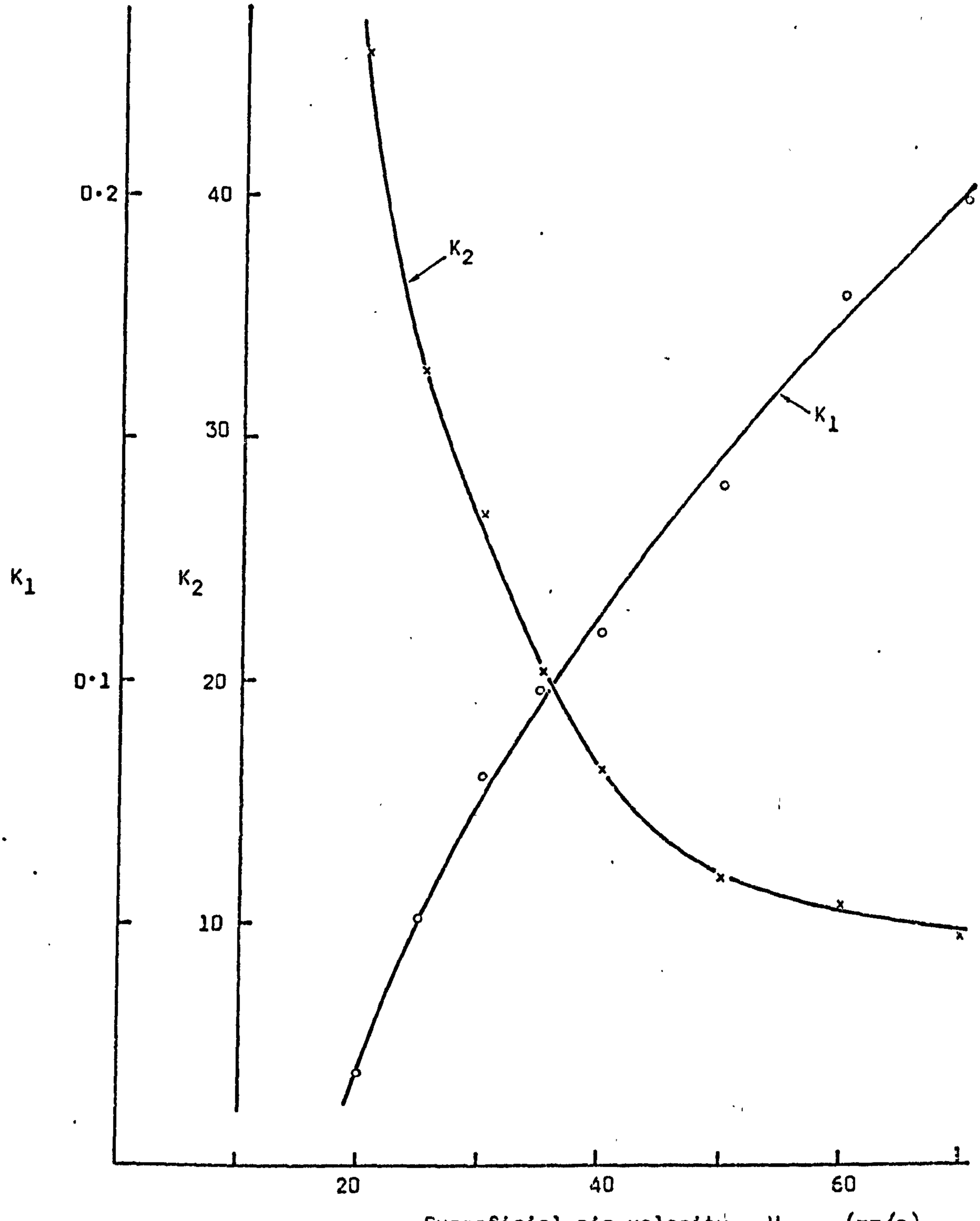

Fig. 9.12 VARIATION OF THE PARAMETERS K_1 AND K_2 WITH SUPERFICIAL AIR VELOCITY. (Data from Fig. 8.23 for Corvic flowing on a Vyon distributor.)

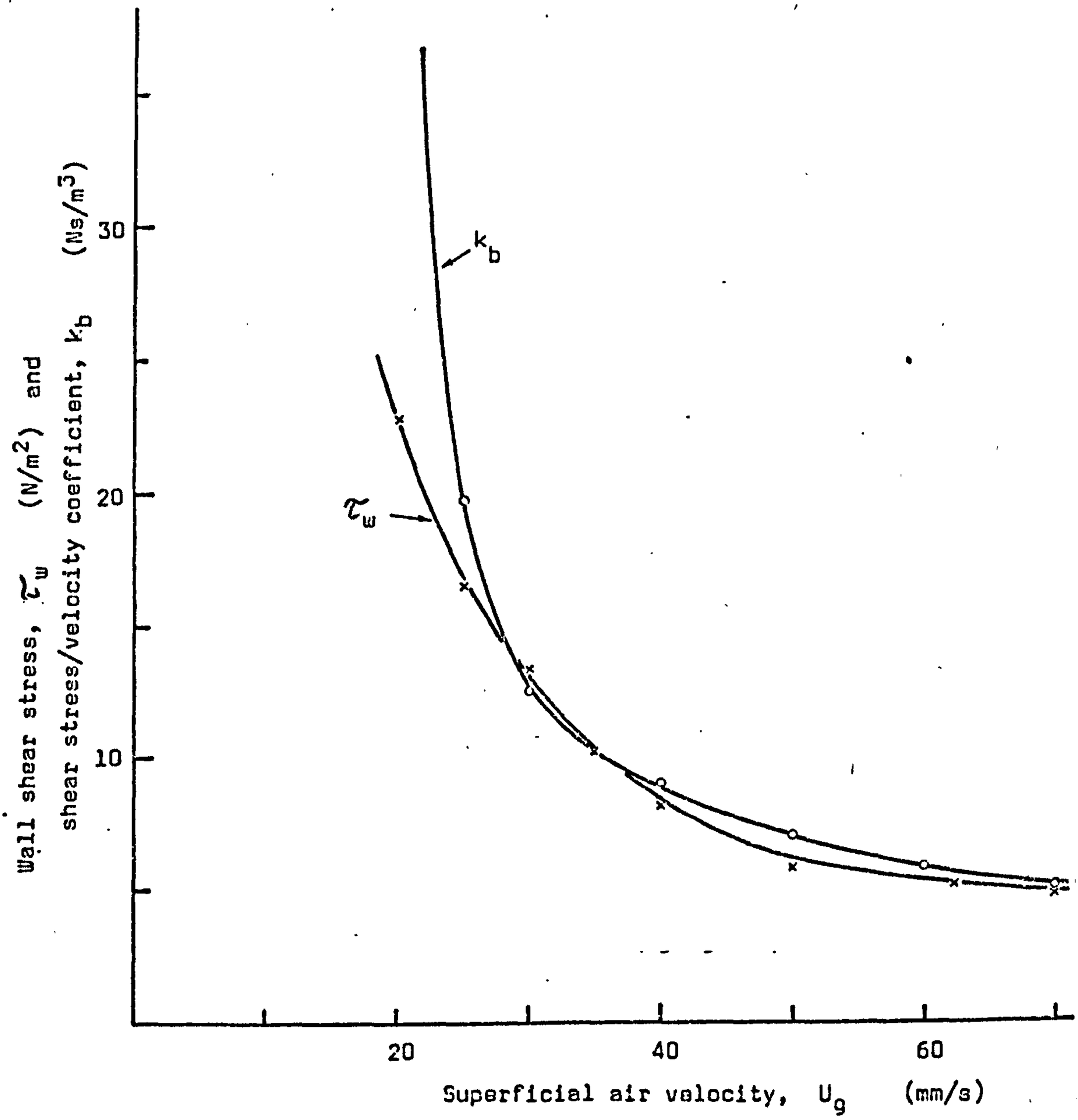

Fig. 9.13 VARIATION OF THE WALL SHEAR STRESS τ_w AND THE SHEAR STRESS/VELOCITY COEFFICIENT k_b WITH SUPERFICIAL AIR VELOCITY. (Data from Fig. 8.23 for Corvic flowing on a Vyon distributor.).

It has been mentioned previously that test results on the channel fitted with the Scandura distributor were generally less consistent than the results of the first series of tests in which Vyon was used. This meant that attempts to plot lines of $\dot{m}/h^2$ against $\sin\alpha$ from the second set of experimental data were largely unsuccessful. The approximate range of values of the parameters K_1 and K_2 was 0.13 to 0.05 and 15 to 22 respectively, as the superficial air velocity was reduced from 65 mm/s down to 25 mm/s. These ranges of K_1 and K_2 corresponded to k_b from 7.7 to 21 Ns/m^3 and τ_w from 7.4 to 11 N/m^2. Although the figures were not considered sufficiently reliable to justify plotting a graph to show the variation of these quantities with superficial air velocity, it can be seen that they are within the ranges determined from the tests with the Vyon distributor.

Clearly a great deal more experimental work needs to be carried out in order to confirm the variation of τ_w and k_b with the superficial air velocity. However, some confidence is given in the results so far obtained by comparing the plot shown on Fig. 9.13 with that produced from the data of Mori et al (Ref. M9) showing the variation of similar coefficients with U_g (Fig. 4.8, page 154). Whilst these two graphs would not be expected to be identical because of differences in the conveyed materials and in the models on which the graphs are based, there is enough similarity to suggest that as further experimental data becomes available a consistent pattern will be established.

9.5 FURTHER COMMENTS ON THE SHEAR STRESSES τ_w AND τ_b

Since no direct measurements were made of the shear stresses at the side walls of the conveying channel and at the channel base (that is, the top surface of the distributor) it is necessary to question whether the values of these stresses inferred from the mathematical model are in fact reasonable. For the charged Corvic flowing in the channel fitted with a Vyon distributor consideration of the model suggested a minimum value of the wall shear stress of around 5 to 6 N/m^2, increasing by some three or four times as the superficial air velocity was reduced towards the point at which flow ceased. In the case of the channel fitted with the Scandura distributor the wall shear stress seemed to have been rather greater, from

a minimum of around 7 N/m^2 , although it was not found to be possible to achieve the flow conditions in this second series of tests that gave wall shear stresses of more than about 11 N/m^2 .

In the proposed model the wall shear stress depends only upon the superficial velocity of the fluidising air, but the shear stress at the channel base is a function of the superficial air velocity and also of the solids flow velocity. Thus in order to calculate the shear stress at the channel base from a value of k_b it is necessary to specify the flow conditions. For example, for the Corvic flowing on the Vyon distributor in a relatively well fluidised condition (k_b = 5 Ns/m^2, say) at a rate of 3 kg/s in a 100 mm wide by 40 mm deep bed, the average shear stress at the base of the channel should be about 12 N/m^2. For a lower solids mass flowrate in a deeper bed the shear stress would of course be proportionately less, but any reduction in the superficial air velocity would cause an increase in the coefficient k_b and thus an increase in the base shear stress.

Direct measurements of the drag on the side walls of a channel conveying fluidised sand have been reported by Botterill and Bessant (Refs. B16, B17) who used a freely supported plate, fitted with a strain gauge transducer and inserted between two sections of channel wall. These authors commented that their measurements were of the same order as values predicted from shear curves and furthermore, they concluded from their results that at low solids flow velocities the drag at the distributor can be greater than that at the side walls of the channel, although at higher shear rates (that is, higher solids flow velocities, as would occur where the superficial air velocity was greater) the drag at the distributor surface could be almost negligible. It is interesting to compare these observations with the requirements of the new modelling approach developed for the flow of either sand or Corvic. For this model the shear stress at the base of the channel decreases with increasing superficial air velocity but increases with increasing solids flow velocity. This does not appear to be an unreasonable state of affairs, but seems partly to conflict with the experimental findings of Botterill and Bessant concerning the increased drag on the distributor at low shear rates. One possible cause of such annomalies in the flow behaviour of fluidised solids is segregation. McGuigan and Pugh (Ref. M6) for instance, found that whilst the shear stress

generally increased with increasing shear rate, under some conditions the reverse could occur, apparently as a result of the coarser particles tending to settle out at the bottom of the channel. However, they did not distinguish between the shear stresses at the side walls and at the channel base.

9.6 CONCLUSIONS

In this Chapter a detailed study of the correlation between the experimental data for the flow of aerated Corvic and the model proposed in Section 4.3.4 has been undertaken. Whilst it is clear that much more experimental work is necessary before suggesting acceptance of the model, the conclusion reached at this stage is that the modelling approach is at least worth examining further. The relationship amongst the three basic variables, solids mass flowrate, channel slope and the depth of the flowing bed has been represented with acceptable accuracy by a simple mathematical model in which there are just two "flexible" parameters incorporating the shear stresses at the side walls and at the base of the channel. These parameters would be functions of the superficial air velocity, the nature of the particulate solid and the roughness of the internal surfaces of the channel.

Modelling the influence of the superficial velocity of the fluidising air was perhaps less satisfactory, the approach at this stage being simply to indicate the relationship between this velocity and the parameters K_1 and K_2 by means of graphs. With further work in this area it should be possible to develop a model which takes into account directly this important variable.

PART III

CHAPTER TEN

GENERAL CONCLUSIONS

10.1 FINAL SUMMARY

The programme of study described in this thesis set out initially to collect together as much as possible of the published work relevant to the air-assisted gravity conveying of bulk particulate solids, and then from an analysis of this literature, supported by new experimental data, to develop a useful approach to the modelling of fluidised flow in inclined channels. The extent to which these objectives have been achieved is perhaps mixed. A considerable proportion of the time allocated to the programme was spent on the literature survey and, as stated in Chapter One, this is believed to have been the most extensive study yet undertaken of literature relevant to air-gravity conveying. A further substantial part of the available time was devoted to different aspects of modelling the flow of fluidised solids, leading up to the approach proposed in Section 4.3.4. Rather less time than would have been desirable was then left for experimental work, but despite this, it is felt that a worthwhile contribution has been made to available data on the flow of aerated powders in inclined channels. In addition, a useful comparative study of various types of porous materials has been undertaken, together with a series of tests on the fluidisation of a number of powders in stationary beds.

The literature survey began with a study of the fluidisation phenomena and an attempt was made to consolidate some of the enormous wealth of published information on this subject into brief discussions of areas that are relevant to the air-assisted gravity flow of powders. Perhaps the most important of these topics relates to incipient fluidisation and the prediction of minimum fluidising velocity. Correlations published by a number of authors were considered and compared and it was concluded that, for the range of particle sizes of bulk solids likely to be handled in air-gravity conveyors, the very simple expression

$$U_{mf} = 420\ \rho_p\ d_v^2$$

would usually give an adequately reliable prediction of the minimum fluidising velocity. (In this expression ρ_p is the particle density in kg/m^3 and d_v is the mean particle size in metres, giving U_{mf} in m/s.) There are of course many more complex expressions than this one, most of

which could be expected to give a slightly more accurate prediction of U_{mf}, but it could often be the case that, if such accuracy were required, it would be better to undertake a practical test on a sample of the powder in a simple fluidisation rig.

The prediction of the superficial air velocity at which entrainment of fines from the surface of a bed of fluidised powder could occur was also considered. As a result, a chart was produced (Fig. 2.13) from which could be quickly estimated the minimum fluidising velocity and the terminal velocity of particles from 20 μm up to 500 μm when fluidised with air at normal ambient conditions. It is felt that a chart of this type could be especially useful to designers of air-assisted gravity conveyors.

Further aspects of the fluidisation of bulk solids were discussed at some length and then a detailed study of the air-assisted gravity conveying of bulk solids was undertaken. It was concluded from this study that the construction of air-assisted gravity conveyors is basically very straightforward and they usually tend to operate satisfactorily (for a short time at least) irrespective of the amount of care taken over their design. However, there are a number of pitfalls to be avoided and it seems probable that the unfortunate experiences of some manufacturers and users have resulted in an unjustified wariness of what should be, for many powders and granular bulk solids, a remarkably convenient and economical method of transport.

Only one width of conveying duct was used in the present investigation and at 100 mm this was at the lower end of the scale as far as industrial applications were concerned. Whilst it would have been useful to have carried out tests in wider channels it seems unlikely that there would have been much deviation from a simple square law relationship between the solids mass flowrate and the channel width. In Section 3.2.3 a convenient "rule-of-thumb" was proposed for estimating the width of channel required for a given application and which should prove useful to designers of air-gravity conveying installations. The expression, which ought to be fairly reliable for most particulate solids normally transported in this type of conveyor, is

$$b \simeq 1.6\left(\frac{\dot{m}}{\rho_p}\right)^{\frac{1}{2}}$$

where $\dot{m}$ is the solids mass flowrate in kg/s and ρ_p is the particle density in kg/m^3, giving the width b in metres.

One of the difficulties faced by the designer of air-gravity conveyors is the lack of reliable techniques for assessing whether a given bulk solid is suitable for conveying by this method, and if so, how it will flow in the channel and what is the optimum quantity of air that should be supplied. Some mathematical equations have been proposed in the published literature but most of these appear to be of limited use without the support of experimental data which is generally not available. It is in a similar respect that the present work does not reach an entirely satisfactory conclusion, although it is felt that a significant step forward has been made. The new modelling approach presented in Chapter Four, supported by the experimental data on the flow of Corvic, suggests that it should be possible, with further experimental work, to establish a reliable method for predicting the flow behaviour of aerated particulate solids in inclined channels. The major requirement of future work is to determine the dependence of the parameters K_1 and K_2 in the proposed mathematical model on the nature of the particulate solid concerned. For instance, it may well be found that there is some correlation between these parameters and the classification of the fluidisation behaviour of the powder according to Geldart and, if this proves to be the case, work on this modelling approach will have been fully justified.

10.2 RECOMMENDATIONS FOR FURTHER WORK

Throughout the planned programme interesting avenues that appeared to be worthy of closer examination were continually opening up. These avenues covered areas of work ranging from simple tests on powders in stationary fluidised beds to a more rigorous analytical investigation of non-Newtonian fluid models for the air-assisted gravity flow of aerated powders.

Reference has been made in the present work (Section 7.5.2) to the influence of particle size on the behaviour of fluidised powder, especially with regard to their minimum fluidising velocity. Geldart (Ref. G2) has published some experimental data on the effect of particle size and size distribution but there appears to be a need for a great deal more research

in this area. Many aspects of such work would be interesting, for instance, the fluidisation of mixtures of powders having different size distributions but the same mean particle size, and also the interaction between the influences of particle size and particle density.

An important feature of commercial air-gravity conveyors that needs further study is the porous air distributor that forms the base of the conveying channel. Almost all of the materials at present available seem to be prone to deterioration through blinding of the pores on the top surface. (Blockage of the underside of the distributor should be controllable with careful filtration of the air supply.) Admittedly some suppliers of the porous materials claim that their product is less susceptible to blinding than others, but there is still a need for investigation of the features which render a given material particularly inclined to suffer deterioration in this way.

Amongst the many practical aspects of air-gravity conveying that need further investigation there are the method of feeding the powder to the channel (for example, flooded feed, or controlled feed, as by a rotary valve), control of the solids flow by a weir or sluice at the outlet end of the channel, and the use of the conveyor in process operations such as heating or cooling the conveyed material by contacting it with a gas. One practical application of this type of conveyor that seems in the literature to have been given more than its fair share of attention concerns their ability to convey powders on an upward slope. The ingenious modifications to the basic "Airslide" that have been developed for this purpose are interesting and a brief discussion of some of them has already been undertaken (Section 3.1.5) but it should be recognised that much simpler dense-phase pneumatic conveyors for lifting powders and granular bulk solids are already well established. The whole point of the air-gravity conveyor is to take advantage of the benefits of gravity to achieve a substantial saving in power consumption when transporting these materials horizontally and energy expended by investigators researching methods of defeating gravity with "airslides operating uphill" seems unlikely to be recovered in the form of useful results, except possibly with difficult materials that cannot be transported in more conventional pipeline conveyors.

Much has been written in this work on the problems created by the development of electrostatic charges during the handling of Corvic. Although the decision was taken to carry out most of the channel flow tests on the Corvic in its charged condition (in which condition it appeared to be representative of a typical slightly cohesive powder) this was largely as an expedient. Discussion with various authorities on electrostatic phenomena associated with powders revealed that this whole area of study was fraught with difficulties, ranging from the formulation of satisfactory explanations of observed behaviour, through the measurement of electrostatic charge, to attempts to achieve good repeatability of experimental results. There would be ample scope for a full study on the electrostatic charging of powders in air-assisted gravity conveyors and the control of charging by adjustment of the humidity of the fluidising air.

Probably a more important contribution to the work on air-gravity conveyors would be the acquisition and publication of experimental data relating to the fluidised flow in inclined channels of a wide variety of different bulk particulate solids. In the first instance this data should concern simply the solids mass flowrate, the channel slope, the superficial air velocity and the depth of the flowing bed, but further work involving the measurement of velocity profiles and of shear stresses on the internal surfaces of the channel should prove interesting and rewarding. Experimental data of this kind would be valuable in the further development of the modelling techniques that have been discussed in Chapter Four. Not only the fundamental model examined in the results analysis of Chapter Nine would benefit from additional research data, but also the various modelling techniques based on the flow of non-Newtonian fluids, as outlined in Chapter Four and in Appendix AIII.

PART IV

APPENDICES

APPENDIX A.I.

CHARACTERISATION OF PARTICULATE BULK SOLIDS

A.I.1 Definition of particle size, shape and size distribution.

A mass of homogeneous, spherical particles can be described by a single dimension - the particle diameter - and a mass of spherical particles of varying size can be described by a mean particle diameter together with some information on the distribution of sizes about that mean. However, where the particles are non-spherical it becomes necessary to define more carefully the parameters used for "size" and "shape".

Thus, for example, a "volume diameter" d_v can be defined as the diameter of a sphere having the same volume as the particle.

That is to say,

$$d_v = \left(\frac{6 V_p}{\pi}\right)^{\frac{1}{3}} = 1.241 V_p^{\frac{1}{3}} \qquad \text{.....A.I.1}$$

where V_p is the volume of the particle.

(It may be noted that for a cube of unit side, the "volume diameter" is 1.241, compared with the maximum dimension of the cube which is 1.732.)

In general, the manner of describing the particle size depends upon the method of measurement, and it follows that the type of particle "diameter" used should depend upon the reason for specifying it! For instance, if a particulate solid is to be used as a catalyst, the surface area of the particles is the significant quantity and therefore it is the "surface diameter" that should be used for particle size.

That is,

$$d_s = \left(\frac{A_{sp}}{\pi}\right)^{\frac{1}{2}} = 0.564 A_{sp}^{\frac{1}{2}} \qquad \text{.....A.I.2}$$

where A_{sp} is the surface area of the particle.

(Again, note that for the cube of unit side, the "surface diameter" is 1.382, so that the ratio d_v/d_s is 0.898.)

Various other particle diameters have been defined and a list of these has been published by Allen (Ref. A2). For convenience this list is reproduced here as Table A.I.1.

The ratio of any pair of the listed "diameters" (often known as a "shape factor") is found to be fairly constant over quite wide size ranges for any one material which has all been produced in the same way or derived from the same source (Ref. A2 p 80). Thus it is possible, for instance, to correlate analyses in which the coarser fraction of a material has been subjected to a sieve analysis and the sub-sieve fraction has been sized in some other way. Some typical values of these ratios (quoted in Ref. B23 Part 4) are given in Table A.I.2, but it should be emphasised that caution is required in the use of these figures, especially where the particles of the material are of extreme shapes.

To convert	Multiply by
Sieve diam. to projected area diam.	1.40
Sieve diam. to Stokes diam.	0.94
Projected area diam. to sieve diam.	0.71
Projected area diam. to Stokes diam.	0.67
Stokes diam. to sieve diam.	1.07
Stokes diam. to projected area diam.	1.50

Table A.I.2 PARTICLE DIAMETER CONVERSION FACTORS (B.S. 3406)

In an industrial situation it is probable that bulk solids comprising a large number of particles of non-uniform size would be encountered. In order to describe such a material completely it is necessary to specify some kind of "mean particle diameter" and to state the "particle size distribution".

Clearly the mean particle diameter can be defined in various ways. For example, a simple arithmetic mean could be used, or alternatively a median diameter for which 50% of the particles in the mixture are less than the stated size. The average particle size can also be defined in

Name	Symbol	Formula	Definition
Volume diameter	d_v	$V = \frac{\pi}{6} d_v^3$	Diameter of a sphere having the same volume as the particle.
Surface diameter	d_s	$S = \pi d_s^2$	Diameter of a sphere having the same surface area as the particle.
Surface volume diameter	d_{sv}	$d_{sv} = d_v^3/d_s^2$	Diameter of a sphere having the same external surface to volume ratio as the particle.
Drag diameter	d_d	$F_D = \frac{1}{2} C_D A \rho u^2$ where $C_D A = f(d_d)$	Diameter of a sphere having the same resistance to motion as the particle in a fluid of the same viscosity and at the same velocity.
		$F_D = 3\pi d_d \mu u$ for $Re < 0.2$	(d_d approximates to d_s when Re is small)
Free-falling diameter	d_f		Diameter of a sphere having the same density and the same free-falling speed as the particle in a fluid of the same density and viscosity.
Stokes diameter	d_{st}	$d_{st} = \left(\frac{d_v^3}{d_d}\right)^{\frac{1}{2}}$	The free-falling diameter of a particle in the laminar flow region ($Re < 0.2$).
Projected area diameter	d_a	$A = \frac{\pi}{4} d_a^2$	Diameter of a circle having the same area as the projected area of the particle resting in a stable position.
Projected area diameter	d_{pa}		Diameter of a circle having the same area as the projected area of the particle in random orientation. (Mean value for all possible orientations; $d_{pa} = d_s$ for convex particles)
Perimeter diameter	d_c	$d_F = d_c$	Diameter of a circle having the same perimeter as the projected outline of the particle.
Sieve diameter	d_A		The width of the minimum square aperture through which the particle will pass.
Feret's diameter	d_F		The mean value of the distance between pairs of parallel tangents to the projected outline of the particle.
Martin's diameter	d_M		The mean chord length of the projected outline of the particle.

Table A.I.1 DEFINITIONS OF PARTICLE SIZE (Ref. A2)

terms of the diameter of a particle of average surface area or of average volume. Thus, for example, the average surface area of a number of particles is given by

$$A_{sm} = \frac{1}{N}\Sigma(\pi d_s^2) \qquad \text{.....A.I.3}$$

so that the diameter of this particle of average surface area (the "surface-mean diameter") is given by

$$d_{sm} = \left(\frac{A_{sm}}{\pi}\right)^{\frac{1}{2}} = \frac{1}{N}\Sigma d_s^2 \qquad \text{.....A.I.4}$$

Similarly the "volume-mean diameter" is given by

$$d_{vm} = \left(\frac{6V_{pm}}{\pi}\right)^{\frac{1}{3}} = \frac{1}{N}\Sigma d_v^3 \qquad \text{.....A.I.5}$$

These and other definitions of mean particle size are listed in Table A.I.3.

The assumption that the particles in a bulk solid are of spherical shape is also obviously unrealistic in the majority of industrial situations and consequently some means of describing the shape is necessary. A number of terms are used to describe qualitatively the shape of individual particles (see for example Ref. A2 p.76) such as granular, acicular, flaky and so on. Defining the shape of non-spherical particles in mathematical terms is not easy but many attempts have been made to establish the use of shape factors to indicate the extent to which particles differ from the spherical.

Probably the most commonly used of these shape factors is the "sphericity" ϕ_s, defined as the reciprocal of the ratio of the surface area of a particle to that of a sphere of the same volume.

That is,

$$\phi_s = \left.\frac{\text{surface area of sphere}}{\text{surface area of particle}}\right\} \text{of the same volume}$$

It will be noted that ϕ_s must be less than unity and that

Name	Symbol	Formula	Definition
Median	d_{wm}		The particle diameter for which 50% of the particles in the mixture are less than the stated size.
Arithmetic mean	d_{am}	$\frac{1}{N}\Sigma d_v$ or $\frac{1}{N}\Sigma d_s$	
Geometric mean	d_{gm}	$(d_{v_1} . d_{v_2} . d_{v_3} \ldots d_{v_N})^{\frac{1}{N}}$ or $\exp(\frac{1}{N}\Sigma \ln d_v)$	
Surface mean	d_{sm}	$(\frac{1}{N}\Sigma d_s^{\,2})^{\frac{1}{2}}$	The diameter of a particle having a surface area equal to the average for all the particles in the mixture.
Volume mean	d_{vm}	$(\frac{1}{N}\Sigma d_v^{\,3})^{\frac{1}{3}}$	The diameter of a sphere having the average volume for the mixture.
Surface-diameter mean	d_{sdm}	$\frac{\Sigma d_s^{\,2}}{\Sigma d_s} = \frac{d_{sm}^{\,2}}{d_{am}}$	The diameter of a sphere having a ratio of surface to diameter equal to the average for the mixture.
Volume-diameter mean	d_{vdm}	$\left(\frac{\Sigma d_v^{\,3}}{\Sigma d_v}\right)^{\frac{1}{2}} = \left(\frac{d_{vm}^{\,3}}{d_{am}}\right)^{\frac{1}{2}}$	The diameter of a sphere having a ratio of volume to diameter equal to the average for the mixture.
Volume-surface mean	d_{vsm}	$\frac{\Sigma d_v^{\,3}}{\Sigma d_s^{\,2}} = \frac{d_{vm}^{\,3}}{d_{sm}^{\,2}}$	The diameter of a sphere having a ratio of volume to surface equal to the average for the mixture (that is, the diameter of a sphere having the same volume as the particle of average surface area for the mixture).

Table A.I.3 DEFINITIONS OF MEAN PARTICLE SIZE (Ref. K2 p.251)

$$\phi_s = \frac{\pi d_v^2}{A_{sp}} = \left(\frac{d_v}{d_s}\right)^2 \qquad \text{.....A.I.6}$$

and thus d_v is always less than d_s for a non-spherical particle.

Also, from equations A.I.1 and A.I.2,

$$\phi_s = \left(\frac{1.241\, V_p^{\frac{1}{3}}}{0.564\, A_{sp}^{\frac{1}{2}}}\right)^2 = 4.838\, \frac{V_p^{\frac{2}{3}}}{A_{sp}} \qquad \text{.....A.I.7}$$

from which it can be seen that the determination of sphericity requires the measurement of the volume and the surface area of particles.

A rigorous discussion of shape factors is undertaken by Allen in Ref. A2.

Another parameter that is of importance in many practical applications is the surface area of a particle divided by its volume; that is, the surface area per unit volume, or "specific surface".

For a single particle the specific surface is thus given by

$$S_p = (\pi d_s^2)/(\tfrac{\pi}{6} d_v^3)$$

from which

$$S_p = \frac{6}{\phi_s d_v} \qquad \text{.....A.I.8}$$

It has been mentioned already that in order to describe completely a polydisperse material it is necessary to state the particle size distribution in addition to specifying a mean or average particle diameter. For such a material it is generally more convenient to present information on the size distribution graphically as a histogram or a fractional percentage plot.

A suitable histogram (Fig. A.I.1) can be developed by constructing rectangles over each class interval (the widths of which would usually be chosen in geometric progression), the area under the rectangles being

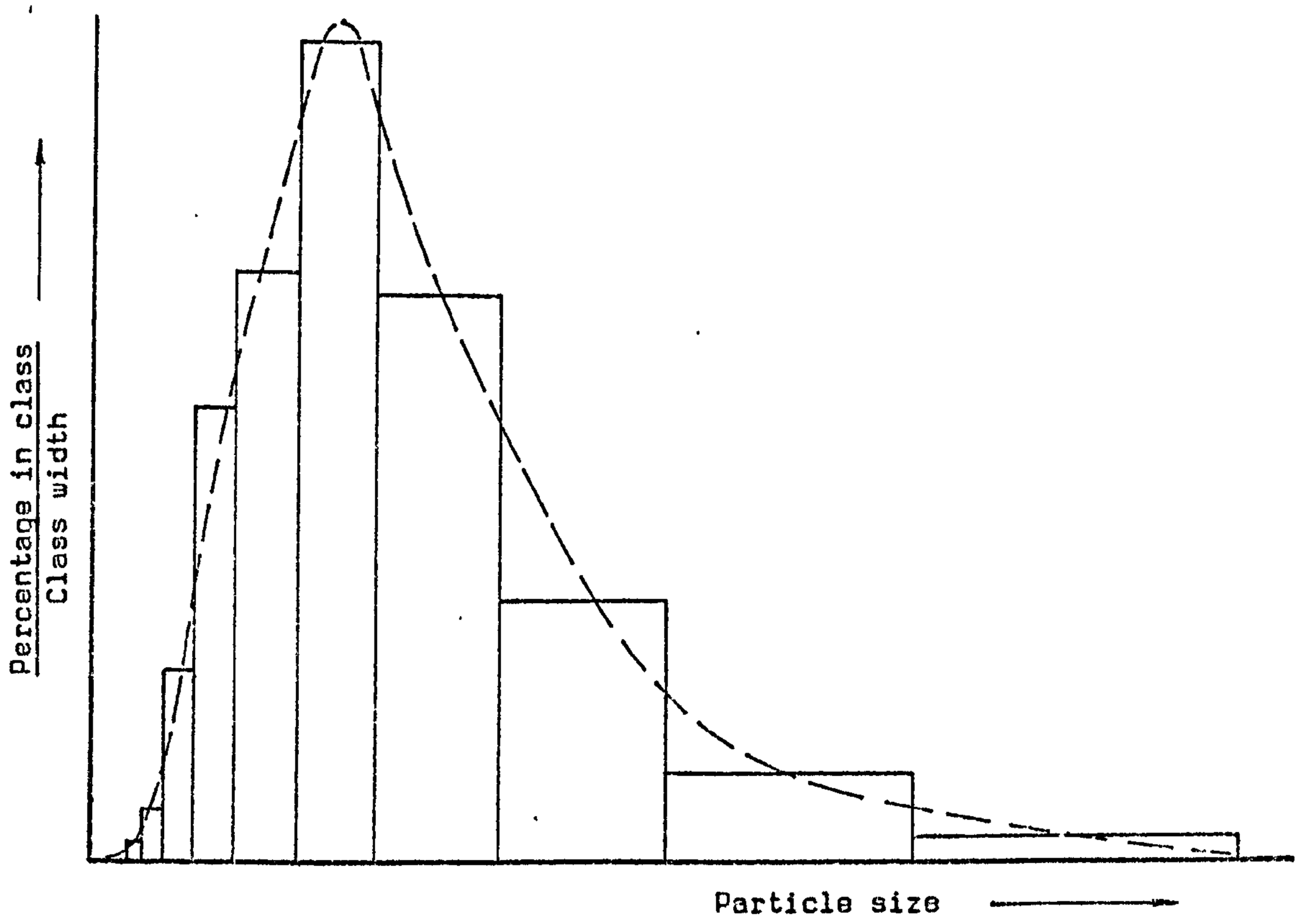

Fig. A.I.1 RELATIVE PERCENTAGE FREQUENCY DISTRIBUTION BY NUMBER.

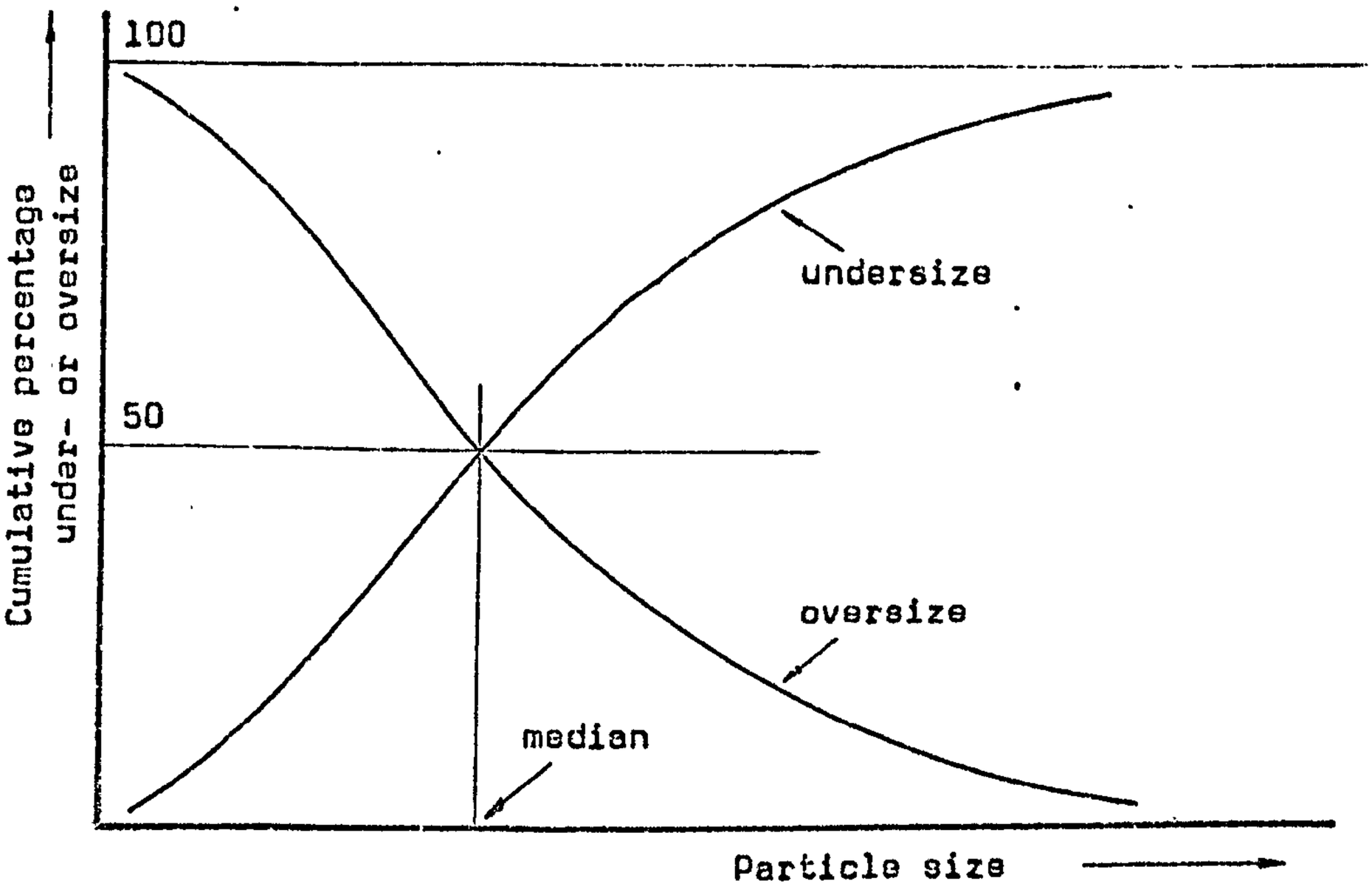

Fig. A.I.2 PARTICLE SIZE DISTRIBUTION PRESENTED AS PLOTS OF CUMULATIVE UNDER- AND OVERSIZE.

proportional to the percentage of particles in the classes (Ref. A2 p.91).

A smooth curve drawn through the histogram of Fig. A.I.1 would yield a frequency distribution, but it is often more useful to present the data as a cumulative plot (Fig. A.I.2). In this case particle size is plotted along the horizontal axis and the ordinate represents cumulative percentage undersize or oversize. The principal advantages of this type of graph are that values not determined experimentally are reliably predicted, and the median size can be read off directly.

It is usually worthwhile plotting cumulative percentage graphs on log-log axes as it frequently happens that a linear relationship results. The reason for this is that many practical particulate solids follow approximately a Gaussian or normal distribution for log d_v, corresponding to a skew distribution of the particle size itself (Ref. K2 p.253).

A.I.2 Measurement of particle properties.

For a full and detailed discussion of the very complex science of particle size analysis reference should be made to one of the specialised works on the subject, such as that of Allen (Ref. A2) or Jelinek (Ref. J2). Useful guidance can also be found in the relevant British Standards Institution publications (Refs. B23, B24). The following notes are restricted to methods of sampling and particle measurement that have been used in the present research programme, and serve merely to outline the procedures actually adopted.

a. SAMPLING

Before making measurements of any kind on a sample of a particulate bulk solid, great care has to be taken to ensure that the sample is truly representative of the total quantity of the material being examined. The importance of sampling cannot be over-emphasised as there is clearly little point in going to a great deal of trouble to obtain an accurate size analysis if the sample used is not of identical composition to the remainder of the material. The problem is perhaps put into perspective

when it is appreciated that for a microscope analysis a few grains of powder may have to be assumed to represent a quantity of a tonne or more of the parent material.

Where possible the sample should be taken from a moving stream of the particulate solid in question by diverting the whole stream for a series of short intervals of time spaced over the period of flow of the complete batch. This technique minimizes the effects of segregation which may occur either across a section of the flow (therefore causing trouble if only part of the flow is sampled) or within the batch giving rise to a variation of composition with time.

Smaller quantities of material can be divided to produce the required sample size by one of a number of techniques. One method that is still widely practised is the familiar "cone-and-quartering" but this has been shown to be rather unreliable as a result of uneven segregation of particles as the heap of material is poured. Much better results are likely to be obtained with some form of spinning riffling device or rotary sample splitter. However, failing these, it is possible to obtain a reliably divided sample from a stationary riffler or chute splitter, although such devices may be prone to some operator bias.

b. SIEVE ANALYSIS

The most popular (and cheapest) method of particle size analysis, especially with relatively coarse materials, is sieving, although the actual mechanism of the process and the influence of such variables as aperture shape and spacing, and the method of vibration seem to be not well understood (Ref. S1).

Essentially sieve analysis is the successive classification of the sample on sieves of suitable mesh size. The number of sieves required to give a satisfactory cumulative size distribution would normally be about five to eight, the mesh sizes being selected to conform to a $\sqrt{2}$ series or, for more accurate work, a $\sqrt[4]{2}$ series.

The lower size limit for material on a wire mesh sieve is around 50 μm, and the recommended mass of sample to be used on standard 8 inch diameter

sieves is 50 g for materials of true density between 1200 and 3000 kg/m^3, and 100 g for materials of density greater than 3000 kg/m^3 (Ref. B24).

There has been a certain amount of debate about whether an experienced operator sieving by hand can produce more consistently reliable results than a mechanical sieve-shaker. However, there is no doubt that the sieve-shaker is quicker, cheaper and generally more convenient. The method of use of the sieve-shaker, particularly with regard to the length of time for which the sieve stack is vibrated, is detailed in the relevant British Standard (Ref. B24).

Measurement of the quantity of material retained on each sieve in the stack then allows direct determination of the cumulative weight percentages under- and oversize.

The sieve size, d_A, is the minimum square aperture through which the particles can pass, and may be related approximately to other "particle diameters" by the factors given in Table A.I.2. As has been pointed out previously (Section 2.7.1), the volume-surface mean diameter is probably a more relevant parameter than the median size for fluidisation studies and can be determined fairly reliably from a sieve analysis by using the expression

$$d_{vsm} \simeq \left(\Sigma \frac{x}{d_A}\right)^{-1} \qquad \text{.....A.I.9}$$

where x is the weight fraction and d_A is the sieve aperture size (Ref. G6.).

c. PHOTOSEDIMENTOMETRY

An alternative method of determining the size of particles involves observation of their rate of free fall in a gravitational field.

For a spherical particle falling at terminal velocity under conditions such that the Reynolds number is low, the viscous drag on the particle is given by Stokes law as

$$F_D = 3 U_t \pi d \mu \qquad \text{.....A.I.10}$$

Now the gravity force on the particle can be expressed as

$$F_G = \frac{\pi}{6} d^3 (\rho_p - \rho) g \qquad \text{.....A.I.11}$$

so that combining these equations we have for a particle falling at steady velocity U_t

$$d = \left(\frac{18 \mu U_t}{(\rho_p - \rho) g} \right)^{\frac{1}{2}} \qquad \text{.....A.I.12}$$

Although the discussion up to this point applies to spherical particles, it is clear that irregular shaped particles will also tend to reach a steady terminal velocity which is dependent upon their size and which in fact allows the definition of a parameter known as Stokes diameter.

The Stokes diameter, d_{st}, of a particle is defined as the diameter of a sphere of the same material which, falling in the same fluid, has the same terminal velocity as the particle.

Thus, for fine particles in general, the sedimentation equation can be written as

$$d_{st} = \left(\frac{18 \mu U_t}{(\rho_p - \rho) g} \right)^{\frac{1}{2}} \qquad \text{.....A.I.13}$$

and it is on this equation that size analysis by sedimentation methods is based.

A reasonable indication of the upper size limits of particles that can be examined by this method is given by the expression

$$d_{crit} = \left(\frac{3.6 \mu^2}{(\rho_p - \rho) \rho g} \right)^{\frac{1}{3}} \qquad \text{.....A.I.14}$$

which is derived from the supposition that the laminar flow condition implicit in Stokes law begins to break down at a Reynolds number of 0.2 (Ref. A2 p.157). Some typical values of this critical particle size, which is of course dependent upon the fluid used, are given in Table A.I.4.

Material	Critical diameter (μm)		
	Settling in water	Settling in air	Settling in ethylene glycol
Sand (ρ_p = 2700 kg/m^3)	60	31.6	560
PVC (ρ_p = 1400 kg/m^3)	97.2	39.4	1000

Table A.I.4 APPROXIMATE UPPER SIZE LIMITS FOR PARTICLES IN SEDIMENTATION ANALYSIS (From equation A.I.14)

In the case of polydisperse systems of particles the situation is very complex, with interactions occurring amongst the particles themselves and between the particles and the boundary walls, all of which may influence observed settling velocities (Ref. A2 p.159, 176). Nevertheless, a quite reliable size analysis can be made since for an initially homogeneous system the mass concentration at any point will remain constant only until the largest particles present have fallen past that point, and thereafter will gradually decrease until all the particles have settled. Thus, from Fig. A.I.3 it is seen that the size of the largest particle in the system would be given by

$$d_{st_{max}} = \left(\frac{18\,\mu H}{(\rho_p - \rho)\,g\,t_o}\right)^{\frac{1}{2}} \qquad \text{.....A.I.15}$$

where H is the distance from the surface of the sedimentation fluid to the measurement zone and t_o is the time after which the concentration on XX first begins to fall. At any instant subsequently the mass concentration on XX will depend upon the proportion of particles of diameter less than that given by equation A.I.15 for the time interval concerned.

The wide-angle scanning photosedimentometer (WASP), illustrated in Fig. A.I.4, is an instrument which will determine the relationship between mass concentration, time and depth below the surface, thus allowing a full particle size analysis to be carried out. In essence the WASP comprises a single light source which provides two similar beams of light directed onto two separate photocells. One photocell forms the

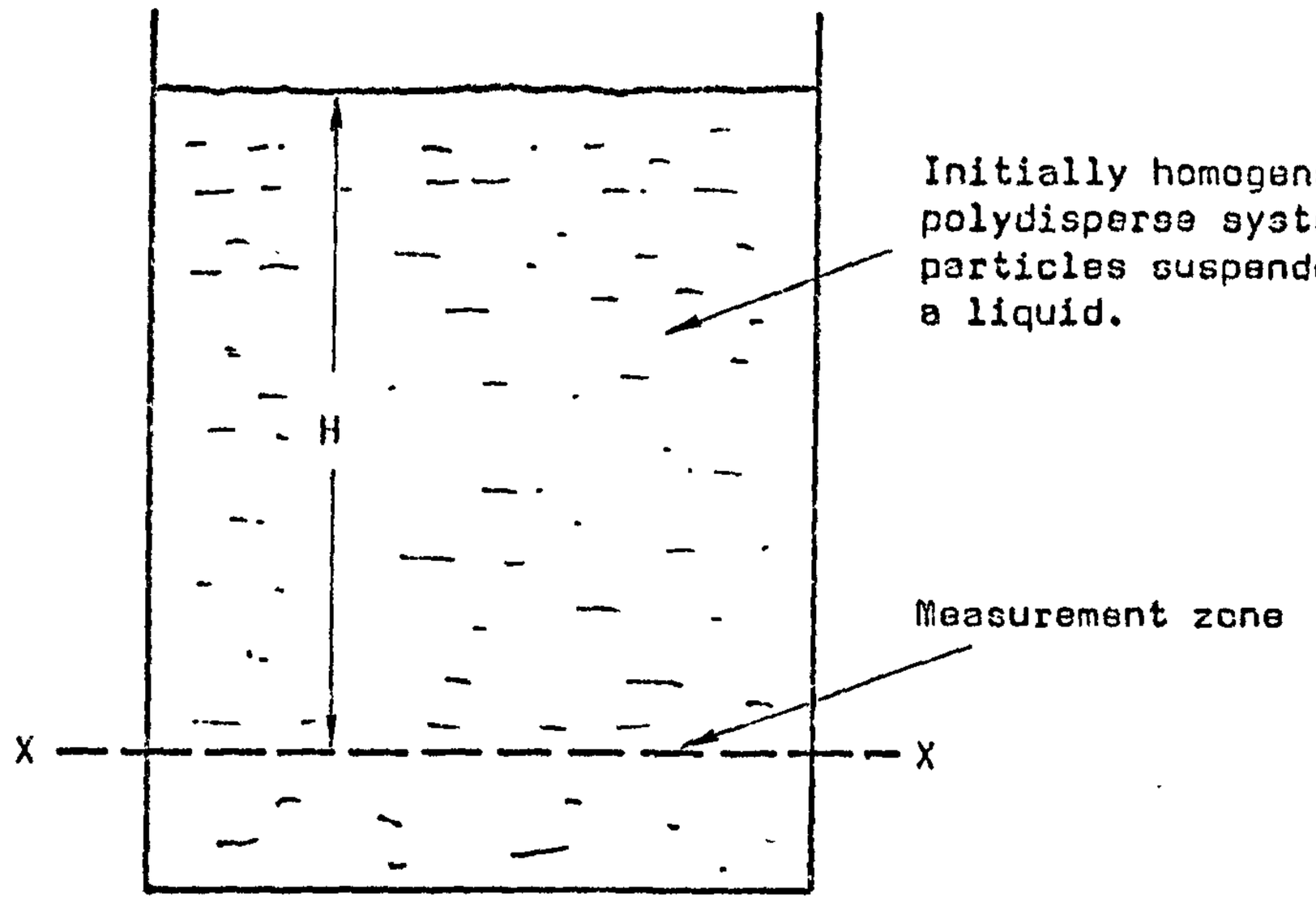

Fig. A.I.3 PARTICLE SIZE ANALYSIS BY SEDIMENTATION.

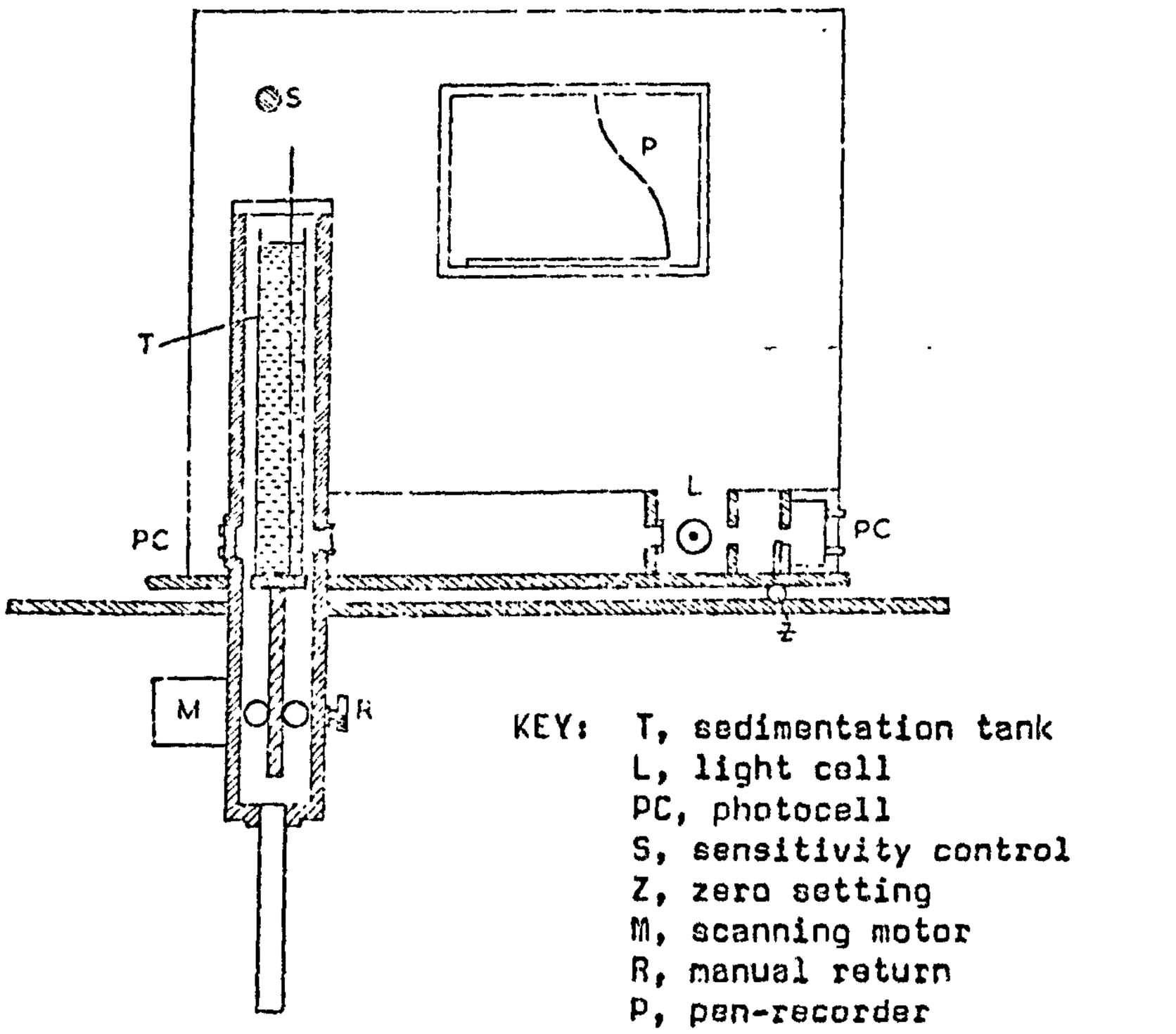

Fig. A.I.4 WIDE-ANGLE SCANNING PHOTOSEDIMENTOMETER (WASP) (Ref. A2)

reference (adjustable using optical filters) whilst the other receives the beam of light attenuated by its passage through the suspension. A pen recorder indicates the difference between the outputs of the two photocells, thus showing a high reading initially for the homogeneous suspension and zero when all the particles have settled. An additional refinement is the scanning device which speeds up the analysis considerably by allowing the light beam to scan the suspension vertically at a rate of 10 mm/min.

The procedure for the use of the WASP is summarised below:-

1. Using a clean sedimentation tank containing clear dispersant, balance the two photocells to give zero output.
2. Adjust sensitivity to give FSD with the filter/stop turned to the "stop" position.
3. Add the prepared sample of powder to the dispersant to give an optical density of about 0.5 to 0.7, and stir the suspension until a reproducible maximum is obtained.
4. Start chart of chart recorder.
5. Switch on scanning device, and allow analysis to proceed until surface of dispersant passes through the light beam (shown by a large peak on the chart as the beam is deflected away from the photocell).

Analysis of the output trace from the pen recorder, following the method set out by Allen (Ref. A2 p.214) then allows a plot to be made of cumulative percentage under- or oversize against Stokes diameter.

d. OPTICAL MICROSCOPY

As a technique for size analysis of particulate solids, optical microscopy has become well established for particles ranging in size from about 0.8 μm up to 150 μm (Ref. B23 Part 4). It has the advantage of allowing examination and measurement of individual particles of the material in question, and the method can often be used where other techniques fail.

Disadvantages may be summarised as:

1. Difficulty of obtaining a very small representative sample for study.
2. Small depth of focus.
3. Time consuming procedure for counting particles.

Numerous variations on the basic technique have been used with a view to minimising the problems, so that there is a considerable choice of method available to the analyst. Many of these different approaches have been reviewed by Allen (Ref. A2). In the present work only the simple manual method of particle sizing, using a conventional bench microscope, is considered.

The basic procedure for size analysis uses a microscope fitted with a micrometer stage and an eyepiece in which a glass disc engraved with a suitable scale is positioned against the field stop. This ocular scale is calibrated against a linear scale engraved on a microscope slide by bringing the two images into sharp coincidence and the engraved slide is then replaced by a slide carrying the prepared powder sample. The sample is scanned in strips, each particle being sized and counted as its image passes over the scale.

A linear scale in the eyepiece gives Feret's diameters of the particles examined, but there have been a number of alternative forms of graticule developed which enable the particle images to be compared with engraved circles, thus giving projected area diameters. One of these, shown with its relative dimensions in Fig. A.I.5, has been adopted as the British Standard graticule (Ref. B23 Part 4).

The full procedure to be followed when carrying out a size analysis can be found in various publications (for example, Refs. B23 Part 4; P8) but a summary is given below:-

1. With the graticule in place in the microscope eyepiece, adjust the magnification so that the diameters of the reference circles correspond to the size range of the particles to be examined.
2. Select a suitable regular pattern of sample fields in order

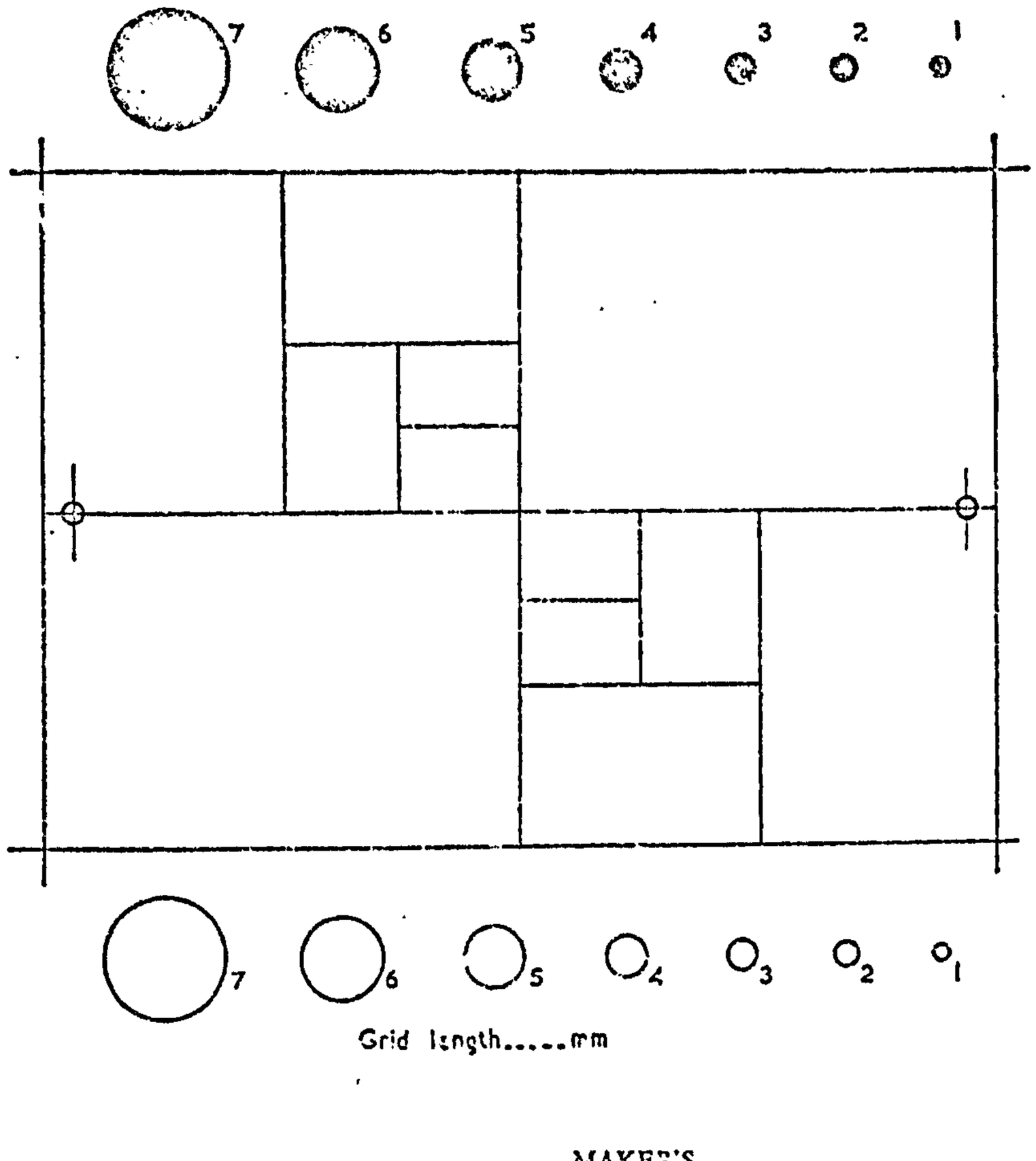

B.S. 3625 MAKER'S SYMBOL

Relative dimensions of British Standard Graticule	
	Numerical value (units)
Grid length	64
Grid breadth	45.3
Distance between calibration marks	60.4
Diameter of circle 1	1.00
2	1.41
3	2.00
4	2.83
5	4.00
6	5.66
7	8.00

Fig. A.I.5 BRITISH STANDARD GRATICULE (BS 3265) (Ref.B23 Part 4).

to cover the whole sample of powder on the slide. (This step is simplified by using a suitably engraved slide or counting cell.)

3. Adjust the micrometer stage to position the graticule in the centre of the first sample field.
4. For particles within the graticule area (and on the boundary lines on two adjacent sides) count the number within each size class by visual comparison with the graticule circles.
5. Repeat the counting of particles in this way with the graticule positioned at the centre of each field area in turn until the whole sample of powder on the slide has been scanned. (Note: the total number of particles of all size classes counted should be not less than 625, and the number of fields examined for any size class should preferably be not less than 24.)

The size distribution can then be determined by using the expression

$$w_r = \frac{100(N_r d_r^3/n_r a_r)}{\Sigma (N_r d_r^3/n_r a_r)} \qquad \text{.....A.I.16}$$

which gives the percentage weight w_r in each class size, where N_r is the total number of particles in a class of mean size d_r and $n_r a_r$ is the field area scanned.

A.I.3 Other properties of particles and beds: voidage, bulk density, angle of repose.

Before entering into any discussion of the flow of air through fixed or free beds of particles it is necessary to establish definitions of a number of parameters characterising the bed and the particles of which it is comprised.

For a packed bed of solid particles we can define a VOIDAGE (also called POROSITY or VOID FRACTION) as

$$\varepsilon_o = \frac{\text{volume of voids}}{\text{total volume of bed}} \qquad \text{.....A.I.17}$$

Thus in a bed of unit volume, the volume of solid particles is $(1-\varepsilon_o)$.

Some typical values of fractional solids content $(1 - \varepsilon_o)$ in packed beds have been collected by Brown and Richards (Ref. B26), ranging from 0.52 for regular cubic packing of spheres to 0.74 for regular hexagonal packing of spheres. Values of random packing of spherical particles and closely graded irregular particles would normally be between these extremes, inclining towards the lower value for looser packings, and a reasonable average figure is about 0.62 for spheres or slightly less for irregular spheroidal particles. However, for materials comprising particles of extreme shape, and especially for fine cohesive powders, the fractional solids content may be very much lower; down to 0.1 or even less (Ref. B26).

The BULK DENSITY of the bed of particles, defined as the total volume of the bed divided by its mass, can be expressed in terms of the voidage and particle density as

$$\rho_b = (1-\varepsilon_o)\rho_p \qquad \text{.....A.I.18}$$

The determination of the voidage and bulk density of a bed of particulate material clearly requires a knowledge of the mass of the bed, its total volume and the volume of the solid particles. The measurement of each of these quantities is essentially straightforward, the problems arising more from the need to decide the conditions under which the volumes should be measured than from the actual measuring techniques. In the case of particle volume, a liquid displacement method (for example, using a standard specific gravity bottle) would normally be satisfactory, but difficulties arise with materials that are porous or that have internal voids since the definition of particle volume becomes uncertain.

With bulk density the problem of definition is even greater since with any particulate material the voidage, and therefore the bulk density, depends upon the packing arrangement. Some attempts have been made to establish a standardised method for determining bulk density so that some uniformity can be maintained amongst quoted values. For instance, the volume of a given mass of powder in a vessel could be measured

after subjecting it to a set "packing" procedure, such as dropping the vessel a number of times from a height of one or two centimetres.

"Minimum bulk density" is a useful parameter which may be defined in terms of the loosest possible stable packing arrangement that can exist in the material. It is measured by fluidising a sample of the material in a suitable vessel and then slowly shutting off the air in order to determine the maximum volume that the sample can occupy with zero airflow. Naturally the measurement of the minimum bulk density of particulate bulk solids that do not fluidise well presents some difficulties, but one possible method is to place a sample of the material in a closed vessel and aerate it by shaking in order to estimate the maximum volume that the sample can occupy.

When the particulate material is actually fluidised its "bulk density" is of course less than the "minimum" previously defined, and its actual value will then depend on the superficial velocity of the fluidising air. Therefore in any situation involving the flow of fluidised particulate solids the bulk density may be a somewhat indefinite parameter and caution should be exercised in its use. (For further discussion on this, see Section 3.4.3.)

Various other properties of bulk particulate solids have been defined when attempting to characterise their behaviour under different conditions. For instance, tests to determine tensile strength may give an indication of the cohesiveness of the material, and this property together with shear strength is obviously of interest when attempting to predict how a bulk solid will flow under gravity (Ref. B26 p.82). Also very relevant to the gravity flow of powders is the property known as ANGLE OF REPOSE which is the maximum angle to the horizontal made by the sides of a stable heap of the powder. Different methods of forming the heap of powder have been considered by Train (Ref. T2) since the method used may well influence the maximum angle that can be measured. Angles of repose of "free-flowing" particulate solids are typically within the range 30^{o} to 45^{o}. (Some values for various industrial materials are listed in Ref. K10 p.370)

As has been described in Section 3.1.1, aeration of a heap of particles can result in a substantial reduction in the angle of repose, in some cases of very free-flowing materials causing the heap to flow outwards until it is almost level. Whilst it is possible to conceive of a "fluidised angle of repose" as a parameter characterising the ability of an aerated powder to flow, the angle is likely to be very small and accurate measurement of it would present considerable practical difficulties, especially with powders that are slightly cohesive and therefore do not fluidise well.

APPENDIX A.II

MATHEMATICAL MODELS FOR GAS FLOW THROUGH BEDS OF PARTICLES

A.II.1 Pressure drop through fixed beds

The analytical approach leading to the development of various forms of the so-called Carman-Kozeny equation for flow in packed beds is now well established. (See for example, Ref. K2, page 262 et seq.)

One version of the Carman-Kozeny equation gives the pressure drop across a packed bed in terms of the thickness h, voidage ε_o, specific surface S_b of the bed, dynamic viscosity μ_g, and superficial velocity U of the flowing fluid, as

$$\Delta p_b = k\left(\frac{1}{\varepsilon_o^3}\right) S_b^2 \mu_g Uh \qquad \text{.....A.II.1}$$

where k is an empirical coefficient.

Substituting for the specific surface S_b in terms of the voidage of the bed ε_o, sphericity ϕ_s and volume diameter d_v of the particles that comprise it, leads to

$$\Delta p_b = k' \frac{(1 - \varepsilon_o)^2}{\phi_s^2 \varepsilon_o^3} \cdot \frac{\mu_g Uh}{d_v^2} \qquad \text{.....A.II.2}$$

the coefficient k' being found to have a value usually between 130 and 200. The value given by Ergun (Ref. E2) from correlation of his own experimental data and that of other workers is 150.

The analysis considered up to now is based on laminar flow through the bed, but as the velocity of the fluid is increased the nature of the flow between the particles changes gradually from laminar to turbulent. Turbulence is likely to occur initially in the larger voidage channels, extending eventually to the smaller ones.

An alternative approach leads to an expression for pressure drop in terms of the kinetic energy of the flowing fluid, which is thus analogous to

the Darcy formula for head loss in closed conduits.

Thus

$$\Delta p_b = 3k_f\left(\frac{1-\varepsilon_o}{\phi_s \varepsilon_o^3}\right)\frac{h\rho_g U^2}{d_v} \qquad \text{.....A.II.3}$$

where k_f is a dimensionless friction coefficient for the void passages, corresponding to the Darcy friction factor for closed conduits.

From equation A.II.3

$$k_f = \frac{1}{3}\left(\frac{\phi_s \varepsilon_o^3}{1-\varepsilon_o}\right)\frac{\Delta p_b}{h}\cdot\frac{d_v}{\rho_g U^2} \qquad \text{.....A.II.4}$$

It might be anticipated that k_f would be a function of a Reynolds number for the bed. Various dimensionless groupings of the relevant bed parameters might be chosen as the Reynolds number, one such group being

$$Re_b = \frac{2}{3}\left(\frac{\phi_s}{1-\varepsilon_o}\right)\frac{d_v U}{\nu_g} \qquad \text{.....A.II.5}$$

As in the case of the Darcy formula for pipe flow, equation A.II.3 derives from a general analysis of the flow through the system and should therefore be applicable whether the flow is laminar or turbulent, provided that an appropriate value of the coefficient k_f is used. It is thus possible to derive an expression relating k_f and Re_b by combining equations A.II.2, A.II.3 and A.II.5 and simplifying as

$$k_f = \frac{k''}{Re_b} \qquad \text{.....A.II.6}$$

It is found that for highly turbulent flow the value of k_f tends to become constant (as the pressure drop becomes proportional to U^2) and an empirical relationship has been proposed by Ergun (Ref. E2) which seems to correlate available experimental data quite well -

$$k_f = \frac{100}{3Re_b} + 0.58 \qquad \text{.....A.II.7}$$

This expression is shown in Fig. A.II.1 plotted to a log-log scale, indicating that the transition from laminar to turbulent flow in the

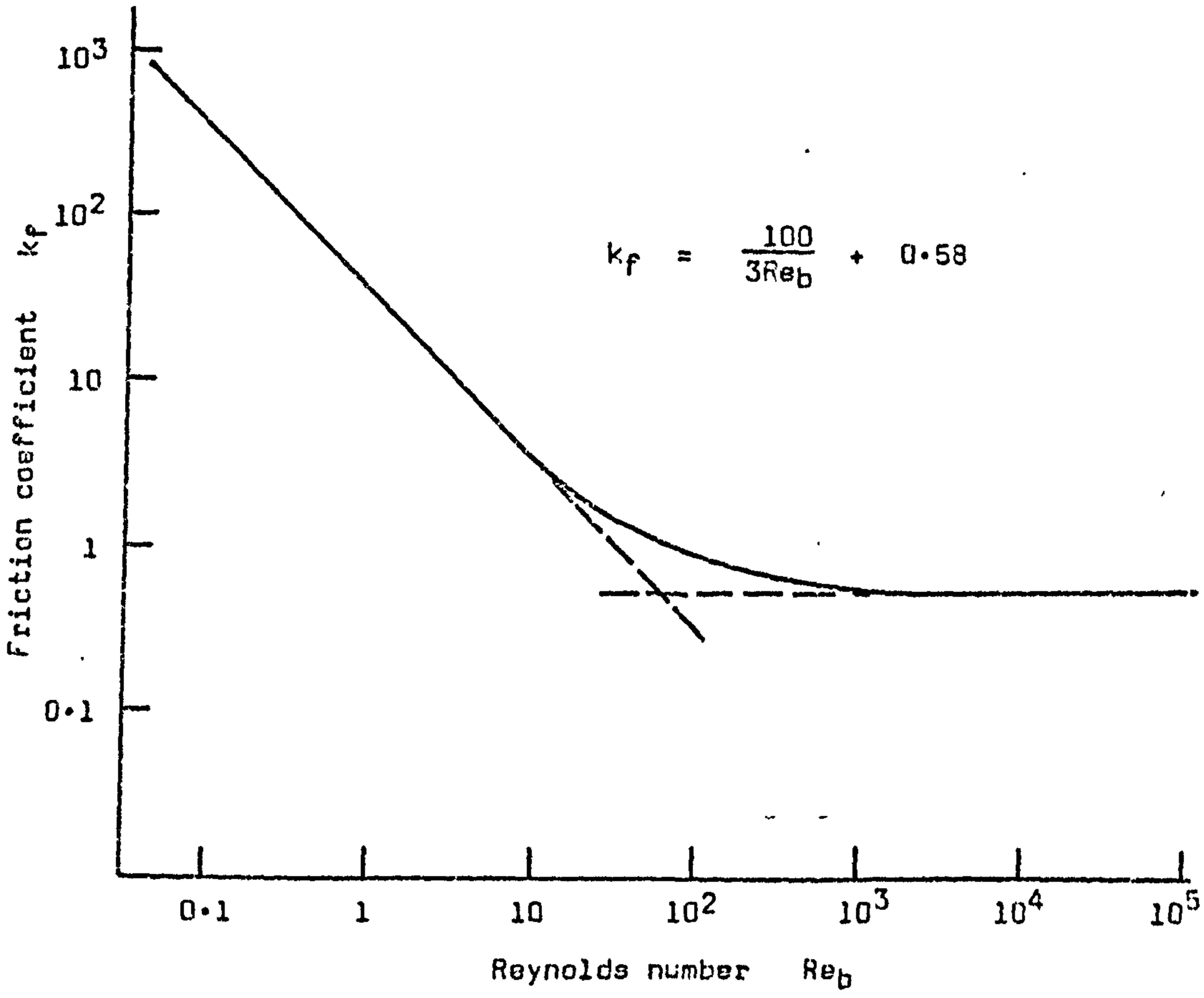

Fig. A.II.1. DIMENSIONLESS PLOT OF FRICTION COEFFICIENT, k_f, AGAINST REYNOLDS NUMBER, Re_b, FOR FLOW THROUGH A PACKED BED.
(After Ergun, Ref. E2)

packed bed occurs over a range of values of Re_b given approximately by

$$10 < Re_b < 1000$$

Now substituting equation A.II.7 into equation A.II.3 we get a general equation for pressure drop as

$$\frac{\Delta p_b}{h} = \frac{1 - \varepsilon_o}{\phi_s \varepsilon_o^3} \cdot \frac{\rho_g U^2}{d_v} \left(\frac{100}{Re_b} + 1.75 \right) \qquad \text{.....A.II.8}$$

which on expanding becomes the full Ergun equation

$$\frac{\Delta p_b}{h} = 150 \frac{(1 - \varepsilon_o)^2}{\phi_s^2 \varepsilon_o^3} \cdot \frac{\mu_g U}{d_v^2} + 1.75 \frac{1 - \varepsilon_o}{\phi_s \varepsilon_o^3} \cdot \frac{\rho_g U}{d_v} \qquad \text{.....A.II.9}$$

It will be noted that this expression represents the pressure drop as the sum of the viscous effect and the kinetic energy effect.

Although strictly this analysis has been developed on the basis of particles of the same size, the more general case of a bed of particles of similar shape but non-uniform size could be covered by the use of a volume-surface mean diameter d_{vsm} in place of the volume diameter d_v.

A.II.2 Fluidised beds - the prediction of minimum fluidising velocity

When the bed of solid particles is fully supported by the upward flowing gas, the total gravity force on the bed can be expressed as

$$W_b = (\rho_p - \rho_g) g A h (1 - \varepsilon) \qquad \text{.....A.II.10}$$

where ρ_p and ρ_g are the densities of the solid particles and of the fluidising gas respectively, A is the cross-sectional area of the fluidised bed, and h and ε are the depth and voidage of the bed.

The term $h(1 - \varepsilon)$ remains constant irrespective of the expansion of the bed so that the equation can be written in terms of the conditions at the onset of fluidisation as

$$W_b = (\rho_p - \rho_g)\, g\, A\, h_{mf}\, (1 - \varepsilon_{mf}) \qquad \text{.....A.II.11}$$

If the gravity force per unit area of the fully supported bed is regarded as being balanced by the pressure drop across the bed, that is, without any supporting contribution from either the distributor surface or the walls of the vessel, we can write

$$\Delta p_b = (\rho_p - \rho_g)\, g\, h_{mf}\, (1 - \varepsilon_{mf}) \qquad \text{.....A.II.12}$$

At the condition where the bed is on the point of becoming fluidised it is not unreasonable to suppose that the expressions developed for flow through a packed bed might still be valid. Thus Δp could be expressed in terms of one of the correlations developed in Section A.II.1.

For example, using the Ergun model, we have from equation A.II.9

$$\Delta p_b = 150\left(\frac{1 - \varepsilon_{mf}}{\phi_s\, d_v}\right)^2 \frac{1}{\varepsilon_{mf}^3} \cdot \mu_g\, U_{mf}\, h_{mf} + 1.75\, \frac{1 - \varepsilon_{mf}}{\phi_s\, \varepsilon_{mf}^3} \cdot \frac{h_{mf}}{d_v} \cdot \rho_g\, U_{mf}^2$$

.....A.II.13

Combining with equation A.II.12 and rearranging, we get

$$\frac{\rho_g(\rho_p - \rho_g)\, g\, d_v^3}{\mu_g^2} = 150\left(\frac{1 - \varepsilon_{mf}}{\phi_s^2\, \varepsilon_{mf}^3}\right)\frac{\rho_g\, d_v\, U_{mf}}{\mu_g} + 1.75\left(\frac{1}{\phi_s\, \varepsilon_{mf}^3}\right)\left(\frac{\rho_g\, d_v\, U_{mf}}{\mu_g}\right)^2 \qquad \text{...A.II.14}$$

Now the left-hand side of this equation is a form of Archimedes number for the bed,

$$Ar_b = \frac{\rho_g(\rho_p - \rho_g)\, g\, d_v^3}{\mu_g^2} \qquad \text{.....A.II.15}$$

and the right-hand side is a function of the bed Reynolds number at the minimum fluidisation condition,

$$Re_{mf} = \frac{\rho_g\, d_v\, U_{mf}}{\mu_g} \qquad \text{.....A.II.16}$$

Thus equation A.II.14 can be simplified to a relationship between these two dimensionless parameters as

$$Ar_b = 150\left(\frac{1-\varepsilon_{mf}}{\phi_s^2\,\varepsilon_{mf}^3}\right)Re_{mf} + 1.75\left(\frac{1}{\phi_s\,\varepsilon_{mf}^3}\right)Re_{mf}^2 \qquad \text{.....A.II.17}$$

This expression tends to be inconvenient to use in this form because of the shortage of readily available information relating to the sphericity ϕ_s and the voidage ε_{mf}. However, Wen and Yu (Ref. W4) have pointed out that ε_{mf} increases as ϕ_s decreases, and also ε_{mf} is nearly independent of the particle diameter, and they go on to show that available experimental data correlates reasonably well with the expressions

$$\frac{1-\varepsilon_{mf}}{\phi_s^2\,\varepsilon_{mf}^3} = 11 \qquad \text{.....A.II.18}$$

and

$$\frac{1}{\phi_s\,\varepsilon_{mf}^3} = 14 \qquad \text{.....A.II.19}$$

It has been suggested subsequently that this approach is not entirely satisfactory (Ref. R1) but nevertheless, substitution of these values into equation A.II.17 does lead to a very convenient correlation between the Archimedes and Reynolds numbers for the bed at the minimum fluidising condition.

Thus $$Re_{mf}^2 + 67.3\,Re_{mf} - 0.0408\,Ar_b = 0 \qquad \text{.....A.II.20}$$

For approximately spherical particles Richardson (Ref. R1) suggests a value of 0.4 for ε_{mf} and arrives at a similar expression relating Re_{mf} and Ar_b as

$$Re_{mf}^2 + 51.4\,Re_{mf} - 0.0366\,Ar_b = 0 \qquad \text{.....A.II.21}$$

In order to apply this correlation to non-spherical particles, Richardson comments that the "diameter" used must be that of a sphere with the same specific surface as the particles, that is, $\phi_s d_v$. This means effectively multiplying the Archimedes and Reynolds numbers for spherical particles by ϕ_s^3 and ϕ_s respectively, so that, for example, equation A.II.21 would become

$$(\phi_s Re_{mf})^2 + 51.4(\phi_s Re_{mf}) - 0.0366\ \phi_s^3 Ar_b = 0 \qquad \text{.....A.II.22}$$

However, this appears to result in a very considerable underestimate of U_{mf} for non-spherical particles.

It is clearly not easy to predict the behaviour at incipient fluidisation of irregular particles. A decrease in the sphericity of an isolated particle would cause an increase in the drag exerted on it at a given velocity. However, in a bed of particles a decrease in sphericity would normally be accompanied by an increase in the bed voidage, which in turn would cause a reduction in the interstitial velocity. The effects might be expected to oppose each other to some extent so that particles of the same size and density should in general become fluidised at around the same value of superficial gas velocity. There is thus good justification in using a correlation, such as equation A.II.20 or A.II.21 that is independent of ϕ_s and ε_{mf}.

An empirical correlation rather similar to these two, but which is perhaps a little more reliable, has been proposed by Baeyens and Geldart (Ref. B3) as

$$Ar_b = 1823\ (Re_{mf})^{1.07} + 21.7\ (Re_{mf})^2 \qquad \text{.....A.II.23}$$

This expression is shown in Fig. A.II.2 as a plot of Re_{mf} against Ar_b, and whilst some caution should be exercised because of the unreliable correlation between ϕ_s and ε_{mf}, this graph should still allow a fairly quick assessment of the minimum fluidising velocity of a material by first calculating Ar_b, and then reading off a value of Re_{mf} and from this estimating U_{mf}.

By way of comparison, also plotted on Fig. A.II.2 are the correlations of Wen and Yu (Ref. W4) and Richardson (Ref. R1) from equations A.II.20 and A.II.21 respectively.

The foregoing analysis is a general one endeavouring to cover the whole range of flow behaviour from laminar through transitional to turbulent.

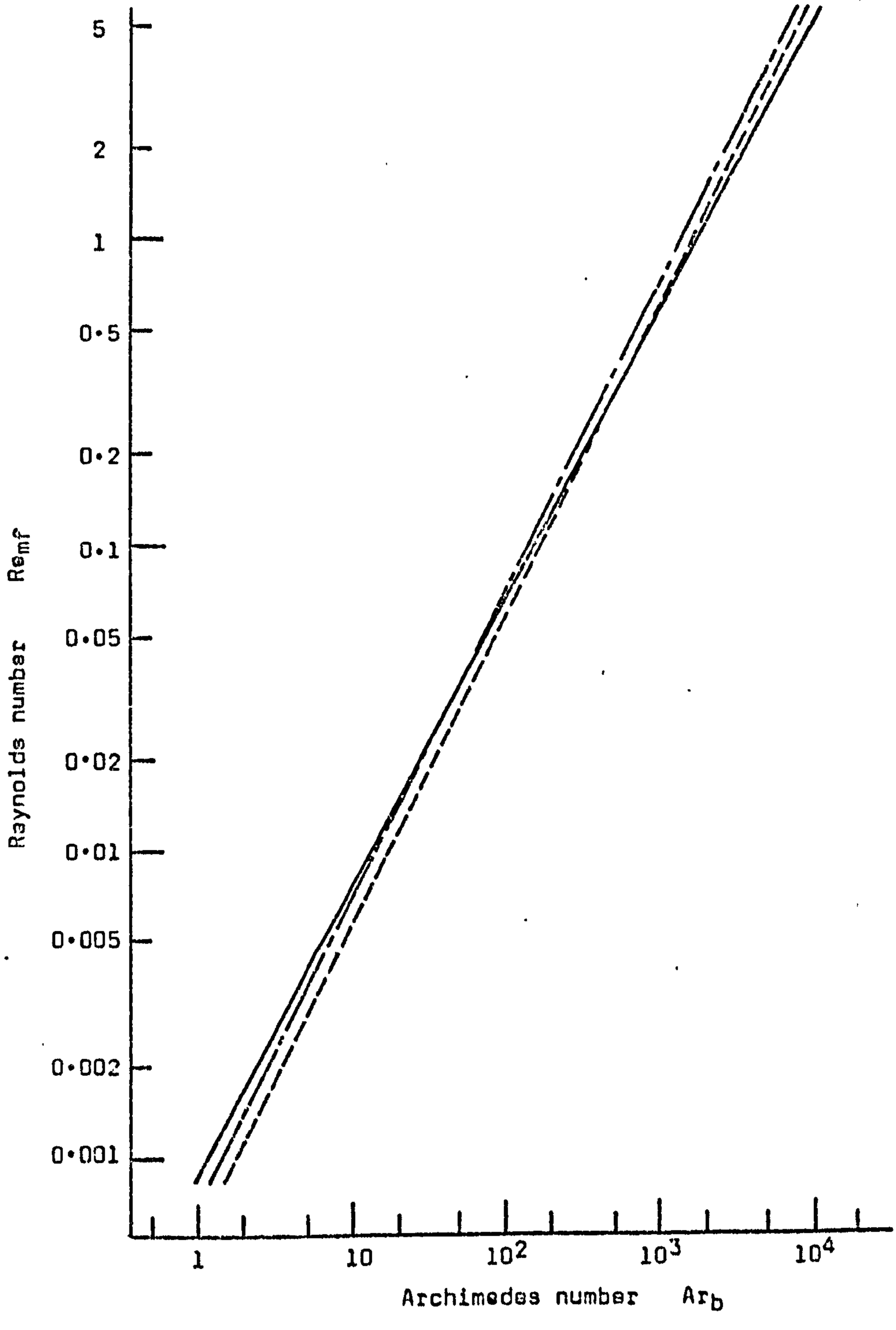

Fig. A.II.2. CORRELATIONS FOR MINIMUM FLUIDISING VELOCITY, PRESENTED AS PLOTS OF REYNOLDS NUMBER, Re_{mf}, AGAINST ARCHIMEDES NUMBER, Ar_b,

——————— Equation A.II.23 (Baeyens and Geldart, Ref.B3)

– – – – – – – Equation A.II.20 (Wen and Yu, Ref. W4)

——— – ——— Equation A.II.21 (Richardson, Ref. R1)

However, at normal atmospheric pressures and temperatures the gas flow through a bed of solid particles tends to be laminar for particles having diameters less than about 500 μm. For such relatively fine particles viscous effects predominate and the expressions for minimum fluidising velocity can therefore be simplified by ignoring the kinetic energy term.

Thus, for example, equation A.II.13 reduces to

$$\Delta p_b = 150 \left(\frac{1 - \varepsilon_{mf}}{\phi_s d_v}\right)^2 \frac{1}{\varepsilon_{mf}^3} \cdot \mu_g U_{mf} h_{mf} \qquad \text{.....A.II.24}$$

and combining with equation A.II.12 gives

$$U_{mf} = \frac{d_v^2}{150} \left(\frac{\phi_s^2 \varepsilon_{mf}^3}{1 - \varepsilon_{mf}}\right)\left(\frac{\rho_p - \rho_g}{\rho_g}\right)\frac{g}{\nu_g} \qquad \text{.....A.II.25}$$

Following Wen and Yu (Ref. W4) in eliminating ϕ_s and ε_{mf} using equation A.II.18 we get

$$U_{mf} = \frac{6.1 \ . 10^{-4} d_v^2 g}{\nu_g} \left(\frac{\rho_p - \rho_g}{\rho_g}\right) \qquad \text{.....A.II.26}$$

This can of course be regarded merely as a variant of the simple expression attributed to Graf (Ref. Z1, p 28)

$$U_{mf} = K d_v^2 g \frac{\rho_p - \rho_g}{\mu_g} \qquad \text{.....A.II.27}$$

in which K is a constant.

The same equation is easily derived from Stokes Law for the drag force on an isolated particle in a laminar flow region, writing k as the ratio of the drag force on a single particle in a packed array to the drag force on a single isolated particle;

so that $k . 3\pi \mu_g d_v U_{mf} = \frac{\pi}{6} d_v^3 (\rho_p - \rho_g) g$ A.II.28

from which equation A.II.27 is obtained with K = 1/18k.

Various values of K have been proposed, for example:-

5.9×10^{-4}	.....Richardson (Ref. R1)
6.1×10^{-4}	.....Wen and Yu (Ref. W4)
7.8×10^{-4}	.....Davies and Richardson (Ref. D3)
8.1×10^{-4}	.....Rowe (Ref. R7)
10.7×10^{-4}	.....Frantz (Ref. F1)

According to recent experimental data reported by Butt (Ref. B30), a value of K of about 8×10^{-4} in equation A.II.27 should generally give the closest prediction, although it does appear that this form of equation is inclined to overestimate U_{mf} for materials having very fine particles and underestimate U_{mf} for the coarser materials.

Attempting to get closer agreement with experimental data Leva et al (Ref. L4) developed a more complex correlation by combining equation A.II.25 with an empirical expression relating the function $\phi_s^2 \varepsilon_{mf}^3/(1-\varepsilon_{mf})$ to the bed Reynolds number.

Thus
$$\frac{\phi_s^2 \varepsilon_{mf}^3}{1-\varepsilon_{mf}} = 0.106\ (Re_{mf})^{-0.063} \qquad \text{.....A.II.29}$$

which is said to hold for $Re_{mf} < 5$, and this leads to

$$U_{mf} = 10.86 \cdot 10^{-4} \frac{d_v^{1.82}}{\nu_g^{0.88}} \left[\left(\frac{\rho_p - \rho_g}{\rho_g}\right) g\right]^{0.94} \qquad \text{.....A.II.30}$$

Whilst this expression agrees fairly closely with the experimental results as reported by Butt (Ref. B30), it is doubtful whether much advantage is gained over the more simple equation A.II.27.

A.II.3 Entrainment - the prediction of terminal velocity

Where the upward velocity of a gas through a fluidised bed exceeds the terminal velocity of the particles (that is, the velocity of free fall of the particles in the gas) it is likely that these particles will tend to become entrained in the gas stream leaving the surface of the bed. In order to predict the occurrence of entrainment it is therefore helpful

to be able to estimate the terminal velocity of the particles, and a number of modelling techniques have been proposed for this purpose. The simplest model uses the basic fluid mechanics approach in which the drag on a particle falling at a steady terminal velocity U_t is balanced by the net gravity force on the particle.

Thus $$U_t = \left[\frac{4\, g\, d_v (\rho_p - \rho_g)}{3\, \rho_p\, C_d}\right]^{\frac{1}{2}} \qquad \text{.....A.II.31}$$

where C_d is an experimentally determined drag coefficient and is a function of the particle Reynolds number $Re_p = d_v \rho_g U_t / \mu_g$.

The form of the relationship between the dimensionless parameters C_d and Re_p is not easily modelled mathematically, although for an isolated sphere at relatively low Reynolds numbers (up to about 1000) the expression of Schiller and Naumann (Ref. S3) seems now to be generally accepted.

This model gives C_d as

$$C_d = \frac{24}{Re_p}\,(1 + 0.15\, Re_p^{0.687}) \qquad \text{.....A.II.32}$$

and is shown plotted on Fig. A.II.3.

The part of the C_d vs. Re_p curve that is relevant to the present work (that is, for Re_p less than about 600) may be more conveniently represented by two linear expressions on the log plot, the first of which derives directly from Stokes law for spherical particles in a laminar flow. Thus Kunii and Levenspiel (Ref. K10, p 76) give

$$C_d = \frac{24}{Re_p} \quad \text{for} \quad Re_p < 0.4 \qquad \text{.....A.II.33a}$$

$$C_d = 10\, Re_p^{-0.5} \quad \text{for} \quad 0.4 < Re_p < 500 \qquad \text{.....A.II.33b}$$

It is seen on Fig. A.II.3 that this model deviates markedly from the curve of Schiller and Naumann, and furthermore the limit of the Stokes Law expression given as $Re_p \simeq 0.4$ appears to be incorrect. A much

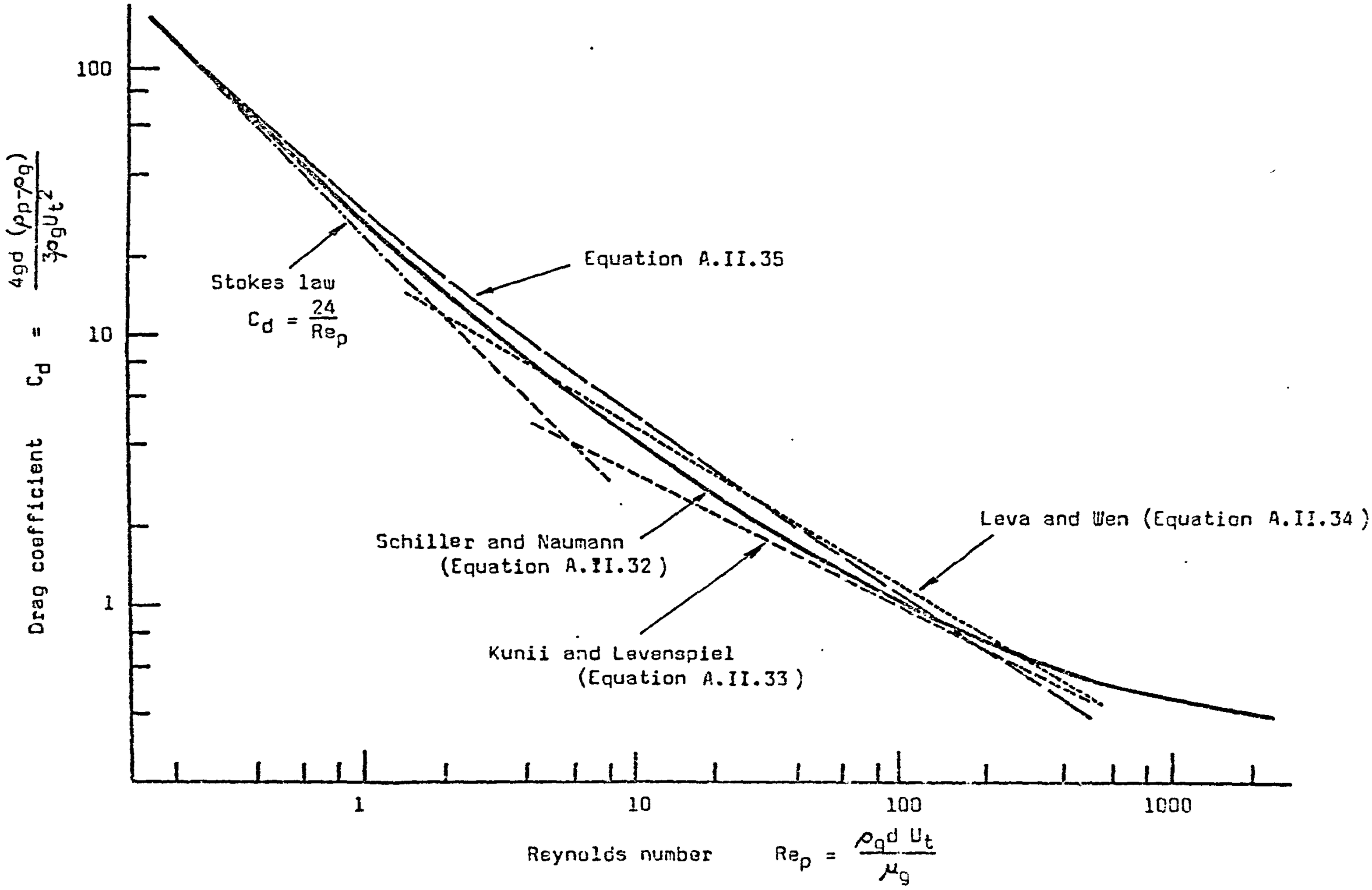

Fig. A.II.3. COMPARISON BETWEEN VARIOUS MODELS OF THE RELATIONSHIP BETWEEN DRAG COEFFICIENT AND REYNOLDS NUMBER FOR SPHERICAL PARTICLES IN AIR.

closer correlation is that of Leva and Wen (Ref. L5) who give

$$C_d = \frac{24}{Re_p} \quad \text{for} \quad Re_p < 2.0 \qquad \text{.....A.II.34a}$$

$$C_d = 18.5\, Re_p^{-0.6} \quad \text{for} \quad 2.0 < Re_p < 500 \qquad \text{.....A.II.34b}$$

It is possible to represent the relationship between C_d and Re_p reasonably well with a single expression rather simpler than that of Schiller and Naumann if some loss of accuracy can be accepted. For example, the curve

$$C_d = \frac{24}{Re_p}(1 + Re_p)^{\frac{1}{3}} \qquad \text{.....A.II.35}$$

when plotted on Fig. A.II.3 is seen to compare favourably with the two lines of Leva and Wen.

However, expressions such as equations A.II.32 and A.II.35 have the disadvantage that they do not allow derivation of any relationship explicit in U_t, whereas from the equation A.II.34 writing $Re_p = d_p \rho_g U_t / \mu_g$ and then substituting into equation A.II.31 we get

$$U_t = \frac{g(\rho_p - \rho_g)d_v^2}{18\mu_g} \quad \text{for} \quad Re_p < 2.0 \qquad \text{.....A.II.36a}$$

$$U_t = 0.152\, \frac{g^{0.71}(\rho_p - \rho_g)^{0.71} d_v^{1.14}}{\mu_g^{0.43} \rho_g^{0.29}}$$

$$\text{for } 2.0 < Re_p < 500 \qquad \text{...A.II.36b}$$

For spherical particles fluidised in air at normal ambient conditions these can be reduced to convenient analytical expressions for terminal velocity as

$$U_t = 2.95 \cdot 10^4 \rho_p d_v^2 \quad \text{for} \quad Re_p < 2.0 \qquad \text{.....A.II.37a}$$

$$U_t = 79.1 \cdot 10^4 \rho_p^{0.71} d_v^{1.14} \quad \text{for } 2.0 < Re_p < 500 \qquad \text{..A.II.37b}$$

where ρ_p is in kg/m^3 and d_v is in metres giving U_t in m/s.

In order to give an impression of the form of this model for a relationship between U_t, ρ_p and d_v the equations A.II.37 are plotted over an appropriate range in Fig. A.II.4.

As with the correlations proposed for the prediction of minimum fluidising velocity, the limitations of the expressions A.II.37 must be recognised. These equations are useful as a guide to the fluidising air velocity at which entrainment could begin from relatively shallow beds as would normally be encountered in air-assisted gravity conveyors. However, for deep beds they could be unreliable as the pressure drop, and therefore the change in air density, across the bed may well be significant. Furthermore, the expressions are based on an analysis for spherical particles and for irregular particles the values of U_t may be rather lower.

Comparatively little has been published on the terminal velocities of non-spherical particles, and virtually nothing on such particles falling in air. The main work on the subject is probably that of Pettyjohn and Christiansen (Ref. P6). Their extensive experimental study dealt only with isometric particles having $\phi_s > 0.67$, but covering a wide range of particle size and density, and resulted in the suggestion that in the laminar flow region the terminal velocity could be given by multiplying the value for spherical particles by a factor K_t where

$$K_t = 0.366 \ln \frac{\phi_s}{0.065} \qquad \text{.....A.II.38}$$

Some caution should be exercised when applying this result to particles settling in gases since Pettyjohn and Christiansen worked only with liquids, and also there is likely to have been a significant wall effect (Ref.A2, p 159). Nevertheless, combining equations A.II.37a and A.II.38 would give

$$U_t = 1.08 \cdot 10^4 \left(\ln \frac{\phi_s}{0.065}\right) \rho_p d_v^{\,2} \qquad \text{.....A.II.39}$$

At Reynolds numbers above about 2, orientation effects may be significant and the influence of sphoricity predicted by equation A.II.38

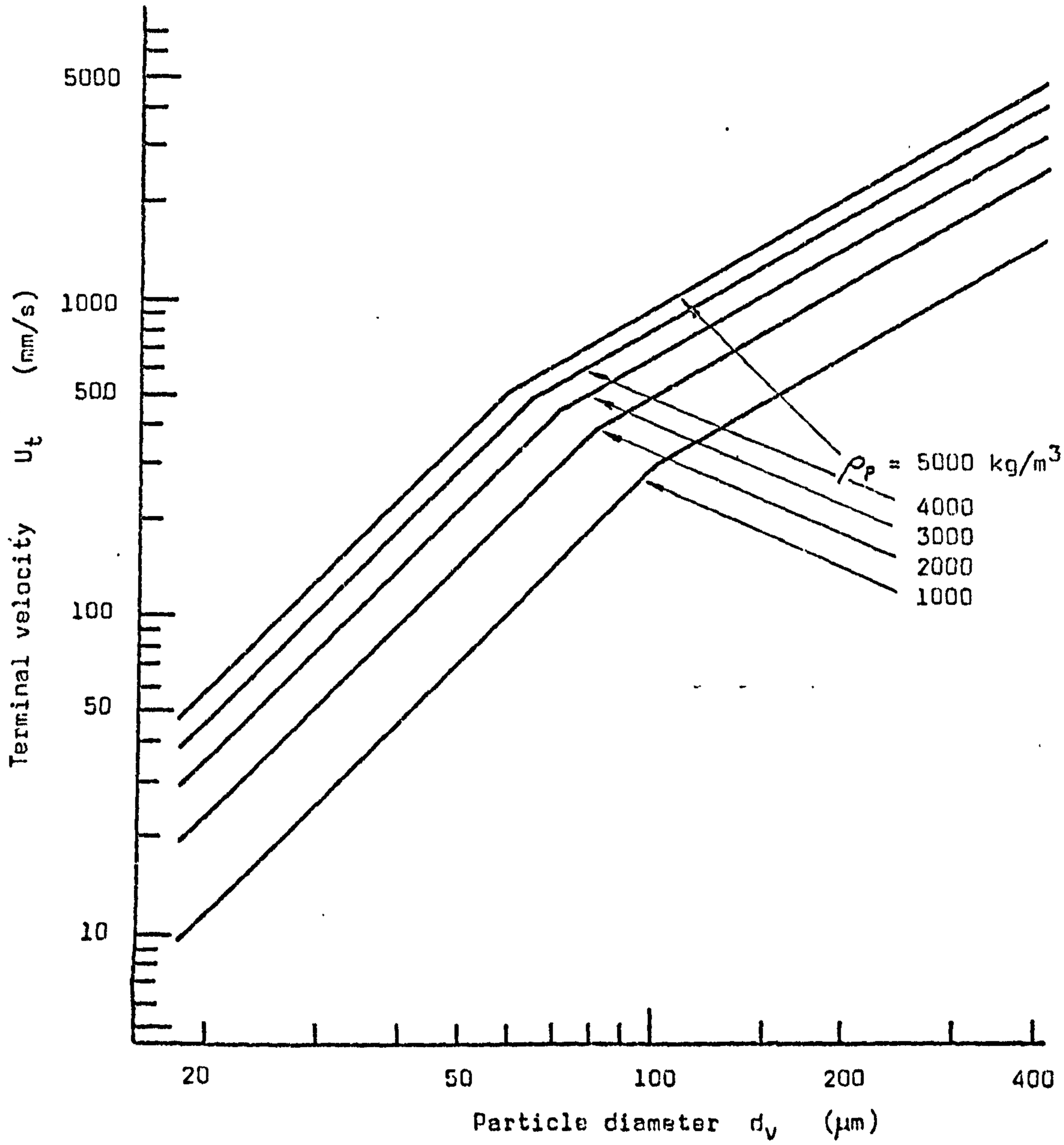

Fig. A.II.4. THE RELATIONSHIP BETWEEN THE TERMINAL VELOCITY OF SPHERICAL PARTICLES IN AIR, PARTICLE DIAMETER AND PARTICLE DENSITY, AS PREDICTED BY EQUATIONS A.II.37.

appears to become increasingly unreliable. Pettyjohn and Christiansen are able only to show the relationship between C_d and Re_p in graphical form for the transition region with Re_p up to 2000. Probably a quite acceptable approximation would be obtained by following the suggestion of Hawksley (Ref. H4) that the drag on a spherical particle is the same as that on a sphere having the same surface area.

In an earlier paper a useful proposal by Hawksley (Ref. H3) was that the C_d vs. Re_p relationship for spherical particles could be used for irregular shaped particles provided that C_d and Re_p are redefined by

$$C_d' = \phi_s \frac{4 g d_v (\rho_p - \rho_g)}{3 \rho_g U_t^2} \qquad \text{.....A.II.40a}$$

$$Re_p' = \frac{1}{\sqrt{\phi_s}} \cdot \frac{\rho_g d_v U_t}{\mu_g} \qquad \text{.....A.II.40b}$$

A chart relating C_d and Re_p for non-spherical particles is also given by Kunii and Levenspiel (Ref. K10, p 77) which is based on experimental work undertaken by various researchers between 1851 and 1928, all of whom used water or other liquids. The results of these workers were presented by Waddell (Ref. W1) as a plot of C_d against Re_p for sphericities of 0.125, 0.220, 0.806 (cubes) and 1.00 (spheres). Brown et al. (Ref. B25) later published an "improved" version of Waddell's chart (see Fig. A.II.5), and this in turn was developed into the plot of $C_d Re_p^2$ against Re_p preferred by Kunii and Levenspiel (see Fig. A.II.6). The scarcity of recent experimental data on terminal velocities of irregular particles, especially in gases, is very evident.

The advantage of using the parameter $C_d Re_p^2$ is that it is independent of velocity, and noting that

$$\text{Archimedes number, } Ar = \tfrac{3}{4} C_d Re_p^2 \qquad \text{.....A.II.41}$$

there is clearly a good justification for extending the use of Re_p against Ar plots to the correlation of terminal velocity data.

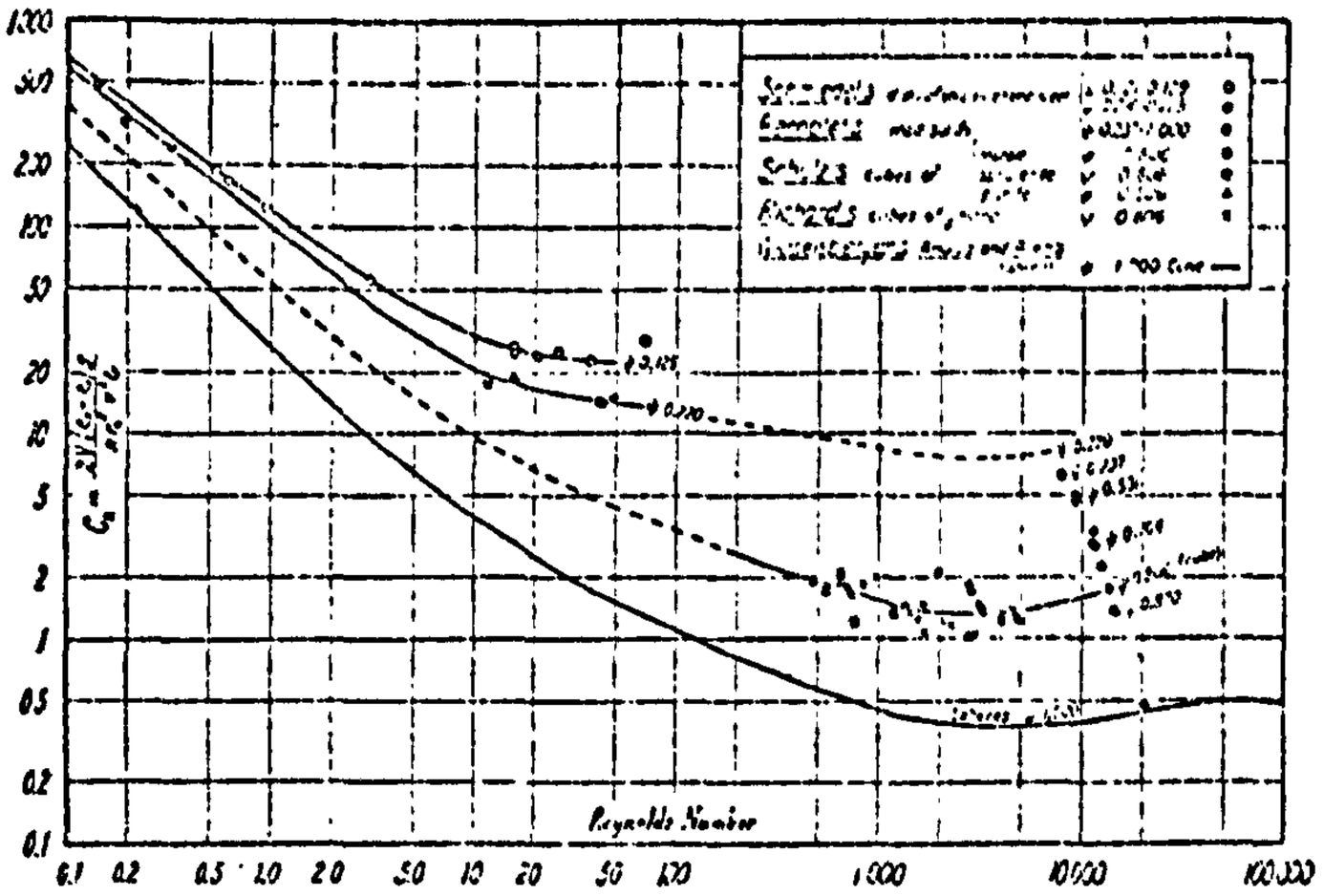

The coefficient of resistance as a function of Reynolds number for solids of different sphericity values.

a.

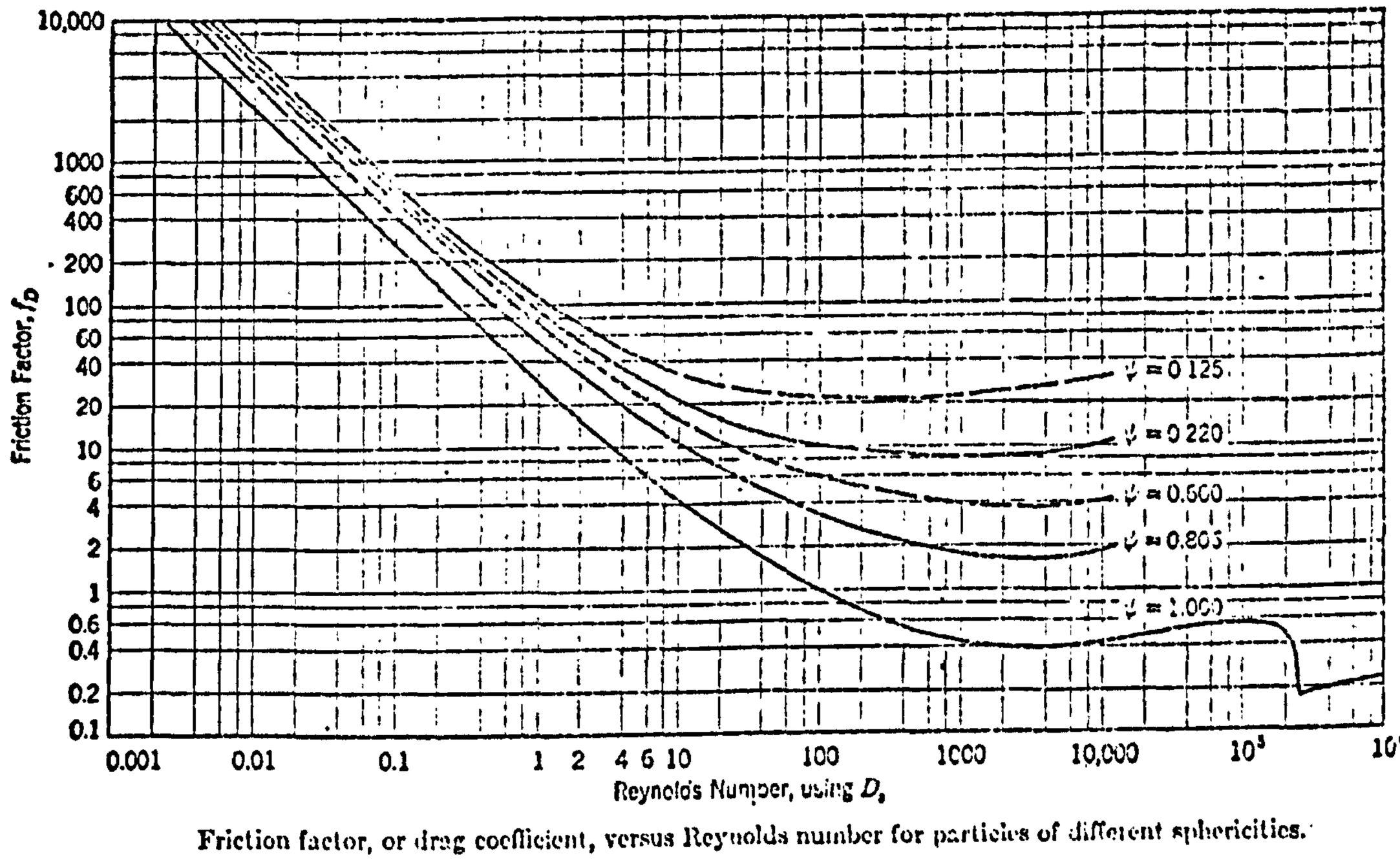

Friction factor, or drag coefficient, versus Reynolds number for particles of different sphericities.

b.

Fig. A.II.5. PLOTS OF DRAG COEFFICIENT AGAINST REYNOLDS NUMBER FOR PARTICLES OF DIFFERENT SPHERICITIES:

a) Chart prepared by Waddell (Ref. W1) in 1934 from the experimental data of various research workers.

b) Later version published in 1950 by Brown et al (Ref. B25).

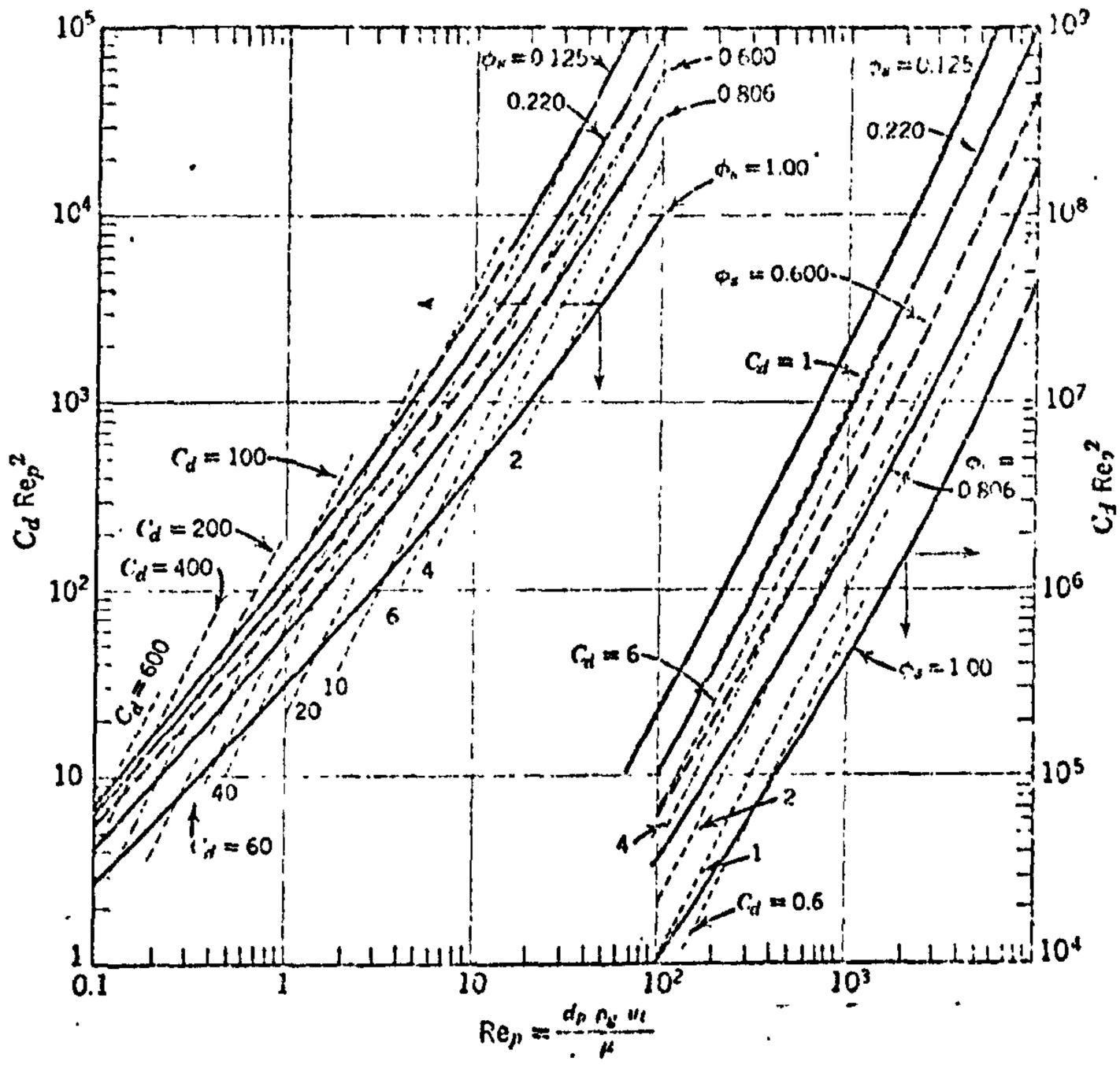

Fig. A.II.6 TERMINAL VELOCITY CORRELATIONS PLOTTED AS $C_d Re_p^2$ AGAINST Re_p, prepared by Kunii and Levenspiel (Ref. K10, p77) from information in Brown et al. (Ref. B25).

Fig. A.II.7 shows such a plot for particles having sphericity from unity down to 0.2, prepared from the model of Schillar and Naumann (equation A.II.32) modified according to the suggestion of Hawksley (equations A.II.40). Whilst quite reasonable agreement would seem to be found between terminal velocities predicted using Fig. A.II.7 (Hawksley) and equation A.II.39 (Pettyjohn and Christiansen), the chart (Fig. A.II.8) prepared from that of Kunii and Levenspiel suggests a rather more drastic effect of reduced sphericity. However, for the reasons set out above, any prediction of the terminal velocity of non-spherical particles in air must be treated with caution and there is a great need for more experimental work in this area.

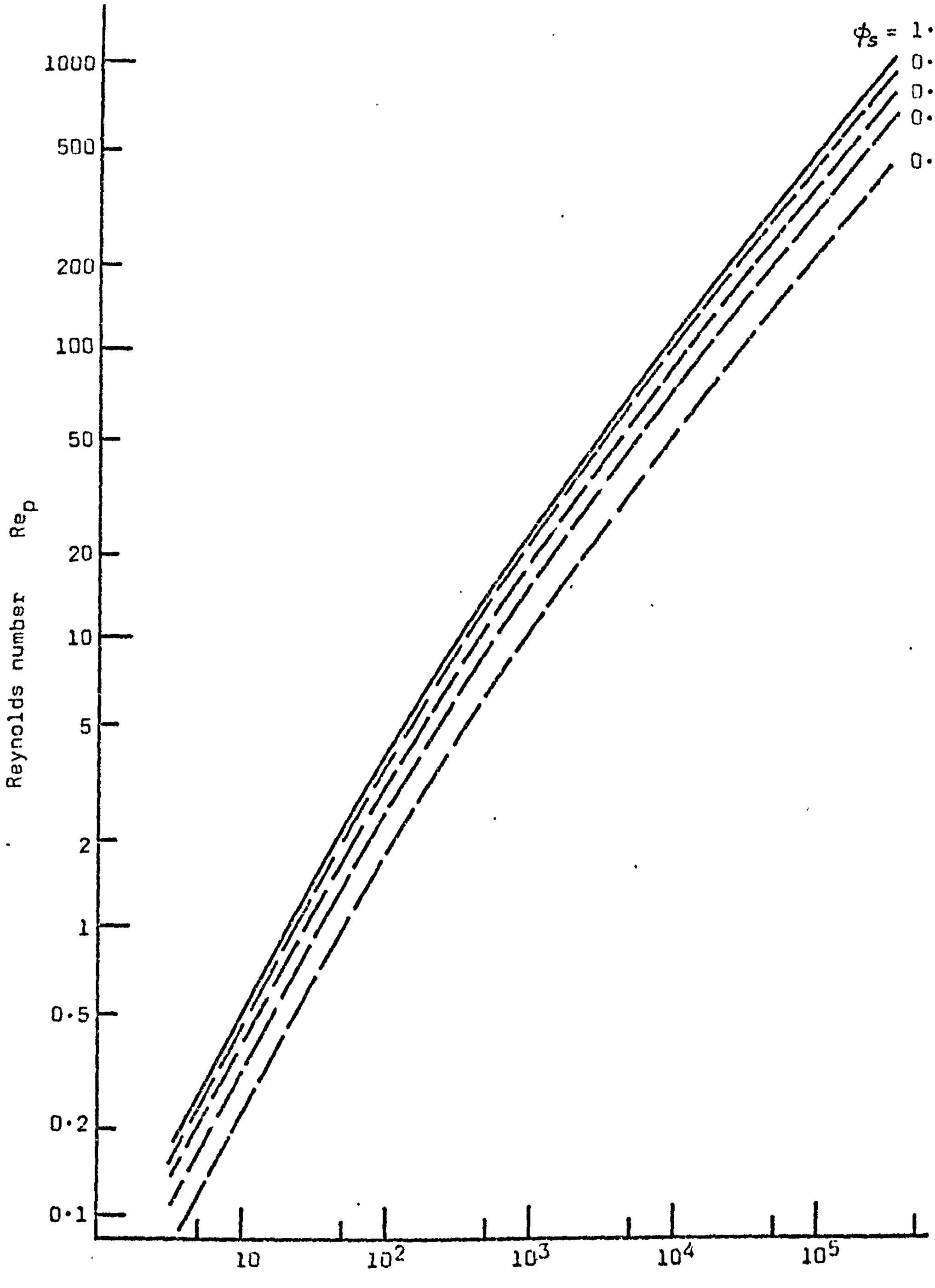

Fig. A.II.7. PLOT OF REYNOLDS NUMBER AGAINST ARCHIMEDES NUMBER FOR ISOLATED PARTICLES AT TERMINAL (FREE-FALL) VELOCITY. Based on the equation of Schiller and Naumann (Ref. S3) modified according to Hawksley (Ref. H3) for irregular particles.

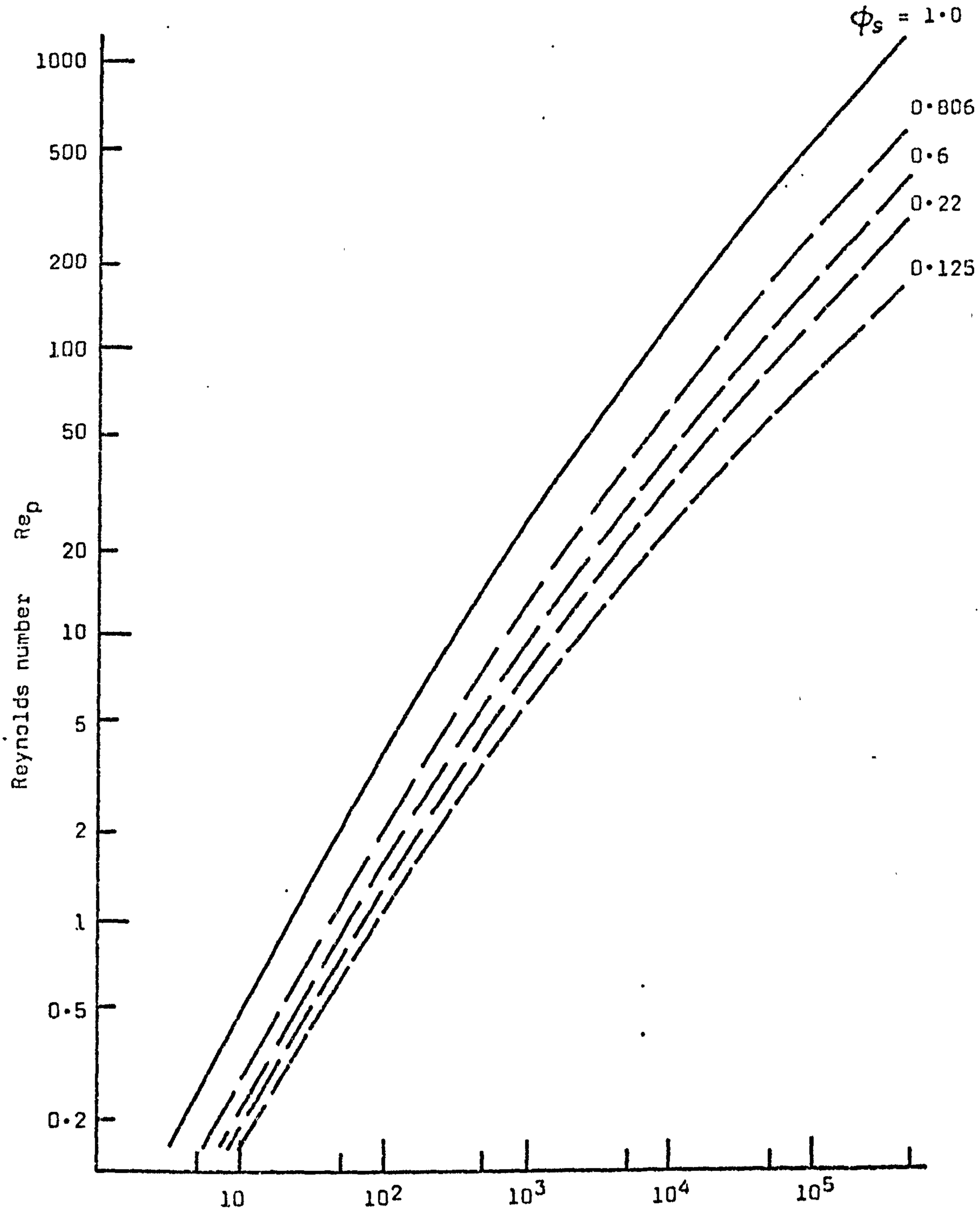

Fig. A.II.8. PLOT OF REYNOLDS NUMBER AGAINST ARCHIMEDES NUMBER FOR ISOLATED PARTICLES AT TERMINAL (FREE-FALL) VELOCITY. Based on chart in Kunii and Levenspiel (Ref. K10, p 77)

APPENDIX A.III

NON-NEWTONIAN FLOW IN AN INCLINED CHANNEL

A.III.1 The power law model of non-Newtonian fluid behaviour

The simplest mathematical model of the laminar flow behaviour of time-independent non-Newtonian fluids is the power law due to Ostwald, normally expressed as

$$\tau = k\dot{\gamma}^n \qquad \text{.....A.III.1}$$

where τ and $\dot{\gamma}$ are the local shear stress and shear rate, and k and n are constants. The value of k gives an indication of the consistency of the fluid, and n indicates the amount of deviation from Newtonian behaviour.

It may be noted that for Newtonian fluids n = 1, for pseudoplastics (shear-thinning fluids) n < 1 and for dilatant (shear-thickening) fluids n > 1. The behaviour of these three fluid models is illustrated on Figs. A.III.1 and A.III.2 as plots of τ against $\dot{\gamma}$ and $\ln\tau$ against $\ln\dot{\gamma}$. The logarithmic plot is useful since the model becomes

$$\ln\tau = n\ln\dot{\gamma} + \ln k \qquad \text{.....A.III.2}$$

and therefore values of n and k can be determined from the slope and intercept of the straight line.

Two inherent limitations of the power law model are:-

1. For real fluids n is unlikely to be constant over the entire range of flow conditions.
2. The "consistency constant" k has dimensions which depend upon the value of n.

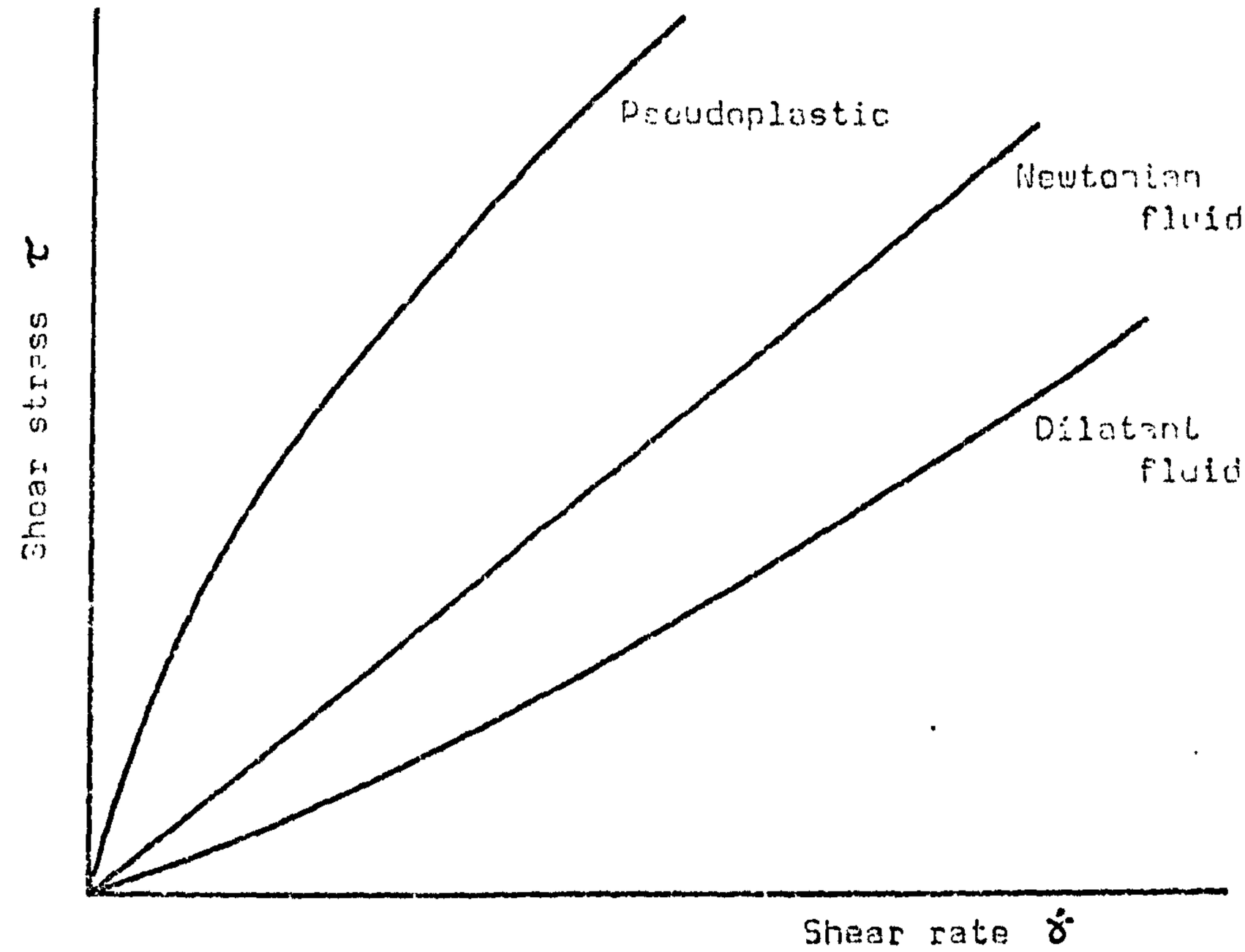

Fig. A.III.1 VARIATION OF SHEAR STRESS WITH SHEAR RATE FOR TYPICAL NEWTONIAN AND POWER-LAW FLUIDS.

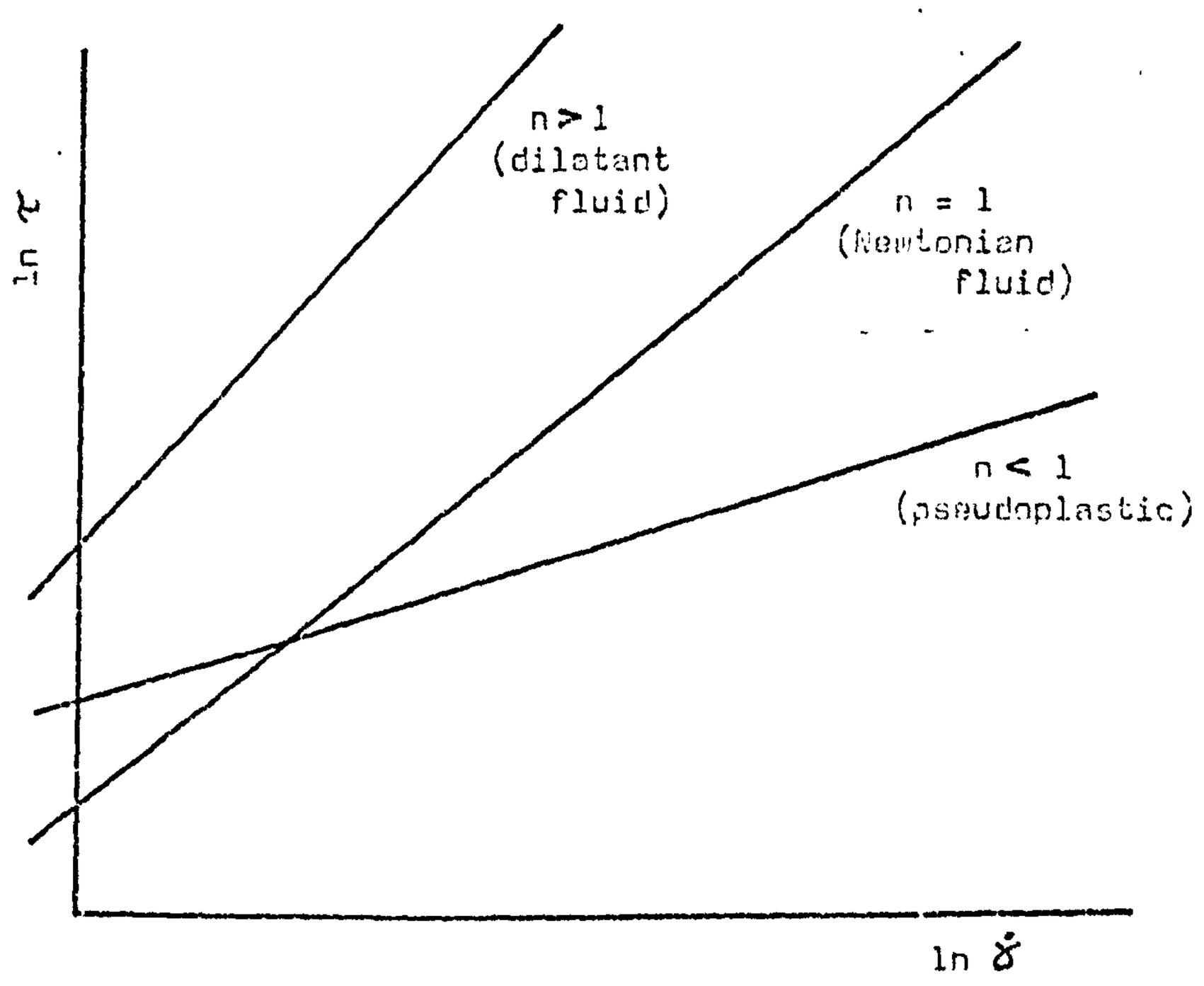

Fig. A.III.2 LOG. PLOT OF SHEAR STRESS AGAINST SHEAR RATE, SHOWING LINEAR RELATIONSHIP FOR NEWTONIAN AND POWER-LAW FLUIDS.

A.III.2 The apparent viscosity of power law fluids

Whilst it is often convenient to define an "apparent viscosity" μ_a in the same way as dynamic viscosity is defined for a Newtonian fluid, that is,

$$\mu_a = \frac{\tau}{\dot{\gamma}} \qquad \text{.....A.III.3}$$

it must be appreciated that, unlike dynamic viscosity, μ_a is not constant but is a function of $\dot{\gamma}$. Thus the term "viscosity" has no meaning for a non-Newtonian fluid unless it is related to a particular shear rate.

From Fig. A.III.3 it can be seen that μ_a is in fact the slope of a line from the origin to a point on the curve of τ against $\dot{\gamma}$. For pseudo-plastics μ_a decreases with increasing rate of shear (shear-thinning behaviour) and for dilatant fluids μ_a increases with increasing rate of shear (shear-thickening).

For the power-law model, combining equations A.III.1 and A.III.3, we have

$$\mu_a = k\dot{\gamma}^{n-1} \qquad \text{.....A.III.4}$$

A.III.3 The uniform laminar flow of a power-law fluid in an inclined channel: two-dimensional model with velocity varying in the lateral direction.

Referring to Fig. A.III.4 it is seen that a force balance on a lamina at distance x from the channel centreline gives

$$\frac{\partial \tau}{\partial x} = \rho g \sin\alpha$$

so that for τ dependent upon x only, and noting that $\tau = 0$ at $x = 0$, we get

$$\tau = \rho g x \sin\alpha \qquad \text{.....A.III.5}$$

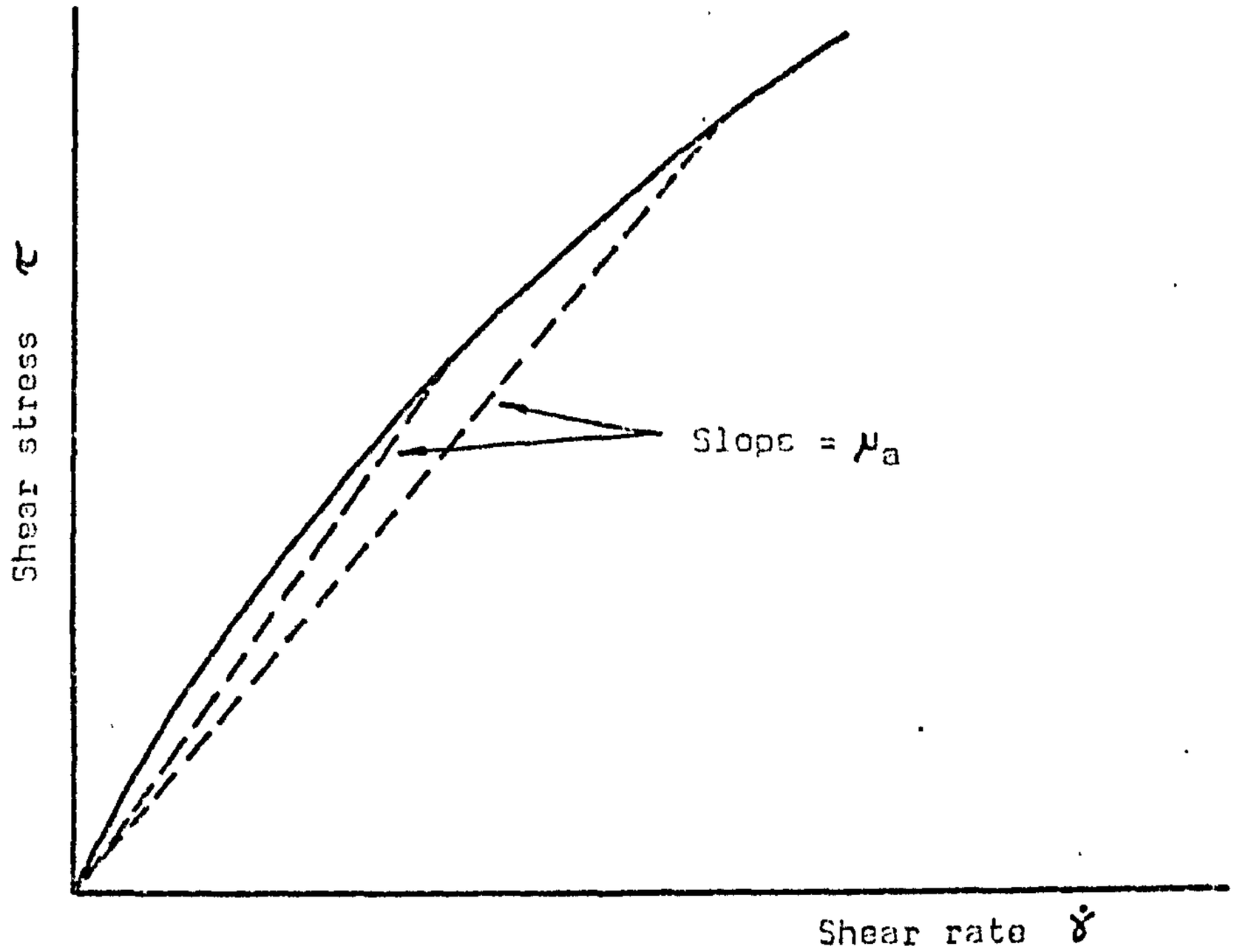

a. pseudoplastic

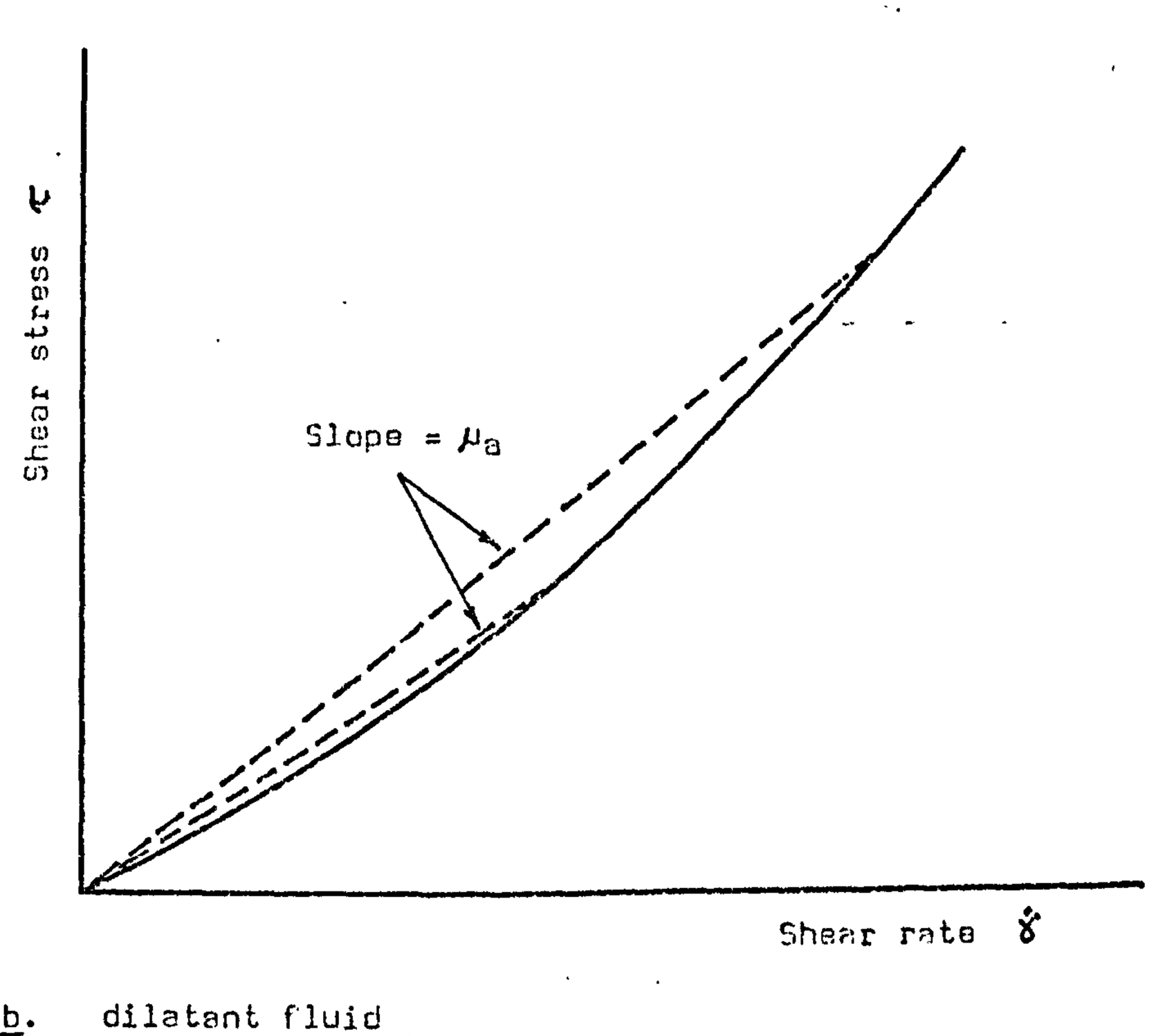

b. dilatant fluid

Fig. A.III.3 APPARENT VISCOSITY OF POWER LAW FLUIDS.

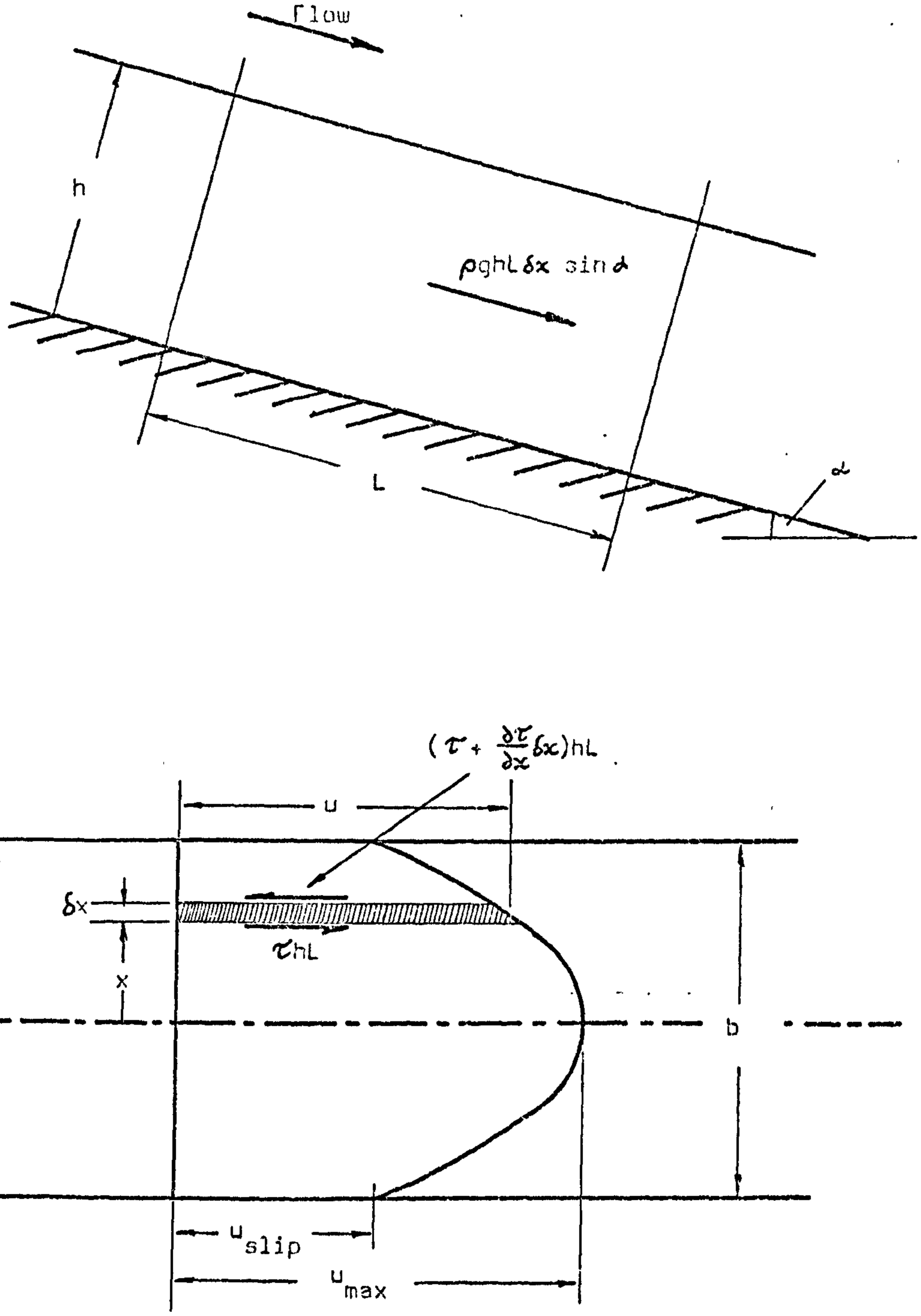

Fig. A.III.4 TWO-DIMENSIONAL LAMINAR FLOW OF A POWER-LAW FLUID IN AN INCLINED CHANNEL (WITH VELOCITY VARYING IN THE LATERAL DIRECTION).

Here τ is the local shear stress at distance x from the central axis of the channel.

For the power-law model $\tau = k\dot{\gamma}^n$

$$\text{or} \quad \tau = -k\left(\frac{du}{dx}\right)^n$$

$$\text{so} \quad du = -\left(\frac{\tau}{k}\right)^{\frac{1}{n}} dx$$

$$= -\left(\frac{\rho g x \sin\alpha}{k}\right)^{\frac{1}{n}} dx$$

$$\text{and} \quad u = -\left(\frac{\rho g \sin\alpha}{k}\right)^{\frac{1}{n}} \int x^{\frac{1}{n}} dx$$

$$\text{or} \quad u = -\left(\frac{\rho g \sin\alpha}{k}\right)^{\frac{1}{n}} \frac{n}{n+1} x^{\frac{n+1}{n}} + C \qquad \text{.....A.III.6}$$

For the case of zero slip at the channel walls ($u_{slip} = 0$), $u = 0$ at $x = b/2$,

$$\text{i.e.} \quad C = \left(\frac{\rho g \sin\alpha}{k}\right)^{\frac{1}{n}} \frac{n}{n+1} \left(\frac{b}{2}\right)^{\frac{n+1}{n}}$$

and the velocity distribution across the channel is then given by

$$u = \left(\frac{\rho g \sin\alpha}{k}\right)^{\frac{1}{n}} \frac{n}{n+1} \left[\left(\frac{b}{2}\right)^{\frac{n+1}{n}} - x^{\frac{n+1}{n}}\right] \qquad \text{.....A.III.7}$$

Now the volume flowrate can be written

$$\dot{V} = 2\int_0^{b/2} h\,u\,dx$$

so that, substituting for u we have

$$\dot{V} = 2h\left(\frac{\rho g \sin\alpha}{k}\right)^{\frac{1}{n}} \frac{n}{n+1} \int_0^{b/2} \left[\left(\frac{b}{2}\right)^{\frac{n+1}{n}} - x^{\frac{n+1}{n}}\right] dx$$

Simplifying this expression and dividing by the cross-sectional area of the channel, bh, then gives

$$u_{av} = \left(\frac{\rho g b \sin\alpha}{2k}\right)^{\frac{1}{n}} \frac{b}{2} \cdot \frac{n}{2n+1} \qquad \text{.....A.III.8}$$

or

$$u_{av} = \left(\frac{\tau_w}{k}\right)^{\frac{1}{n}} \frac{b}{2} \cdot \frac{n}{2n+1} \qquad \text{.....A.III.9}$$

where τ_w is the shear stress at the channel walls (that is, $\tau = \tau_w$ at $x = \pm b/2$).

$$\therefore \quad \tau_w = k\left(\frac{2u_{av}}{b}\right)^n \left(\frac{2n+1}{n}\right)^n \qquad \text{.....A.III.10}$$

and comparing with equation A.III.1 suggests that the shear rate at the walls could be expressed as

$$\dot{\gamma}_w = \frac{2u_{av}}{b} \cdot \frac{2n+1}{n} \qquad \text{.....A.III.11}$$

In log form, equation A.III.10 becomes

$$\ln \tau_w = n \ln\left(\frac{2u_{av}}{b}\right) + \ln\left[k\left(\frac{2n+1}{n}\right)^n\right] \qquad \text{.....A.III.12}$$

or, in terms of directly measurable quantities,

$$\ln\left(\frac{\rho g b \sin\alpha}{2}\right) = n \ln\left(\frac{2\dot{m}}{\rho b^2 h}\right) + \ln\left[k\left(\frac{2n+1}{n}\right)^n\right] \qquad \text{.....A.III.13}$$

and thus a log plot of τ_w against $2u_{av}/b$ for the two dimensional flow of a power-law fluid in an open channel would, for this model, yield a straight line of slope n and intercept $k\left(\frac{2n+1}{n}\right)^n$ from which k could be determined (Fig. A.III.5).

Also for this model, using equation A.III.8, the mass flowrate can be

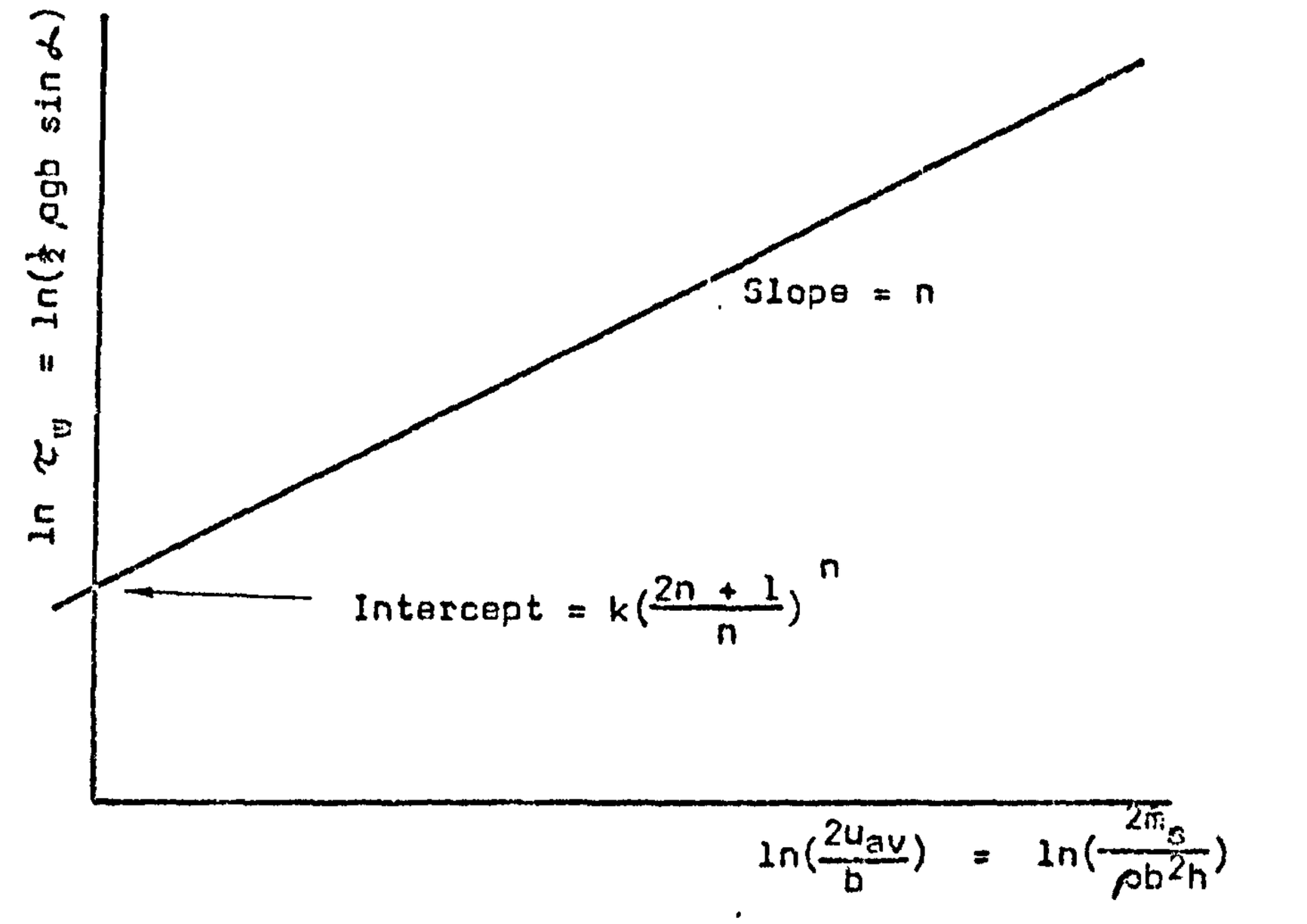

Fig. A.III.5 LOG PLOT OF τ_w AGAINST $2u_{av}/b$ TO DETERMINE n AND k FOR THE TWO-DIMENSIONAL MODEL OF A POWER-LAW FLUID IN AN INCLINED CHANNEL.

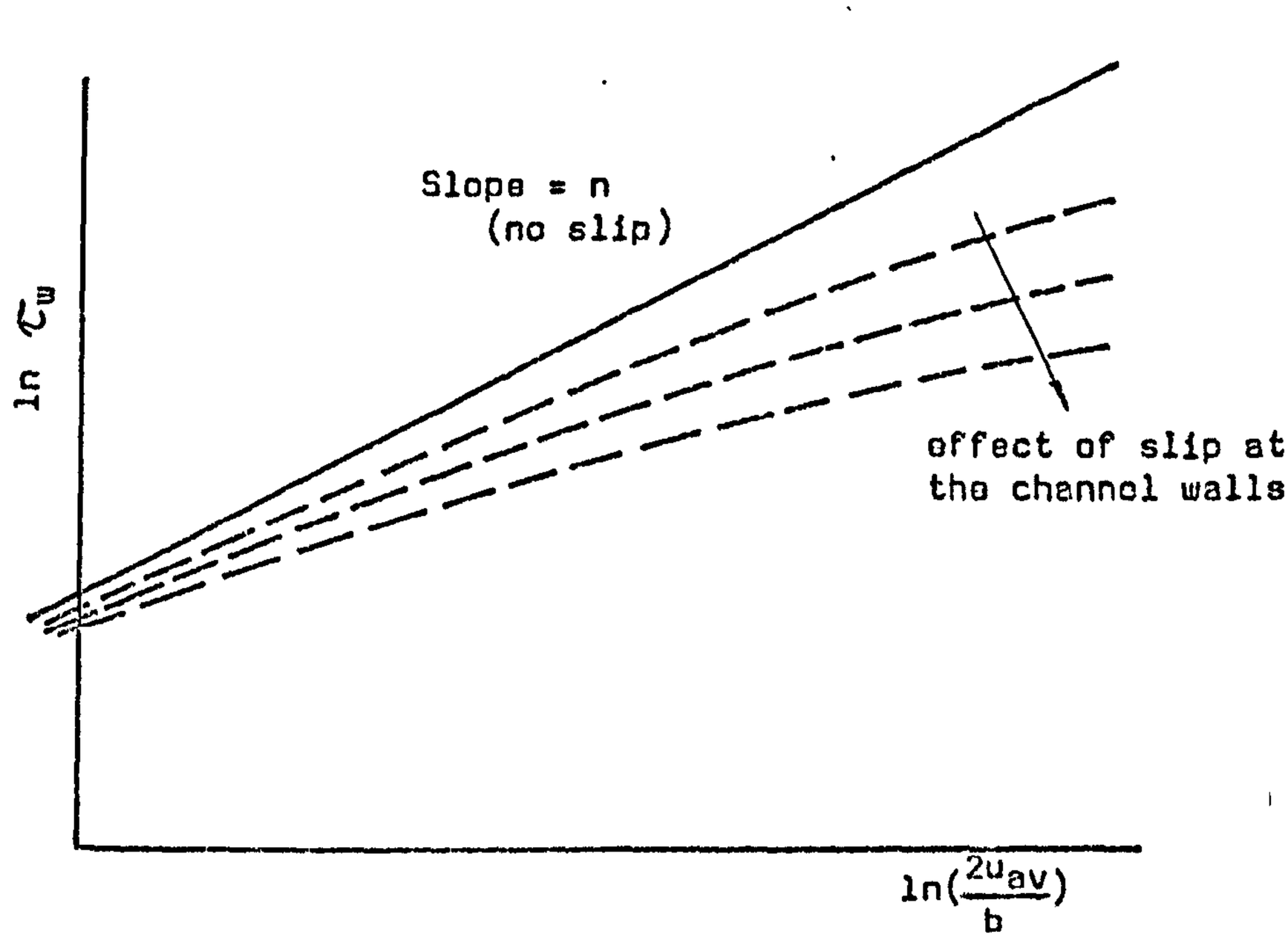

Fig. A.III.6 LOG PLOT OF τ_w AGAINST $2u_{av}/b$ FOR THE TWO-DIMENSIONAL MODEL, SHOWING THE INFLUENCE OF SLIP AT THE CHANNEL WALLS.

expressed as

$$\dot{m} = \frac{\rho b^2 h}{2} \cdot \frac{n}{2n+1} \left(\frac{\rho g b \sin\alpha}{2k}\right)^{\frac{1}{n}} \qquad \text{.....A.III.14}$$

In the special case of Newtonian behaviour, n = 1 and k = μ so that this equation reduces to

$$\dot{m} = \frac{\rho^2 g b^3 h \sin\alpha}{12\mu} \qquad \text{.....A.III.15}$$

The effect of slip at the channel walls can be incorporated in the model by adjusting the limits of integration in the expression for velocity distribution. Thus the constant in equation A.III.6 is modified to include u_{slip}, so that equation A.III.7 becomes

$$u = u_{slip} - \left(\frac{\rho g \sin\alpha}{k}\right)^{\frac{1}{n}} \frac{n}{n+1} x^{\frac{n+1}{n}} \qquad \text{.....A.III.16}$$

Substituting for u in the expression for $\dot{V}$ and then integrating and dividing by bh as before, leads to an expression for u_{av}.

Thus

$$u_{av} = u_{slip} + \left(\frac{\tau_w}{k}\right)^{\frac{1}{n}} \frac{b}{2} \cdot \frac{n}{2n+1} \qquad \text{.....A.III.17}$$

from which

$$\tau_w = \left[\frac{2(u_{av} - u_{slip})}{b}\right]^n k\left(\frac{2n+1}{n}\right)^n \qquad \text{.....A.III.18}$$

This expression can be written

$$\tau_w = \left(\frac{2u_{av}}{b}\right)^n \left(1 - \frac{u_{slip}}{u_{av}}\right)^n k\left(\frac{2n+1}{n}\right)^n \qquad \text{.....A.III.19}$$

or in log form

$$\ln\tau_w = n \ln\left(\frac{2u_{av}}{b}\right) + n \ln\left(1 - \frac{u_{slip}}{u_{av}}\right) + \ln\left[k\left(\frac{2n+1}{n}\right)^n\right] \qquad \text{.....A.III.20}$$

The term $n \ln (1 - \frac{u_{slip}}{u_{av}})$ must be negative, lying between zero for $u_{slip} = 0$, and minus infinity for $u_{slip} = u_{av}$ which corresponds to total slip over the walls and a uniform velocity distribution. Thus, for the two-dimensional model under consideration, the effect of slip at the walls would appear as a downward deviation of the line on the plot of $\ln \tau_w$ against $\ln(2 u_{av}/b)$ as shown on Fig. A.III.6.

The influence of slip on mass flowrate can be examined by substituting for u_{av} and τ_w in equation A.III.17 to give

$$\dot{m} = \rho b h u_{slip} + \frac{\rho b^2 h}{2} \left(\frac{\rho g b \sin \alpha}{2k}\right)^{\frac{1}{n}} \cdot \frac{n}{2n+1} \qquad \text{.....A.III.21}$$

or, for a Newtonian fluid, setting $n = 1$ and $k = \mu$,

$$\dot{m} = \rho b h u_{slip} + \frac{\rho^2 g b^3 h \sin \alpha}{12 \mu} \qquad \text{.....A.III.22}$$

For zero slip this naturally reduces to equation A.III.15 and it is seen that (as might be expected) for a given mass flowrate an increase in the slip velocity causes a reduction in the depth of the flowing fluid.

It is of interest to note that a dimensionless velocity profile for this power-law fluid model may be obtained by combining equations A.III.7 and A.III.8 as

$$\frac{u}{u_{av}} = \frac{2n+1}{n+1} \left[1 - \left(\frac{2x}{b}\right)^{\frac{n+1}{n}}\right] \qquad \text{.....A.III.23}$$

which for $n = 1$ reduces to

$$\frac{u}{u_{av}} = \frac{3}{2} \left[1 - \left(\frac{2x}{b}\right)^2\right] \qquad \text{.....A.III.24}$$

the velocity profile for a Newtonian fluid in laminar flow in an open channel.

From equation A.III.23 it is seen that for the extreme case of $n = \infty$, the maximum velocity is twice the average, and as n decreases the profile

becomes "flatter", passing through the parabolic shape at n = 1. For low values of n the profile becomes very flat with effectively only the fluid near the channel wall being sheared. Thus the velocity profile approximates to a case of uniform velocity over a central zone of the flow with a relatively steep velocity gradient near the channel wall. This situation now approaches the Bingham plastic model in which the flow in the region close to the walls is Newtonian and that in the central zone (where the shear stress is less than some "yield value" τ_y) moves effectively as a solid mass.

A.III.4 The uniform laminar flow of a power-law fluid in an open channel: two-dimensional model with velocity varying with depth.

The model is illustrated in Fig. A.III.7 and corresponds to the case of flow over an infinite plane surface.

Now τ is a function of y only and $\tau = 0$ at $y = h$ (free surface) so that the distribution of shear stress with distance from the surface of the plane is given by

$$\tau = \rho g (h - y) \sin \alpha \qquad \text{.....A.III.25}$$

Writing $\tau = k(du/dy)^n$ and following a similar procedure to that set out in Section A.III.3, expressions can be derived for the velocity distribution and average velocity as follows:-

$$u = \left(\frac{\rho g \sin \alpha}{k}\right)^{\frac{1}{n}} \left[h^{\frac{1}{n}} y - \frac{n}{n+1} y^{\frac{n+1}{n}}\right] + C \qquad \text{.....A.III.26}$$

where C is a constant of integration, which is zero for the case of zero slip, so that

$$u = \left(\frac{\rho g h \sin \alpha}{k}\right)^{\frac{1}{n}} \left[y - \frac{n}{n+1} h^{-\frac{1}{n}} y^{\frac{n+1}{n}}\right] \qquad \text{.....A.III.27}$$

Also

$$u_{av} = \left(\frac{\rho g h \sin \alpha}{k}\right)^{\frac{1}{n}} h\left[\frac{3n+1}{2(n+1)(2n+1)}\right] \qquad \text{.....A.III.28}$$

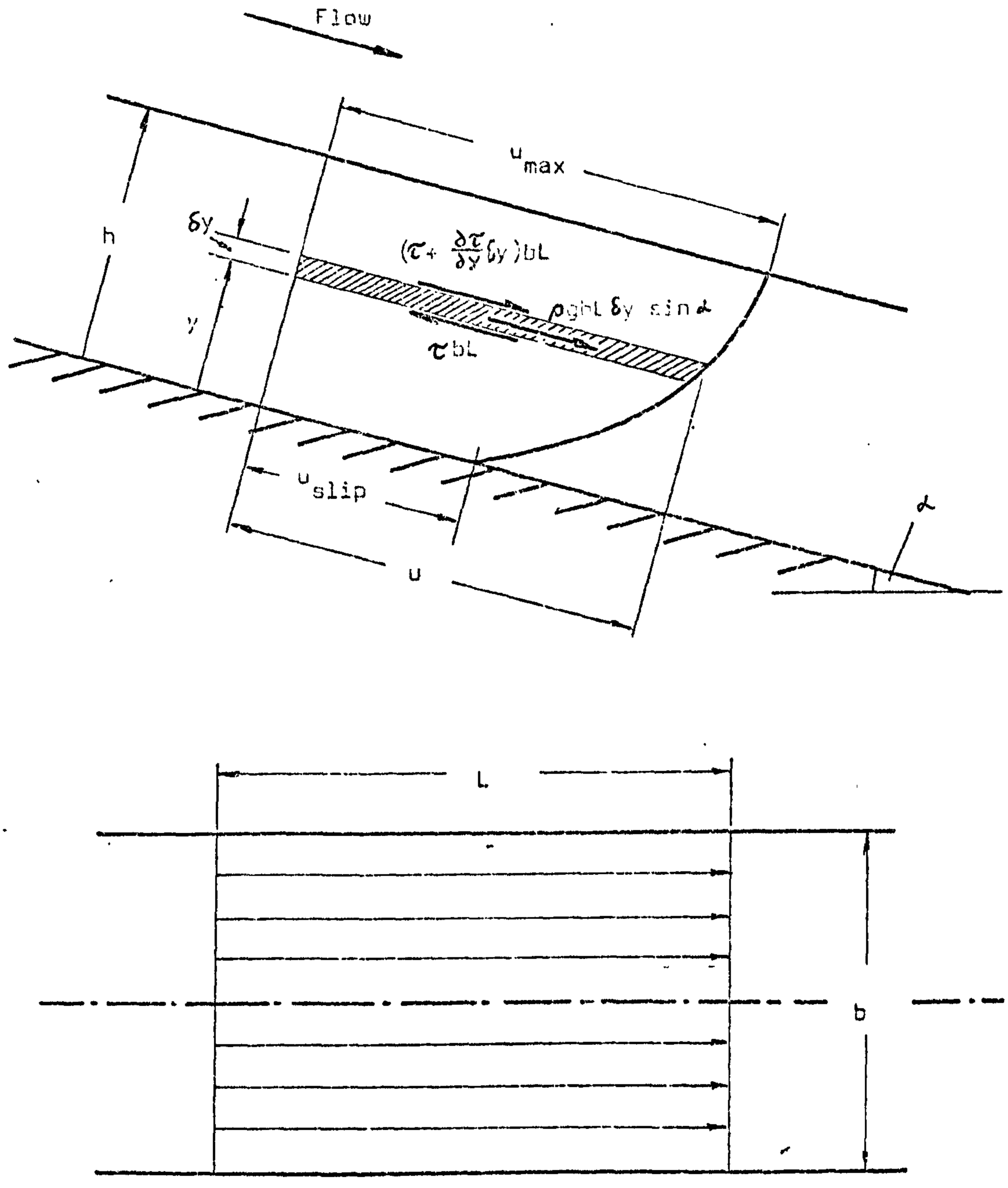

Fig. A.III.7 TWO-DIMENSIONAL LAMINAR FLOW OF A POWER-LAW FLUID IN AN INCLINED CHANNEL (WITH VELOCITY VARYING WITH DEPTH).

Again, writing the shear stress at the surface of the plane (y = 0) as $\tau_b = \rho g h \sin\alpha$, we have on rearranging equation A.III.28,

$$\tau_b = \left(\frac{u_{av}}{h}\right)^n k\left[\frac{2(n+1)(2n+1)}{3n+1}\right] \qquad \text{.....A.III.29}$$

and comparison with equation A.III.1 suggests that for this model the shear rate at the base could be expressed as

$$\dot{\gamma} = \frac{u_{av}}{h} \cdot \frac{2(n+1)(2n+1)}{3n+1} \qquad \text{.....A.III.30}$$

In log. form equation A.III.29 becomes

$$\ln\tau_b = n\ln\left(\frac{u_{av}}{h}\right) + \ln\left[k\left(\frac{2(n+1)(2n+1)}{3n+1}\right)\right] \qquad \text{.....A.III.31}$$

$$\ln(\rho g h \sin\alpha) = n\ln\left(\frac{\dot{m}}{\rho b h^2}\right) + \ln\left[k\left(\frac{2(n+1)(2n+1)}{3n+1}\right)\right] \qquad \text{.....A.III.32}$$

Thus, for this model a log. plot of τ_b against u_{av}/h would yield a straight line of slope n. The "consistency constant" k could again be determined from the intercept (Fig. A.III.8).

The mass flowrate, $\dot{m} = \rho b h u_{av}$, so that from equation A.III.28,

$$\dot{m} = \rho b h^2\left[\frac{3n+1}{2(n+1)(2n+1)}\right]\left(\frac{\rho g h \sin\alpha}{k}\right)^{\frac{1}{n}} \qquad \text{.....A.III.33}$$

or, for a Newtonian fluid, setting n = 1 and k = μ,

$$\dot{m} = \frac{\rho^2 g b h^3 \sin\alpha}{3\mu} \qquad \text{.....A.III.34}$$

To examine the effect of slip at the surface of the inclined plane (corresponding to slip at the base of a wide channel) an exactly similar approach to that leading up to equations A.III.18 and A.III.20 can be followed.

Thus $$\tau_b = \left(\frac{u_{av} - u_{slip}}{h}\right)^n k\left(\frac{2(n+1)(2n+1)}{3n+1}\right)^n \qquad \text{.....A.III.35}$$

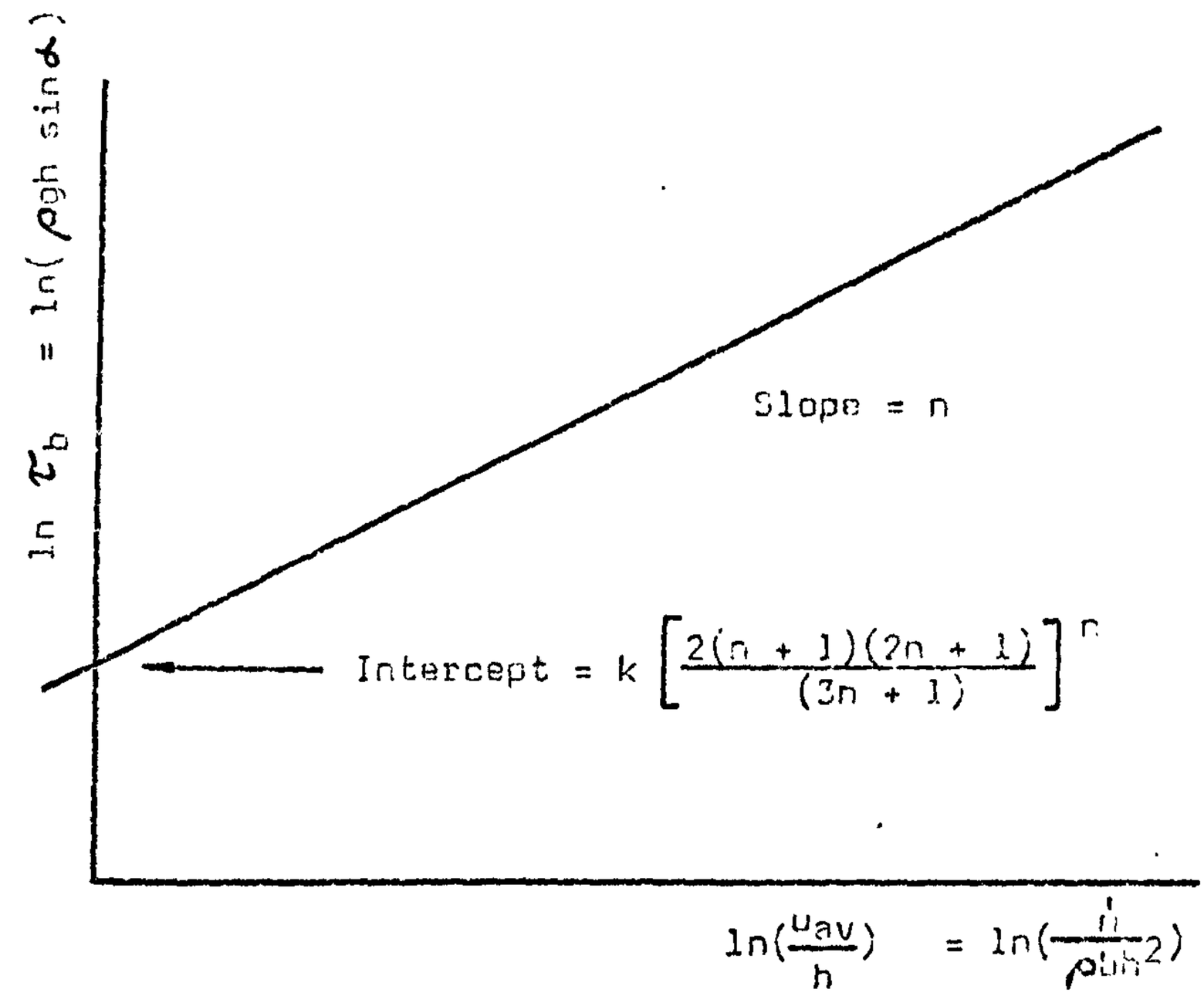

Fig. A.III.8 LOG PLOT OF τ_b AGAINST u_{av}/h TO DETERMINE n AND k FOR THE TWO-DIMENSIONAL FLOW OF A POWER-LAW FLUID ON AN INCLINED PLANE SURFACE.

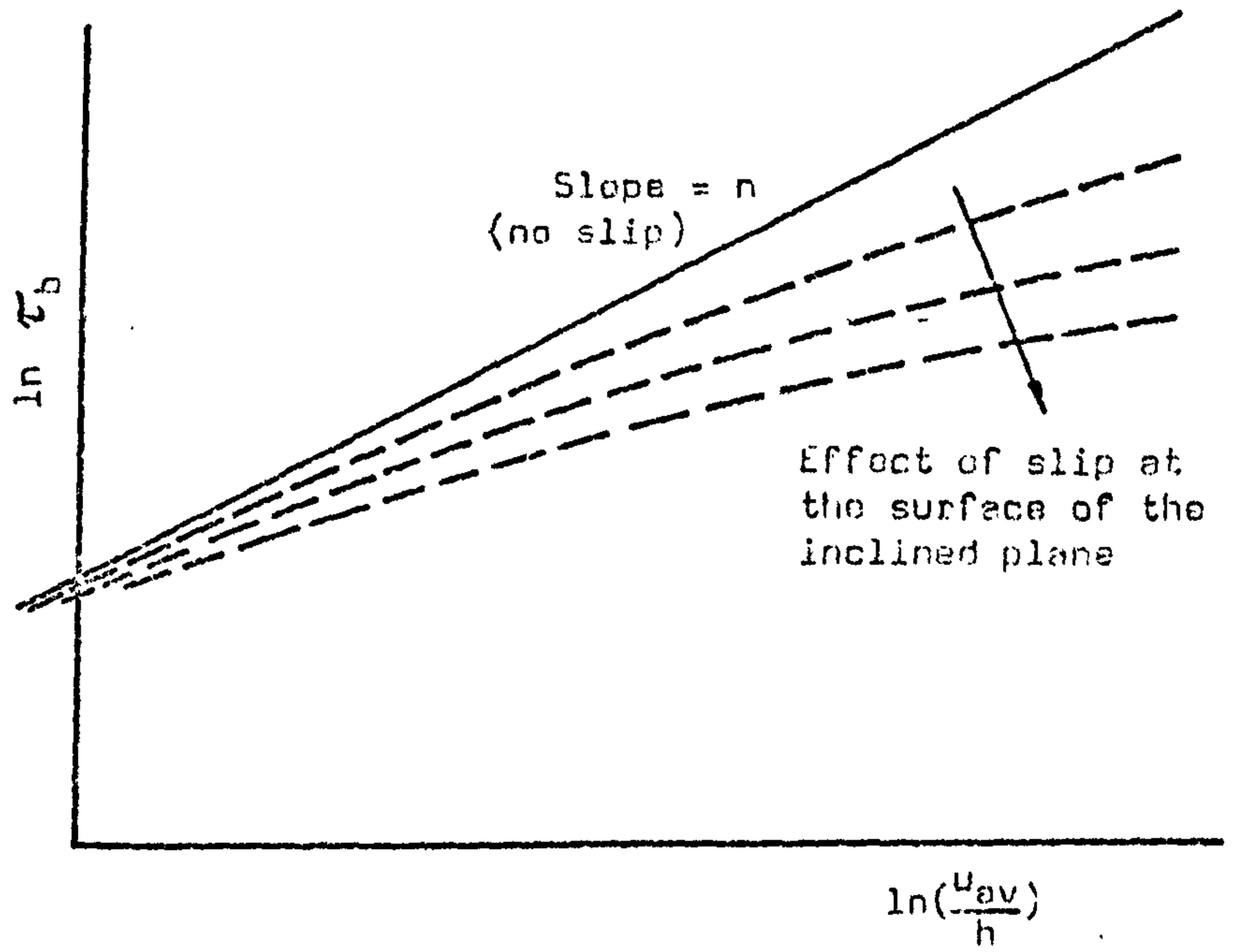

Fig. A.III.9 LOG PLOT OF τ_b AGAINST u_{av}/h FOR THE TWO-DIMENSIONAL MODEL, SHOWING THE INFLUENCE OF SLIP AT THE SURFACE OF THE PLANE (CORRESPONDING TO THE BASE OF A WIDE INCLINED CHANNEL).

and

$$\ln \tau_b = n \ln \left(\frac{u_{\varepsilon v}}{h}\right) + n \ln \left(1 - \frac{u_{slip}}{u_{av}}\right) + \ln \left[k \left(\frac{2(n+1)(2n+1)}{3n+1} \right) \right] \quad \ldots A.III.36$$

As before, the effect of slip should be evident from a downward deviation from the linear plot of $\ln \tau_b$ against $\ln(u_{av}/h)$ as shown on Fig. A.III.9.

As for the previous model, a dimensionless velocity profile may be obtained by combining equations A.III.27 and A.III.28 to yield

$$\frac{u}{u_{av}} = \frac{2(n+1)(2n+1)}{3n+1} \left[\frac{y}{h} - \frac{n}{n+1} \left(\frac{y}{h}\right)^{\frac{n+1}{n}} \right] \quad \ldots A.III.37$$

For n = 1 this expression becomes

$$\frac{u}{u_{av}} = 3 \left[\frac{y}{h} - \frac{1}{2} \left(\frac{y}{h}\right)^2 \right] \quad \ldots A.III.38$$

which represents a parabolic profile and corresponds to the case of a Newtonian fluid in laminar flow on an infinite inclined plane. Again, the shape of the velocity profile varies with the value of n, tending towards the Bingham plastic model as n falls below unity.

A.III.5 The uniform flow of a power-law fluid in an inclined channel: three-dimensional model with equal shear stress and equal slip at base and walls.

An analysis of the three-dimensional model tends to be rather more difficult, but a possible approach, based on an extension of the Rabinowitsch-Mooney equation for flow in channels of arbitrary shape, has been shown by Kozicki and Tiu (Ref. K7). In this model the equation of motion of the flow in the channel is first expressed as

$$\tau_o = \rho g \lambda \sin \alpha \quad \ldots A.III.39$$

where τ_o is the boundary shear stress (which is the same at the channel walls and at the channel base) and λ is the hydraulic mean depth of the flow, defined by

$$\lambda = \frac{bh}{b + 2h} \qquad \text{.....A.III.40}$$

The effect of slip on the channel surfaces is taken into account in the analysis of Kozicki and Tiu (although, like the shear stress, it is assumed to be the same at the walls and base of the channel) and the expression derived by them for the average velocity of a power-law fluid in an inclined channel is thus

$$u_{av} = u_{slip} + \frac{\lambda}{2}\left(\frac{\tau_o}{k}\right)^{\frac{1}{n}}\left(\frac{n}{A + Bn}\right) \qquad \text{.....A.III.41}$$

where A and B are "geometric coefficients", the values of which depend upon the cross-sectional shape of the channel and the aspect ratio of the flow.

Equation A.III.41 can be rearranged to give shear stress as

$$\tau_o = k\left(\frac{u_{av} - u_{slip}}{\lambda}\right)^n \left[\frac{2(A + Bn)}{n}\right]^n \qquad \text{.....A.III.42}$$

which is of the same form as the corresponding expressions for shear stresses at the base and walls in the two-dimensional models (equations A.III.18 and A.III.35) and, in the same way, suggests that a plot of $\ln \tau_o$ against $\ln(u_{av}/\lambda)$ could give information on the existence of slip. Thus, writing equation A.III.42 in log form

$$\ln \tau_o = n \ln\left(\frac{u_{av}}{\lambda}\right) + n \ln\left(1 - \frac{u_{slip}}{u_{av}}\right) + \ln\left[k\left(\frac{2A + 2Bn}{n}\right)\right]^n \qquad \text{.....A.III.43}$$

it is seen that a plot of $\ln \tau_o$ against $\ln(u_{av}/\lambda)$ could only be expected to be linear if the slip is zero.

In order to gain an impression of the deviation of equation A.III.42 from a simple power-law relationship, the term involving the geometric coefficients A and B (which is a function of aspect ratio and power-law

index) is shown plotted against h/b for various values of n in Fig. A.III.10. It is seen that for values of aspect ratio within the range 0.3 to 1.0 (a realistic range for most practical channel flow applications) the function is virtually constant, depending only upon the power-law index n. For n = 1 the function has a value of around 1.8, so that for a Newtonian fluid with zero slip, the shear stress would be given by

$$\tau_o \simeq 1.8\frac{\mu u_{av}}{\lambda} \qquad \text{.....A.III.44}$$

from which an expression for mass flowrate can be derived as

$$\dot{m} \simeq \frac{\rho^2 g \lambda^2 b h \sin\alpha}{1.8\mu} \qquad \text{.....A.III.45}$$

A.III.6 The relationship between "friction factor" and "Reynolds number" for the laminar flow of power-law fluids in inclined channels.

The convenience of the correlation f = 16/Re for the laminar flow of Newtonian fluids has led many authors to look for a corresponding correlation that would apply generally to fluids whether they exhibit Newtonian or time-independent non-Newtonian behaviour. Metzner and Reed (Ref. M8) proposed generalized parameters for the flow of a fluid in a circular pipe of diameter D as

$$f' = \frac{16\ k'\ 8^{n'-1}}{D^{n'}\ u_{av}^{\ 2-n'}\ \rho} \qquad \text{.....A.III.46}$$

and

$$Re' = \frac{D^{n'}\ u_{av}^{\ 2-n'}\ \rho}{k'\ 8^{n'-1}} \qquad \text{.....A.III.47}$$

where n' defines the extent of divergence from Newtonian behaviour and is effectively the same as the index in the power law model (equation A.III.1) and k' is a factor defining the consistency of the fluid.

Following this approach, friction factor and Reynolds number parameters can be defined for fluid flow in inclined channels using the model

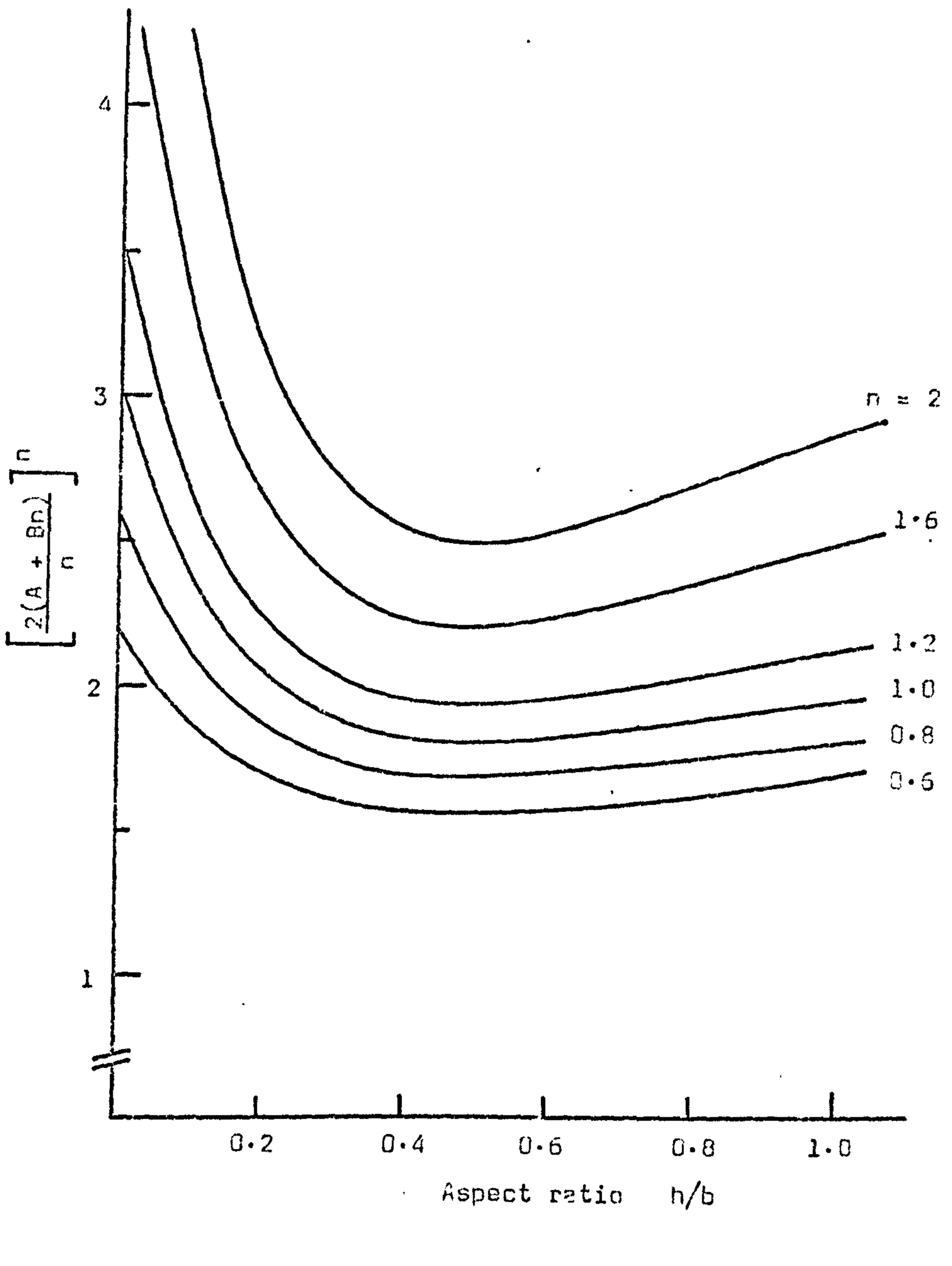

Fig. A.III.10 VARIATION OF FUNCTION IN EQUATION A.III.42 WITH ASPECT RATIO OF THE FLOW IN THE CHANNEL.

discussed in the previous Section.

Thus, writing $f_c = \tau_o / \frac{1}{2} \rho u_{av}^2$, we have from equation A.III.42, for zero slip

$$f_c = \frac{2k}{\rho \lambda^n u_{av}^{2-n}} \left[\frac{2(A + Bn)}{n}\right]^n \qquad \text{.....A.III.48}$$

and setting $f_c = 16/Re'$

$$Re' = \frac{8 \rho \lambda^n u_{av}^{2-n}}{k} \left[\frac{n}{2(A + Bn)}\right]^n \qquad \text{.....A.III.49}$$

where again FigA.III.10 can be consulted for values of the term involving the geometric coefficients A and B.

A.III.7 The Bingham plastic model of non-Newtonian fluid behaviour.

A certain class of real fluids exhibit a behaviour that is characterised by an initial resistance to shear deformation until a yield stress is reached. Once deformation has started, equal increments of stress tend to produce equal increments in velocity with the fluid flowing in a more or less Newtonian manner. A convenient model to represent this type of behaviour is the Bingham plastic which is illustrated in Fig. A.III.11 in the form of a plot of shear stress against shear rate.

It may be noted that, as in the case of power law fluids, the "apparent viscosity" μ_a, defined as

$$\mu_a = \frac{\tau}{\dot{\gamma}} \qquad \text{.....A.III.50}$$

depends upon the rate of shear. However, for the Bingham plastic an alternative parameter can be defined as the slope of the plot of τ against $\dot{\gamma}$ after flow has commenced.

Thus
$$\eta = \frac{\tau - \tau_y}{\dot{\gamma}} \qquad \text{.....A.III.51}$$

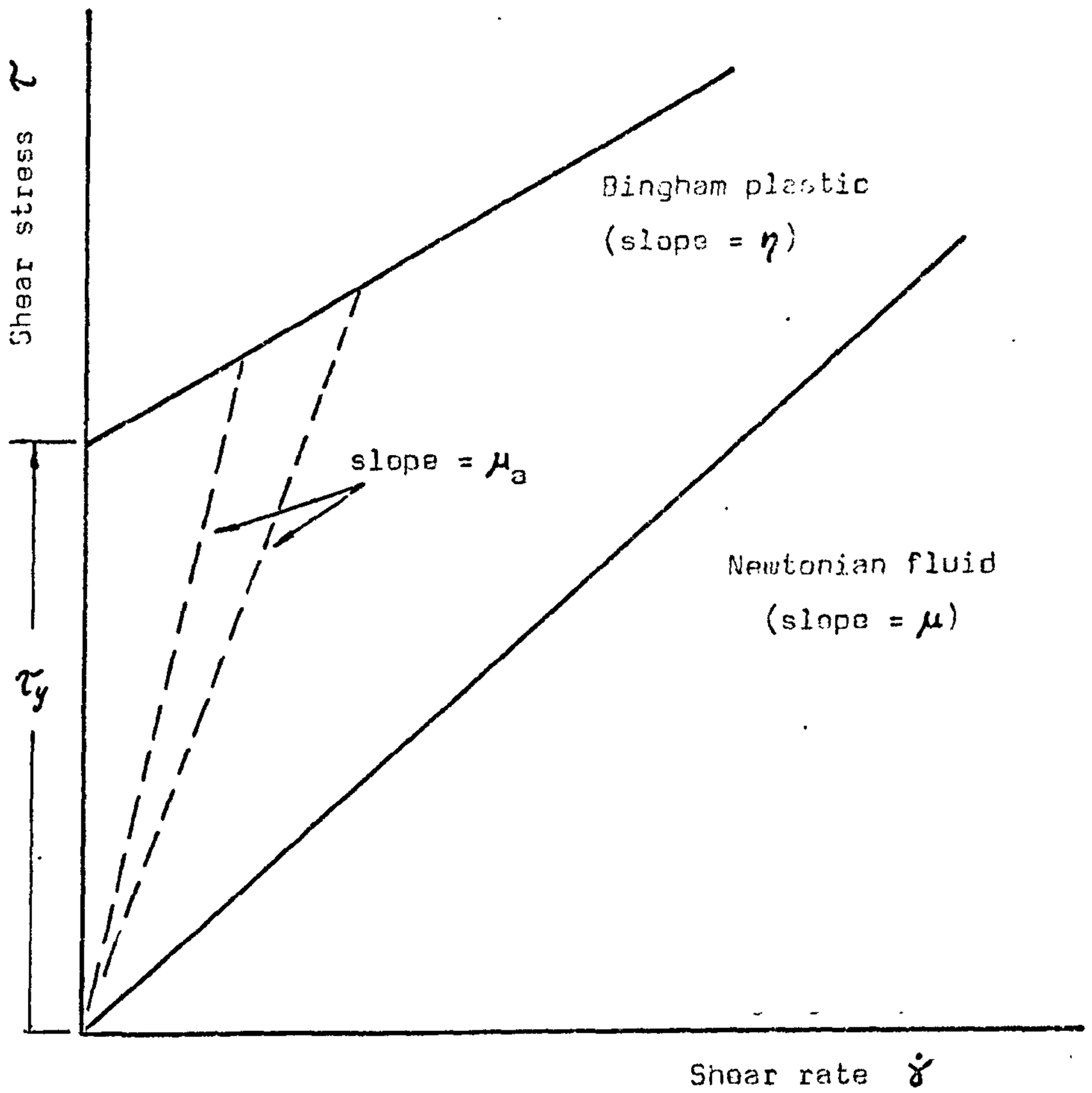

Fig. A.III.11 VARIATION OF SHEAR STRESS WITH SHEAR RATE FOR A BINGHAM PLASTIC, SHOWING "COEFFICIENT OF RIGIDITY η", YIELD STRESS τ_y AND APPARENT VISCOSITY μ_a.

where τ_y is the yield stress and η is usually called the "coefficient of rigidity" of the fluid.

A.III.8 <u>The uniform laminar flow of a Bingham plastic in an inclined channel: two-dimensional model with velocity varying in the lateral direction.</u>

A force balance on a lamina at distance x from the channel centreline (Fig. A. III.12) gives, as in the case of the power-law model (Section A.III.3)

$$\tau_w = \rho g x \sin\alpha \qquad \text{.....A.III.52}$$

Now for a Bingham plastic, the shear stress may be written (from equation A.III.51)

$$\tau = \tau_y + \eta\left(-\frac{du}{dx}\right) \qquad \text{.....A.III.53}$$

so that

$$-\frac{du}{dx} = \frac{\tau - \tau_y}{\eta} \qquad \text{.....A.III.54}$$

and

$$u = \frac{\tau_y x}{\eta} - \frac{\rho g x^2 \sin\alpha}{2\eta} + C \qquad \text{.....A.III.55}$$

For no slip at the channel walls, u = 0 at x = b/2

i.e. $$C = \frac{\rho g b^2 \sin\alpha}{8\eta} - \frac{\tau_y b}{2\eta} .$$

so that

$$u = \frac{\tau_o}{4\eta b}(b^2 - 4x^2) - \frac{\tau_y}{2\eta}(b - 2x) \qquad \text{.....A.III.56}$$

The velocity distribution for the two-dimensional flow of a Bingham plastic is best expressed in two parts:-

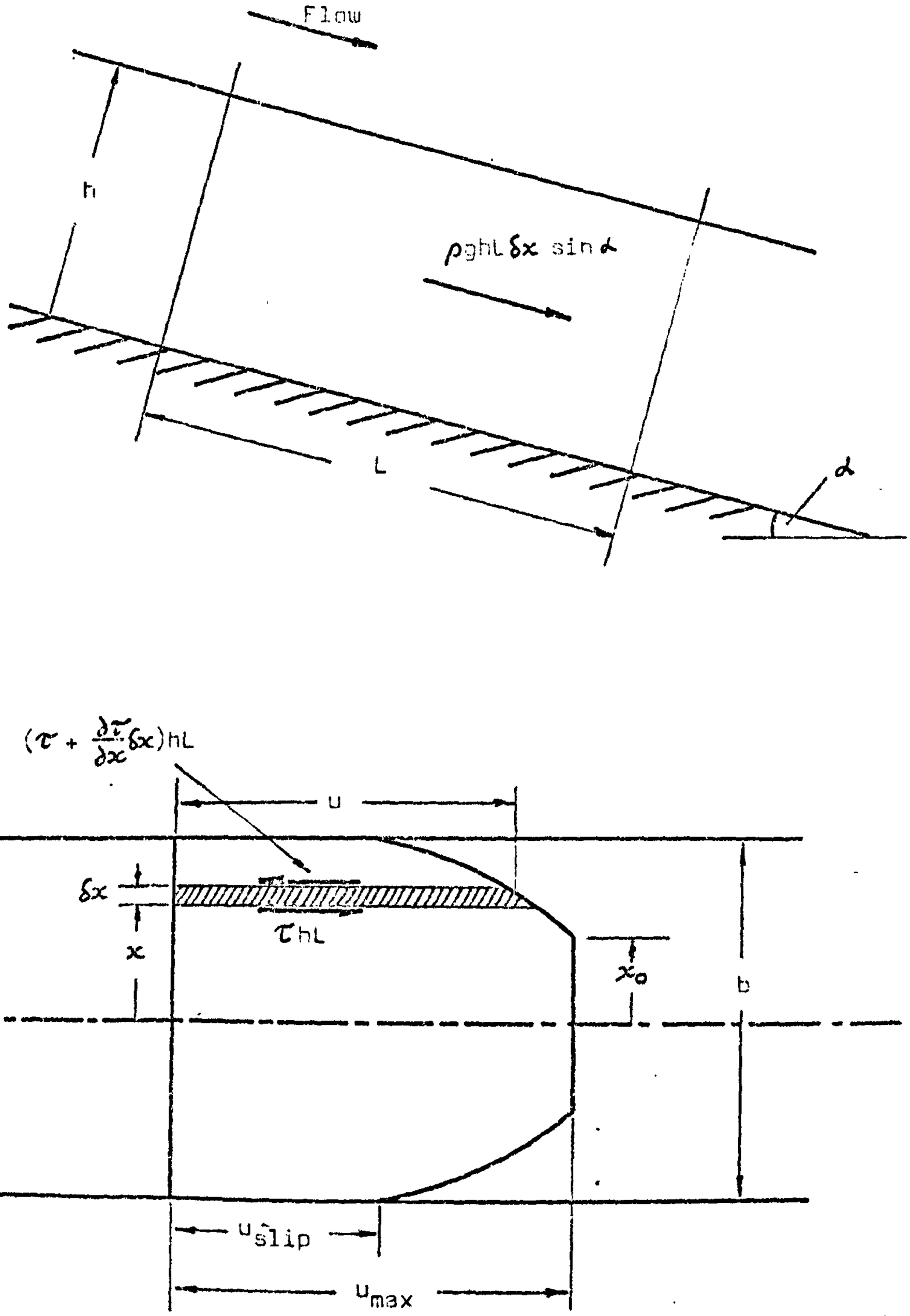

Fig. A.III.12 TWO-DIMENSIONAL LAMINAR FLOW OF A BINGHAM PLASTIC IN AN INCLINED CHANNEL (WITH VELOCITY VARYING IN THE LATERAL DIRECTION).

For $x_o < b < b/2$ the velocity is given by equation A.III.56.
For $0 < x < x_o$ the velocity is uniform and is given by the expression

$$u = u_{max} = \frac{\tau_w}{4\eta b}(b^2 - 4x_o) - \frac{\tau_y}{2\eta}(b - 2x_o) \qquad \text{.....A.III.57}$$

where $x = x_o$ gives the position where $\tau = \tau_y$.

Volume flowrate can then be determined from

$$\dot{V} = 2hx_o u_{max} + 2h\int_{x_o}^{\frac{b}{2}} u\,dx \qquad \text{.....A.III.58}$$

Substituting for u_{max} and u and carrying out the integration leads to

$$\dot{V} = \frac{1}{6}\frac{hb^2}{\eta}\tau_w - \frac{4}{3}\frac{hx_o^3}{\eta b}\tau_w - \frac{1}{4}\frac{hb^2}{\eta}\tau_y + \frac{hx_o^2}{\eta}\tau_y$$

and noting that

$$x_o = \frac{\tau_y}{\rho g \sin\alpha} = \frac{\tau_y}{\tau_w}\cdot\frac{b}{2}$$

a further substitution for x_o leads to

$$\dot{V} = \frac{hb^2}{12\eta}\left(2\tau_w - 3\tau_y + \frac{\tau_y^3}{\tau_w^2}\right) \qquad \text{.....A.III.59}$$

from which

$$u_{av} = \frac{b\tau_w}{6\eta}\left[1 - \frac{3}{2}\left(\frac{\tau_y}{\tau_w}\right) + \frac{1}{2}\left(\frac{\tau_y}{\tau_w}\right)^3\right] \qquad \text{.....A.III.60}$$

Following now the suggestion of Caldwell and Babbitt (Ref. C1) who developed expressions of this form for the flow of a Bingham plastic in a circular pipe, the final term in equation A.III.60 can be omitted with only a small error, so that an approximate expression for the average velocity in an inclined channel is

$$u_{av} = \frac{b}{6\eta}\left(\tau_w - \frac{3\tau_y}{2}\right) \qquad \text{.....A.III.61}$$

Rearranging,

$$\tau_w = \frac{6\,u_{av}}{b}\,\eta + \frac{3\,\tau_y}{2} \qquad \text{.....A.III.62}$$

Now Caldwell and Babbit (Ref. C1) report that Bingham showed η and τ_y to be properties of the flowing material (independent of the characteristics of the channel) and their own work on circular pipes tended to confirm this conclusion. Thus for this two-dimensional model of the flow of a Bingham plastic, a plot of τ_w against $6\,u_{av}/b$ should yield a straight line of slope η and intercept $3\,\tau_y/2$. (Fig. A.III.13)

The effect of slip at the channel walls can be taken into account, as before, by writing $(u - u_{slip})$ for u. Thus equation A.III.52 becomes

$$\tau_w = \frac{6\,u_{av}}{b}\,\eta\,\left(1 - \frac{u_{slip}}{u_{av}}\right) + \frac{3}{2}\,\tau_y \qquad \text{.....A.III.63}$$

from which it is evident that the effect of slip might be to reduce the slope of the plot of τ_w against $6\,u_{av}/b$ as shown on Fig. A.III.13.

A.III.9 The uniform laminar flow of a Bingham plastic in an inclined channel: two dimensional model with velocity varying with depth.

Following an analysis very similar to those of the previous models, we find that the velocity distribution in this case is:-

For $0 < y < y_o$

$$u = u_{slip} + \left(\frac{\tau_b - \tau_y}{\eta}\right) y - \frac{\tau_b}{2\,h\,\eta}\,y^2 \qquad \text{.....A.III.64}$$

For $y_o < y < h$

$$u = u_{max} = u_{slip} + \left(\frac{\tau_b - \tau_y}{\eta}\right) y_o - \frac{\tau_b}{2\,h\,\eta}\,y_o^2 \qquad \text{.....A.III.65}$$

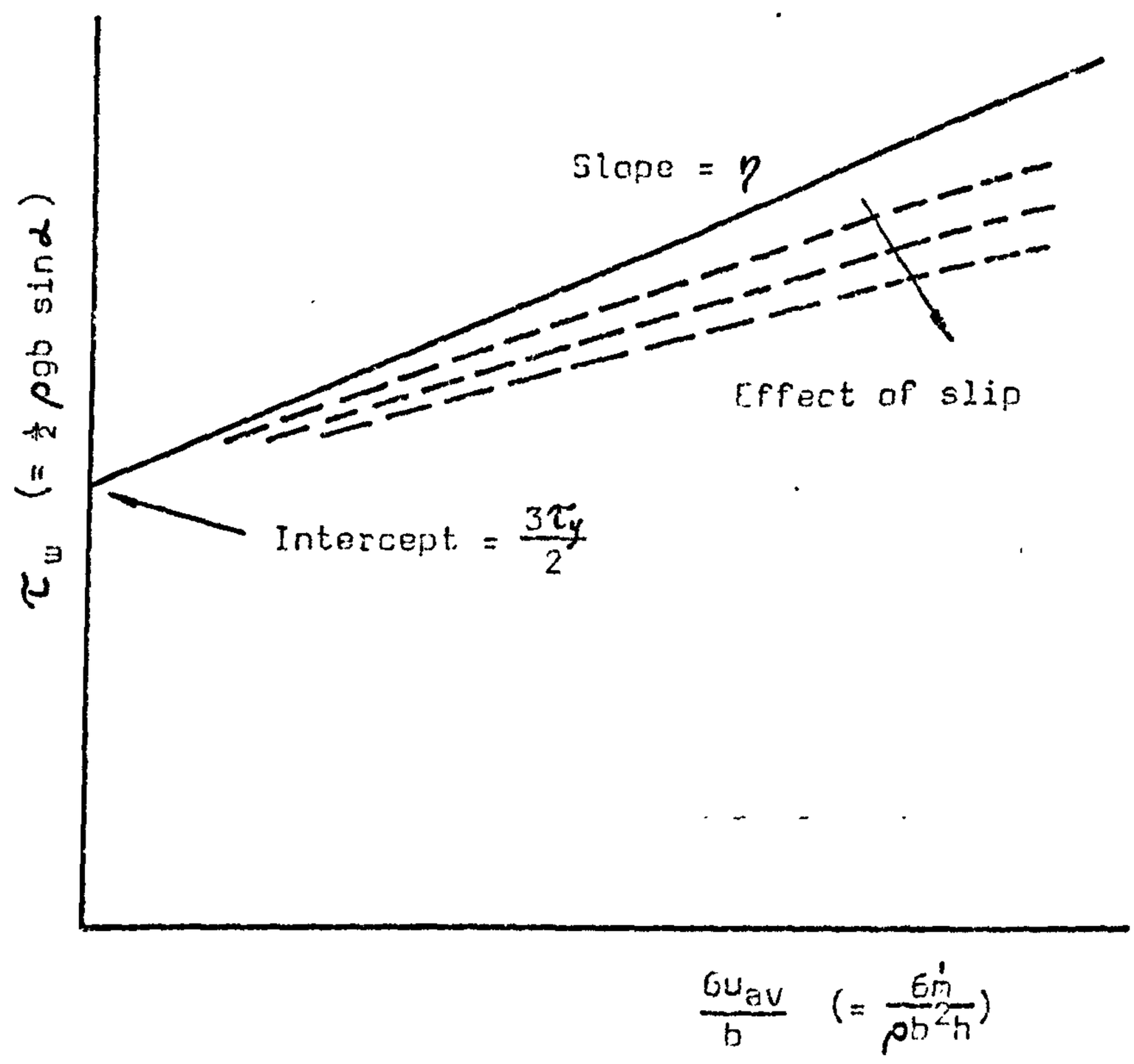

Fig. A.III.13 PLOT OF τ_w AGAINST $6u_{av}/b$ FOR THE TWO-DIMENSIONAL BINGHAM PLASTIC MODEL.

The average velocity in the channel can be shown to be given by

$$u_{av} = \frac{h\tau_b}{3\eta}\left[1 - \frac{3}{2}\left(\frac{\tau_y}{\tau_b}\right) + \frac{1}{2}\left(\frac{\tau_y}{\tau_b}\right)^3\right] \qquad \text{.....A.III.66}$$

and the similarity to equation A.III.60, for the other two-dimensional model, is clear.

Simplifying this expression, as before, we get

$$\tau_b = \frac{3u_{av}}{h}\eta + \frac{3\tau_y}{2} \qquad \text{.....A.III.67}$$

and it is seen that once again, a plot of τ_b against $3u_{av}/h$ should result in a straight line from which η and τ_y could be found, if there is no slip.

A.III.10 <u>The uniform flow of a Bingham plastic in an inclined channel: three-dimensional model with equal shear stress and equal slip at base and walls.</u>

As remarked previously, the rigorous analysis of the three-dimensional model is not easy. However, Kozicki and Tiu (Ref. K7) include the Bingham plastic as one of the model fluids in their generalized analysis of non-Newtonian fluid flow in open channels. The full expressions for average velocity and Reynolds number, as given by Kozicki and Tiu, are unfortunately somewhat unwieldy owing to the presence of the geometric coefficients A and B. However, it is of interest to note that the form of the relationships is similar to those developed for the two-dimensional cases.

Thus, for example, for average velocity (without slip) Kozicki and Tiu give

$$u_{av} = \frac{\lambda\tau_o}{2\eta}\left[\frac{1}{A+B} - \frac{1}{B}\left(\frac{\tau_y}{\tau_o}\right) + \frac{A}{B(A+B)}\left(\frac{\tau_y}{\tau_o}\right)^{\frac{A+B}{A}}\right] \qquad \text{.....A.III.68}$$

which in fact reduces to equation A.III.60 as $h/b \to \infty$ and to equation A.III.66 to $h/b \to 0$.

Simplifying Kozicki and Tiu's equation by omitting the last term, we get an approximate expression for τ_o as

$$\tau_o = \frac{2\eta (A+B) u_{av}}{\lambda} + \left(\frac{A+B}{B}\right) \tau_y \qquad \text{.....A.III.69}$$

This suggests that, unless experimental measurements can be carried out at constant aspect ratio, a plot of τ_o against u_{av}/λ may not allow the determination of η and τ_y, since the contribution of the yield stress of the fluid to the overall flow resistance is dependent upon the aspect ratio of the flow.

For convenience, values of Kozicki and Tiu's geometric coefficients, A and B, are plotted on Fig. A.III.14 over a moderate range of aspect ratio.

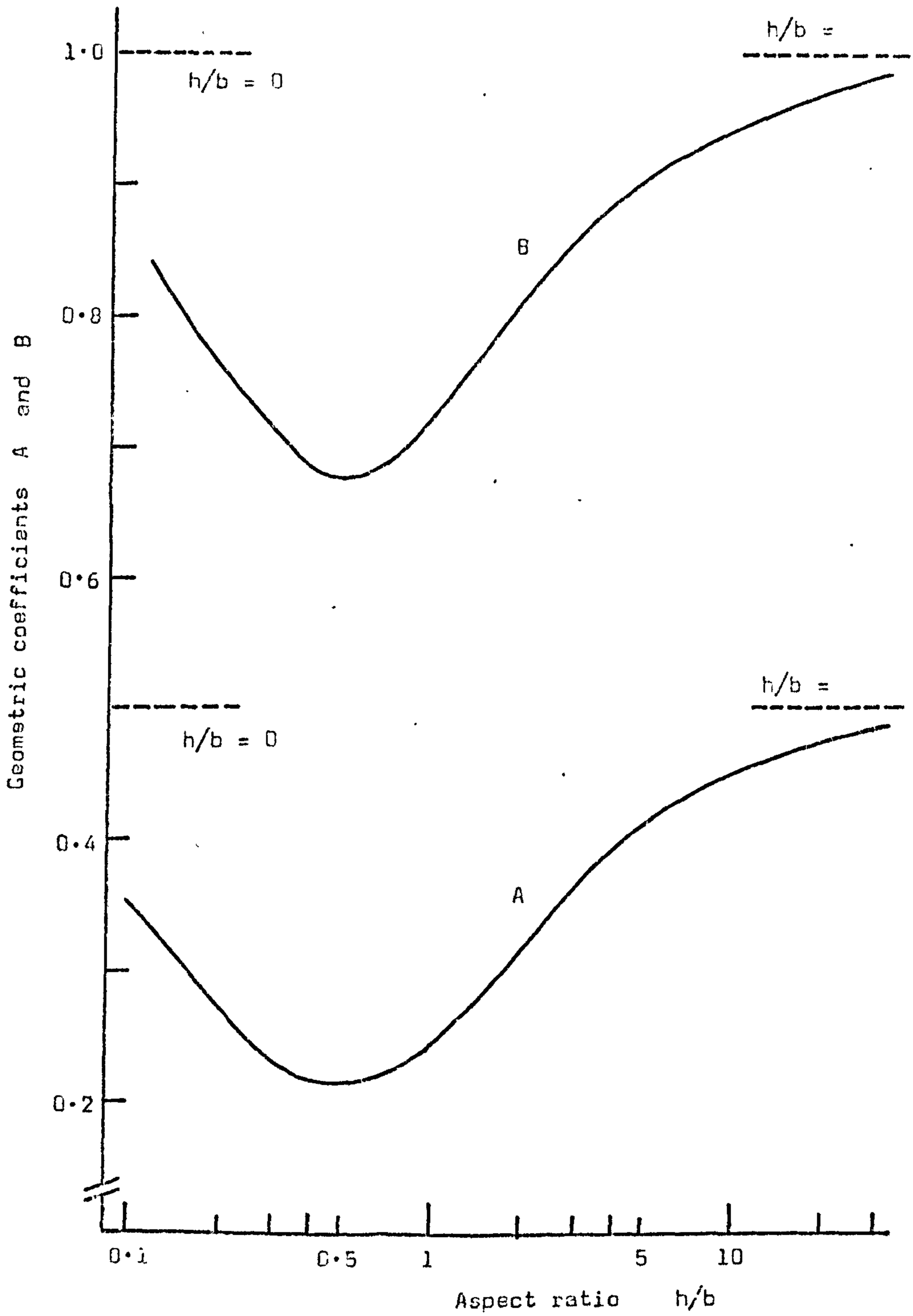

Fig. A.III.14 GEOMETRIC COEFFICIENTS FOR CHANNELS OF RECTANGULAR CROSS SECTION (Kozicki and Tiu; Ref. K7)

APPENDIX A.IV

SUPPLIERS/MANUFACTURERS OF AIR-ASSISTED GRAVITY CONVEYING EQUIPMENT

A.IV.1 Conveyors and component units.

POLYSIUS LTD., "Fluidor"
The Brackens,
Ascot, Berks.
Tel: Winkfield Row (034 47)2011

GEO. W. KING LTD., "Gravitair"
P.O. Box No. 18,
Stevenage,
Hertfordshire SG1 2AA.
Tel: Stevenage (0438) 4400

SHEEPBRIDGE EQUIPMENT LTD.,
Chesterfield,
Derbyshire S41 9QD.
Tel: Chesterfield (0246) 5471 & 51631

GATX-FULLER LTD., "Airslide"
Radnor House,
1272 London Road,
London SW16 4DX.
Tel: 01-764 9571

LING SYSTEMS LTD., "JetStream"
Unit Eight,
Station Road,
Gamlingay,
Sandy,
Bedfordshire SG19 3HG.
Tel: Gamlingay (0767) 50101

DOULTON INDUSTRIAL PRODUCTS LTD.,
Filleybrooks,
Stone,
Staffordshire.
Tel: Stone (078 583) 3241

S.A. DES ETABLISSEMENTS NEU,
Siege Social: 47, rue Fourier,
59000 Lille,
France.

SKET,
Veb Zementanlagenbau Dessau,
DDR - 45 Dessau, Brauereistrasse 13

FULLER COMPANY, "Airslide"
124 Bridge Street,
Catasauqua,
Pa. 18032, U.S.A.

AERODYNE MACHINERY, "Fluid-Slide"
General Resource Corp.,
201 South Third Street,
Hopkins,
Minnesota 55343, U.S.A.

WHIRL-AIR-FLOW, "Whirl-Slide"
1515 Central Avenue, Northeast,
Minneapolis,
Minnesota 55413, U.S.A.

DUCON FLUID TRANSPORT, "FLO/tray"
840 First Avenue,
King of Prussia,
Pennsylvania 19406, U.S.A.

HALLIBURTON SERVICES, "Air Trough"
Special Products Division,
P.O. Drawer 1431,
Duncan,
Oklahoma 73533, U.S.A.

A.IV.2 Porous distributor materials

PORVAIR LTD., "Vyon" (sintered plastic sheet)
Estuary Road,
Kings Lynn,
Norfolk PE30 2HS
Tel: Kings Lynn (0553) 61111

SCANDURA LTD., "Top Line" woven cotton, polyester
P.O. Box No.18, and asbestos belting.
Cleckheaton,
Yorkshire BD19 3UJ
Tel: Cleckheaton (097-62) 5711

DOULTON INDUSTRIAL PRODUCTS LTD., "Pyrolith" (sintered ceramic
Filleybrooks, tiles)
Stone,
Staffordshire.
Tel: Stone (078 583) 3241

GANDY LTD., "Wocot" (woven cotton belting)
P.O. Box No.2,
Wallesey,
Cheshire L44 7EL
Tel: Wallesey (051-638) 6432/7

ACCUMATIC ENGINEERING LTD., "Sintercon" (sintered bronze
Llay Hall, sheet)
Cefn-y-Bedd,
Wrexham,
North Wales LL2 9YH
Tel: Caergwrle (0978) 760751

MICHIGAN DYNAMICS, 32400 Ford Road, Garden City, Michigan 48135, U.S.A.	"Dynapore" (woven wire mesh laminate)
FACET ENTERPRISES, INC., Filter Products Division, 434, West Twelve Mile Road, P.O. Box 135, Madison Heights, Michigan 48071, U.S.A.	"Poroflow" (woven wire mesh laminate)
OY NOKIA AB, Finnish Cable Works, Lapinlahdenkatu 1 G, 00180 Helsinki 18, Finland.	"Nopol" (porous plastic sheeting)
HEIN, LEHMANN AG, Postfach 4109, Fichtenstrasse 75, 4000 Dusseldorf, West Germany.	"Conidor" fine-hole perforated metal sheeting)

APPENDIX A.V.

CALIBRATION CURVES AND GENERAL INFORMATION ON EQUIPMENT USED IN EXPERIMENTAL INVESTIGATION.

A.V.1 Rotameters

Manufactured by: GEC-Elliott Process Instruments Ltd.,
Rotameter Works,
330 Purley Way,
Croydon, CR9 4PG

Types used:

Metric Series,	size 10	float A	}	small fluidising rig
	" 24X	" A	}	
	size 35	float A	}	main channel flow rig
	" 65	" A	}	
	" 65X	" K	}	

Calibration:

For the three rotameters used on the air supply to the main channel the manufacturer's calibration curves were considered to be adequate (Figs. A.V.1 to A.V.3).

However, the two rotameters on the small fluidising rig had to provide a continuous range of flow from virtually zero to the maximum indicated on the larger instrument and consequently it was decided to calibrate them together on a specially constructed apparatus. This apparatus, which is illustrated in Fig. A.V.4, consisted of a tank of about 140 litre capacity, connected by a 50 mm diameter pipe to the mains water supply. A control valve on this inlet pipe allowed the water flow to be adjusted from zero up to about 150 litres/min, the flowrate being measured by timing the rise of the level in a sight glass fitted to the tank. The rotameter to be calibrated was connected to the air outlet from the top of the tank, the rate of air displaced being equal to the rate of water inflow. Figs. A.V.5 and A.V.6 are the calibrations obtained by this method.

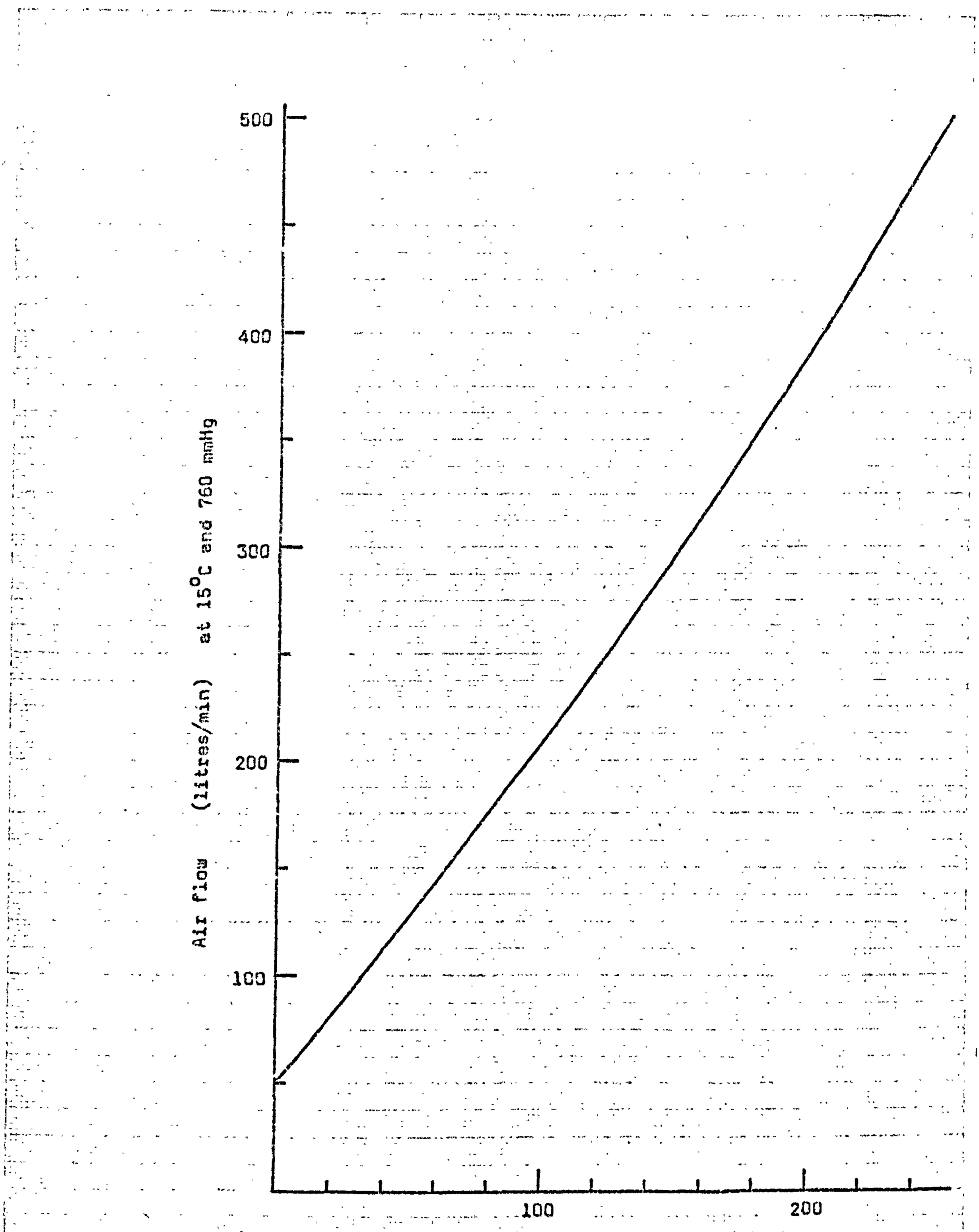

Fig. A.V.1 ROTAMETER CALIBRATION CHART (AIR)

Tube size 35; float type A.

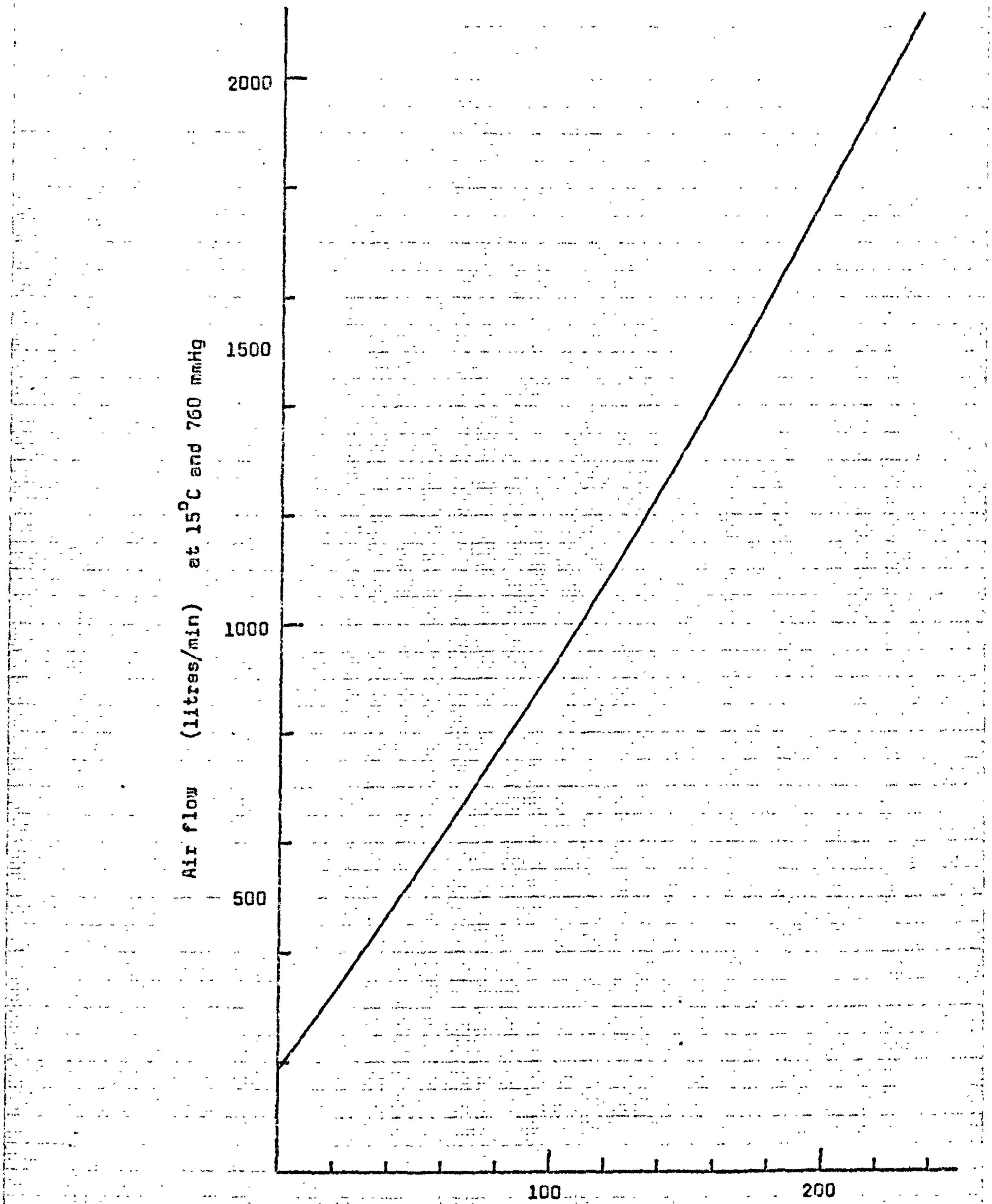

Fig. A.V.2 ROTAMETER CALIBRATION CHART (AIR)

Tube size 65; float type A.

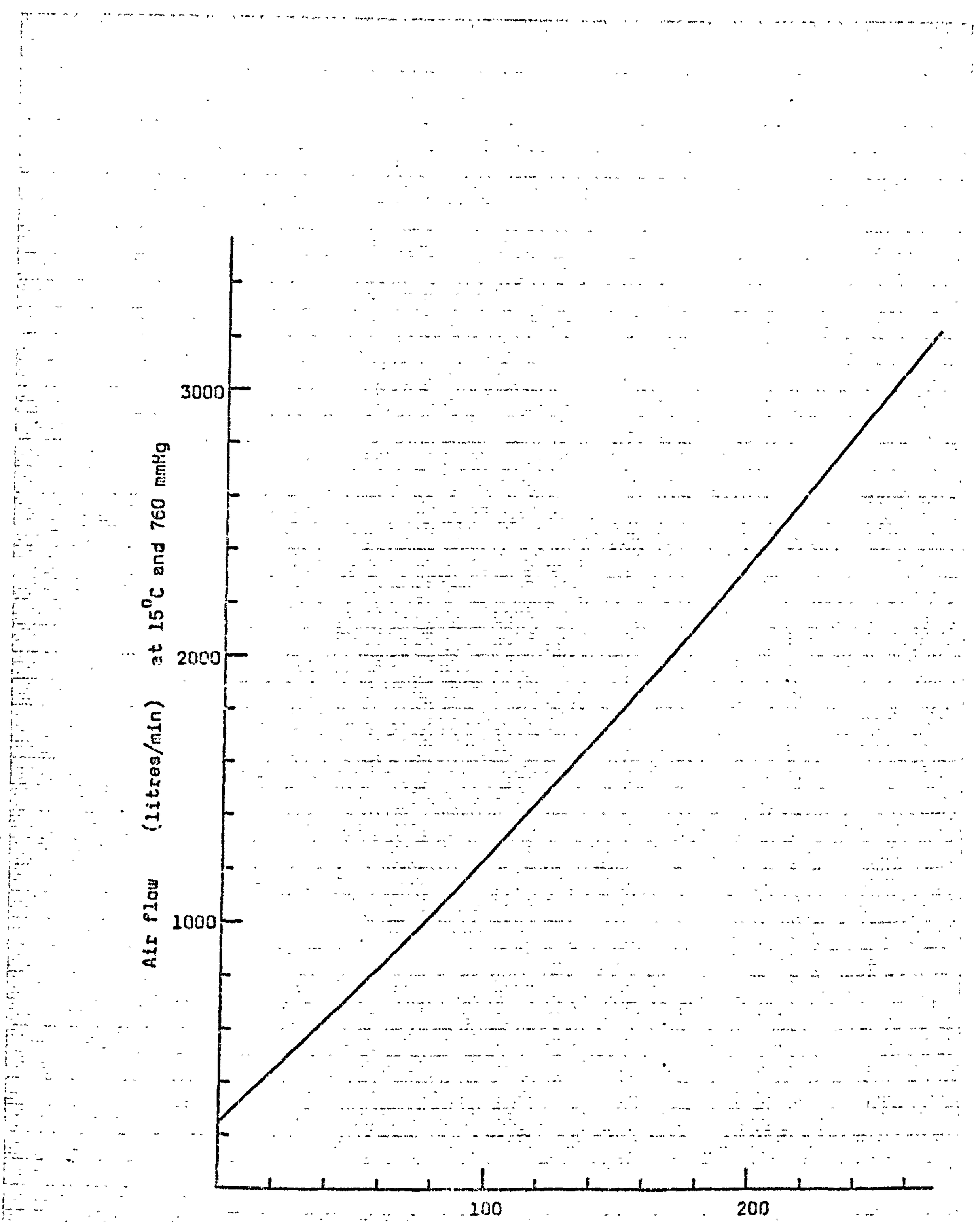

Fig. A.V.3 ROTAMETER CALIBRATION CHART (AIR)

Tube size 65X; float type K.

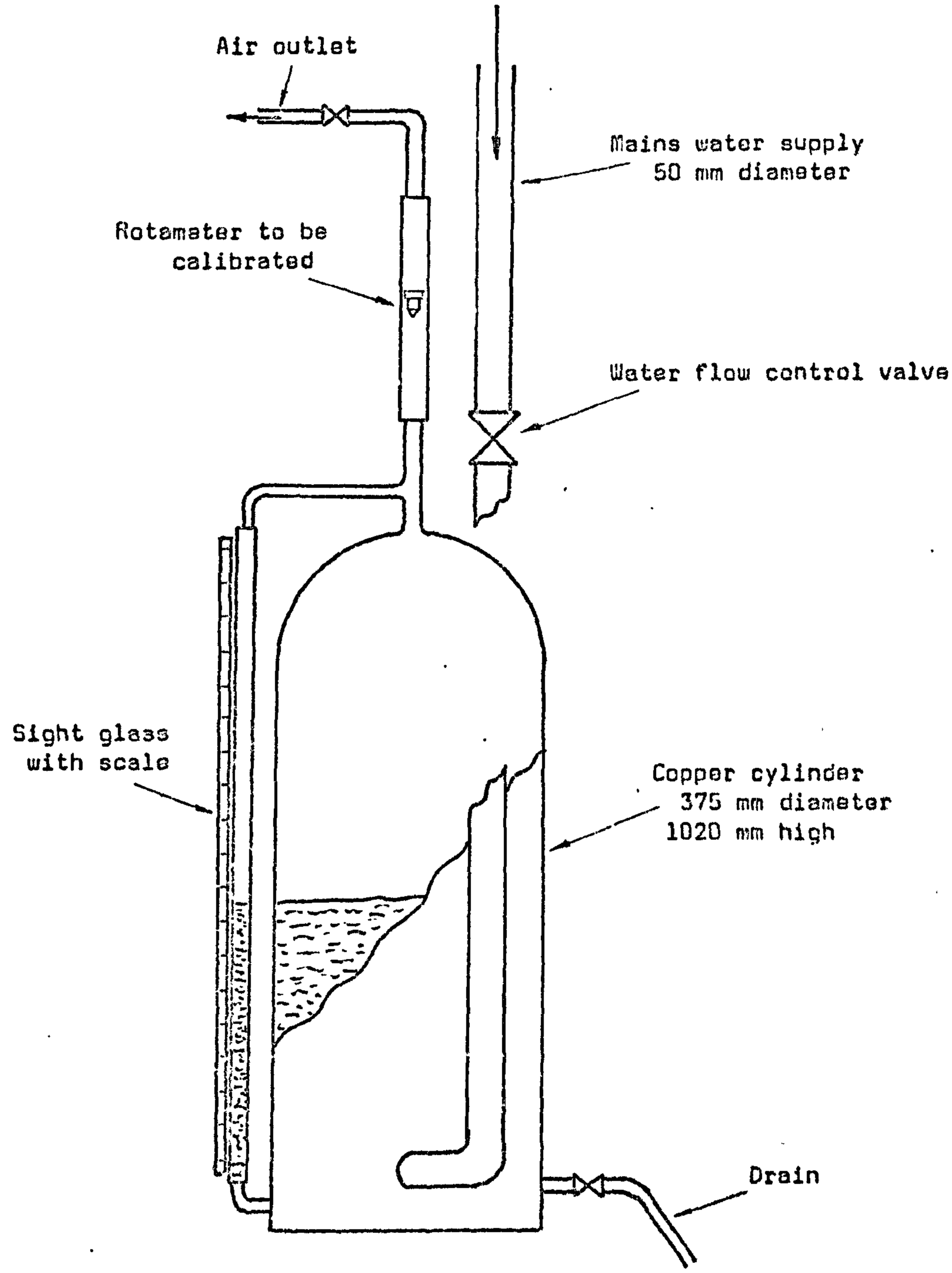

Fig. A.V.4 ROTAMETER CALIBRATION RIG

(Air flowrates up to 150 litres/min)

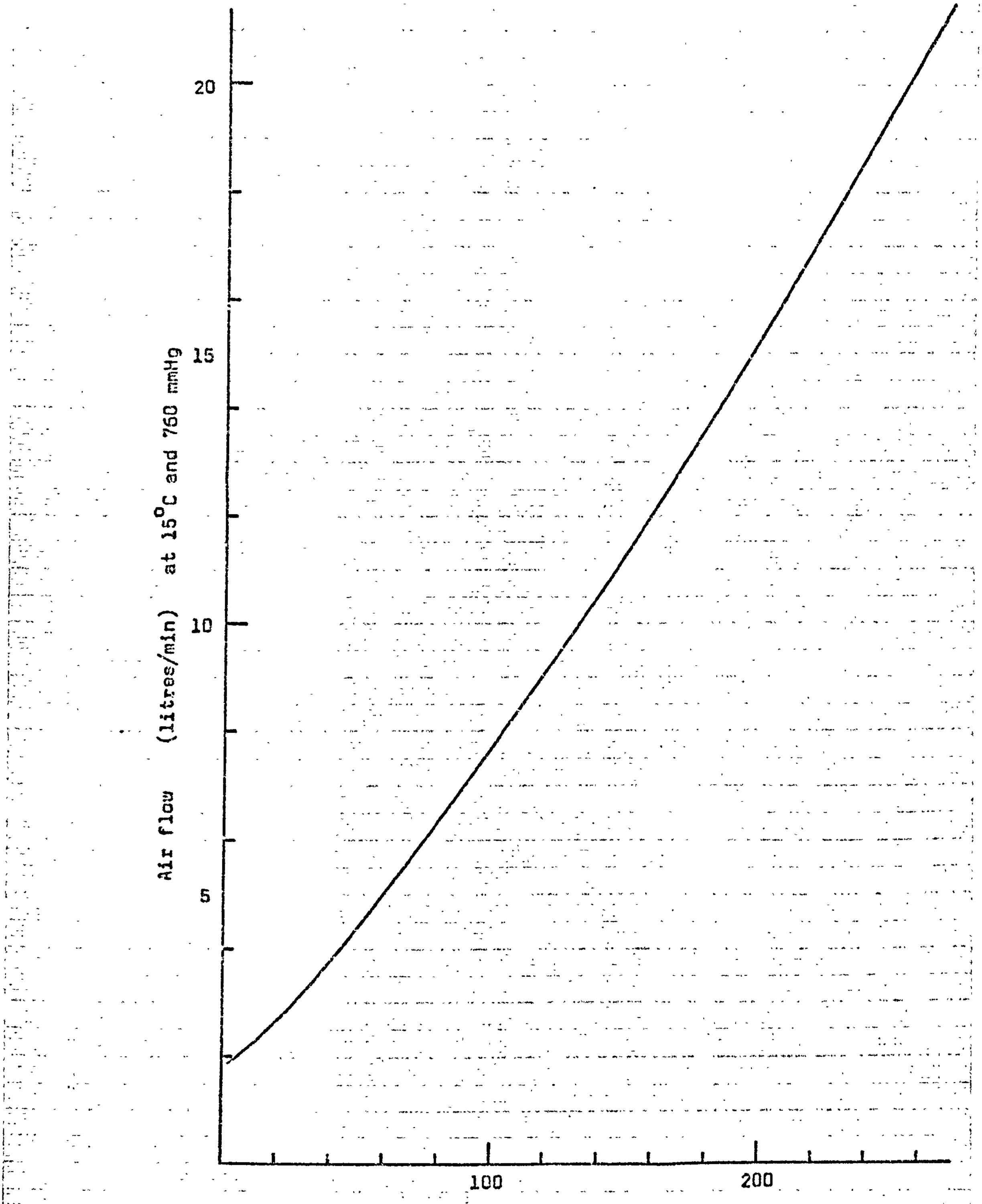

Fig. A.V.5 ROTAMETER CALIBRATION CHART (AIR)

Tube size 10; float type A.

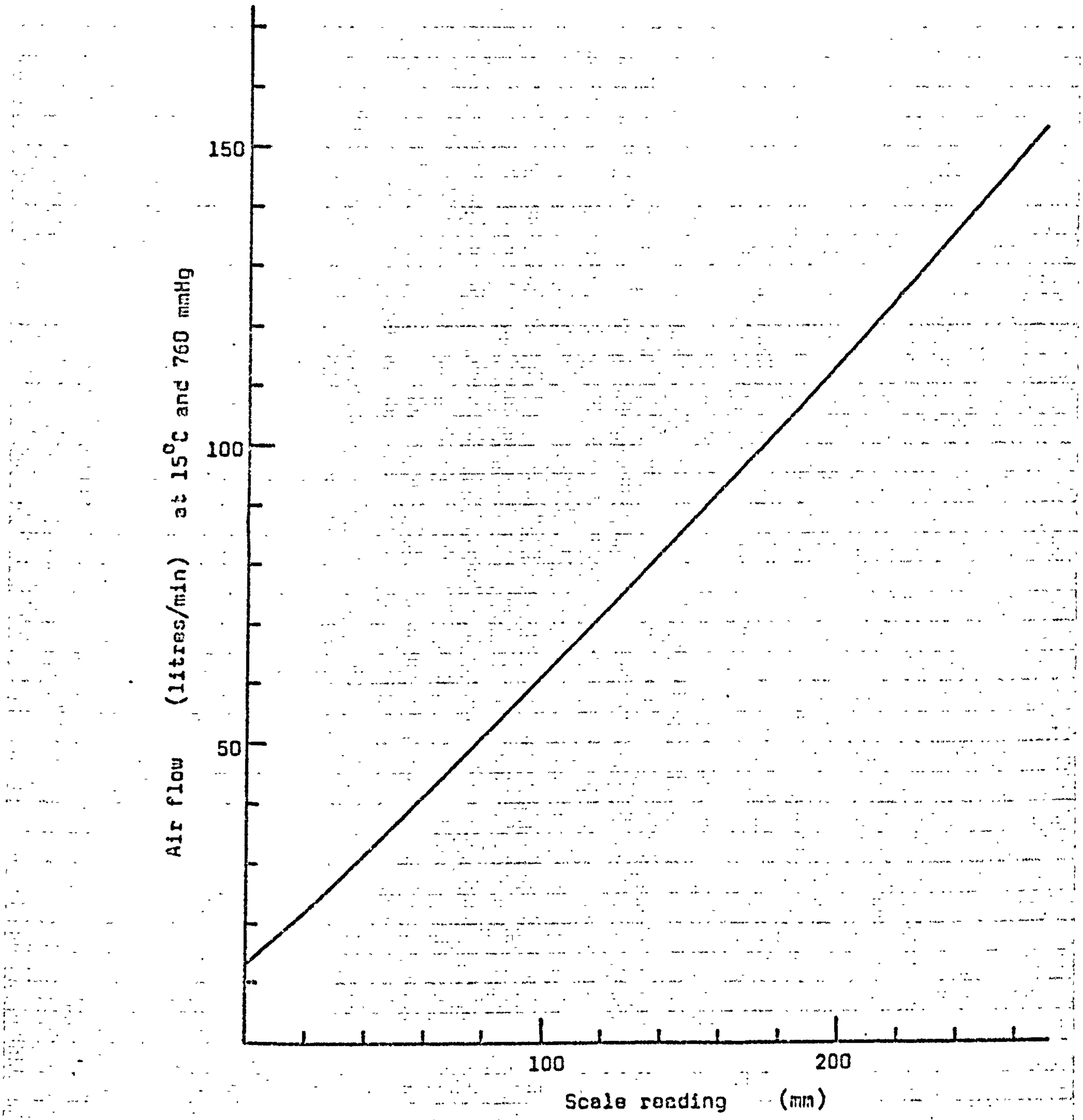

Fig. A.V.6 ROTAMETER CALIBRATION CHART (AIR)

Tube size 24X; float type A.

A.V.2 Hygrometer.

Manufactured by: Moisture Control and Measurement Ltd.,
Thorp Arch Trading Estate,
Wetherby,
Yorkshire LS23 7BJ

Model No. 600

The MCM hygrometer measures humidity by means of a moisture sensitive capacitance probe. This probe is produced by winding a fine insulated wire over an anodic layer which has been formed onto an aluminium rod. The wire and the aluminium rod form the two electrodes of the capacitor and the anodic layer acts as the dielectric. Because the dielectric is only a few microns thick the response to a change in the vapour pressure of the atmosphere (which causes a change in the number of water molecules held in the pores of the dielectric) is virtually instantaneous.

The instrument was calibrated by the manufacturer and Fig. A.V.7 is based on the curve provided by them.

A.V.3 Load cells.

Manufactured by: GEC-Elliott Automation Ltd.,
Process Instruments Division,
Century Works,
Lewisham,
London, SE13 7LN

Type: D1-00, capacity 1 ton.

The weigh-bin was mounted on a set of three identical load cells as described in Section 8.2. In order to obtain an indication of the combined load on the cells the three outputs were fed to the summing and amplifying circuit described in the following paragraph.

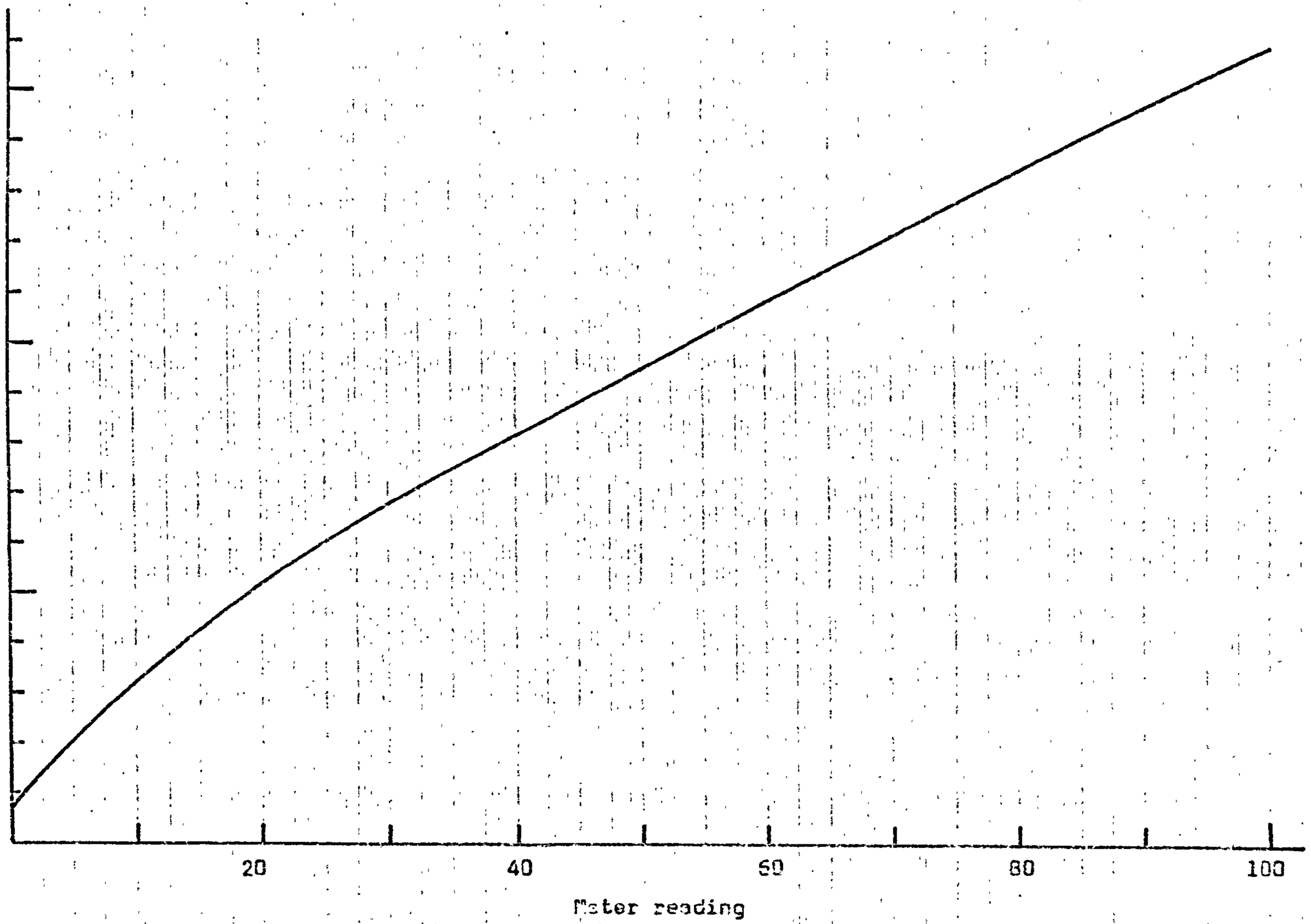

Fig. A.V.7 CALIBRATION CHART FOR MCM HYGROMETER

A.V.4 Mass flow meter.

This unit was designed and constructed by Mr. N. A. Livermore of the Division of Engineering Systems and Instrumentation at the Thames Polytechnic. The circuit is shown in Fig. A.V.8 and the unit itself in Plate XII.

The complete weigh-bin assembly, comprising the bin itself, mounted on the three load cells which were in turn connected to the mass flow meter, was calibrated by stacking cast iron weights on the top cover of the bin and plotting the relationships between the meter reading and the load applied. The resulting calibration curves are shown as Figs. A.V.9 and A.V.10. This calibration procedure was repeated at intervals during the programme of work, but drift of the instrument was found to be minimal.

A.V.5 Rotary valve.

Manufacturer/supplier: Geo. W. King Ltd.,
P. O. Box 18,
Stevenage,
Herts. SG1 2AA

Type: RV12

The King-Semco rotary valve was a conventional air-lock valve, chain driven from the Carter Variable-Speed drive, adjusted by a remote control handwheel. Fig. A.V.11 is a calibration of the handwheel indicator dial against the speed of rotation of the valve.

A.V.6 Return conveyor ('Floveyor').

Manufacturer: Entecon Ltd.,
Blackwater Bridge,
London Road,
Blackwater,
Camberley,
Surrey GU17 9AP

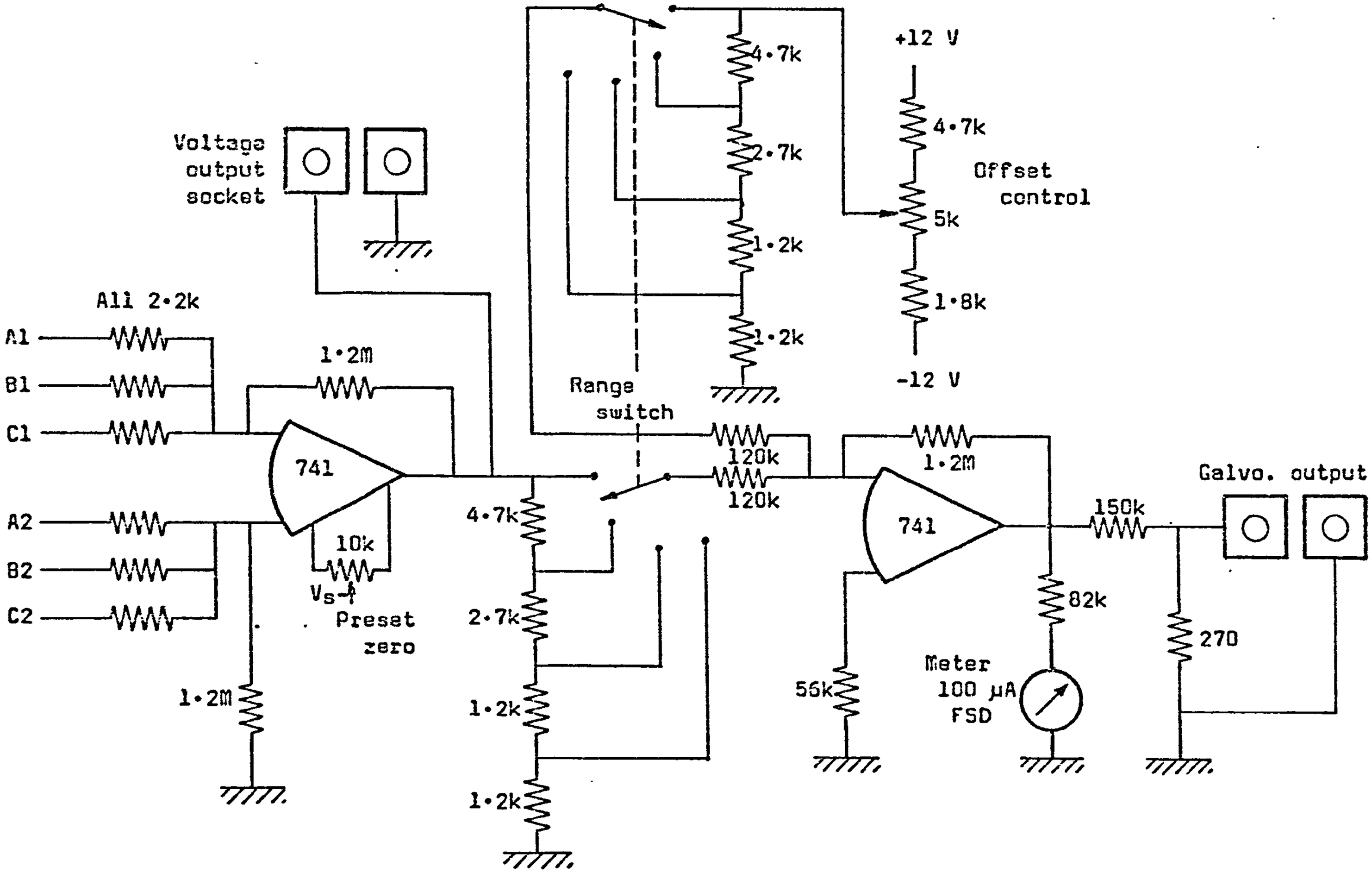

Fig. A.V.8 CIRCUIT DIAGRAM FOR MASS FLOW METER.

Plate XII. THE MASS FLOW METER; USED IN CONJUNCTION WITH THE LOAD CELLS TO INDICATE THE QUANTITY OF POWDER IN THE WEIGH-BIN.

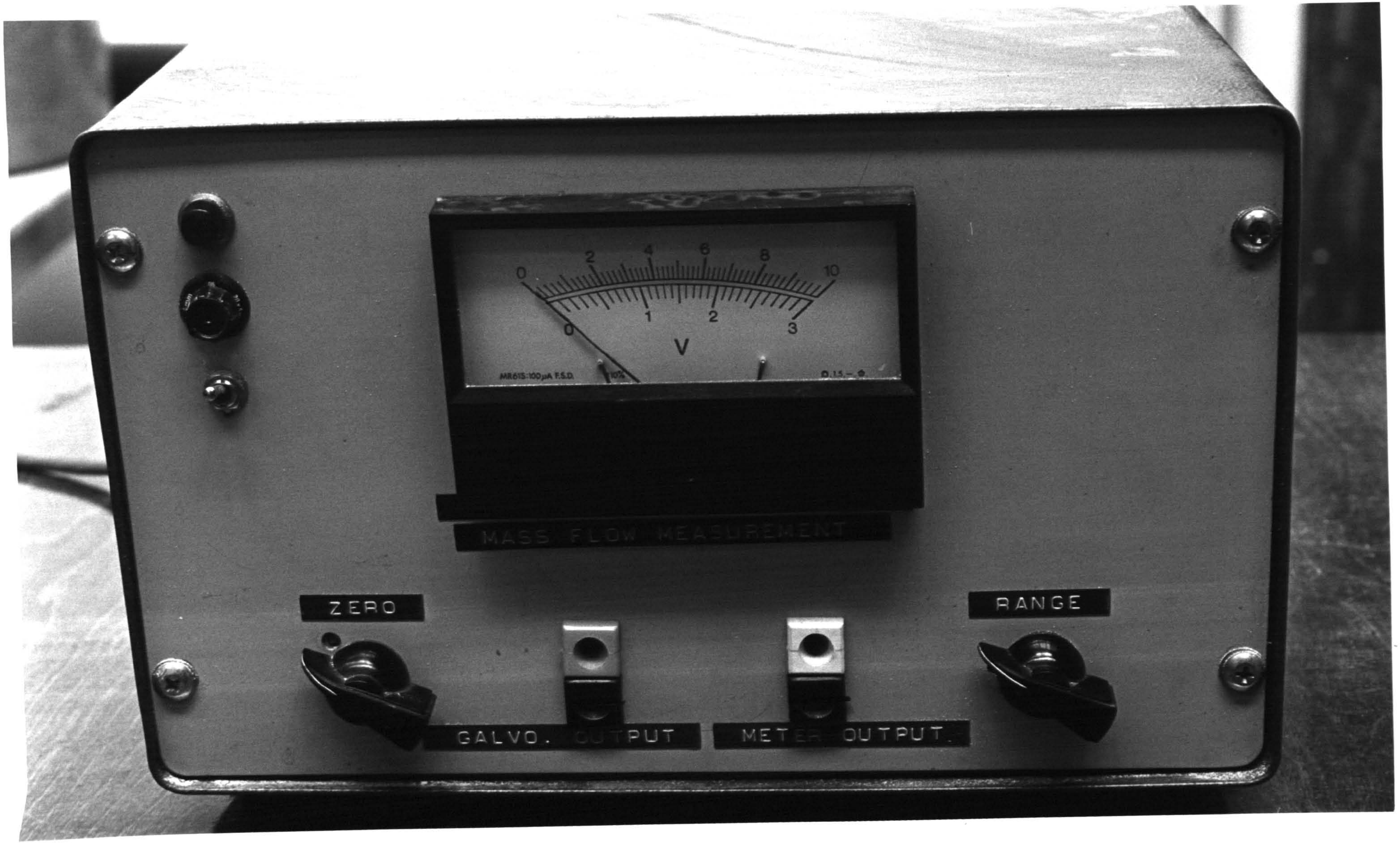
0
2
4
6
8
10
0
1
2
3
V
MR61S:100μA F.S.D.
D.15.—Φ
MASS FLOW MEASUREMENT
ZERO
RANGE
GALVO. OUTPUT
METER OUTPUT

Plate XII. THE MASS FLOW METER; USED IN CONJUNCTION WITH THE LOAD CELLS TO INDICATE THE QUANTITY OF POWDER IN THE WEIGH-BIN.

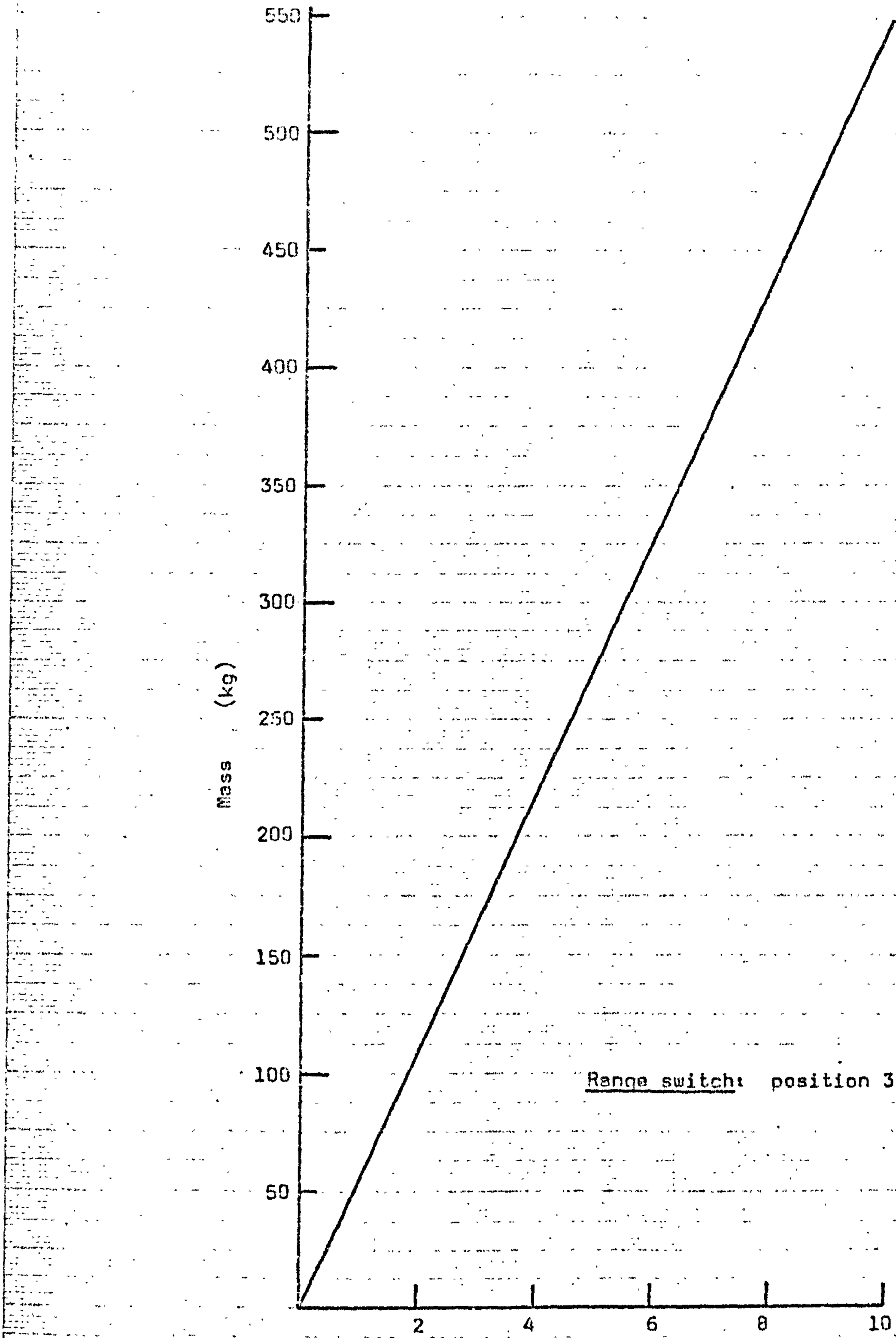

Fig. A.V.9 WEIGH-BIN CALIBRATION.

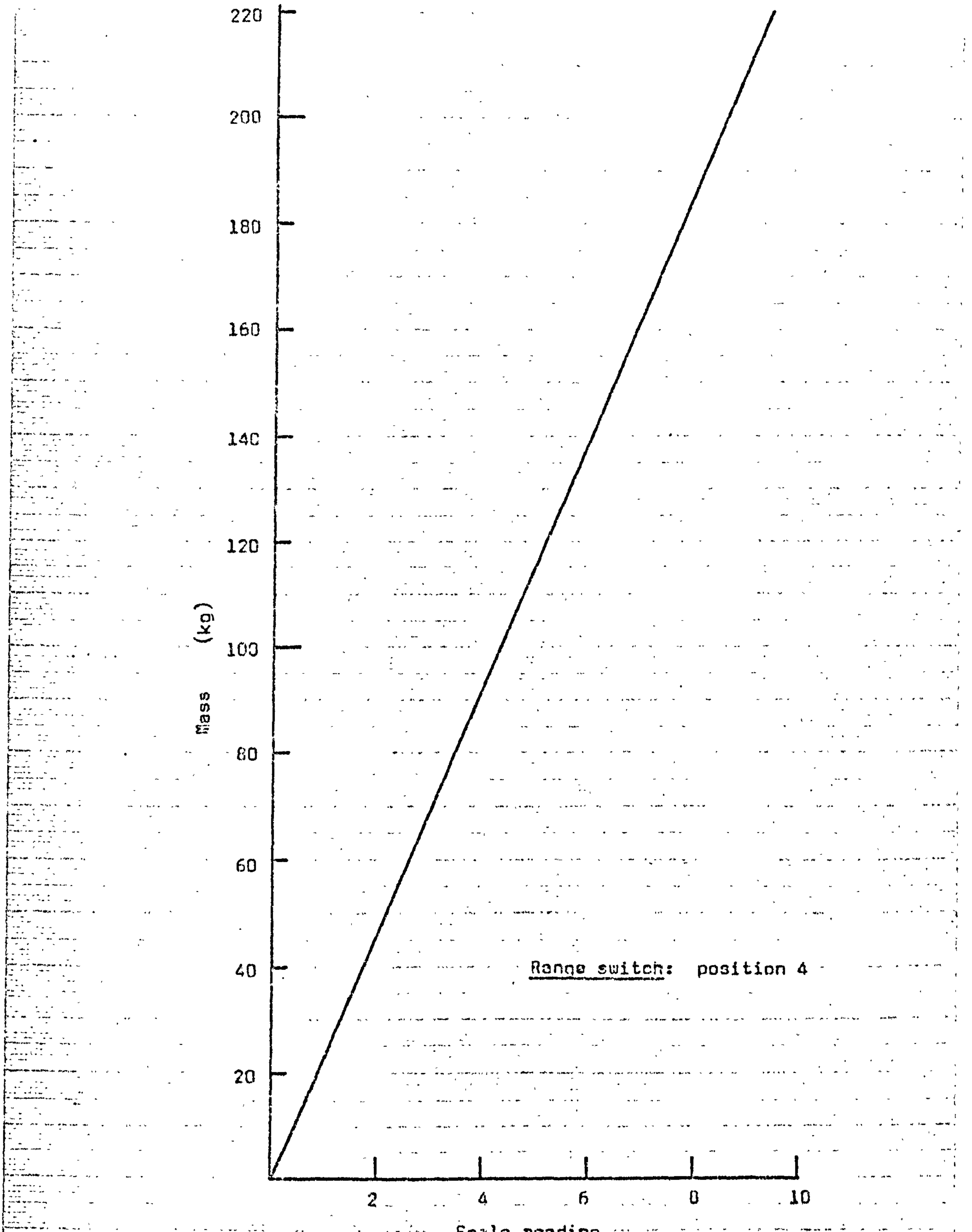

Fig. A.V.10 WEIGH-BIN CALIBRATION.

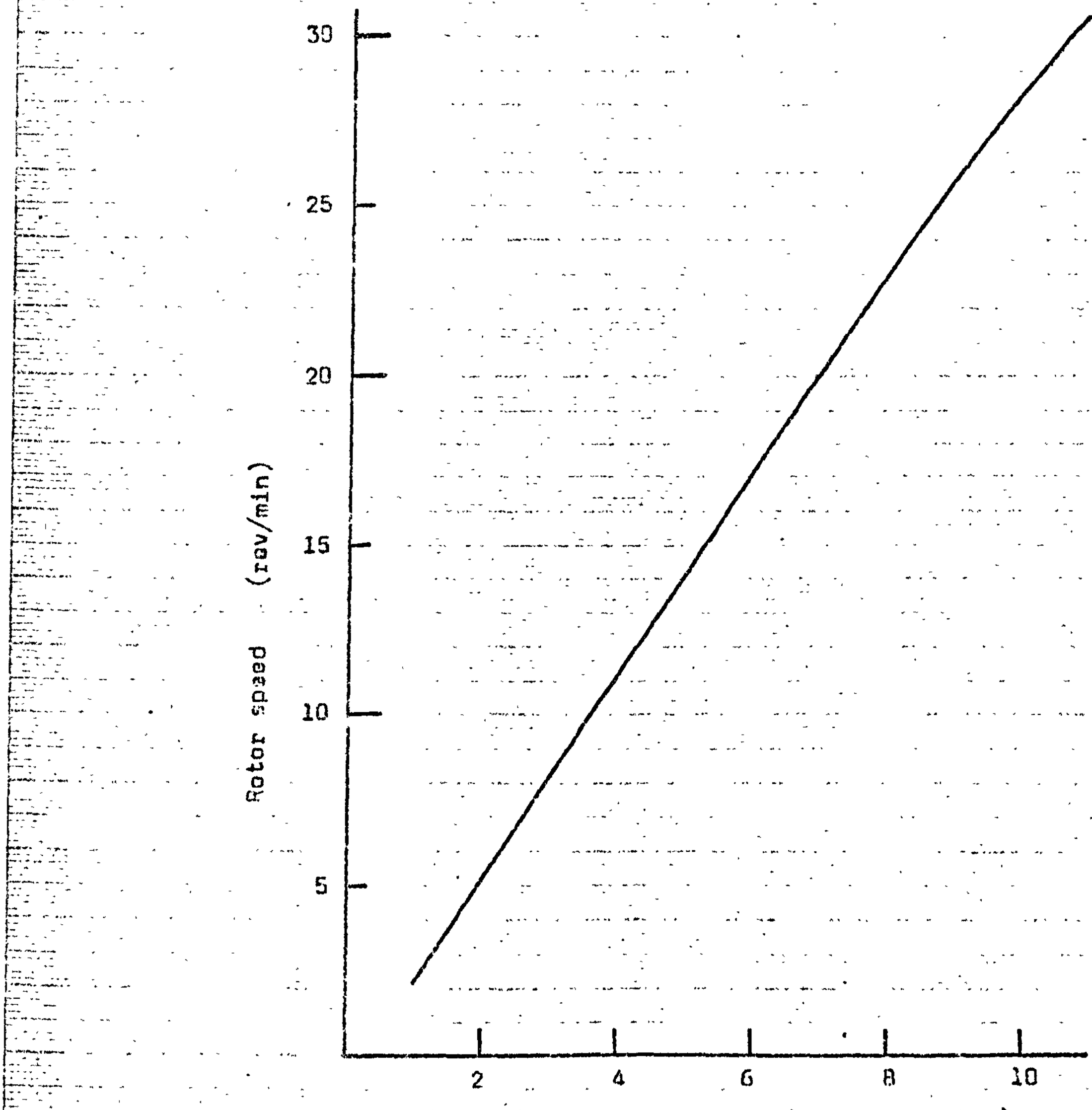

Fig. A.V.11 CALIBRATION OF ROTARY VALVE SPEED CONTROL.

The Floveyor is a tubular 'aero-mechanical' conveyor in which material is conveyed by a series of discs spaced at equal intervals along a continuous steel rope. The rope passes over sprockets at each end of the unit and travels at a velocity of around 3 m/s.

A.V.7 Air blower.

Manufacturer: Godfrey Blowers,
Howden and Godfrey House,
Godfrey Way,
Hounslow,
Middlesex TW4 5PW

Model: MU 1000 Roots-type positive displacement blower.

Performance chart (based on a chart in British Imperial units, supplied by the manufacturer) is reproduced as Fig. A.V.12.

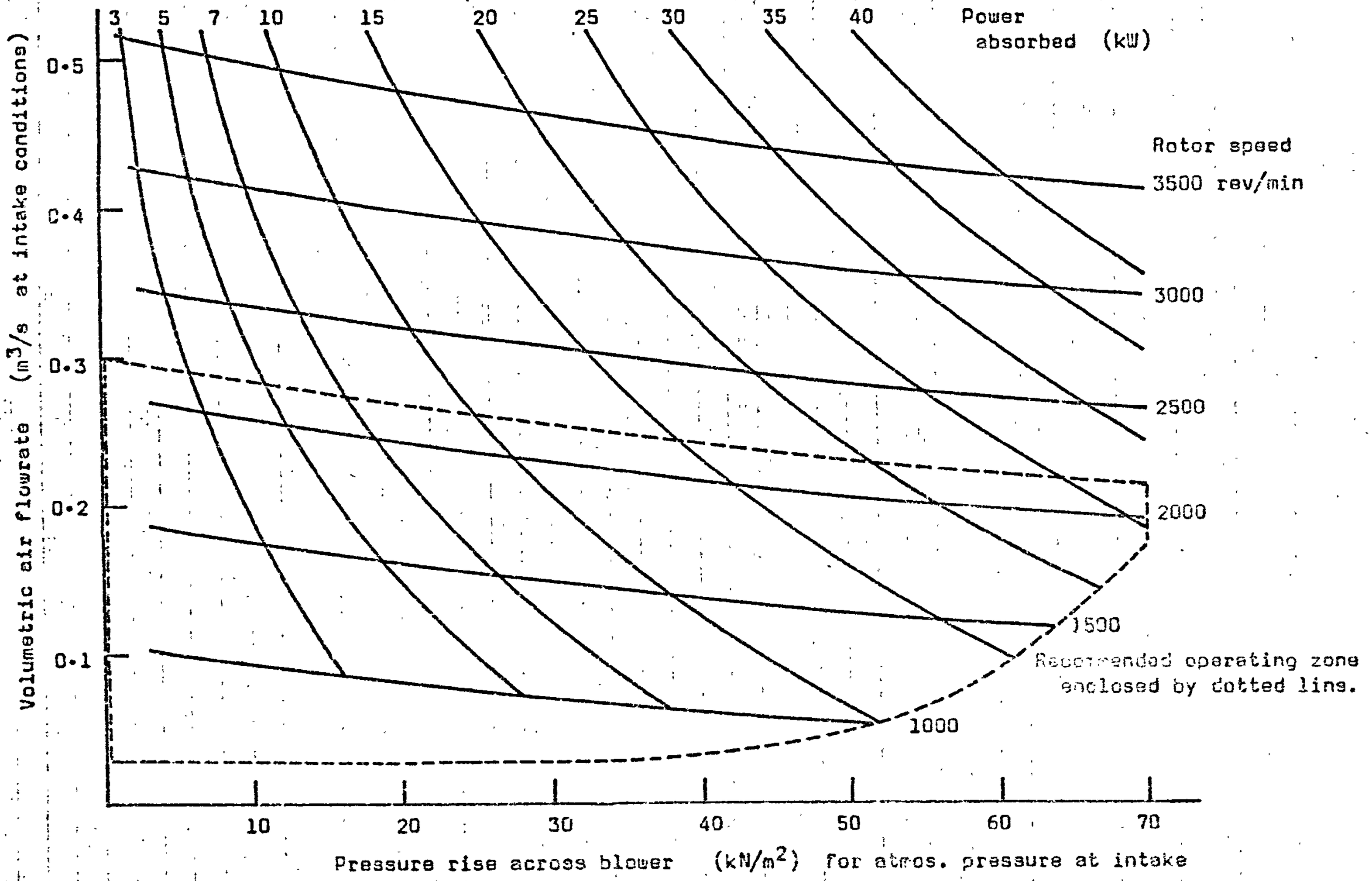

Fig. A.V.12 PERFORMANCE CHART FOR GODFREY MU1000 INDUSTRIAL BLOWER.

REFERENCES

A1. Agarwal, J.C.; Davis, W.L.; King, D.T., "Fluidised bed coal dryer". Chem. Eng. Progr. v 58 n 11 (November 1962) pp 85-90.

A2. Allen, T., "Particle Size Measurement". 2nd Edn. Chapman and Hall, London, 1975.

A3. Alston, G.L., "Advances in rockdusting procedures". Mechanization, January 1961, pp 46-48.

A4. Anon., "Arten und Einsatzmöglichkeiten pneumatischer Förderinnen". (Types of pneumatic conveying channel and their application) Klepzig-Fachberichte, v 73 n 9 (September 1965) pp 408-410. (In German).

A5. Anon., "Fluidised solids conveyors". Fluid Handling, August 1952, pp 233-234.

A6. Anon., "Hot dust is conveyed pneumatically from precipitators to furnaces". Engg. and Mining J., v 155 n 7 (1954) p 91.

A7. Anon., "Newest case handling system: a river of air!" J. Modern Materials Handling, v 22 n 9 (September 1967) pp 42-44.

A8. Anon., "Pneumatische Förderung mit offenem Luftstrom". (Pneumatic handling using open air-stream). Fördern und Heben, v 18 n 1 (1968) pp 56-57. (In German)

A9. Arai, N.; Sugiyama, S., "Studies of fluidization of moist particles". J. Chem. Engg. of Japan, v 7 n 4 (August 1974) pp 247-251.

A10. Ashwin, B.S.; Hagyard, T.; Saunders, I.C.B.; Young, T.E., "Viscometers having damped torsional oscillation". J. Scientific Instr., v 37 (December 1960) pp 480-485.

A11. Astarita, G.; Marrucci, G.; Palumbo, G., "Non-Newtonian gravity flow along inclined plane surfaces". Ind. and Engg. Chem. Fundam., v 3 n 4 (November 1964) pp 333-339.

A12. Avery, W.M., "Meet the airslide". Pit and Quarry, v 41 n 2 (February 1949) pp 62-67).

A13. Anon., "Neues pneumatisches Förderverfahren". (New techniques in pneumatic conveying.) Chemie-Ing. Techn., v 36 n 5 (1964) pp 555-556. (In German)

B1. Baerg, A.; Klassen, J.; Gishler, P.E., "Heat transfer in a fluidised solids bed". Canadian J. of Res., v 28F n 8 (August 1950) pp 287-307.

B2. Baerns, M., "Effect of interparticle adhesive forces on fluidization of fine particles". Ind. and Engg. Chem. Fundam., v 5 n 4 (November 1966) pp 508-516.

B3. Baeyens, J.; Geldart, D., "Predictive calculations of flow parameters in gas fluidized beds and fluidization behaviour of various powders". Proc. Conf. "La Fluidisation et ses Applications", Toulouse, October 1973, pp 263-273.

B4. Bakker, P.J.; Heertjes, P.M., "Porosity distributions in a fluidized bed". Chem. Engg. Sci., v 12 (1960) pp 260-271.

B5. Barnea, E.; Mednick, R.L., "Correlation for minimum fluidisation velocity". Trans. Instn. Chem. Engrs., v 53 n 4 (October 1975) pp 278-281.

B6. Baumgarten, P.K.; Pigford, R.L, "Density fluctuations in fluidised beds". A.I.Ch.E. Jour., v 6 n 1 (March 1960) pp 115-123.

B7. Benenati, R.F.; Brosilow, C.B., "Void fraction distribution in beds of spheres". A.I.Ch.E. Jour., v 8 n 3 (July 1962) pp 359-361.

B8. Bessant, D.J., "The flow of fluidised solids". Ph.D. Thesis, Univ. of Birmingham, 1973.

B9. Bessant, D.J.; Botterill, J.S.M., "The flow properties of fluidised solids". Proc. Conf. "La Fluidisation et ses Applications", Toulouse, October 1973, pp 81-89.

B10. Boland, D.; Al-Salim, Q.A.W.; Geldart, D., "Static electrification in fluidised beds". Chem. Engg. Sci., v 24 (1969) pp 1389-1390.

B11. Boland, D.; Geldart, D., "Electrostatic charging in gas fluidised beds". Proc. Powtech '71: Int. Powder Tech. and Bulk Granular Solids Conf., Harrogate, May 1971, pp 243-249.

B12. Boland, D.; Geldart, D., "Electrostatic charging in gas fluidised beds". Powder Technol., v 5 (1971/72) pp 289-297.

B13. Boothroyd, R.G., "Flowing Gas-Solids Suspeusions". Chapman and Hall, London, 1971.

B14. Boothroyd, R.G.; Arundel, P.A., "Measurement of local solids velocity in a pneumatic conveyor from correlated electrostatic signals". Proc. Pneumotransport 1, BHRA Conf., Cambridge, September 1971.

B15. Botterill, J.S.M., "Fluid-Bed Heat Transfer". Academic Press, London, 1975.

B16. Botterill, J.S.M.; Bessant, D.J., "The flow properties of fluidised solids". Symp. on Rheol. of Particulate Systems, Harrogate, March 1973.

B17. Botterill, J.S.M; Bessant, D.J., "The flow properties of fluidised solids". Proc. Pneumotransport 3, BHRA Conf., Bath, Paper E3, April 1976.

B18. Botterill, J.S.M.; Bessant, D.J., "Tho flow properties of fluidised solids". Powder Technol., v 14 n 1 (May/June 1976) pp 131-137.

B19. Botterill, J.S.M.; Chandrasekhar, R.; van der Kolk, M., "Heat transfer and pressuro loss for the flow of fluidised solid across banks of tubes". Brit. Chem. Engg., v 15 n 6 (June 1970) pp 769-772.

B20. Botterill, J.S.M.; Chandrasekhar, R.; van der Kolk, M., "The flow of fluidised solids past arrays of tubes - heat transfer and pressure loss studies". Chem. Engg. Progr. Symp. Series, v 66 n 101 (1970) pp 61-69.

B21. Botterill, J.S.M.; van der Kolk, M., "The flow properties of fluidised solids". Chem. Engg. Progr. Symp. Series, v 67 n 116 (1971) pp 70-76.

B22. Botterill, J.S.M.; van der Kolk, M.; Elliott, D.E.; McGuigan, S., "The flow of fluidised solids". Proc. Powtech '71: Int. Powder Tech. and Bulk Granular Solids Conf., Harrogate, May 1971, pp 215-221.

B23. British Standard 3406: "Methods for the determination of particle size of powders". Part 1:1961, Parts 2 to 4:1963.

B24. British Standard 1796: 1952, "Methods for the use of British Standard fine mesh test sieves".

B25. Brown, G.G. et al, "Unit Operations". Wiley, 1950.

B26. Brown, R.L.; Richards, J.C., "Principles of Powder Mechanics". Pergamon Press, Oxford, 1970.

B27. Bushell, E.; Maskell, R.C., "Fluidised handling of alumina powder". Mech. Handling, v 47 n 3 (March 1960) pp 126-131.

B28. Bushell, E.; Maskell, R.C., "Eine pneumatische Anlage für Tonerde-Pulver". (Fluidised handling of alumina powder.) Aufbereitungs-Technik, v 1 n 6 (June 1960) pp 259-263. (In German)

B29. Butler, P., "No-moving-parts conveyor shifts dry powdered solids". Process Engg., August 1974, p 65.

B30. Butt, M.H.D., "The effects of particle properties on heat transfer to gas fluidised beds". Ph.D. Thesis, Univ. of Birmingham, 1966.

C1. Caldwell, D.H.; Babbitt, H.E., "Flow of muds, sludges, and suspensions in circular pipe". Ind. and Engg. Chem., v 33 n 2 (February 1941) pp 249-256.

C2. Carman, P.C., "Fluid flow through granular beds". Trans. Instn. Chem. Engrs. (London), v 15 n 1 (1937) pp 150-166.

C3. Chandelle, V., "Manutention des produits granuleux par air-slides et air-lifts". (Transportation of granular materials in air-slides and air-lifts). Annales des Mines de Belgique, n 2 (1971) pp 191-208. (In French and Flemish)

C4. Ciborowski, J.; Wlodarski, A., "On electrostatic effects in fluidised beds". Chem. Engg. Sci., v 17 (1962) pp 23-32.

C5. Cole, B.N.; Baum, M.R.; Mobbs, F.R., "An investigation of electrostatic charging effects in high-speed gas-solids pipe flows". Proc. I. Mech. E. v 184 pt 3C (1969-70) pp 77-83.

C6. Craik, D.J.; Miller, B.F., "The flow properties of powders under humid conditions". J. Pharmacy and Pharmacology, v 10 (suppl.) (December 1958) pp 136-144.

D1. Davidson, J.F.; Harrison, D.; Guedes de Carvalho, J.R.F., "On the liquidlike behaviour of fluidized beds". Ann. Rev. Fluid Mechs., v 9 (1977) pp 55-86.

D2. Davies, G.; Robinson, D.B., "A study of aggregative fluidization". Can. J. Chem. Engg., v 38 n 6 (December 1960) pp 175-183.

D3. Davies, L.; Richardson, J.F., "Gas interchange between bubbles and the continuous phase in a fluidised bed". Trans. Instn. Chem. Engrs., v 44 (1966) pp T293-T305.

D4. Descamps, P.; Jodlowski, C., "Principes et bases du transport pneumatique et de la fluidisation". (Fundamentals of pneumatic conveying and fluidisation.) Air Industriel (France), v 11 (October 1973) pp 23-27. (In French)

D5. Diekman, R.; Forsythe, W.L, "Laboratory prediction of flow properties of fluidized solids". Ind. and Engg. Chem., v 45 n 6 (June 1953) pp 1174-1177.

D6. Donald, M.B., "Electrostatic separation of minerals". Research, (Lond.), v 11 (1958) pp 19-25.

D7. Dodge, J., "Verfahren zum Fortschaffen von Materialien in Förderrinnen mittels Luftdruck". (Procedure for transportation of materials in conveying channels using pressurised air.) DRP 88402, 1895. (German Patent)

D8. Donsi, G.; Massimilla, L., "Particle to particle forces in fluidisation of fine powders". Proc. Conf. "La Fluidisation et ses Applications", Toulouse, October 1973, pp 41-51.

D9. Dotson, J.M., "Factors affecting density transients in a fluidized bed". A.I.Ch.E. Jour., v 5 n 2 (June 1959 pp 169-174).

D10. Duckworth, R.A.; Chan, T.K., "The influence of electrostatic charges on the pressure gradient during pneumatic transport". Proc. Pneumotransport 2, BHRA Conf., Guildford, Paper A5, September 1973.

E1. E.E.U.A. Handbook No. 15, "Pneumatic handling of powdered materials". Constable & Co., London, 1963.

E2. Ergun, S., "Fluid flow through packed columns". Chem. Engg. Progr., v 48 (1952) pp 89-94.

F1. Frantz, J.F., "Minimum fluidization velocities and pressure drop in fluidized beds". Chem. Engg. Progr. Symp. Series, v 62 n 62 (1966) pp 21-31.

F2. Fuller Company, "Self-unloading bin". Brit. Patent 724719, 1953.

F3. Furukawa, J.; Ohmae, T., "Liquidlike properties of fluidized systems". Ind. and Engg. Chem., v 50 n 5 (May 1958) pp S21-828.

F4. Futer, R.E., "Conveying solids with cooperating series of air jets". ASME Paper 68-MH-31, (1968).

G1. Geldart, D., "Predicting the expansion of gas fluidised beds". Proc. Int. Fluidization Conf., Asilomar, Calif., U.S.A., June 1975. "Fluidization Technology", Vol. I, pp 237-244.

G2. Geldart, D., "The effect of particle size and size distribution on the behaviour of gas-fluidised beds". Powder Technology, v 6 (1972) pp 201-215.

G3. Geldart, D., "Types of gas fluidization". Powder Technology, v 7 (1973) pp 285-292.

G5. Geldart, D.; Kelsey, J.R., "The influence of the gas distributor on bed expansion, bubble size, and bubble frequency in fluidised beds". I.Chem.E. Symp. Series, n 30 (1968) pp 114-125.

G6. Gel'perin, N.I.; Ainshtein, V.G.; Lapshenkov, G.I.; Mikhailov, V.A., "Effective viscosity of a fluidised bed of granular materials". Theor. Foundations of Chem. Engg. v 2 n 4 (July-August 1968) pp 526-531.

G7. Godard, K.; Richardson, J.F., "The behaviour of bubble-free fluidised beds". I.Chem.E. Symp. Series, n 30 (1968) pp 126-135.

G8. Grace, J.R., "The viscosity of fluidised beds". Can. Jour. Chem. Engg., v 48 (February 1970) pp 30-33.

G9. Gregoraszczuk, M.; Fedoryszyn, A., "Podstawowe obliczenia przenosnikow aeracyjnych". (Basic calculations of air-lift conveyors.) Przeglad Mechaniczny, v 33 n 22 (November 1974) pp 761-764. (In Polish)

G10. Grohse, E.W., "Analysis of gas fluidized solid systems by X-ray absorption". A.I.Ch.E. Jour., v 1 n 3 (September 1955) pp 358-365.

H1. Hagyard, T.; Sacerdote, A.M., "Viscosity of suspensious of gas fluidized spheres". Ind. and Engg. Chem. Fundam., v 5 n 4 (November 1966) pp 501-508.

H2. Harris, W.F., "Pneumatic conveying - special problems of density". Mech. Handling, v 52 n 11 (November 1965) pp 521-527.

H3. Hawksley, P.G.W., "The physics of particle size measurement. Part I. Fluid dynamics and the Stokes diameter". BCURA Bull., v 15 n 4 (April 1951) pp 105-146.

H4. Hawksley, P.G.W., "Survey of the relative motion of particles and fluids". Brit. J. Appl. Physics, Suppl. n 3 (1954) pp S1-S5.

H5. Hiby, J.W., "Untersuchungen über den kritischen Mindestdruckverlust des Anströmbodens bei Fluidabbetten (Fliessbetten)". (Critical minimum pressure drop of the gas distribution plate in fluidised bed units.) Chemie-Ing-Techn., v 36 n 3 (January 1964) pp 228-229. (In German)

H6. Hudson, W.G., "Give your handling problems the air". Mill and Factory, January 1959, pp 95-97.

H7. Hudson, W.G., "Why use pneumatic conveyors?" Chem. Engg., April 1954, pp 191-194.

H8. Huron Portland Cement Company, "Improvements in or relating to the conveying of pulverulent or finely divided materials". Brit. Patent 677891, February 1949.

I1. Isler, W., "Die horizontal und schräg aufwärts fördernde pneumatische Rinne". (An air-slide type conveyor for horizontal and upward inclined transport) Zement-Kalk-Gips, n 10 (1960) pp 482-486. (In German)

J1. Jakab, E.; Kucsera, Gy,; Marjan, Gy.; Loibl, S., "Pilot-plant investigations on aerodynamic conveying channel". Proc. 2nd Conf. on Pneumatic Conveying, Pécs, Hungary, March 1978, Paper B3, pp 117-123.

J2. Jelinek, Z.K., "Particle Size Analysis". Ellis Horwood, Chichester, 1970.

J3. Jolley, L.J.; Stantan, J.E., "Fluidization in beds of coal and coke particles: some effects of size of particles and viscosity, density and velocity of gas". J. Appl. Chem., v 2 Suppl. Issue No. 1, (1952) pp S62-S68.

K1. Katz, H.M., "Studies of particle size distribution in fluidized beds". Argonne Nat. Lab. Report No. ANL-5725, 1957.

K2. Kay, J.M.; Nedderman, R.M., "Fluid Mechanics and Heat Transfer". 3rd Edn., Cambridge University Press, 1974.

K3. Keuneke, K., "Fluidisierung und Fliessbettförderung von Schüttgütern kleiner Teilchengrösse". (Fluidisation and fluidised bed conveying of solid materials with small particle sizes.) VDI-Forschungsheft 509, 1965. (In German)

K4. Kisel'nikov, V.N.; Vyalkov, V.V.; Filatov, V.M., "On the problem of electrostatic phenomena in a fluidized bed". Int. Chem. Engg., v 7 n 3 (July 1967) pp 428-431.

K5. Kosa, L.; Verba, A.; Tallian, A., "Berechnung der Treibkraft in aerokinetische Rinne". (Estimating the power consumption of pneumatic conveying channels.) Proc. 2nd Conf. on Pneumatic Conveying, Pécs, Hungary, March 1978, Paper B9, pp 125-129. (In German).

K6. Kovacs, L.; Varadi, S., "Kristallzuckerförderung mittels Aerationsrinne, bzw. einer mit geschlitztem Boden versehenen Rinne". (Conveying granulated sugar through aerated channels, for example, in a channel fitted with a slotted base-plate.) Proc. 2nd Conf. on Pneumatic Conveying, Pécs, Hungary, March 1978, Paper B10, pp 131-139. (In German)

K7. Kozicki, W.; Tiu, C., "Non-Newtonian flow through open channels". Can. J. Chem. Engg. v 45 (June 1967) pp 127-134.

K8. Kramers, H., "On the 'viscosity' of a bed of fluidised solids". Chem. Engg. Sci., v 1 n 1 (1951) pp 35-37.

K9. Kraus, M. N., "Pneumatic Conveying of Bulk Materials". The Ronald Press Co., New York, 1968.

K10. Kunii, D.; Levenspiel, O., "Fluidization Engineering". John Wiley and Sons, 1969.

K11. Kunkel, W.B., "The static electrification of dust particles on dispersion into a cloud". J. Appl. Physics, v 21 (August 1950) pp 821-832.

L1. Leitzel, R.E.; Morrisey, W.M., "Air float conveyors". In "Bulk Materials Handling", Vol. I, Ed. M.C. Hawk, University of Pittsburgh, School of Mech. Engg., 1971, pp 307-325.

L2. Leont'ev, A.P.; Vakhrushev, I.A., "Experimental determination of effective viscosity of fluidized beds by falling-ball method". Chem. and Technol. of Fuel Oils (USSR), v 12 n 4 (April 1976) pp 294-297.

L3. Leva, M., "Fluidization". McGraw-Hill, 1959.

L4. Leva, M.; Shirai, T.; Wen, C.Y., "La prévision de début de fluidisation dans les lits solides granulaires". (Prediction of the onset of fluidisation in granular solid beds.) Genie Chimique, v 75 n 2 (February 1956) pp 33-42. (In French)

L5. Leva, M.; Wen, C.Y., "Elutriation". In "Fluidization", Ed. by J. F. Davidson and D. Harrison, Academic Press, 1971, pp 627-650.

L6. Lewis, W.K.; Gilliland, E.R.; Bauer, W.C., "Characteristics of fluidised particles". Ind. and Engg. Chem., v 41 n 6 (June 1949) pp 1104-1117.

L7. Lewis, W.K.; Gilliland, E.R.; Lang, P.M., "Entrainment from fluidised beds". Chem. Engg. Progr. Symp. Series, v 58 n 38 (1962) pp 65-78.

L8. Liu, F.F-K.; Orr, C., "Apparent viscosity of gas-solid fluidised systems". J. Chem. and Engg. Data, v 5 n 4 (October 1960) pp 430-432.

M1. Martin, D., "No-transfer-point open air conveyor". Process Engg., July 1975, p 39.

M2. Masterson, S.G., "Dense-phase conveying: pro and con". Ceramic Age, October 1970, p 21-22.

M3. Matheson, G.L.; Herbst, W.A.; Holt, P.H., "Characteristics of fluid-solid systems". Ind. and Engg. Chem., v 41 n 6 (June 1949) pp 1099-1104.

M4. McGuigan, S.J., "The flow behaviour of shallow fluidised beds". Ph.D. Thesis, Univ. of Aston in Birmingham, 1974.

M5. McGuigan, S.J.; Elliott, D.E., "The viscosity of shallow fluidised beds". 4th Int. Congr. CHISA, Prague, Czech., September 1972.

M6. McGuigan, S.J.; Pugh, R.R., "The flow of fluidised solids in an open channel". Proc. Pneumotransport 3, BHRA Conf., Bath, Paper E2, April 1976.

M7. Mendies, P.J.; Wheeldon, J.M.; Williams, J.C., "The velocity of granular material flowing in a pneumatic conveyor". Proc. Pneumotransport 2, BHRA Conf., Guildford, Paper D1, September 1973.

M8. Metzner, A.B.; Reed, J.C., "Flow of non-Newtonian fluids - correlation of the laminar, transition, and turbulent-flow regions". A.I.Ch.E. Jour., v 1 n 4 (December 1955) pp 434-440.

M9. Mori, Y.; Aoki, R.; Oya, K.; Ishikawa, H., "Transportation of solid material by an air-slide conveyor". Kagaku Kogaku (Japan), v 19 n 1 (1955) pp 16-22. (In Japanese)

M10. Morse, R.D., "Fluidization of granular solids". Ind. and Engg. Chem., v 41 n 6 (June 1949) pp 1117-1124.

M11. Morse, R.D.; Ballou, C.O., "The uniformity of fluidization - its measurement and use". Chem. Engg. Progr., v 47 n 4 (April 1951) pp 199-204.

M12. Motamedi, M.; Jameson, G.J., "A new method for the measurement of the incipient fluidizing velocity". Chem. Engg. Sci., v 23 (1968) pp 791-793.

M13. Mumby, K., "Crossroads for fluidized conveying". Mech. Handling, v 52 n 11 (November 1965) pp 513-520.

M14. Muskett, W.J.; Leicester, A.R.; Mason, J.S., "The fluidised transport of powdered materials in an air-gravity conveyor". Proc. Pneumotransport 2, BHRA Conf., Guildford, Paper F1, September 1973.

M15. Montgomery, D.J., "Static electrification of solids". In "Solid State Physics" Vol. IX, Ed. by F. Seitz and D. Turnbull, Academic Press, 1959, pp 139-197.

N1. Neuzil, L.; Turcajova, M., "Fluidised bed viscosity". Coll. Czech. Chem. Commun., v 34 (1969) pp 3652-3655.

N2. Neuzil, L.; Turcajova, M., "Relative viscosity of fluidised bed". Coll. Czech. Chem. Commun., v 42 n 2 (1977) pp 599-611.

N3. Nordberg, B., "Air activated gravity conveyors". Rock Products, v 52 (August 1949) pp 115-124.

P1. Parker, H.W.; Stevens, W.F., "Effect of liquid on interparticle forces in gas-fluidised beds". A.I.Ch.E. Jour., v 5 n 3 (Sept. 1959) pp 314-318.

P2. Partridge, B.A.; Rowe, P.N., "Analysis of gas flow in a bubbling fluidised bed when cloud formation occurs". Trans. Instn. Chem. Engrs., v 44 (1966) pp T349-T356.

P3. Pay, F.J., "Electrostatic - a potential hazard when handling powders in bulk". Bulk, v 4 n 3 (January/February 1978) pp 51-55.

P4. Peters, C.; Rose, R., "Air assisted gravity conveyors and silo fluidizing". S. African Mech. Engr., v 26 n 6 (June 1976) pp 249-253.

P5. Peters, K.; Schmidt, A., "Untersuchungen über das Wirbelschicht-verfahren". (Studies of the fluidised bed process.) Ost. Chem.-Zeitung, v 54 (September 1953) pp 253-258. (In German)

P6. Pettyjohn, E.S.; Christiansen, E.B., "Effect of particle shape on free-settling rates of isometric particles". Chem. Engg. Progr., v 44 n 2 (February 1948) pp 157-172.

P7. Pfrunder, V.R., "Erfahrungen mit dem pneumatischen Zementtransport". (Experience on the pneumatic conveying of cement.) Zement-Kalk-Gips, v 4 n 3 (March 1951) pp 52-55. (In German)

P8. Pharmaceutical Society of Great Britain, "Characterisation and Manipulation of Powders". Pharmaceutical Press, 1967.

P9. Pugh, R.R., "The flow of fluidised solids". Ph.D.Thesis, Univ. of Aston in Birmingham, 1975.

Q1. Qassim, R.Y., "On the flow of fluidised suspensions". Ph.D. Thesis, Univ. of London, 1970.

R1. Richardson, J.F., "Incipient fluidization and particulate systems". In "Fluidization", Ed. J.F. Davidson and D. Harrison, Academic Press, 1971, pp 25-64.

R2. Richardson, J.F.; McLeman, M., "Pneumatic conveying: Part II. Solids velocities and pressure gradients in a one-inch horizontal pipe". Trans. Instn. Chem. Engrs., v 38 (1960) pp 257-266.

R3. Richardson, J.F.; Zaki, W.N., "Sedimentation and fluidisation: Part I". Trans. Instn. Chem. Engrs., v 32 (1954) pp 35-53.

R4. Rietema, K.; Mutsers, S.M.P., "On the elasticity of gas-fluidised systems". Proc. Int. Fluidization Conf., Asilomar, Calif., U.S.A., June 1975, "Fluidization Technology", Vol. I, pp 53-57.

R5. Rietema, K.; Mutsers, S.M.P., "The effect of interparticle forces on the expansion of a homogeneous gas-fluidised bed". Proc. Conf. "La Fluidisation et ses Applications", Toulouse, October 1973, pp 28-40.

R6. Rowe, P.N., "Experimental properties of bubbles". In "Fluidization", Ed. by J.F. Davidson and D. Harrison, Academic Press, 1971, pp 121-191.

R7. Rowe, P.N., "Drag forces in a hydraulic model of a fluidised bed: Part II". Trans. Instn. Chem. Engrs., v 39 (1961) pp 175-180.

S1. Scarlett, B., "Particle size analysis". Chem. and Process Engg., April 1965.

S2. Schauki, N., "Genugsames Fliessbett. Pneumatische Rinnen für die Schuttgutförderung". (Satisfactory fluidised bed. Pneumatic channels for material transport.) Maschinenmarkt Industrie-journal, v 77 n 80 (1971) pp 1813-1818. (In German)

S3. Schiller, L.; Naumann, A., "Uber die grundlegenden Berechnungen bei der Schwerkraftaufbereitung". (On the fundamental calculations for gravitational classification.) Zeit. Ver. Deutsch. Ing., v 77 n 12 (March 1933) pp 318-320. (In German)

S4. Schugerl, K., "Rheological behaviour of fluidised systems". In "Fluidization", Ed. by J. F. Davidson and D. Harrison, Academic Press, 1971, pp 261-292.

S5. Selig, H-J., "Flow bottoms made of composite plates (perm-porous plastics on perforated plate) for pneumatic storage mixing and handling applications". Fördern und Heben, v 17 n 15 (1967) pp 891-895. (In German)

S6. Selig, H-J., "Initial flow bottoms of porous sintered plastics for pneumatic storage, mixing and handling". Fördorn und Heben, v 15 n 11 (1965) pp 800-802. (In German)

S7. Shinohara, K.; Hayashi, K.; Tanaka, T., "Residence time distribution of particles with pneumatic escalator". J. Chem. Engg. of Japan, v 6 n 5 (1973) pp 447-453.

S8. Shinohara, K.; Saito, K.; Tanaka, T., "Flow properties of particles on air-slide". Micromeritics, v 19 (1974) pp 64-72. (In Japanese)

S9. Shinohara, K.; Tanaka, T., "A new device for pneumatic transport of particles". J. Chem. Engg. of Japan, v 5 n 3 (1972) pp 279-285.

S10. Shuster, W.W.; Haas, F.C., "Point viscosity measurements in a fluidised bed". J. Chem.and Engg. Data, v 5 n 4 (October 1960) pp 525-530.

S11. Seigel, R., "Effect of distributor plate-to-bed resistance ratio on onset of fluidized bed channelling". A.I.Ch.E. Jour., v 22 n 3 (May 1976) pp 590-592.

S12. Siemes, W., "Förderung von körnigem Gut in geneigten Fliessbetten". (Transport of granular material in inclined fluidised beds.) Chemie-Ing. Tech., v 31 n 3 (January 1959) pp 212-213. (In German)

S13. Siemes, W.; Hellmer, L., "Die Messung der Wirbelschichtviskosität mit der pneumatischen Rinne". (Measurement of fluidised bed viscosity with pneumatic duct.) Chem. Engg. Sci., v 17 (1962) pp 555-571. (In German)

S14. Stacey, R.B., "Fluidised bed conveying systems". Unpublished communication to Pneumotransport Panel of BHRA, June 1974.

S15. Stegmaier, W., "Goulottes pneumatiques de transport horizontal". (Horizontally conveying pneumatic chutes.) Fördern und Heben, v 26 n 6 (1976) pp 621-624. (In German)

S16. Stoess, H.A., "Pneumatic Conveying". Wiley-Interscience, 1970.

S17. Straub, L.G.; Silberman, E.; Nelson, H.C., "Open channel flow at small Reynolds numbers". Trans. Am. Soc. Civil Engrs., v 123 Paper No. 2935 (1958) pp 685-706.

S18. Sutherland, J.P., "The measurement of pressure drop across a gas fluidised bed". Chem. Engg. Sci., v 19 (1964) pp 839-841.

S19. Suzuki, A.; Tanaka, T., "Measurement of flow properties of powders along an inclined plane". Ind. and Engg. Chem. Fundam., v 10 n 1 (1971) pp 84-91.

S20. Szonyi, J., "Förderleistungsfähigkeit der pneumatischen Förderrinne". (Operational performance of pneumatic conveying channels.) Proc. 2nd Conf. on Pneumatic Conveying, Pécs, Hungary, March 1978, Paper B7, pp 111-116. (In German)

S21. Singh, B.; Callcott, T.G.; Rigby, G.R., "Flow of fluidized solids and other fluids in open channels". Powder Techn., v 20 (May/June 1978) pp 99-113.

S22. Stankovich, I. "Classification of pneumatic handling". Proc. Pneumotransport 4, BHRA Conf., Carmel, Calif., Paper F7, June 1978.

T1. Toomey, R.D.; Johnstone, H.F., "Gaseous fluidization of solid particles". Chem. Engg. Progr., v 48 n 5 (May 1952) pp 220-226.

T2. Train, D., "Some aspects of the property of angle of repose of powders". J. Pharmacy and Pharmacology, v 10 (suppl.) (December 1958) pp 127-135.

T3. Trivedi, R.C.; Rice, W.J., "Effect of bed depth, air velocity, and distributor on pressure drop in an air-fluidized bed". Chem. Engg. Progr. Symp. Series, v 62 n 67 (1966) pp 57-63.

T4. Turcajova, M.; Neuzil, L., "Friction factor for flow of a fluidized bed in an airslide". Coll. Czech. Chem. Commun., v 42 n 2 (1977) pp 612-619.

V1. Vitunac, E.A., "Considerations in the selection of a pneumatic conveying system". Mining Engineering, May 1968, pp 83-87.

V2. Vollkommer, T.J., "Improvements in pneumatic apparatus for the transport and guidance of band or sheet or plate material". Brit. Patent 17472, 1902.

W1. Waddell, H., "The coefficient of resistance as a function of Reynolds number for solids of various shapes". J. Franklin Inst., v 217 n 4 (April 1934) pp 459-490.

W2. Weber, M., "Fliessförderung in Rinnen und Rohrleitungen". (Fluidised flow in channels and pipelines.) Maschinenmarkt Industriejournal, v 74 n 102 (1968) pp 161-164. (In German)

W3. Wen, C.Y.; Yu, Y.H., "A generalized method for predicting the minimum fluidization velocity". A.I.Ch.E. Jour., v 12 n 3 (May 1966) pp 610-612.

W4. Wen, C.Y.; Yu, Y.H., "Mechanics of fluidization". Chem. Engg. Progr. Symp. Series, v 62 n 62 (1966) pp 100-111.

W5. West, R.F., "Bulk materials handling of alumina". ASME Paper No. 61-WA-80, 1962.

Z1. Zabrodsky, S.S., "Hydrodynamics and Heat Transfer in Fluidized Beds". M.I.T. Press, 1966.

Z2. Zabrodsky, S.S., "On operation of gas-distributors in fluidised bed equipment". Proc. Conf. "La Fluidisation et ses Applications", Toulouse, October 1973, pp 99-106.

APPENDIX A.VII

CONFERENCE PAPERS AND PUBLICATIONS ARISING FROM THE RESEARCH PROGRAMME

1. Woodcock, C.R. and Mason, J.S. "Fluidised bed conveying - art or science?" Proc. Pneumotransport 3, BHRA Conference, Paper E1, Bath, U.K., April 1976.

2. Woodcock, C.R. and Mason, J.S. "The flow characteristics of a fluidised p.v.c. powder in an inclined channel". Proc. Int. Powder and Bulk Solids Handling and Processing Conf., Chicago, U.S.A., May 1977, pp 466-475.

3. Woodcock, C.R. and Mason, J.S. "Air-assisted gravity conveying to transport powders economically". Presented at Conf. Powder Europa, Wiesbaden, W. Germany, January 1978.

4. Woodcock, C.R. and Mason, J.S. "The modelling of air-assisted bulk particulate solids flow in inclined channels". Proc. Pneumotransport 4, BHRA Conference, Paper D2, Carmel-by-the-Sea, California, U.S.A., June 1978.

5. Woodcock, C.R. and Mason, J.S. "Aspects of the design of air-assisted gravity conveyors for the transport of bulk particulate solids". To be presented at A.I.Chem. E. Conf., Florida, U.S.A., Nov. 1978.